Cranfield Institute of Technology

College of Aeronautics

Ph.D. Thesis

M.S.Ryan

The Dynamic Analysis of Flexible Riser Systems

Supervisor: Prof.C.L.Kirk

January 1988

ABSTRACT

The aim of this thesis is to provide a design tool for the engineering analysis of the dynamics of a flexible riser system. The design tool is provided in the form of a computer program.

The two main requirements of such a program are that it is realistic and practical to use. The necessary theory is developed to allow these requirements to be satisfied.

To ensure accuracy checks are made against model tests and known analytical solutions.

How the computer program may be used is shown by analysing a particular riser configuration.

ACKNOWLEDGEMENTS

I wish to thank Professor C.L.Kirk for his help and guidance; past and present members of the Offshore Structures Group including Drs. R.S.Langley, A.D.Trim and R.Ghadimi; John Carter of Dunlop Oil and Marine Limited; S.E.R.C. who provided financial support; the computer manager Dr. L. Oswald and finally all those people who have been unfortunate enough to live with me during the past three years.

CONTENTS

FIGURES

NOTATION

The usage of symbols is made clear in the relevant part of the text. For purposes of reference the notation used in the two more mathematical chapters is given here. Note that a given symbol might be used to denote several different quantities.

CHAPTER TWO:

t :Time.

t_o :Reference time.

s_o :Arc-length parameter in reference state.

s :Arc-length parameter in strained state.

s_m :Arc-length parameter for centre of mass of segment.

$\underset{\sim}{t}$:Tangent vector to a space curve.

$\underset{\sim}{b}$:Binormal vector to a space curve.

$\underset{\sim}{n}$:Normal vector to a space curve.

κ :Curvature of space curve.

τ :Torsion of a space curve.

$\underset{\sim}{F}_b$:Body force per unit volume.

$\underset{\sim}{F}_e$:Surface traction force over S_e .

$\underset{\sim}{F}_i$:Surface traction force over S_i .

$\underset{\sim}{F}_R$:Surface traction force over A_R .

$\underset{\sim}{F}_L$:Surface traction force over A_L .

$\underset{\sim}{F}_T$:Surface traction force over A .

V :Volume of segment.

S_e :Total curved external surface of segment. (excluding end surfaces)

S_i :Total curved internal surface of segment.

(excluding end surfaces)

A_R :Right-hand end surface of segment.

A_L :Left-hand end surface of segment.

A :Appropriate cross-sectional area. (either left-hand or rigth-hand end surface)

$\underset{\sim}{F}_u$:Upthrust force per unit arc-length.

$\underset{\sim}{F}_m$:Morison loading force per unit arc-length.

$\underset{\sim}{R}$:Reaction force per unit arc-length due to internal fluid flow.

$\underset{\sim}{Q}$:Resultant load vector.

$\underset{\sim}{v}_f$:Velocity of internal fluid flow.

$\underset{\sim}{F}_p$:Hydrostatic pressure force term (detailed usage explained in text).

$\underset{\sim}{F}_p^*$:Hydrostatic pressure force term (detailed usage explained in text).

$\underset{\sim}{q}$:Position vector from the centre-line to a point on the cross-section.

P_I :Internal fluid pressure.

L :Net length of continuous riser.

CHAPTER THREE:

$\underset{\sim}{r}_i$:Position vector of the ith node.

L_i^* :Unstrained length of the ith mass-less spring.

L_i :Strained length of the ith mass-less spring.

$\underset{\sim}{t}_i$:Tangent vector defined by the ith mass-less spring.

m_i :Mass of ith lumped mass.

T_i :Tension in ith element.

k_i :Spring constant of ith mass-less spring.

N :Number of mass-less springs employed in

discretization.

$\underset{\sim}{F}_i$:Nodal force acting at ith lumped mass.

g :Gravitational constant.

$\underset{\sim}{r}, \underset{\sim}{R}$:Position vectors of the ends of an element.

E :Young's Modulus.

A :Cross-sectional area of the riser.

$\underset{\sim}{F}_{ei}$:Element force on ith element.

$\underset{\sim}{M}_{ei}$:Element Morison force on ith element.

$\underset{\sim}{G}_{ei}$:Element gravity force on ith element.

$\underset{\sim}{U}_{ei}$:Element upthrust force on ith element.

V_i :Volume of ith element.

$\underset{\sim}{D}_{ei}$:Element drag force on ith element.

$\underset{\sim}{I}_{ei}$:Element inertia force on ith element.

$\underset{\sim}{A}_{ei}$:Element added mass force on ith element.

D_i :Diameter of ith element in the strained state.

D_i^* :Diameter of ith element in the unstrained state.

$\dot{x}$:First derivative of variable $x=x(t)$ with respect to time i.e. $\dot{x}=\frac{dx}{dt}$.

$\ddot{x}$:Second derivative of variable $x=x(t)$ with respect to time i.e. $\ddot{x}=\frac{d^2x}{dt^2}$.

$\frac{\partial r}{\partial s_0}, \frac{\overline{\partial r}}{\partial s_0}$:Values of $\frac{\partial r}{\partial s_0}$ at either end of the ith element.

$\mathcal{L}, \bar{\mathcal{L}}, \mathcal{K}, \mathcal{H}$:Hermite interpolating polynomials.

$\underset{\sim}{\chi}|_m$:Value of the variable $\underset{\sim}{\chi}$ evaluated at the middle of the element.

$\underset{\sim}{E}_e$:External force on an element per unit of unstrained length.

ρ_i :Density of ith element per unit of unstrained length.

H :Unstrained length of an element.

h :Strained length of an element.

$L, \bar{L}$:Linear interpolating polynomials for general element.

$L_i, \bar{L}_i$:Linear interpolating polynomials for ith element.

$\underset{\sim}{r}_t$:Position vector of a point on an element.

$\underset{\sim}{x}|^n$:Value of the variable $\underset{\sim}{x}$ after n timesteps.

$\underset{\sim}{V}_i$:Defined by $\underset{\sim}{V}_i = L_i \underset{\sim}{\bar{V}}_i$.

$\underset{\sim}{U}_i$:Defined by $\underset{\sim}{U}_i = L_i \underset{\sim}{\bar{U}}_i$.

$\underset{\sim}{\bar{V}}_i$:Defined by $\underset{\sim}{\bar{V}}_i = -\cos\theta_i \sin\psi_i \underset{\sim}{i} + \cos\theta_i \cos\psi_i \underset{\sim}{j}$.

$\underset{\sim}{\bar{U}}_i$:Defined by $\underset{\sim}{\bar{U}}_i = -\sin\theta_i \cos\psi_i \underset{\sim}{i} - \sin\theta_i \sin\psi_i \underset{\sim}{j} - \cos\theta_i \underset{\sim}{k}$.

$[A_i]$:Defined by $[A_i] = m_i [I] + F_i [\hat{T}_i]$ $(i = 1, \ldots, N-1)$.

$\underset{\sim}{A}_i$:Nodal added mass force.

$\{\underset{\sim}{e}_x, \underset{\sim}{e}_y, \underset{\sim}{e}_z\}$:Orthonormal basis ($\underset{\sim}{e}_z$ generally points upward).

Δt :Timestep.

δ :Either variational operator or denotes a small quantity (usage made clear in text).

$\tilde{\underset{\sim}{r}}$:Global finite element approximation of position vector of riser centre-line.

ϕ_i :Basis function.

Ω :Differential operator.

$\underset{\sim}{r}'_i$:Defined by $\underset{\sim}{r}'_i = \left(\frac{\partial \underset{\sim}{r}}{\partial s_0}\right)_i$.

$\underset{\sim}{\bar{r}}'_i$:Defined by $\underset{\sim}{\bar{r}}'_i = \left(\frac{\partial \underset{\sim}{\bar{r}}}{\partial s_0}\right)_i$.

$\bar{T}_m$:Tension at the midpoint of an element.

θ_i, ψ_i :Euler angles (defined in section 2.6.2) for ith element.

$[M]$:Mass matrix of system.

$\underset{\sim}{F}$:Force vector for system.

ρ_w :Density of seawater per unit volume.

$\underset{\sim}{r}_{ei}$:Defined by $\underset{\sim}{r}_{ei} = \frac{1}{2}(\underset{\sim}{r}_{i-1} + \underset{\sim}{r}_i)$.

$\underset{\sim}{v}_{fi}$:Element fluid velocity.

α_i :Defined by $4\alpha_i = \frac{1}{4}\pi\rho_w D_i^2 C_A L_i$

$\underset{\sim}{x}|_{n_i}$:"Normal" component of variable $\underset{\sim}{x}$ with respect to the ith element i.e. $\underset{\sim}{x}|_{n_i} = \underset{\sim}{x} - (\underset{\sim}{x}\cdot\underset{\sim}{t}_i)\underset{\sim}{t}_i$.

$[T_i]$:Defined by $[\underset{\sim}{x}|_{n_i}] = [T_i][\underset{\sim}{x}]$.

$[I]$:3×3 identity matrix.

$(\underset{\sim}{x})_x$:Defined by $(\underset{\sim}{x})_x = (\underset{\sim}{x}\cdot\underset{\sim}{e}_x)$ where $\underset{\sim}{e}_x$ is a unit vector and is a member of the basis $\{\underset{\sim}{e}_x, \underset{\sim}{e}_y, \underset{\sim}{e}_z\} = \{\underset{\sim}{i}, \underset{\sim}{j}, \underset{\sim}{k}\}$.

$\hat{\underset{\sim}{t}}_i$:"Average" tangent vector defined by $\hat{\underset{\sim}{t}}_i = \frac{L_{i+1}\underset{\sim}{t}_i + L_i\underset{\sim}{t}_{i+1}}{|L_{i+1}\underset{\sim}{t}_i + L_i\underset{\sim}{t}_{i+1}|}$.

$\underset{\sim}{x}|_{\hat{n}_i}$:"Normal" component of variable $\underset{\sim}{x}$ with respect to the "average" tangent vector i.e. $\underset{\sim}{x}|_{\hat{n}_i} = \underset{\sim}{x} - (\underset{\sim}{x}\cdot\hat{\underset{\sim}{t}}_i)\hat{\underset{\sim}{t}}_i$.

$[\hat{T}_i]$:Defined by $[\underset{\sim}{x}|_{\hat{n}_i}] = [\hat{T}_i][\underset{\sim}{x}]$.

β_i :Defined by $\beta_i = 2\alpha_i + 2\alpha_{i+1}$ $(i=1,\ldots,N-1)$

$(AE)_i$:Value of AE for ith element.

$\underset{\sim}{R}$:Defined by $\underset{\sim}{R} = \bar{\underset{\sim}{E}} - \underset{\sim}{C}$.

Δ :Defined by $\Delta = \frac{2\underset{\sim}{R}\cdot\delta\underset{\sim}{R} + \delta\underset{\sim}{R}\cdot\delta\underset{\sim}{R}}{\underset{\sim}{R}\cdot\underset{\sim}{R}}$.

$\bar{\underset{\sim}{F}}_{ei}$:Defined by $\bar{\underset{\sim}{F}}_{ei} = \underset{\sim}{F}_{ei} - \underset{\sim}{A}_{ei}$.

t_j^* :Tangent vector for cubic element.

$\underset{\sim}{Q}, \bar{\underset{\sim}{Q}}$:Interpolating functions.

CHAPTER ONE:INTRODUCTION

1.1:Overview.

In this chapter a brief history of U.K. offshore oil and gas production is given along with the probable future developments. The importance of flexible risers is explained. Possible operational problems are described.

The previous relevant literature is reviewed, the aims of this thesis are given and the chapters to follow are briefly described.

1.2:History of U.K. Oil and Gas production.

An excellent description of the growth of the U.K. offshore oil and gas industry is given by the U.K. Offshore Operators Association[1986] and much of what follows in section 1.2 follows this reference.

The first major discovery in the North Sea was the Groningen Gas field in the late 1950's. After this discovery it was thought that the geology of the North Sea area was such that there might be significant gas bearing formations in the Southern North Sea. And by 1967 three major gas fields had been discovered; Hewett, Leman and Indefatigable. In 1975 Britain became virtually self-sufficient with these three large gas fields contributing over 75% of the nation's gas supply.

In the 1970's O.P.E.C. forced oil prices to rise sharply. Thus interest was switched to producing oil from

the then newly discovered oil fields. In 1969 the giant Ekofisk field was discovered in the Norwegian sector of the North Sea along with the Montrose field in the Central North Sea Basin.

The Montrose field was the first commercial oil discovery in the U.K. sector. However the first oil to come ashore from the U.K. sector was from the Argyll field in June 1975. Five months later oil flowed ashore from the Forties field. By the end of 1980 there were a total of 15 fields "on stream" producing about 1.6 million barrels of oil per day. The producing oil and gas fields at present are shown in figure 1.2(a).

In recent years companies have been encouraged by the Government to explore for new gas reserves in order that the dependence on gas imports could be reduced. In 1984 the Department of Energy gave approval for seven new gas field projects. It is estimated that these new developments along with recent discoveries will make Britain self-sufficient until at least the next century.

Now the total number of offshore exploration wells has exceeded 1000 producing more than 200 significant discoveries. There are 30 offshore fields producing 2.65 million barrels of oil per day and 9 offshore gas fields producing 4.1 billion cubic feet of gas per day. The total investment by the oil industry has exceeded 40 billion pounds and employment has been provided for over 100,000 people.

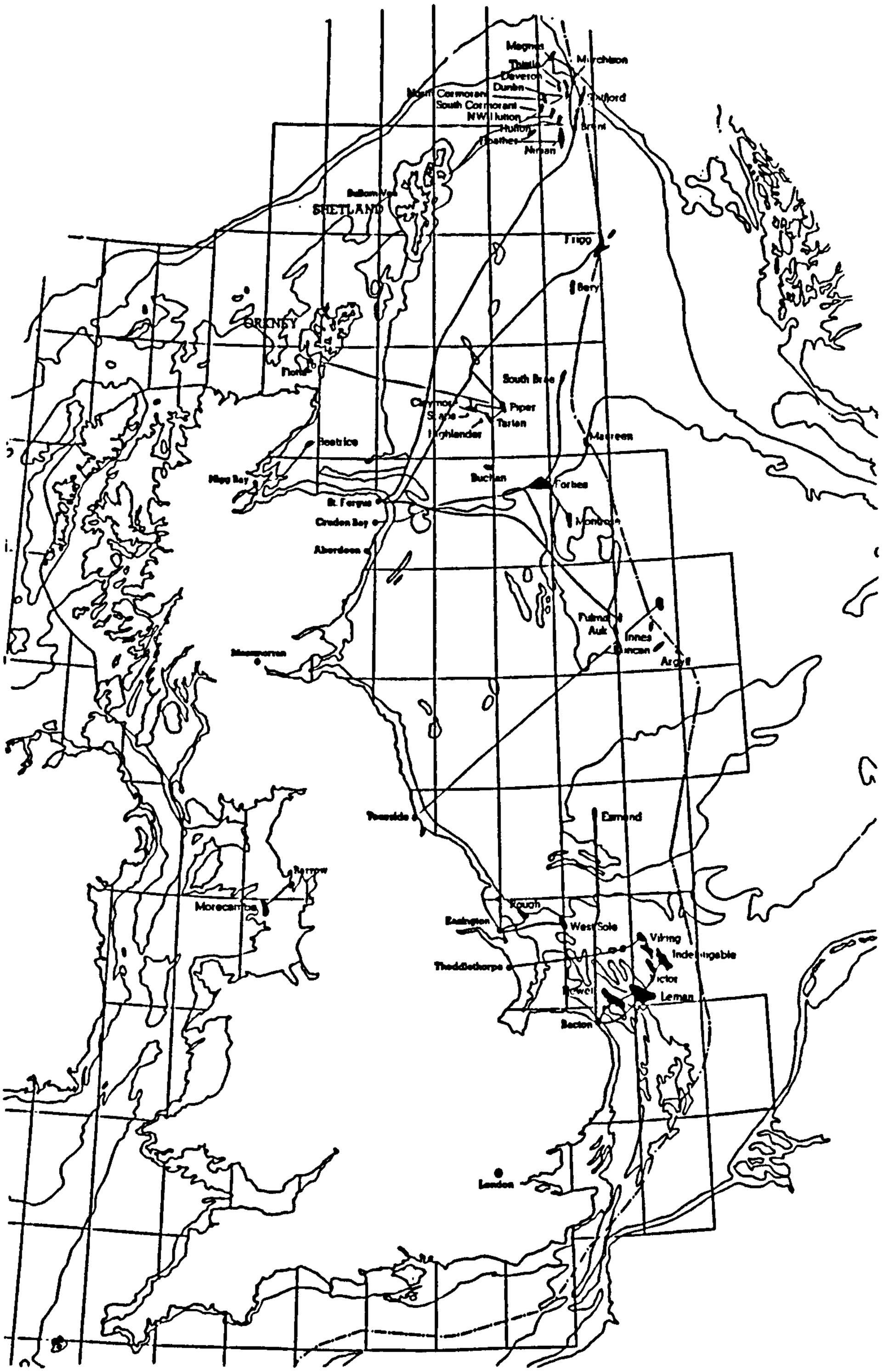

Figure 1.2(a): Producing Oil and Gas Fields in 1986

For every barrel of oil produced about 54% of its cash value goes in revenue to the government (by royalty, petroleum revenue tax and corporation tax), approximately 33% goes on capital and operating costs and only 13% is profit. For example in the financial year 1984-1985 20 billion pounds worth of oil and gas were produced and the government received 12 billion pounds in revenue.

1.3:The Future.

It is thought that all the major oil fields in the Central North Sea Basin, in the Northern North Sea Basin and in the East Shetland Basin have now been discovered. Hence new fields will be either much smaller or in deeper more hostile water such as in the area west of Shetland. The likely size of new fields in the more mature areas of the North Sea is around 80 million barrels which is about a fifth of the size of a typical field now.

Oil companies are developing new techniques for producing residual oil from existing fields by injecting chemicals, gases and hot water/steam into the oil reservoir. These techniques have proved to be prohibitively expensive so far but may be used in the future.

Recently the oil price has dropped considerably and it is unlikely to reach its previous level in the near future. Hence if oil is going to be worth producing in the future more economic ways must be found to do so; one way to do this is to use flexible riser systems.

It is not only the oil price that controls the development of new fields; the Government has substantial control also. If the Government were to reduce the Petroleum Revenue Tax this would encourage further development as the oil companies could then make a reasonable profit.

1.4:Flexible Riser Systems.

Before oil is produced the well is first drilled using a jack-up barge, a semi-submersible rig or a drill-ship as shown in figure 1.4 (a). Oil is then produced by using a rigid riser (a tensioned steel tube) with either a fixed platform (examples of which are shown in figure 1.4(b)) or with a semi-submersible (in this context often called a floating production vessel). For a small field it is not economic to use a fixed platform neither is it economic if the field is in deep water. Hence in the future it is more likely that floating production vessel technology shall be used. It is possible to use a floating production vessel with a flexible riser (a reinforced rubber hose) as shown in figure 1.4(c) rather than with a rigid riser. In this context flexible risers have several advantages over rigid risers:

1.They can remain connected in any sea state.

2.They leave the area around the well template free for diving and other underwater operations.

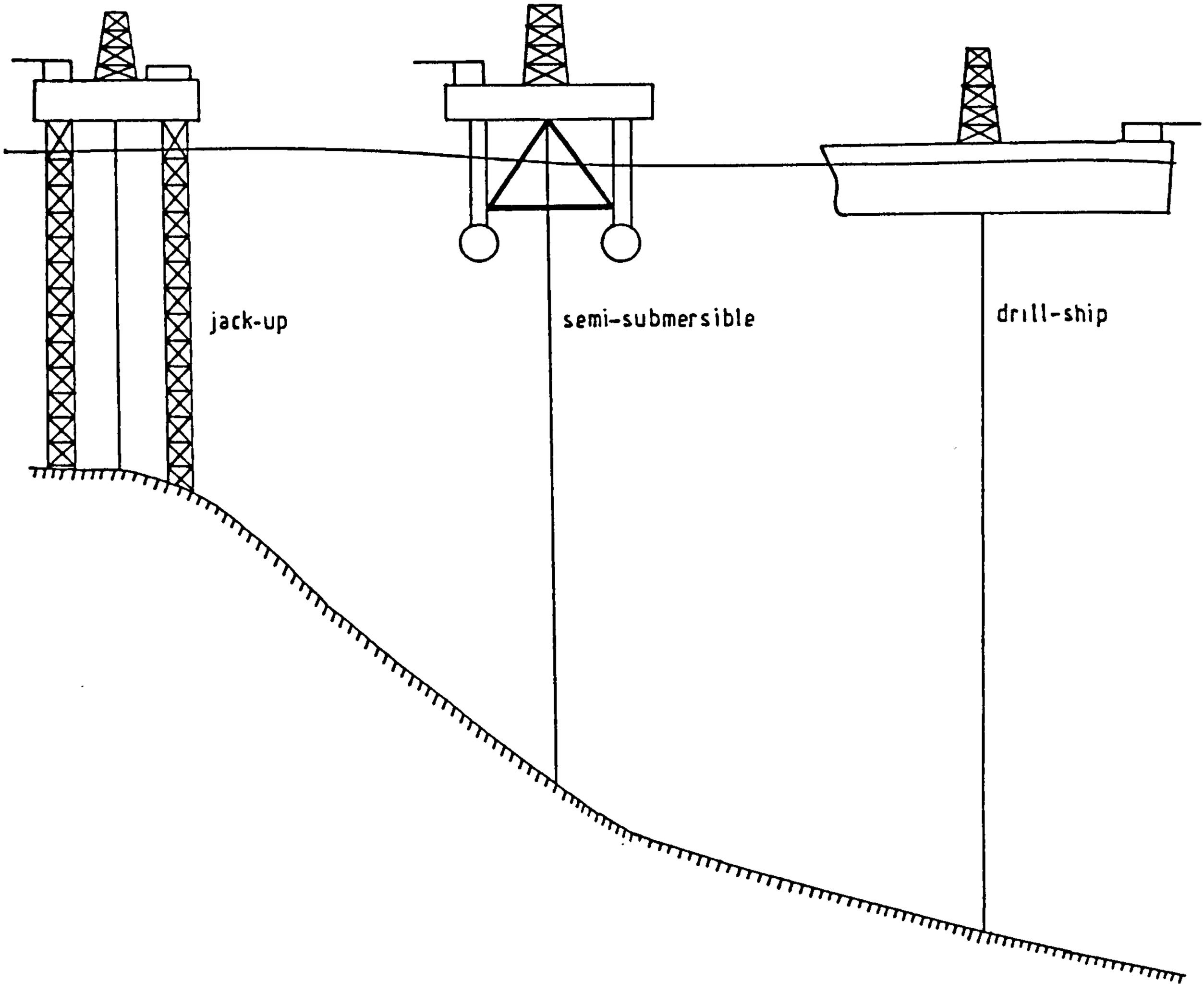

Figure 1.4 (a): Jack-Up, Semi-Submersible and Drill-Ship

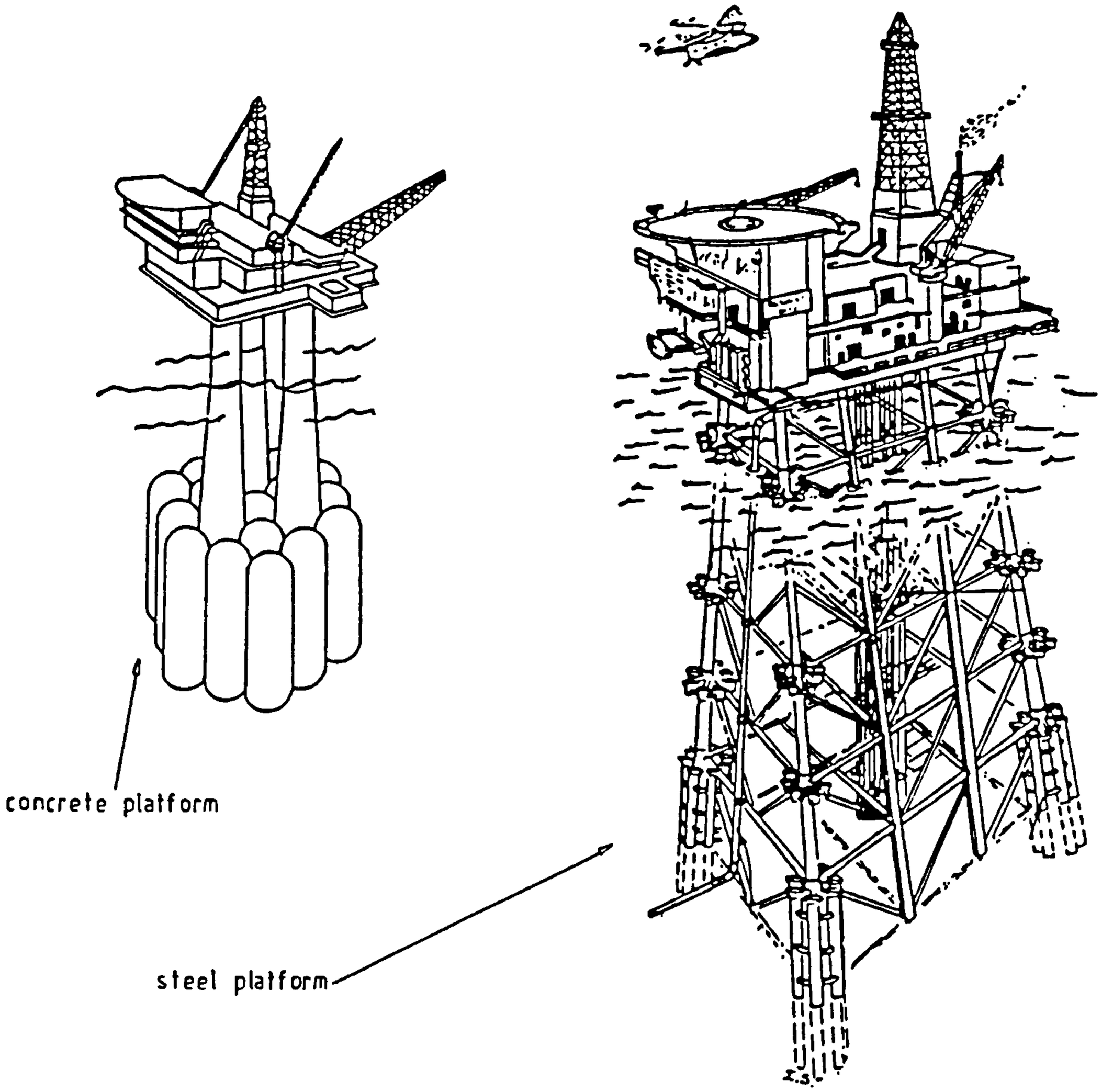

Figure 1.4(b): Examples of Fixed Platforms (not to scale)

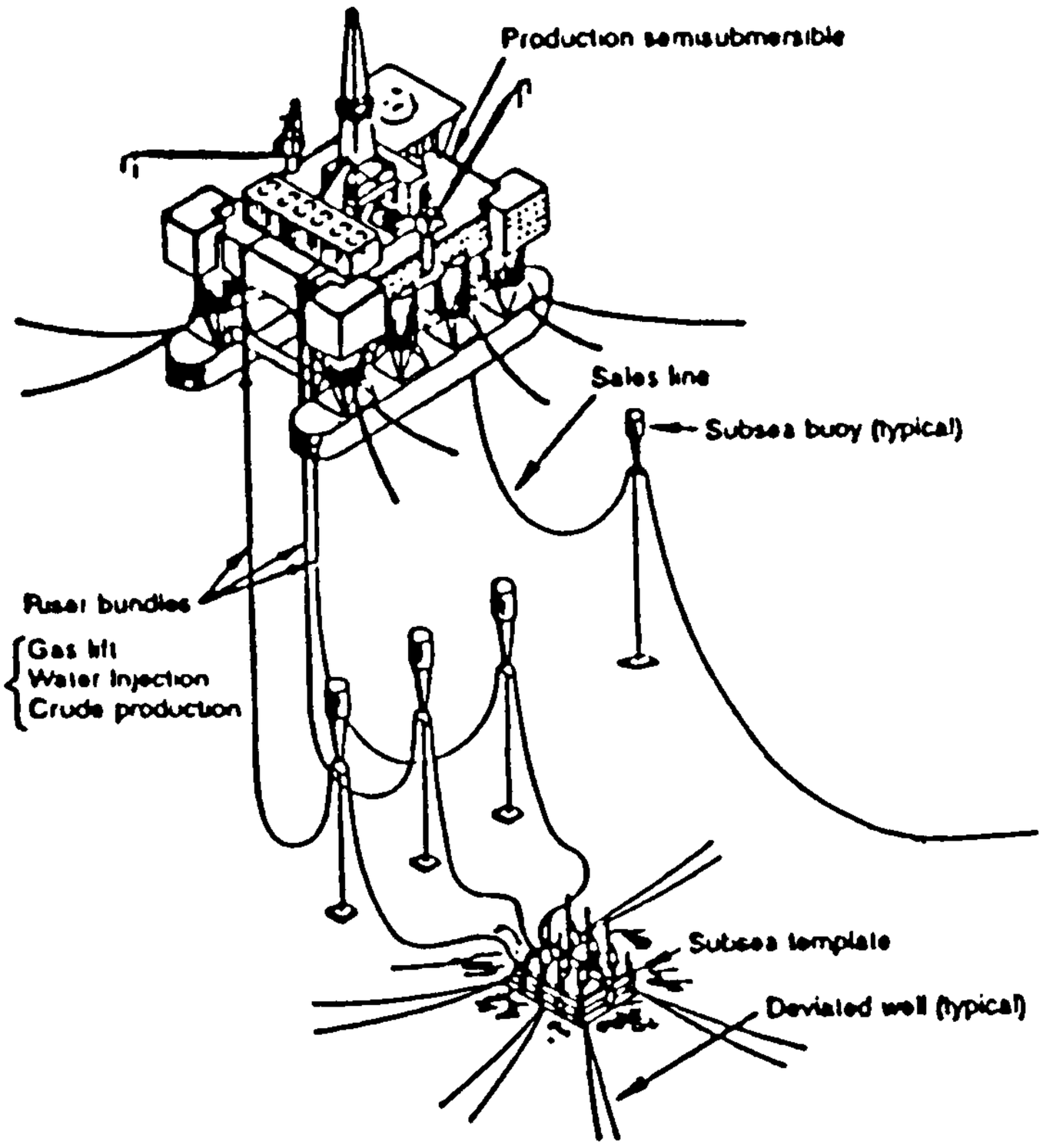

DP-120

DP-120 is suited for 100,000 to 240,000-bopd production capacity.

Figure 1.4(c): Floating Production Vessel with a Flexible Riser

3.They can produce oil in very bad weather conditions.

There are five types of flexible riser configuration as shown in figure 1.4(d). The choice of configuration is dependent on economic and environmental factors.

The first purpose built floating production vessel has been constructed in 1986 for the Balmoral field. It has been designed to use a flexible riser. Oil production using this floating production vessel started in 1987.

Flexible risers were first used in the Campos Basin off Brazil in the mid 1970's. When oil was first discovered there, there was termendous pressure on the national oil company Petrobras to bring oil ashore as quickly as possible because of the poor state of the Brazilian economy. Hence Petrobras used floating production vessels with flexible risers rather than conventional fixed platforms as to do so would mean the earlier production of oil. The original intention was to replace the floating production vessels by fixed platforms with rigid risers however this was found to be unnecessary. All the technology was largely untried however it proved to be successful. Conditions in the North Sea are much more hostile than in the Campos Basin hence careful evaluation of floating production technology is required.

Flexible risers are subject to some extremely complex motions and the following operational problems may

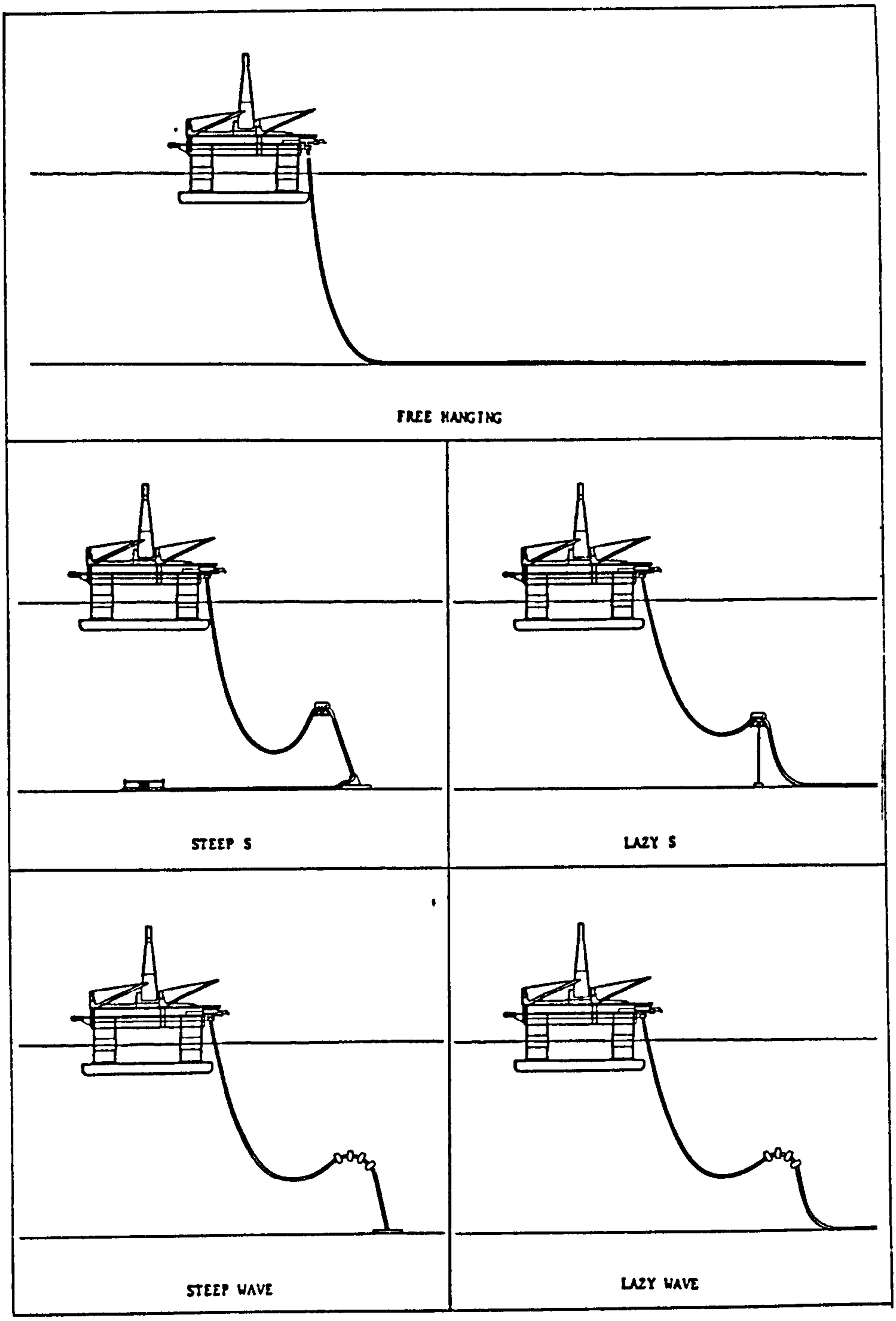

Figure 1.4 (d): Types of Flexible Riser Configuration (Pettenati-Auziere [1985])

occur:

1.Chafing from contact with itself (only likely in a multiple riser system) or with the seabed or with other bodies such as buoys etc..

2.Kinking due to high local bending stresses.

3.Entanglement of the riser with mooring cables etc..

4.Fatigue of the riser material due to the motions of the riser system.

A designer might try to overcome these problems by changing the dynamic or static properties of the riser system. The aim of this thesis is to develop sufficient theory so that a riser system might be modelled realistically by a computer program and then to show how this computer program may be used. Such a computer program would be of considerable practical use to a design engineer.

There are a number of non-trivial things that must be included in the model so that it is realistic:

1.The bending stiffness of the riser must be modelled to ascertain its effect on both the static and dynamic behaviour of the riser. Even if the bending stiffness of the riser has little effect on the riser behaviour it may still be important to include it so that the riser bending moments may be calculated for use in fatigue calculations.

2.The flexible riser usually has a liquid flowing through it

e.g. water, oil etc.. This liquid may effect the behaviour of the riser and it must be allowed for in the model. Note that in some circumstances the riser might have gas (for gas injection, gas lift etc.) flowing in it but because of the low density of the gas compared with that of the riser it is unlikely to have any significant effect.

3.In some riser configurations the lower part of the riser might lie on the seabed.

4.The top end of the riser is usually above the water surface. The change in loading that this causes must be included.

5.The movement of the top end of the riser caused by the motion of the semi-submersible.

The principle manufacturers of flexible risers are Dunlop in England and Coflexip in France. Coflexip has had a monoply in the market until recently when Dunlop developed the facility to manufacture continuous lengths of riser. Previously Dunlop could not do this and therefore its products were only suitable for flow-lines, jumper connections and for other similar uses. Data for the flexible risers made by Dunlop and Coflexip is given in Appendix D. The data given in this appendix is approximate. Normally risers are made to a specification given by the customer. Both makes of flexible riser have a spiral wound interlocked inner steel core with a plastic coating to retain the fluid that is to be transported. There are then

layers of either textile reinforcements, wound steel cable reinforcements or elastomeric materials. These layers ensure that the riser is able to resist weathering and abrasion. In figure 1.4(e) the structures of two types of Coflexip riser are shown.

There are several types of flexible riser configuration and these are shown in figure 1.4(d). Each of these configurations has certain advantages and disadvantages dependent on external factors. For example the free hanging configuration has the advantage that it is simple to install and the disadvantage that it performs badly in hostile weather conditions.

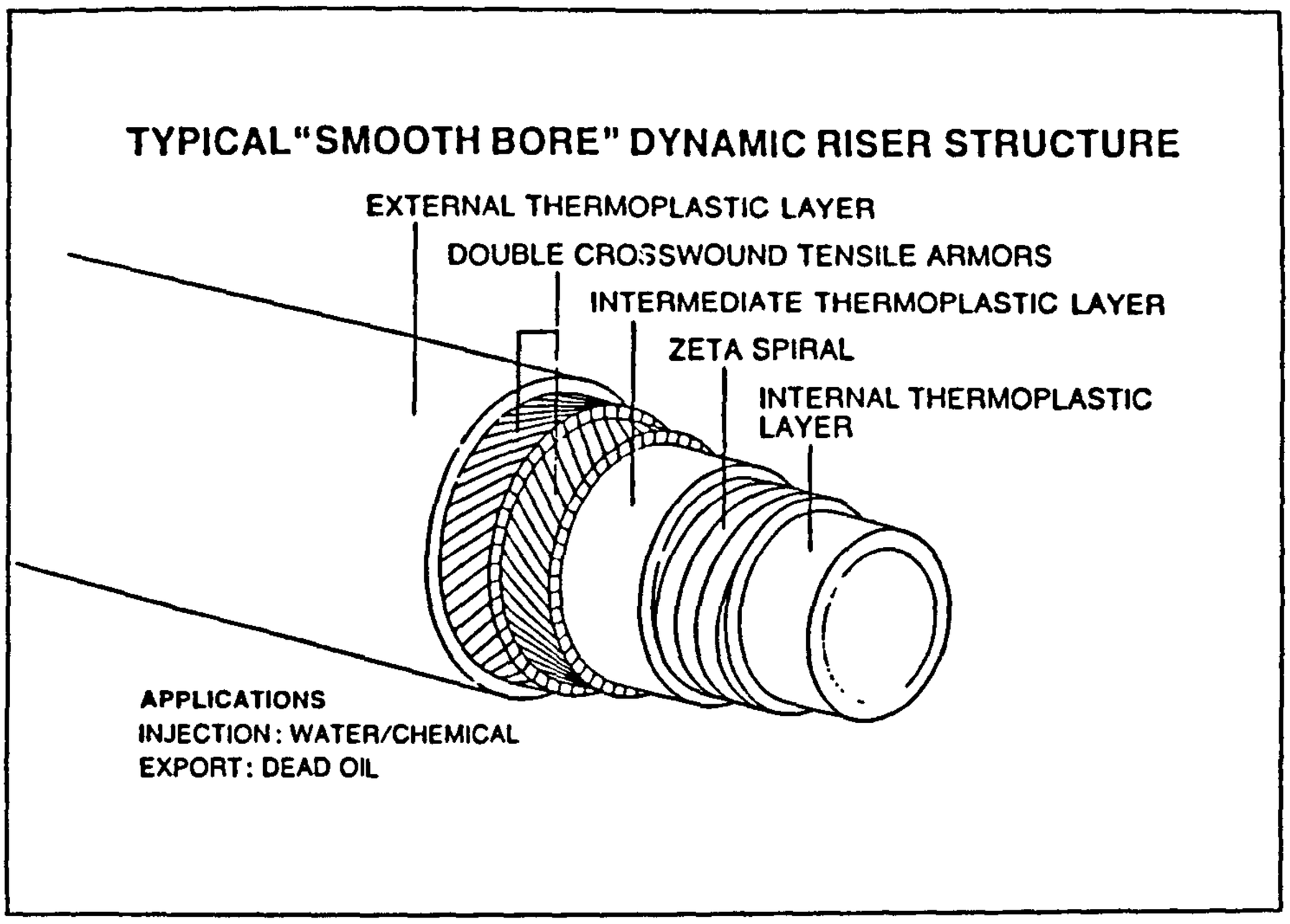

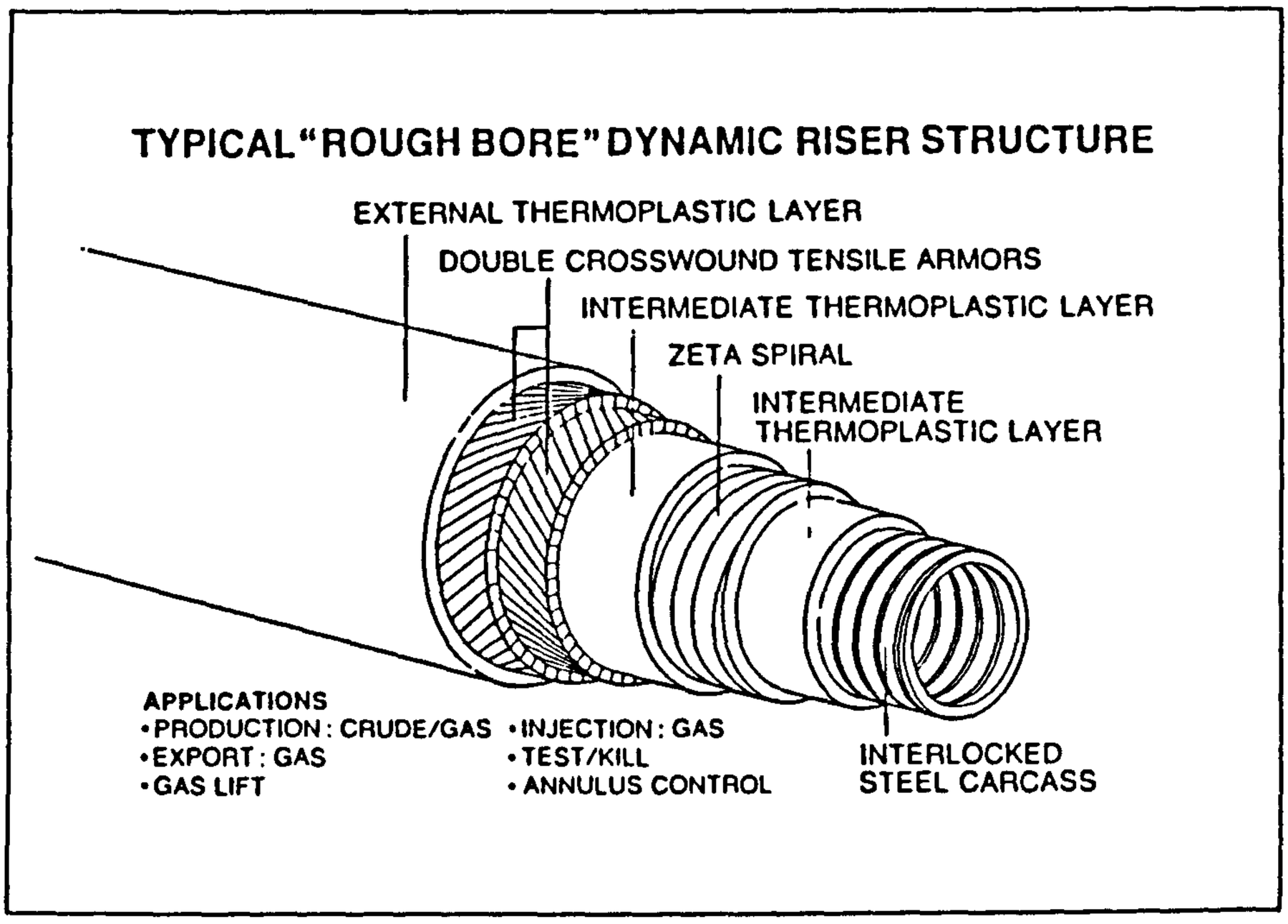

Figure 1.4(e): Typical Internal Structures of Coflexip Risers (Pettenati-Auziere (1985))

1.5:Objectives, Contents and Literature Review.

1.5.1:Introduction.

As mentioned previously the aim of this work is to develop a realistic design tool for the dynamic analysis of flexible risers in the form of a computer program. This tool will help the designer to choose the appropriate riser configuration and the appropriate riser parameters for the given expected environmental conditions. It will also help to overcome various possible operational problems as described in section 1.4. Previous computer models are not adequate for the following reasons:

1.Too inefficient; for example the Flexan program (C.I.S.I. Petrole Services[1984]) needs to run on a Cray supercomputer.

2.Too complicated; for example the programs based on the elements derived by O'Brien, McNamara and Dunne[1987] and O'Brien, McNamara and Gilroy[1986].

3.The theory on which they are based is not adequately justified; for example the program developed by Ractliffe[1984].

4.They can only deal with some of the practical requirements; which are usually for example the modelling of ground contact, top motion, bending stiffness, internal fluid flow etc..

5.None of them have been validated against an analytical

dynamic solution.

In the rest of section 1.5 for each of the chapters of this thesis a brief description of the work contained within the chapter is given along with a brief description of the relevant literature.

1.5.2:Chapter Two.

In Chapter Two a mathematical description is provided for the dynamics of a riser in terms of two types of equation; a differential equation and a variational equation. The differential equation derived includes as special cases all the previous relevant differential equations i.e. the equation derived by Cristescu[1967] for an extensible string and the equation derived by Nordgren[1974] for an inextensible rod. Derivation of the variational equation is equivalent to deriving an expression for the strain energy of the riser. This has not previously been done. It is shown how the variational equation may be used to obtain the differential equation.

The remaining chapters of this thesis are based to a large extent on the work done in Chapter Two. The variational equation in particular forms the basis of several very useful finite element discretizations that are developed in Chapter Three.

For the first time a mathematical model for the description of the internal fluid flow is presented. In

essence the riser is modelled as a slender tensioned beam that is subject to large displacements. If the bending stiffness of the riser is included then the strain in the riser must be small.

1.5.3:Chapter Three.

In Chapter Three the mathematical descriptions given in Chapter Two are used to find computational methods that describe the dynamics of the riser; these are called discretizations. Most of the discretizations result in sets of ordinary differential equations in time (called equations of motion) which may be integrated using a standard scheme such as the Newmark one (see Cook[1974]). The discretization which does not model the elasticity of the riser results in a set of linear equations. All of the discretizations given in Chapter Three are completely new apart from the elastic lumped mass method which was originally developed by Nakajima et.al.[1982].

Many of the discretizations give equations of motion that are similar but this does not imply that the choice of the discretization is not important, since some of them are more versatile and adaptable than others. In particular the variational finite element methods developed in Chapter Three have many advantages over other discretizations.

The discretizations given in Chapter Three can be divided into two types; one type describes the dynamics of

the riser through describing the dynamics of a much simpler structural system and the other directly discretizes one of the mathematical equations developed in Chapter Two.

In Chapter Three several simplifying assumptions were made:

1.The bending stiffness of the riser is zero.

2.The effects of the internal fluid flow are negligible.

3.There is no ground contact of the riser with the seabed.

4.The riser is totally immersed in the sea.

5.Both ends of the riser are fixed.

1.5.4:Chapter Four.

In practice the assumptions listed in section 1.5.3 are not valid and it is very important to allow for the appropriate effects in a computer model. How this may be done is shown in Chapter Four. There has been very little published research in these areas.

The only reference that allows for the incorporation of bending stiffness into a linear finite element discretization is Ractliffe[1985]. However it is believed that for reasons of commercial security this reference is incomplete. Because the forces that act on the riser due to the bending stiffness are dependent on the curvature of the riser special care must be taken when incorporating the bending stiffness into a linear

discretization i.e. a discretization that uses either a linear structural element or a finite element. In Chapter Four the bending stiffness is incorporated into a linear discretization using a particularly simple method. Extensive validation is carried out against known analytical solutions for a beam; the large displacement elastica solution and the small displacement uniformly loaded beam solution. The results obtained are in excellent agreement and are suprisingly accurate considering the crudity of the method. There has been other work done by O'Brien, McNamara and Dunne[1987] and by O'Brien, McNamara and Gilroy[1986] using much more complicated elements. In Chapter Four it is also shown how it is possible to include the bending stiffness when cubic elements are used.

Using the theory developed for the bending stiffness and the mathematical description of the internal fluid provided in Chapter Two it is shown how to allow for internal fluid flow effects when a linear discretization is used. Because of the accuracy achieved for the bending stiffness similar accuracy is to be expected for the modelling of the internal fluid flow.

The top end of the riser is normally subject to movement due to the motion of the floating production vessel. There are no references that adequately take account of this. In certain circumstances extra force terms are generated. The extra force terms that are generated for a linear discretization are given.

For some riser configurations e.g. lazy "s" the lower part of the riser might lie on the seabed. To model contact with the seabed a very simple approach is used; the seabed is modelled as a fluid with gradually increasing density. Hence as the riser enters the seabed (note that in practice many seabeds are composed of silt and thus it is reasonable to model them as fluids) the upthrust force on the riser increases and constrains the riser to lie just beneath the seabed level.

The top end of the riser usually lies above the water surface. Hence special care must be taken to take account of the change in loading that this causes. In the modelling of both ground contact and the sections of the riser above the water surface there is always at least one element that has a discontinuity of loading. It is important to allow for the change in the loading mechanism on these elements. In Chapter Four the changes necessary are given. Using this modified loading mechanism allows longer length elements to be used near the water surface and also in the region near the seabed. There are no references that deal with elements that have a discontinuity of loading and the resulting changes in the equations of motion (e.g. the changes to the added mass matrix) that these elements cause.

1.5.5:Chapter Five.

In Chapter Five various results are given. The effects of various parameters such as the amplitude of the top motion, the wave height and the wave period are examined for the steep "s" configuration. To analyse the performance of a riser system fully, many parameters must be varied. To do so would generate an enormous amount of data and would require a lot of C.P.U. time. It is the aim of this chapter only to indicate some of the parameters which would effect the dynamic behaviour of the riser the most.

It is important to validate any computer program for the dynamic analysis of flexible riser systems against either full size tests, model tests or analytical solutions. It is not practical to use full size test as this would be very expensive. However validation is carried out against both model tests and relevant analytical solutions. The program is found to be in agreement with model tests and in very close agreement with analytical solutions.

In certain circumstances a riser system might undergo vortex shedding (King[1977]). This may cause premature failure of the riser because of fatigue. Ways to reduce vortex shedding (if it occurs) are found for a steep "s" configuration.

1.5.6:Chapter Six.

In Chapter Six a brief summary of the conclusions about the work done in this thesis is given. Recommendations are made about the possibilities for future work.

CHAPTER TWO:MATHEMATICAL DESCRIPTION OF A FLEXIBLE RISER

2.1:Introduction.

In this chapter a mathematical description is provided for the dynamics of a finite, continuous, length of riser that is shown in figure 2.1(a). The mathematical description is given in terms of two types of equation; a variational equation and a partial differential equation. These equations are vital to understanding about the dynamics of risers. In Chapter Three these equations are used extensively to obtain various numerical solutions using standard techniques. The forces acting on the length of riser are shown in figure 2.1(a).

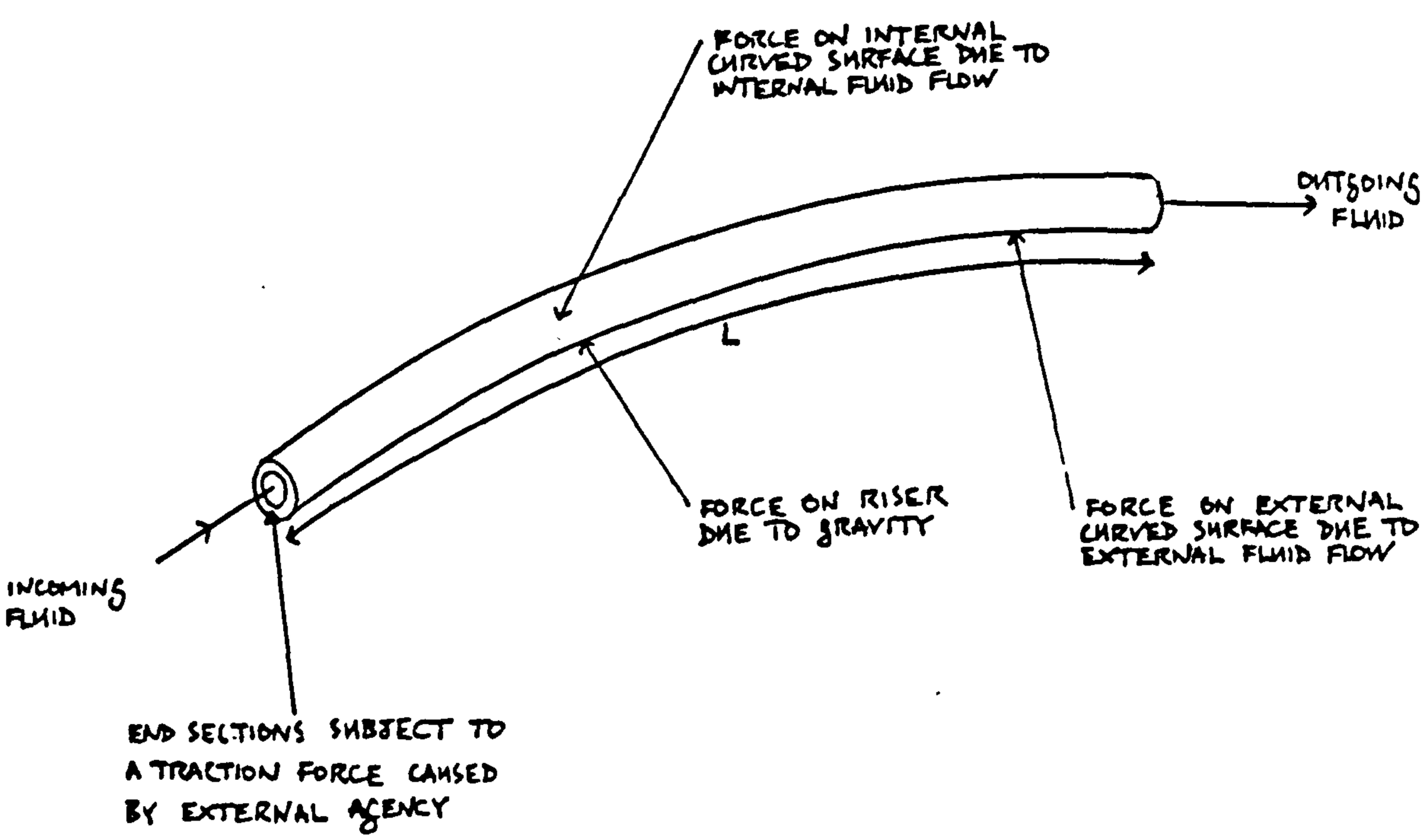

FIGURE 2.1 (a) : ARBITRARY LENGTH OF RISER SUBJECT TO EXTERNAL FORCES

It is supposed, with no loss of generality, that the length of riser has non-zero bending stiffness and is elastic and that the cross-section of the riser is circular and that it always remains so. It is also necessary to make further assumptions both about the mathematical description of the external forces and about the nature of the response of the material of the riser when under load. These assumptions are detailed in the text of this chapter.

Internal fluid flow effects are modelled and in order to do this it is necessary to make several assumptions about the nature of the flow and the deformation in the riser.

The variational equation and partial differential equation, whilst being closely related, are obtained by applying physical laws in two different ways; the variational equation is obtained by applying physical laws globally and the partial differential equation is obtained by applying physical laws locally. Both types of equation are of considerable use.

Some numerical solutions (see Chapter Three for examples) for the dynamics of risers are not based directly on either a partial differential equation or a variational equation. These numerical solutions however can nearly always be obtained by using these equations and are best understood by doing so (the reasons for this are given later).

The riser is modelled as a slender tensioned beam that is subjected to small strain and large displacements. It is also assumed that the riser is sufficiently slender so that rotational kinetic energy terms can be neglected. Hence some of the theory developed in this chapter is closely related to standard, slender, small strain and large displacement theory as developed by Love[1952] for example.

If the bending stiffness can be considered to be effectively zero (i.e. the riser can be modelled as a string) then large axial strains are permissible in the formulation. However where the bending stiffness is included the strain in the riser must be small.

Very general theories for slender beams are given in Antman[1972], Green, Knops and Laws[1968], Green and Laws[1966] and Cohen[1966]. These theories whilst being more rigorous than the theory developed here are too complicated however to be directly applied to the dynamics of risers. However they provide validations for some of the assumptions made.

References which are useful in enabling the description of internal fluid flow are Ortloff and Ives[1969], Triantafyllou and Chryssostomidis[1985], Paidoussis[1966,1973], Blevins[1977] and Paidoussis and Luu[1985]. All of these references are concerned with small displacement problems only. Paidoussis and Luu[1985] and Blevins[1977] deal specifically with

internal fluid flow so are thus most relevant.

Bernitsas and Kokarakis[1985] derive in detail sets of partial differential equations which are equivalent to the differential equations obtained by Love[1952]. The equations obtained are general and can be applied to risers with non-circular cross-sections. Internal fluid flow effects are accounted for. However they are accounted for in a way that makes numerical computation difficult. At no stage do Bernitsas and Kokarakis[1985] reduce the problem to a single partial differential equation which is what is required for an efficient numerical solution.

Nordgren[1974] has simplified the problem considerably by deriving a single partial differential equation for an inextensible riser. This equation can then be solved by using standard techniques. Nordgren[1974] chose a finite difference scheme to do this. Nordgren[1974] also derived the partial differential equation using Hamilton's Principle with the constraint condition of inextensibility enforced using a Lagrange multiplier. How the Lagrange multiplier term is obtained is difficult to understand however. In this chapter we derive a partial differential equation which can be reduced to Nordgren's partial differential equation for the case when the riser is inextensible.

In this chapter a partial differential equation is obtained for a riser that is more general than the previous partial differential equations that have been obtained. For certain special cases it is shown that this equation reduces to the partial differential equations obtained by Nordgren[1974] and by Cristescu[1967]. In Chapter Three finite element discretizations are given based on this equation. The strain energy for the riser is obtained after having found the internal virtual work for the riser. No references have been found in the literature that derive the strain energy for a riser. The obtaining of the strain energy allows a number of versatile finite element discretizations to be obtained easily (these are given in Chapter Three). As will be shown not only are these discretzations easy to obtain they are also well-suited to the analysis of structural problems like the one that is being analysed here.

2.1.1:Forces acting on a Riser.

Consider the following forces acting on the finite continuous length of riser shown in figure 2.1(a).

1.Weight load due to gravity force acting on the riser and its contents.

2.An upthrust load due to the hydrostatic component of the external fluid pressure. In reality some of the riser might be above the water surface and hence no upthrust load would act. This effect of only partial submergence is not taken account of in this chapter.

3.Traction loads on the end cross-sections of the riser. These traction loads arise due to attachment to a floating production vessel or other external agency or due to the presence of the adjacent riser. The traction load is composed of tension and shear components.

4.Due to wave motion the external fluid exerts a hydrodynamic pressure load and due to wave and riser motion it exerts a viscous drag load on the riser. This load is modelled by an equation called Morison's equation which is described in section 2.1.2.

5.The load on the riser due to the internal fluid flow.

2.1.2:Morison's Equation.

Morison's equation (Morison, O'Brien, Johnson and Schaaf[1950], Langley[1984], Sarpkaya and Isaacson[1981]) is a semi-empirical equation which states that the normal force $\underset{\sim}{F}$ per unit length acting at a point on a slender rod, as shown in figure 2.1.2(a), due to the external flow is given by Morison's equation, which for three dimensional flow can be written in the vector form

$$\underset{\sim}{F} = \tfrac{1}{2}\rho_w D C_D (\underset{\sim}{u}_f - \dot{\underset{\sim}{r}})|_n \, |(\underset{\sim}{u}_f - \dot{\underset{\sim}{r}})|_n| \qquad (A)$$

$$+\tfrac{1}{4}\pi\rho_w D^2 (1+C_A)\,\dot{\underset{\sim}{u}}_f|_n - \tfrac{1}{4}\pi\rho_w D^2 C_A\,\ddot{\underset{\sim}{r}}|_n$$

where ρ_w = density of sea-water (i.e.the external fluid), D = diameter of the rod, $\underset{\sim}{u}_f$ = resultant fluid velocity due to current and wave motion at the point on the rod at which the force is being evaluated, $\underset{\sim}{r}$ = position vector at the point on the rod at which the force is being evaluated and C_D and C_A are constants. C_D is called the drag coefficient and C_A is called the added mass coefficient ($\approx$1.0). C_D and C_A are usually determined from experiment and depend on the nature of the external flow (in particular Reynolds number). For a vector $\underset{\sim}{v}$ the normal component $\underset{\sim}{v}|_n$ is defined as

$$\underset{\sim}{v}|_n = \underset{\sim}{v} - (\underset{\sim}{v}\cdot\underset{\sim}{t})\underset{\sim}{t} \qquad (B)$$

where $\underset{\sim}{t}$ = tangent vector of the rod. In matrix form this equation can be written

$$\begin{bmatrix} (\underset{\sim}{x}\ln)_x \\ (\underset{\sim}{x}\ln)_y \\ (\underset{\sim}{x}\ln)_z \end{bmatrix} = \begin{bmatrix} 1-(\underset{\sim}{t})_x^2 & -(\underset{\sim}{t})_x(\underset{\sim}{t})_y & -(\underset{\sim}{t})_x(\underset{\sim}{t})_z \\ & 1-(\underset{\sim}{t})_y^2 & -(\underset{\sim}{t})_y(\underset{\sim}{t})_z \\ \text{sym.} & & 1-(\underset{\sim}{t})_z^2 \end{bmatrix} \qquad (c)$$

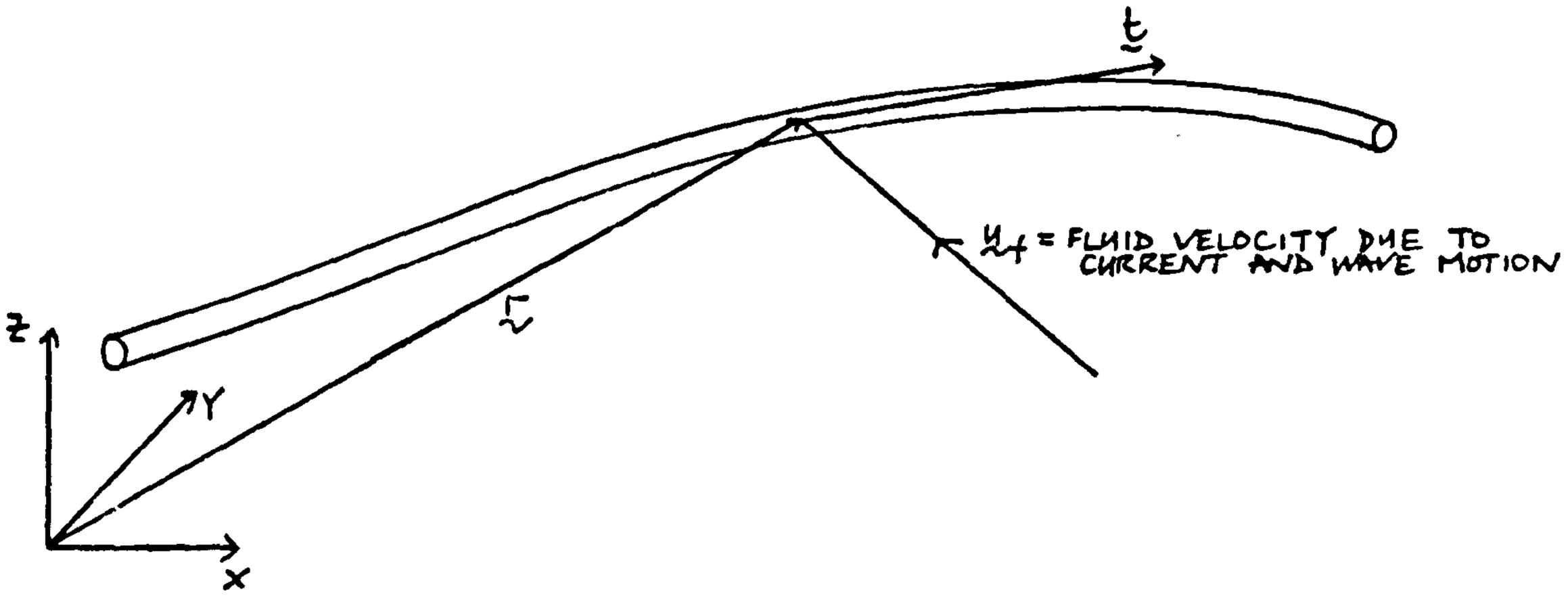

FIGURE 2.1.2 (b) : ILLUSTRATION FOR MORISON'S EQUATION

2.2:Resultant Force and Moment acting on a Segment of Riser.

2.2.1:Introduction.

In this section expressions are derived for the resultant force and moment due to the forces acting on a segment of the riser as shown in figure 2.2.1(a). These expressions are useful in formulating the partial differential equation and the variational equation for the riser.

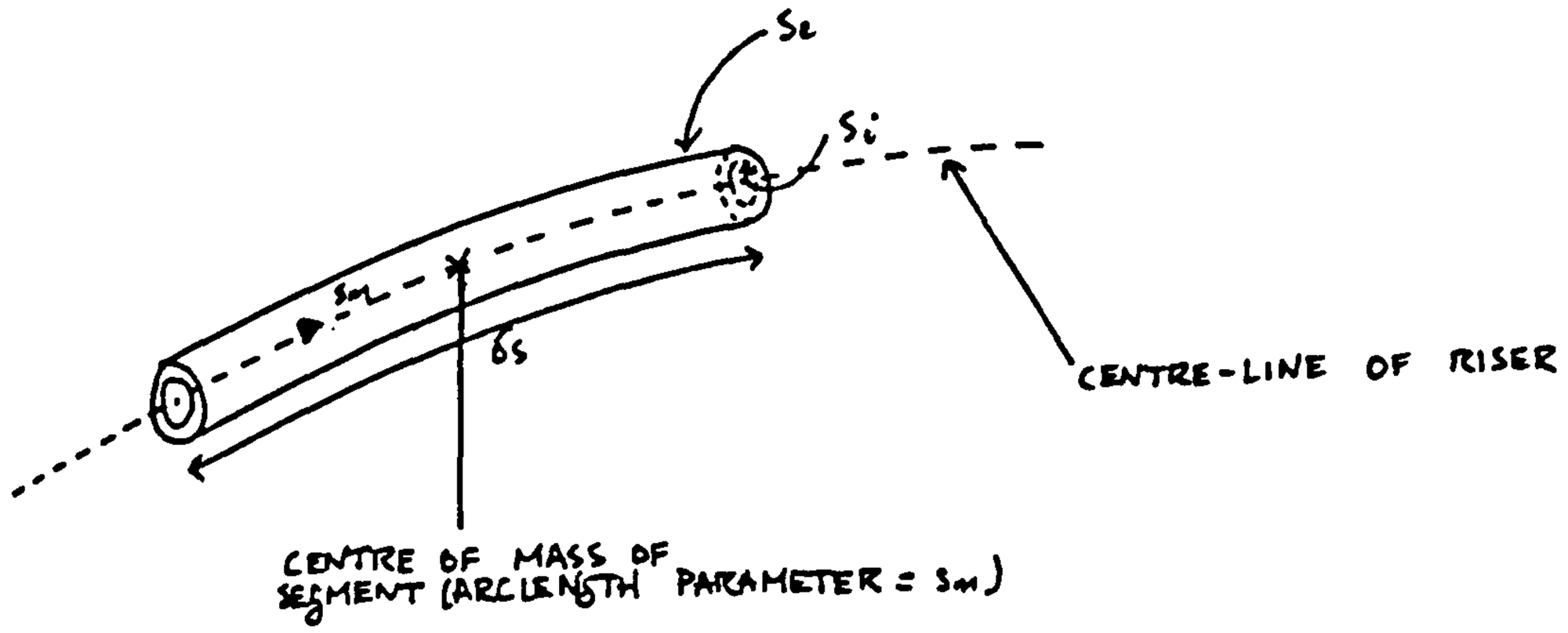

FIGURE 2.2.1(a): SEGMENT OF THE RISER

The Bernoulli-Euler hypothesis (Washizu[1975]) is: "Cross-sections which are perpendicular to the centroid locus before bending remain plane and perpendicular to the deformed locus and suffer no strains in their planes." The centroid locus for the problem here is the centre-line of the riser. The Bernoulli-Euler hypothesis is invoked here and again in section 2.3 when the constitutive equations for the riser are formulated.

The assumption that the cross-section of the riser is circular and remains so allows the definition of a centre-line along the riser. The dynamics of the riser are formulated in terms of the dynamics of the centre-line. In section 2.3 an expression is given for the force resultant of the traction forces acting over a cross-section in terms of the stretch of the centre-line. Also in section 2.3 an expression is given for the moment resultant of the traction forces acting over a cross-section in terms of the curvature of the centre-line.

Consider figure 2.2.1(b) which shows the hypothetical path of the riser from an unstrained reference state. The left hand end of the riser is the reference point for the measurement of arc-length. Note it is pointless to formulate the partial differential equation and variational equation for the dynamics of the riser in terms of the current arc-length parameter s, because s is precisely one of the quantities that is to be determined. Therefore here the formulation of the expressions for the resultant force and the resultant moment acting on a segment is sought in terms of the unstrained arc-length parameter s_o.

From the differential geometry of space curves (Appendix A) it is possible to define an orthonormal basis at each point on the riser. The vectors that compose this basis are called the tangent vector $\underset{\sim}{t}$, the binormal

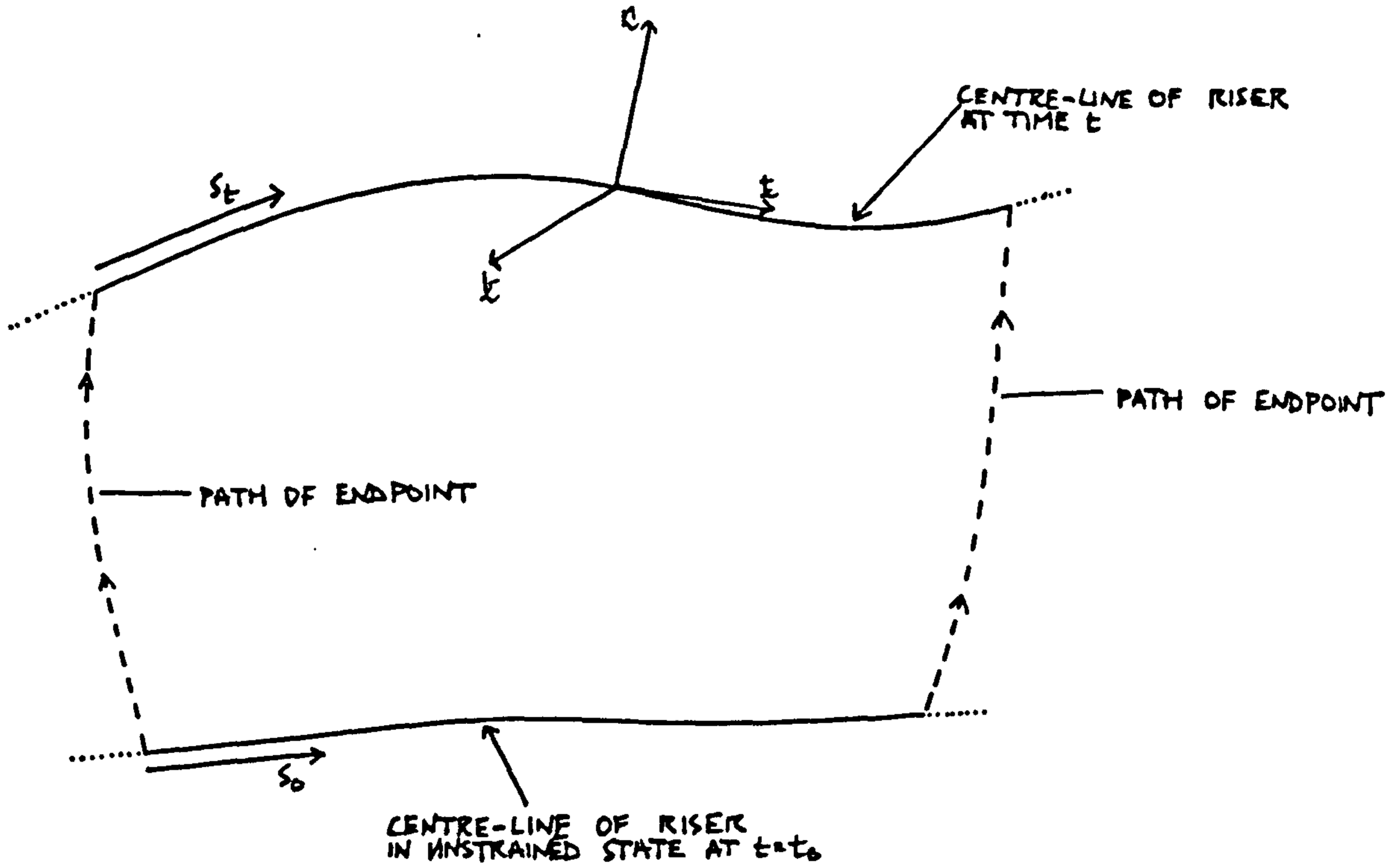

FIGURE 2.2.1 (b): HYPOTHETICAL PATH OF RISER FROM UNSTRAINED REFERENCE STATE

vector $\underset{\sim}{b}$ and the normal vector $\underset{\sim}{n}$. This basis is very useful in the formulation of the resultant force and the resultant moment.

2.2.2:Resultant Force.

Consider a segment of riser as shown in figure 2.2.1(a) of length δs and subjected to a body force $\underset{\sim}{F}_b$ per unit volume of the segment due to gravity, a surface traction force $\underset{\sim}{F}_e$ per unit area over the external curved surface S_e due to the external fluid, a surface traction force $\underset{\sim}{F}_i$ per unit area over the internal curved surface S_i due to the internal fluid flow, a surface traction force $\underset{\sim}{F}_R$ per unit area over the right-hand end surface of the segment A_R due to the presence of the adjacent sections of riser or floating production vessel or other external agency, and a similar surface traction force $\underset{\sim}{F}_L$ over the left-hand end surface of the segment A_L. Note that the surface traction forces over the left-hand and right-hand end surfaces are composed of shear and tension force components. The net force on the segment is

$$\int_V \underset{\sim}{F}_b \, dV + \int_{S_e} \underset{\sim}{F}_e \, dS + \int_{S_i} \underset{\sim}{F}_i \, dS + \int_{A_R} \underset{\sim}{F}_R \, dA + \int_{A_L} \underset{\sim}{F}_L \, dA \qquad (A)$$

It is assumed that

$$\int_V \underset{\sim}{F}_b \, dV = \delta s \, \underset{\sim}{F}_g \qquad (B)$$

where $\underset{\sim}{F}_g$ =gravity force per unit arc-length.

By integrating the hydrostatic pressure over and the two end surfaces it is found

$$\int_{S_e} \underset{\sim}{F}_e \, dS = \delta s \, (\underset{\sim}{F}_u + \underset{\sim}{F}_m) - \int_{A_R} \underset{\sim}{F}_p \, dA - \int_{A_L} \underset{\sim}{F}_p \, dA \qquad (C)$$

where $\underset{\sim}{F}_u$ is the upthrust buoyancy force per unit arc-length due to the hydrostatic fluid pressure, $\underset{\sim}{F}_m$ is the Morison loading force per unit arc-length as described in section 2.1.2 and where $\underset{\sim}{F}_p$ is the hydrostatic pressure force per unit area on the end surfaces, and

$$\int_{S_i} \underset{\sim}{F}_i \, dS = \delta s \underset{\sim}{R} \qquad (D)$$

where $\underset{\sim}{R}$ is a reaction force per unit arc-length due to change in momentum of the internal fluid flow and is described in section 2.4. The resultants $\int_{A_R} \underset{\sim}{F}_R \, dA$ and $\int_{A_L} \underset{\sim}{F}_L \, dA$ are described in detail later in this chapter.

Thus the net force on the segment is

$$\delta s (\underset{\sim}{F}_u + \underset{\sim}{F}_m + \underset{\sim}{R} + \underset{\sim}{F}_g) + \int_{A_R} (\underset{\sim}{F}_R - \underset{\sim}{F}_p) \, dA + \int_{A_L} (\underset{\sim}{F}_L - \underset{\sim}{F}_p) \, dA \qquad (E)$$

as shown in figure 2.2.2(a).

Now let $\underset{\sim}{F}_T$ denote the surface traction force per unit area due to the presence of the adjacent lengths of riser or floating production vessel or other external agency, on a portion of an end section of a segment of the riser whose outward normal is in the same direction as the tangent vector of the centre-line (see figure 2.2.2(b)). Then

$$\int_{A_R} \underset{\sim}{F}_R \, dA = \int_{A} \underset{\sim}{F}_T \, dA \qquad (F)$$

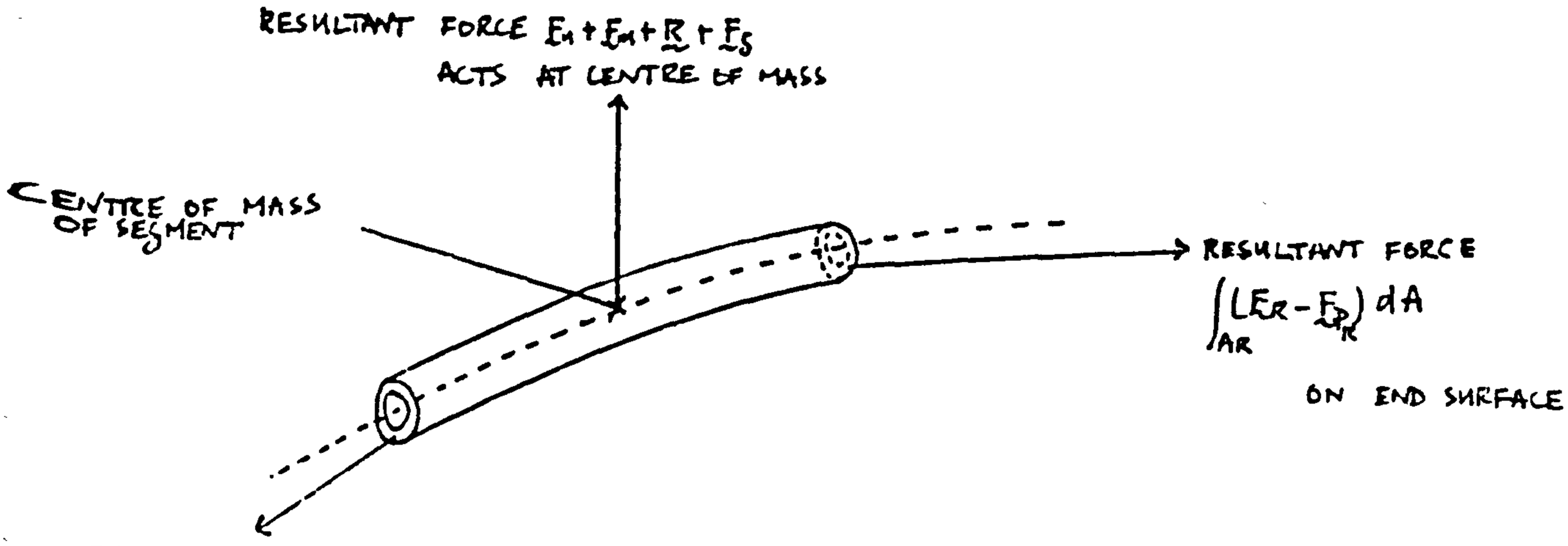

FIGURE 2.2.2(a) : RESULTANT FORCES ACTING ON A SEGMENT OF THE RISER

with A taken at $s = s_M + \frac{\delta s}{2}$. And

$$\int_{A_L} \underset{\sim}{E}_L \, dA = - \int_A \underset{\sim}{E}_T \, dA \qquad (H)$$

with A taken at $s = s_M - \frac{\delta s}{2}$. A denotes the appropriate area of cross-section of the riser and may either be the left-hand end area A_L or the right-hand end area A_R .

Similarly let $\underset{\sim}{F}_p^*$ denote the hydrostatic pressure force per unit area on a portion of the surface of an isolated end section of the segment of the riser whose outward normal is in the same direction as the tangent vector of the centre-line. Then

$$\int_{A_R} \underset{\sim}{E}_p \, dA = \int_A \underset{\sim}{E}_p^* \, dA \qquad (I)$$

evaluated at $s = s_M + \frac{\delta s}{2}$. And

$$\int_{A_L} \underset{\sim}{E}_p \, dA = - \int_A \underset{\sim}{E}_p^* \, dA \qquad (J)$$

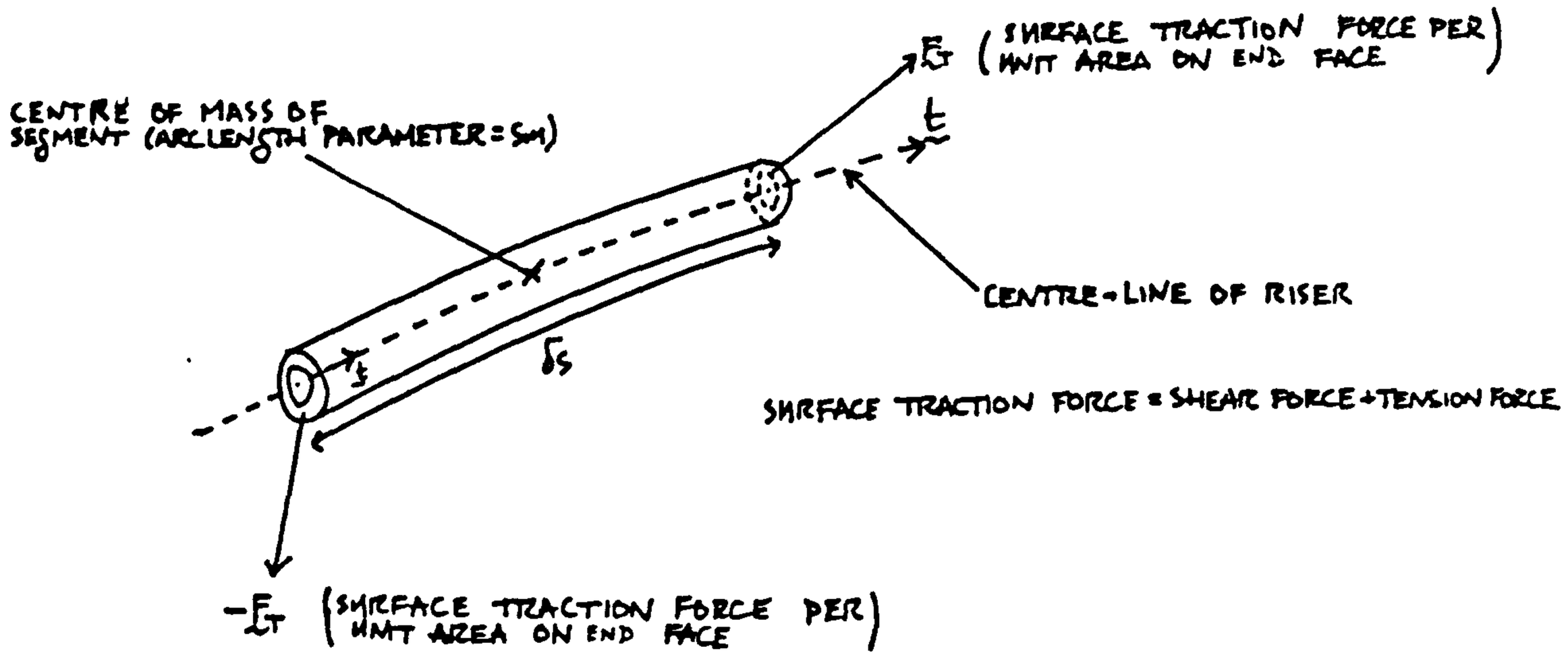

FIGURE 2.2.2(b): EXPLANATION OF $\underset{\sim}{F}_T$ TERM

evaluated at $s = s_M - \frac{\delta s}{2}$. $\underset{\sim}{F}_p^*$ is given by $\underset{\sim}{F}_p^* = -\rho g z \underset{\sim}{t}$ where z is the distance of the point on the end surface from the sea-surface.

In the above two paragraphs Newton's Law of action and reaction has been used.

In the limit as $\delta s \to 0$

$$\int_{A_R} (\underset{\sim}{F}_R - \underset{\sim}{F}_p)\, dA + \int_{A_L} (\underset{\sim}{F}_L - \underset{\sim}{F}_p)\, dA = \delta s \frac{\partial}{\partial s} \left\{ \int_A (\underset{\sim}{F}_T - \underset{\sim}{F}_p^*)\, dA \right\} \quad (K)$$

$$= \delta s_0 \frac{\partial}{\partial s_0} \left\{ \int_A (\underset{\sim}{F}_T - \underset{\sim}{F}_p^*)\, dA \right\}$$

Thus in the limit as $\delta s \to 0$ the net force on the segment is

$$\delta s\, (\underset{\sim}{F}_H + \underset{\sim}{F}_M + \underset{\sim}{R} + \underset{\sim}{F}_G) + \delta s \frac{\partial}{\partial s} \left\{ \int_A (\underset{\sim}{F}_T - \underset{\sim}{F}_p^*)\, dA \right\} \quad (a)$$

2.2.3:Resultant Moment.

It is assumed that there is no net moment about the centre of mass of the segment caused by the hydrodynamic pressure of the external fluid, that the internal fluid produces no net moment about the centre of mass of the segment and that the gravity force acting on the segment produces no moment about the centre of mass of the segment.

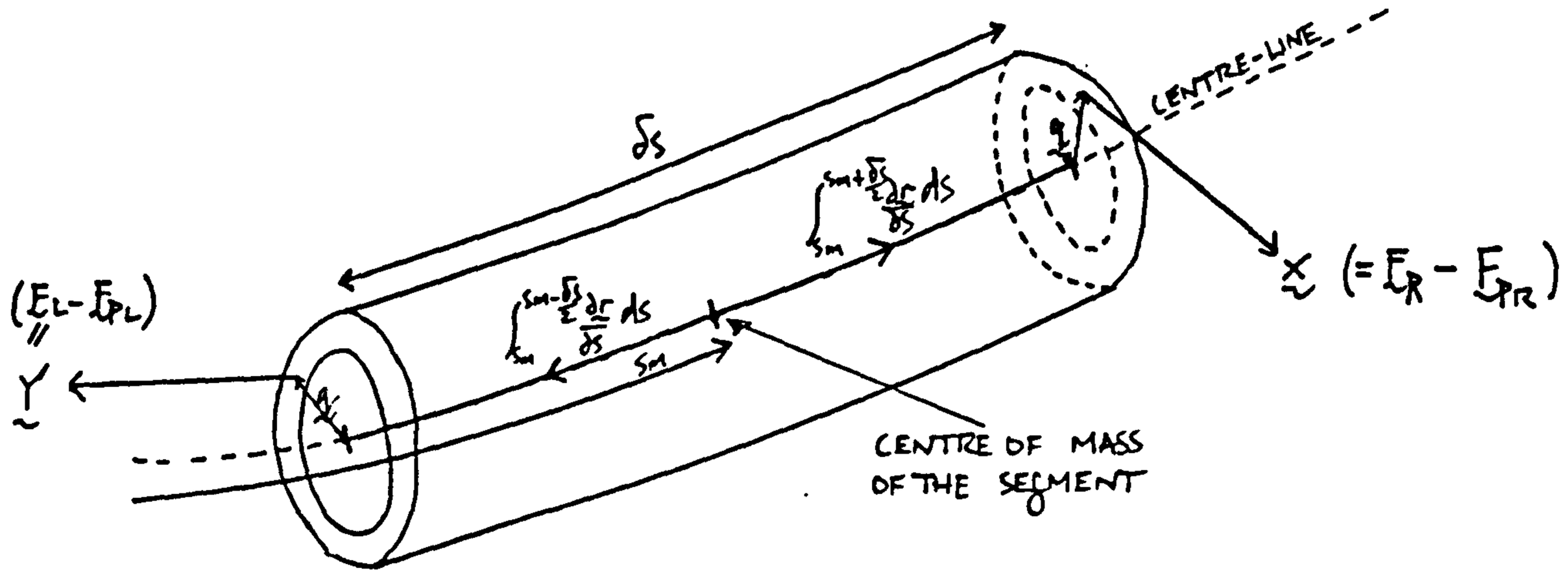

MOMENT OF FORCE X ACTING ON RIGHT-HAND FACE ABOUT THE CENTRE OF MASS OF THE SEGMENT IS

$$\left\{ \int_{s_m}^{s_m+\frac{\delta s}{2}} \frac{\partial r}{\partial s} ds + q \right\} \wedge X$$

MOMENT OF FORCE Y ACTING ON LEFT-HAND FACE ABOUT THE CENTRE OF MASS OF THE SEGMENT IS

$$\left\{ \int_{s_m}^{s_m-\frac{\delta s}{2}} \frac{\partial r}{\partial s} ds + q \right\} \wedge Y$$

FIGURE 2.2.3(a): DETERMINATION OF MOMENTS

From figure 2.2.3(a) the net moment of the forces acting on the segment, about the centre of mass is

$$\int_{A_R} \left\{ \underset{\sim}{r} + \int_{s_m}^{s_m+\frac{\delta s}{2}} \frac{\partial \underset{\sim}{r}}{\partial s}\, ds \right\} \wedge (\underset{\sim}{F}_R - \underset{\sim}{F}_p)\, dA$$

$$+ \int_{A_L} \left\{ \underset{\sim}{r} + \int_{s_m}^{s_m-\frac{\delta s}{2}} \frac{\partial \underset{\sim}{r}}{\partial s}\, ds \right\} \wedge (\underset{\sim}{F}_L - \underset{\sim}{F}_p)\, dA \qquad (A)$$

But to first order in δs

$$\int_{s_m}^{s_m+\frac{\delta s}{2}} \frac{\partial \underset{\sim}{r}}{\partial s}\, ds = \frac{\delta s}{2} \left.\frac{\partial \underset{\sim}{r}}{\partial s}\right|_{s=s_m} \qquad (B)$$

and

$$\int_{s_m}^{s_m-\frac{\delta s}{2}} \frac{\partial \underset{\sim}{r}}{\partial s}\, ds = -\frac{\delta s}{2} \left.\frac{\partial \underset{\sim}{r}}{\partial s}\right|_{s=s_m}$$

which gives if it is assumed that the riser is slender enough so terms like

$$\int_A \underset{\sim}{r} \wedge \underset{\sim}{F}_p\, dA$$

can be neglected, that the net moment about the centre of mass of the segment is given by

$$\int_{A_R} \underset{\sim}{r} \wedge \underset{\sim}{F}_T\, dA + \int_{A_L} \underset{\sim}{r} \wedge \underset{\sim}{F}_T\, dA$$

$$+ \frac{\delta s}{2} \frac{\partial \underset{\sim}{r}}{\partial s} \wedge \left\{ \int_{A_R} (\underset{\sim}{F}_T - \underset{\sim}{F}_p)\, dA + \int_{A_L} (\underset{\sim}{F}_T - \underset{\sim}{F}_p)\, dA \right\} \qquad (C)$$

in the limit as $\delta s \to 0$ using a Taylor's series expansion this gives

$$\delta s \frac{\partial}{\partial s} \left\{ \int_A \underset{\sim}{r} \wedge \underset{\sim}{F}_T\, dA \right\} + \delta s \frac{\partial \underset{\sim}{r}}{\partial s} \wedge \left\{ \int_A (\underset{\sim}{F}_T - \underset{\sim}{F}_p^*)\, dA \right\} \qquad (a)$$

2.3:Constitutive Relationships.

2.3.1:Introduction.

The aim of this section is to relate the force and the moment resultant on a cross-section of the riser to the geometric properties of the centre-line. These resultants cannot be found by using any dynamical consideration.

As in section 2.2 the Bernoulli-Euler hypothesis is invoked.

2.3.2:Relationship for the Force Resultant.

From section 2.2.2 the net force acting on a segment is given by equation 2.2.2(a)

$$\delta s\left(\underset{\sim}{F}_M + \underset{\sim}{F}_m + \underset{\sim}{R} + \underset{\sim}{F}_g\right) + \delta s \frac{\partial}{\partial s}\left\{\int_A \left(\underset{\sim}{F}_T - \underset{\sim}{F}_p^*\right) dA\right\} \qquad (A)$$

Since only end forces effect the strain of the centre-line of the segment a simple linear relationship is assumed to hold

$$\underset{\sim}{t} \cdot \int_A \left(\underset{\sim}{F}_T - \underset{\sim}{F}_p^*\right) dA = AE\left(\frac{\partial s}{\partial s_0} - 1\right) \qquad (B)$$

The quantity

$$T_e = AE\left(\frac{\partial s}{\partial s_0} - 1\right) \qquad (q)$$

is called the effective tension. The notion of effective tension is discussed in Goodman and Breslin[1976]. A is the cross-sectional area of the riser in the deformed

state.

If it is supposed that the material of the riser is volume conserving then

$$A\delta s = A_0 \delta s_0 \qquad (C)$$

where A_0 is the cross-sectional area in the undeformed reference state. Then

$$A = A_0 \left(\frac{\partial s}{\partial s_0}\right)^{-1} \qquad (D)$$

and

$$T_e = A_0 E \left(\frac{\partial s}{\partial s_0} - 1\right)\left(\frac{\partial s}{\partial s_0}\right)^{-1} \qquad (E)$$

For small strain this becomes

$$T_e = A_0 E \left(\frac{\partial s}{\partial s_0} - 1\right) \qquad (E)$$

The assumption of volume conservation is true for materials that have a Poisson's ratio equal to 0.5. This is likely to be the case for rubber-like materials but not for steel. In fact as is shown later any function of the form

$$T_e = T_e \left(\frac{\partial s}{\partial s_0}\right) \qquad (F)$$

is easily adapted to fit into one of the numerical schemes developed in Chapter Three. Thus it is possible to allow, to some extent, for non-linear materials.

If the riser had no reinforcements and was made entirely of a rubber-like material then the following relationship (Beatty and Chow[1983]) can be used

$$T_e = \frac{A_0 E}{3}\left\{\frac{\partial s}{\partial s_0} - \frac{1}{\left(\frac{\partial s}{\partial s_0}\right)^2}\right\} \qquad (a)$$

This equation reduces to equation (a) in the limit of small strain i.e. as $\frac{\partial s}{\partial s_0} \longrightarrow 1$.

2.3.3:Relationship for the Moment Resultant.

Here the moment resultant expression ($EI\kappa\underset{\sim}{b}$) that is found in the Bernoulli-Euler theory of rods (Love[1952]) is derived. This expression will nearly always need to be modified for a riser since risers are made of an anisotropic material.

Consider the cross-section of the riser shown in figure 2.3.3(a). The cross-section of the riser lies in the plane formed by the normal vector and binormal vector which are defined at the point where the cross-section is bisected by the centre-line. The two areas shown are symmetric images of one another with respect to the axis defined by the normal vector. By symmetry, if no torsion is allowed, the traction forces $\underset{\sim}{F}_{T_1}$ and $\underset{\sim}{F}_{T_2}$ per unit area on the respective areas must be symmetric with respect to the $\underset{\sim}{n}$ axis. Thus

$$\underset{\sim}{F}_{T_2} = \alpha\underset{\sim}{t} + \beta\underset{\sim}{n} + \gamma\underset{\sim}{b} \qquad (A)$$

and

$$\underset{\sim}{F}_{T_1} = \alpha\underset{\sim}{t} + \beta\underset{\sim}{n} - \gamma\underset{\sim}{b} \qquad (B)$$

where α , β and γ depend on the position of the two symmetric areas on the cross-section of the riser. Similarly for the two respective position vectors to the two areas from the centre-point of the cross-section on the centre-line of the riser

$$\underset{\sim}{q}_2 = \eta \underset{\sim}{k} + \epsilon \underset{\sim}{n} \qquad (C)$$

and

$$\underset{\sim}{q}_1 = -\eta \underset{\sim}{k} + \epsilon \underset{\sim}{n} \qquad (D)$$

where η and ϵ depend on the position of the two symmetric areas on the cross-section of the riser. Thus the resultant moment is

$$(\underset{\sim}{q}_1 \wedge \underset{\sim}{F}_{T_1})\,\delta A_1 + (\underset{\sim}{q}_2 \wedge \underset{\sim}{F}_{T_2})\,\delta A_2 = -\alpha\epsilon \underset{\sim}{k}\,\delta A_1 - \alpha\epsilon \underset{\sim}{k}\,\delta A_2 \qquad (E)$$

From previous arguments $\alpha = \alpha(s)$ only, therefore

$$\int \underset{\sim}{q} \wedge \underset{\sim}{F}_T \, dA = -\int \alpha\epsilon \underset{\sim}{k} \, dA \qquad (A)$$

hence all that remains to do in order to evaluate the moment resultant integral is to find α . This is done in the next section.

2.3.3.1:Calculation of α .

The position vector of any point on a cross-section of the riser can be written

$$\underset{\sim}{r} = \underset{\sim}{r}_c + \epsilon \underset{\sim}{n} + \eta \underset{\sim}{k} \qquad (A)$$

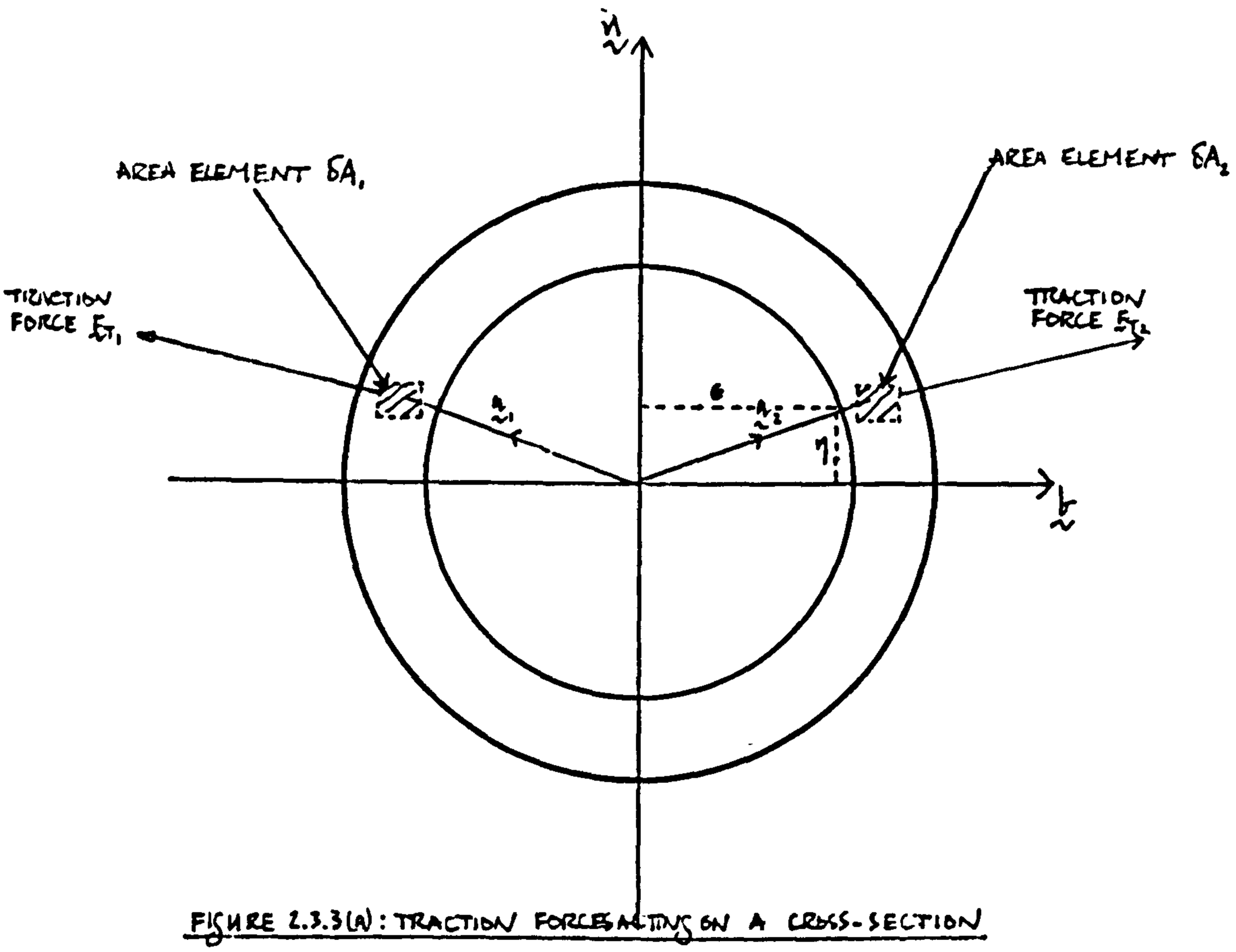

FIGURE 2.3.3(A): TRACTION FORCES ACTING ON A CROSS-SECTION

where $\underset{\sim}{r}_c$ is the position vector of the centre-point of the riser and, ϵ and η, depend on the position of the point on the cross-section. Keeping ϵ and η constant defines a series of curves that are at right angles to the centre-line. One such line is shown in figure 2.3.3.1(a). Suppose that the arc-length parameter for one of these curves is $\bar{s}$ then the relevant strain measure of the curve is $\frac{\partial \bar{s}}{\partial s_0}$. Now

$$\delta \underset{\sim}{r} = \delta \underset{\sim}{r}_c + \epsilon \, \delta \underset{\sim}{n} + \eta \, \delta \underset{\sim}{b} \qquad (B)$$

But consider a point $\underset{\sim}{\chi}$ on the centre-line of the riser.

For a distance δs along the centre-line

$$\delta \underset{\sim}{\chi} = \underset{\sim}{t} \delta s + \kappa \underset{\sim}{n} \delta s^2 + O(\delta s^3) \qquad (C)$$

hence locally the centre-line can be considered to lie in a plane formed by the normal and the tangent vectors. Hence provided δs is small enough $\delta \underline{r} = \underline{0}$ and $\delta \underline{n} . \underline{t} = 0$ (i.e. $\tau = 0$) can be considered to hold true to obtain using Appendix A

$$|\delta \underline{r}| = (1 - \epsilon\kappa)\delta s \qquad (b)$$

This gives the extra stretch or compression of a part of the riser due to the curvature of the centre-line. It is this extra stretch or compression that gives rise to a resultant moment across a cross-section of the riser.

If a constitutive equation similar to equation 2.3.2(a) is assumed to hold for the tangential traction force then

$$\alpha = E\left(\frac{\delta \bar{s}}{\delta s_0} - 1\right) = E\left[(1-\epsilon\kappa)\frac{\delta s}{\delta s_0} - 1\right] \qquad (a)$$

s = ARC-LENGTH PARAMETER OF CENTRE-LINE
ζ = ARC-LENGTH PARAMETER OF ---- LINE

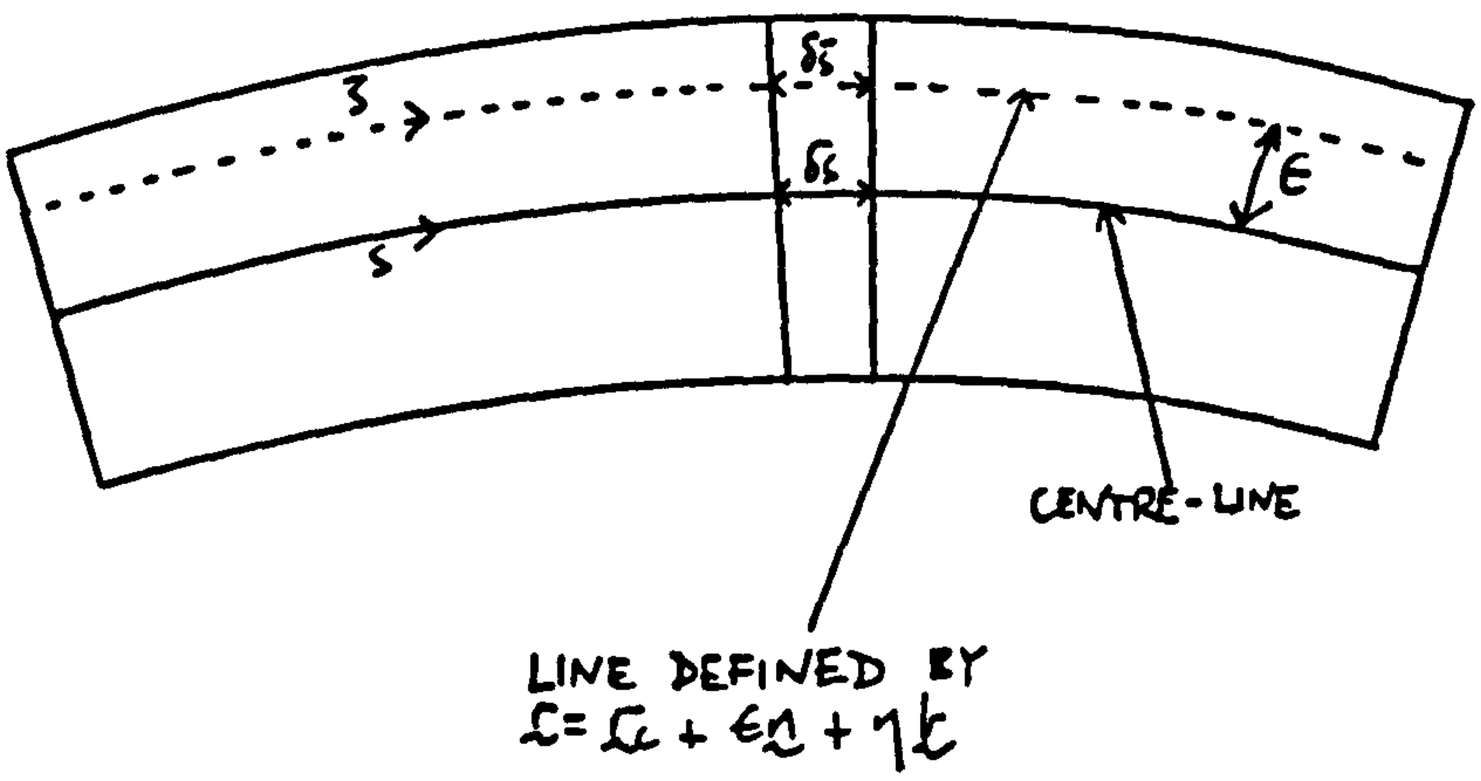

FIGURE 2.3.1(a): CALCULATION OF α

2.3.3.2:Derivation of Bending Moment.

Using equations 2.3.3(a) and 2.3.3.1(a) gives the bending moment as

$$\int \underset{\sim}{q} \wedge \underset{\sim}{E}_T \, dA = -\int \left[E(1-\epsilon\kappa)\frac{\partial s}{\partial s_0} - E \right] \epsilon \underset{\sim}{b} \, dA$$

$$= E\kappa \underset{\sim}{b} \frac{\partial s}{\partial s_0} \int \epsilon^2 \, dA = E\kappa \underset{\sim}{b} \frac{\partial s}{\partial s_0} I \qquad (A)$$

where I is known as the second moment of area of the cross-section about the binormal axis. It is simple to show that for a circular riser

$$I = \frac{\pi}{4}\left(r_E^4 - r_I^4 \right) \qquad (B)$$

where r_E and r_I are the external and internal radii of the riser respectively. For small strain $\frac{\partial s}{\partial s_0}$ may be set equal to 1. If the constitutive equation 2.3.2(d) was used instead of equation 2.3.2(a) then an alternative bending moment expression would have been derived. This equation would give the bending moment for a rubber-like material and would reduce to equation (a) in the limit of small strain.

The quantity EI is known as the bending stiffness of the riser. Note that the argument that has been given assumes that the riser material is isotropic. In practice this rarely is the case and equation 2.3.3.2(a) must be replaced by

$$\int \underset{\sim}{q} \wedge \underset{\sim}{E}_T \, dA = EI \lambda \kappa \underset{\sim}{b} \qquad (C)$$

where E is the Young's modulus for the material of the riser in longitudinal extension and λ is a factor that depends on the anisotropy of the material. In practice we determine the value of $EI\lambda$ from experiment.

2.4:Internal Fluid Flow Effects.

2.4.1:Introduction.

In order to describe internal fluid flow effects fully further consideration must be given to the reaction force $\underset{\sim}{R}$ in the force resultant expression (equation 2.2.2(a)) for a segment of the riser. It will be shown that it must be assumed that the axial strain in the riser is small in order that the problem is tractable. Several simplifying assumptions about the nature of the internal fluid flow are also made for the same reason.

2.4.2:Equation of Motion for Internal Fluid.

Consider the fluid flowing through the length of riser shown in figure 2.4.2(a). An internal force normal to the riser is caused by internal fluid flow. This force arises due to the change in the momentum of the fluid. Initially no assumptions are made about the strain in the riser to illustrate the simplification obtained by making a small strain assumption. It is assumed that the fluid speed across the cross-section of the riser is constant (alternatively the equations of motion could be formulated in terms of an average speed across a cross-section). The fluid speed relative to the riser (V) can be written in three different but equivalent forms

$$V = V(s_0, t) \qquad (A)$$

(i.e.the fluid speed at a point of the riser depends on

the unstrained arc-length parameter of that point of the riser in the unstrained state and on time) or

$$v = v(s,t) \qquad (B)$$

(i.e.the fluid speed at a point of the riser depends on the strained arc-length parameter of that point of the riser and on time) or

$$v = v(s_4,t) \qquad (C)$$

(i.e.the fluid speed at a point of the riser depends on the original arc-length parameter of that fluid in the unstrained state and on time).

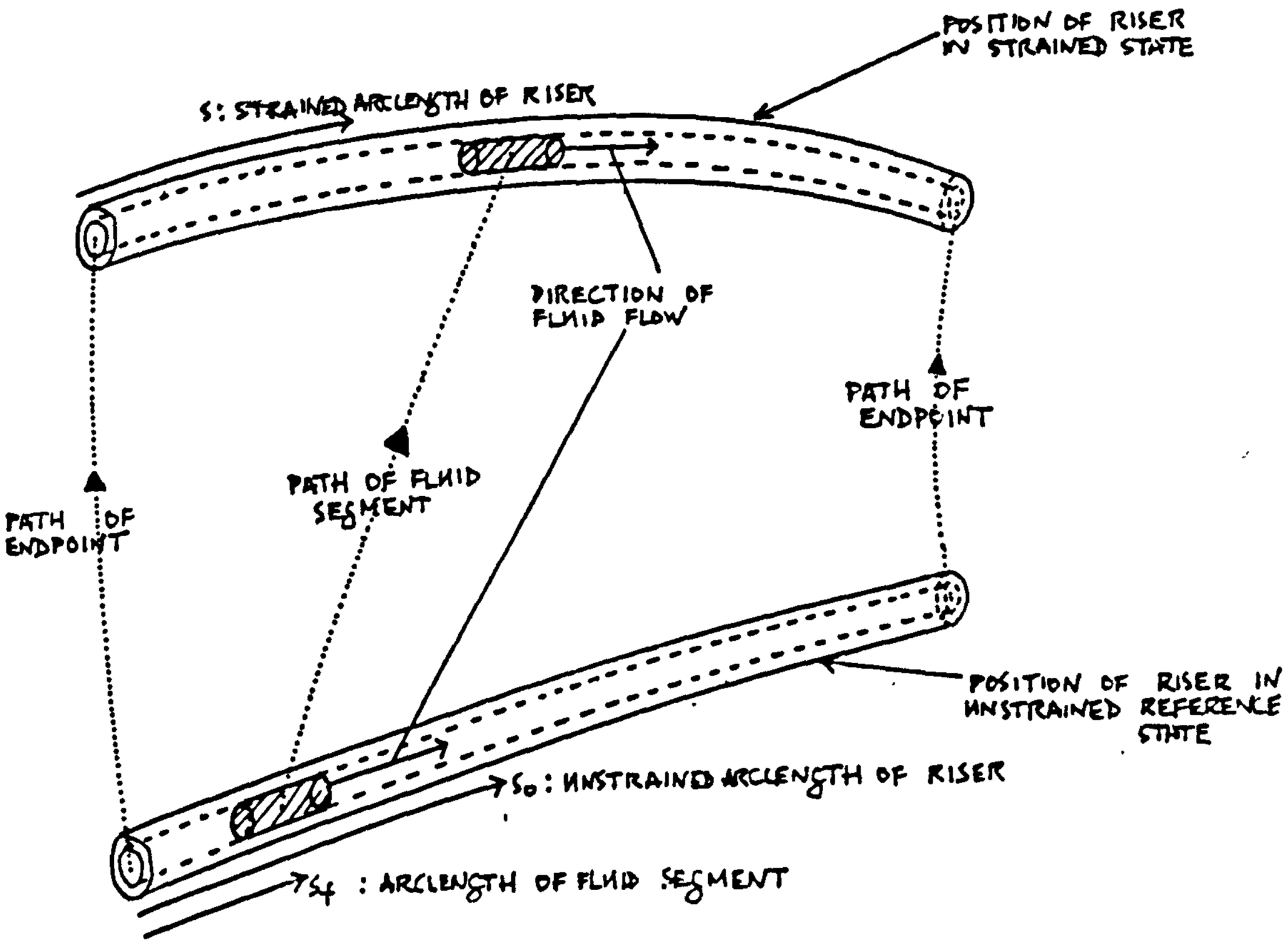

FIGURE 2.4.2(a) : INTERNAL FLUID FLOW

Similarly for the absolute fluid velocity $\underset{\sim}{\sigma}_f$

$$\underset{\sim}{\sigma}_f = \underset{\sim}{\sigma}_f (s_0, t) \qquad (D)$$

or

$$\underset{\sim}{\sigma}_f = \underset{\sim}{\varepsilon}_f (s, t) \qquad (E)$$

or

$$\underset{\sim}{\sigma}_f = \underset{\sim}{\sigma}_f (s_f, t) \qquad (F)$$

The absolute velocity of the fluid consists of the velocity of the riser plus the tangential velocity of the fluid relative to the riser

$$\underset{\sim}{\sigma}_f = \underset{\sim}{\varepsilon}_f (s_0, t) = \frac{\partial \underset{\sim}{r}(s_0, t)}{\partial t} + v(s_0, t)\, \underset{\sim}{t}(s_0, t) \qquad (G)$$

Now the incremental change in absolute fluid velocity in time δt is

$$\delta \underset{\sim}{\varepsilon}_f = \frac{\partial \underset{\sim}{\varepsilon}_f (s_f, t)}{\partial t} \delta t + \frac{\partial \underset{\sim}{\sigma}_f (s_f, t)}{\partial s_f} \delta s_f = \frac{\partial \underset{\sim}{\sigma}_f (s_0, t)}{\partial t} \delta t + \frac{\partial \underset{\sim}{\sigma}_f (s_0, t)}{\partial s_0} \delta s_0 \qquad (H)$$

but in the strained state the point at s_0 as moved axially to s hence

$$s_0 = s_0 (s, t) \qquad (I)$$

and for the internal fluid

$$s = s (s_f, t) \qquad (J)$$

hence the incremental displacement of the fluid in time δt is

$$\delta s = \frac{\partial s (s_f, t)}{\partial t} \delta t + \frac{\partial s (s_f, t)}{\partial s_f} \delta s_f \qquad (K)$$

and

$$\delta s_0 = \frac{\partial s_0(s,t)}{\partial t}\,\delta t + \frac{\partial s_0(s,t)}{\partial s}\,\delta s \qquad (L)$$

hence

$$\frac{\partial \underset{\sim}{\varepsilon}_f(s_f,t)}{\partial t} = \frac{\partial \underset{\sim}{\varepsilon}_f(s_0,t)}{\partial t} + \left\{\frac{\partial s_0(s,t)}{\partial t} + v\,\frac{\partial s_0(s,t)}{\partial s}\right\}\frac{\partial \underset{\sim}{\varepsilon}_f(s_0,t)}{\partial s_0} \qquad (M)$$

where

$$v(s_f,t) = \frac{\partial s(s_f,t)}{\partial t} \qquad (N)$$

From figure 2.4.2(b) the equation of motion of a segment of the fluid is

$$\begin{aligned}\rho_f A(s_f,t)\,\delta s_f\,\frac{\partial \underset{\sim}{\varepsilon}_f(s_f,t)}{\partial t} = {} & -A(s+\delta s,t)\,p(s+\delta s,t)\,\underset{\sim}{t}(s+\delta s,t) \\ & + A(s,t)\,p(s,t)\,\underset{\sim}{t}(s,t) \\ & - \rho_f A(s_f,t)\,\delta s_f\,g\,\underset{\sim}{k} + \underset{\sim}{R}\,\delta s\end{aligned} \qquad (O)$$

where ρ_f = density of the fluid per unit volume, A = internal cross-sectional area of the riser and $\underset{\sim}{R}$ = reaction force per unit arc-length in the strained configuration due to the inside walls of the riser. By mass conservation

$$\rho_f A(s_f,t)\,\delta s_f = \rho_f A(s,t)\,\delta s \qquad (P)$$

The assumption is made that the fluid is incompressible so ρ_f is constant. Hence the equation of motion becomes

$$\begin{aligned}\rho_f A(s,t)\,\delta s\,\frac{\partial \underset{\sim}{\varepsilon}_f(s_f,t)}{\partial t} = {} & -A(s+\delta s,t)\,p(s+\delta s,t)\,\underset{\sim}{t}(s+\delta s,t) \\ & + A(s,t)\,p(s,t)\,\underset{\sim}{t}(s,t) \\ & - \rho_f A(s,t)\,\delta s\,g\,\underset{\sim}{k} + \underset{\sim}{R}\,\delta s\end{aligned} \qquad (Q)$$

which gives in the limit as $\delta s \to 0$

$$\rho_f A \frac{\partial \underset{\sim}{v}_f(s_f,t)}{\partial t} = - \frac{\partial (p A \underset{\sim}{t})}{\partial s} - \rho_f g A \underset{\sim}{k} + \underset{\sim}{R} \qquad (R)$$

which when substituting equation (a) gives

$$\rho_f A \left(\frac{\partial}{\partial t} + \lambda \frac{\partial}{\partial s_o}\right)\left(\frac{\partial}{\partial t} + v\left(\frac{\partial s}{\partial s_o}\right)^{-1}\frac{\partial}{\partial s_o}\right)\underset{\sim}{r}(s_o,t) = - \frac{\partial}{\partial s}(pA\underset{\sim}{t}) - \rho_f g A \underset{\sim}{k} + \underset{\sim}{R} \qquad (S)$$

where

$$\lambda = \frac{\partial s_o(s,t)}{\partial t} + v \frac{\partial s_o(s,t)}{\partial s} \qquad (T)$$

The assumption of small strain is now made to simplify the equation of motion for the fluid. For infinitesimally small strain

$$s = s_o \qquad (U)$$

for all time. Hence from equation (a) for small strain

$$\frac{\partial s_o}{\partial t} = 0 \qquad (V)$$

and

$$\frac{\partial s_o}{\partial s} = 1 \qquad (W)$$

Therefore the equation of motion of the fluid for small strain is

$$\rho_f A \left(\frac{\partial}{\partial t} + v \frac{\partial}{\partial s}\right)^2 \underset{\sim}{r}(s,t) = - \frac{\partial (p A \underset{\sim}{t})}{\partial s} - \rho_f A g \underset{\sim}{k} + \underset{\sim}{R} \qquad (a)$$

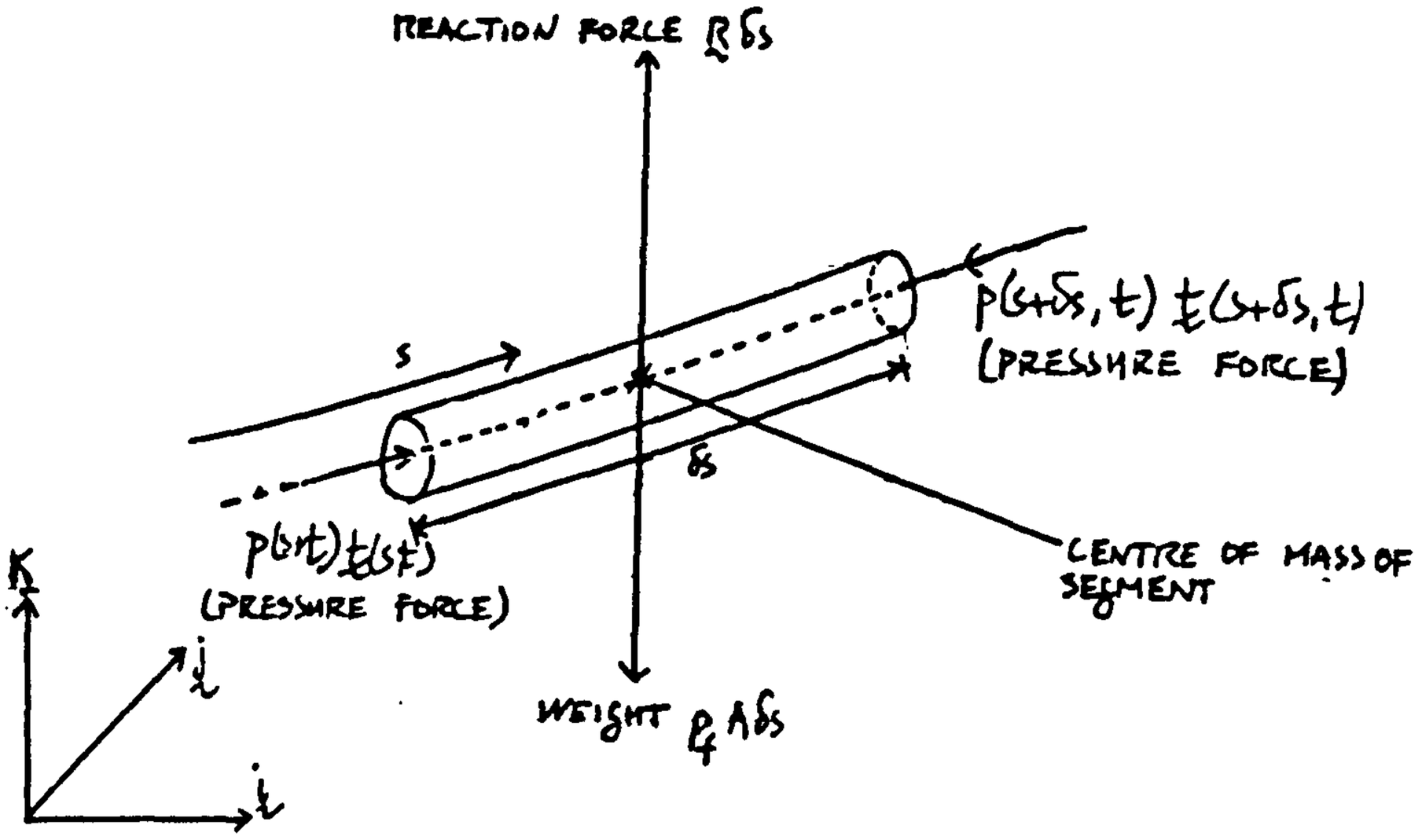

FIGURE 2.4.2(b): FORCES ACTING ON A SEGMENT OF FLUID

2.4.3: Resolved Components of Equation of Motion for the Internal Fluid.

Expanding the term on the left hand side of equation 2.4.2(c) gives

$$\rho_f A \left\{ \frac{\partial^2 \underset{\sim}{r}}{\partial t^2} + \frac{\partial v}{\partial t}\frac{\partial \underset{\sim}{r}}{\partial s} + 2v\frac{\partial}{\partial t}\left(\frac{\partial \underset{\sim}{r}}{\partial s}\right) + v^2\frac{\partial^2 \underset{\sim}{r}}{\partial s^2} + v\frac{\partial v}{\partial s}\frac{\partial \underset{\sim}{r}}{\partial s} \right\} \quad (A)$$

Hence since from Appendix A

$$\underset{\sim}{t}\cdot\underset{\sim}{t} = 1 \quad (B)$$

and

$$\frac{d\underset{\sim}{t}}{dt}\cdot\underset{\sim}{t} = 0 \quad (C)$$

resolution of the equations of motion in the tangential

direction gives

$$\rho_f A\left\{\frac{\partial^2 \underset{\sim}{r}}{\partial t^2}\cdot\underset{\sim}{t}+\frac{\partial v}{\partial t}+v\frac{\partial v}{\partial s}\right\}=-\frac{\partial(pA)}{\partial s}-\rho_f A g\,\underset{\sim}{k}\cdot\underset{\sim}{t}+\underset{\sim}{R}\cdot\underset{\sim}{t}\qquad(a)$$

and in the normal direction

$$\rho_f A\left\{\frac{\partial^2 \underset{\sim}{r}}{\partial t^2}\cdot\underset{\sim}{n}+2v\frac{\partial \underset{\sim}{t}}{\partial t}\cdot\underset{\sim}{n}+v^2\kappa\right\}=-pA\kappa-\rho_f g A\,\underset{\sim}{k}\cdot\underset{\sim}{n}+\underset{\sim}{R}\cdot\underset{\sim}{n}\qquad(b)$$

and finally resolution of the equation of motion in the binormal direction gives

$$\rho_f A\left\{\frac{\partial^2 \underset{\sim}{r}}{\partial t^2}\cdot\underset{\sim}{b}+2v\frac{\partial \underset{\sim}{t}}{\partial t}\cdot\underset{\sim}{b}\right\}=-\rho_f g A\,\underset{\sim}{k}\cdot\underset{\sim}{b}+\underset{\sim}{R}\cdot\underset{\sim}{b}\qquad(c)$$

2.4.4:Bernoulli's Equation.

The purpose of this section is to show that the equations developed in the previous sections for the motion of the fluid are consistant with Bernoulli's equation. To simplify the problem it is assumed that the riser is stationary and that the flow in the riser is both steady (i.e. $v=v(s)$ only) and inviscid. Note as mentioned before only circular risers are considered here, hence the position vector of any point on the internal surface is

$$\underset{\sim}{r}=\underset{\sim}{r}_c+a(\cos\theta\,\underset{\sim}{b}+\sin\theta\,\underset{\sim}{n})\qquad(0\le\theta\le 2\pi)\qquad(A)$$

where $\underset{\sim}{r}_c$ =position vector of the appropriate point on the centre-line of the riser, $a=a(s)$ =internal radius and θ =angular measure. Thus for an element $\delta\bar{A}$ of the internal surface with outward normal $\underset{\sim}{n}^*$

$$\underset{\sim}{n}^*\delta\bar{A}=\left(\frac{\partial \underset{\sim}{r}}{\partial s}\wedge\frac{\partial \underset{\sim}{r}}{\partial\theta}\right)\delta s\,\delta\theta=\begin{vmatrix}\underset{\sim}{t} & \underset{\sim}{k} & \underset{\sim}{n}\\ (1-a\kappa\sin\theta) & \left(a\sin\theta\tau+\frac{\partial a}{\partial s}\cos\theta\right) & \left(-a\tau\cos\theta+\frac{\partial a}{\partial\theta}s\right)\\ 0 & -a\sin\theta & a\cos\theta\end{vmatrix}\qquad(B)$$

$$=-\delta s\,\delta\theta\left\{\underset{\sim}{t}\left[a\frac{\partial a}{\partial s}\right]+\underset{\sim}{k}\left[-a\cos\theta(1-a\kappa\sin\theta)\right]+\underset{\sim}{n}\left[-a\sin\theta(1-a\kappa\sin\theta)\right]\right\}$$

using Appendix A. Hence

$$-\delta s\,\underset{\sim}{R} = \int p\,\underset{\sim}{n}^{*}\,d\bar{A} = \int p\left\{-a\frac{\partial a}{\partial s}\underset{\sim}{t} + a\cos\theta(1-a\kappa\sin\theta)\underset{\sim}{k} + a\sin\theta(1-a\kappa\sin\theta)\underset{\sim}{n}\right\}ds\,d\theta$$

$$= \int \left\{-2\pi a\frac{\partial a}{\partial s}\underset{\sim}{t} - a^{2}\kappa\pi\,\underset{\sim}{n}\right\}p\,ds \qquad (C)$$

where the integral is taken over the internal surface of a segment of the riser. But

$$A = \pi a^{2} \qquad (D)$$

gives

$$\delta s\,\underset{\sim}{R} = \int p\frac{d}{ds}(A\underset{\sim}{t})\,ds \qquad (E)$$

Substituting this result into equation 2.4.3(a) gives

$$\rho_f A v\frac{\partial v}{\partial s} = -\frac{\partial(pA)}{\partial s} - \rho_f g A\,\underset{\sim}{k}.\underset{\sim}{t} + p\frac{\partial A}{\partial s} \qquad (F)$$

therefore since $\underset{\sim}{k}.\underset{\sim}{t} = \frac{\partial z}{\partial s}$ (z vertical)

$$\rho_f A\frac{\partial(\frac{1}{2}v^{2})}{\partial s} = -A\frac{\partial p}{\partial s} - \rho_f g A\frac{\partial z}{\partial s} \qquad (G)$$

which integrates to give Bernoulli's equation

$$\frac{1}{2}\rho_f v^{2} + p + \rho_f g z = C \qquad (H)$$

where C is a constant. Note that this equation will approximately apply for small movements of the riser since $\frac{\partial^{2}\underset{\sim}{r}}{\partial t^{2}} \approx \underset{\sim}{0}$ for this case.

If in the unstrained state the cross-section of the riser is constant then if it is assumed that it suffers small strain and is volume conserving then the cross-section of the riser is approximately constant for all time. This means that v is approximately constant and Bernoulli's equation gives

$$p + \rho_f g z = D \qquad \text{(I)}$$

where D is a constant.

2.4.5:Modification to the Constitutive Relationships caused by Internal Fluid Flow.

For small strain one of the constitutive relationships that has been assumed to hold true is equation 2.3.2(a)

$$\underset{\sim}{t} \cdot \int_A (\underset{\sim}{F}_T - \underset{\sim}{F}_p^*)\, dA = AE\left(\frac{\partial s}{\partial s_0} - 1\right) \qquad \text{(A)}$$

This relationship needs to be modified if there is internal fluid flow in the riser. Equation 2.4.2(a) means a relationship

$$\underset{\sim}{t} \cdot \left\{ \int_A (\underset{\sim}{F}_T - \underset{\sim}{F}_p^*)\, dA - p_I A \underset{\sim}{t} \right\} = AE\left(\frac{\partial s}{\partial s_0} - 1\right) = T_e \qquad \text{(B)}$$

must be used, where p_I is the internal fluid pressure.

2.5: Derivation of Partial Differential Equation of Riser Motion.

2.5.1: Introduction.

In this section the governing partial differential equation for the riser motion are derived using the results of the previous sections. As before a general segment of the riser is initially considered and then the results are simply extended to apply at any point along the length of the riser.

2.5.2: Force Equilibrium Equation.

By the conservation of mass for the segment

$$\delta s_0 \rho(s_0) = \delta s \rho(s,t) \qquad (A)$$

where δs_0 = original length of the segment in the unstrained reference state, δs = length of the segment in the strained state, $\rho=\rho(s_0)$ = density distribution in the unstrained state and $\rho=\rho(s,t)$ = density distribution in the strained state. Hence using equation 2.2.2(a) and Newton's second law gives the dynamic equilibrium equation

$$\rho(s_0)\frac{\partial^2 \underset{\sim}{r}(s_0,t)}{\partial t^2} = \frac{\partial s}{\partial s_0}\underset{\sim}{Q} + \frac{\partial}{\partial s_0}\left\{ \int_A (\underset{\sim}{E}_T - \underset{\sim}{E}_T^*)\,dS - p_i A \underset{\sim}{t} \right\} \qquad (B)$$

where $\underset{\sim}{Q} = \underset{\sim}{F}_H + \underset{\sim}{F}_M + \underset{\sim}{R}^* + \underset{\sim}{F}_g$ and $\underset{\sim}{R}^*$ is defined by

$$\underset{\sim}{R}^* = -\rho_f A\left(\frac{\partial}{\partial t} + v\frac{\partial}{\partial s}\right)^2 \underset{\sim}{r}(s,t) - \rho_f g A \underset{\sim}{k} \qquad (C)$$

2.5.3:Moment Equilibrium Equation.

Since the net moment about the centre of mass of the forces on the segment is zero then using equation 2.2.3(a) gives

$$\underset{\sim}{0} = \frac{\partial}{\partial s}\left\{\int_A \underset{\sim}{q} \wedge \underset{\sim}{F}_T \, dA\right\} + \frac{\partial \underset{\sim}{r}}{\partial s} \wedge \left[\int_A (\underset{\sim}{F}_T - \underset{\sim}{F}_P^*)\, dA - p_I A \underset{\sim}{t}\right] \quad (a)$$

2.5.4:Derivation of Partial Differential Equation.

Taking the vector product of equation 2.5.3(a) with the tangent vector $\underset{\sim}{t}$ and using the constitutive relationship $\int \underset{\sim}{q} \wedge \underset{\sim}{F}_T dA = EI\kappa \underset{\sim}{b}$ and the vector identity $\underset{\sim}{a} \wedge (\underset{\sim}{b} \wedge \underset{\sim}{c}) = (\underset{\sim}{a} \cdot \underset{\sim}{c})\underset{\sim}{b} - (\underset{\sim}{a} \cdot \underset{\sim}{b})\underset{\sim}{c}$ gives

$$\underset{\sim}{t} \wedge \frac{\partial}{\partial s}\left\{EI\kappa \underset{\sim}{b}\right\} + T_e \underset{\sim}{t} = \left\{\int_A (\underset{\sim}{F}_T - \underset{\sim}{F}_P^*)\, dA - p_I A \underset{\sim}{t}\right\} \quad (A)$$

Thus substituting this equation into equation 2.5.2(a) gives

$$\rho(s_0)\frac{\partial^2 \underset{\sim}{r}(s_0,t)}{\partial t^2} = \frac{\partial s}{\partial s_0}\underset{\sim}{Q} + \frac{\partial}{\partial s_0}\left\{T_e \underset{\sim}{t} + \underset{\sim}{t} \wedge \frac{\partial}{\partial s}(EI\kappa \underset{\sim}{b})\right\} \quad (B)$$

But using the vector identity $\underset{\sim}{a} \wedge (\underset{\sim}{b} \wedge \underset{\sim}{c}) = (\underset{\sim}{a} \cdot \underset{\sim}{c})\underset{\sim}{b} - (\underset{\sim}{a} \cdot \underset{\sim}{b})\underset{\sim}{c}$ once again gives

$$\underset{\sim}{t} \wedge \frac{\partial}{\partial s}(EI\kappa \underset{\sim}{b}) = EI\, \underset{\sim}{t} \wedge \frac{\partial}{\partial s}\left(\underset{\sim}{t} \wedge \frac{\partial \underset{\sim}{t}}{\partial s}\right) = EI\, \underset{\sim}{t} \wedge \left(\underset{\sim}{t} \wedge \frac{\partial^2 \underset{\sim}{t}}{\partial s^2}\right) \quad (C)$$

$$= EI\left[\left(\underset{\sim}{t} \cdot \frac{\partial^2 \underset{\sim}{t}}{\partial t^2}\right)\underset{\sim}{t} - \frac{\partial^2 \underset{\sim}{t}}{\partial s^2}\right] = -EI\left[\kappa^2 \underset{\sim}{t} + \frac{\partial^2 \underset{\sim}{t}}{\partial s^2}\right]$$

Hence noting that $\underset{\sim}{t} = \frac{\partial \underset{\sim}{r}}{\partial s}$ and substituting gives

$$\rho(s_0)\frac{\partial^2 \underset{\sim}{r}(s_0,t)}{\partial t^2} = \underset{\sim}{Q}\frac{\partial s}{\partial s_0} - EI\frac{\partial}{\partial s_0}\left\{\frac{1}{\frac{\partial s}{\partial s_0}}\frac{\partial}{\partial s_0}\left[\frac{1}{\frac{\partial s}{\partial s_0}}\frac{\partial}{\partial s_0}\left(\frac{1}{\frac{\partial s}{\partial s_0}}\frac{\partial \underset{\sim}{r}}{\partial s_0}\right)\right]\right\}$$

$$+\frac{\partial}{\partial s_0}\left\{(T_e - EIK^2)\frac{1}{\frac{\partial s}{\partial s_0}}\frac{\partial \underset{\sim}{r}}{\partial s_0}\right\} \qquad (a)$$

In the limit of small strain as the variable s becomes the variable s_0

$$\rho(s_0)\frac{\partial^2 \underset{\sim}{r}(s_0,t)}{\partial t^2} = \underset{\sim}{Q} - EI\frac{\partial^4 \underset{\sim}{r}}{\partial s_0^4} + \frac{\partial}{\partial s_0}\left\{(T_e - EIK^2)\frac{\partial \underset{\sim}{r}}{\partial s_0}\right\} \qquad (b)$$

This equation is identical that derived by Nordgren[1974].

If $EI=0$ then equation (b) reduces to

$$\rho(s_0)\frac{\partial^2 \underset{\sim}{r}}{\partial t^2} = \underset{\sim}{Q}\frac{\partial s}{\partial s_0} + \frac{\partial}{\partial s_0}\left\{\frac{T_e}{\frac{\partial s}{\partial s_0}}\frac{\partial \underset{\sim}{r}}{\partial s_0}\right\} \qquad (c)$$

which is identical to that derived by Cristescu[1967].

2.5.5:Boundary Conditions.

Since a finite continuous length of riser is being considered the mathematical boundary conditions on the differential equation arise from the physical boundary conditions imposed on the two ends of the riser.

Consider for example the top end of the riser where the possible physical boundary conditions are:

1.The end is constrained to move along some known path and is clamped at known angles to the path.

2.The end is constrained to move along some known path and is pinned in its motion along this path.

3.The end is free of constraint.

Case 1. implies that $\underset{\sim}{r}$ and $\frac{\partial \underset{\sim}{r}}{\partial s_0}$ are known at all times at the end.

Case 2. implies that $\underset{\sim}{r}$ is known at all times at the end, however since the end is pinned there can be no net moment about about the centre-line at the end and thus at the end

$$k = 0 \qquad (A)$$

or

$$\frac{\partial^2 \underset{\sim}{r}}{\partial s^2} = \underset{\sim}{0} \qquad (B)$$

Case 3. implies that at the end

$$Q = \int_A \underset{\sim}{r} \wedge \underset{\sim}{F}_T \, dA = \int_A \underset{\sim}{F}_T \, dA \qquad (C)$$

hence as in case 2. at the end

$$K = 0 \qquad (D)$$

must hold but also since $\int \underset{\sim}{F}_T dA = 0$ from equation 2.5.3(a) at the end

$$Q = \frac{\partial}{\partial s}(K \underset{\sim}{b}) = \dot{K} \underset{\sim}{b} \qquad (E)$$

$$= \left(\underset{\sim}{n} \cdot \frac{\partial^3 \underset{\sim}{r}}{\partial s_0^3} \right) \underset{\sim}{b}$$

hence $\frac{\partial^3 \underset{\sim}{r}}{\partial s_0^3} = \underset{\sim}{0}$ at the end.

2.5.6:Reduction to the Standard Small Displacement, Small Strain, Rigid Riser Differential Equation.

Consider the rigid riser shown in figure 2.5.6(a). The rigid riser is subject to small strain only and a small displacement u in the y direction. From Kirk[1984] the partial differential equation for the dynamics of the riser is

$$-EI \frac{\partial^4 u}{\partial x^4} + \frac{\partial}{\partial x}\left\{ T_e \frac{\partial u}{\partial x} \right\} + f = \rho \frac{\partial^2 u}{\partial t^2} \qquad (a)$$

where f is the force on the riser acting in the y direction. It shall be illustrated how equation 2.5.4(b) can be reduced to the rigid riser equation.

Equation 2.5.4(b) can be written

$$\rho \frac{\partial^2 \underset{\sim}{r}}{\partial t^2} = \underset{\sim}{Q} - EI \left\{ \frac{\partial^2 (\kappa \underset{\sim}{n})}{\partial s_0^2} + \frac{\partial (\kappa^2 \underset{\sim}{t})}{\partial s_0} \right\} + \frac{\partial}{\partial s_0}(T_e \underset{\sim}{t}) \qquad (A)$$

using the Frenet-Serret formulae (Appendix A) gives

$$\rho \frac{\partial^2 \underset{\sim}{r}}{\partial t^2} = \underset{\sim}{Q} - EI \left\{ \frac{\partial}{\partial s_0}\left[\frac{\partial \kappa}{\partial s_0} \underset{\sim}{n} - \kappa^2 \underset{\sim}{t} \right] + \frac{\partial (\kappa^2 \underset{\sim}{t})}{\partial s_0} \right\} + \frac{\partial}{\partial s_0}(T_e \underset{\sim}{t}) \qquad (B)$$

since the rigid riser is assumed to move in the x-y plane the geometric torsion of the centre-line must be zero (i.e. $\tau = 0$). Therefore

$$\rho \frac{\partial^2 \underset{\sim}{r}}{\partial t^2} = \underset{\sim}{Q} - EI \frac{\partial}{\partial s_0}\left\{ \frac{\partial \kappa}{\partial s_0} \underset{\sim}{n} \right\} + \frac{\partial}{\partial s_0}(T_e \underset{\sim}{t}) \qquad (C)$$

but for small displacements the variable s_0 becomes the variable x to give

$$\rho \frac{\partial^2 \underset{\sim}{r}}{\partial t^2} = \underset{\sim}{Q} - EI \frac{\partial}{\partial x}\left\{ \frac{\partial \kappa}{\partial x} \frac{1}{\kappa} \frac{\partial^2 \underset{\sim}{r}}{\partial x^2} \right\} + \frac{\partial}{\partial x}(T_e \underset{\sim}{t}) \qquad (D)$$

$$= \underset{\sim}{Q} - EI \frac{\partial}{\partial x}\left\{ \left(\frac{\partial^2 \underset{\sim}{r}}{\partial x^2} \cdot \frac{\partial^3 \underset{\sim}{r}}{\partial x^3} \right)\left(\frac{\partial^2 \underset{\sim}{r}}{\partial x^2} \cdot \frac{\partial^2 \underset{\sim}{r}}{\partial x^2} \right)^{-1} \frac{\partial^2 \underset{\sim}{r}}{\partial x^2} \right\} + \frac{\partial}{\partial x}(T_e \underset{\sim}{t})$$

For small displacements of the riser

$$\mathcal{L} = x\,\ell_x + y\,\ell_y \qquad (E)$$

hence if $\underset{\sim}{Q}.\,\ell_y = f$ then taking the component of the partial differential equation in the y direction gives

$$\rho \frac{\partial^2 y}{\partial t^2} = f - EI \frac{\partial^4 y}{\partial x^4} + \frac{\partial}{\partial x}\left(T_e \frac{\partial y}{\partial x}\right) \qquad (F)$$

as required.

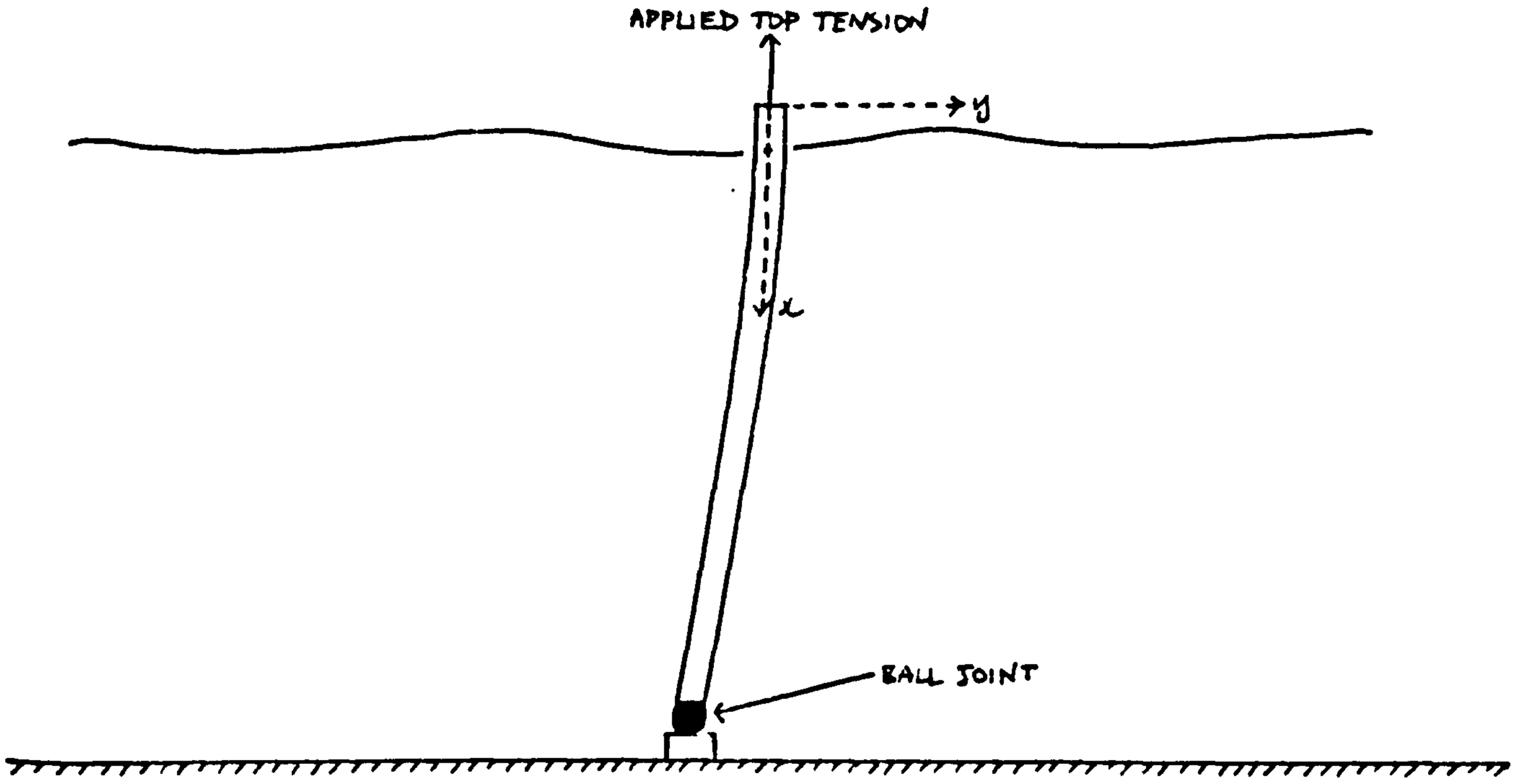

FIGURE 2.5.6(a): A RIGID (TENSIONED) RISER

2.6:Derivation of Variational Equation for Riser.

2.6.1:Introduction.

In this section a variational equation for the finite continuous length of riser shown in figure 2.1(a) is derived. The derivation of the variational equation gives greater insight than the previous derivation in section 2.5 of the governing partial differential equation. In the derivation of the variational equation the work of Washizu[1975] on the dynamics of elastic bodies is used. The variational calculus used in this section is described in detail in Milne[1980].

2.6.2:Preliminaries.

Consider an individual segment of the riser of length δs as shown in figure 2.6.2(a). $\underset{\sim}{k}_1$, $\underset{\sim}{k}_2$ and $\underset{\sim}{k}_3$ is a set of axes fixed in the material of the segment at t=0. After time t this set of axes goes to the new set $\underset{\sim}{k}_1'$, $\underset{\sim}{k}_2'$ and $\underset{\sim}{k}_3'$. $\underset{\sim}{k}_1$ is defined here such that $\underset{\sim}{k}_1 = \underset{\sim}{t}$ and for all time $\underset{\sim}{k}_1' = \underset{\sim}{t}$.

Let us consider an arbitrary vector $\underset{\sim}{q}$ then

$$\underset{\sim}{q} = \sum_{i=1}^{i=3} p_i' \underset{\sim}{k}_i' \qquad (A)$$

and hence

$$\frac{d\underset{\sim}{q}}{dt} = \sum_{i=1}^{i=3} \left\{ \frac{dp_i'}{dt} \underset{\sim}{k}_i' + p_i' \frac{d\underset{\sim}{k}_i'}{dt} \right\} \qquad (B)$$

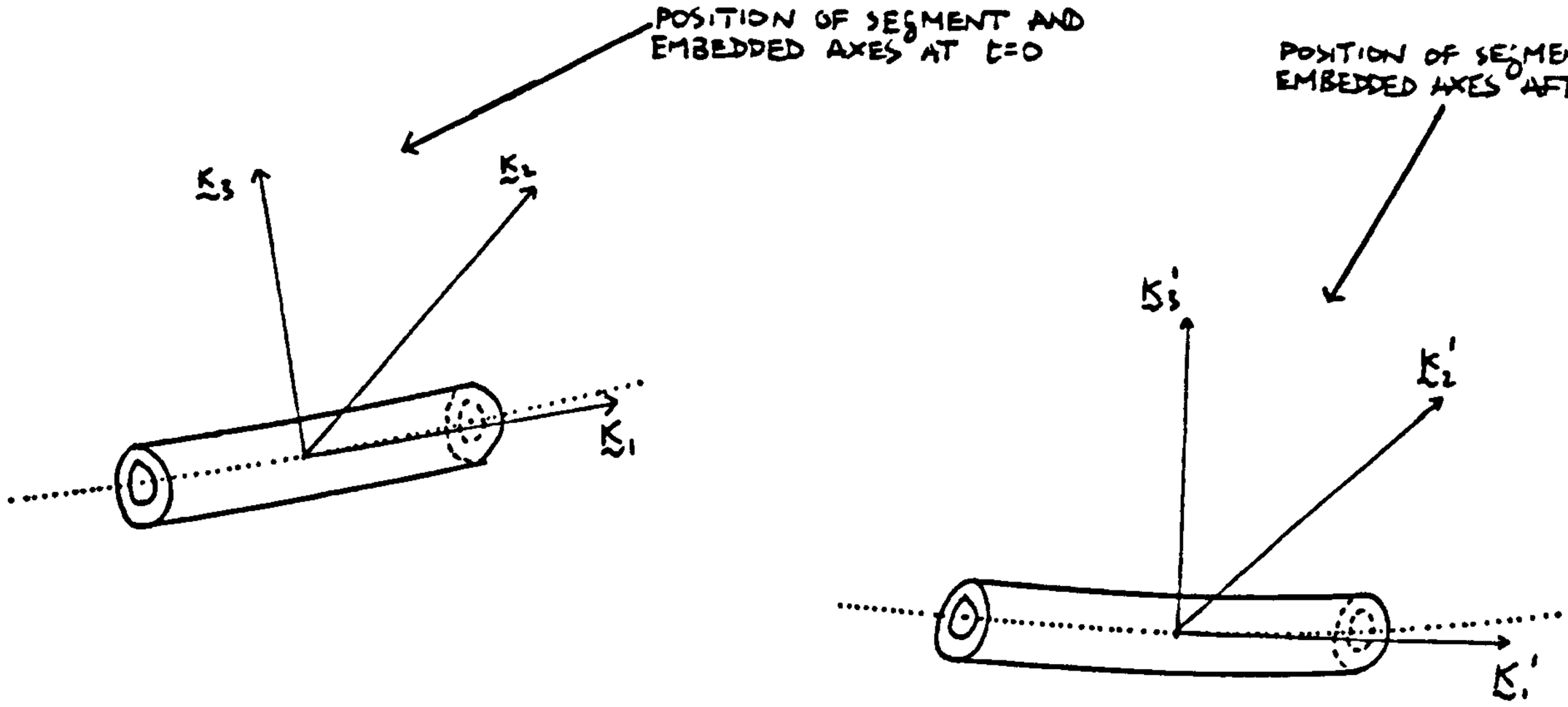

FIGURE 2.6.2(a) : THE EMBEDDED AXES

but $\underset{\sim}{k}_i'$ is a unit vector so for all time

$$\frac{d\underset{\sim}{k}_i'}{dt} \cdot \underset{\sim}{k}_i' = 0 \qquad (C)$$

This means

$$\frac{d\underset{\sim}{k}_1'}{dt} = \alpha_{12}\,\underset{\sim}{k}_2' + \alpha_{13}\,\underset{\sim}{k}_3' \qquad (D)$$

$$\frac{d\underset{\sim}{k}_2'}{dt} = \alpha_{21}\,\underset{\sim}{k}_1' + \alpha_{23}\,\underset{\sim}{k}_3'$$

$$\frac{d\underset{\sim}{k}_3'}{dt} = \alpha_{31}\,\underset{\sim}{k}_1' + \alpha_{32}\,\underset{\sim}{k}_2'$$

Using the orthogonality of $\underset{\sim}{k}_1'$, $\underset{\sim}{k}_2'$ and $\underset{\sim}{k}_3'$ gives relations like

$$\frac{d\underset{\sim}{k}_1'}{dt} \cdot \underset{\sim}{k}_2' + \underset{\sim}{k}_1' \cdot \frac{d\underset{\sim}{k}_2'}{dt} = 0 \qquad (E)$$

which means

$$\alpha_{12} = -\alpha_{21}\ ,\quad \alpha_{13} = -\alpha_{31}\ ,\quad \alpha_{23} = -\alpha_{32} \qquad (F)$$

Hence it is shown that

$$\frac{d\underset{\sim}{k}_i'}{dt} = (-\alpha_{23}\ ,\ \alpha_{13}\ ,\ -\alpha_{12}) \wedge \underset{\sim}{k}_i' \qquad (G)$$

i.e. that there is a vector $\underset{\sim}{w}$ such that

$$\frac{d\underset{\sim}{k}_i'}{dt} = \underset{\sim}{w} \wedge \underset{\sim}{k}_i' \qquad (H)$$

Using the standard Eulerian angles (Goldstein[1980]) θ , ψ and ϕ as shown in figure 2.6.2(b) the primed axes can be related to the unprimed axes

$$\begin{bmatrix} \underset{\sim}{k}_1' \\ \underset{\sim}{k}_2' \\ \underset{\sim}{k}_3' \end{bmatrix} = \begin{bmatrix} \cos\theta\cos\psi & \cos\theta\sin\psi & -\sin\theta \\ -\cos\phi\sin\psi + \sin\phi\sin\theta\cos\psi & \cos\phi\cos\psi + \sin\phi\sin\theta\sin\psi & \sin\phi\cos\theta \\ \sin\phi\sin\psi + \cos\phi\sin\theta\cos\psi & -\sin\phi\cos\psi + \cos\phi\sin\theta\sin\psi & \cos\phi\cos\theta \end{bmatrix} \begin{bmatrix} \underset{\sim}{k}_1 \\ \underset{\sim}{k}_2 \\ \underset{\sim}{k}_3 \end{bmatrix} \qquad (I)$$

The inverse matrix can simply be found. Hence using (a) gives

$$\underset{\sim}{w} = (\dot{\phi} - \dot{\psi}\sin\theta)\,\underset{\sim}{k}_1' + (\dot{\theta}\cos\phi + \dot{\psi}\sin\phi\cos\theta)\,\underset{\sim}{k}_2' + (-\dot{\theta}\sin\phi + \dot{\psi}\cos\phi\cos\theta)\,\underset{\sim}{k}_3' \qquad (J)$$

2.6.3:Kinetic Energy of the Segment.

For any point in the segment the displacement vector $\underset{\sim}{r}$ is given by

$$\underset{\sim}{r} = \underset{\sim}{r}_\delta + \underset{\sim}{r}^\circ + \underset{\sim}{u} \qquad (A)$$

where $\underset{\sim}{u}$ = elastic deformation vector and $\underset{\sim}{r}^\circ$ = position vector in the undeformed state from the centre of mass of the segment whose position vector is $\underset{\sim}{r}_\delta$ to a point in the segment.

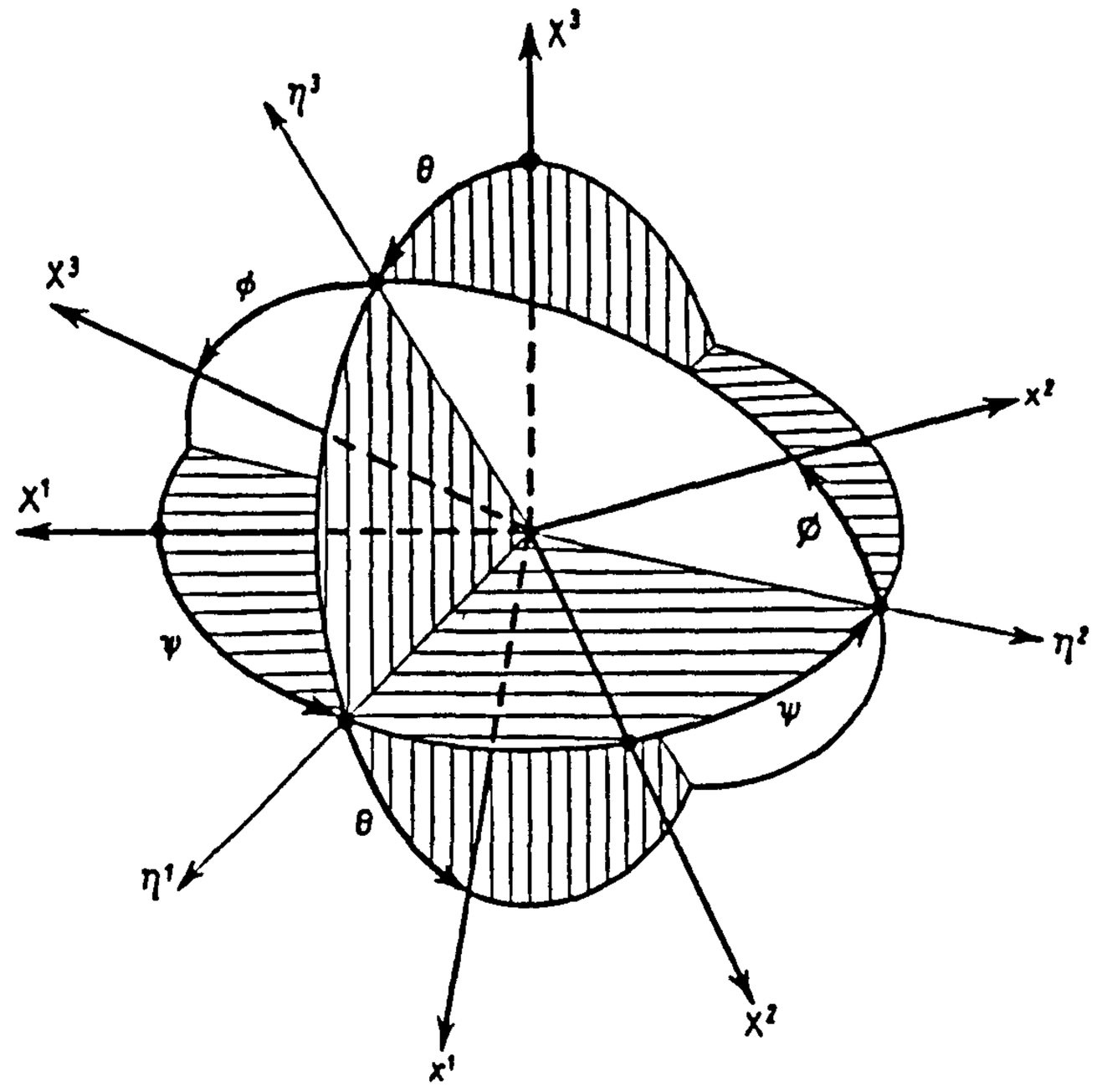

The transformation from the space fixed axes (X^1, X^2, X^3) to the moving axes (x^1, x^2, x^3) is defined by three successive angles of rotation. First, the (X^1, X^2, X^3) axes are rotated around the X^3-axis by the angle ψ to obtain (η^1, η^2, X^3) axes. Second, the (η^1, η^2, X^3) axes are rotated around the η^2-axis by the angle θ to obtain (x^1, η^2, η^3) axes. Finally, the (x^1, η^2, η^3) axes are rotated around the x^1-axis by the angle ϕ to obtain (x^1, x^2, x^3) axes. The three angles ϕ, θ and ψ, called the Eulerian angles, specify the orientation of the (x^1, x^2, x^3) axes uniquely.

Figure 2.6.2(b): The Eulerian Angles (from Washizu [1975])

It is assumed that the contribution to the kinetic energy T by elastic deformation is negligible. Thus the kinetic energy of the segment is given by

$$T = \int \frac{1}{2}\rho \left(\frac{d\underset{\sim}{\xi}}{dt} + \frac{d\underset{\sim}{\xi}^{\circ}}{dt} \right)^2 dV \qquad (B)$$

$$= \int \frac{1}{2}\rho \left\{ \left(\frac{d\underset{\sim}{\xi}}{dt} \right)^2 + 2(\underset{\sim}{\omega} \wedge \underset{\sim}{\xi}^{\circ}) \cdot \frac{d\underset{\sim}{\xi}}{dt} + (\underset{\sim}{\omega} \wedge \underset{\sim}{\xi}^{\circ})^2 \right\} dV$$

$$= \int \frac{1}{2}\rho \left\{ \left(\frac{d\underset{\sim}{\xi}}{dt} \right)^2 + (\underset{\sim}{\omega} \wedge \underset{\sim}{\xi}^{\circ})^2 \right\} dV + \rho \left(\frac{d\underset{\sim}{\xi}}{dt} \wedge \underset{\sim}{\omega} \right) \cdot \int \underset{\sim}{\xi}^{\circ} dV$$

(n.b. $\underset{\sim}{a} \cdot (\underset{\sim}{b} \wedge \underset{\sim}{c}) = \underset{\sim}{c} \cdot (\underset{\sim}{a} \wedge \underset{\sim}{b})$)

In deriving the above expression equation 2.6.2(a) has been used. But $\underset{\sim}{r}_g$ is the centre of mass of the segment hence

$$T = \int \frac{1}{2}\rho \left\{ \left(\frac{d\underset{\sim}{r}_s}{dt}\right)^2 + (\underset{\sim}{\omega} \wedge \underset{\sim}{r}^o)^2 \right\} dV \qquad (C)$$

This expression consists of a translational component and a rotational component. If the segment is sufficiently slender then

$$T = \frac{1}{2}\rho(s_o)\,\delta s_o \left(\frac{d\underset{\sim}{r}_s}{dt}\right)^2 + \frac{1}{2}\rho(s_o)\,\delta s_o \left[\frac{1}{12}\delta s_o^2\right]\left\{ |\underset{\sim}{\omega}|^2 - (\underset{\sim}{\omega}.\underset{\sim}{k}_1')^2 \right\} \qquad (D)$$

and hence the kinetic energy of the whole of the riser length is given by

$$T = \int \frac{1}{2}\rho(s_o) \left(\frac{d\underset{\sim}{r}}{dt}\right)^2 ds_o \qquad (a)$$

if second order terms are neglected.

Note that the above derivation is only applicable if the riser is slender in comparison to its length.

2.6.4:Virtual Work Done on a Segment.

From section 2.6.2 for the relevant virtual displacements

$$\delta\underset{\sim}{\omega} = (\delta\phi - \delta\psi\sin\theta)\,\underset{\sim}{k}_1' + (\delta\theta\cos\phi + \delta\psi\sin\phi\cos\theta)\,\underset{\sim}{k}_2' + (-\delta\theta\sin\phi + \delta\psi\cos\phi\cos\theta)\,\underset{\sim}{k}_3' \qquad (A)$$

and

$$\delta\underset{\sim}{r} = \delta\underset{\sim}{r}_g + \delta\underset{\sim}{\omega} \wedge \underset{\sim}{r}^o \qquad (B)$$

Thus the net virtual work done (including the virtual work done on the ends of the segment) is

$$\delta W = \int \underset{\sim}{P} \cdot [\delta \underset{\sim}{r}_g + \delta \underset{\sim}{\omega} \wedge \underset{\sim}{r}^\circ] \, dV + \int \underset{\sim}{F} \cdot [\delta \underset{\sim}{r}_g + \delta \underset{\sim}{\omega} \wedge \underset{\sim}{r}^\circ] \, dS \qquad (C)$$

$$+ \int_{A_{Le}} \underset{\sim}{F}_{Le} \cdot [\delta \underset{\sim}{r}_{Le} + \delta \underset{\sim}{\omega}_{Le} \wedge \underset{\sim}{q}] \, dS + \int_{A_{Ri}} \underset{\sim}{F}_{Ri} \cdot [\delta \underset{\sim}{r}_{Ri} + \delta \underset{\sim}{\omega}_{Ri} \wedge \underset{\sim}{q}] \, dS$$

$$= \delta \underset{\sim}{r}_g \cdot \left\{ \int \underset{\sim}{P} \, dV + \int \underset{\sim}{F} \, dS \right\} + \delta \underset{\sim}{\omega} \cdot \left\{ \int \underset{\sim}{r}^\circ \wedge \underset{\sim}{P} \, dV + \int \underset{\sim}{r}^\circ \wedge \underset{\sim}{F} \, dS \right\}$$

$$+ \delta \underset{\sim}{r}_{Le} \cdot \int_{A_{Le}} \underset{\sim}{F}_{Le} \, dS + \delta \underset{\sim}{r}_{Ri} \cdot \int_{A_{Ri}} \underset{\sim}{F}_{Ri} \, dS$$

$$+ \delta \underset{\sim}{\omega}_{Le} \cdot \int_{A_{Le}} \underset{\sim}{q} \wedge \underset{\sim}{F}_{Le} \, dS + \delta \underset{\sim}{\omega}_{Ri} \cdot \int_{A_{Ri}} \underset{\sim}{q} \wedge \underset{\sim}{F}_{Ri} \, dS$$

where $\underset{\sim}{P}$ = force per unit volume acting on the segment and $\underset{\sim}{F}$ = force per unit area acting on the curved surfaces of the segment. Note to avoid confusion in notation Le denotes the left-hand of the segment and Ri denotes the right-hand end of the segment. In the next section L denotes the net length of continuous riser

2.6.5:Virtual Work done on the Riser

Using section 2.2, section 2.6.4 and Newton's Law of Action and Reaction gives the net virtual work done on the riser

$$\delta W = \int \underset{\sim}{\delta r} \cdot \left\{ \underset{\sim}{Q} \frac{\partial s}{\partial s_0} + \frac{\partial}{\partial s_0} \left[\int_A (\underset{\sim}{F}_T - \underset{\sim}{F}_P^*)\, dA \right] \right\} ds_0 \qquad (A)$$

$$+ \int \underset{\sim}{\delta\omega} \cdot \left\{ \frac{\partial}{\partial s_0} \left[\int \underset{\sim}{q} \wedge \underset{\sim}{E}_T\, dA \right] + \underset{\sim}{t} \wedge \int_A (\underset{\sim}{F}_T - \underset{\sim}{F}_P^*)\, dA \right\} ds_0$$

$$+ \underset{\sim}{\delta r}_0 \cdot \left\{ \int \underset{\sim}{\bar{F}}_0\, dA + \int (\underset{\sim}{F}_T - \underset{\sim}{F}_P^*) dA \Big|_0 \right\} + \underset{\sim}{\delta r}_L \cdot \left\{ \int \underset{\sim}{\bar{F}}_L\, dA - \int (\underset{\sim}{F}_T - \underset{\sim}{F}_P^*) dA \Big|_L \right\}$$

$$+ \underset{\sim}{\delta\omega}_0 \cdot \left\{ \int_{A_0} \underset{\sim}{r} \wedge \underset{\sim}{\bar{F}}_0\, dA + \int \underset{\sim}{q} \wedge \underset{\sim}{E}_T\, dA \Big|_0 \right\} + \underset{\sim}{\delta\omega}_L \cdot \left\{ \int_{A_L} \underset{\sim}{r} \wedge \underset{\sim}{\bar{F}}_L\, dA - \int \underset{\sim}{q} \wedge \underset{\sim}{E}_T\, dA \Big|_L \right\}$$

The bar over the appropriate force terms denotes the applied force terms at the ends of the riser. $\underset{\sim}{\chi}|_0$ denotes the value of the variable $\underset{\sim}{\chi}$ evaluated at the end of the riser where the arc-length parameter is defined to be 0 and $\underset{\sim}{\chi}|_L$ denotes the value of $\underset{\sim}{\chi}$ evaluated at the end of the riser with arc-length parameter equal to L .

2.6.6:Differential Equations for a Riser with Boundary Conditions.

Using section 2.6.5, equation 2.6.3(a) and the principle of virtual work gives

$$\rho(s_o)\frac{\partial^2 \underset{\sim}{r}}{\partial t^2} = \underset{\sim}{Q}\frac{\partial s}{\partial s_o} + \frac{\partial}{\partial s_o}\left\{\int_A (\underset{\sim}{E}_T - \underset{\sim}{E}_p^*)\,dA\right\} \qquad (A)$$

and

$$\underset{\sim}{Q} = \frac{\partial}{\partial s_o}\left\{\int \underset{\sim}{q}\wedge \underset{\sim}{E}_T\,dA\right\} + \underset{\sim}{t}\wedge\int_A(\underset{\sim}{E}_T - \underset{\sim}{E}_p^*)\,dA \qquad (B)$$

(These partial differential equations are identical to the ones derived in section 2.5 if it is noted that for simplification internal fluid effects are not dealt with here). Together with the boundary conditions

$$\int \bar{\underset{\sim}{E}}_o\,dA = -\int(\underset{\sim}{E}_T - \underset{\sim}{E}_p^*)\,dA\Big|_o \qquad (C)$$

$$\int \bar{\underset{\sim}{E}}_L\,dA = \int(\underset{\sim}{E}_T - \underset{\sim}{E}_p^*)\,dA\Big|_L$$

$$\int_{A_L} \underset{\sim}{q}\wedge \bar{\underset{\sim}{E}}_o\,dA = -\int \underset{\sim}{q}\wedge \underset{\sim}{E}_T\,dA\Big|_o$$

$$\int_{A_R} \underset{\sim}{q}\wedge \bar{\underset{\sim}{E}}_L\,dA = \int \underset{\sim}{q}\wedge \underset{\sim}{E}_T\,dA\Big|_L$$

2.6.7:Derivation of the Strain Energy Functional.

The strain energy functional $\checkmark$ is that functional such that

$$\delta V = -\int \delta\underset{\sim}{r}\cdot\frac{\partial}{\partial s_o}\left\{\int(\underset{\sim}{E}_T - \underset{\sim}{E}_p^*)\,dA\right\}ds_o + \int \underset{\sim}{E}_T\Big|_L\cdot\delta\underset{\sim}{r}\Big|_L\,dA - \int \underset{\sim}{E}_T\Big|_o\cdot\delta\underset{\sim}{r}\Big|_o\,dA \qquad (A)$$

$$+\delta\underset{\sim}{w}\Big|_L\cdot\int\underset{\sim}{q}\wedge\underset{\sim}{E}_T\,dA\Big|_L - \delta\underset{\sim}{w}\Big|_o\cdot\int\underset{\sim}{q}\wedge\underset{\sim}{E}_T\,dA\Big|_o$$

$$= -\int\delta\underset{\sim}{r}\cdot\frac{\partial}{\partial s_o}\left\{\int(\underset{\sim}{E}_T - \underset{\sim}{E}_p^*)\,dA\right\}ds_o + \int\underset{\sim}{E}_T\cdot\delta\underset{\sim}{r}\,dA\Big|_o^L + \left[\delta\underset{\sim}{w}\cdot\int\underset{\sim}{q}\wedge\underset{\sim}{E}_T\,dA\right]_o^L$$

It will be shown that the required functional V is given by

$$V = \int_0^L \left\{ \left[\int T_e \left(\frac{\partial s}{\partial s_0} \right) d\left(\frac{\partial s}{\partial s_0} \right) \right] + \frac{EI}{2} \kappa^{*2} \left(3 - 2 \frac{\partial s}{\partial s_0} \right) \right\} ds_0 \qquad (B)$$

where

$$\kappa^{*2} = \frac{\partial^2 \underset{\sim}{r}}{\partial s_0^2} \cdot \frac{\partial^2 \underset{\sim}{r}}{\partial s_0^2} \qquad (C)$$

which is the small strain approximation to

$$\kappa^2 = \frac{\partial^2 \underset{\sim}{r}}{\partial s^2} \cdot \frac{\partial^2 \underset{\sim}{r}}{\partial s^2} \qquad (D)$$

Note no assumptions are made about the exact nature of the function T_e thus non-linear materials are allowed for. If the bending stiffness of the riser is zero then this strain energy functional is valid for small or large strain. In Appendix B the pure stretching energy, for particular cases, for both linear and non-linear materials is obtained.

The proof is done in the following steps

STEP A:

$$\delta \int_0^L \left[\int T_e \left(\frac{\partial s}{\partial s_0} \right) d\left(\frac{\partial s}{\partial s_0} \right) \right] ds_0 = \int_0^L T_e \, \delta \left(\frac{\partial s}{\partial s_0} \right) ds_0 \qquad (E)$$

$$= \int_0^L T_e \, \frac{\partial \underset{\sim}{r}}{\partial s_0} \Big/ \frac{\partial s}{\partial s_0} \cdot \frac{\partial \, \delta \underset{\sim}{r}}{\partial s_0} \, ds_0$$

$$= T_e \underset{\sim}{t} \cdot \delta \underset{\sim}{r} \Big|_0^L - \int_0^L \delta \underset{\sim}{r} \cdot \frac{\partial (T_e \underset{\sim}{t})}{\partial s_0} \, ds_0$$

Note in the above step in the proof no assumption has been made about the magnitude of the strain. However for the following steps the small strain assumption is used.

STEP B:

$$\int_0^L \left[\delta\left(\frac{EI}{2}\kappa^{*2}\right)\right]\left[3-2\frac{\partial s}{\partial s_0}\right] ds_0 = \int_0^L \delta\left(\frac{EI}{2}\kappa^{*2}\right) ds_0 = \int_0^L EI\,\frac{\partial^2 \underset{\sim}{r}}{\partial s_0^2}\cdot\frac{\partial^2 \delta\underset{\sim}{r}}{\partial s_0^2}\, ds_0$$

$$= EI\,\frac{\partial \delta\underset{\sim}{r}}{\partial s_0}\cdot\frac{\partial^2 \underset{\sim}{r}}{\partial s_0^2}\Bigg|_0^L - \int_0^L EI\,\frac{\partial \delta\underset{\sim}{r}}{\partial s_0}\cdot\frac{\partial^3 \underset{\sim}{r}}{\partial s_0^3}\, ds_0$$

$$= EI\,\frac{\partial \delta\underset{\sim}{r}}{\partial s_0}\cdot\frac{\partial^2 \underset{\sim}{r}}{\partial s_0^2}\Bigg|_0^L - EI\,\delta\underset{\sim}{r}\cdot\frac{\partial^3 \underset{\sim}{r}}{\partial s_0^3} + \int_0^L EI\,\delta\underset{\sim}{r}\cdot\frac{\partial^4 \underset{\sim}{r}}{\partial s_0^4}\, ds_0 \qquad (F)$$

(n.b. $\frac{\partial s}{\partial s_0} \to 1 \Rightarrow 3-2\frac{\partial s}{\partial s_0} \to 1$)

STEP C:

$$\int_0^L \frac{EI\kappa^{*2}}{2}\,\delta\left(3-2\frac{\partial s}{\partial s_0}\right) ds_0 = \int_0^L \frac{EI\kappa^{*2}}{2}\left(-2\underset{\sim}{t}\cdot\frac{\partial \delta\underset{\sim}{r}}{\partial s_0}\right) ds_0 \qquad (G)$$

$$= -\delta\underset{\sim}{r}\cdot EI\kappa^{*2}\underset{\sim}{t}\Bigg|_0^L + \int_0^L \delta\underset{\sim}{r}\cdot\frac{\partial}{\partial s_0}\left\{EI\kappa^{*2}\underset{\sim}{t}\right\} ds_0$$

Hence

$$\delta V = \left[T_e \frac{\partial \underset{\sim}{r}}{\partial s_0} - EI \frac{\partial^3 \underset{\sim}{r}}{\partial s_0^3} - EI\kappa^2 \frac{\partial \underset{\sim}{r}}{\partial s_0} \right] \cdot \delta \underset{\sim}{r} \Big|_0^L + EI \frac{\partial^2 \underset{\sim}{r}}{\partial s_0^2} \cdot \delta \left(\frac{\partial \underset{\sim}{r}}{\partial s_0} \right) \Big|_0^L$$

$$- \int_0^L \frac{\partial}{\partial s_0} \left\{ T_e \frac{\partial \underset{\sim}{r}}{\partial s_0} - EI \frac{\partial^3 \underset{\sim}{r}}{\partial s_0^3} - EI\kappa^2 \frac{\partial \underset{\sim}{r}}{\partial s_0} \right\} \cdot \delta \underset{\sim}{r} \, ds_0 \qquad (H)$$

However from section 2.5.4

$$\int (\underset{\sim}{F}_T - \underset{\sim}{F}_p^*) \, dA = - EI \frac{\partial^3 \underset{\sim}{r}}{\partial s_0^3} + [T_e - EI\kappa^2] \frac{\partial \underset{\sim}{r}}{\partial s_0} \qquad (I)$$

Hence

$$\delta V = \int (\underset{\sim}{F}_T - \underset{\sim}{F}_p^*) dA \cdot \delta \underset{\sim}{r} \Big|_0^L + EI \frac{\partial^2 \underset{\sim}{r}}{\partial s_0^2} \cdot \delta \left(\frac{\partial \underset{\sim}{r}}{\partial s_0} \right) \Big|_0^L - \int_0^L \frac{\partial}{\partial s_0} \left\{ \int (\underset{\sim}{F}_T - \underset{\sim}{F}_p^*) dA \right\} \cdot \delta \underset{\sim}{r} \, ds_0 \qquad (J)$$

Therefore all that remains to complete the proof is to show

$$EI \frac{\partial^2 \underset{\sim}{t}}{\partial s_0^2} \cdot \delta \left(\frac{\partial \underset{\sim}{r}}{\partial s_0} \right) \Big|_0^L = \delta \underset{\sim}{\omega} \cdot \int \underset{\sim}{q} \wedge \underset{\sim}{F}_T \, dA \Big|_0^L \qquad (K)$$

or

$$EI\kappa \underset{\sim}{n} \cdot \delta (\underset{\sim}{t}) \Big|_0^L = \delta \underset{\sim}{\omega} \cdot EI\kappa \underset{\sim}{b} \Big|_0^L \qquad (L)$$

but this follows immediately since $\delta \underset{\sim}{t} = \delta \underset{\sim}{\omega} \wedge \underset{\sim}{t}$ gives

$$\underset{\sim}{n} \cdot \delta (\underset{\sim}{t}) = \underset{\sim}{n} \cdot (\delta \underset{\sim}{\omega} \wedge \underset{\sim}{t}) = \delta \underset{\sim}{\omega} \cdot \underset{\sim}{b} \qquad (M)$$

and as required it has been shown that

$$\delta V = \left\{ \int \underset{\sim}{F}_T \, dA \cdot \delta \underset{\sim}{r} \right\} \Big|_0^L + \delta \underset{\sim}{\omega} \cdot \int \underset{\sim}{q} \wedge \underset{\sim}{F}_T \, dA \Big|_0^L \qquad (N)$$

$$- \int_0^L \delta \underset{\sim}{r} \cdot \frac{\partial}{\partial s_0} \left\{ \int \underset{\sim}{F}_T - \underset{\sim}{F}_p^* \, dA \right\} ds_0$$

CHAPTER THREE:DISCRETIZATIONS FOR A FLEXIBLE RISER.

3.1:Introduction.

In this chapter several discretizations are provided for the dynamic description of a continuous length of flexible riser as shown in figure 2.1(a). All of the discretizations given in this thesis, apart from the elastic lumped mass discretization, are completely new. Many of the discretizations give equations of motion that are similar but this does not imply that the choice of the discretization is not important, since some of them are more versatile and adaptable than others. In particular the variational finite element methods, for reasons given later, have many advantages over other discretizations.

The discretizations given in this thesis are compared with each other and with those in the literature. Recommendations are made for their use.

Using the techniques given in this chapter other new discretizations can also be derived. Details about these discretizations are given in section 3.8. Other techniques e.g. finite difference methods, that are not used in this chapter, could also be used to generate new discretizations and further details of such new discretiztions are also given in section 3.8.

The discretizations given can be divided into two types. One type describes the dynamics of the riser through modelling the dynamics of a much simpler structural system.

For example the elastic lumped mass method consists of the description of a collection of masses connected together by mass-less springs and the inelastic lumped mass method consists of a description of infinitely stiff rigid rods that are hinged together. The second type consists of directly discretizing one of the continuum equations (either a partial differential equation or a variational equation) that was derived in chapter two. Only finite element discretizations of the continuum equations are given although other discretizations are possible such as finite difference discretizations.

The inelastic lumped mass method simultaneously with a discretization in space for the system also employs a discretization in time i.e. it is a space-time discretization. All the other models use a discretization in space at first to obtain a system of equations of the form

$$[M][\ddot{r}] = [F] \tag{A}$$

where $[M=M(r)]$ =the mass matrix, $[r]$ =column vector of appropriate degrees of freedom for the system and $[F=F(\dot{r},r,t)]$ =column vector of both internal and external forces. This set of ordinary differential equations is then discretized in time using the Newmark or other similar time-stepping scheme.

In this chapter a number of simplifying assumptions are made:

1.The bending stiffness of the riser is zero.

2.The effects of internal fluid flow are negligible

3.There is no ground contact of the riser with the seabed.

4.The riser is totally immersed in the sea.

5.Both ends of the riser are fixed.

These constraints are relaxed in chapter four. Note no restrictions are made on the magnitude of the strain in the riser.

3.2:Elastic Lumped Mass Discretization.

3.2.1:Introduction.

The riser is modelled by a series of masses connected together by mass-less spring elements as shown in figure 3.2.1. In essence a continuous structure is being approximated by a much simpler discrete one. As will be shown later in this chapter there is an intrinsic error in the lumped mass discretization. The error is caused by neglecting rotational kinetic energy and mass coupling effects.

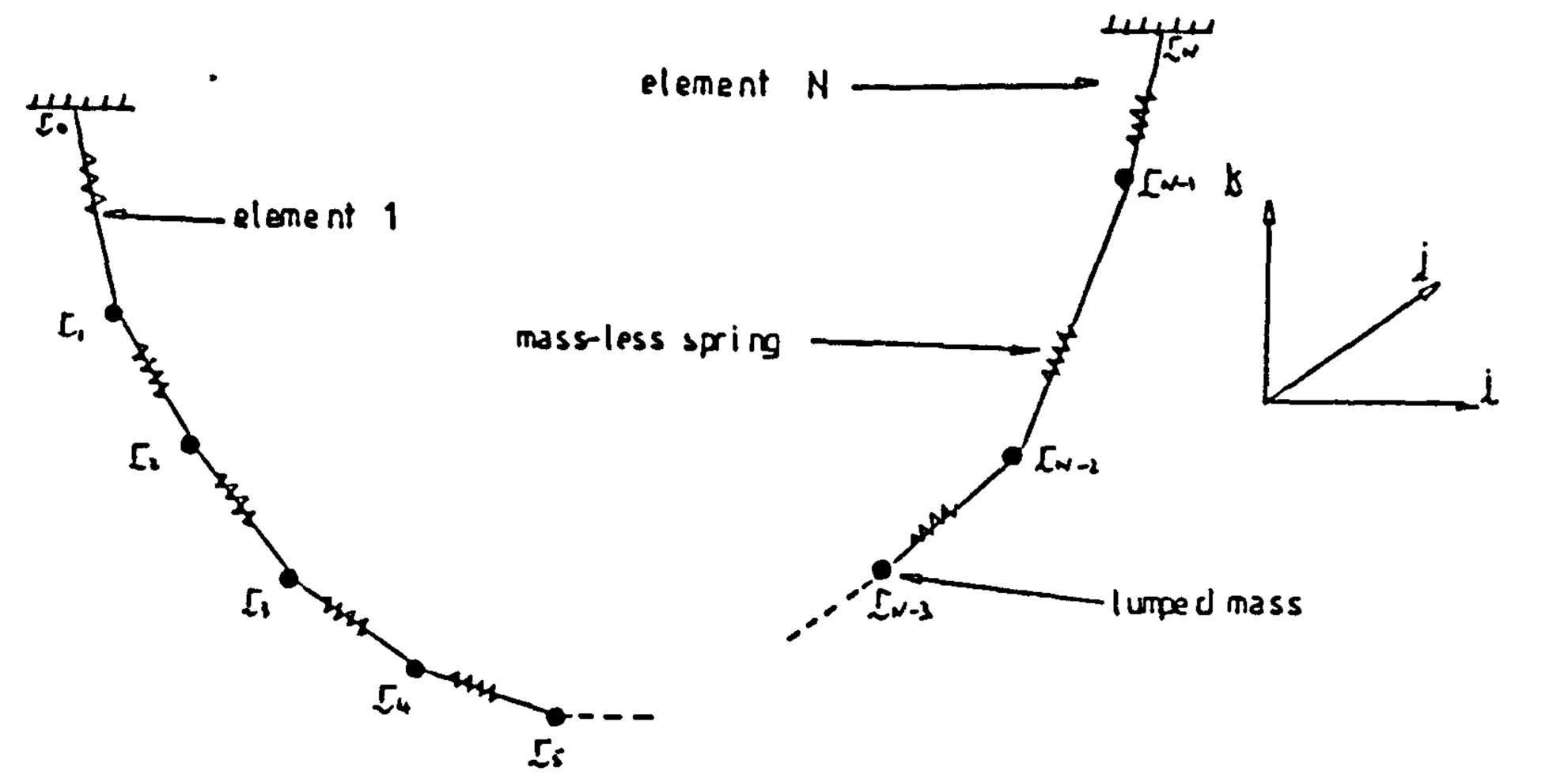

Figure 3.2.1: The Elastic Lumped Mass Method

Elastic lumped mass discretizations are given in Nakajima, Motora and Fujino[1982], Nath and Thresher[1975] and Ractliffe[1984]. Nakajima et. al. and Nath et. al. deal with two dimensions only whereas Ractliffe's

discretization is three dimensional. Nakajima et. al. use the Houboult time stepping integration method and employ a complicated method for linearising the elastic forces. Nath et. al. use a second order predictor-corrector method. Ractliffe decouples the transverse motion from the longitudinal motion (see section 3.10.3 on the method of characteristics) and obtains equations of motion for the transverse motion and for the longitudinal motion. These equations are then integrated seperately with timesteps that are not equal. This is supposed to reduce the C.P.U. time required by allowing a larger timestep, than would otherwise have been possible, for the integration of the transverse motion. Ractliffe allows for the modelling of bending stiffness and for the modelling of internal fluid flow. However it is thought that for commercial reasons full details of his discretization have not been given.

3.2.2:Equations of motion.

Consider figure 3.2.1. Applying Newton's second law to each of the masses gives

$$
\begin{aligned}
m_1 \ddot{\underline{r}}_1 &= \underline{F}_1 + T_2 \underline{t}_2 - T_1 \underline{t}_1 , \\
m_2 \ddot{\underline{r}}_2 &= \underline{F}_2 + T_3 \underline{t}_3 - T_2 \underline{t}_2 , \\
&\vdots \\
m_{N-1} \ddot{\underline{r}}_{N-1} &= \underline{F}_{N-1} + T_N \underline{t}_N - T_{N-1} \underline{t}_{N-1} ,
\end{aligned}
\qquad (a)
$$

where M_i $(i=1,\ldots,N-1)$ = lumped mass at the ith node, $\underset{\sim}{r}_i (i=0,\ldots,N)$ = position vector of the ith node, $T_i (i=1,\ldots,N)$ = tension in the ith spring $\underset{\sim}{F}_i$ $(i=1,\ldots,N-1)$ = modal force and $\underset{\sim}{t}_i (i=1,\ldots,N)$ = tangent vector defined by each of the springs. There are also N equations of elastic constraint

$$
\begin{aligned}
T_1 &= K_1 (L_1 - L_1^*) , \\
T_2 &= K_2 (L_2 - L_2^*) , \\
&\vdots \\
T_N &= K_N (L_N - L_N^*) ,
\end{aligned}
\qquad (b)
$$

where $K_i (i=1,\ldots,N)$ = itth spring constant (it is assumed that the springs are linear but non-linear springs could easily be included to model non-linear material behaviour), $L_i (i=1,\ldots N)$ = strained length and $L_i^* (i=1,\ldots,N)$ = unstrained length of the ith spring.

There are $3(N-1)$ equations from equations (a) and N equations from equations (b), hence in total there are $4N-3$ equations. There are $3(N-1)$ variables in $\underset{\sim}{r}_1$, $\underset{\sim}{r}_2, \ldots\ldots, \underset{\sim}{r}_{N-1}$ and N variables in $T_1, T_2, \ldots\ldots, T_N$ hence in total there are $4N-3$ variables. The number of variables is equal to the number of equations therefore the system of equations obtained is complete.

3.2.3:Relationship of Parameters to the Continuum.

Figure 3.2.3(a) shows the hypothetical path of a section of the riser from an unstrained reference state. It is supposed that the arc-length between $\underset{\sim}{r}_K$ and $\underset{\sim}{r}_{K+1}$ is given by L^*_{K+1} . The lumped mass discretzation uses the distance $L_{K+1}=|\underset{\sim}{r}_{K+1}-\underset{\sim}{r}_K|$ between the two points $\underset{\sim}{r}_{K+1}$ and $\underset{\sim}{r}_K$ in its formulation. The real strained state of the riser does not necessarily pass through the appropriate points. Similarly the net length of the riser in the strained state is not neccesarily the same as the net length of the mass-less springs. As the number of structural elements is increased a better approximation both to the nodal points of the riser and to the net length of the riser is obtained.

The mass of the ith lumped mass is related to the continuum through the equations

$$m_1=\frac{1}{2}(\rho_1 L_1^* + \rho_2 L_2^*) \qquad (A)$$

$$m_2=\frac{1}{2}(\rho_2 L_2^* + \rho_3 L_3^*)$$

$$\vdots$$

$$m_{N-1}=\frac{1}{2}(\rho_{N-1} L_{N-1}^* + \rho_N L_N^*)$$

where $\rho_i\ (i=1,\ldots,N)$ is the density per unit length of the riser at the point midway between the appropriate nodes in the unstrained reference configuration. Note that the net mass of the approximating structure is

$$\frac{1}{2}\rho_1 L_1^* + \rho_2 L_2^* + \rho_3 L_3^* + \ldots + \rho_{N-1} L_{N-1}^* + \frac{1}{2}\rho_N L_N^* \qquad (B)$$

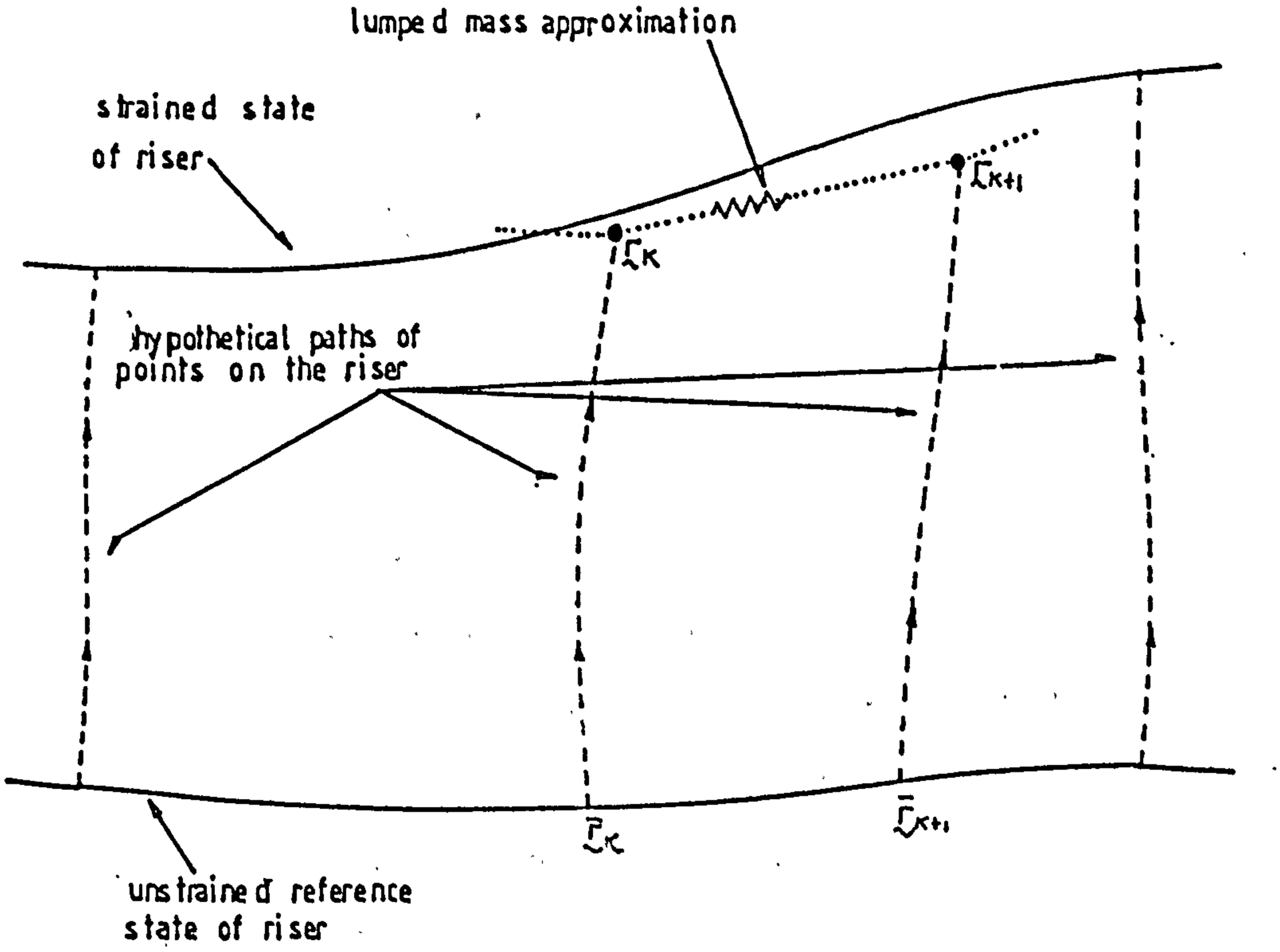

Figure 3.2.3 (a): The Elastic Lumped Mass Method

If the density of the riser is constant in the unstrained reference state so that $\rho_i = \rho \ (i=1,\ldots,N)$ then the net mass of the approximating structure may be written

$$\rho(L_1^* + L_2^* + \ldots + L_N^*) - \tfrac{1}{2}\rho L_1^* - \tfrac{1}{2}\rho L_N^* \qquad (C)$$

Hence the net mass of the approximating structure is not the same as the net mass of the riser and only in the limit of infinite lumped masses are the two masses equal. It is however possible to define M_1 and M_{N-1} so that the net masses are equal for any number of lumped masses, but this is not thought worthwhile as it destroys the simplicity of the formulation. In addition it can be supposed that the "missing" masses $\frac{1}{2}\rho L_1^*$ and $\frac{1}{2}\rho L_N^*$ are "lumped" at the appropriate fixed points of the riser.

Similarly the spring constants are related

$$K_1 = (EA)_1 / L_1^* \qquad (P)$$

$$K_2 = (EA)_2 / L_2^*$$

$$\vdots$$

$$K_N = (EA)_N / L_N^*$$

where $(EA)_i$ =longitudinal stiffness of the riser measured at the point midway between the appropriate nodes of the riser in the unstrained reference configuration. E =Young's Modulus of the material of the riser and A =cross-sectional area of the riser.

3.2.4:Relationship of Nodal Forces to the Continuum.

The following relationships are used to find the nodal forces

$$\underset{\sim}{F}_1 = \frac{1}{2}(\underset{\sim}{F}_{e1} + \underset{\sim}{F}_{e2}) \qquad (A)$$

$$\underset{\sim}{F}_2 = \frac{1}{2}(\underset{\sim}{F}_{e2} + \underset{\sim}{F}_{e3})$$

$$\vdots$$

$$\underset{\sim}{F}_{N-1} = \frac{1}{2}(\underset{\sim}{F}_{eN-1} + \underset{\sim}{F}_{eN})$$

where $\underset{\sim}{F}_{ei}\ (i=1,\ldots,N)$ =force on element i (which is usually estimated at the centre of the element). Note that there are other methods of finding the nodal forces.

The element force $\underset{\sim}{F}_{ei}\ (i=1,\ldots,N)$ may be written in the form

$$\underset{\sim}{F}_{ei} = \underset{\sim}{M}_{ei} + \underset{\sim}{G}_{ei} + \underset{\sim}{U}_{ei} \qquad (B)$$

where $\underset{\sim}{M}_{ei}$ =element force due to Morison forces, $\underset{\sim}{G}_{ei}$ =element force due to the gravity force and $\underset{\sim}{U}_{ei}$ =element force due to the upthrust force caused by the hydrostatic pressure.

The nodal gravity forces $\underset{\sim}{G}_{ei}$ can be related to the continuum through the equations

$$\underset{\sim}{G}_{e1} = -\rho_1 L_1^* g \underset{\sim}{k} \qquad (C)$$

$$\underset{\sim}{G}_{e2} = -\rho_2 L_2^* g \underset{\sim}{k}$$

$$\vdots$$

$$\underset{\sim}{G}_{eN} = -\rho_N L_N^* g \underset{\sim}{k}$$

where g =acceleration due to gravity. Similarly for the element buoyancy forces

$$\underset{\sim}{U}_{e1} = \rho_w V_1 g \underset{\sim}{k} \qquad (D)$$

$$\underset{\sim}{U}_{e2} = \rho_w V_2 g \underset{\sim}{k}$$

$$\vdots$$

$$\underset{\sim}{U}_{eN} = \rho_w V_N g \underset{\sim}{k}$$

where ρ_w =density of seawater per unit volume and $V_i\ (i=1,\ldots,N)$ =volume of element. Note that the volume of an element is not necessarily constant and may for example depend on the strain in the riser.

3.2.5:Element Morison Forces.

From section 2.1.2 the element hydrodynamic Morison forces on the riser $\underset{\sim}{M}_{ei}$ $(i=1,\ldots,N)$ may be written in the form

$$\underset{\sim}{M}_{ei} = \underset{\sim}{D}_{ei} + \underset{\sim}{I}_{ei} + \underset{\sim}{A}_{ei} \qquad (A)$$

where $\underset{\sim}{D}_{ei}$ =element drag force, $\underset{\sim}{I}_{ei}$ =element inertia force and $\underset{\sim}{A}_{ei}$ = element added mass force. These forces are found by utilising the geometry and dynamics of an element.

The element inertia forces $\underset{\sim}{I}_{ei}$ are given by

$$\begin{aligned} I_{e1} &= \tfrac{1}{4}\pi\rho_w D_1^2 L_1 (1+C_A)\, \dot{\underset{\sim}{v}}_{f1}|_{n_1} \\ &\vdots \\ I_{e2} &= \tfrac{1}{4}\pi\rho_w D_2^2 L_2 (1+C_A)\, \dot{\underset{\sim}{v}}_{f2}|_{n_2} \\ &\vdots \\ I_{eN} &= \tfrac{1}{4}\pi\rho_w D_N^2 L_N (1+C_A)\, \dot{\underset{\sim}{v}}_{fN}|_{n_N} \end{aligned} \qquad (B)$$

where $\underset{\sim}{v}|_{n_j} = \underset{\sim}{v} - (\underset{\sim}{v}\cdot\underset{\sim}{t}_j)\underset{\sim}{t}_j$ for an arbitrary vector $\underset{\sim}{v}$, $\underset{\sim}{v}_{fi}$ =fluid velocity (includes current and wave velocities) evaluated at the middle of the ith element, C_A =added mass coefficient and D_i $(i=1,\ldots,N)$ = diameter of the element. Note that the diameter of an element is not necessarily equal to D_i^* $(i=1,\ldots,N)$ and may for example depend on the strain in an element (this effect is usually negligible in practice).

The element drag forces are given by

$$\begin{aligned} \underset{\sim}{D}_{e1} &= \tfrac{1}{2}\rho_w D_1 L_1 (\underset{\sim}{v}_{f1} - \dot{\underset{\sim}{r}}_{e1})|_{n_1} \left|(\underset{\sim}{v}_{f1} - \dot{\underset{\sim}{r}}_{e1})|_{n_1}\right| \\ \underset{\sim}{D}_{e2} &= \tfrac{1}{2}\rho_w D_2 L_2 (\underset{\sim}{v}_{f2} - \dot{\underset{\sim}{r}}_{e2})|_{n_2} \left|(\underset{\sim}{v}_{f2} - \dot{\underset{\sim}{r}}_{e2})|_{n_2}\right| \\ &\vdots \\ \underset{\sim}{D}_{eN} &= \tfrac{1}{2}\rho_w D_N L_N (\underset{\sim}{v}_{fN} - \dot{\underset{\sim}{r}}_{eN})|_{n_N} \left|(\underset{\sim}{v}_{fN} - \dot{\underset{\sim}{r}}_{eN})|_{n_N}\right| \end{aligned} \qquad (C)$$

where $\dot{\underset{\sim}{r}}_{ei} = \frac{1}{2}(\dot{\underset{\sim}{r}}_i + \dot{\underset{\sim}{r}}_{i-1})$ $(i=1,\ldots,N)$. $\dot{\underset{\sim}{r}}_{ei}$ is the midpoint velocity of a spring element.

The element added mass forces are given by

$$\underset{\sim}{A}_{e1} = -\tfrac{1}{4}\pi\rho_w D_1^2 C_A \ddot{\underset{\sim}{r}}_{e1}|_{n_1} L_1 = -4\alpha_1 \ddot{\underset{\sim}{r}}_{e1}|_{n_1} \qquad (D)$$

$$\underset{\sim}{A}_{e2} = -\tfrac{1}{4}\pi\rho_w D_2^2 C_A \ddot{\underset{\sim}{r}}_{e2}|_{n_2} L_2 = -4\alpha_2 \ddot{\underset{\sim}{r}}_{e2}|_{n_2}$$

$$\vdots$$

$$\underset{\sim}{A}_{eN} = -\tfrac{1}{4}\pi\rho_w D_N^2 C_A \ddot{\underset{\sim}{r}}_{eN}|_{n_N} L_N = -4\alpha_N \ddot{\underset{\sim}{r}}_{eN}|_{n_N}$$

where α_i $(i=1,\ldots,N)$ is defined so that $4\alpha_i = \frac{1}{4}\pi\rho_w D_i^2 C_A L_i$ and $\ddot{\underset{\sim}{r}}_{ei} = \frac{1}{2}(\ddot{\underset{\sim}{r}}_i + \ddot{\underset{\sim}{r}}_{i-1})$.

3.2.6:Assembly of the Equations of Motion.

From previous sections the equations of motion may be assembled

$$\begin{bmatrix} m_1 \ddot{\underset{\sim}{r}}_1 \\ m_2 \ddot{\underset{\sim}{r}}_2 \\ \vdots \\ m_{N-1} \ddot{\underset{\sim}{r}}_{N-1} \end{bmatrix} = \begin{bmatrix} T_2 \underset{\sim}{t}_2 - T_1 \underset{\sim}{t}_1 \\ T_3 \underset{\sim}{t}_3 - T_2 \underset{\sim}{t}_2 \\ \vdots \\ T_N \underset{\sim}{t}_N - T_{N-1} \underset{\sim}{t}_{N-1} \end{bmatrix} + \begin{bmatrix} \frac{1}{2}(\underset{\sim}{F}_{e1} + \underset{\sim}{F}_{e2}) \\ \frac{1}{2}(\underset{\sim}{F}_{e2} + \underset{\sim}{F}_{e3}) \\ \vdots \\ \frac{1}{2}(\underset{\sim}{F}_{eN-1} + \underset{\sim}{F}_{eN}) \end{bmatrix} \qquad (a)$$

For the purposes of numerical computation the added mass

term needs to be absorbed on the left hand side (so that the equations of motion are of the form $[M][\ddot{\xi}]=[F]$) to form

$$[M]\begin{bmatrix}\ddot{\xi}_1\\ \ddot{\xi}_2\\ \vdots\\ \ddot{\xi}_{N-2}\\ \ddot{\xi}_{N-1}\end{bmatrix}=\begin{bmatrix}T_2\xi_2-T_1\xi_1\\ T_3\xi_3-T_2\xi_2\\ \vdots\\ T_{N-1}\xi_{N-1}-T_{N-2}\xi_{N-2}\\ T_N\xi_N-T_{N-1}\xi_{N-1}\end{bmatrix}+\begin{bmatrix}\frac{1}{2}(\bar{F}_{e1}+\bar{F}_{e2})\\ \frac{1}{2}(\bar{F}_{e2}+\bar{F}_{e3})\\ \vdots\\ \frac{1}{2}(\bar{F}_{N-2}+\bar{F}_{N-1})\\ \frac{1}{2}(\bar{F}_{N-1}+\bar{F}_N)\end{bmatrix} \qquad (A)$$

where

$$[M]=\begin{bmatrix}m_1I & & & & \\ & m_2I & & & \\ & & \ddots & & \\ & & & m_{N-1}I & \\ & & & & m_NI\end{bmatrix}+\begin{bmatrix}K_1T_1+\alpha_2T_2 & \alpha_2T_2 & & & \\ \alpha_2T_2 & \alpha_2T_2+\alpha_3T_3 & \alpha_3T_3 & & \\ & \ddots & \ddots & \ddots & \\ & & \alpha_{N-1}T_{N-1} & \alpha_{N-1}T_{N-1}+\alpha_NT_N & \alpha_NT_N\end{bmatrix} \qquad (B)$$

and where I = 3×3 identity matrix, $\bar{F}_{ei}$ $(i=1,\ldots,N)$ includes all the external forces apart from the added mass forces and the matrix $[T_i]$ is defined by

$$[\xi|_{n_i}]=[T_i][\xi] \qquad (C)$$

where $[T_i]$ is given by

$$[T_i]=\begin{bmatrix}1-(\xi_i)_x^2 & -(\xi_i)_x(\xi_i)_y & -(\xi_i)_x(\xi_i)_z\\ & 1-(\xi_i)_y^2 & -(\xi_i)_y(\xi_i)_z\\ \text{sym.} & & 1-(\xi_i)_z^2\end{bmatrix} \qquad (D)$$

$$\left[\text{n.b.}\ (\xi_i)_x=(\xi_i\cdot\underset{\sim}{i})\right]$$

3.3.7:An Alternative Added Mass Matrix.

The equations of motion can also be written in the form

$$\begin{bmatrix} m_1 \ddot{\underset{\sim}{r}}_1 \\ m_2 \ddot{\underset{\sim}{r}}_2 \\ \vdots \\ m_{N-1} \ddot{\underset{\sim}{r}}_{N-1} \end{bmatrix} = \begin{bmatrix} T_2 \underset{\sim}{t}_2 - T_1 \underset{\sim}{t}_1 \\ T_3 \underset{\sim}{t}_3 - T_2 \underset{\sim}{t}_2 \\ \vdots \\ T_N \underset{\sim}{t}_N - T_{N-1} \underset{\sim}{t}_{N-1} \end{bmatrix} + \begin{bmatrix} \frac{1}{2}(\bar{\underset{\sim}{F}}_{e_1} + \bar{\underset{\sim}{F}}_{e_2}) \\ \frac{1}{2}(\bar{\underset{\sim}{F}}_{e_2} + \bar{\underset{\sim}{F}}_{e_3}) \\ \vdots \\ \frac{1}{2}(\bar{\underset{\sim}{F}}_{e_N} + \bar{\underset{\sim}{F}}_{e_{N-1}}) \end{bmatrix} + \begin{bmatrix} \underset{\sim}{A}_1 \\ \underset{\sim}{A}_2 \\ \vdots \\ \underset{\sim}{A}_{N-1} \end{bmatrix} \qquad (A)$$

where A_i $(i=1,\ldots,N)$ are direct nodal estimates of the added mass forces. These nodal estimates of the added mass forces are defined as follows

$$\underset{\sim}{A}_1 = -\frac{1}{2}(4\alpha_1 + 4\alpha_2)\,\ddot{\underset{\sim}{r}}|_{\hat{n}_1} = -\beta_1\,\ddot{\underset{\sim}{r}}_1|_{\hat{n}_1} \qquad (B)$$

$$\underset{\sim}{A}_2 = -\frac{1}{2}(4\alpha_2 + 4\alpha_3)\,\ddot{\underset{\sim}{r}}|_{\hat{n}_2} = -\beta_2\,\ddot{\underset{\sim}{r}}_2|_{\hat{n}_2}$$

$$\vdots$$

$$\underset{\sim}{A}_{N-1} = -\frac{1}{2}(4\alpha_{N-1} + 4\alpha_N)\,\ddot{\underset{\sim}{r}}_{N-1}|_{\hat{n}_{N-1}} = -\beta_{N-1}\,\ddot{\underset{\sim}{r}}_{N-1}|_{\hat{n}_{N-1}}$$

where

$$\underset{\sim}{v}|_{\hat{n}_i} = \underset{\sim}{v} - (\underset{\sim}{v}\cdot\hat{\underset{\sim}{t}}_i)\hat{\underset{\sim}{t}}_i \qquad (C)$$

and $\hat{\underset{\sim}{t}}_i$ $(i=1,\ldots,N-1)$ is an "average" tangent vector given by

$$\hat{\underset{\sim}{t}}_1 = \frac{L_2\underset{\sim}{t}_1 + L_1\underset{\sim}{t}_2}{|L_2\underset{\sim}{t}_1 + L_1\underset{\sim}{t}_2|}\,, \quad \hat{\underset{\sim}{t}}_2 = \frac{L_3\underset{\sim}{t}_2 + L_2\underset{\sim}{t}_3}{|L_3\underset{\sim}{t}_2 + L_2\underset{\sim}{t}_3|}\,, \quad \ldots, \quad \hat{\underset{\sim}{t}}_{N-1} = \frac{L_N\underset{\sim}{t}_{N-1} + L_{N-1}\underset{\sim}{t}_N}{|L_N\underset{\sim}{t}_{N-1} + L_{N-1}\underset{\sim}{t}_N|} \qquad (D)$$

This will give an added mass matrix

$$\begin{bmatrix} \beta_1\hat{T}_1 & & & & \\ & \beta_2\hat{T}_2 & & & \\ & & \ddots & & \\ & & & \beta_{N-2}\hat{T}_{N-2} & \\ & & & & \beta_{N-1}\hat{T}_{N-1} \end{bmatrix} \qquad (E)$$

where $[\hat{T}_i]\ (i=1,\ldots,N-1)$ is defined as

$$[\hat{T}_i] = \begin{bmatrix} 1-(\hat{t}_i)_x & -(\hat{t}_i)_x(\hat{t}_i)_y & -(\hat{t}_i)_x(\hat{t}_i)_z \\ & 1-(\hat{t}_i)_y^2 & -(\hat{t}_i)_y(\hat{t}_i)_z \\ \text{sym.} & & 1-(\hat{t}_i)_z^2 \end{bmatrix} \qquad (F)$$

The added mass matrix is now in the form of a block diagonal matrix. The addition of the added mass matrix to the structural mass matrix which is diagonal leads to an overall mass matrix that can easily be inverted. This may lead to a numerically more efficient solution.

3.2.8:Incremental Calculation of the Tensions.

When the discretization is carried out in time (i.e. when the equations of motion are integrated with respect to time) the tensions in the spring elements need to be calculated at each timestep. One way to do this would be to use the equation

$$T_i = (EA)_i \frac{(L_i - L_i^*)}{L_i^*} \qquad (A)$$

However to do so would lead to (Conte and deBoor[1972]) a loss of significant digits (even using FORTRAN double precision on the D.E.C. Vax series of computers). The loss of significant digits gives an error in the calculation of the tensions that eventually leads to numerical instability.

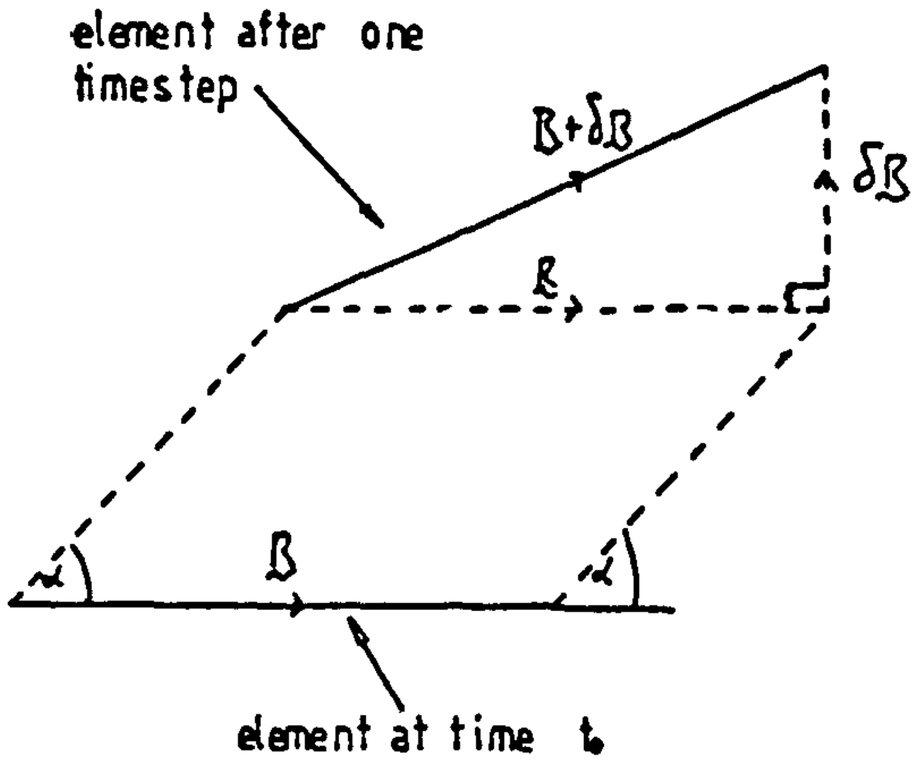

Figure 3.2.8: Calculation of the Incremental Tensions

Suppose after one timestep that the change in the length of a spring element is δL_i then the change in the tension of the spring element is

$$\delta T_i = (EA)_i \frac{\delta L_i}{L_i^*} \qquad (B)$$

δL_i is calculated using a Taylor series

$$\delta L_i = \left\{ (\underset{\sim}{R} + \delta\underset{\sim}{R}).(\underset{\sim}{R} + \delta\underset{\sim}{R}) \right\}^{\frac{1}{2}} - \left\{ \underset{\sim}{R}.\underset{\sim}{R} \right\}^{\frac{1}{2}} \qquad (C)$$

where $\underset{\sim}{R} = \bar{\underset{\sim}{r}} - \underset{\sim}{r}$ (represents a vector between the ends of the element) and $\delta\underset{\sim}{R}$ is the change in $\underset{\sim}{R}$ after one timestep , therefore

$$\delta L_i = (\underset{\sim}{R}.\underset{\sim}{R})^{\frac{1}{2}} \left\{ 1 + \frac{2\underset{\sim}{R}.\delta\underset{\sim}{R} + \delta\underset{\sim}{R}.\delta\underset{\sim}{R}}{\underset{\sim}{R}.\underset{\sim}{R}} \right\}^{\frac{1}{2}} - (\underset{\sim}{R}.\underset{\sim}{R})^{\frac{1}{2}}$$

$$= (\underset{\sim}{R}.\underset{\sim}{R})^{\frac{1}{2}} \left\{ 1 + \frac{1}{2}\Delta - \frac{1}{8}\Delta^2 + \dots \right\}^{\frac{1}{2}} - (\underset{\sim}{R}.\underset{\sim}{R})^{\frac{1}{2}}$$

$$= (\underset{\sim}{R}.\underset{\sim}{R})^{\frac{1}{2}} \left\{ \frac{1}{2}\Delta - \frac{1}{8}\Delta^2 + \dots \right\}^{\frac{1}{2}} \qquad (a)$$

where $\Delta = \frac{2\underset{\sim}{R}.\delta\underset{\sim}{R} + \delta\underset{\sim}{R}.\delta\underset{\sim}{R}}{\underset{\sim}{R}.\underset{\sim}{R}}$. In implementation on a computer Δ is a very small quantity and certainly $|\Delta| < |$. This means δL_i can be calculated to any desired degree of accuracy.

For efficiency it might be thought advantageous to use the equation

$$\delta T_i = (EA)_i \frac{\underset{\sim}{t}_i.\delta\underset{\sim}{R}_i}{L_i} \quad (b)$$

i.e. equation (a) to first order in $\delta\underset{\sim}{R}$. However this is not the case as is illustrated in figure 3.2.8. Suppose the element moves so that $\delta\underset{\sim}{R}.\underset{\sim}{R} = 0$, then using equation (b) would give $\delta T_i = 0$. Patently for the specified movement of the element there must be an increase in the tension of the element. Hence the conclusion can be drawn that it would be prudent to use higher order terms in equation (a).

3.3:Inelastic Lumped Mass Discretization

3.3.1:Introduction.

This method is similar to the elastic lumped mass method given in section 3.2. The length of riser is modelled as a series of masses connected together by mass-less rigid rods. Direct reduction of the equations of motion to the discretized system of equations $[M][\ddot{r}] = [F]$ is not possible. Hence a space-time discretization must be carried out.

An inelastic lumped mass discretization was first given by Walton and Polachek[1959,1960] and was the first numerical work done on cable dynamics. Walton and Polacheks' discretization is for two dimensions only but has since been extended to three dimensions by Tsinipizoglou[1981]. The discretization given here however is different to that of Walton and Polachek.

3.3.2:Equations of Motion.

Applying Newton's second law to each of the masses gives

$$m_1 \frac{d^2 L_1 \underset{\sim}{t}_1}{dt^2} = \underset{\sim}{F}_1 + T_2 \underset{\sim}{t}_2 - T_1 \underset{\sim}{t}_1$$

$$m_2 \frac{d^2(L_1 \underset{\sim}{t}_1 + L_2 \underset{\sim}{t}_2)}{dt^2} = \underset{\sim}{F}_2 + T_3 \underset{\sim}{t}_3 - T_2 \underset{\sim}{t}_2 \qquad (a)$$

$$\vdots$$

$$m_{N-1} \frac{d^2(L_1 \underset{\sim}{t}_1 + L_2 \underset{\sim}{t}_2 + \ldots + L_{N-1} \underset{\sim}{t}_{N-1})}{dt^2} = \underset{\sim}{F}_{N-1} + T_N \underset{\sim}{t}_N - T_{N-1} \underset{\sim}{t}_{N-1}$$

since it is assumed that the ends of the riser are fixed. The nodal forces are determined in exactly the same way they were determined in section 3.2. However note that in this case there is no stretching of the elements. In addition there is the equation of constraint relating to the riser length

$$L_1 \underset{\sim}{t}_1 + L_2 \underset{\sim}{t}_2 + \ldots + L_N \underset{\sim}{t}_N = \underset{\sim}{r}_N - \underset{\sim}{r}_0 \qquad (b)$$

There are $3(N-1)$ equations from equations (a) and 3 equations from equations (b) hence in total there are $3N$ equations. There are $2N$ variables for $\underset{\sim}{t}_1, \underset{\sim}{t}_2, \ldots, \underset{\sim}{t}_N$ (each tangent vector $\underset{\sim}{t}_i$ needs two linearly independent variables to fully describe it) and N variables in $T_1, T_2, \ldots, T_N$ hence in total there are $3N$ variables. The number of variables is equal to the number of equations hence the system of equations is complete.

3.3.3:Added Mass.

The dynamic equations can be rewritten in the form

$$\begin{bmatrix} m_1 I + \rho_1 \hat{T}_1 & & & \\ & m_2 I + \rho_2 \hat{T}_2 & & \\ & & \ddots & \\ & & & m_{N-1} I + \rho_{N-1} \hat{T}_{N-1} \end{bmatrix} \frac{d^2}{dt^2} \begin{bmatrix} L_1 \underset{\sim}{t}_1 \\ L_2 \underset{\sim}{t}_2 + L_1 \underset{\sim}{t}_1 \\ \vdots \\ L_{N-2} \underset{\sim}{t}_{N-2} + \ldots + L_1 \underset{\sim}{t}_1 \\ L_{N-1} \underset{\sim}{t}_{N-1} + \ldots + L_1 \underset{\sim}{t}_1 \end{bmatrix} = \begin{bmatrix} T_2 \underset{\sim}{t}_2 - T_1 \underset{\sim}{t}_1 \\ T_3 \underset{\sim}{t}_3 - T_2 \underset{\sim}{t}_2 \\ \vdots \\ T_{N-1} \underset{\sim}{t}_{N-1} - T_{N-2} \underset{\sim}{t}_{N-2} \\ T_N \underset{\sim}{t}_N - T_{N-1} \underset{\sim}{t}_{N-1} \end{bmatrix} + \begin{bmatrix} \frac{1}{2}(\bar{\underset{\sim}{F}}_{e_1} + \bar{\underset{\sim}{F}}_{e_2}) \\ \frac{1}{2}(\bar{\underset{\sim}{F}}_{e_2} + \bar{\underset{\sim}{F}}_{e_3}) \\ \vdots \\ \frac{1}{2}(\bar{\underset{\sim}{F}}_{e_{N-2}} + \bar{\underset{\sim}{F}}_{e_{N-1}}) \\ \frac{1}{2}(\bar{\underset{\sim}{F}}_{e_{N-1}} + \bar{\underset{\sim}{F}}_{e_N}) \end{bmatrix} \qquad (a)$$

where all the quantities are defined as in section 3.2. For

simplicity the block diagonal added mass matrix is chosen to be added to the L.H.S. in the above equation. However there would be no great difficulty in using the added mass matrix that is not block diagonal.

3.3.4:Discretization Procedure in Time.

In order to perform the discretization procedure in time both the standard Euler angles (Goldstein[1980]) and the central difference method must be used.

From section 2.6.2 the ith unit tangent vector is

$$\underset{\sim}{t}_i = \cos\theta_i \cos\psi_i \, \underset{\sim}{i} + \cos\theta_i \sin\psi_i \, \underset{\sim}{j} - \sin\theta_i \, \underset{\sim}{k} \qquad (A)$$

where θ_i and ψ_i are the standard Euler angles and $\underset{\sim}{i}$, $\underset{\sim}{j}$, $\underset{\sim}{k}$ are defined in figure 3.2.1. Thus for a small change $\delta\underset{\sim}{t}_i$ in the tangent vector

$$\delta\underset{\sim}{t}_i = \delta\theta_i(-\sin\theta_i\cos\psi_i \, \underset{\sim}{i} - \sin\theta_i\sin\psi_i \, \underset{\sim}{j} - \cos\theta_i \, \underset{\sim}{k}) \qquad (B)$$

$$+ \delta\psi_i(-\cos\theta_i\sin\psi_i \, \underset{\sim}{i} + \cos\theta_i\cos\psi_i \, \underset{\sim}{j})$$

ie.

$$\delta\underset{\sim}{t}_i = \delta\theta_i \, \underset{\sim}{\bar{u}}_i + \delta\psi_i \, \bar{\chi}_i \qquad (a)$$

where

$$\underset{\sim}{\bar{u}}_i = -\sin\theta_i\cos\psi_i \, \underset{\sim}{i} - \sin\theta_i\sin\psi_i \, \underset{\sim}{j} - \cos\theta_i \, \underset{\sim}{k} \qquad (C)$$

and

$$\underset{\sim}{\bar{v}}_i = -\cos\theta_i\sin\psi_i \, \underset{\sim}{i} + \cos\theta_i\cos\psi_i \, \underset{\sim}{j} \qquad (D)$$

In the central difference method the acceleration at the nth timestep $\ddot{\underset{\sim}{x}}|^n$ is approximated by the central difference equation

$$\ddot{\underset{\sim}{x}}|^n = (\delta\underset{\sim}{x}|^{n+1} - \delta\underset{\sim}{x}|^n)/\Delta t^2 \qquad (E)$$

where

$$\delta\underset{\sim}{x}|^n = \underset{\sim}{x}|^n - \underset{\sim}{x}|^{n-1} \qquad (F)$$

and $\underset{\sim}{x}|^n$ denotes the value of $\underset{\sim}{x}$ at the nth timestep.

3.3.5:Use of Central Differences and Euler Angles.

The equations of motion (equations 3.3.3(a)) can be written in the form

$$\begin{bmatrix} A_1 & & & & \\ A_2 & A_2 & & & \\ & \ddots & \ddots & & \\ A_{N-2} & A_{N-2} & \cdots & A_{N-2} & \\ A_{N-1} & A_{N-1} & \cdots & A_{N-1} & A_{N-1} \end{bmatrix} \begin{bmatrix} \frac{d^2 L_1 t_1}{dt^2} \\ \frac{d^2 L_2 t_2}{dt^2} \\ \vdots \\ \frac{d^2 L_{N-2} t_{N-2}}{dt^2} \\ \frac{d^2 L_{N-1} t_{N-1}}{dt^2} \end{bmatrix} = \begin{bmatrix} T_2 t_2 - T_1 t_1 \\ T_3 t_3 - T_2 t_2 \\ \vdots \\ T_{N-1} t_{N-1} - T_{N-2} t_{N-2} \\ T_N t_N - T_{N-1} t_{N-1} \end{bmatrix} + \begin{bmatrix} \frac{1}{2}(\bar{F}_{e_1} + \bar{F}_{e_1}) \\ \frac{1}{2}(\bar{F}_{e_2} + \bar{F}_{e_1}) \\ \vdots \\ \frac{1}{2}(\bar{F}_{e_{N-1}} + \bar{F}_{e_{N-2}}) \\ \frac{1}{2}(\bar{F}_{e_N} + \bar{F}_{e_{N-1}}) \end{bmatrix} \qquad (A)$$

where $[A_i] = M_i[I] + \beta_i[\hat{T}_i]$. Applying central differences as described in section 3.3.4 gives

$$\begin{bmatrix} A_1 & & & & \\ A_2 & A_2 & & & \\ \vdots & \vdots & \ddots & & \\ A_{N-2} & A_{N-2} & \cdots & A_{N-2} & \\ A_{N-1} & A_{N-1} & \cdots & A_{N-1} & A_{N-1} \end{bmatrix} \begin{bmatrix} \delta(L_1 t_1)\rceil^{n+1} \\ \delta(L_2 t_2)\rceil^{n+1} \\ \vdots \\ \delta(L_{N-2} t_{N-2})\rceil^{n+1} \\ \delta(L_{N-1} t_{N-1})\rceil^{n+1} \end{bmatrix} =$$

$$\begin{bmatrix} A_1 & & & & \\ A_2 & A_2 & & & \\ \vdots & \vdots & \ddots & & \\ A_{N-2} & A_{N-2} & \cdots & A_{N-2} & \\ A_{N-1} & A_{N-1} & \cdots & A_{N-1} & A_{N-1} \end{bmatrix} \begin{bmatrix} \delta(L_1 t_1)\rceil^{n} \\ \delta(L_2 t_2)\rceil^{n} \\ \vdots \\ \delta(L_{N-2} t_{N-2})\rceil^{n} \\ \delta(L_{N-1} t_{N-1})\rceil^{n} \end{bmatrix}$$

$$+ \left\{ \begin{bmatrix} T_2 \underset{\sim}{t}_2 - T_1 \underset{\sim}{t}_1 \\ T_3 \underset{\sim}{t}_3 - T_2 \underset{\sim}{t}_2 \\ \vdots \\ T_{N-1} \underset{\sim}{t}_{N-1} - T_{N-2} \underset{\sim}{t}_{N-2} \\ T_N \underset{\sim}{t}_N - T_{N-1} \underset{\sim}{t}_{N-1} \end{bmatrix} + \begin{bmatrix} \frac{1}{2}(\bar{\underset{\sim}{F}}_{e_1} + \bar{\underset{\sim}{F}}_{e_2}) \\ \frac{1}{2}(\bar{\underset{\sim}{F}}_{e_2} + \bar{\underset{\sim}{F}}_{e_3}) \\ \vdots \\ \frac{1}{2}(\bar{\underset{\sim}{F}}_{e_{N-1}} + \bar{\underset{\sim}{F}}_{e_{N-2}}) \\ \frac{1}{2}(\bar{\underset{\sim}{F}}_{e_N} + \bar{\underset{\sim}{F}}_{e_{N-1}}) \end{bmatrix} \right\} \Delta t^2$$

(9)

Using equation 3.3.4(a) gives

$$\begin{bmatrix} \delta(L_1 t_1)^{n+1} \\ \delta(L_2 t_2)^{n+1} \\ \vdots \\ \delta(L_{N-2} t_{N-2})^{n+1} \\ \delta(L_{N-1} t_{N-1})^{n+1} \end{bmatrix} = \underset{3(N-1)\times 2(N-1)}{\begin{bmatrix} \underset{\sim}{u}_1 & \underset{\sim}{v}_1 & 0 & \cdots & 0 \\ 0 & 0 & \underset{\sim}{u}_2 & \underset{\sim}{v}_2 & 0 \\ \vdots & & & & \\ 0 & \cdots & & \underset{\sim}{u}_{N-2} & \underset{\sim}{v}_{N-2} \\ 0 & \cdots & 0 & 0 & \underset{\sim}{u}_{N-1} \; \underset{\sim}{v}_{N-1} \end{bmatrix}} \underset{2(N-1)\times 1}{\begin{bmatrix} \delta\theta_1 \\ \delta\psi_1 \\ \delta\theta_2 \\ \delta\psi_2 \\ \vdots \\ \delta\theta_{N-2} \\ \delta\psi_{N-2} \\ \delta\theta_{N-1} \\ \delta\psi_{N-1} \end{bmatrix}} \qquad (B)$$

$3(N-1)\times 1$

where θ_i and ψ_i are the relevant Euler angles for the ith element and where $\underset{\sim}{u}_i$ and $\underset{\sim}{v}_i$ are defined so that

$$\underset{\sim}{u}_i = L_i \underset{\sim}{\bar{u}}_i \qquad (C)$$

and

$$\underset{\sim}{v}_i = L_i \underset{\sim}{\bar{v}}_i \qquad (D)$$

Using equation (a) this gives

$$\underset{3(N-1)\times 2(N-1)}{\begin{bmatrix} A_1\underset{\sim}{u}_1 & A_1\underset{\sim}{v}_1 & & & \\ A_2\underset{\sim}{u}_1 & A_2\underset{\sim}{v}_1 & A_2\underset{\sim}{u}_2 & A_2\underset{\sim}{v}_2 & \\ \vdots & \vdots & \vdots & \vdots & \\ A_{N-2}\underset{\sim}{u}_1 & A_{N-2}\underset{\sim}{v}_1 & A_{N-2}\underset{\sim}{u}_2 & A_{N-2}\underset{\sim}{v}_2 \cdots & A_{N-2}\underset{\sim}{u}_{N-2} \; A_{N-2}\underset{\sim}{v}_{N-2} \; 0 \quad 0 \\ A_{N-1}\underset{\sim}{u}_1 & A_{N-1}\underset{\sim}{v}_1 & A_{N-1}\underset{\sim}{u}_2 & A_{N-1}\underset{\sim}{v}_2 \cdots & A_{N-1}\underset{\sim}{u}_{N-2} \; A_{N-1}\underset{\sim}{v}_{N-2} \; A_{N-1}\underset{\sim}{u}_{N-1} \; A_{N-1}\underset{\sim}{v}_{N-1} \end{bmatrix}} \underset{2(N-1)\times 1}{\begin{bmatrix} \delta\theta_1 \\ \delta\psi_1 \\ \delta\theta_2 \\ \delta\psi_2 \\ \vdots \\ \delta\theta_{N-2} \\ \delta\psi_{N-2} \\ \delta\theta_{N-1} \\ \delta\psi_{N-1} \end{bmatrix}^{n+1}} = \qquad (E)$$

$$\begin{bmatrix} A_1 & 0 \cdots & \cdots 0 \\ A_2 & A_2 \cdots & \cdots 0 \\ \vdots & \vdots \quad \ddots & \\ A_{N-2} & A_{N-2} \cdots & A_{N-2} \; 0 \\ A_{N-1} & A_{N-1} \cdots & A_{N-1} \; A_{N-1} \end{bmatrix} \begin{bmatrix} \delta(L_1 t_1)|^n \\ \delta(L_2 t_2)|^n \\ \vdots \\ \delta(L_{N-1} t_{N-1})|^n \\ \delta(L_N t_N)|^n \end{bmatrix}$$

$$+ \left\{ \begin{bmatrix} T_2 t_{c_2} - T_1 t_{c_1} \\ T_3 t_{c_3} - T_2 t_{c_2} \\ \vdots \\ T_{N-1} t_{c_{N-1}} - T_{N-2} t_{c_{N-2}} \\ T_N t_{c_N} - T_{N-1} t_{c_{N-1}} \end{bmatrix} \begin{bmatrix} \frac{1}{2}(\bar{E}_{e_1} + \bar{E}_{e_2}) \\ \frac{1}{2}(\bar{E}_{e_2} + \bar{E}_{e_3}) \\ \vdots \\ \frac{1}{2}(\bar{E}_{e_{N-1}} + \bar{E}_{e_{N-2}}) \\ \frac{1}{2}(\bar{E}_{e_N} + \bar{E}_{e_{N-1}}) \end{bmatrix} \right\} \Delta t^2 .$$

The tension terms can be included as additional terms on the left hand side to give

$$\underbrace{\begin{bmatrix} A_1 y_1 & A_1 x_1 & 0 & \cdots & & & & \cdots & 0 & \Delta t^2 t_1 & \Delta t^2 t_2 & 0 & \cdots & & 0 \\ A_2 y_1 & A_2 x_1 & A_2 y_2 & A_2 x_2 & 0 & \cdots & & \cdots & 0 & 0 & \Delta t^2 t_2 & -\Delta t^2 t_3 & \cdots & & 0 \\ \vdots & \vdots & \vdots & \vdots & & & & & \vdots & \vdots & & & & & \vdots \\ A_{N-2} y_1 & A_{N-2} x_1 & A_{N-2} y_2 & A_{N-2} x_2 & \cdots & A_{N-2} y_{N-2} & A_{N-2} x_{N-2} & 0 & 0 & 0 & \cdots & 0 & \Delta t^2 t_{N-2} & -\Delta t^2 t_{N-1} & 0 \\ A_{N-1} y_1 & A_{N-1} x_1 & A_{N-1} y_2 & A_{N-1} x_2 & \cdots & A_{N-1} y_{N-2} & A_{N-1} x_{N-2} & A_{N-1} y_{N-1} & A_{N-1} x_{N-1} & 0 & \cdots & 0 & 0 & \Delta t^2 t_{N-1} & -\Delta t^2 t_N \end{bmatrix}}_{3(N-1) \times [2(N-1)+N]} \underbrace{\begin{bmatrix} \delta\theta_1|^{n+1} \\ \delta\psi_1|^{n+1} \\ \delta\theta_2|^{n+1} \\ \delta\psi_2|^{n+1} \\ \vdots \\ \delta\theta_{N-2}|^{n+1} \\ \delta\psi_{N-2}|^{n+1} \\ \delta\theta_{N-1}|^{n+1} \\ \delta\psi_{N-1}|^{n+1} \\ T_1|^n \\ T_2|^n \\ \vdots \\ T_{N-1}|^n \\ T_N|^n \end{bmatrix}}_{[2(N-1)+N] \times 1}$$

$$= \begin{bmatrix} A_1 & 0 & \cdots & & 0 \\ A_2 & A_2 & 0 & \cdots & 0 \\ \vdots & \vdots & & & \vdots \\ A_{N-2} & A_{N-2} & \cdots & A_{N-2} & 0 \\ A_{N-1} & A_{N-1} & \cdots & A_{N-1} & A_{N-1} \end{bmatrix} \begin{bmatrix} \delta(L_1 t_1)|^n \\ \delta(L_2 t_2)|^n \\ \vdots \\ \delta(L_{N-2} t_{N-2})|^n \\ \delta(L_{N-1} t_{N-1})|^n \end{bmatrix} + \begin{bmatrix} \frac{1}{2}(\bar{F}_{\ell 1} + \bar{F}_{\ell 2}) \\ \frac{1}{2}(\bar{F}_{\ell 2} + \bar{F}_{\ell 3}) \\ \vdots \\ \frac{1}{2}(\bar{F}_{\ell N-1} + \bar{F}_{\ell N-2}) \\ \frac{1}{2}(\bar{F}_{\ell N} + \bar{F}_{\ell N-1}) \end{bmatrix} . \Delta t^2 \qquad (F)$$

However from the constraint condition

$$\delta(L_1 \underset{\sim}{t}_1) + \delta(L_2 \underset{\sim}{t}_2) + \ldots + \delta(L_N \underset{\sim}{t}_N) = \underset{\sim}{0} \qquad (G)$$

or put into matrix form

$$\underset{3 \times 2N}{\begin{bmatrix} \underset{\sim}{u}_1 & \underset{\sim}{v}_1 & \underset{\sim}{u}_2 & \underset{\sim}{v}_2 & \cdots & \underset{\sim}{u}_{N-2} & \underset{\sim}{v}_{N-2} & \underset{\sim}{u}_{N-1} & \underset{\sim}{v}_{N-1} & \underset{\sim}{u}_N & \underset{\sim}{v}_N \end{bmatrix}} \underset{2N \times 1}{\begin{bmatrix} \delta\theta_1 \\ \delta\psi_1 \\ \delta\theta_2 \\ \delta\psi_2 \\ \vdots \\ \delta\theta_{N-2} \\ \delta\psi_{N-2} \\ \delta\theta_{N-1} \\ \delta\psi_{N-1} \\ \delta\theta_N \\ \delta\psi_N \end{bmatrix}} = \underset{\sim}{0} \qquad (H)$$

Thus finally the equations of motion are obtained

$$
\begin{bmatrix} \bar{M} \end{bmatrix}
\begin{bmatrix} \delta\theta_1|^{n+1} \\ \delta\psi_1|^{n+1} \\ \delta\theta_2|^{n+1} \\ \delta\psi_2|^{n+1} \\ \vdots \\ \delta\theta_{N-2}|^{n+1} \\ \delta\psi_{N-2}|^{n+1} \\ \delta\theta_{N-1}|^{n+1} \\ \delta\psi_{N-1}|^{n+1} \\ \delta\theta_N|^{n+1} \\ \delta\psi_N|^{n+1} \\ T_1|^n \\ T_2|^n \\ \vdots \\ T_{N-1}|^n \\ T_N|^n \end{bmatrix}
=
\begin{bmatrix} A_1 & 0 & \cdots & 0 & 0 \\ A_2 & A_2 & 0 & 0 & 0 \\ \vdots & \vdots & & \vdots & \vdots \\ A_{N-2} & A_{N-2} & \cdots & A_{N-2} & 0 \\ A_{N-1} & A_{N-1} & \cdots & A_{N-1} & A_{N-1} \\ 0 & 0 & \cdots & 0 & 0 \end{bmatrix}
\begin{bmatrix} \delta(L_1 \underset{\sim}{t}_1)|^n \\ \delta(L_2 \underset{\sim}{t}_2)|^n \\ \vdots \\ \delta(L_{N-2} \underset{\sim}{t}_{N-2})|^n \\ \delta(L_{N-1} \underset{\sim}{t}_{N-1})|^n \\ 0 \end{bmatrix}
$$

$$
+ \begin{bmatrix} \frac{1}{2}(\bar{\underset{\sim}{F}}_{e_1} + \bar{\underset{\sim}{F}}_{e_2}) \\ \frac{1}{2}(\bar{\underset{\sim}{F}}_{e_2} + \bar{\underset{\sim}{F}}_{e_3}) \\ \vdots \\ \frac{1}{2}(\bar{\underset{\sim}{F}}_{e_{N-1}} + \bar{\underset{\sim}{F}}_{e_{N-2}}) \\ \frac{1}{2}(\bar{\underset{\sim}{F}}_{e_N} + \bar{\underset{\sim}{F}}_{e_{N-1}}) \\ 0 \end{bmatrix} \cdot \Delta t^2 \qquad (6)
$$

where

$$[\bar{M}] = \qquad (I)$$

$3N \times 3N$

$$\begin{bmatrix}
A_1\underset{\sim}{u}_1 & A_1\underset{\sim}{v}_1 & 0 & \cdots & & & \cdots & 0 & 0 & 0 & \Delta t^2\underset{\sim}{t}_1 & -\Delta t^2\underset{\sim}{t}_2 & 0 & \cdots & 0 \\
A_2\underset{\sim}{u}_1 & A_2\underset{\sim}{v}_1 & A_2\underset{\sim}{u}_2 & A_2\underset{\sim}{v}_2 & 0 & \cdots & & & & 0 & \Delta t^2\underset{\sim}{t}_2 & -\Delta t^2\underset{\sim}{t}_3 & 0 & \cdots & \vdots \\
\vdots & \vdots & \vdots & \vdots & & & & & & 0 & \vdots & & & & \\
A_{N-2}\underset{\sim}{u}_1 & A_{N-2}\underset{\sim}{v}_1 & A_{N-2}\underset{\sim}{u}_2 & A_{N-2}\underset{\sim}{v}_2 & \cdots & -A_{N-2}\underset{\sim}{u}_{N-1} & A_{N-2}\underset{\sim}{v}_{N-2} & 0 & 0 & & & \Delta t^2\underset{\sim}{t}_{N-2} & -\Delta t^2\underset{\sim}{t}_{N-1} & 0 \\
A_{N-1}\underset{\sim}{u}_1 & A_{N-1}\underset{\sim}{v}_1 & A_{N-1}\underset{\sim}{u}_2 & A_{N-1}\underset{\sim}{v}_2 & \cdots & A_{N-1}\underset{\sim}{u}_{N-1} & A_{N-1}\underset{\sim}{v}_{N-1} & 0 & 0 & 0 & \cdots & 0 & \Delta t^2\underset{\sim}{t}_{N-1} & -\Delta t^2\underset{\sim}{t}_N \\
\underset{\sim}{u}_1 & \underset{\sim}{v}_1 & \underset{\sim}{u}_2 & \underset{\sim}{v}_2 & \cdots & \underset{\sim}{u}_{N-1} & \underset{\sim}{v}_{N-1} & \underset{\sim}{u}_N & \underset{\sim}{v}_N & 0 & \cdots & & \vdots & 0
\end{bmatrix}$$

3.2.6:Initialisation.

Because of the form of equations 3.2.6(b) to start off the time-stepping procedure $\delta(L_1\underset{\sim}{t}_1)|'$, $\delta(L_2\underset{\sim}{t}_2)|'$,....., $\delta(L_{N-1}\underset{\sim}{t}_{N-1})|'$ must be known. Using a Taylor's series gives

$$\delta(L_1\underset{\sim}{t}_1)|' = \Delta t \left.\frac{d(L_1\underset{\sim}{t}_1)}{dt}\right|^{\circ} + \frac{\Delta t^2}{2}\left.\frac{d^2(L_1\underset{\sim}{t}_1)}{dt^2}\right|^{\circ} + \ldots \qquad (A)$$

$$\delta(L_1\underset{\sim}{t}_1+L_2\underset{\sim}{t}_2)|' = \Delta t \left.\frac{d(L_1\underset{\sim}{t}_1+L_2\underset{\sim}{t}_2)}{dt}\right|^{\circ} + \frac{\Delta t^2}{2}\left.\frac{d^2(L_1\underset{\sim}{t}_1+L_2\underset{\sim}{t}_2)}{dt^2}\right|^{\circ} + \ldots$$

$$\vdots$$

$$\delta(L_1\underset{\sim}{t}_1+L_2\underset{\sim}{t}_2+\ldots+L_{N-1}\underset{\sim}{t}_{N-1})|' = \Delta t \left.\frac{d(L_1\underset{\sim}{t}_1+L_2\underset{\sim}{t}_2+\ldots+L_{N-1}\underset{\sim}{t}_{N-1})}{dt}\right|^{\circ} + \frac{\Delta t^2}{2}\left.\frac{d^2(L_1\underset{\sim}{t}_1+L_2\underset{\sim}{t}_2+\ldots+L_{N-1}\underset{\sim}{t}_{N-1})}{dt^2}\right|^{\circ}$$

It is supposed that in the starting position the riser is strain free and stationary. Then from the equations of motion

$$\delta(L_1\underset{\sim}{t}_1)|' = \frac{\Delta t^2}{2} A_1^{-1}\cdot\frac{1}{2}(\bar{\underset{\sim}{F}}_{e_1}+\bar{\underset{\sim}{F}}_{e_2}) \qquad (B)$$

$$\delta(L_1\underset{\sim}{t}_1+L_2\underset{\sim}{t}_2)|' = \frac{\Delta t^2}{2} A_2^{-1}\cdot\frac{1}{2}(\bar{\underset{\sim}{F}}_{e_2}+\bar{\underset{\sim}{F}}_{e_3})$$

$$\vdots$$

$$\delta(L_1\underset{\sim}{t}_1+L_2\underset{\sim}{t}_2+\ldots+L_{N-1}\underset{\sim}{t}_{N-1})|' = \frac{\Delta t^2}{2} A_{N-1}^{-1}\cdot\frac{1}{2}(\bar{\underset{\sim}{F}}_{e_{N-1}}+\bar{\underset{\sim}{F}}_{e_N})$$

This system of equations can be trivially solved by elementary substitution to give $\delta(L_1\underset{\sim}{t}_1)|', \delta(L_2\underset{\sim}{t}_2)|', \ldots, \delta(L_{N-1}\underset{\sim}{t}_{N-1})|'$.

3.4:Elastic Rod Discretization.

3.4.1:Introduction.

In this section the length of riser is modelled as a series of elastic rods hinged together as shown in figure 3.4.1. The finite element method (Zienkiewicz[1977], Meirovitch[1975,1980], Tong and Rossetos[1977] and Cook[1974]) is used to formulate the equations of motion for the system. Although the equations of motion are obtained in a totally different way to the elastic lumped mass method the resulting system of equations are identical apart from the structure of the mass matrix.

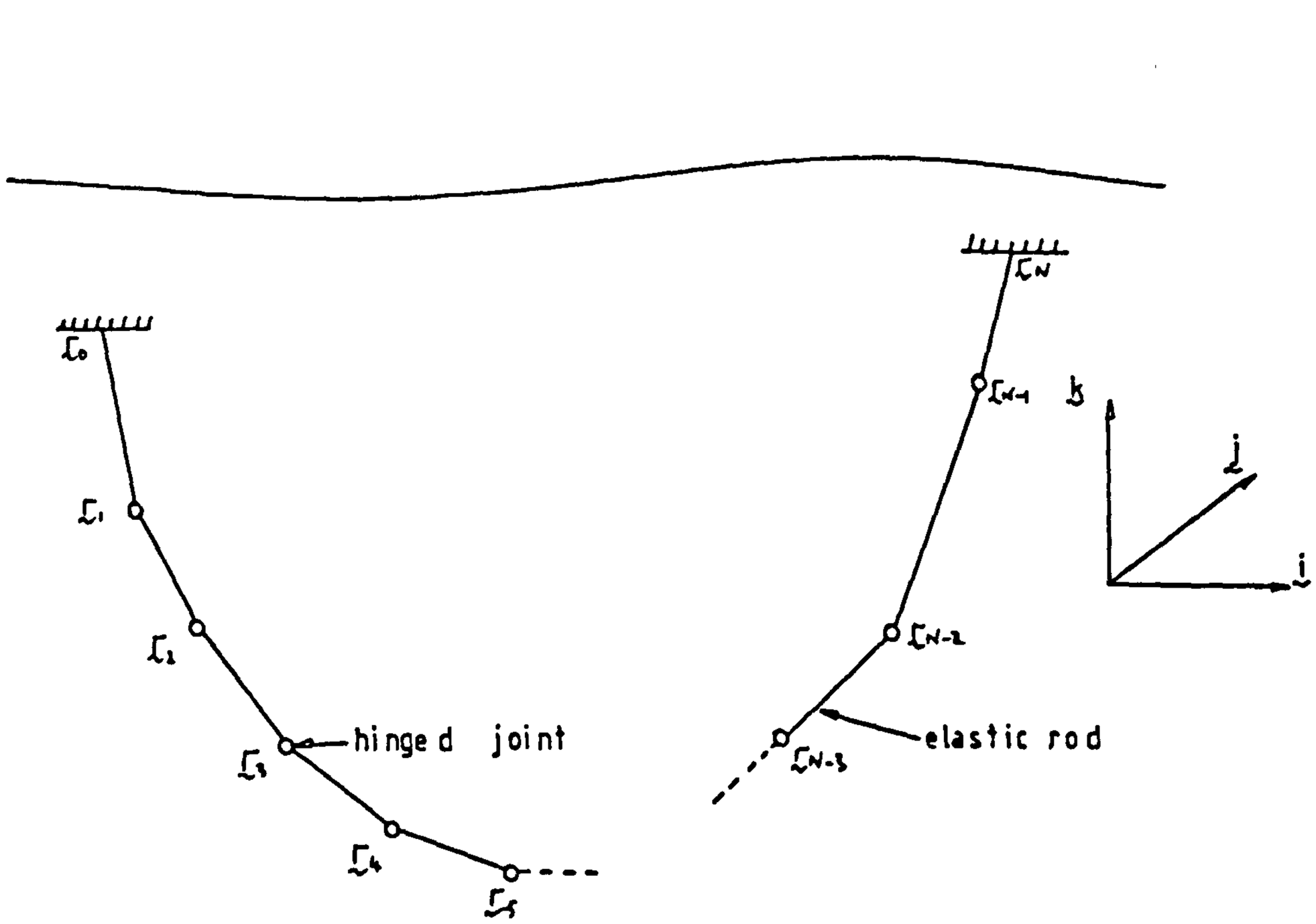

Figure 3.4.1: The Elastic Rod Method

3.4.2:Elastic Rod Element.

Consider the elastic rod element shown in figure 3.4.2(a). The position vector $\underset{\sim}{r}_e$ of a point on the element is given by

$$\underset{\sim}{r}_e = L\underset{\sim}{r} + \bar{L}\underset{\sim}{\bar{r}} = [L \;\; \bar{L}]\begin{bmatrix}\underset{\sim}{r}\\ \underset{\sim}{\bar{r}}\end{bmatrix} \qquad (a)$$

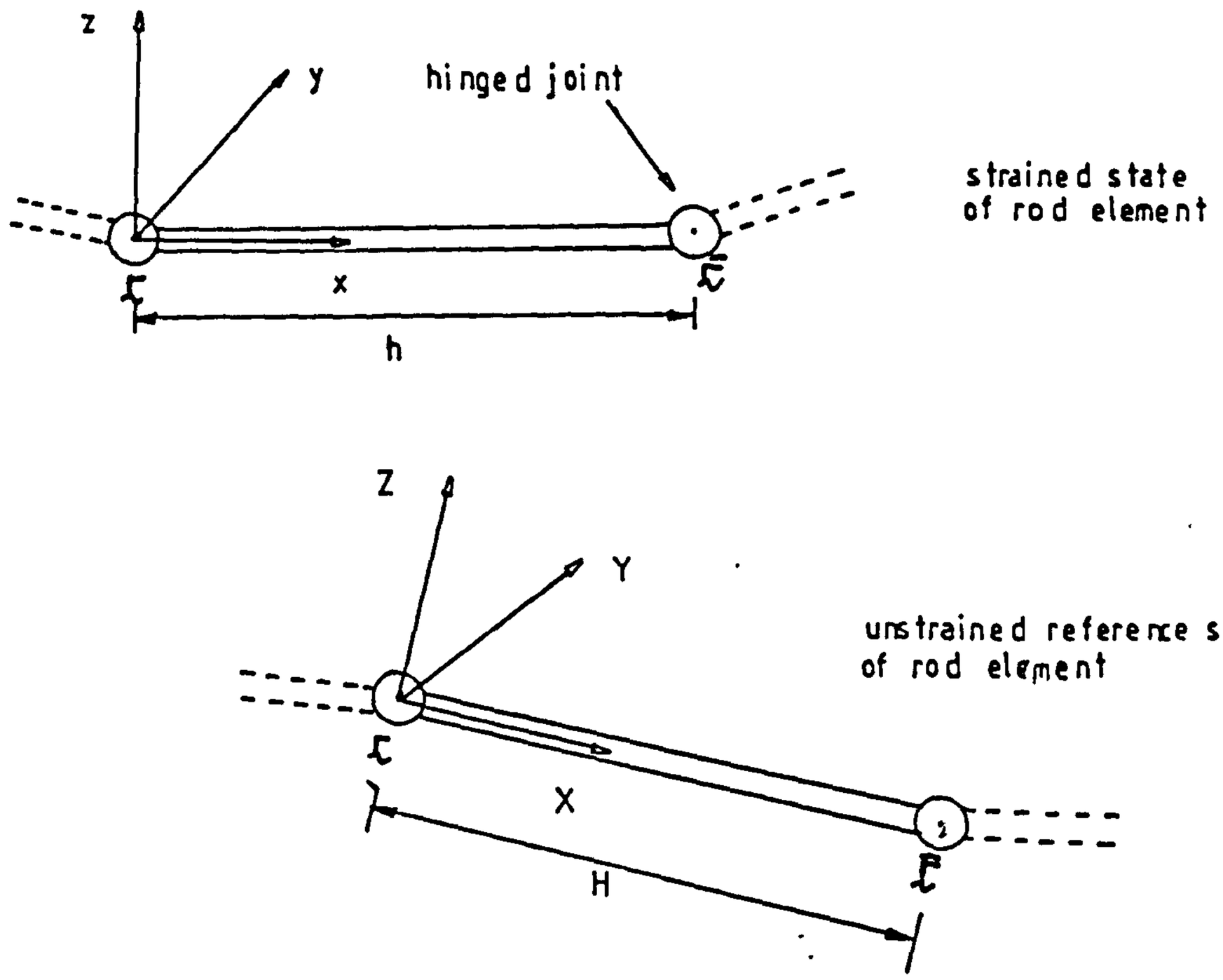

Figure 3.4.2(a): The Elastic Rod Element

where $\underset{\sim}{r}$ and $\underset{\sim}{\bar{r}}$ are the position vectors of the ends of the element and L and $\bar{L}$ are linear polynomials given by

$$L = \frac{x-H}{-H} \quad , \quad \bar{L} = \frac{x}{H} \qquad (b)$$

These polynomials are shown in figure 3.4.2(b). Note expressed in full matrix form equation (a) is

$$\begin{bmatrix} (\underline{r}_e)_x \\ (\underline{r}_e)_y \\ (\underline{r}_e)_z \end{bmatrix} = \left[\begin{array}{ccc:ccc} L & 0 & 0 & \bar{L} & 0 & 0 \\ 0 & L & 0 & 0 & \bar{L} & 0 \\ 0 & 0 & L & 0 & 0 & \bar{L} \end{array}\right] \left[\begin{array}{c} (\underline{r})_x \\ (\underline{r})_y \\ (\underline{r})_z \\ \hdashline (\bar{\underline{r}})_x \\ (\bar{\underline{r}})_y \\ (\bar{\underline{r}})_z \end{array}\right] \qquad (A)$$

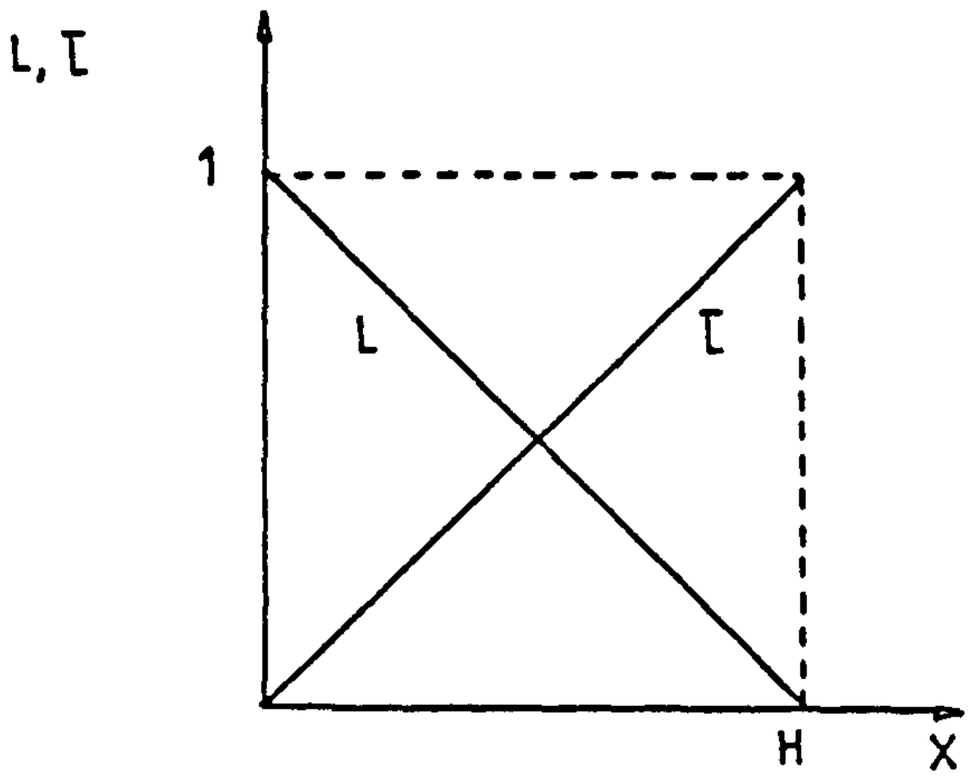

Figure 3.4.2(b) The Linear Interpolating Polynomials $L, \bar{L}$

where $(\underset{\sim}{r}_e)_x = \underset{\sim}{r}_e \cdot \underset{\sim}{i}$ etc.. For convenience the simpler form shall always be used.

3.4.2.1:Kinetic Energy of a Rod Element.

Refering to figure 3.4.2 the kinetic energy of the rod element (denoted by K.E.) is

$$\int_e \frac{1}{2}\rho(X)\,\frac{\partial \underset{\sim}{r}}{\partial t}\cdot\frac{\partial \underset{\sim}{r}}{\partial t}\,dX \qquad (A)$$

where $\rho=\rho(X)$ is the density of the riser per unit of unstrained length. Substituting in equation 3.4.2(a) gives

$$K.E._e = \int_e \frac{1}{2}\rho(X)\left\{[L\ \bar{L}]\begin{bmatrix}\dot{\underset{\sim}{r}}\\ \dot{\underset{\sim}{\bar{r}}}\end{bmatrix}\right\}^T[L\ \bar{L}]\begin{bmatrix}\dot{\underset{\sim}{r}}\\ \dot{\underset{\sim}{\bar{r}}}\end{bmatrix}dX \qquad (B)$$

It is now assumed that the length of the element is sufficiently small so that

$$K.E._e = \frac{1}{2}\rho(X_m)\int_e [L\dot{\underset{\sim}{r}}\ \dot{\underset{\sim}{\bar{r}}}]\begin{bmatrix}L^2 & L\bar{L}\\ L\bar{L} & \bar{L}^2\end{bmatrix}\begin{bmatrix}\dot{\underset{\sim}{r}}\\ \dot{\underset{\sim}{\bar{r}}}\end{bmatrix}dX \qquad (C)$$

where X_m is the value of X at the middle of the unstrained element of length H. Integrating the polynomials in the matrix gives

$$K.E._e = \frac{1}{2}\rho(X_m)H\left[\dot{\underset{\sim}{r}}\ \ \dot{\underset{\sim}{\bar{r}}}\right]\begin{bmatrix}\frac{2}{6} & \frac{1}{6}\\ \frac{1}{6} & \frac{2}{6}\end{bmatrix}\begin{bmatrix}\dot{\underset{\sim}{r}}\\ \dot{\underset{\sim}{\bar{r}}}\end{bmatrix} \qquad (D)$$

3.4.2.2:Strain Energy of a Rod Element.

The strain energy of the rod element is given by (Spiegel[1967])

$$S.E._e = \frac{1}{2}\frac{(EA)_e}{H}(h-H)^2 \qquad (A)$$

Hence the variation in the strain energy is given by

$$\delta S.E._e = \frac{(EA)_e}{H}(h-H)\,\delta h = \frac{(EA)_e}{H}(h-H)\,\delta\left\{(\bar{\xi}-\xi).(\bar{\xi}-\xi)\right\}^{\frac{1}{2}}$$

$$= \frac{(EA)_e}{H}(h-H)\frac{1}{2h}.2.\left\{(\bar{\xi}-\xi).(\delta\bar{\xi}-\delta\xi)\right\}^{\frac{1}{2}} \qquad (B)$$

$$= T\underset{\sim}{t}\cdot(\delta\bar{\xi}-\delta\xi)$$

where $T = \frac{EA(h-H)}{H}$ =tension in the element and $\underset{\sim}{t} = \frac{\bar{\xi}-\xi}{h}$ =tangent vector of the element.

3.4.2.3:Virtual Work Done on a Rod Element.

If the external force per unit of strained length on the element is $\underset{\sim}{E}_e$ then the element virtual work is

$$\delta W_e = \int_e \underset{\sim}{E}_e \frac{dx}{dX}\cdot\delta\underset{\sim}{r}_e\,dX \qquad (A)$$

Now

$$x = |L\xi + \bar{L}\bar{\xi} - \xi| = |(L-1)\xi + \bar{L}\bar{\xi}| \qquad (B)$$

$$= |\bar{L}(\bar{\xi}-\xi)| = \bar{L}\,|\bar{\xi}-\xi|$$

since from equation 3.4.2(b) $L+\bar{L}=1$ .Therefore

$$\frac{\partial x}{\partial X} = \frac{\partial \bar{L}}{\partial X} h = \frac{h}{H} \qquad (C)$$

which gives

$$\delta W_e = \frac{h}{H} \int_e \underset{\sim}{E}_e \cdot \delta \underset{\sim}{r}_e \, dX \qquad (D)$$

Now if the element is short enough

$$\delta W_e = \frac{h}{H} \underset{\sim}{E}_e|_m \cdot \int_e \delta \underset{\sim}{r}_e \, dX \qquad (E)$$

where $|_m$ denotes evaluated at the middle of the element.

Using the linear interpolating polynomials gives

$$\delta W_e = (\underset{\sim}{E}_e)|_m \frac{h}{H} \int_e \begin{bmatrix} L & \bar{L} \end{bmatrix} \begin{bmatrix} \delta \underset{\sim}{r} \\ \delta \bar{\underset{\sim}{r}} \end{bmatrix} dX = (\underset{\sim}{E}_e)|_m \cdot \frac{h}{2H} \times H (\delta \underset{\sim}{r} + \delta \bar{\underset{\sim}{r}}) \qquad (F)$$

$$= h \, \underset{\sim}{E}_e|_m \cdot \frac{1}{2} (\delta \underset{\sim}{r} + \delta \bar{\underset{\sim}{r}})$$

This equation corresponds to the lumping of forces used in the lumped mass discretization given in sections 3.2 and 3.3. Note there are other ways of estimating the virtual work. For example $\underset{\sim}{E}_e$ may be interpolated within an element by

$$\underset{\sim}{E}_e = L \underset{\sim}{E} + \bar{L} \bar{\underset{\sim}{E}} \qquad (H)$$

where $\underset{\sim}{E}$ and $\bar{\underset{\sim}{E}}$ are nodal estimates of the force per unit of strained length. Then

$$\delta W_e = \frac{h}{H} \int_e \left\{ \begin{bmatrix} L & \bar{L} \end{bmatrix} \begin{bmatrix} \underset{\sim}{E} \\ \bar{\underset{\sim}{E}} \end{bmatrix} \right\} \left\{ \begin{bmatrix} L & \bar{L} \end{bmatrix} \begin{bmatrix} \delta \underset{\sim}{r} \\ \delta \bar{\underset{\sim}{r}} \end{bmatrix} \right\}^T dX \qquad (I)$$

$$= \frac{h}{H} \cdot H \begin{bmatrix} \delta \underset{\sim}{r} & \delta \bar{\underset{\sim}{r}} \end{bmatrix} \begin{bmatrix} \frac{2}{6} & \frac{1}{6} \\ \frac{1}{6} & \frac{2}{6} \end{bmatrix} \begin{bmatrix} \underset{\sim}{E} \\ \bar{\underset{\sim}{E}} \end{bmatrix}$$

3.4.3:Assembly of the Equations of Motion.

Hamilton's principle for the system is

$$0 = \delta \int_{t_1}^{t_2} \left\{ \sum_{\text{elements}} K.E._e \; - \sum_{\text{elements}} S.E._e \right\} dt \qquad (A)$$

$$+ \int_{t_1}^{t_2} \sum_{\text{elements}} \delta W_e \, dt$$

Note that there is no virtual work done on the end cross-sections of the end elements since the ends are assumed to be fixed. Hamilton's principle is used to assemble the equations of motion for the system and for N elastic rod elements gives

(B)

$$D = \delta \int_{t_1}^{t_2} \left\{ \frac{1}{2} \begin{bmatrix} \dot{\underset{\sim}{r}}_1 & \dot{\underset{\sim}{r}}_2 & \cdots & \dot{\underset{\sim}{r}}_{N-2} & \dot{\underset{\sim}{r}}_{N-1} \end{bmatrix} \begin{bmatrix} \frac{1}{3}\rho_1 H_1 & \frac{1}{6}\rho_1 H_1 + \frac{1}{6}\rho_2 H_2 & & & \\ \frac{1}{6}\rho_1 H_1 + \frac{1}{6}\rho_2 H_2 & \frac{1}{3}\rho_2 H_2 + \frac{1}{3}\rho_3 H_3 & \ddots & & \\ & \ddots & \ddots & \frac{1}{6}\rho_{N-1} H_{N-1} + \frac{1}{6}\rho_N H_N & \\ & & \frac{1}{6}\rho_{N-1} H_{N-1} + \frac{1}{6}\rho_N H_N & \frac{1}{3}\rho_{N-1} H_{N-1} + \frac{1}{3}\rho_N H_N & \\ & & & \frac{1}{6}\rho_N H_N & \frac{1}{3}\rho_N H_N \end{bmatrix} \begin{bmatrix} \dot{\underset{\sim}{r}}_1 \\ \dot{\underset{\sim}{r}}_2 \\ \vdots \\ \dot{\underset{\sim}{r}}_{N-2} \\ \dot{\underset{\sim}{r}}_{N-1} \end{bmatrix} \right\} dt$$

$$+ \int_{t_1}^{t_2} \left\{ \begin{bmatrix} \delta\underset{\sim}{r}_1 & \delta\underset{\sim}{r}_2 & \cdots & \delta\underset{\sim}{r}_{N-2} & \delta\underset{\sim}{r}_{N-1} \end{bmatrix} \left(\begin{bmatrix} T_2 \underset{\sim}{t}_2 - T_1 \underset{\sim}{t}_1 \\ T_3 \underset{\sim}{t}_3 - T_2 \underset{\sim}{t}_2 \\ \vdots \\ T_{N-1} \underset{\sim}{t}_{N-1} - T_{N-2} \underset{\sim}{t}_{N-2} \\ T_N \underset{\sim}{t}_N - T_{N-1} \underset{\sim}{t}_{N-1} \end{bmatrix} + \begin{bmatrix} \frac{1}{2}(\underset{\sim}{F}_{e_1} + \underset{\sim}{F}_{e_2}) \\ \frac{1}{2}(\underset{\sim}{F}_{e_2} + \underset{\sim}{F}_{e_3}) \\ \vdots \\ \frac{1}{2}(\underset{\sim}{F}_{e_{N-2}} + \underset{\sim}{F}_{e_{N-1}}) \\ \frac{1}{2}(\underset{\sim}{F}_{e_{N-1}} + \underset{\sim}{F}_{e_N}) \end{bmatrix} \right) \right\} dt$$

since for an arbitrary element $h\underset{\sim}{\Xi}| = \underset{\sim}{F}_e$. The value of $\underset{\sim}{F}_e$ can be found in exactly the same way it was found in section 3.2. If the equality holds for all variations $\delta\underset{\sim}{r}_1 , \delta\underset{\sim}{r}_2 , \ldots\ldots , \delta\underset{\sim}{r}_{N-1}$ then

$$\begin{bmatrix} \frac{2}{6}\rho_1 H_1 + \frac{2}{6}\rho_2 H_2 & \frac{1}{6}\rho_2 H_2 & & \\ \frac{1}{6}\rho_2 H_2 & \frac{2}{6}\rho_2 H_2 + \frac{2}{6}\rho_3 H_3 & \ddots & \\ & \ddots & \frac{2}{6}\rho_{N-1} H_{N-1} + \frac{2}{6}\rho_N H_N & \end{bmatrix} \begin{bmatrix} \ddot{\underset{\sim}{r}}_1 \\ \ddot{\underset{\sim}{r}}_2 \\ \vdots \\ \ddot{\underset{\sim}{r}}_{N-1} \end{bmatrix} = \begin{bmatrix} T_2\underset{\sim}{t}_2 - T_1\underset{\sim}{t}_1 \\ T_3\underset{\sim}{t}_3 - T_2\underset{\sim}{t}_2 \\ \vdots \\ T_N\underset{\sim}{t}_N - T_{N-1}\underset{\sim}{t}_{N-1} \end{bmatrix} + \begin{bmatrix} \frac{1}{2}(\underset{\sim}{F}_{e_1} + \underset{\sim}{F}_{e_2}) \\ \frac{1}{2}(\underset{\sim}{F}_{e_2} + \underset{\sim}{F}_{e_3}) \\ \vdots \\ \frac{1}{2}(\underset{\sim}{F}_{e_{N-1}} + \underset{\sim}{F}_{e_N}) \end{bmatrix} \qquad (C)$$

The added mass matrix can be extracted in exactly the same way it was extracted in section 3.2.6 to give the final equations of motion

$$[M] \begin{bmatrix} \ddot{\underset{\sim}{r}}_1 \\ \ddot{\underset{\sim}{r}}_2 \\ \vdots \\ \ddot{\underset{\sim}{r}}_{N-1} \end{bmatrix} = \begin{bmatrix} T_2\underset{\sim}{t}_2 - T_1\underset{\sim}{t}_1 \\ T_3\underset{\sim}{t}_3 - T_2\underset{\sim}{t}_2 \\ \vdots \\ T_N\underset{\sim}{t}_N - T_{N-1}\underset{\sim}{t}_{N-1} \end{bmatrix} + \begin{bmatrix} \frac{1}{2}(\underset{\sim}{F}_{e_1} + \underset{\sim}{F}_{e_2}) \\ \frac{1}{2}(\underset{\sim}{F}_{e_2} + \underset{\sim}{F}_{e_3}) \\ \vdots \\ \frac{1}{2}(\underset{\sim}{F}_{e_{N-1}} + \underset{\sim}{F}_{e_N}) \end{bmatrix} \qquad (D)$$

where

$$[M] = \begin{bmatrix} \frac{2}{6}\rho_1 H_1 & \frac{1}{6}\rho_2 H_2 & & & \\ \frac{1}{6}\rho_2 H_2 & \frac{2}{6}\rho_2 H_2 + \frac{2}{6}\rho_3 H_3 & & & \\ & \ddots & \ddots & & \\ & & \frac{2}{6}\rho_{N-2} H_{N-2} & \frac{1}{6}\rho_{N-1} H_{N-1} & \\ & & \frac{1}{6}\rho_{N-1} H_{N-1} & \frac{2}{6}\rho_{N-1} H_{N-1} + \frac{2}{6}\rho_N H_N & \end{bmatrix} + \begin{bmatrix} \alpha_1 T_1 + \alpha_2 T_2 & \alpha_2 T_2 & & & \\ \alpha_2 T_2 & \alpha_2 T_2 + \alpha_3 T_3 & & & \\ & \ddots & \ddots & & \\ & & \alpha_{N-2} T_{N-2} + \alpha_{N-1} T_{N-1} & \alpha_{N-1} T_{N-1} & \\ & & \alpha_{N-1} T_{N-1} & \alpha_{N-1} T_{N-1} + \alpha_N T_N & \end{bmatrix} \qquad (E)$$

In a computer implementation of the discretization, in order to avoid numerical instability, the tensions in the elements must be calculated incrementally using the method given in section 3.2.8.

3.5:Galerkin Discretization with Linear Elements

3.5.1:Introduction.

In this section the Cristescu form of equation 2.5.4(a) is used

$$\rho(s_0)\frac{\partial^2 \underset{\sim}{r}}{\partial t^2} = \underset{\sim}{Q}\frac{\partial s}{\partial s_0} + \frac{\partial}{\partial s_0}\left\{\frac{T_e}{\frac{\partial s}{\partial s_0}}\frac{\partial \underset{\sim}{r}}{\partial s_0}\right\} \qquad (a)$$

where $\underset{\sim}{Q}$ =external force per unit of strained length and T_e =effective tension. The equation is discretized in space using linear finite elements with the Galerkin method (Jain[1985]).

3.5.2:Basis Functions.

For any element as in section 3.4 the element position vector $\underset{\sim}{r}_e$ may be interpolated

$$\underset{\sim}{r}_e = \underset{\sim}{r}_e(s_0) = L\underset{\sim}{r} + L\bar{\underset{\sim}{r}} \qquad (a)$$

Hence an approximate solution $\tilde{\underset{\sim}{r}}$ can be written in the form

$$\tilde{\underset{\sim}{r}} = L_1\underset{\sim}{r}_0 + (\bar{L}_1 \oplus L_2)\underset{\sim}{r}_1 + \ldots + (\bar{L}_{N-1} \oplus L_N)\underset{\sim}{r}_{N-1} + \bar{L}_N\underset{\sim}{r}_N \qquad (A)$$

The "addition" in the above expression needs to be carefully explained (Oden and Reddy[1976]). It is defined as follows

$$\bar{L}_i \oplus \bar{L}_{i+1} = \begin{cases} \bar{L}_i & \text{on element } i \\ L_{i+1} & \text{on element } i+1 \end{cases}$$

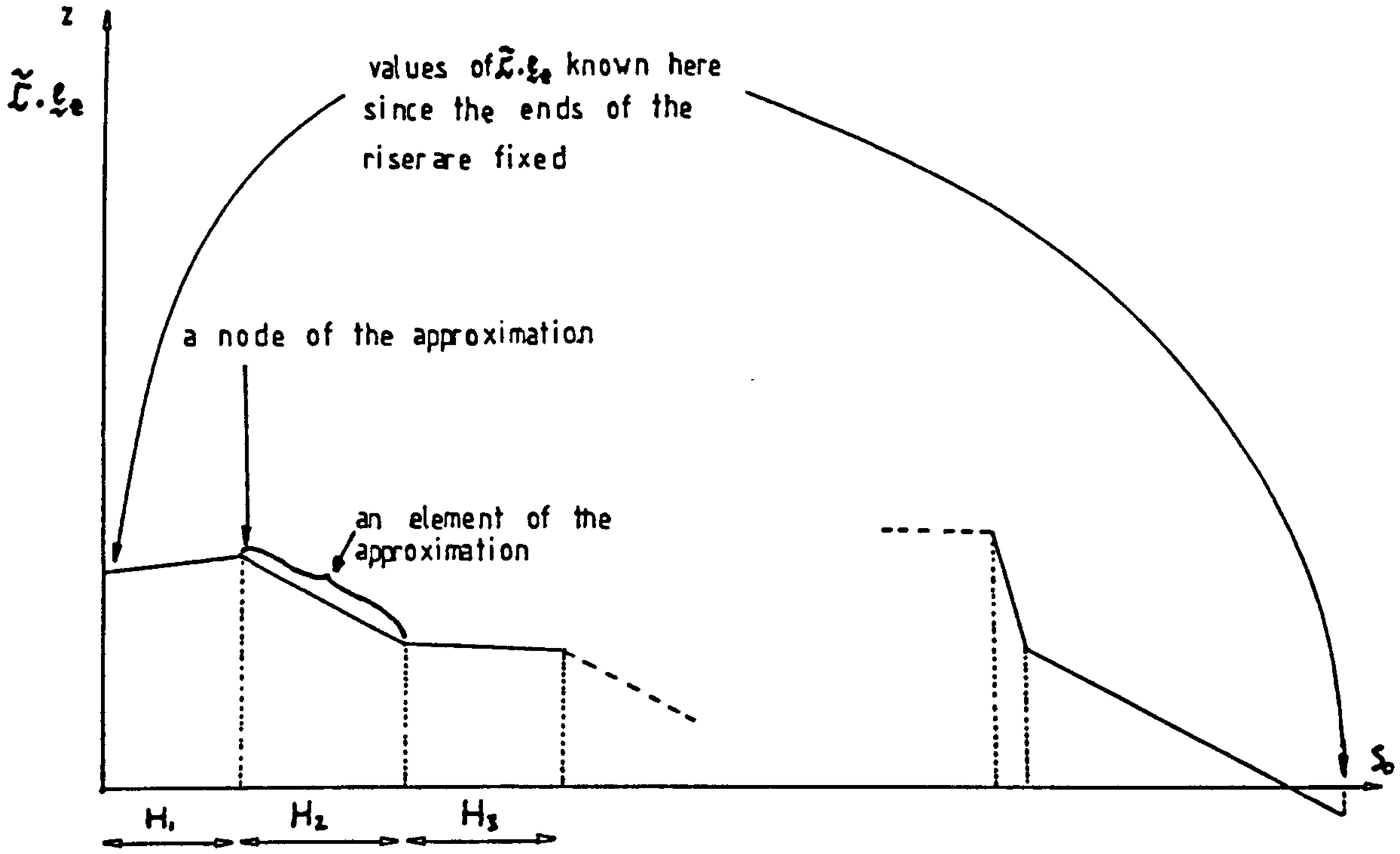

Figure 3.5.2: A Component of the Approximating Function for ξ

Note that there are no discontinuities in $T_i \oplus L_{i+1}$ at the central node. The function $T_i \oplus L_{i+1}$ is a "hat" shaped function and takes the value of zero outside the ith and (i+1)th elements. Now $\underset{\sim}{\xi}_0$ and $\underset{\sim}{\xi}_N$ are known since both ends of the riser are assumed to be fixed, hence the functions $T_1 \oplus L_2$, $T_2 \oplus L_3$, ..., $T_{N-1} \oplus L_N$ are like basis functions that span the space of the approximate solution.

3.5.3:Galerkin Solution.

The Galerkin weighted residual formulation of equation 3.5.1(a) is now considered. Integrating by parts gives

$$\int_0^L \phi_i \left\{ -\rho \frac{\partial^2 \tilde{\underset{\sim}{\xi}}}{\partial t^2} + \underset{\sim}{Q} \frac{\partial \tilde{s}}{\partial s_0} + \frac{\partial}{\partial s_0}\left[\frac{T_e}{\frac{\partial \tilde{s}}{\partial s_0}} \frac{\partial \tilde{\underset{\sim}{\xi}}}{\partial s_0} \right] \right\} ds_0 \qquad (A)$$

$$= \phi_i \frac{T_e}{\frac{\partial \tilde{s}}{\partial s_0}} \frac{\partial \tilde{\underset{\sim}{\xi}}}{\partial s_0} \Big|_0^L + \int_0^L \left[\phi_i \left\{ -\rho \frac{\partial^2 \tilde{\underset{\sim}{\xi}}}{\partial t^2} + \underset{\sim}{Q} \frac{\partial \tilde{s}}{\partial s_0} \right\} - \phi_i' \frac{T_e}{\frac{\partial \tilde{s}}{\partial s_0}} \frac{\partial \tilde{\underset{\sim}{\xi}}}{\partial s_0} \right] ds_0$$

where L =length of riser and $\tilde{s}$ is the approximate value of s determined using the approximation $\tilde{\underset{\sim}{\xi}}$.

Define $\phi_i = T_i \oplus L_{i+1}$ $(i=1,\ldots,N-1)$ then (B)

$$\int_0^L \phi_i \left\{ -\rho \frac{\partial^2 \tilde{\underset{\sim}{\xi}}}{\partial t^2} + \underset{\sim}{Q} \frac{\partial \tilde{s}}{\partial s_0} + \frac{\partial}{\partial s_0}\left[\frac{T_e}{\frac{\partial \tilde{s}}{\partial s_0}} \frac{\partial \tilde{\underset{\sim}{\xi}}}{\partial s_0} \right] \right\} ds_0 = \int_0^L \left[\phi_i \left\{ -\rho \frac{\partial^2 \tilde{\underset{\sim}{\xi}}}{\partial t^2} + \underset{\sim}{Q} \frac{\partial \tilde{s}}{\partial s_0} \right\} - \phi_i' \frac{T_e}{\frac{\partial \tilde{s}}{\partial s_0}} \frac{\partial \tilde{\underset{\sim}{\xi}}}{\partial s_0} \right] ds_0$$

since all of the basis functions are zero at the ends of the riser. Hence if for all of the basis functions

$$0 = \int_0^L \left[\phi_i \left\{ -\rho \frac{\partial^2 \tilde{\underset{\sim}{\xi}}}{\partial t^2} + \underset{\sim}{Q} \frac{\partial \tilde{s}}{\partial s_0} \right\} - \phi_i' \frac{T_e}{\frac{\partial \tilde{s}}{\partial s_0}} \frac{\partial \tilde{\underset{\sim}{\xi}}}{\partial s_0} \right] ds_0 \qquad (a)$$

is enforced the approximate solution $\tilde{\underset{\sim}{\xi}}$ is forced to satisfy approximately (see Wait and Mitchell on weak and strong solutions)

$$-\rho \frac{\partial^2 \tilde{\underset{\sim}{\xi}}}{\partial t^2} + \underset{\sim}{Q} \frac{\partial \tilde{s}}{\partial s_0} + \frac{\partial}{\partial s_0}\left[\frac{T_e}{\frac{\partial \tilde{s}}{\partial s_0}} \frac{\partial \tilde{\underset{\sim}{\xi}}}{\partial s_0} \right] = \underset{\sim}{0} \qquad (C)$$

Define

$$\langle \phi_i \mid \tilde{\underline{\xi}} \rangle = \int_0^L \left[\phi_i \left\{ -\rho \frac{\partial^2 \tilde{\underline{\xi}}}{\partial t^2} + \underset{\sim}{Q} \frac{\partial \tilde{s}}{\partial s_0} \right\} - \phi_i' \frac{T_e}{\frac{\partial \tilde{s}}{\partial s_0}} \frac{\partial \tilde{\underline{\xi}}}{\partial s_0} \right] ds_0 \quad (b)$$

Note that $\langle \phi_i \mid \tilde{\underline{\xi}} \rangle = 0$ is equivalent to enforcing equation (a). Now evaluating $\frac{\partial \tilde{s}}{\partial s_0}$ within an element using the interpolation gives

$$\frac{\partial \tilde{s}}{\partial s_0} = \left\{ \frac{\partial \tilde{\underline{\xi}}}{\partial s_0} \cdot \frac{\partial \tilde{\underline{\xi}}}{\partial s_0} \right\}^{\frac{1}{2}} = \left\{ \left([L' \; \bar{L}'] \begin{bmatrix} \underline{\xi} \\ \bar{\underline{\xi}} \end{bmatrix} \right)^T \left([L' \; \bar{L}'] \begin{bmatrix} \underline{\xi} \\ \bar{\underline{\xi}} \end{bmatrix} \right) \right\}^{\frac{1}{2}} \quad (D)$$

$$= \left\{ \left(\left[\frac{-1}{H}, \frac{1}{H} \right] \begin{bmatrix} \underline{\xi} \\ \bar{\underline{\xi}} \end{bmatrix} \right)^T \left(\left[\frac{-1}{H}, \frac{1}{H} \right] \begin{bmatrix} \underline{\xi} \\ \bar{\underline{\xi}} \end{bmatrix} \right) \right\}^{\frac{1}{2}} = \frac{1}{H} \left\{ (\bar{\xi} - \xi) \cdot (\bar{\xi} - \xi) \right\}^{\frac{1}{2}} = \frac{h}{H}$$

which on substitution into equation (b) gives

$$\langle \bar{L}_i \oplus L_{i+1} \mid \tilde{\underline{\xi}} \rangle = \int_{e_i} \left[\bar{L}_i \left\{ -\rho_i \frac{\partial^2 \tilde{\underline{\xi}}}{\partial t^2} + \frac{h_i}{H_i} \underset{\sim}{Q}_{e_i} \right\} - L_i' \frac{T_i}{\left(\frac{h_i}{H_i} \right)} \frac{\partial \tilde{\underline{\xi}}}{\partial s_0} \right] ds_0 \quad (E)$$

$$+ \int_{e_{i+1}} \left[L_{i+1} \left\{ -\rho_{i+1} \frac{\partial^2 \tilde{\underline{\xi}}}{\partial t^2} + \frac{h_{i+1}}{H_{i+1}} \underset{\sim}{Q}_{e_{i+1}} \right\} - L_{i+1}' \frac{T_{i+1}}{\left(\frac{h_{i+1}}{H_{i+1}} \right)} \frac{\partial \tilde{\underline{\xi}}}{\partial s_0} \right] ds_0$$

$$= \int_{e_i} \left[\bar{L}_i \left\{ -\rho_i [L L_i, \bar{L}_i] \begin{bmatrix} \ddot{\underline{\xi}}_{i-1} \\ \ddot{\underline{\xi}}_i \end{bmatrix} + \frac{h_i}{H_i} \underset{\sim}{Q}_{e_i} \right\} - L_i' \frac{T_i}{\left(\frac{h_i}{H_i} \right)} [L_i', \bar{L}_i'] \begin{bmatrix} \underline{\xi}_{i-1} \\ \underline{\xi}_i \end{bmatrix} \right] ds_0$$

$$+ \int_{e_{i+1}} \left[L_{i+1} \left\{ -\rho_{i+1} [L L_{i+1}, \bar{L}_{i+1}] \begin{bmatrix} \ddot{\underline{\xi}}_i \\ \ddot{\underline{\xi}}_{i+1} \end{bmatrix} + \frac{h_{i+1}}{H_{i+1}} \underset{\sim}{Q}_{e_{i+1}} \right\} - L_{i+1}' \frac{T_{i+1}}{\left(\frac{h_{i+1}}{H_{i+1}} \right)} [L_{i+1}', \bar{L}_{i+1}'] \begin{bmatrix} \underline{\xi}_i \\ \underline{\xi}_{i+1} \end{bmatrix} \right] ds_0$$

$$= -\rho_i H_i \left[\frac{1}{6}, \frac{2}{6} \right] \begin{bmatrix} \ddot{\underline{\xi}}_{i-1} \\ \ddot{\underline{\xi}}_i \end{bmatrix} + \frac{1}{2} h_i \underset{\sim}{Q}_{e_i} - \frac{T_i}{\left(\frac{h_i}{H_i} \right)} \left[\frac{-1}{H_i}, \frac{1}{H_i} \right] \begin{bmatrix} \underline{\xi}_{i-1} \\ \underline{\xi}_i \end{bmatrix}$$

$$-\rho_{i+1} H_{i+1} \left[\frac{2}{6}, \frac{1}{6} \right] \begin{bmatrix} \ddot{\underline{\xi}}_i \\ \ddot{\underline{\xi}}_{i+1} \end{bmatrix} + \frac{1}{2} h_{i+1} \underset{\sim}{Q}_{e_{i+1}} - \frac{(-T_{i+1})}{\left(\frac{h_{i+1}}{H_{i+1}} \right)} \left[\frac{-1}{H_{i+1}}, \frac{1}{H_{i+1}} \right] \begin{bmatrix} \underline{\xi}_i \\ \underline{\xi}_{i+1} \end{bmatrix}$$

where $\underset{\sim}{Q}_{ei}$ is defined to be the value of $\underset{\sim}{Q}$ evaluated at the middle of the ith element. Therefore

$$\langle \bar{L}_i \oplus L_{i+1} | \tilde{\xi} \rangle = -\rho_i H_i \left[\tfrac{1}{6}, \tfrac{2}{6}\right] \begin{bmatrix} \ddot{\underset{\sim}{\xi}}_{i-1} \\ \ddot{\underset{\sim}{\xi}}_i \end{bmatrix} + \frac{1}{2} h_i \underset{\sim}{Q}_{ei} - T_i \underset{\sim}{t}_i \qquad (F)$$

$$-\rho_{i+1} H_{i+1} \left[\tfrac{2}{6}, \tfrac{1}{6}\right] \begin{bmatrix} \ddot{\underset{\sim}{\xi}}_i \\ \ddot{\underset{\sim}{\xi}}_{i+1} \end{bmatrix} + \frac{1}{2} h_{i+1} \underset{\sim}{Q}_{ei+1} + T_{i+1} \underset{\sim}{t}_{i+1}$$

Hence demanding $\langle \bar{L}_i \oplus L_{i+1} | \tilde{\xi} \rangle = 0$ for $i = 1, \ldots, N-1$ gives the matrix equations of motion

$$\begin{bmatrix} \frac{2}{6}\rho_1 H_1 + \frac{2}{6}\rho_2 H_2 & \frac{1}{6}\rho_2 H_2 & & & \\ \frac{1}{6}\rho_2 H_2 & \frac{2}{6}\rho_2 H_2 + \frac{2}{6}\rho_3 H_3 & \ddots & & \\ & \ddots & \frac{2}{6}\rho_{N-2} H_{N-2} + \frac{2}{6}\rho_{N-1} H_{N-1} & \frac{1}{6}\rho_{N-1} H_{N-1} & \\ & & \frac{1}{6}\rho_{N-1} H_{N-1} & \frac{2}{6}\rho_{N-1} H_{N-1} + \frac{2}{6}\rho_N H_N \end{bmatrix} = \begin{bmatrix} \frac{1}{2}(h_1 \underset{\sim}{Q}_{e1} + h_2 \underset{\sim}{Q}_{e2}) \\ \frac{1}{2}(h_2 \underset{\sim}{Q}_{e2} + h_3 \underset{\sim}{Q}_{e3}) \\ \vdots \\ \frac{1}{2}(h_{N-2} \underset{\sim}{Q}_{eN-2} + h_{N-1} \underset{\sim}{Q}_{eN-1}) \\ \frac{1}{2}(h_{N-1} \underset{\sim}{Q}_{eN-1} + h_N \underset{\sim}{Q}_{eN}) \end{bmatrix} + \begin{bmatrix} T_2 \underset{\sim}{t}_2 - T_1 \underset{\sim}{t}_1 \\ T_3 \underset{\sim}{t}_3 - T_2 \underset{\sim}{t}_2 \\ \vdots \\ T_{N-1} \underset{\sim}{t}_{N-1} - T_{N-2} \underset{\sim}{t}_{N-2} \\ T_N \underset{\sim}{t}_N - T_{N-1} \underset{\sim}{t}_{N-1} \end{bmatrix}$$

Note it can be written that and the force terms can be determined in exactly the same way they were determined in sections 3.2.4 and 3.2.5. The added mass matrix may also be extracted in exactly the same way it was in section 3.2.6.

In a computer implementation of the discretization that has just been given, in order to avoid numerical instability the tensions in the elements of the approximation must be calculated incrementally using the method given in section 3.2.8.

3.6:Variational Discretization with Linear Elements.

3.6.1:Introduction.

From equation 2.6.7(a), since the bending stiffness of the riser is assumed to be zero, the appropriate variational equation is

$$0 = \delta \int_{t_1}^{t_2} \left[\int_0^L \frac{1}{2} \rho \frac{\partial \underset{\sim}{r}}{\partial t} \cdot \frac{\partial \underset{\sim}{r}}{\partial t} - \frac{1}{2EA} T_e^2 \, ds_0 \right] dt \qquad (A)$$

$$+ \int_{t_1}^{t_2} \left[\int_0^L \frac{\partial s}{\partial s_0} \underset{\sim}{Q} \cdot \delta \underset{\sim}{r} \, ds_0 \right] dt$$

where $\underset{\sim}{Q}$ =external force per unit of strained length and T_e =effective tension. In this section linear polynomials are used to discretize this variational equation. The linear polynomials used are exactly the same as the ones that have been used in sections 3.4 and 3.5.

3.6.2:Properties of an Element.

3.6.2.1:Kinetic Energy of an Element.

The kinetic energy of an element is given by

$$\int_e \frac{1}{2} \rho(s_0) \frac{\partial \underset{\sim}{r}}{\partial t} \cdot \frac{\partial \underset{\sim}{r}}{\partial t} \, ds_0 = \frac{1}{2} \rho_e \int_e \left\{ [L \; \underset{\sim}{L}] \begin{bmatrix} \dot{\xi} \\ \dot{\underset{\sim}{\xi}} \end{bmatrix} \right\}^T \left\{ [L \; \underset{\sim}{L}] \begin{bmatrix} \dot{\xi} \\ \dot{\underset{\sim}{\xi}} \end{bmatrix} \right\} ds_0 \qquad (A)$$

$$= \frac{1}{2} \rho_e \int_e [\dot{\xi} \; \dot{\underset{\sim}{\xi}}] \begin{bmatrix} L^2 & L\underset{\sim}{L} \\ L\underset{\sim}{L} & \underset{\sim}{L}^2 \end{bmatrix} \begin{bmatrix} \dot{\xi} \\ \dot{\underset{\sim}{\xi}} \end{bmatrix} ds_0 = \frac{1}{2} \rho_e H_e [\dot{\xi} \; \dot{\underset{\sim}{\xi}}] \begin{bmatrix} \frac{2}{6} & \frac{1}{6} \\ \frac{1}{6} & \frac{2}{6} \end{bmatrix} \begin{bmatrix} \dot{\xi} \\ \dot{\underset{\sim}{\xi}} \end{bmatrix}$$

where H_e =unstrained length of an element.

3.6.2.2:Strain Energy of an Element.

The strain energy of an element is

$$(S.E.)_e = \frac{1}{2(EA)_e} \int_e T_e^2 \, ds_o \qquad (A)$$

but

$$\frac{\partial s}{\partial s_o}\Big|_m = \left\{ \frac{\partial \underset{\sim}{r}}{\partial s_o} \cdot \frac{\partial \underset{\sim}{r}}{\partial s_o} \right\}^{\frac{1}{2}} = \left\{ \frac{1}{H} (\underset{\sim}{\bar{r}} - \underset{\sim}{r}) \cdot \frac{1}{H} (\underset{\sim}{\bar{r}} - \underset{\sim}{r}) \right\}^{\frac{1}{2}} = \frac{h}{H} \qquad (B)$$

therefore

$$(S.E.)_e = \frac{1}{2(EA)_e} (EA)_e^2 \int_e \left(\frac{h}{H} - 1 \right)^2 ds_o = \frac{1}{2} (EA)_e \left(\frac{h}{H} - 1 \right)^2 H \qquad (C)$$

$$= \frac{1}{2} \frac{(EA)_e}{H} (h - H)^2$$

This has the same form as the strain energy of an elastic rod element (see section 3.4.2.2) and as before

$$\delta(S.E.)_e = \underset{\sim}{T} \underset{\sim}{t} \cdot (\delta \underset{\sim}{\bar{r}} - \delta \underset{\sim}{r}) \qquad (D)$$

3.6.2.3:Virtual Work done on an Element.

The element virtual work is approximated by evaluating $\underset{\sim}{Q}$ at the middle of an element

$$\delta W_e = \int_e \frac{\partial s}{\partial s_o} \underset{\sim}{Q} \cdot \delta \underset{\sim}{r} \, ds_o = \frac{h}{H} \underset{\sim}{Q}|_m \cdot \int_e [L \; \bar{L}] \begin{bmatrix} \delta \underset{\sim}{r} \\ \delta \underset{\sim}{\bar{r}} \end{bmatrix} ds_o$$

$$= \frac{h}{H} \underset{\sim}{Q}|_m \cdot \frac{1}{2} H (\delta \underset{\sim}{r} + \delta \underset{\sim}{\bar{r}}) = \frac{1}{2} h \underset{\sim}{Q}|_m \cdot (\delta \underset{\sim}{r} + \delta \underset{\sim}{\bar{r}}) \qquad (A)$$

$$= \frac{1}{2} \underset{\sim}{F}_e \cdot (\delta \underset{\sim}{r} + \delta \underset{\sim}{\bar{r}})$$

using the same notation that was used in previous sections. The above expression has exactly the same form as the corresponding expression for an elastic rod element (see section 3.4.2.3) and indeed $\underset{\sim}{F}_e$ is calculated in exactly the same way.

3.6.3:Assembly of Equations of Motion.

Substituting the results for an element into the variational principle given in section 3.6.1 gives

$$\delta \int_{t_1}^{t_2} \left\{ \begin{bmatrix} \dot{\underset{\sim}{r}}_1 & \dot{\underset{\sim}{r}}_2 & \cdots & \dot{\underset{\sim}{r}}_{N-1} \end{bmatrix} \begin{bmatrix} \frac{1}{3}\rho_1 H_1 + \frac{1}{3}\rho_2 H_2 & \frac{1}{6}\rho_2 H_2 & & & \\ \frac{1}{6}\rho_2 H_2 & \frac{1}{3}\rho_2 H_2 + \frac{1}{3}\rho_3 H_3 & \ddots & & \\ & \ddots & \ddots & \frac{1}{6}\rho_{N-2} H_{N-2} & \\ & & \frac{1}{6}\rho_{N-2} H_{N-2} & \frac{1}{3}\rho_{N-2} H_{N-2} + \frac{1}{3}\rho_{N-1} H_{N-1} & \frac{1}{6}\rho_{N-1} H_{N-1} \\ & & & \frac{1}{6}\rho_{N-1} H_{N-1} & \frac{1}{3}\rho_{N-1} H_{N-1} + \frac{1}{3}\rho_N H_N \end{bmatrix} \begin{bmatrix} \ddot{\underset{\sim}{r}}_1 \\ \ddot{\underset{\sim}{r}}_2 \\ \vdots \\ \ddot{\underset{\sim}{r}}_{N-1} \end{bmatrix} \right. \qquad (A)$$

$$\left. + \frac{1}{2}\frac{(EA)_1}{H_1}(h_1 - H_1)^2 + \frac{1}{2}\frac{(EA)_2}{H_2}(h_2 - H_2)^2 + \ldots + \frac{1}{2}\frac{(EA)_N}{H_N}(h_N - H_N)^2 \right\} dt$$

$$+ \int_{t_1}^{t_2} \begin{bmatrix} \delta\underset{\sim}{r}_1 & \delta\underset{\sim}{r}_2 & \cdots & \delta\underset{\sim}{r}_{N-1} \end{bmatrix} \begin{bmatrix} \frac{1}{2}(\underset{\sim}{F}_{e_1} + \underset{\sim}{F}_{e_2}) \\ \frac{1}{2}(\underset{\sim}{F}_{e_2} + \underset{\sim}{F}_{e_3}) \\ \vdots \\ \frac{1}{2}(\underset{\sim}{F}_{eN} + \underset{\sim}{F}_{eN-1}) \end{bmatrix} dt = \underset{\sim}{0}$$

which gives the equations of motion

$$\begin{bmatrix} \frac{1}{6}AH_1 & & & & \\ + & & & & \\ \frac{2}{6}\rho_2 H_2 & \frac{1}{6}\rho_2 H_2 & & & \\ \frac{1}{6}\rho_2 H_2 & \frac{2}{6}\rho_2 H_2 & & & \\ & + & & & \\ & \frac{2}{6}A_2 H_3 & & & \\ & & \ddots & & \\ & & & \frac{2}{6}\rho_{N-2} H_{N-2} & \\ & & & + & \\ & & & \frac{2}{6}\rho_{N-1} H_{N-1} & \frac{1}{6}\rho_{N-1} H_{N-1} \\ & & & \frac{1}{6}\rho_{N-1} H_{N-1} & \frac{2}{6}\rho_{N-1} H_{N-1} \\ & & & & + \\ & & & & \frac{2}{6}\rho_N H_N \end{bmatrix} \begin{bmatrix} \ddot{\underset{\sim}{r}}_1 \\ \ddot{\underset{\sim}{r}}_2 \\ \vdots \\ \ddot{\underset{\sim}{r}}_{N-1} \end{bmatrix} = \begin{bmatrix} \frac{1}{2}(\underset{\sim}{F}_{e1} + \underset{\sim}{F}_{e2}) \\ \frac{1}{2}(\underset{\sim}{F}_{e2} + \underset{\sim}{F}_{e3}) \\ \vdots \\ \frac{1}{2}(\underset{\sim}{F}_{eN-1} + \underset{\sim}{F}_{eN}) \end{bmatrix} + \begin{bmatrix} T_2 \underset{\sim}{t}_2 - T_1 \underset{\sim}{t}_1 \\ T_3 \underset{\sim}{t}_3 - T_2 \underset{\sim}{t}_2 \\ \vdots \\ T_N \underset{\sim}{t}_N - T_{N-1} \underset{\sim}{t}_{N-1} \end{bmatrix} \qquad (B)$$

Note that Hamilton's principle requires $\delta \underset{\sim}{r}_i|_{t_1} = \delta \underset{\sim}{r}_i|_{t_2} = 0$ and since $\underset{\sim}{r}_0$ and $\underset{\sim}{r}_N$ are known $\delta \underset{\sim}{r}_0 = \delta \underset{\sim}{r}_N = 0$

In a computer implementation of the discretization that has been just given, in order to avoid numerical instability the tensions in the elements of the approximation must be calculated incrementally using the method given in section 3.2.8.

3.7:Variational Discretization with Cubic Elements.

3.7.1:Introduction.

As in section 3.6 the variational equation

$$0=\delta\int_{t_1}^{t_2}\left\{\int_0^L \frac{1}{2}\rho\frac{\partial\underset{\sim}{r}}{\partial t}\cdot\frac{\partial\underset{\sim}{r}}{\partial t}\,ds_0-\int_0^L\frac{1}{2EA}T_e^2\,ds_0\right\}dt \qquad (a)$$

$$+\int_{t_1}^{t_2}\left\{\int_0^L\frac{\partial s}{\partial s_0}\underset{\sim}{Q}\cdot\delta\underset{\sim}{r}\,ds_0\right\}dt$$

is discretized. $\underset{\sim}{Q}$ =external force per unit of unstrained length and T_e =effective tension. For an element the following interpolation

$$\underset{\sim}{r}_e=\mathcal{L}\underset{\sim}{r}+\bar{\mathcal{L}}\bar{\underset{\sim}{r}}+\mathcal{H}\frac{\partial\underset{\sim}{r}}{\partial s_0}+\bar{\mathcal{H}}\frac{\partial\bar{\underset{\sim}{r}}}{\partial s_0}=\begin{bmatrix}\mathcal{L} & \mathcal{H} & \bar{\mathcal{L}} & \bar{\mathcal{H}}\end{bmatrix}\begin{bmatrix}\underset{\sim}{r}\\ \underset{\sim}{r}'\\ \bar{\underset{\sim}{r}}\\ \bar{\underset{\sim}{r}}'\end{bmatrix} \qquad (b)$$

is used where $\mathcal{L}$, $\bar{\mathcal{L}}$, $\mathcal{H}$ and $\bar{\mathcal{H}}$ are the standard cubic Hermite interpolating polynomials (Wait and Mitchell[1985]) as shown in figure 3.7.1(a). The Hermite polynomials may be defined in terms of the standard linear polynomials L and $\bar{L}$ which were defined in section 3.4

$$\mathcal{L}=L^2(3-2L)\ ,\quad \bar{\mathcal{L}}=\bar{L}^2(3-2\bar{L})\ ,\quad \mathcal{H}=HL^2\bar{L}\ ,\quad \bar{\mathcal{H}}=-HL\bar{L}^2 \qquad (A)$$

When using this interpolation the approximating function $\tilde{\underset{\sim}{r}}$ given by

$$\tilde{\underset{\sim}{r}}=\underset{\sim}{r}_{e_1}\oplus\underset{\sim}{r}_{e_2}\oplus\cdots\oplus\underset{\sim}{r}_{e_N} \qquad (B)$$

is constrained to be continuous in $\underset{\sim}{r}$ and $\frac{\partial\underset{\sim}{r}}{\partial s_0}$ at the nodes of the approximation. N is the number of elements

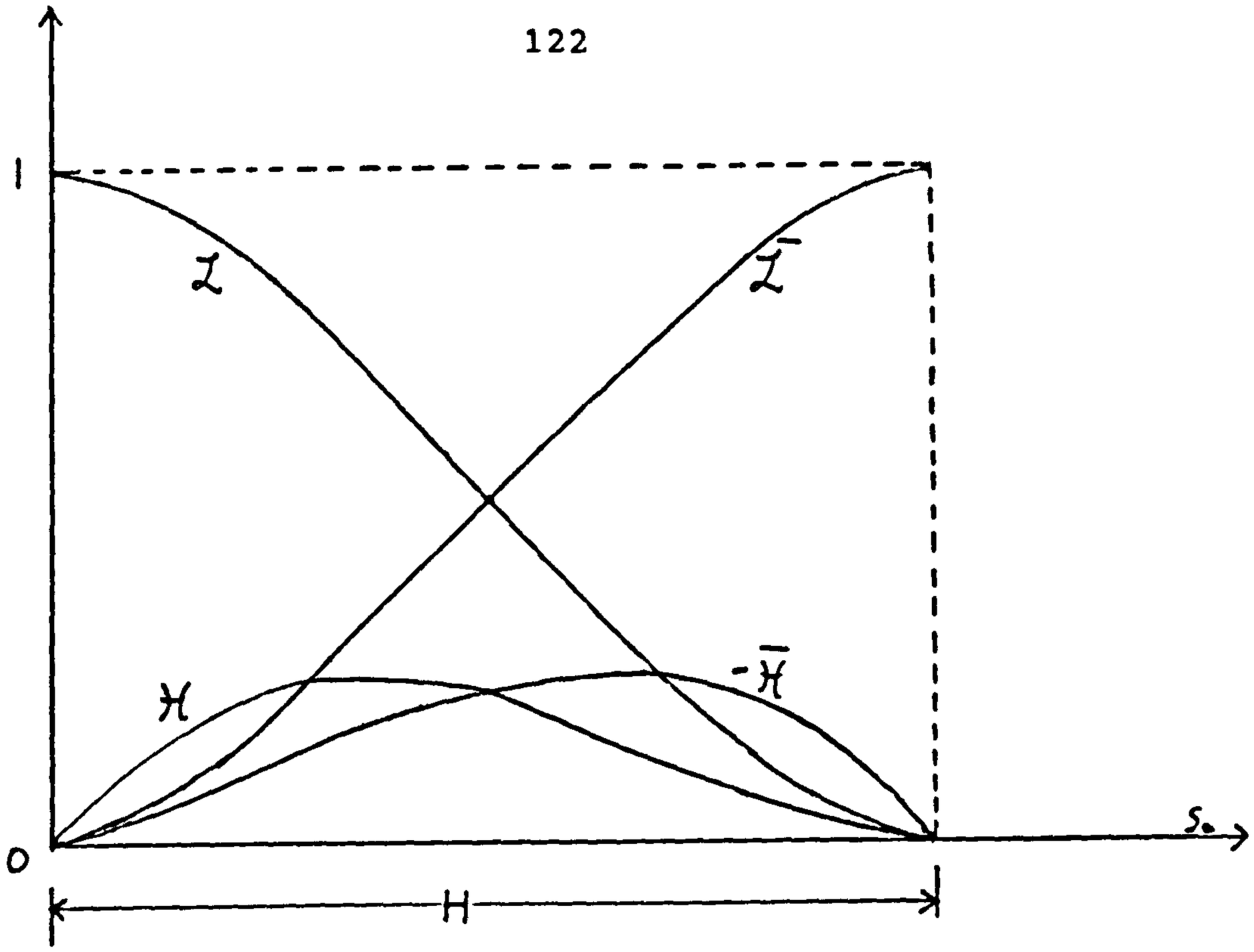

Hermite Polynomials $\mathcal{L}, \bar{\mathcal{L}}, \mathcal{H}, \bar{\mathcal{H}}$ defined so that

$$\mathcal{L}(\xi) = 1, \ \mathcal{L}(\bar{\xi}) = 0, \ \mathcal{L}'(\xi) = 0, \ \mathcal{L}'(\bar{\xi}) = 0$$
$$\bar{\mathcal{L}}(\xi) = 0, \ \bar{\mathcal{L}}(\bar{\xi}) = 1, \ \bar{\mathcal{L}}'(\xi) = 0, \ \bar{\mathcal{L}}'(\bar{\xi}) = 0$$
$$\mathcal{H}(\xi) = 0, \ \mathcal{H}(\bar{\xi}) = 0, \ \mathcal{H}'(\xi) = 1, \ \mathcal{H}'(\bar{\xi}) = 0$$
$$\bar{\mathcal{H}}(\xi) = 0, \ \bar{\mathcal{H}}(\bar{\xi}) = 0, \ \bar{\mathcal{H}}'(\xi) = 0, \ \bar{\mathcal{H}}'(\bar{\xi}) = 1$$

Figure 3.7.1(a): The Hermite Polynomials defined on an Element

in the approximation. One component of the approximation is shown in figure 3.7.1(b). This interpolation can be easily adapted to allow for the bending stiffness of the riser as will be shown in the next chapter.

The curved elements used in section 3.7 are more accurate than the straight line elements that have been used previously. However by their very nature they are more complicated. Unlike straight line elements the bending

stiffness of the riser can be included in a consistent way. They are also more suited to modelling sections of the riser that have high curvature. See sections 3.9 and 3.10 for further discussions about the merits of curved elements.

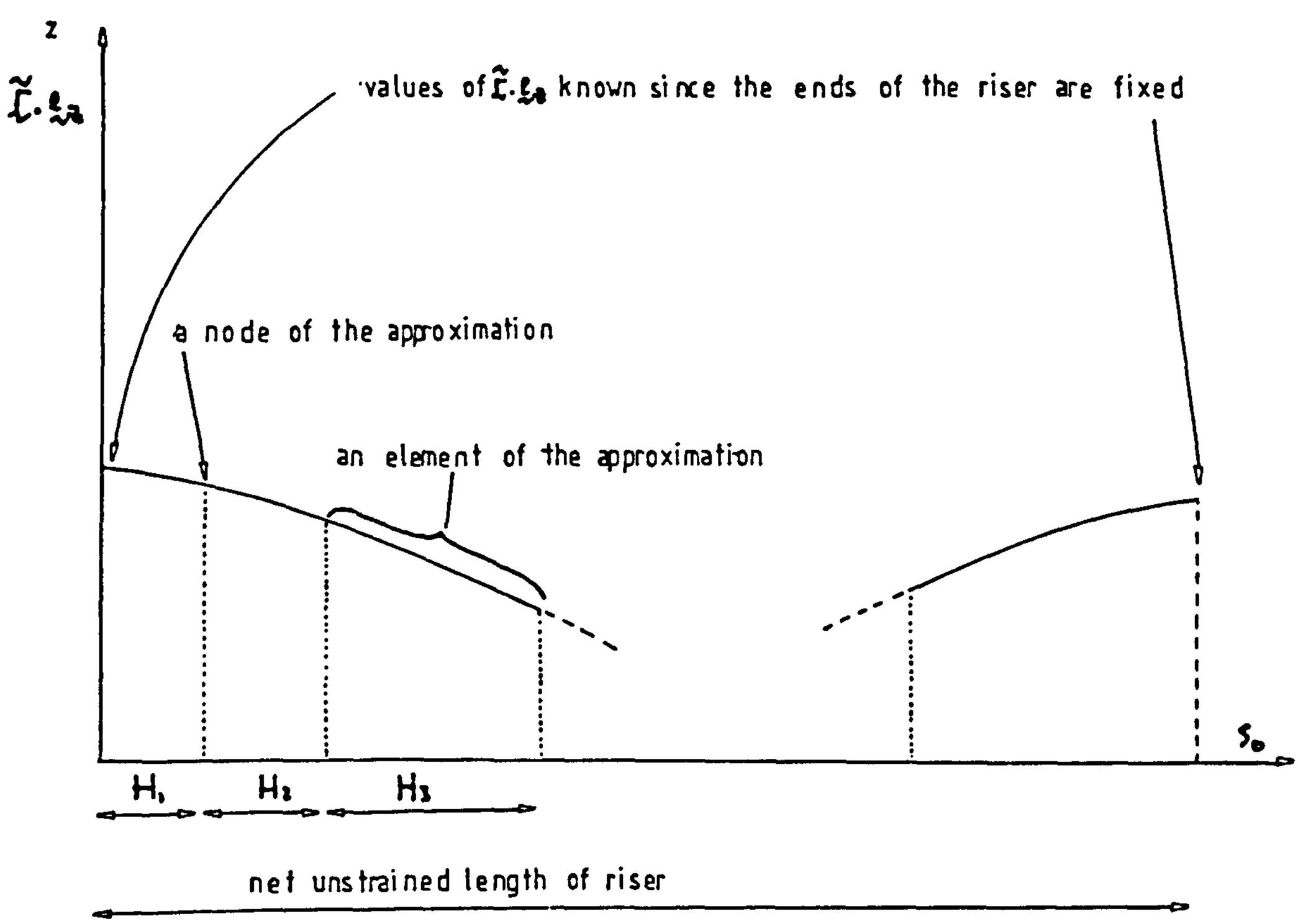

Figure 3.7.1(b): A Component of the Approximating Function for $\tilde{\underset{\sim}{\Sigma}}$

3.7.2:Properties of an Element.

A typical element of the approximation is shown in figure 3.7.2. Note that because of the nature of the interpolation unlike the other elements that have been used this element is curved. Also since the strain in an element is not necessarily constant neither necessarily is the tension.

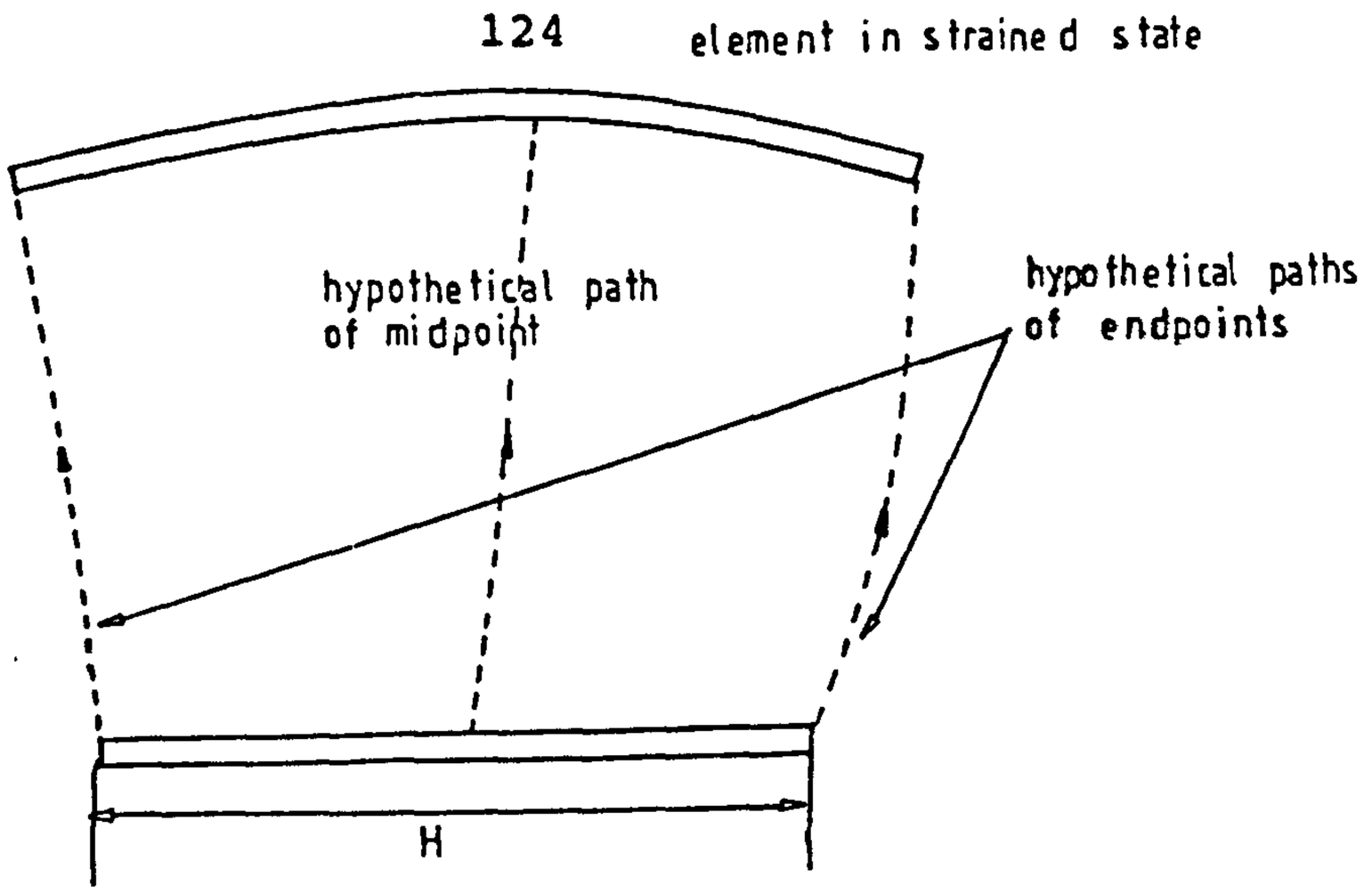

Figure 3.7.2: A Cubic Element

Because the strain in the element is not necessarily constant along its length the mid-point of the element in an unstrained reference state is not necessarily the mid-point of the element in a strained state. When the mid-point of an element is refered to in section 3.7 it is defined to be the point on the element that was originally the mid-point of the element in an unstrained reference state.

3.7.2.1:Kinetic Energy of an Element.

Using equation 3.7.1(b) gives the kinetic energy of an element

$$\int_e \frac{1}{2}\rho \frac{\partial \underset{\sim}{r}_e}{\partial t} \cdot \frac{\partial \underset{\sim}{r}_e}{\partial t}\, ds_o = \qquad (A)$$

$$\int_e \frac{1}{2}\rho \begin{bmatrix} \dot{\underset{\sim}{r}} & \dot{\underset{\sim}{r}}' & \ddot{\underset{\sim}{r}} & \ddot{\underset{\sim}{r}}' \end{bmatrix} \begin{bmatrix} \mathcal{L}^2 & \mathcal{L}\mathcal{H} & \mathcal{L}\bar{\mathcal{L}} & \mathcal{L}\bar{\mathcal{H}} \\ & \mathcal{H}^2 & \mathcal{H}\bar{\mathcal{L}} & \mathcal{H}\bar{\mathcal{H}} \\ & \text{Sym} & \bar{\mathcal{L}}^2 & \bar{\mathcal{L}}\bar{\mathcal{H}} \\ & & & \bar{\mathcal{H}}^2 \end{bmatrix} \begin{bmatrix} \dot{\underset{\sim}{r}} & \dot{\underset{\sim}{r}}' & \ddot{\underset{\sim}{r}} & \ddot{\underset{\sim}{r}}' \end{bmatrix}^T ds_o$$

$$= \frac{1}{2}\frac{\rho_e H}{420} \begin{bmatrix} \dot{\underset{\sim}{r}} & \dot{\underset{\sim}{r}}' & \ddot{\underset{\sim}{r}} & \ddot{\underset{\sim}{r}}' \end{bmatrix} \begin{bmatrix} 156 & 22H & 54 & -13H \\ & 4H^2 & 13H & -3H^2 \\ & & 156 & -22H \\ & \text{Sym} & & 4H^2 \end{bmatrix} \begin{bmatrix} \dot{\underset{\sim}{r}} \\ \dot{\underset{\sim}{r}}' \\ \ddot{\underset{\sim}{r}} \\ \ddot{\underset{\sim}{r}}' \end{bmatrix}$$

where for example $\underset{\sim}{\Gamma}'$ denotes differentiation of $\underset{\sim}{\Gamma}$ with repect to s_o .

3.7.2.2:Pure Stretching Energy of an Element.

From section 2.6.7

$$\delta(S.E.)_e = \delta \int_e \frac{1}{2EA} T_e^2 \, ds_o = T_m \int_e \frac{\frac{\partial \underset{\sim}{r}}{\partial s_o}}{\frac{ds}{ds_o}} \cdot \frac{\partial \delta \underset{\sim}{r}}{\partial s_o} \, ds_o \qquad (A)$$

where T_m is the tension at the midpoint of the element.

Therefore using equation 3.7.1(b) gives

$$\delta \int_e \frac{1}{2EA} T_e^2 \, ds_o = \frac{T_m}{\frac{ds}{ds_o}\Big|_m} \int_e \begin{bmatrix} \delta \underset{\sim}{r} & \delta \underset{\sim}{r}' & \delta \underset{\sim}{\bar{r}} & \delta \underset{\sim}{\bar{r}}' \end{bmatrix} \begin{bmatrix} \mathcal{L}^{1^2} & \mathcal{L}'\mathcal{H}' & \mathcal{L}'\bar{\mathcal{L}}' & \mathcal{L}\bar{\mathcal{H}}' \\ & \mathcal{H}'^2 & \mathcal{H}\bar{\mathcal{L}}' & \mathcal{H}'\bar{\mathcal{H}}' \\ & & \bar{\mathcal{L}}'^2 & \bar{\mathcal{L}}'\bar{\mathcal{H}}' \\ \text{SYMM} & & & \bar{\mathcal{H}}'^2 \end{bmatrix} \begin{bmatrix} \underset{\sim}{r} \\ \underset{\sim}{r}' \\ \underset{\sim}{\bar{r}} \\ \underset{\sim}{\bar{r}}' \end{bmatrix}$$

$$= \frac{T_m}{\frac{ds}{ds_o}\Big|_m} \begin{bmatrix} \delta \underset{\sim}{r} & \delta \underset{\sim}{r}' & \delta \underset{\sim}{\bar{r}} & \delta \underset{\sim}{\bar{r}}' \end{bmatrix} \begin{bmatrix} \frac{6}{5H} & \frac{1}{10} & -\frac{6}{5H} & \frac{1}{10} \\ & \frac{2}{15}H & -\frac{1}{10} & -\frac{1}{30}H \\ & & \frac{6}{5}H & -\frac{1}{10} \\ \text{SYMM} & & & \frac{2}{15}H \end{bmatrix} \begin{bmatrix} \underset{\sim}{r} \\ \underset{\sim}{r}' \\ \underset{\sim}{\bar{r}} \\ \underset{\sim}{\bar{r}}' \end{bmatrix}$$

$$= \frac{T_m}{\frac{ds}{ds_o}\Big|_m} \begin{bmatrix} \delta \underset{\sim}{r} & \delta \underset{\sim}{r}' & \delta \underset{\sim}{\bar{r}} & \delta \underset{\sim}{\bar{r}}' \end{bmatrix} \begin{bmatrix} -\underset{\sim}{\epsilon} \\ -\underset{\sim}{\eta} \\ +\underset{\sim}{\epsilon} \\ -\underset{\sim}{\eta}^* \end{bmatrix} \qquad (a)$$

where $\frac{ds}{ds_o}\Big|_m$ denotes the value of $\frac{ds}{ds_o}$ evaluated at the middle of the element and

$$\underset{\sim}{\epsilon} = \left[-\frac{ds}{ds_o}\Big|_m\right]^{-1}\left(\frac{6}{5H}\underset{\sim}{r} + \frac{1}{10}\underset{\sim}{r}' - \frac{6}{5H}\underset{\sim}{\bar{r}} + \frac{1}{10}\underset{\sim}{\bar{r}}'\right), \quad \underset{\sim}{\eta} = \left[-\frac{ds}{ds_o}\Big|_m\right]^{-1}\left(\frac{1}{10}\underset{\sim}{r} + \frac{2}{15}H\underset{\sim}{r}' - \frac{1}{10}\underset{\sim}{\bar{r}} - \frac{1}{30}H\underset{\sim}{\bar{r}}'\right),$$

$$\underset{\sim}{\eta}^* = \left[-\frac{ds}{ds_o}\Big|_m\right]^{-1}\left(\frac{1}{10}\underset{\sim}{r} - \frac{1}{30}H\underset{\sim}{r}' - \frac{1}{10}\underset{\sim}{\bar{r}} + \frac{2}{15}H\underset{\sim}{\bar{r}}'\right) \qquad (B)$$

In the above equation $\frac{\partial s}{\partial s_0}\Big|_m$ can be calculated as follows

$$\frac{\partial \underset{\sim}{r}_e}{\partial s_0} = \begin{bmatrix} \mathcal{L}' & \mathcal{H}' & \bar{\mathcal{L}}' & \bar{\mathcal{H}}' \end{bmatrix} \begin{bmatrix} \underset{\sim}{r} \\ \frac{\partial \underset{\sim}{r}}{\partial s_0} \\ \bar{\underset{\sim}{r}} \\ \frac{\partial \bar{\underset{\sim}{r}}}{\partial s_0} \end{bmatrix} \qquad (C)$$

hence at the mid-point of an element

$$\frac{\partial \underset{\sim}{r}_e}{\partial s_0}\Big|_m = \begin{bmatrix} -\frac{3}{2H} & -\frac{1}{4} & \frac{3}{2H} & -\frac{1}{4} \end{bmatrix} \begin{bmatrix} \underset{\sim}{r} \\ \frac{\partial \underset{\sim}{r}}{\partial s_0} \\ \bar{\underset{\sim}{r}} \\ \frac{\partial \bar{\underset{\sim}{r}}}{\partial s_0} \end{bmatrix} \qquad (D)$$

thus $\frac{\partial s}{\partial s_0}\Big|_m$ can be calculated from

$$\frac{\partial s}{\partial s_0}\Big|_m = \left\{ \begin{bmatrix} \mathcal{L} & \mathcal{H}' & \bar{\mathcal{L}} & \bar{\mathcal{H}}' \end{bmatrix} \begin{bmatrix} \frac{9}{4H^2} & \frac{3}{8H} & -\frac{9}{4H^2} & \frac{3}{8H} \\ & \frac{1}{16} & -\frac{3}{8H} & \frac{1}{16} \\ & & \frac{9}{4H^2} & -\frac{3}{8H} \\ \text{SYM} & & & \frac{1}{16} \end{bmatrix} \begin{bmatrix} \underset{\sim}{r} \\ \underset{\sim}{r}' \\ \bar{\underset{\sim}{r}} \\ \bar{\underset{\sim}{r}}' \end{bmatrix} \right\}^{\Sigma} \qquad (E)$$

3.7.2.3:External Virtual Work Done on an Element.

The external virtual work done on an element of the riser is given by

$$\int_e \frac{\partial s}{\partial s_0} \underset{\sim}{Q} \cdot \delta \underset{\sim}{r}\, ds_0 = \frac{\partial s}{\partial s_0}\Big|_m \underset{\sim}{Q}|_m \cdot \int_e \delta \underset{\sim}{r}\, ds_0 = \frac{\partial s}{\partial s_0}\Big|_m \underset{\sim}{Q}|_m \cdot \int_e \left(\mathcal{L}\, \delta \underset{\sim}{r} + \mathcal{H}\, \delta \underset{\sim}{r}' + \bar{\mathcal{L}}\, \delta \bar{\underset{\sim}{r}} + \bar{\mathcal{H}}\, \delta \bar{\underset{\sim}{r}}' \right) ds_0 \qquad (A)$$

$$= \frac{\partial s}{\partial s_0}\Big|_m \underset{\sim}{Q}_m \cdot \left\{ \frac{1}{2} H\, \delta \underset{\sim}{r} + \frac{1}{12} H^2 \delta \underset{\sim}{r}' + \frac{1}{2} H\, \delta \bar{\underset{\sim}{r}} - \frac{1}{12} H^2 \delta \bar{\underset{\sim}{r}}' \right\}$$

or in matrix form

$$\frac{\partial s}{\partial s_0}\Big|_m \left\{ \left[\tfrac{1}{2}H \quad \tfrac{1}{12}H^2 \quad \tfrac{1}{2}H \quad -\tfrac{1}{12}H^2 \right] \begin{bmatrix} \delta\underset{\sim}{r} \\ \delta\underset{\sim}{r}' \\ \delta\underset{\sim}{\bar{r}} \\ \delta\underset{\sim}{\bar{r}}' \end{bmatrix} \right\}^T \left[\underset{\sim}{Q}|_m \right]$$

$$= \frac{\partial s}{\partial s_0}\Big|_m \left[\delta\underset{\sim}{r} \quad \delta\underset{\sim}{r}' \quad \delta\underset{\sim}{\bar{r}} \quad \delta\underset{\sim}{\bar{r}}' \right] \begin{bmatrix} \frac{1}{2}H\underset{\sim}{Q}|_m \\ \frac{1}{12}H^2\underset{\sim}{Q}|_m \\ \frac{1}{2}H\underset{\sim}{Q}|_m \\ -\frac{1}{12}H^2\underset{\sim}{Q}|_m \end{bmatrix} \qquad (4)$$

3.7.2.4:Alternative Virtual Work Interpolation.

The external force $\underset{\sim}{Q}_e$ can also be interpolated within an element by

$$\underset{\sim}{Q}_e = L\underset{\sim}{Q} + \bar{L}\,\underset{\sim}{\bar{Q}} = \begin{bmatrix} L & \bar{L} \end{bmatrix} \begin{bmatrix} \underset{\sim}{Q} \\ \underset{\sim}{\bar{Q}} \end{bmatrix} \qquad (A)$$

where L and $\bar{L}$ are the standard linear interpolating polynomials defined earlier. $\underset{\sim}{Q}$ and $\underset{\sim}{\bar{Q}}$ are the nodal estimates of $\underset{\sim}{Q}_e$. Using this interpolation for $\underset{\sim}{Q}_e$

$$\int_e \frac{\partial s}{\partial s_0}\,\underset{\sim}{Q}\cdot\delta\underset{\sim}{r}\,ds_0 = \frac{\partial s}{\partial s_0}\Big|_m \int_e \left\{ \begin{bmatrix} L & \bar{L} \end{bmatrix} \begin{bmatrix} \underset{\sim}{Q} \\ \underset{\sim}{\bar{Q}} \end{bmatrix} \right\}^T \begin{bmatrix} \mathcal{L} & \mathcal{H} & \bar{\mathcal{L}} & \bar{\mathcal{H}} \end{bmatrix} \begin{bmatrix} \delta\underset{\sim}{r} \\ \delta\underset{\sim}{r}' \\ \delta\underset{\sim}{\bar{r}} \\ \delta\underset{\sim}{\bar{r}}' \end{bmatrix} ds_0$$

$$= \begin{bmatrix} \delta\underset{\sim}{r} & \delta\underset{\sim}{r}' & \delta\underset{\sim}{\bar{r}} & \delta\underset{\sim}{\bar{r}}' \end{bmatrix} \begin{bmatrix} \frac{7}{20}H & \frac{3}{20}H \\ \frac{1}{20}H^2 & \frac{1}{30}H^2 \\ \frac{3}{20}H & \frac{7}{20}H \\ -\frac{1}{30}H^2 & -\frac{1}{20}H^2 \end{bmatrix} \begin{bmatrix} \underset{\sim}{Q} \\ \underset{\sim}{\bar{Q}} \end{bmatrix} \times \frac{\partial s}{\partial s_0}\Big|_m \qquad (B)$$

3.7.3:Assembly of the Equations of Motion.

The variational equation in section 3.7.1 with equations 3.7.2.1(a), 3.7.2.2(a) and the virtual work interpolation given in section 3.7.2.3 gives

$$
\begin{aligned}
0=\delta\int_{t_1}^{t_2}\Bigg\{ & \frac{H_1}{2}\frac{\rho_1}{420}\begin{bmatrix}\dot{\underset{\sim}{r}}_0 & \dot{\underset{\sim}{r}}_0' & \dot{\underset{\sim}{r}}_1 & \dot{\underset{\sim}{r}}_1'\end{bmatrix}\begin{bmatrix}156 & 22H_1 & 54 & -13H_1\\ & 4H_1^2 & 13H_1 & -3H_1^2\\ & & 156 & -22H_1\\ \text{sym.} & & & 4H_1^2\end{bmatrix}\begin{bmatrix}\dot{\underset{\sim}{r}}_0\\ \dot{\underset{\sim}{r}}_0'\\ \dot{\underset{\sim}{r}}_1\\ \dot{\underset{\sim}{r}}_1'\end{bmatrix} \\
& +\frac{H_2}{2}\frac{\rho_2}{420}\begin{bmatrix}\dot{\underset{\sim}{r}}_1 & \dot{\underset{\sim}{r}}_1' & \dot{\underset{\sim}{r}}_2 & \dot{\underset{\sim}{r}}_2'\end{bmatrix}\begin{bmatrix}156 & 22H_2 & 54 & -13H_2\\ & 4H_2^2 & 13H_2 & -3H_2^2\\ & & 156 & -22H_2\\ \text{sym.} & & & 4H_2^2\end{bmatrix}\begin{bmatrix}\dot{\underset{\sim}{r}}_1\\ \dot{\underset{\sim}{r}}_1'\\ \dot{\underset{\sim}{r}}_2\\ \dot{\underset{\sim}{r}}_2'\end{bmatrix} \qquad (A)\\
& + \ldots \\
& +\frac{H_N}{2}\frac{\rho_N}{420}\begin{bmatrix}\dot{\underset{\sim}{r}}_{N-1} & \dot{\underset{\sim}{r}}_{N-1}' & \dot{\underset{\sim}{r}}_N & \dot{\underset{\sim}{r}}_N'\end{bmatrix}\begin{bmatrix}156 & 22H_N & 54 & -13H_N\\ & 4H_N^2 & 13H_N & -3H_N^2\\ & & 156 & -22H_N\\ \text{sym.} & & & 4H_N^2\end{bmatrix}\begin{bmatrix}\dot{\underset{\sim}{r}}_{N-1}\\ \dot{\underset{\sim}{r}}_{N-1}'\\ \dot{\underset{\sim}{r}}_N\\ \dot{\underset{\sim}{r}}_N'\end{bmatrix}\Bigg\}\,dt
\end{aligned}
$$

$$-\int_{t_1}^{t_2}\Bigg\{\frac{T_1}{\left.\frac{\partial s}{\partial s_0}\right|_1}\begin{bmatrix}\delta\underset{\sim}{r}_0 & \delta\underset{\sim}{r}_0' & \delta\underset{\sim}{r}_1 & \delta\underset{\sim}{r}_1'\end{bmatrix}\begin{bmatrix}-\underset{\sim}{\epsilon}_1\\ -\underset{\sim}{\eta}_1\\ \underset{\sim}{\epsilon}_1\\ -\underset{\sim}{\eta}_1^*\end{bmatrix}+\frac{T_2}{\left.\frac{\partial s}{\partial s_0}\right|_2}\begin{bmatrix}\delta\underset{\sim}{r}_1 & \delta\underset{\sim}{r}_1' & \delta\underset{\sim}{r}_2 & \delta\underset{\sim}{r}_2'\end{bmatrix}\begin{bmatrix}-\underset{\sim}{\epsilon}_2\\ -\underset{\sim}{\eta}_2\\ \underset{\sim}{\epsilon}_2\\ -\underset{\sim}{\eta}_2^*\end{bmatrix}$$

$$+\ \cdots\ +\frac{T_N}{\left.\frac{\partial s}{\partial s_0}\right|_N}\begin{bmatrix}\delta\underset{\sim}{r}_{N-1} & \delta\underset{\sim}{r}_{N-1}' & \delta\underset{\sim}{r}_N & \delta\underset{\sim}{r}_N'\end{bmatrix}\begin{bmatrix}-\underset{\sim}{\epsilon}_N\\ -\eta_N\\ \underset{\sim}{\epsilon}_N\\ -\eta_N^*\end{bmatrix}\Bigg\}\,dt$$

$$+\int_{t_1}^{t_2}\Bigg\{\left.\frac{\partial s}{\partial s_0}\right|_1\begin{bmatrix}\delta\underset{\sim}{r}_0 & \delta\underset{\sim}{r}_0' & \delta\underset{\sim}{r}_1 & \delta\underset{\sim}{r}_1'\end{bmatrix}\begin{bmatrix}\frac{1}{2}H_1\underset{\sim}{Q}_1\\ \frac{1}{12}H_1^2\underset{\sim}{Q}_1\\ \frac{1}{2}H_1\underset{\sim}{Q}_1\\ -\frac{1}{12}H_1^2\underset{\sim}{Q}_1\end{bmatrix}+\left.\frac{\partial s}{\partial s_0}\right|_2\delta\underset{\sim}{r}_0\ \delta r$$

$$+\left.\frac{\partial s}{\partial s_0}\right|_2\begin{bmatrix}\delta\underset{\sim}{r}_1 & \delta\underset{\sim}{r}_1' & \delta\underset{\sim}{r}_2 & \delta\underset{\sim}{r}_2'\end{bmatrix}\begin{bmatrix}\frac{1}{2}H_2\underset{\sim}{Q}_2\\ \frac{1}{12}H_2^2\underset{\sim}{Q}_2\\ \frac{1}{2}H_2\underset{\sim}{Q}_2\\ -\frac{1}{12}H_2^2\underset{\sim}{Q}_2\end{bmatrix}$$

$$+\ \cdots\ +\left.\frac{\partial s}{\partial s_0}\right|_N\begin{bmatrix}\delta\underset{\sim}{r}_{N-1} & \delta\underset{\sim}{r}_{N-1}' & \delta\underset{\sim}{r}_N & \delta\underset{\sim}{r}_N'\end{bmatrix}\begin{bmatrix}\frac{1}{2}H_N\underset{\sim}{Q}_N\\ \frac{1}{12}H_N^2\underset{\sim}{Q}_N\\ \frac{1}{2}H_N\underset{\sim}{Q}_N\\ -\frac{1}{12}H_N^2\underset{\sim}{Q}_N\end{bmatrix}\Bigg\}\,dt$$

after simplification this becomes

$$0=\int_{t_1}^{t_2}\frac{1}{420}\left[\delta r_0\ \delta r_0'\ \delta r_1\ \delta r_1'\ \delta r_2\ \delta r_2'\ \ldots\ \delta r_{N-1}\ \delta r_{N-1}'\ \delta r_N\ \delta r_N'\right][M]\begin{bmatrix}\vdots\\ r_0\\ \dot{r}_0\\ \vdots\\ r_1\\ \dot{r}_1\\ \vdots\\ r_2\\ \dot{r}_2\end{bmatrix}\ dt \qquad (B)$$

$$+\int_{t_1}^{t_2}\left[\delta\underset{\sim}{r}_0 \;\; \delta\underset{\sim}{r}_0' \;\; \delta\underset{\sim}{r}_1 \;\; \delta\underset{\sim}{r}_1' \;\; \delta\underset{\sim}{r}_2 \;\; \delta\underset{\sim}{r}_2' \;\; \ldots\ldots \;\; \delta\underset{\sim}{r}_{N-1} \;\; \delta\underset{\sim}{r}_{N-1}' \;\; \delta\underset{\sim}{r}_N \;\; \delta\underset{\sim}{r}_N'\right]\begin{bmatrix} T_1^*\underset{\sim}{\epsilon}_1 \\ T_1^*\underset{\sim}{\eta}_1 \\ -T_1^*\underset{\sim}{\epsilon}_1 + T_2^*\underset{\sim}{\epsilon}_2 \\ T_1^*\underset{\sim}{\eta}_1^* + T_2^*\underset{\sim}{\eta}_2 \\ \vdots \\ -T_2^*\underset{\sim}{\epsilon}_2 \\ T_2^*\underset{\sim}{\eta}_2^* \\ \vdots \\ +T_N^*\underset{\sim}{\epsilon}_N - T_{N-1}^*\underset{\sim}{\epsilon}_{N-1} \\ +T_N^*\underset{\sim}{\eta}_N + T_{N-1}^*\underset{\sim}{\eta}_{N-1} \\ -T_N^*\underset{\sim}{\epsilon}_N \\ T_N^*\underset{\sim}{\eta}_N^* \end{bmatrix} dt$$

$$+\int_{t_1}^{t_2}\left[\delta\underset{\sim}{r}_0 \;\; \delta\underset{\sim}{r}_0' \;\; \delta\underset{\sim}{r}_1 \;\; \delta\underset{\sim}{r}_1' \;\; \delta\underset{\sim}{r}_2 \;\; \delta\underset{\sim}{r}_2' \;\; \ldots\ldots \;\; \delta\underset{\sim}{r}_{N-1} \;\; \delta\underset{\sim}{r}_{N-1}' \;\; \delta\underset{\sim}{r}_N \;\; \delta\underset{\sim}{r}_N'\right]\begin{bmatrix} \frac{1}{2}H_1\underset{\sim}{Q}_1^* \\ \frac{1}{12}H_1^2Q_1^* \\ \frac{1}{2}H_1\underset{\sim}{Q}_1^* + \frac{1}{2}H_2\underset{\sim}{Q}_2^* \\ -\frac{1}{12}H_1^2\underset{\sim}{Q}_1^* + \frac{1}{12}H_2^2\underset{\sim}{Q}_2^* \\ \vdots \\ +\frac{1}{2}H_2\underset{\sim}{Q}_2^* \\ -\frac{1}{12}H_2^2\underset{\sim}{Q}_2^* \\ \vdots \\ \frac{1}{2}H_{N-1}\underset{\sim}{Q}_{N-1}^* + \frac{1}{2}H_N\underset{\sim}{Q}_N^* \\ -\frac{1}{12}H_{N-1}^2\underset{\sim}{Q}_{N-1}^* + \frac{1}{12}H_N^2\underset{\sim}{Q}_N^* \\ +\frac{1}{2}H_N\underset{\sim}{Q}_N^* \\ -\frac{1}{12}H_N^2\underset{\sim}{Q}_N^* \end{bmatrix} dt$$

where

$$[M] =$$

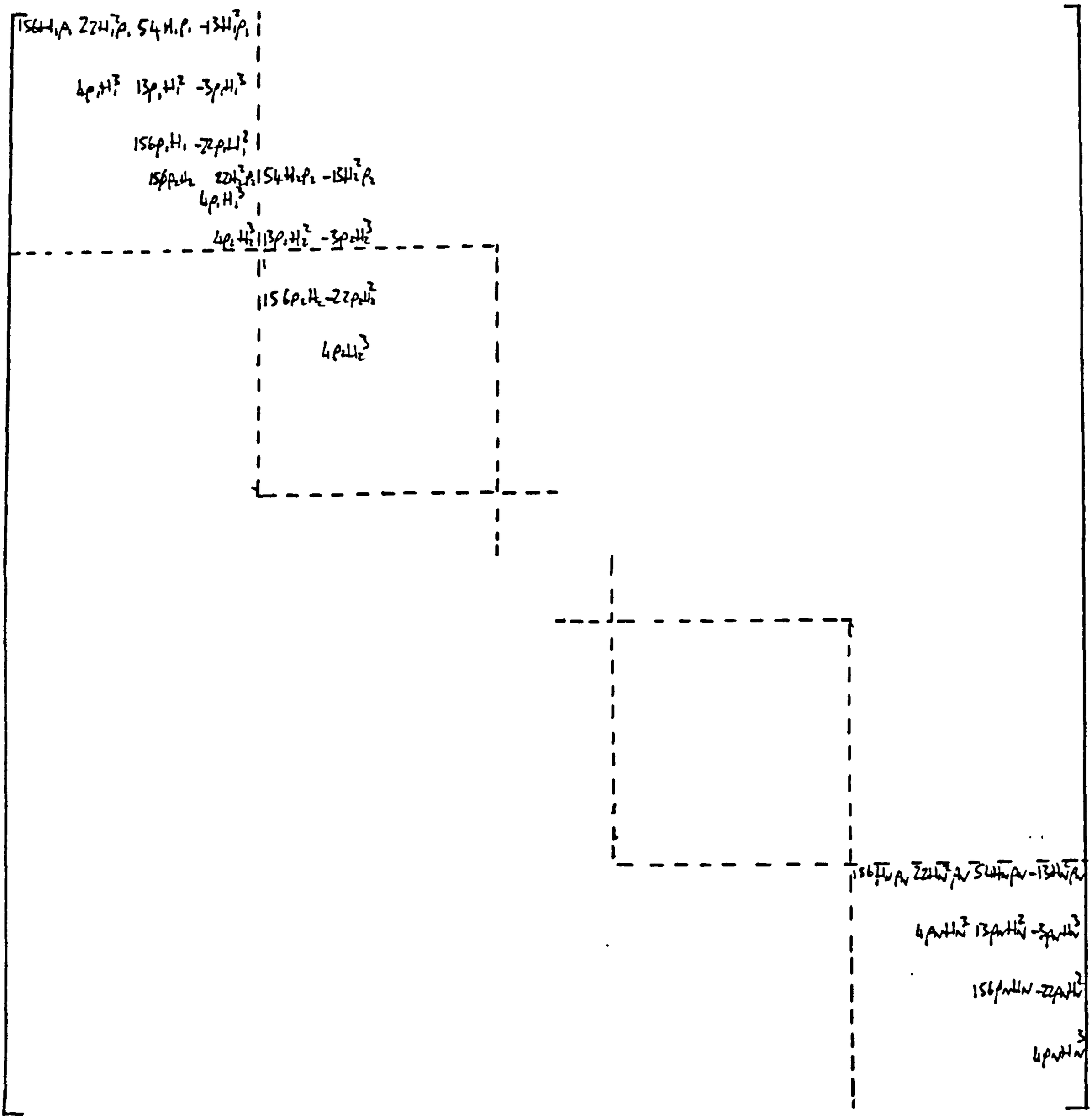

(C)

where $T_i^* = T_i \Big/ \frac{\delta s}{\delta s_0}\Big|_M$ and $\underset{\sim}{Q}_i^* = \underset{\sim}{Q}_i \frac{\delta s}{\delta s_0}\Big|_M$. This gives the equation of motion

$$[M]\begin{bmatrix} \delta\underset{\sim}{r}_0' \\ \delta\underset{\sim}{r}_1 \\ \delta\underset{\sim}{r}_1' \\ \delta\underset{\sim}{r}_2 \\ \delta\underset{\sim}{r}_2' \\ \vdots \\ \delta\underset{\sim}{r}_{N-1} \\ \delta\underset{\sim}{r}_{N-1}' \\ \delta\underset{\sim}{r}_N \end{bmatrix} = \begin{bmatrix} T_1^*\underset{\sim}{\eta}_1 \\ -T_1^*\underset{\sim}{\epsilon}_1 + T_2^*\underset{\sim}{\epsilon}_2 \\ T_1^*\underset{\sim}{\eta}_1^* + T_2\underset{\sim}{\eta}_2 \\ -T_2^*\underset{\sim}{\epsilon}_2 \\ +T_2^*\underset{\sim}{\eta}_2^* \\ \vdots \\ T_N^*\underset{\sim}{\epsilon}_N - T_{N-1}^*\underset{\sim}{\epsilon}_{N-1} \\ T_N^*\underset{\sim}{\eta}_N - T_{N-1}^*\underset{\sim}{\eta}_{N-1}^* \\ T_N^*\underset{\sim}{\eta}_N^* \end{bmatrix} + \begin{bmatrix} \frac{1}{12}H_1^2\underset{\sim}{Q}_1^* \\ \frac{1}{2}H_1\underset{\sim}{Q}_1^* + \frac{1}{2}H_2\underset{\sim}{Q}_2^* \\ -\frac{1}{12}H_1^2\underset{\sim}{Q}_1^* + \frac{1}{12}H_2^2\underset{\sim}{Q}_2^* \\ +\frac{1}{2}H_2\underset{\sim}{Q}_2^* \\ -\frac{1}{12}H_2\underset{\sim}{Q}_2^* \\ \vdots \\ \frac{1}{2}H_{N-1}\underset{\sim}{Q}_{N-1}^* + \frac{1}{2}H_N\underset{\sim}{Q}_N^* \\ -\frac{1}{12}H_{N-1}^2\underset{\sim}{Q}_{N-1}^* + \frac{1}{12}H_N^2\underset{\sim}{Q}_N^* \\ -\frac{1}{12}H_N^2\underset{\sim}{Q}_N^* \end{bmatrix} \qquad (A)$$

where

$$[M] = \frac{1}{420}\times\begin{bmatrix} 4\rho_1H_1^3 & 13\rho_1H_1^2 & -3\rho_1H_1^3 & & & & & & \\ & 156\rho_1H_1 \;\; 156\rho_2H_2 & -22\rho_1H_1^2 \;\; 22\rho_2H_2^2 & 54\rho_2H_2 & -13H_2^2\rho_2 & & & & \\ & & 4\rho_1H_1^3 \;\; 4\rho_2H_2^3 & 13\rho_2H_2^2 & -3\rho_2H_2^3 & & & & \\ & & & 156\rho_2H_2 & -22\rho_2H_2^2 & & & & \\ & & & & 4\rho_2H_2^3 & & & & \\ & & & & & \ddots & & & \\ & & & & & & 156\rho_NH_N & 22\rho_NH_N^2 & -13\rho_NH_N^2 \\ & & & & & & 22\rho_NH_N^2 & 4\rho_NH_N^3 & -3\rho_NH_N^3 \\ & & & & & & & -3\rho_NH_N^3 & 4\rho_NH_N^3 \end{bmatrix} \qquad (D)$$

Note that $\underset{\sim}{\Gamma}_0$ and $\underset{\sim}{\Gamma}_N$ are constant so $\delta\underset{\sim}{\Gamma}_0 = \delta\underset{\sim}{\Gamma}_N = \dot{\underset{\sim}{\Gamma}}_0 = \dot{\underset{\sim}{\Gamma}}_N = 0$.

3.7.4:Alteration to the Equations of Motion caused by Alternative Interpolation for Virtual Work.

With the alternative virtual work interpolation given in section 3.7.5 the net virtual work done on the riser may be written

$$\left[\delta\underset{\sim}{\Gamma}_0 \quad \delta\underset{\sim}{\Gamma}_0' \quad \delta\underset{\sim}{\Gamma}_1 \quad \delta\underset{\sim}{\Gamma}_1'\right]\begin{bmatrix} \frac{7}{20}H_1\underset{\sim}{Q}_0^* + \frac{3}{20}H_1\underset{\sim}{Q}_1^* \\ \frac{1}{20}H_1^2\underset{\sim}{Q}_0^* + \frac{1}{30}H_1^2\underset{\sim}{Q}_1^* \\ \frac{3}{20}H_1\underset{\sim}{Q}_0^* + \frac{7}{20}H_1\underset{\sim}{Q}_1^* \\ -\frac{1}{30}H_1^2\underset{\sim}{Q}_0^* - \frac{1}{20}H_1^2\underset{\sim}{Q}_1^* \end{bmatrix} + \left[\delta\underset{\sim}{\Gamma}_1 \quad \delta\underset{\sim}{\Gamma}_1' \quad \delta\underset{\sim}{\Gamma}_2 \quad \delta\underset{\sim}{\Gamma}_2'\right]\begin{bmatrix} \frac{7}{20}H_2\underset{\sim}{Q}_1^* + \frac{3}{20}H_2\underset{\sim}{Q}_2^* \\ \frac{1}{20}H_2^2\underset{\sim}{Q}_1^* + \frac{1}{30}H_2^2\underset{\sim}{Q}_2^* \\ \frac{3}{20}H_2\underset{\sim}{Q}_1^* + \frac{7}{20}H_2\underset{\sim}{Q}_2^* \\ -\frac{1}{30}H_2^2\underset{\sim}{Q}_1^* - \frac{1}{20}H_2^2\underset{\sim}{Q}_2^* \end{bmatrix} + \ldots$$

$$\ldots + \left[\delta\underset{\sim}{\Gamma}_{N-1} \quad \delta\underset{\sim}{\Gamma}_{N-1}' \quad \delta\underset{\sim}{\Gamma}_N \quad \delta\underset{\sim}{\Gamma}_N'\right]\begin{bmatrix} \frac{7}{20}H_N\underset{\sim}{Q}_{N-1}^* + \frac{3}{20}H_N\underset{\sim}{Q}_N^* \\ \frac{1}{20}H_N^2\underset{\sim}{Q}_{N-1}^* + \frac{1}{30}H_N^2\underset{\sim}{Q}_N^* \\ \frac{3}{20}H_N\underset{\sim}{Q}_{N-1}^* + \frac{7}{20}H_N\underset{\sim}{Q}_N^* \\ -\frac{1}{30}H_N^2\underset{\sim}{Q}_{N-1}^* - \frac{1}{20}H_N^2\underset{\sim}{Q}_N^* \end{bmatrix} \qquad (A)$$

Note that the $\underset{\sim}{Q}_i$ in the above equation is the nodal value of $\underset{\sim}{Q}$ and not the element value of $\underset{\sim}{Q}$. With the alternative force interpolation if the above equation is used then the force term on the right hand side of equations (a) must be replaced by the alternative force term

$$
\begin{bmatrix}
\frac{1}{20}H_1^2\underset{\sim}{Q}_0^* + \frac{1}{30}H_1^2\underset{\sim}{Q}_1^* & \\
\frac{3}{20}H_1\underset{\sim}{Q}_0^* + \frac{7}{20}H_1\underset{\sim}{Q}_1^* & + \frac{7}{20}H_2\underset{\sim}{Q}_1^* + \frac{3}{20}H_2\underset{\sim}{Q}_2^* \\
-\frac{1}{30}H_1^2\underset{\sim}{Q}_0^* - \frac{1}{20}H_1^2\underset{\sim}{Q}_1^* & + \frac{1}{20}H_2^2\underset{\sim}{Q}_1^* + \frac{1}{30}H_2^2\underset{\sim}{Q}_2^* \\
 & + \frac{3}{20}H_2\underset{\sim}{Q}_1^* + \frac{7}{20}H_2\underset{\sim}{Q}_2^* \\
 & - \frac{1}{30}H_2^2\underset{\sim}{Q}_1^* - \frac{1}{20}H_2^2\underset{\sim}{Q}_2^* \\
 & \vdots \\
 & \frac{7}{20}H_{N-1}\underset{\sim}{Q}_{N-2}^* + \frac{3}{20}H_{N-1}\underset{\sim}{Q}_{N-1}^* \\
 & \frac{1}{20}H_{N-1}^2\underset{\sim}{Q}_{N-2}^* + \frac{1}{30}H_{N-1}^2\underset{\sim}{Q}_{N-1}^* \\
\frac{7}{20}H_N\underset{\sim}{Q}_{N-1}^* + \frac{3}{20}H_N\underset{\sim}{Q}_N^* & + \frac{3}{20}H_{N-1}\underset{\sim}{Q}_{N-2}^* + \frac{7}{20}H_{N-1}\underset{\sim}{Q}_{N-1}^* \\
\frac{1}{20}H_N^2\underset{\sim}{Q}_{N-1}^* + \frac{1}{30}H_N^2\underset{\sim}{Q}_N^* & - \frac{1}{30}H_{N-1}^2\underset{\sim}{Q}_{N-2}^* - \frac{1}{20}H_{N-1}^2\underset{\sim}{Q}_{N-1}^* \\
-\frac{1}{30}H_N^2\underset{\sim}{Q}_{N-1}^* + \frac{1}{20}H_N^2\underset{\sim}{Q}_N^* &
\end{bmatrix} \qquad (B)
$$

3.7.5:Relationships the Element Forces.

In this section expressions are given for the evaluation of the element force terms $\underset{\sim}{Q}|_m$. For the ith element $\underset{\sim}{Q}|_m$ will be denoted by $\underset{\sim}{Q}_i\ (i=1,\ldots,N)$ in this section. $\underset{\sim}{Q}_i$ may be written

$$\underset{\sim}{Q}_i = \underset{\sim}{M}_{ei}^* + \underset{\sim}{f}_{pi}^* + \underset{\sim}{U}_{ei}^* \qquad (A)$$

where $\underset{\sim}{M}^*_{e_i}$ = element Morison force per unit of strained arc-length, $\underset{\sim}{G}^*_{e_i}$ = element force per unit of strained arc-length due to gravity and $\underset{\sim}{U}^*_{e_i}$ = element upthrust force per unit of strained arc-length.

$\underset{\sim}{G}^*_{e_i}$ is calculated using the equations

$$\underset{\sim}{G}^*_{e_1} = -\rho_1 g \underset{\sim}{k} \Big/ \frac{\partial s}{\partial s_0}\Big|_1$$

$$\underset{\sim}{G}^*_{e_2} = -\rho_2 g \underset{\sim}{k} \Big/ \frac{\partial s}{\partial s_0}\Big|_2 \qquad (B)$$

$$\vdots$$

$$\underset{\sim}{G}^*_{e_N} = -\rho_N g \underset{\sim}{k} \Big/ \frac{\partial s}{\partial s_0}\Big|_N$$

where ρ_i $(i=1,\ldots,N)$ = density per unit length of the riser in an unstrained reference state at the middle of the ith element and $\frac{\partial s}{\partial s_0}\Big|_i$ $(i=1,\ldots,N)$ denotes the value of $\frac{\partial s}{\partial s_0}$ at the middle of the ith element.

$\underset{\sim}{U}^*_{e_i}$ is calculated using the equations

$$\underset{\sim}{U}^*_{e_1} = A_1 \rho_w g \underset{\sim}{k}$$

$$\underset{\sim}{U}^*_{e_2} = A_2 \rho_w g \underset{\sim}{k} \qquad (C)$$

$$\vdots$$

$$\underset{\sim}{U}^*_{e_N} = A_N \rho_w g \underset{\sim}{k}$$

where A_i = cross-sectional area of the middle of the ith

element in the strained state. A_i is not necessarily constant and may for example depend on the strain in an element.

3.7.5.1:Element Morison Forces.

From section 2.1.2 the element Morison forces $\underset{\sim}{M}_{ei}^{*}$ may be written in the form

$$\underset{\sim}{M}_{ei}^{*} = \underset{\sim}{D}_{ei}^{*} + \underset{\sim}{I}_{ei}^{*} + \underset{\sim}{A}_{ei}^{*} \qquad (A)$$

where $\underset{\sim}{D}_{ei}^{*}$ = element drag force, $\underset{\sim}{I}_{ei}^{*}$ = element inertia force and $\underset{\sim}{A}_{ei}^{*}$ = element added mass force. $\underset{\sim}{D}_{ei}^{*}$, $\underset{\sim}{I}_{ei}^{*}$ and $\underset{\sim}{A}_{ei}^{*}$ are all evaluated per unit of strained arc-length.

$\underset{\sim}{I}_{ei}^{*}$ is calculated using the equations

$$\underset{\sim}{I}_{e1}^{*} = \frac{1}{4}\pi\rho_w D_1^2 (1+C_A)\, \dot{\underset{\sim}{u}}_{f1}|_{n_1^*} \qquad (B)$$

$$\underset{\sim}{I}_{e2}^{*} = \frac{1}{4}\pi\rho_w D_2^2 (1+C_A)\, \dot{\underset{\sim}{u}}_{f2}|_{n_2^*}$$

$$\vdots$$

$$\underset{\sim}{I}_{eN}^{*} = \frac{1}{4}\pi\rho_w D_N^2 (1+C_A)\, \dot{\underset{\sim}{u}}_{fN}|_{n_N^*}$$

where $\underset{\sim}{u}_{fi}$ = fluid velocity evaluated at the middle of the ith element and D_i = diameter of the element. Note that D_i is not necessarily constant. $\underset{\sim}{v}|_{n_j^*}$ is defined by

$$\underset{\sim}{v}|_{n_j^*} = \underset{\sim}{v} - (\underset{\sim}{v}\cdot\underset{\sim}{t}_j^{*})\,\underset{\sim}{t}_j^{*} \qquad (C)$$

where $\underset{\sim}{t}_j^{*}$ =unit tangent vector at the middle of the element

$$\underset{\sim}{t}_j^{*} = \frac{\partial \underset{\sim}{r}_e}{\partial s_0}\Big|_m \Big/ \frac{ds}{ds_0}\Big|_m \qquad (D)$$

where $\left.\frac{\partial \underset{\sim}{r}_e}{\partial s_0}\right|_m$ and $\left.\frac{\partial s}{\partial s_0}\right|_m$ have been given in section 3.7.3.

The element drag force $\underset{\sim}{D}^*_{e_i}$ is given by the equations

$$\underset{\sim}{D}^*_{e_1} = \tfrac{1}{2}\rho_w D_1 \left(\underset{\sim}{u}_{f_1} - \dot{\underset{\sim}{r}}_{e_1}\right)\Big|_{n_1^*} \left| \left(\underset{\sim}{u}_{f_1} - \dot{\underset{\sim}{r}}_{e_1}\right)\Big|_{n_1^*} \right| \qquad (E)$$

$$\underset{\sim}{D}^*_{e_2} = \tfrac{1}{2}\rho_w D_2 \left(\underset{\sim}{u}_{f_2} - \dot{\underset{\sim}{r}}_{e_2}\right)\Big|_{n_2^*} \left| \left(\underset{\sim}{u}_{f_2} - \dot{\underset{\sim}{r}}_{e_2}\right)\Big|_{n_2^*} \right|$$

$$\vdots$$

$$\underset{\sim}{D}^*_{e_N} = \tfrac{1}{2}\rho_w D_N \left(\underset{\sim}{u}_{f_N} - \dot{\underset{\sim}{r}}_{e_N}\right)\Big|_{n_N^*} \left| \left(\underset{\sim}{u}_{f_N} - \dot{\underset{\sim}{r}}_{e_N}\right)\Big|_{n_N^*} \right|$$

where $\dot{\underset{\sim}{r}}_{e_i}$ is found from

$$\dot{\underset{\sim}{r}}_{e_i} = \begin{bmatrix} \mathcal{L} & \mathcal{H} & \bar{\mathcal{L}} & \bar{\mathcal{H}} \end{bmatrix} \left[\begin{array}{c} \underset{\sim}{r} \\ \dot{\underset{\sim}{r}} \\ \underset{\sim}{r}' \\ \dot{\underset{\sim}{r}}' \end{array}\right]\Bigg|_m = \begin{bmatrix} \frac{1}{2} & \frac{1}{8}H & \frac{1}{2} & -\frac{1}{8}H \end{bmatrix} \left[\begin{array}{c} \underset{\sim}{r} \\ \dot{\underset{\sim}{r}} \\ \underset{\sim}{r}' \\ \dot{\underset{\sim}{r}}' \end{array}\right] \qquad (F)$$

The element added mass force $\underset{\sim}{A}^*_{e_i}$ is given by the equations

$$\underset{\sim}{A}^*_{e_1} = -\tfrac{1}{4}\pi\rho_w D_1^2 C_A \ \ddot{\underset{\sim}{r}}_{e_1}\Big|_{n_1^*} \qquad (G)$$

$$\underset{\sim}{A}^*_{e_2} = -\tfrac{1}{4}\pi\rho_w D_2^2 C_A \ \ddot{\underset{\sim}{r}}_{e_2}\Big|_{n_2^*}$$

$$\vdots$$

$$\underset{\sim}{A}^*_{e_N} = -\tfrac{1}{4}\pi\rho_w D_N^2 C_A \ \ddot{\underset{\sim}{r}}_{e_N}\Big|_{n_N^*}$$

where $\ddot{\underset{\sim}{r}}_{e_i}$ is found from

$$\ddot{\underset{\sim}{r}}_{e_i} = \begin{bmatrix} \frac{1}{2} & \frac{1}{8}H & \frac{1}{2} & -\frac{1}{8}H \end{bmatrix} \left[\begin{array}{c} \dot{\underset{\sim}{r}} \\ \ddot{\underset{\sim}{r}} \\ \dot{\underset{\sim}{r}}' \\ \ddot{\underset{\sim}{r}}' \end{array}\right] \qquad (H)$$

3.7.6:Extraction of the Added Mass Matrix.

From the force term occuring in the equations of motion those parts that are due to the added mass forces may be extracted as

$$\begin{bmatrix} \frac{1}{2}H_1\bar{A}_1^{\cdot\cdot} \\ \frac{1}{12}H_1^2\bar{A}_1^{\cdot\cdot} \\ \frac{1}{2}H_1\bar{A}_1^{\cdot\cdot} + \frac{1}{2}H_2\bar{A}_2^{\cdot\cdot} \\ -\frac{1}{12}H_1^2\bar{A}_1^{\cdot\cdot} + \frac{1}{12}H_2\bar{A}_2^{\cdot\cdot} \\ \frac{1}{2}H_2\bar{A}_2^{\cdot\cdot} + \frac{1}{2}H_2\bar{A}_2^{\cdot\cdot} \\ \frac{1}{12}H_2\bar{A}_2^{\cdot\cdot} - \frac{1}{12}H_2\bar{A}_2^{\cdot\cdot} \\ \vdots \\ \frac{1}{2}H_N\bar{A}_N^{\cdot\cdot} + \frac{1}{2}H_{N-1}\bar{A}_{N-1}^{\cdot\cdot} \\ \frac{1}{12}H_N\bar{A}_N^{\cdot\cdot} - \frac{1}{12}H_{N-1}^2\bar{A}_{N-1}^{\cdot\cdot} \\ \frac{1}{2}H_N\bar{A}_N^{\cdot\cdot} \\ -\frac{1}{12}H_N^2\bar{A}_N^{\cdot\cdot} \end{bmatrix} \qquad (A)$$

where $\bar{A}_i^{**} = \frac{-1}{\partial s/\partial s_0|_m} \cdot \frac{1}{4}\pi\rho_w D_i^2 C_A \ddot{r}_{ei}|_{n_i^*}$. If T_i is defined so that $H_i\bar{A}_i^{**} = T_i\ddot{r}_{ei}$ then using equation 3.7.5.1(a) allows the added mass force term to be written in the matrix form

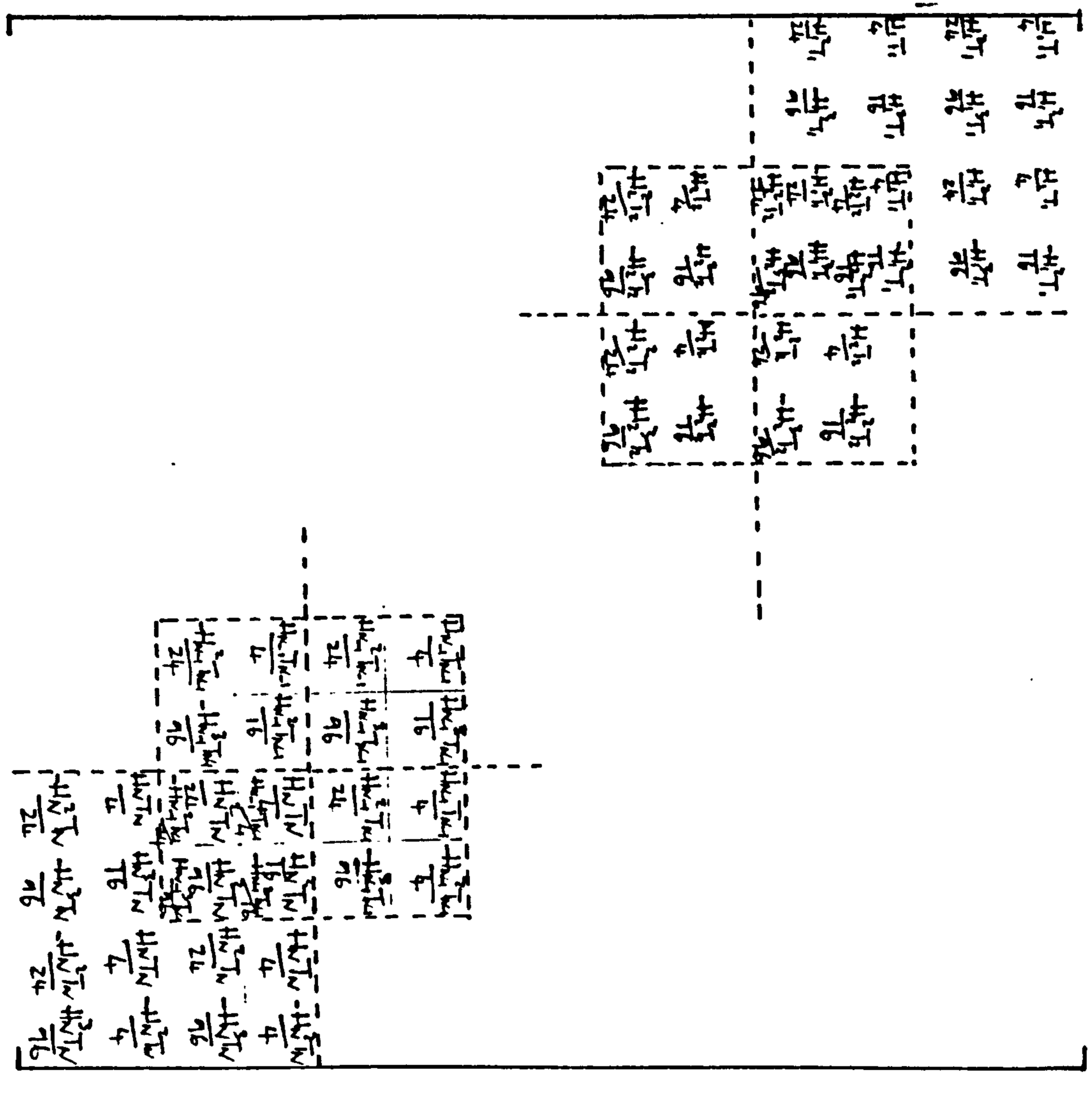

(B)

3.7.7:Calculation of Riser Curvature.

Manufacturers normally specify the maximum curvature that is permissible for a flexible riser of a given diameter and construction. It is thus useful to be able to estimate the riser curvature from the computed results of a given discretization. With the discretization of section 3.7 it is particularly simple to do this.

The curvature K is given by

$$K = \left\{ \frac{\partial^2 \underset{\sim}{r}}{\partial s^2} \cdot \frac{\partial^2 \underset{\sim}{r}}{\partial s^2} \right\}^{\frac{1}{2}} \qquad (A)$$

$\frac{\partial^2 \underset{\sim}{r}}{\partial s^2}$ can be calculated from

$$\frac{\partial^2 \underset{\sim}{r}}{\partial s^2} = \frac{1}{\left(\frac{\partial s}{\partial s_0}\right)^2} \left\{ \frac{\partial^2 \underset{\sim}{r}}{\partial s_0^2} - \frac{1}{\left(\frac{\partial s}{\partial s_0}\right)} \frac{\partial \underset{\sim}{r}}{\partial s_0} \frac{\partial^2 s}{\partial s_0^2} \right\} \qquad (B)$$

(the above expression is obtained by simple differentiation)

now

$$\frac{\partial^2 \underset{\sim}{r}}{\partial s_0^2} = \begin{bmatrix} \mathcal{Z}'' & \mathcal{H}'' & \bar{\mathcal{Z}}'' & \bar{\mathcal{H}}'' \end{bmatrix} \begin{bmatrix} \underset{\sim}{r} \\ \underset{\sim}{r}' \\ \bar{\underset{\sim}{r}} \\ \bar{\underset{\sim}{r}}' \end{bmatrix} \qquad (C)$$

and similarly

$$\frac{\partial \underset{\sim}{r}}{\partial s_0} = \begin{bmatrix} \mathcal{Z}' & \mathcal{H}' & \bar{\mathcal{Z}}' & \bar{\mathcal{H}}' \end{bmatrix} \begin{bmatrix} \underset{\sim}{r} \\ \underset{\sim}{r}' \\ \bar{\underset{\sim}{r}} \\ \bar{\underset{\sim}{r}}' \end{bmatrix} \qquad (D)$$

also

$$\frac{\partial^2 s}{\partial s_0^2} = \frac{\partial}{\partial s_0}\left\{\frac{\partial \underset{\sim}{r}}{\partial s_0}\cdot\frac{\partial \underset{\sim}{r}}{\partial s_0}\right\}^{\frac{1}{2}} \qquad (E)$$

$$= \frac{1}{\frac{\partial s}{\partial s_0}}\ \frac{\partial^2 \underset{\sim}{r}}{\partial s_0^2}\cdot\frac{\partial \underset{\sim}{r}}{\partial s_0}$$

therefore at any point within an element

$$\frac{\partial^2 \underset{\sim}{r}}{\partial s^2} = \frac{1}{\left(\frac{\partial s}{\partial s_0}\right)^2}\left\{\frac{\partial^2 \underset{\sim}{r}}{\partial s_0^2} - \frac{1}{\left(\frac{\partial s}{\partial s_0}\right)^2}\ \frac{\partial \underset{\sim}{r}}{\partial s_0}\left(\frac{\partial \underset{\sim}{r}}{\partial s_0}\cdot\frac{\partial^2 \underset{\sim}{r}}{\partial s_0^2}\right)\right\} \qquad (F)$$

$$= \frac{1}{\left(\frac{\partial s}{\partial s_0}\right)^2}\left\{\begin{bmatrix} \mathcal{L}'' & \mathcal{H}'' & \bar{\mathcal{L}}'' & \bar{\mathcal{H}}'' \end{bmatrix}\begin{bmatrix} \underset{\sim}{r} \\ \underset{\sim}{r}' \\ \bar{\underset{\sim}{r}} \\ \bar{\underset{\sim}{r}}' \end{bmatrix}\right.$$

$$\left. - \frac{1}{\left(\frac{\partial s}{\partial s_0}\right)^2}\begin{bmatrix} \mathcal{L}' & \mathcal{H}' & \bar{\mathcal{L}}' & \bar{\mathcal{H}}' \end{bmatrix}\begin{bmatrix} \underset{\sim}{r} \\ \underset{\sim}{r}' \\ \bar{\underset{\sim}{r}} \\ \bar{\underset{\sim}{r}}' \end{bmatrix}\left(\begin{bmatrix} \underset{\sim}{r} & \underset{\sim}{r}' & \bar{\underset{\sim}{r}} & \bar{\underset{\sim}{r}}' \end{bmatrix}\begin{bmatrix} \mathcal{L}'\mathcal{L}'' & \mathcal{L}'\mathcal{H}'' & \mathcal{L}'\bar{\mathcal{L}}'' & \mathcal{L}'\bar{\mathcal{H}}'' \\ \mathcal{H}'\mathcal{L}'' & \mathcal{H}'\mathcal{H}'' & \mathcal{H}'\bar{\mathcal{L}}'' & \mathcal{H}'\bar{\mathcal{H}}'' \\ \bar{\mathcal{L}}'\mathcal{L}'' & \bar{\mathcal{L}}'\mathcal{H}'' & \bar{\mathcal{L}}'\bar{\mathcal{L}}'' & \bar{\mathcal{L}}'\bar{\mathcal{H}}'' \\ \bar{\mathcal{H}}'\mathcal{L}'' & \bar{\mathcal{H}}'\mathcal{H}'' & \bar{\mathcal{H}}'\bar{\mathcal{L}}'' & \bar{\mathcal{H}}'\bar{\mathcal{H}}'' \end{bmatrix}\begin{bmatrix} \underset{\sim}{r} \\ \underset{\sim}{r}' \\ \bar{\underset{\sim}{r}} \\ \bar{\underset{\sim}{r}}' \end{bmatrix}\right)\right\}$$

where $\frac{\partial s}{\partial s_0}$ is calculated from

$$\frac{\partial s}{\partial s_0} = \left\{\begin{bmatrix} \underset{\sim}{r} & \underset{\sim}{r}' & \bar{\underset{\sim}{r}} & \bar{\underset{\sim}{r}}' \end{bmatrix}\begin{bmatrix} \mathcal{L}'^2 & \mathcal{L}'\mathcal{H}' & \mathcal{L}'\bar{\mathcal{L}}' & \mathcal{L}'\bar{\mathcal{H}}' \\ & \mathcal{H}'^2 & \mathcal{H}'\bar{\mathcal{L}}' & \mathcal{H}'\bar{\mathcal{H}}' \\ & & \bar{\mathcal{L}}'^2 & \bar{\mathcal{L}}'\bar{\mathcal{H}}' \\ \text{symm.} & & & \bar{\mathcal{H}}'^2 \end{bmatrix}\begin{bmatrix} \underset{\sim}{r} \\ \underset{\sim}{r}' \\ \bar{\underset{\sim}{r}} \\ \bar{\underset{\sim}{r}}' \end{bmatrix}\right\}^{\frac{1}{2}} \qquad (G)$$

If the strain in the riser is small enough the approximation

$$\frac{\delta^2 \underset{\sim}{r}}{\delta s^2} = \begin{bmatrix} \mathcal{L}'' & \mathcal{H}'' & \bar{\mathcal{L}}'' & \bar{\mathcal{H}}'' \end{bmatrix} \begin{bmatrix} \underset{\sim}{r} \\ \underset{\sim}{r}' \\ \bar{\underset{\sim}{r}} \\ \bar{\underset{\sim}{r}}' \end{bmatrix} \qquad (G)$$

may be used. The second derivative may now be expressed in terms in terms of the linear interpolating polynomials to give

$$\frac{\delta^2 \underset{\sim}{r}}{\delta s^2} = \begin{bmatrix} \frac{6}{H^2}(1-2L) & , \frac{2}{H}(1-3L) & , \frac{6}{H^2}(1-2\bar{L}) & , -\frac{2}{H}(1-3\bar{L}) \end{bmatrix} \begin{bmatrix} \underset{\sim}{r} \\ \underset{\sim}{r}' \\ \bar{\underset{\sim}{r}} \\ \bar{\underset{\sim}{r}}' \end{bmatrix} \qquad (H)$$

If it is needed to find the curvature at the centres of the elements only then

$$\frac{\delta^2 \underset{\sim}{r}}{\delta s^2} = \frac{1}{H}\left(\bar{\underset{\sim}{r}}' - \underset{\sim}{r}'\right) \qquad (I)$$

may be used.

3.7.8:Incremental Calculation of the Tensions.

To calculate the tensions in the elements at the mid-points the equation

$$T_M = AE\left(\frac{\delta s}{\delta s_0}\Big|_M - 1\right) \qquad (A)$$

could be used, however to do so would give rise to numerical instability for the reasons given in section 3.2.8. The tension terms T_M must therefore be calculated incrementally.

Using equations 3.7.7(a) in equation 3.7.8(a) gives

$$T_M = AE\left\{\left(\begin{bmatrix} \underset{\sim}{r} & \underset{\sim}{r}' & \underset{\sim}{\bar{r}} & \underset{\sim}{\bar{r}}' \end{bmatrix} \begin{bmatrix} \frac{9}{4H^2} & \frac{3}{8H} & \frac{-9}{4H^2} & \frac{3}{8H} \\ & \frac{1}{16} & \frac{-3}{8H} & \frac{1}{16} \\ & & \frac{9}{4H^2} & \frac{-3}{8H} \\ \text{sym.} & & & \frac{1}{16} \end{bmatrix} \begin{bmatrix} \underset{\sim}{r} \\ \underset{\sim}{r}' \\ \underset{\sim}{\bar{r}} \\ \underset{\sim}{\bar{r}}' \end{bmatrix}\right)^{\frac{1}{2}} - 1\right\} \quad (A)$$

therefore for a change $\Delta\underset{\sim}{r}$, $\Delta\underset{\sim}{\bar{r}}$, $\Delta\underset{\sim}{r}'$ and $\Delta\underset{\sim}{\bar{r}}'$ in the nodal degrees of freedom of the element the change ΔT_m in the mid-point tension may be found from

$$T + \Delta T_m = AE\left\{\left(\begin{bmatrix} \underset{\sim}{r} & \underset{\sim}{r}' & \underset{\sim}{\bar{r}} & \underset{\sim}{\bar{r}}' \end{bmatrix} \begin{bmatrix} \frac{9}{4H^2} & \frac{3}{8H} & \frac{-9}{4H^2} & \frac{3}{8H} \\ & \frac{1}{16} & \frac{-3}{8H} & \frac{1}{16} \\ & & \frac{9}{4H^2} & \frac{-3}{8H} \\ \text{sym.} & & & \frac{1}{16} \end{bmatrix} \begin{bmatrix} \underset{\sim}{r} \\ \underset{\sim}{r}' \\ \underset{\sim}{\bar{r}} \\ \underset{\sim}{\bar{r}}' \end{bmatrix}\right.$$

$$+ 2\begin{bmatrix} \Delta\underset{\sim}{r} & \Delta\underset{\sim}{r}' & \Delta\underset{\sim}{\bar{r}} & \Delta\underset{\sim}{\bar{r}}' \end{bmatrix} \begin{bmatrix} \frac{9}{4H^2} & \frac{3}{8H} & \frac{-9}{4H^2} & \frac{3}{8H} \\ & \frac{1}{16} & \frac{-3}{8H} & \frac{1}{16} \\ & & \frac{9}{4H^2} & \frac{-3}{8H} \\ \text{sym.} & & & \frac{1}{16} \end{bmatrix} \begin{bmatrix} \underset{\sim}{r} \\ \underset{\sim}{r}' \\ \underset{\sim}{\bar{r}} \\ \underset{\sim}{\bar{r}}' \end{bmatrix}$$

$$\left. + \begin{bmatrix} \Delta\underset{\sim}{r} & \Delta\underset{\sim}{r}' & \Delta\underset{\sim}{\bar{r}} & \Delta\underset{\sim}{\bar{r}}' \end{bmatrix} \begin{bmatrix} \frac{9}{4H^2} & \frac{3}{8H} & \frac{-9}{4H^2} & \frac{3}{8H} \\ & \frac{1}{16} & \frac{-3}{8H} & \frac{1}{16} \\ & & \frac{9}{4H^2} & \frac{-3}{8H} \\ \text{sym.} & & & \frac{1}{16} \end{bmatrix} \begin{bmatrix} \Delta\underset{\sim}{r} \\ \Delta\underset{\sim}{r}' \\ \Delta\underset{\sim}{\bar{r}} \\ \Delta\underset{\sim}{\bar{r}}' \end{bmatrix}\right)^{\frac{1}{2}} - 1\right\} \quad (B)$$

Let

$$\bar{\Delta} = \left\{ 2 \begin{bmatrix} \Delta\underset{\sim}{\Gamma} & \Delta\underset{\sim}{\Gamma}' & \Delta\bar{\underset{\sim}{\Gamma}} & \Delta\bar{\underset{\sim}{\Gamma}}' \end{bmatrix} \begin{bmatrix} \frac{4}{4H^2} & \frac{3}{8H} & \frac{-9}{4H^2} & \frac{3}{8H} \\ & \frac{1}{16} & \frac{-3}{8H} & \frac{1}{16} \\ & & \frac{9}{4H^2} & \frac{-3}{8H} \\ \text{sym.} & & & \frac{1}{16} \end{bmatrix} \begin{bmatrix} \underset{\sim}{\Gamma} \\ \underset{\sim}{\Gamma}' \\ \bar{\underset{\sim}{\Gamma}} \\ \bar{\underset{\sim}{\Gamma}}' \end{bmatrix} \right.$$

$$\left. + \begin{bmatrix} \Delta\underset{\sim}{\Gamma} & \Delta\underset{\sim}{\Gamma}' & \Delta\bar{\underset{\sim}{\Gamma}} & \Delta\bar{\underset{\sim}{\Gamma}}' \end{bmatrix} \begin{bmatrix} \frac{1}{4H^2} & \frac{3}{8H} & \frac{-9}{4H^2} & \frac{3}{8H} \\ & \frac{1}{16} & \frac{-3}{8H} & \frac{1}{16} \\ & & \frac{9}{4H^2} & \frac{-3}{8H} \\ \text{sym.} & & & \frac{1}{16} \end{bmatrix} \begin{bmatrix} \Delta\underset{\sim}{\Gamma} \\ \Delta\underset{\sim}{\Gamma}' \\ \Delta\bar{\underset{\sim}{\Gamma}} \\ \Delta\bar{\underset{\sim}{\Gamma}}' \end{bmatrix} \right\} \qquad (C)$$

$$\times \left\{ \begin{bmatrix} \underset{\sim}{\Gamma} & \underset{\sim}{\Gamma}' & \bar{\underset{\sim}{\Gamma}} & \bar{\underset{\sim}{\Gamma}}' \end{bmatrix} \begin{bmatrix} \frac{9}{4H^2} & \frac{3}{8H} & \frac{-9}{4H^2} & \frac{3}{8H} \\ & \frac{1}{16} & \frac{-3}{8H} & \frac{1}{16} \\ & & \frac{9}{4H^2} & \frac{-3}{8H} \\ \text{sym.} & & & \frac{1}{16} \end{bmatrix} \begin{bmatrix} \underset{\sim}{\Gamma} \\ \underset{\sim}{\Gamma}' \\ \bar{\underset{\sim}{\Gamma}} \\ \bar{\underset{\sim}{\Gamma}}' \end{bmatrix} \right\}^{-1}$$

therefore using a Taylor series gives the incremental tension

$$\Delta T_M = AE \left.\frac{\partial s}{\partial s_0}\right|_M \left\{ \frac{1}{2}\Delta - \frac{1}{8}\Delta^2 + \dots \right\} \qquad (D)$$

T_M can thus be calculated to any desired degree of accuracy.

3.8:Other Possible New Types of Discretization.

It is thought that the discretizations that have been presented here illustrate the wide range of methods that can be used to produce a discretization. The methods given are perfectly adequate for the dynamic analysis of flexible riser systems and indeed, as will be shown later have a number of advantages over previous methods. It is however possible to produce more new types of discretization, though there would be little practical benefit in doing so.

The riser differential equation (2.5.4(c)) could be discretized using the Galerkin method with the Hermite cubic element that was used in section 3.7. This would give rise to equations of motion that are identical to those obtained in section 3.7. Note that the Galerkin discretization with linear elements in section 3.5 of the Cristescu differential equation (2.5.4(a)) results in equations of motion that are identical to those obtained from the variational discretization with linear elements. It can be shown (see Wait and Mitchell[1985]) that variational finite element discretizations (more properly called Ritz finite element methods) are equivalent to Galerkin finite element discretizations. The Galerkin finite element method is a member of a larger class of F.E. methods called the Petrov-Galerkin F.E. methods (often called weighted residual F.E. methods). Examples of Petrov-Galerkin F.E.

methods are the collacation F.E. method and the least squares F.E. method. The Galerkin F.E. method has been chosen here because of its equivalence with the variational method, however any of the other Petrov-Galerkin methods could have been used.

Various new finite difference discretizations of the riser differential equations (equations 2.5.4(a), (b) and (c)) could have been generated. It is likely (Fletcher[1987]) that some of the discretizations obtained in this way would be equivalent to discretizations obtained using the Petrov-Galerkin F.E. methods.

Higher order finite elements e.g. quintic elements or spline function elements could be used to generate new discretizations. The disadvantage of using finite elements such as these is that the discretization becomes much more complicated.

3.9:Comparison of Discretizations.

3.9.1:Introduction.

In this section comparisons are made between the discretizations that have been given in the previous sections. All of the these apart from the cubic variational one are based on straight line "elements" (some use the notion of a structural element and others of a finite element), these discretizations will be called linear discretizations. The linear discretizations are compared against each other and then against the cubic discretiztion. Recommendations are made about the use of these discretizations.

3.9.2:Comparison of the Linear Discretizations.

All of the linear discretizations allow for the extensibility of the riser apart from the inelastic lumped mass model. Excluding the extensibility of the riser in the discretization means that the possibility of high frequency longitudinal waves travelling down the riser is not permitted. This has the advantage that in the numerical integration of the equations of motion the timestep does not have to be restricted so that it is small enough to follow these wave motions (the longitudinal wave motions have a much higher velocity of propagation than the transverse wave motions: see section 3.10.3 on the method of

characteristics). It is possible however to have a numerical integration scheme that will damp out these high frequency components of the riser motion. However it is thought that it is important to allow for these longitudinal motions and not to damp them out using the integration scheme. This is because they may significantly affect the fatigue life of the riser due to the dynamic variations in the tension. Note that perhaps the longitudinal motions of the riser will be naturally damped out due to internal structural damping, thus the structural damping of the riser should be modelled if possible (this is done in the next chapter).

Due to the fact that the linear discretizations do not have continuous first derivatives at the nodes it might be thought that the modelling of the bending stiffness is not possible. This is not the case as will be shown in the next chapter.

The inelastic discretization is much more complicated to form and to use than the other discretizations. For this reason and the others stated in this section its use is not recommended.

The equations of motion obtained from all of the linear elastic discretizations are exactly the same apart from the structure of the mass matrix (not including the added mass matrix). The mass matrix obtained using the finite element discretization contains off-diagonal terms. In fact it is possible to obtain the mass matrix in the

lumped mass method by using the finite element method. This is done in the following section.

3.9.2.1:Obtaining the Mass Matrix in the Lumped Mass Method by using the Finite Element Method.

The interpolating functions Q and $\bar{Q}$ (Leonard and Nath[1981]) shown in figure 3.9.2.1(a) are used. Thus on an element

$$\underset{\sim}{r}_e = Q\underset{\sim}{r} + \bar{Q}\underset{\sim}{\bar{r}}$$

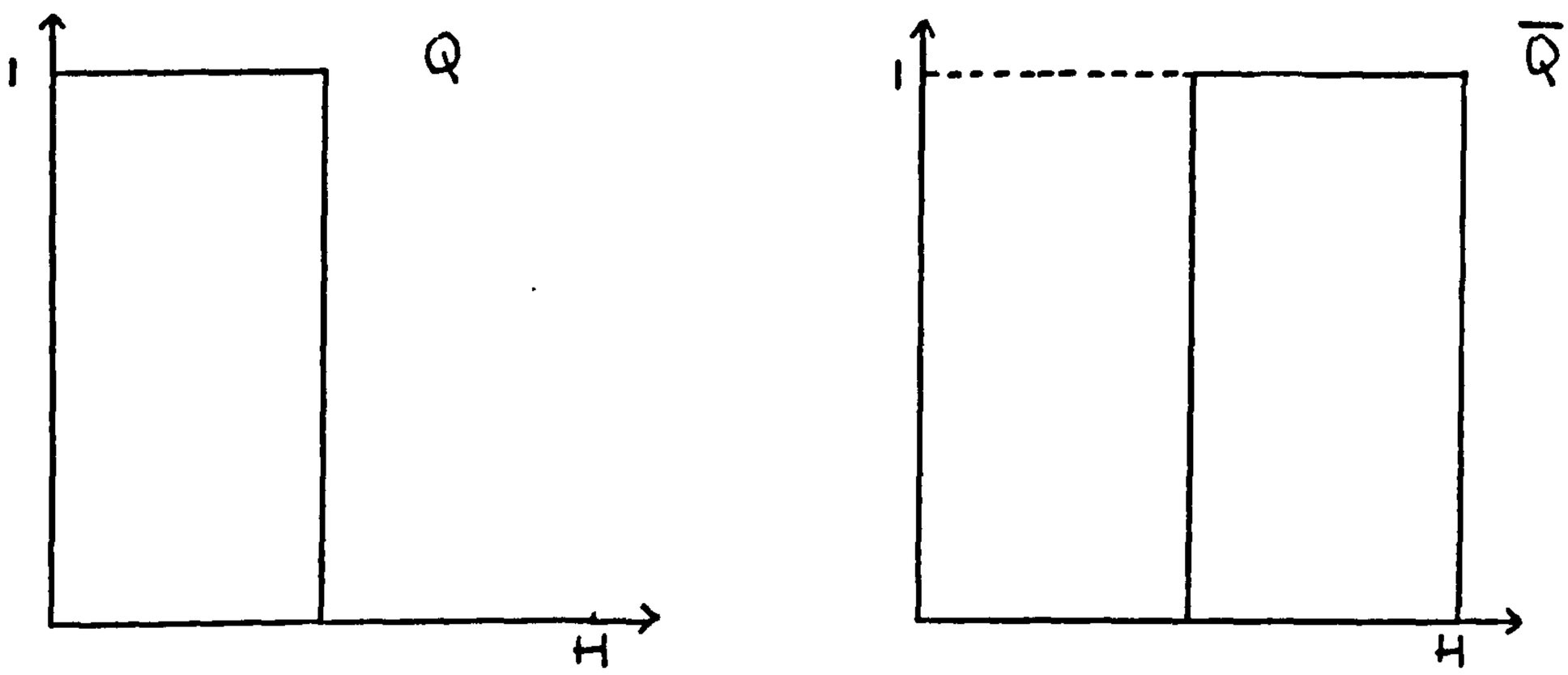

Figure 3.9.2.1 (a): Interpolating Functions Q and $\bar{Q}$

A component of the approximating function for $\underset{\sim}{r}$ is shown in figure 3.9.2.1(b). This approximating function shall be used for discretising the kinetic energy term in the variational principle and the conventional approximating function shall be used for the other terms. The kinetic energy of an element is given by

$$(K.E.)_e = \int_e \frac{1}{2}\rho(s_0)\frac{\partial \underset{\sim}{r}_e}{\partial t}\cdot\frac{\partial \underset{\sim}{r}_e}{\partial t}\,ds_0 = \frac{1}{2}\rho_e\int_e \begin{bmatrix}\dot{\underset{\sim}{r}} & \dot{\underset{\sim}{\bar{r}}}\end{bmatrix}\begin{bmatrix}Q^2 & Q\bar{Q}\\ Q\bar{Q} & \bar{Q}^2\end{bmatrix}\begin{bmatrix}\dot{\underset{\sim}{r}}\\ \dot{\underset{\sim}{\bar{r}}}\end{bmatrix} ds_0 \qquad (A)$$

$$= \frac{1}{2}\rho_e\int_e \begin{bmatrix}\dot{\underset{\sim}{r}} & \dot{\underset{\sim}{\bar{r}}}\end{bmatrix}\begin{bmatrix}Q & 0\\ 0 & \bar{Q}\end{bmatrix}\begin{bmatrix}\dot{\underset{\sim}{r}}\\ \dot{\underset{\sim}{\bar{r}}}\end{bmatrix} ds_0 = \frac{1}{2}\rho_e H_e\begin{bmatrix}\dot{\underset{\sim}{r}} & \dot{\underset{\sim}{\bar{r}}}\end{bmatrix}\begin{bmatrix}\frac{1}{2} & 0\\ 0 & \frac{1}{2}\end{bmatrix}\begin{bmatrix}\dot{\underset{\sim}{r}}\\ \dot{\underset{\sim}{\bar{r}}}\end{bmatrix}$$

Thus the total kinetic energy of the riser is

$$\frac{1}{2}\begin{bmatrix}\dot{\underset{\sim}{\Gamma}}_1 & \dot{\underset{\sim}{\Gamma}}_2 & \cdots & \dot{\underset{\sim}{\Gamma}}_{N-2} & \dot{\underset{\sim}{\Gamma}}_{N-1}\end{bmatrix}\begin{bmatrix}\frac{1}{2}H_1\rho_1 & & & & \\ \frac{1}{2}+H_2\rho_2 & & & & \\ & \frac{1}{2}H_2\rho_2 & & & \\ & \frac{1}{2}+H_3\rho_3 & & & \\ & & \ddots & & \\ & & & \frac{1}{2}H_{N-1}\rho_{N-1} & \\ & & & \frac{1}{2}+H_N\rho_N & \end{bmatrix}\begin{bmatrix}\dot{\underset{\sim}{\Gamma}}_1 \\ \dot{\underset{\sim}{\Gamma}}_2 \\ \vdots \\ \dot{\underset{\sim}{\Gamma}}_{N-2} \\ \dot{\underset{\sim}{\Gamma}}_{N-1}\end{bmatrix} \qquad (B)$$

Hence the mass matrix for the riser is

$$\begin{bmatrix}\frac{1}{2}H_1\rho_1 & & & & \\ \frac{1}{2}+H_2\rho_2 & & & & \\ & \frac{1}{2}H_2\rho_2 & & & \\ & \frac{1}{2}+H_3\rho_3 & & & \\ & & \ddots & & \\ & & & \frac{1}{2}H_{N-1}\rho_{N-1} & \\ & & & \frac{1}{2}+H_N\rho_N & \end{bmatrix} \qquad (C)$$

which is identical to that obtained by the lumped parameter method.

3.9.2.2:Error caused by the use of a Diagonal Mass Matrix.

The approximating function using linear interpolation shown in figure 3.5.2 is a closer estimate to the real shape of the riser than the step function approximation shown in figure 3.9.2.1(b). Hence if the diagonal mass matrix is used rather than the non-diagonal one an error is introduced into the discretization which

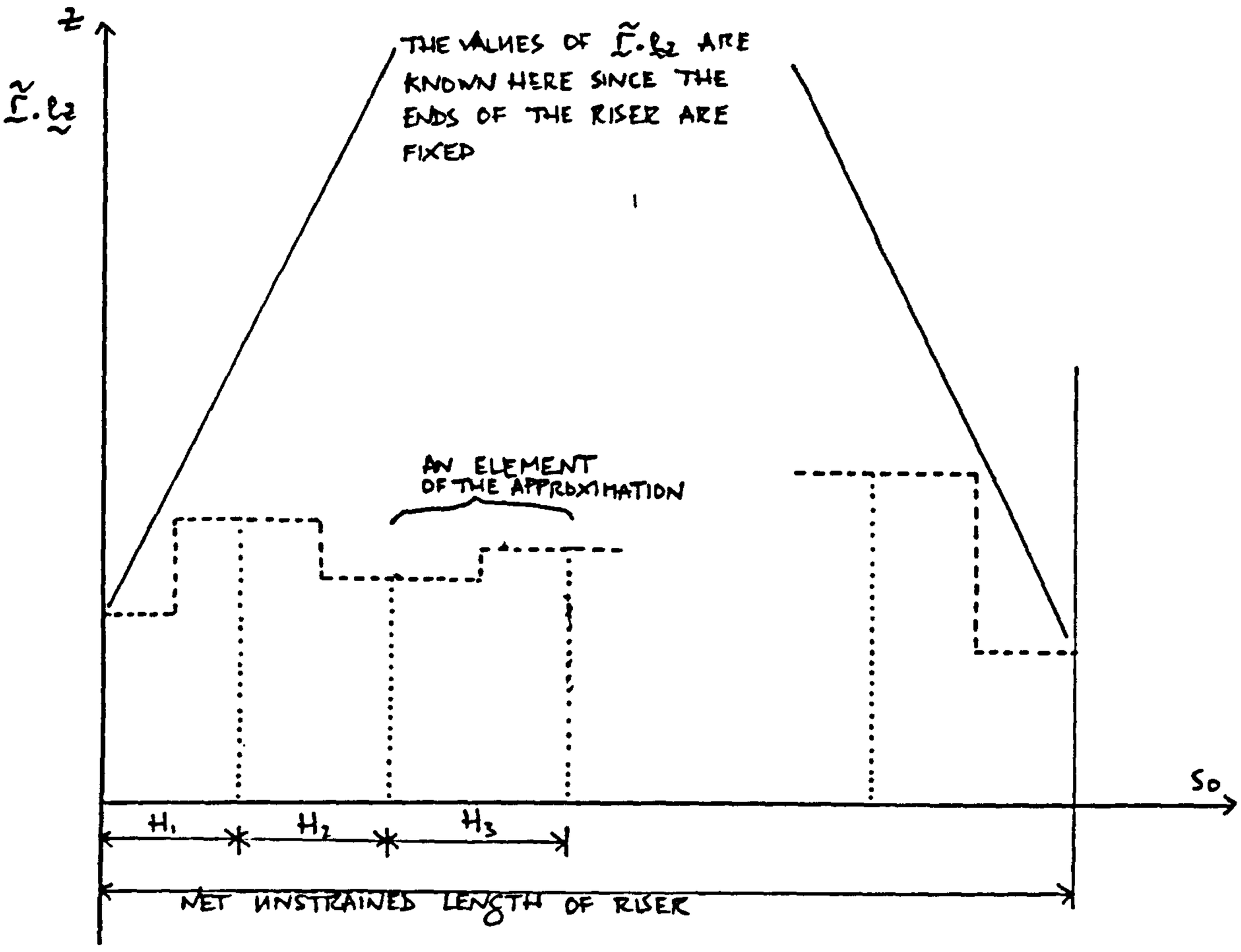

FIGURE 3.9.2.1(F): A COMPONENT OF THE APPROXIMATING FUNCTION $(\tilde{\Gamma}.\underset{\sim}{\ell_2})$ FOR $\underset{\sim}{\Gamma}$

need not be present. The error can be thought of as being introduced because of the neglecting of the rotational kinetic energy and of the mass coupling effects. Note that the overall mass matrix i.e. the mass matrix that has had the added mass matrix added to it will not be diagonal even if the diagonal mass matrix is used. It will be block diagonal however if the appropriate added mass matrix is chosen.

Suppose that the added mass matrix is small in comparison to the riser mass matrix so that it can be

neglected. Then the use of the diagonal mass matrix in a computer implementation will lead, for a given number of elements, to a faster solution because diagonal matrix inversion is trivial.

Consider figure 3.9.2.2(a) from Meggitt, Webster and Migliore[1980]. It shows the comparison between an elastic lumped mass code called SNAPLG and a finite element code using straight line elements called SEADYN. The comparison is for the example shown in figure 3.9.2.2(b). The added mass matrix is not set to zero. Both SNAPLG and SEADYN use the same data for this buoy relaxation example. There is a large difference between the results obtained from the two codes. The SNAPLG result gives a curve that is unrealistically smooth for this problem. The difference between the two results is thought to be due to the use of a diagonal mass matrix in the lumped parameter discretization (results given in the following section support this) however it is noted that since SNAPLG and SEADYN are two totally different programs there might be other reasons for this.

3.9.2.3:Numerical Results.

A computer program was written based on an elastic linear discretization. More details of this program are given in the following chapters. The riser is released from the strain free (i.e. there is no tension in the elements) configuration shown in figure 3.9.2.3(a). The data used is shown in this figure. The riser motion is gradually damped

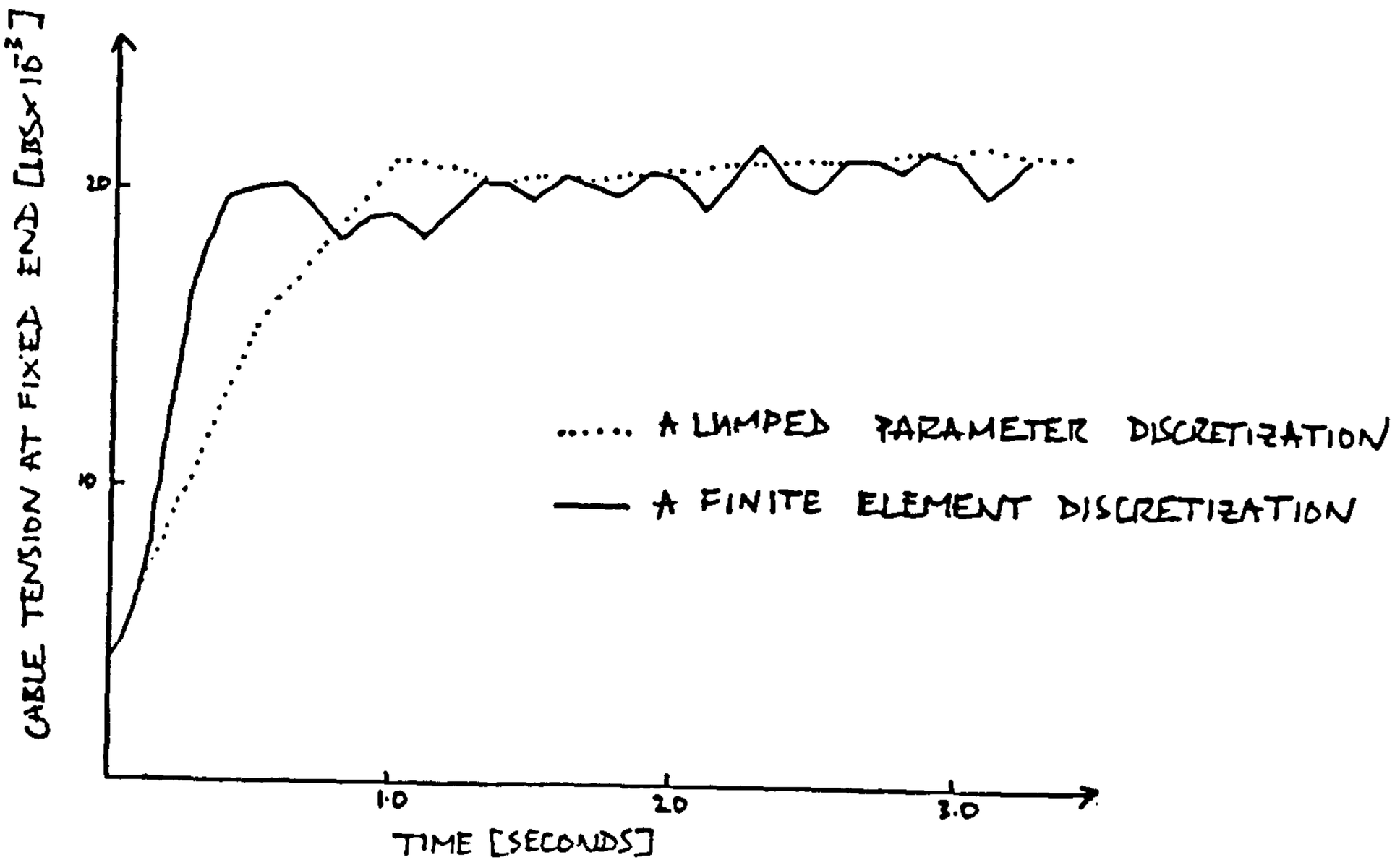

FIGURE 3.9.2.2(a): COMPARISON FOR BUOY RELAXATION PROBLEM

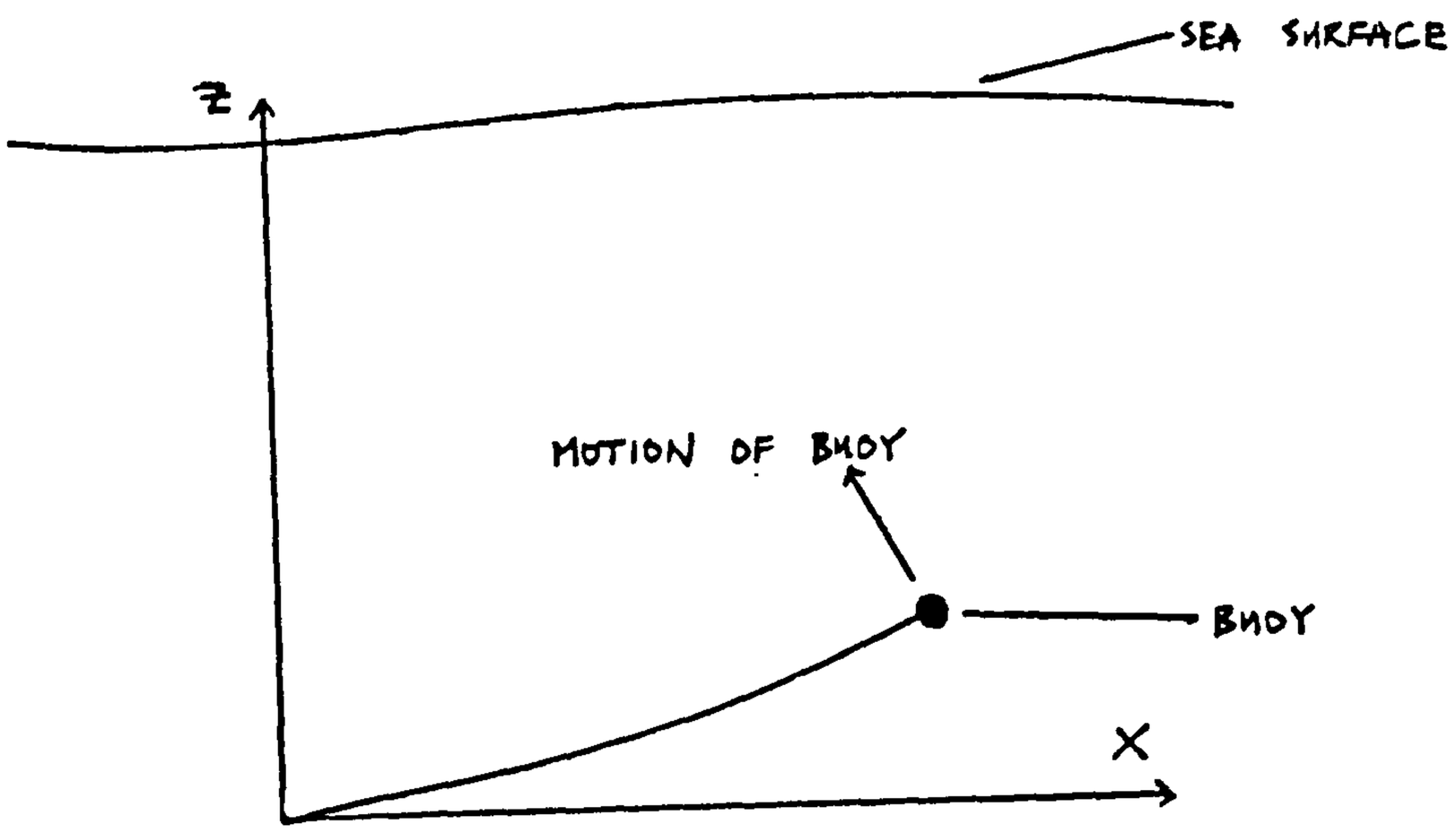

FIGURE 3.9.2.2(b): THE TEST PROBLEM OF KALMAN AND HUSTON [1985]

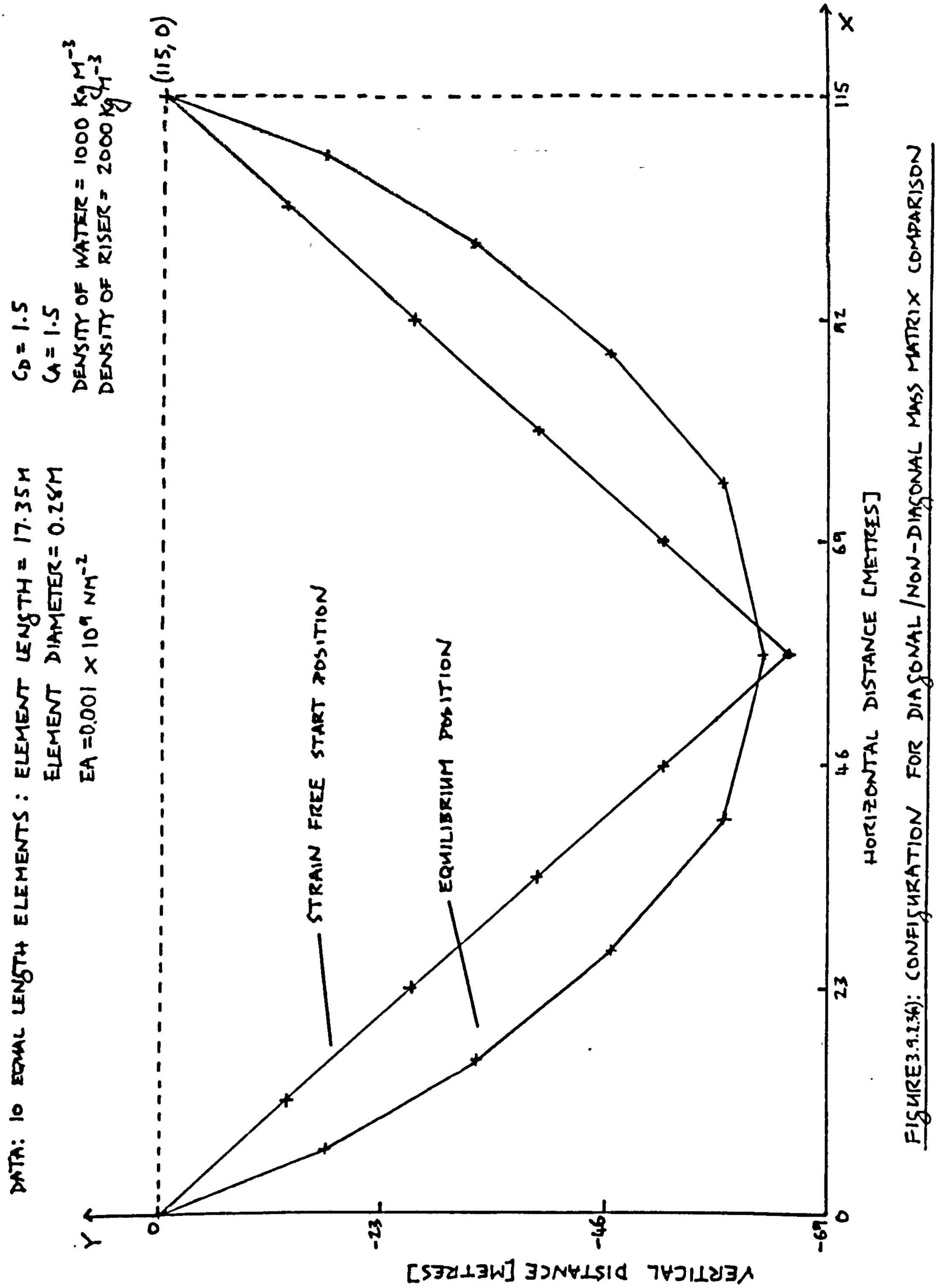

FIGURE 3.9.1.3(b): CONFIGURATION FOR DIAGONAL/NON-DIAGONAL MASS MATRIX COMPARISON

out until it comes to rest in the static equilibrium position.

The displacement time-history of the central node of the configuration is plotted in figure 3.9.2.3(b) for both the case when a diagonal mass matrix is used and for the case when a non-diagonal mass matrix is used. Note that the added mass matrix in this example is set to zero in order that a comparison between the use of the two mass matrices may be made. There is a large difference between the two results. When the riser undergoes small oscillations about the equilibrium position there is phase difference between the two results. The plot obtained with the diagonal mass matrix is smoother than that with the non-diagonal mass matrix.

3.9.2.4:Conclusions about the Structure of the Mass Matrix.

It has been shown theoretically that an error is introduced, that need not be present, by the use of a diagonal mass matrix. That this error is in practice significant has also been shown.

If the added mass matrix can be neglected then use of a diagonal mass matrix will lead to a faster computer program for the reasons given in section 3.9.2.2. However it is not certain that this increase in speed would offset the unnecessary discretization error. To ascertain if this would be the case a number of examples would need to be

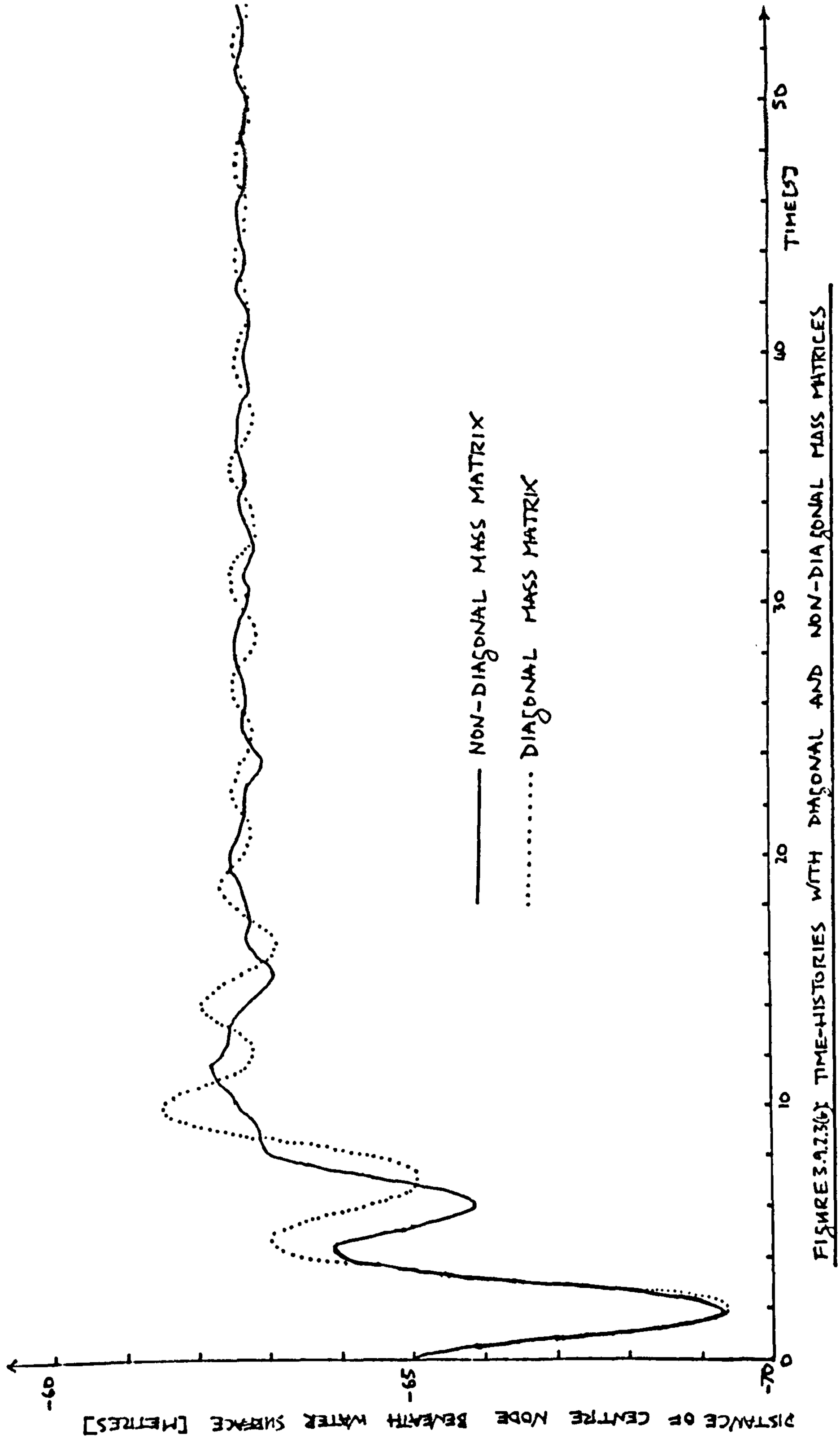
FIGURE 3.9.2.3(b): TIME-HISTORIES WITH DIAGONAL AND NON-DIAGONAL MASS MATRICES
TIME [S]
0
10
20
30
40
50
NON-DIAGONAL MASS MATRIX
DIAGONAL MASS MATRIX
-R 0
-65
-69
DISTANCE OF CENTRE NODE BENEATH WATER SURFACE [METRES]

examined. Clearly because of the increase in the discretization error more elements must be used to achieve comparable accuracy to the case when a non-diagonal mass matrix is used.

The non-diagonal mass matrix is recommended for a dynamic analysis and will be used in this thesis for the following reasons:

1.The added mass matrix for flexible risers cannot be neglected and is not diagonal.

2.To prevent an unnecessary discretization error.

If all that is required is to find the equilibrium position of the riser then it is recommended that a diagonal mass matrix is used with the added mass matrix set to zero. This will allow the equilibrium position to be found more quickly.

3.9.3:Comparison between the Linear and Cubic Discretizations.

The advantages of the cubic discretization over a linear one are:

1.The cubic model is naturally adapted to allow for the modelling of the bending stiffness of the riser whereas the linear models are not. However as shown in the next chapter the linear models can allow for the bending stiffness of the riser.

2.For the end user of a computer program, based on one of the discretizations, it is attractive to model a smooth structure such as a riser by a smooth approximating function such as the one used in the cubic discretization.

3.For a given required accuracy a computer program based on the cubic discretization should be faster.

The advantages of the linear discretization over the cubic one are:

1.Because the linear models have fewer degrees of freedom per element ($\underset{\sim}{\Gamma}$ and $\underset{\sim}{\bar{\Gamma}}$ compared with $\underset{\sim}{\Gamma}$, $\underset{\sim}{\bar{\Gamma}}$, $\frac{\partial \underset{\sim}{\Gamma}}{\partial s_0}$ and $\frac{\partial \underset{\sim}{\bar{\Gamma}}}{\partial s_0}$ for the cubic discretization) a computer program based on a linear discretization is easier to develop.

3.10:Comparison with Discretizations in the Literature.

3.10.1:Introduction.

In section 3.10 the discretizations that have been given are compared with other discretizations in the literature.

There are many other types of discretization in the literature that can be used for the dynamic analysis of flexible riser systems. Many of these discretizations were originally made in order to analyse the dynamics of cables and thus do not allow for the bending stiffness of the riser (this is dealt with in the next chapter). However this may not present great difficulties in the adaptability of these cable dynamics discretizations since as shown in the next chapter it is fairly easy to allow for the bending stiffness. Also since the bending stiffness of a riser is usually small in comparison to the extensional stiffness it might not be important to model the bending stiffness.

Some of the discretizations in the literature involve the numerical solution of one of the riser differential equations (equations 2.5.4(a),(b) and (c)) e.g. the discretizations of Garrett and Nordgren. All such discretizations can not easily deal with the physical boundary conditions on the riser system unlike the variational finite element discretizations that have been given.

Many of the discretizations in the literature could feasibly be used for the dynamic analysis of flexible riser systems however they tend to be over-complicated in comparison to some of the discretizations presented earlier in this chapter.

Some of the discretizations in the literature do not allow for the extensibility of the riser. These discretizations are not recommended for the reasons given in sections 3.9.2 and 3.10.

3.10.2:The Galerkin Discretization of Garrett.

Garrett[1982] discretizes the partial differential equation 2.5.4(b) using the Galerkin method with Hermite cubic elements that are constrained to be inextensible. The partial differential equation used was originally derived by Nordgren[1974]. The equation models the bending stiffness of the riser but does not model the extensional stiffness of the riser. This means that the partial differential equation is not complete on it's own and there is an additional equation of constraint that constrains the riser to be inextensible. This equation of constraint causes considerable difficulties in the numerical solution and adds greatly to the complication of the discretization. Note that although the method does not allow for any extension in the riser it does allow for the calculation of the tension in the riser. The discretization gives the numerical solution for a continuous length of riser and does not deal

with seperate lengths of riser that may be connected together in various ways i.e. clamped or pinned. It does not seem as though this could be done without considerable complication. It would be necessary in fact to have to apply the method to Nordgren's partial differential equation over several different domains and attempt to match the solution at the points of connection. The paper does not show how it would be possible to incorporate the addition of buoys or lumped masses into the discretization. The accuracy of the method for the calculation of the dynamic tensions is in doubt since it is difficult to estimate how much this will depend on the extension of the riser. The method will also not be capable of modelling longitudinal waves that could propagate along the riser giving additional tension variations.

3.10.3:The Method of Characteristics.

The method of characteristics is a numerical method for hyperbolic partial differential equations. It is shown by Cristescu[1967] that equation 2.5.4(c) is in the form of an hyperbolic partial differential equation, provided that geometry dependent terms in the added mass matrix are set to zero.

The fact that equation 2.5.4(c) can be thought to be hyperbolic allows the definition of sets of lines called characteristic lines. These lines have special properties and can give considerable insight into the nature of wave

propagation in the riser. Generally characteristics represent wave fronts. Cristescu shows that for the case when equation 2.5.4(c) reduces to an hyperbolic equation that there are two types of characteristic line, each type representing a different type of possible wave motion in the riser . One type of wave motion is transverse and the other longitudinal. Cristescu shows that the transverse waves affect the the shape of the riser but not the longitudinal strain and that the longitudinal waves propagate elongations of the riser (i.e. effect the tension in the riser) but do not change its shape. If the riser is not initially straight then propagation of any single type of wave on its own is not possible and the two types of wave motion are coupled. Cristescu devises various numerical schemes using the characteristic lines for the integration of equation 2.5.4(c) for various special cases.

Cristescu shows that the speed of propagation of the longitudinal waves (C_L) is

$$\left\{ \frac{1}{\bar{\rho}} \frac{dT}{d\left(\frac{\partial s}{\partial s_0}\right)} \right\}^{\frac{1}{2}} \qquad (A)$$

and the speed of propagation of the transverse waves (C_T) is

$$\left\{ \frac{T}{\bar{\rho} \frac{\partial s}{\partial s_0}} \right\}^{\frac{1}{2}} \qquad (a)$$

for small strain this can be written as

$$\left\{ \frac{T}{\bar{\rho}} \right\}^{\frac{1}{2}} \qquad (B)$$

where $\bar{\rho}$ =net density of the riser per unit of unstrained

length and includes the non-geometry dependent added mass terms. Suppose that the riser material obeys the constitutive relationship given by equation 2.3.2(a) then

$$C_L = \left\{ \frac{A_0 E}{\bar{\rho}} \right\}^{\frac{1}{2}} , \quad C_T = \left\{ \frac{A_0 E \left[\frac{\partial s}{\partial s_0} - 1 \right]}{\bar{\rho}} \right\}^{\frac{1}{2}} \qquad (C)$$

thus it can be seen that the longitudinal waves propagate at constant velocity whereas the transverse waves propagate at a velocity dependent on the tension in the riser (from (a) this is always the case for the velocity of the transverse waves and does not depend on the constitutive relationship).

Consider a typical riser that is in a steep "s" configuration. Take typical values for the riser of

$$EA_0 = 0.1 \times 10^9 N$$

$$\bar{\rho} = 2000 \, kg \, m^{-3}$$

$$T = 50,000N$$

then

$$C_L = 224 \, ms^{-1} , \quad C_T = 5 ms^{-1}$$

Thus the speed of the longitudinal waves is nearly 50 times the speed of the transverse waves. Consider a typical 25m length of riser then a longitudinal wave will take only about 0.1 seconds to travel along the length of riser. This has important implications. A time integration scheme that uses a timestep of around 0.1 seconds for a typical riser configuration must damp out the high frequency components of the riser motion because it cannot follow the longitudinal motion with such a large timestep. Hence in order to

follow the longitudinal motion for a typical riser configuration a timestep of 0.01 seconds or less must be used. As mentioned in section 3.9.2 it is considered here important to model the longitudinal motions of the riser as they may significantly affect its fatigue life.

Ferriss[1982] devises a scheme in order not to model the longitudinal motions of the riser. He does this in order that a bigger timestep can be used. This means that a computer implementation of his scheme should be faster. He reduces the governing equation 2.5.4(c) to a mixed hyperbolic-parabolic set of partial differential equations. Ferriss ignores the added mass forces and it is doubtful if these forces could be included without a great deal of complication.

The method of characteristics whilst giving considerable physical insight into the manner of wave propagation in the riser is not a practical tool for the dynamic analysis of flexible riser systems. It is inefficient, complicated and not very versatile. It would also be extremely difficult to adapt the method to deal with the bending stiffness of the riser, the boundary conditions on the riser at the end-points and the addition of buoys.

3.10.4:Finite Segment Methods.

A systematic method of deriving the equations of motion for complex problems in rigid body dynamics is given in Kane and Levinson[1985]. The method can deal with complex configurations of rigid bodies that are connected together. It provides for the automatic elimination of internal constraint forces without complex calculations and has been used successfully in the analysis of a wide variety of problems.

The method has been applied by Winget and Huston[1976] and Kalmman and Huston[1985] to cable dynamics problems. The cable is divided into a given number of inelastic rod elements (which are called finite segments). Each of the rod elements is a rigid body and hence the method of analysis given in Kane and Levinson may be used. It is possible to calculate the tensions in each of the segments however it is doubtful if these tensions will be accurate since the extension of the segments is not included. This discretization does not have the versatility of a finite element discretization but could be adapted to model the dynamics of a flexible riser.

Kalmman and Huston[1985] have developed a code called UCIN-CABLE based on the finite segment method. They have tested the code against experimental results and against the finite element code SEADYN which is based on the

analysis performed by Webster[1975(i),(ii)]. The particular problem that Kalmman and Huston have chosen to carry out their test on (not a full scale test but a model test) is shown in figure 3.9.2.2(b) and is normally known as a buoy relaxation problem. Some of the results of the model test and the comparison with the results predicted by UCIN-CABLE and SEADYN are shown in figure 3.10.4. Test 1 is with a silicon rubber cable and with X=51in. Z=-24in.. Test 2 is with a silicon rubber cable that has a wire core and with X=51in. Z=-33in.. For both SEADYN and UCIN-CABLE the predicted results for the configuration of the cable is not in close agreement with the result obtained from experiment. UCIN-CABLE is slightly closer to the experimental result than SEADYN. The fixed end cable tension predicted by UCIN-CABLE in both test 1 and test 2 is a smooth curve with no discontinuities of gradient. This does not agree well with either the experimental results or the the results predicted by SEADYN. Prediction of tension peaks might be very important in estimating the fatigue life of a flexible riser. As has been mentioned before it is not really to be expected that an inelastic discretization will give a very good estimate of the dynamic tension (Walton and Polachek[1959]). The dynamic variation in tension predicted by SEADYN is not in very good agreement with the experimental results. The reasons for this are not clear as SEADYN has been tested against model tests before and was shown to give excellent predictions (Meggitt,Webster and Migliore[1980]).

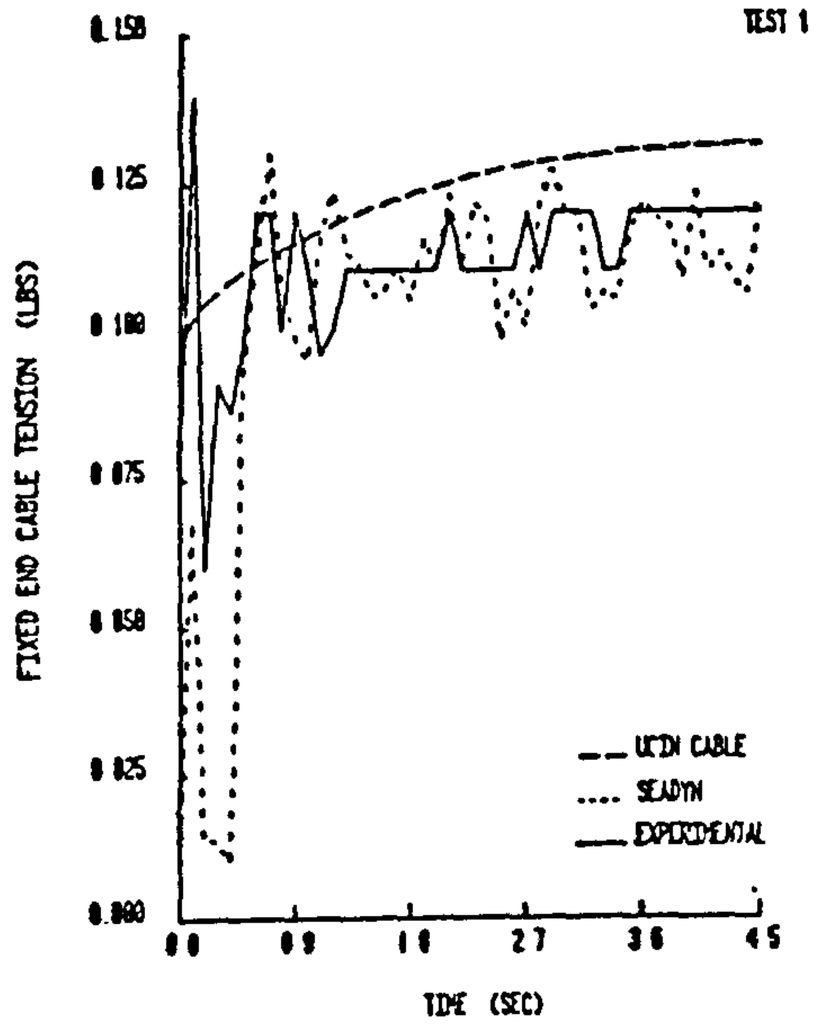

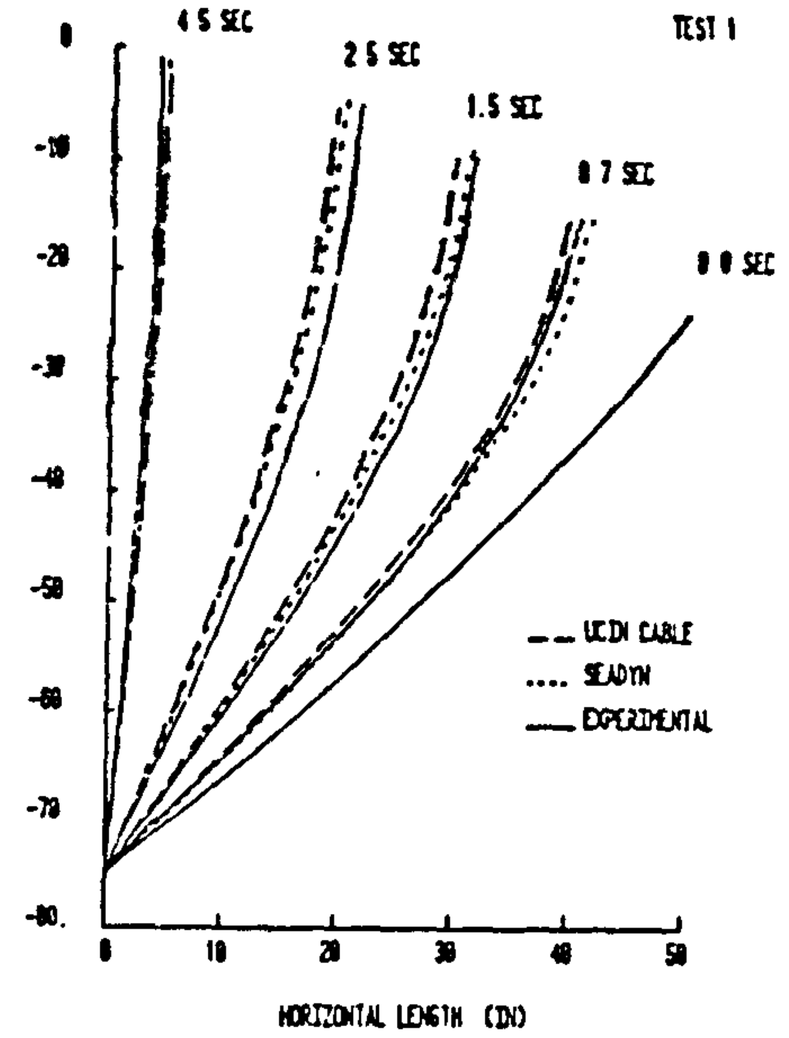

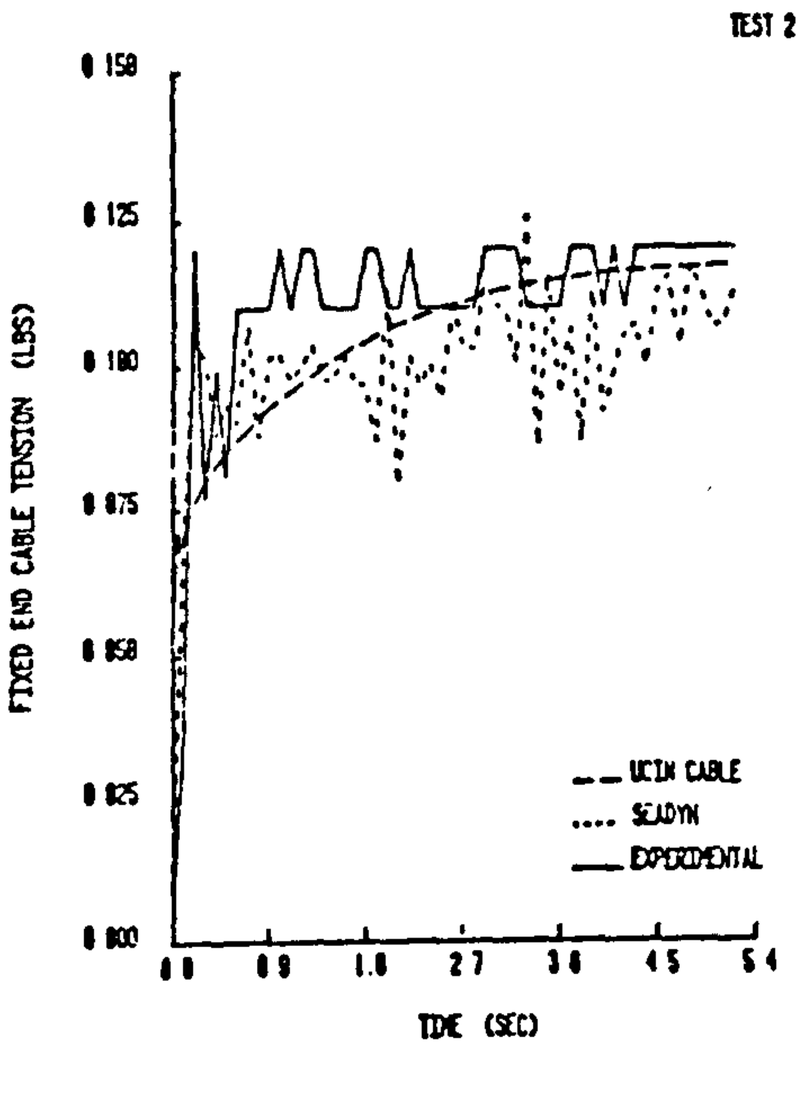

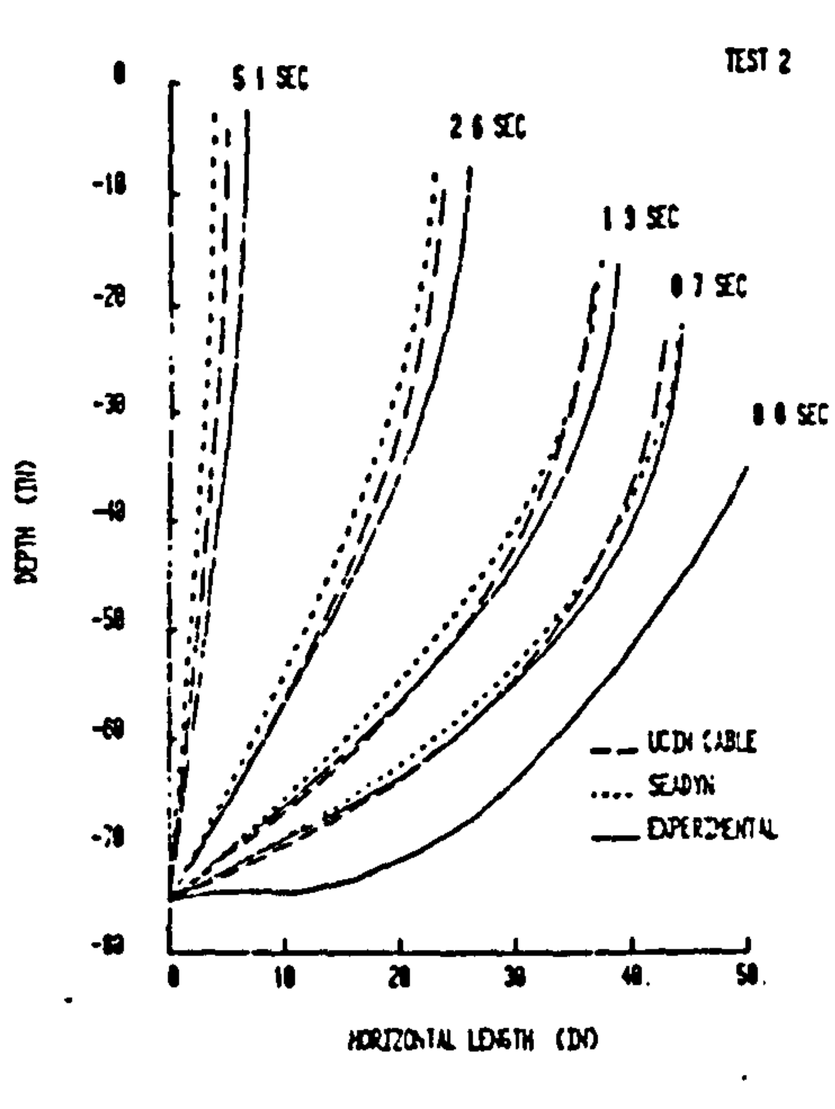

Figure 3.10.4: Comparison with Model Tests

3.10.5:Finite Difference Discretizations.

It is possible to use a finite difference method to numerically solve the partial differential equations derived in chapter two. Nordgren[1974] uses a finite difference method to solve the partial differential equation derived for an inextensible rod (equivalent to an inelastic riser). Chang and Pilkey[1973] also use a finite difference type method to solve a two dimensional mooring line problem.

As commented on by Fletcher[1984] (see section 3.8) most finite difference discretizations can be derived using the F.E. method. In addition the F.E. method is versatile, powerful and particularly well suited for the analysis of structural problems. It is thus thought not worthwhile to use the finite difference method in preference to the F.E. method to analyse flexible riser systems.

3.10.6:The Elastic Catenary Method.

The elastic catenary discretization is described in Peyrot[1980], Peyrot and Goulois[1979] and the FLEXAN user's guide[1984]. The discretization uses a special type of element based on the elastic catenary analytical solution for a cable hanging under gravity load only (O'Brien and Francis[1964]).

The method assumes that on each element the drag load and the inertia load is constant along the element,

thus the method assumes that the net load on an element is constant. Hence the calculated net load on the element and the elastic catenary equations can be used to find the configuration of the element. Note that the added mass load is lumped to the nodes.

The elastic catenary method is an excellent method for static analysis of cable structures or flexible risers under gravity loads only with discrete loads at the nodes of the elements. When drag or inertia loads are present smaller elements will be needed for a static analysis in order that the assumption of constant load over the element is reasonably valid.

The assumption that a cable element will always be in the shape of an elastic catenary is not a reasonable assumption if the element is moving unless very small elements are used. For this reason the elastic catenary discretization is not recommended for the dynamic analysis of a flexible riser. When used for a static analysis the method is adaptable and versatile because it is finite element method. The method will easily be able to model the addition of buoys and weights to the flexible riser.

The elastic catenary method has been coded to form the FLEXAN code (FLEXAN user's guide[1984]) which was originally designed to be run on a CRAY supercomputer. For a simple steep "s" configuration with a regular wave the FLEXAN code runs in real time on a CRAY for a dynamic simulation with 11 elements. In March 1985 a new version of

FLEXAN was implemented on a CRAY-XMP series supercomputer, which is one of the most powerful computers in the world.

The FLEXAN code is used extensively by COFLEXIP.

3.10.7:Updated Lagrangian and Total Lagrangian Methods for Cable Dynamics.

There are special finite element treatments for structures that undergo large displacements. These treatments are incremental in nature and are described in detail in Wunderlich[1977]. There are two types of treatment one is called the updated Lagrangian method and the other the total Lagrangian method. In the total Lagrangian method an unstrained state of the structure is chosen as a reference state for the analysis and in the updated Lagrangian method the last previous estimate of the position of the structure is chosen as a reference state. The application of both of these types of analysis to cable dynamics is described in Ozdemir[1979].

Webster[1975(i),(ii)] uses the total Lagrangian method to formulate the equations of motion of the cable. He has produced the well-tested code SEADYN using this formulation.

Leonard[1972,1973] and Leonard and Recker [1972] use incremental methods with curved elements. The elements used however cannot be condidered to be truly curved like the Hermite cubic element that was used earlier in this

chapter. This is because the effect of curvature is only taken account of for the estimation of the stiffness of the element and not for anything else e.g. the estimation of the kinetic energy of the element. Nevertheless some very good results are obtained. And a computer program based on this discretization is shown not only to be more accurate than one which does not take account of the curvature but also to be faster to run.

The updated and total Lagrangian methods both use the principle of virtual work which has also been used for some of the discretizations given in this chapter. They give no additional advantages in either the formulation of the problem or the solution of the equations of motion. Indeed they are considerably more complicated than the F.E. methods that have been presented in this chapter.

3.10.8:Finite Element Methods for Beams.

Many finite element discretizations have been given for the large displacement (note our problem is a large displacement one) of beams (Wen and Rahimzadeh[1983]). Some of these utiise the updated and total Lagrangian methods that were briefly described in the previous section. For even a simple problem such as the elastica a considerable number of the discretizations (Wen and Rahimzadeh) do not give adequate results. O'Brien, McNamara and Dunne[1987] and O'Brien, McNamara and Gilroy[1986] use large displacement beam finite elements for describing the

dynamics of flexible risers. Bourgat, Dumay and Glowinski[1980] combine the finite element method with non-linear programming methods to describe large dispacement beams.

In the next chapter the bending stiffness of the riser is modelled without introducing the considerable complication associated with large displacement beam F.E. methods.

Conclusions.

It has been shown that it is possible to produce new discretizations ad infinitum. The linear and cubic variational finite element discretizations are perfectly adequate for a dynamic analysis of flexible riser systems. They have a number of advantages over other discretizations. Some of these advantages are:

1.A simple formulation.

2.No unnecessary discretization errors are included in the formulation.

3.They can allow for the effects of the bending stiffness of the riser, internal fluid flow and other various effects in a simple manner. How this is done is dealt with in the next chapter.

4.Since the discretizations are based on a variational F.E. method they are particularly well-suited for the analysis of structural problems.

5.They both model the extensibility of the riser and do not restrict the magnitude of the strain in the riser.

The specific advantages and disadvantages of the cubic discretization in relation to the linear discretization are given in section 3.9.3.

CHAPTER FOUR: PRACTICAL REQUIREMENTS FOR A DISCRETIZATION

4.1:Introduction.

In Chapter Three the following assumptions were made:

1.The bending stiffness of the riser is zero.

2.The effect of the internal fluid flow is negligible.

3.There is no ground contact of the riser with the seabed.

4.The riser is totally immersed in the sea.

5.Both ends of the riser are fixed.

It was necessary to make these assumptions in order to save space and time. In practice these assumptions are not valid and it is important to allow for the appropriate effects in a computer model.

The only reference that allows for both the bending stiffness of the riser and the internal fluid flow of the riser in a simple way is Ractliffe[1984]. However as commented upon before it is believed that for commercial reasons this reference is incomplete. In the reference there is no validation against the analytical solutions available for beams e.g. the elastica solution (Love[1953]). Validation is needed because of the crudity of the modelling of the bending stiffness. The way in which Ractliffe models the bending stiffness means that equal length elements are preferred.

In this chapter the bending stiffness of the riser is modelled by a method that can deal with elements of unequal lengths. The method whilst being very simple achieves an accuracy that is remarkable. The accuracy of the method is illustrated by validation against the elastica analytical solution. It is shown how the bending stiffness may be incorporated into the cubic variational discretization presented in Chapter Three.

Using the theory developed in Chapter Two to describe the internal fluid flow with the theory developed to allow for the bending stiffness it is possible to allow for internal fluid flow effects. How this may be done is illustrated in section 4.7.

The top end of the riser configuration is normally subject to movement due to the motions of the floating production vessel. This means that the equations of motion developed in Chapter Two need to be modified. Details of the required modifications are given for the elastic linear discretization.

Ground contact of the riser with the seabed is modelled using a simple idea; the density of the external fluid is assumed to increase rapidly in the region of the seabed. This means that the upthrust force on the riser becomes greater in the region of the seabed and this constrains the riser so that it cannot move beneath the seabed.

The top end of the riser usually lies above the water surface. Thus special care must be taken to take account of this change in loading. A special element is derived to allow for only partial loading on an element. This element is of considerable use as it reduces the number of elements required not only near the water surface but also near the seabed.

No references deal with the change in the equations of motion due to the motion of the top end of the riser, or deal with the change in the loading mechanism when elements are only partially submerged.

4.2:The Modelling of the Riser Bending Stiffness.

4.2.1:The Linear Discretization.

4.2.1.1:Introduction.

With the linear discretization direct substitution of the approximating function for the riser position into the bending strain energy term developed in section 2.6.7 is not adequate. This is because no matter how many elements are used due to the second derivative terms appearing in the bending strain energy term a zero estimate of the bending strain energy will be obtained. It is thus necessary to use a virtual work formulation to allow for the riser bending stiffness when a linear element is used.

First of all the virtual work done on the riser δW_T by the tension forces is derived in terms of the nodal tension forces. By taking averages of the nodal tension forces a result for the virtual work is obtained that is identical to that obtained by using the strain energy expression developed in section 2.6.7. By analogy an expression is derived, in terms of element estimates of the shear forces, for the virtual work done by the shear forces. This expression enables the simple modelling of the riser bending stiffness.

Validation is carried out against the elastica solution (Love[1952]) and also against a simple small displacement beam solution.

4.2.1.2:Internal Virtual Work Done by the Tension Forces.

Using section 2.6.5 the internal virtual work δW_T done on the riser due to the tension forces is given by

$$\delta W_T = \int \delta \underset{\sim}{r} \cdot \frac{\partial (T \underset{\sim}{t})}{\partial s_o} \, ds_o \qquad (a)$$

where T =tension in the riser, $\underset{\sim}{t}$ =tangent vector of the riser centre-line, $\underset{\sim}{r}$ =position vector of a point on the riser centre-line and s_o =unstretched arc-length parameter. On an element it may be written that

$$(T \underset{\sim}{t})_e = L (T \underset{\sim}{t}) + \bar{L} (\overline{T \underset{\sim}{t}}) \qquad (A)$$

where $(T \underset{\sim}{t})_e$ =value of $T \underset{\sim}{t}$ within an element, L , $\bar{L}$ are the standard linear interpolating polynomials defined in section 3.4.2(a) and $(T \underset{\sim}{t})$, $(\overline{T \underset{\sim}{t}})$ are the nodal estimates of the tension forces. It may also be written that

$$\delta \underset{\sim}{r}_e = L \, \delta \underset{\sim}{r} + \bar{L} \, \delta \underset{\sim}{\bar{r}} \qquad (B)$$

hence

$$\delta W_T = \int \delta \underset{\sim}{r} \cdot \frac{\partial (T \underset{\sim}{t})}{\partial s_o} \, ds_o = \sum_e \int_e \begin{bmatrix} \delta \underset{\sim}{r} & \delta \underset{\sim}{\bar{r}} \end{bmatrix} \begin{bmatrix} L \\ \bar{L} \end{bmatrix} \begin{bmatrix} L' & \bar{L}' \end{bmatrix} \begin{bmatrix} (T \underset{\sim}{t}) \\ (\overline{T \underset{\sim}{t}}) \end{bmatrix} ds_o$$

$$= \sum_e \int_e \begin{bmatrix} \delta \underset{\sim}{r} & \delta \underset{\sim}{\bar{r}} \end{bmatrix} \begin{bmatrix} L \\ \bar{L} \end{bmatrix} \begin{bmatrix} -\frac{1}{H} & \frac{1}{H} \end{bmatrix} \begin{bmatrix} (T \underset{\sim}{t}) \\ (\overline{T \underset{\sim}{t}}) \end{bmatrix} ds_o \qquad (C)$$

$$= \sum_e \begin{bmatrix} \delta \underset{\sim}{r} & \delta \underset{\sim}{\bar{r}} \end{bmatrix} \begin{bmatrix} -\frac{1}{2} & \frac{1}{2} \\ -\frac{1}{2} & \frac{1}{2} \end{bmatrix} \begin{bmatrix} (T \underset{\sim}{t}) \\ (\overline{T \underset{\sim}{t}}) \end{bmatrix}$$

Now consider N elements as shown in figure 4.2.1.2(a). The net internal virtual work done on the elements due to the tension forces is given by

$$\delta W_I = \begin{bmatrix} \delta\underset{\sim}{r}_0 & \delta\underset{\sim}{r}_1 & \cdots & \delta\underset{\sim}{r}_{N-1} & \delta\underset{\sim}{r}_N \end{bmatrix} \begin{bmatrix} -\frac{1}{2} & \frac{1}{2} & & & \\ & -\frac{1}{2} & \frac{1}{2} & & \\ & & \ddots & \ddots & \\ & & & -\frac{1}{2} & \frac{1}{2} \\ & & & & -\frac{1}{2} & \frac{1}{2} \end{bmatrix} \begin{bmatrix} (T\underset{\sim}{t})_0 \\ (T\underset{\sim}{t})_1 \\ \vdots \\ (T\underset{\sim}{t})_{N-1} \\ (T\underset{\sim}{t})_N \end{bmatrix}$$

$$= \begin{bmatrix} \delta\underset{\sim}{r}_0 & \delta\underset{\sim}{r}_1 & \cdots & \delta\underset{\sim}{r}_{N-1} & \delta\underset{\sim}{r}_N \end{bmatrix} \begin{bmatrix} -\frac{1}{2} & \frac{1}{2} & & & \\ -\frac{1}{2} & 0 & \frac{1}{2} & & \\ & \ddots & \ddots & \ddots & \\ & & -\frac{1}{2} & 0 & \frac{1}{2} \\ & & & -\frac{1}{2} & \frac{1}{2} \end{bmatrix} \begin{bmatrix} (T\underset{\sim}{t})_0 \\ (T\underset{\sim}{t})_1 \\ \vdots \\ (T\underset{\sim}{t})_{N-1} \\ (T\underset{\sim}{t})_N \end{bmatrix} \quad (4)$$

$$= \begin{bmatrix} \delta\underset{\sim}{r}_0 & \delta\underset{\sim}{r}_1 & \cdots & \delta\underset{\sim}{r}_{N-1} & \delta\underset{\sim}{r}_N \end{bmatrix} \begin{bmatrix} \frac{1}{2}\{(T\underset{\sim}{t})_1 - (T\underset{\sim}{t})_0\} \\ \frac{1}{2}\{(T\underset{\sim}{t})_2 - (T\underset{\sim}{t})_0\} \\ \vdots \\ \frac{1}{2}\{(T\underset{\sim}{t})_N - (T\underset{\sim}{t})_{N-2}\} \\ \frac{1}{2}\{(T\underset{\sim}{t})_N - (T\underset{\sim}{t})_{N-1}\} \end{bmatrix}$$

when both ends of the riser are free this gives

$$\delta W_t = \begin{bmatrix} \delta\underset{\sim}{r}_0 & \delta\underset{\sim}{r}_1 & \cdots & \delta\underset{\sim}{r}_{N-1} & \delta\underset{\sim}{r}_N \end{bmatrix} \begin{bmatrix} \frac{1}{2}(T\underset{\sim}{t})_1 \\ \frac{1}{2}\{(T\underset{\sim}{t})_2 - (T\underset{\sim}{t})_1\} \\ \vdots \\ \frac{1}{2}\{(T\underset{\sim}{t})_N - (T\underset{\sim}{t})_{N-1}\} \\ -\frac{1}{2}(T\underset{\sim}{t})_{N-1} \end{bmatrix} \qquad (c)$$

since $(T\underset{\sim}{t})_0 = (T\underset{\sim}{t})_N = \underset{\sim}{0}$. And if both ends of the riser undergo some prescribed motion equation (b) gives

$$\delta W_t = \begin{bmatrix} \delta\underset{\sim}{r}_1 & \delta\underset{\sim}{r}_2 & \cdots & \delta\underset{\sim}{r}_{N-2} & \delta\underset{\sim}{r}_{N-1} \end{bmatrix} \begin{bmatrix} (T\underset{\sim}{t})_2 - (T\underset{\sim}{t})_1 \\ (T\underset{\sim}{t})_3 - (T\underset{\sim}{t})_2 \\ \vdots \\ (T\underset{\sim}{t})_{N-1} - (T\underset{\sim}{t})_{N-2} \\ (T\underset{\sim}{t})_N - (T\underset{\sim}{t})_{N-1} \end{bmatrix} \qquad (d)$$

since $\delta\underset{\sim}{r}_0 = \delta\underset{\sim}{r}_N = \underset{\sim}{0}$. This is identical to the result obtained in section 3.6.3. From equations (c) and (d) the appropriate result may be derived for the case when one end of the riser is free and the other end of the riser has some prescribed motion.

Define average element values of the tension forces (denoted by $\widehat{T\underset{\sim}{t}}$) as follows

$$\begin{aligned} (\widehat{T\underset{\sim}{t}})_1 &= \frac{1}{2}\{(T\underset{\sim}{t})_0 + (T\underset{\sim}{t})_1\} \qquad (D) \\ (\widehat{T\underset{\sim}{t}})_2 &= \frac{1}{2}\{(T\underset{\sim}{t})_1 + (T\underset{\sim}{t})_2\} \\ &\vdots \\ (\widehat{T\underset{\sim}{t}})_{N-1} &= \frac{1}{2}\{(T\underset{\sim}{t})_{N-1} + (T\underset{\sim}{t})_{N-2}\} \\ (\widehat{T\underset{\sim}{t}})_N &= \frac{1}{2}\{(T\underset{\sim}{t})_N + (T\underset{\sim}{t})_{N-1}\} \end{aligned}$$

then δW_T may be written in the form

$$\delta W_T = \begin{bmatrix} \delta \underset{\sim}{r}_0 & \delta \underset{\sim}{r}_1 & \dots & \delta \underset{\sim}{r}_{N-1} & \delta \underset{\sim}{r}_N \end{bmatrix} \begin{bmatrix} (\hat{T}\underset{\sim}{t})_1 \\ (\hat{T}\underset{\sim}{t})_2 - (\hat{T}\underset{\sim}{t})_1 \\ \vdots \\ (\hat{T}\underset{\sim}{t})_N - (\hat{T}\underset{\sim}{t})_{N-1} \\ -(\hat{T}\underset{\sim}{t})_N \end{bmatrix} \qquad (E)$$

From equations (c) and (d) it may be seen that this result holds true independently of the boundary conditions on the two ends of the riser. If $(\hat{T}\underset{\sim}{t})_i$ is identified with the element tension force used in Chapter Three then this result is identical to the result obtained when the strain energy formulation was used.

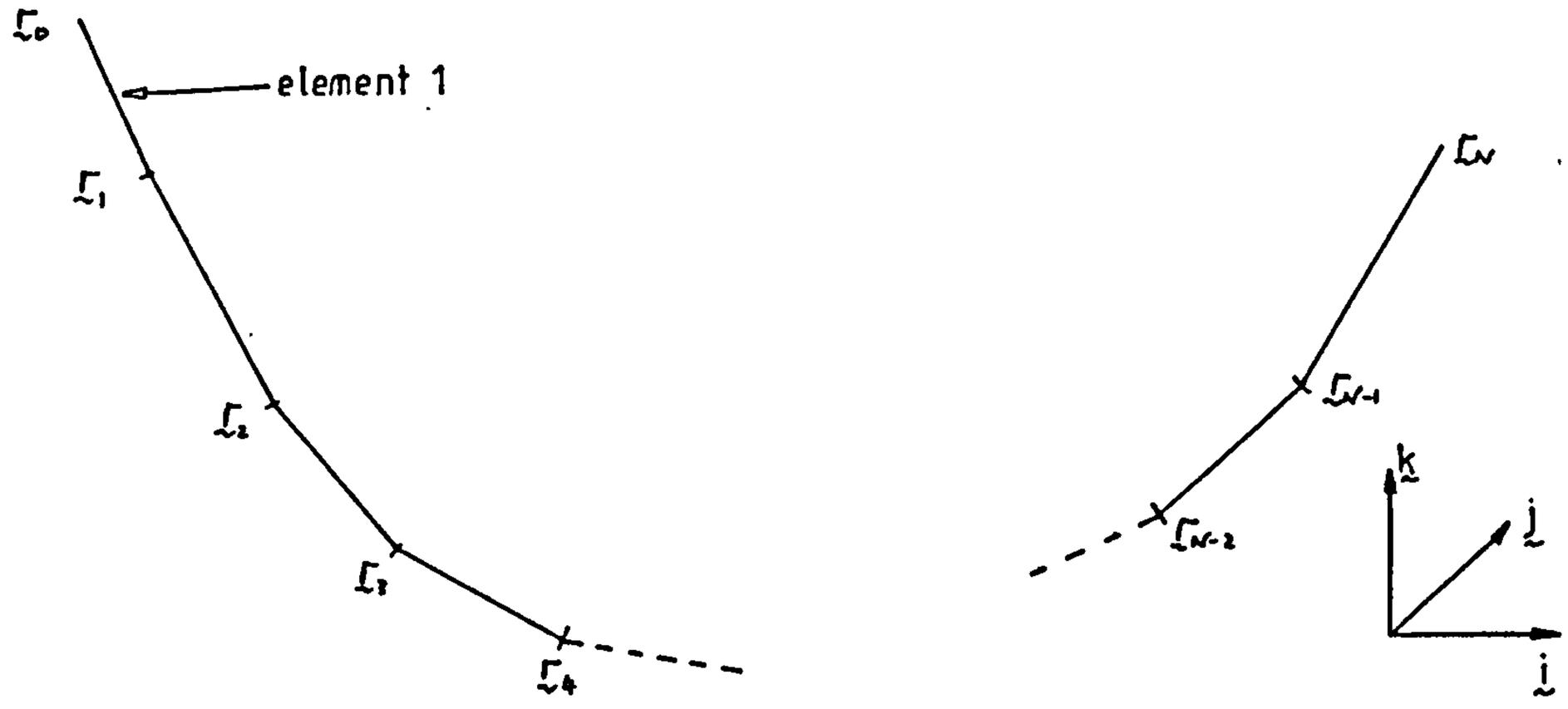

Figure 4.2.1.2(a): Calculating the Virtual Work done by Tension Forces

4.2.1.3:Internal Virtual Work done by Shear Forces.

It is not possible to use a strain energy formulation with a linear discretization. This is because linear interpolating polynomials are not of sufficiently high order. Substitution of a linear finite element into the strain energy expression for bending given in section 2.6.7 will result in zero bending strain energy which is obviously incorrect. It is therefore necessary to estimate the internal virtual work done by the shear forces by using the formulation given in section 4.2.1.1.

From section 2.6.5 the internal virtual work done on the riser by the shear forces (denoted by δW_s) is given by

$$\delta W_s = \int \delta \underset{\sim}{r} \cdot \frac{\partial \underset{\sim}{S}}{\partial s_0} \, ds_0 \qquad (a)$$

where $\underset{\sim}{S}$ =resultant shear force acting on the riser configuration and is given by (see Chapter Two)

$$\underset{\sim}{S} = \underset{\sim}{t} \wedge \frac{\partial}{\partial s_0}(B\kappa \underset{\sim}{b}) \qquad (A)$$

where $\underset{\sim}{t}$ =tangent vector, $\underset{\sim}{b}$ =binormal vector, κ =curvature and B =bending stiffness of the riser (=EI for an isotropic riser).

If it is assumed that both ends of the riser execute some prescribed motion, which is nearly always the case, then since equation (a) has precisely the same form as

equation 4.2.1.2(a) the method given in section 4.2.1.2 may be used. Thus the internal virtual work done on the riser by the shear forces is given by

$$\delta W_s = \begin{bmatrix} \delta\underset{\sim}{\Sigma}_1 & \delta\underset{\sim}{\Sigma}_2 & \cdots & \delta\underset{\sim}{\Sigma}_{N-2} & \delta\underset{\sim}{\Sigma}_{N-1} \end{bmatrix} \begin{bmatrix} \hat{\underset{\sim}{\Sigma}}_2 - \hat{\underset{\sim}{\Sigma}}_1 \\ \hat{\underset{\sim}{\Sigma}}_3 - \hat{\underset{\sim}{\Sigma}}_2 \\ \vdots \\ \hat{\underset{\sim}{\Sigma}}_{N-1} - \hat{\underset{\sim}{\Sigma}}_{N-2} \\ \hat{\underset{\sim}{\Sigma}}_N - \hat{\underset{\sim}{\Sigma}}_{N-1} \end{bmatrix} \qquad (B)$$

where $\hat{\underset{\sim}{\Sigma}}_i$ is the estimate of the shear force for the ith element.

4.2.1.4:Estimate of the Element Shear Force.

The element shear force $\hat{\underset{\sim}{\Sigma}}_i$ can be estimated very simply. First the bending moment $\underset{\sim}{M}_j$ at the jth node is approximated. From the continuum equations developed in Chapter Two

$$\underset{\sim}{M}_j = B_j K_j \underset{\sim}{b}_j \qquad (A)$$

where B_j =bending stiffness of the riser at the jth node, K_j =curvature of the riser centre-line at the jth node and $\underset{\sim}{b}_j$ =the binormal vector at the jth node. From the definition of the binormal vector given in Appendix A

$$\underset{\sim}{M}_j = B_j \hat{\underset{\sim}{t}}_j \wedge \left(\frac{d\underset{\sim}{t}}{ds}\right)_j \qquad (a)$$

where $\hat{\underset{\sim}{t}}_j$ is defined by

$$\hat{\underset{\sim}{t}}_j = \frac{h_j \underset{\sim}{t}_{j+1} + h_{j+1} \underset{\sim}{t}_j}{\left| h_j \underset{\sim}{t}_{j+1} + h_{j+1} \underset{\sim}{t}_j \right|} \qquad (b)$$

and $\left(\frac{d\underset{\sim}{t}}{ds}\right)_j$ is defined by

$$\left(\frac{d\underset{\sim}{t}}{ds}\right)_j = \frac{\underset{\sim}{t}_{j+1} - \underset{\sim}{t}_j}{(h_{j+1} + h_j)/2} \qquad (c)$$

These definitions hold only at those nodes that are not end nodes. $\hat{\underset{\sim}{t}}_j$ can be thought of as an average nodal tangent vector. If one of the adjacent elements is shorter than the other one then $\hat{\underset{\sim}{t}}_j$ is biased towards the shorter one. This is thought to be more accurate when elements of unequal lengths are used. Substituting for $\hat{\underset{\sim}{t}}_j$ and $\left(\frac{d\underset{\sim}{t}}{ds}\right)_j$ from equations (b) and (c) into equation (a) gives

$$\underset{\sim}{M}_j = B_j \left\{ \frac{h_j \underset{\sim}{t}_{j+1} + h_{j+1} \underset{\sim}{t}_j}{\left| h_j \underset{\sim}{t}_{j+1} + h_{j+1} \underset{\sim}{t}_j \right|} \right\} \wedge \left\{ \frac{\underset{\sim}{t}_{j+1} - \underset{\sim}{t}_j}{(h_{j+1} + h_j)/2} \right\}$$

$$= B_j \frac{h_{j+1}(\underset{\sim}{t}_j \wedge \underset{\sim}{t}_{j+1}) - h_j(\underset{\sim}{t}_{j+1} \wedge \underset{\sim}{t}_j)}{\left| h_j \underset{\sim}{t}_{j+1} + h_{j+1} \underset{\sim}{t}_j \right| (h_{j+1} + h_j)/2}$$

$$= B_j \frac{\underset{\sim}{t}_j \wedge \underset{\sim}{t}_{j+1}}{\left| \frac{h_j}{2} \underset{\sim}{t}_{j+1} + \frac{h_{j+1}}{2} \underset{\sim}{t}_j \right|} \qquad (d)$$

This expression has a particularly simple form and the nodal

bending moments may be calculated quickly. Knowledge of the bending moments may be required for fatigue calculations. Thus from equation (d)

$$\underset{\sim}{M}_j = B_j \frac{\underset{\sim}{t}_j \wedge \underset{\sim}{t}_{j+1}}{|\underset{\sim}{t}_j \wedge \underset{\sim}{t}_{j+1}|} \cdot \frac{|\underset{\sim}{t}_j \wedge \underset{\sim}{t}_{j+1}|}{\left|\frac{h_j}{2}\underset{\sim}{t}_{j+1} + \frac{h_{j+1}}{2}\underset{\sim}{t}_j\right|} \qquad (B)$$

hence the nodal estimate of $\underset{\sim}{t}_j$ is

$$\underset{\sim}{t}_j = \frac{\underset{\sim}{t}_j \wedge \underset{\sim}{t}_{j+1}}{|\underset{\sim}{t}_j \wedge \underset{\sim}{t}_{j+1}|} \qquad (e)$$

and the nodal estimate of the curvature K_j is

$$K_j = \frac{|\underset{\sim}{t}_j \wedge \underset{\sim}{t}_{j+1}|}{\left|\frac{h_j}{2}\underset{\sim}{t}_{j+1} + \frac{h_{j+1}}{2}\underset{\sim}{t}_j\right|} \qquad (f)$$

alternatively using the vector identity $(\underset{\sim}{A} \wedge \underset{\sim}{B})^2 = (\underset{\sim}{A}.\underset{\sim}{A})(\underset{\sim}{B}.\underset{\sim}{B}) - (\underset{\sim}{A}.\underset{\sim}{B})^2$ this may be written in the form

$$K_j = \frac{\left\{1 - (\underset{\sim}{t}_j . \underset{\sim}{t}_{j+1})^2\right\}^{\frac{1}{2}}}{\left|\frac{h_j}{2}\underset{\sim}{t}_{j+1} + \frac{h_{j+1}}{2}\underset{\sim}{t}_j\right|} \qquad (C)$$

4.2.1.5:Check on Theory.

When the elements are straight at the jth node i.e. when $\underset{\sim}{t}_j = \underset{\sim}{t}_{j+1}$ then equation 4.2.1.4(d) does not define the binormal vector. Similarly for the continuum the binormal vector is not defined at those points at which the riser is straight i.e. at those points at which $\frac{d\underset{\sim}{t}}{ds} = 0$.

Again suppose that $\underset{\sim}{t}_j = \underset{\sim}{t}_{j+1}$ then equation (f) gives

$$K_j = 0 \qquad (A)$$

Now examine the limit as $N \to \infty$. Then as the limit is approached to a very high order of accuracy it may be written that

$$\underset{\sim}{t}_j = \underset{\sim}{t} \quad , \quad \underset{\sim}{t}_{j+1} = \underset{\sim}{t} + \delta s \frac{d\underset{\sim}{t}}{ds} + \frac{\delta s^2}{2} \frac{d^2\underset{\sim}{t}}{ds^2} \qquad (a)$$

since the discretization in the limit will be a very close appoximation to the continuum. Substituting these results into equation 4.2.1.4(e) gives

$$\underset{\sim}{b}_j = \frac{\underset{\sim}{t}_j \wedge \underset{\sim}{t}_{j+1}}{\left| \underset{\sim}{t}_j \wedge \underset{\sim}{t}_{j+1} \right|} = \frac{\underset{\sim}{t} \wedge \left[\underset{\sim}{t} + \delta s \frac{d\underset{\sim}{t}}{ds} + \frac{\delta s^2}{2} \frac{d^2\underset{\sim}{t}}{ds^2} \right]}{\left| \underset{\sim}{t} \wedge \left[\underset{\sim}{t} + \delta s \frac{d\underset{\sim}{t}}{ds} + \frac{\delta s^2}{2} \frac{d^2\underset{\sim}{t}}{ds^2} \right] \right|} \qquad (B)$$

Thus as $N \to \infty$

$$\underset{\sim}{b}_j \to \frac{\underset{\sim}{t} \wedge \frac{d\underset{\sim}{t}}{ds}}{\left| \underset{\sim}{t} \wedge \frac{d\underset{\sim}{t}}{ds} \right|} = \frac{\kappa \underset{\sim}{t} \wedge \underset{\sim}{n}}{\left| \kappa \underset{\sim}{t} \wedge \underset{\sim}{n} \right|} = \underset{\sim}{t} \wedge \underset{\sim}{n} = \underset{\sim}{b} \qquad (C)$$

Hence equation 4.2.1.4(f) approaches the continuum result as there are more and more elements. Now substitute equation (a) into equation 4.2.1.4(f) to obtain

$$K_j = \frac{\left| \underset{\sim}{t} \wedge \left[\underset{\sim}{t} + \delta s \frac{d\underset{\sim}{t}}{ds} + \frac{\delta s^2}{2} \frac{d^2\underset{\sim}{t}}{ds^2} \right] \right|}{\left| \frac{h_j}{2} \underset{\sim}{t} + \frac{h_{j+1}}{2} \left(\underset{\sim}{t} + \delta s \frac{d\underset{\sim}{t}}{ds} + \frac{\delta s^2}{2} \frac{d^2\underset{\sim}{t}}{ds^2} \right) \right|} \qquad (D)$$

but $\delta s = (h_j + h_{j+1})/2$ therefore as $N \to \infty$

$$K_j \longrightarrow \frac{\delta s \, |K|}{|(h_j + h_{j+1})/2|} = K \qquad (E)$$

Hence equation 4.2.1.4(f) approaches the continuum result as more and more elements are used.

4.2.1.6:Calculation of Bending Moments for End Nodes.

The procedure outlined in section 4.2.1.4 fails if the node considered is an end node, thus an alternative procedure for the end nodes is required. Suppose that the end is pinned then at this node the moment is defined to be zero. Now suppose that the left hand end is clamped at a tangent $\underset{\sim}{t}_L$ then the moment $\underset{\sim}{M}_L$ at this end is defined by

$$\underset{\sim}{M}_L = B_L \underset{\sim}{t}_L \wedge \left\{ \frac{\underset{\sim}{t}_1 - \underset{\sim}{t}_L}{h_1/2} \right\} = B_L \frac{\underset{\sim}{t}_L \wedge \underset{\sim}{t}_1}{h_1/2} \qquad (A)$$

where B_L =bending stiffness evaluated at the left hand end. Similarly if the right hand end is clamped at a tangent $\underset{\sim}{t}_R$

then the moment $\underset{\sim}{M}_R$ at this end is defined by

$$\underset{\sim}{M}_R = B_R \underset{\sim}{t}_R \wedge \left\{ \frac{\underset{\sim}{t}_R - \underset{\sim}{t}_N}{h_N/2} \right\} = B_R \frac{\underset{\sim}{t}_N \wedge \underset{\sim}{t}_R}{h_N/2} \qquad (B)$$

where B_R =bending stiffness evaluated at the right hand end.

4.2.1.7:Validation Against Analytical Solutions.

Consider the beam under an end load as shown in figure 4.2.1.7(a). Then it is possible to analytically determine the equilibrium position of the beam (Love[1953]). The analytical solution is known as the elastica. For the validation of the procedure for incorporating the bending stiffness of the riser against the elastica the following data is used

$B=2.0E+07nm^2$

$EA=0.327E+09n$

Length of beam L=162m

Two different element discretizations are used; one with all the elements of equal length and one where this is not the case. For the case when some of the elements have unequal lengths

ELEMENT NUMBER	ELEMENT LENGTH[metres]
1	6.0

2	6.0
3	6.0
4	12.0
5	12.0
6	12.0
7	24.0
8	42.0
9	42.0

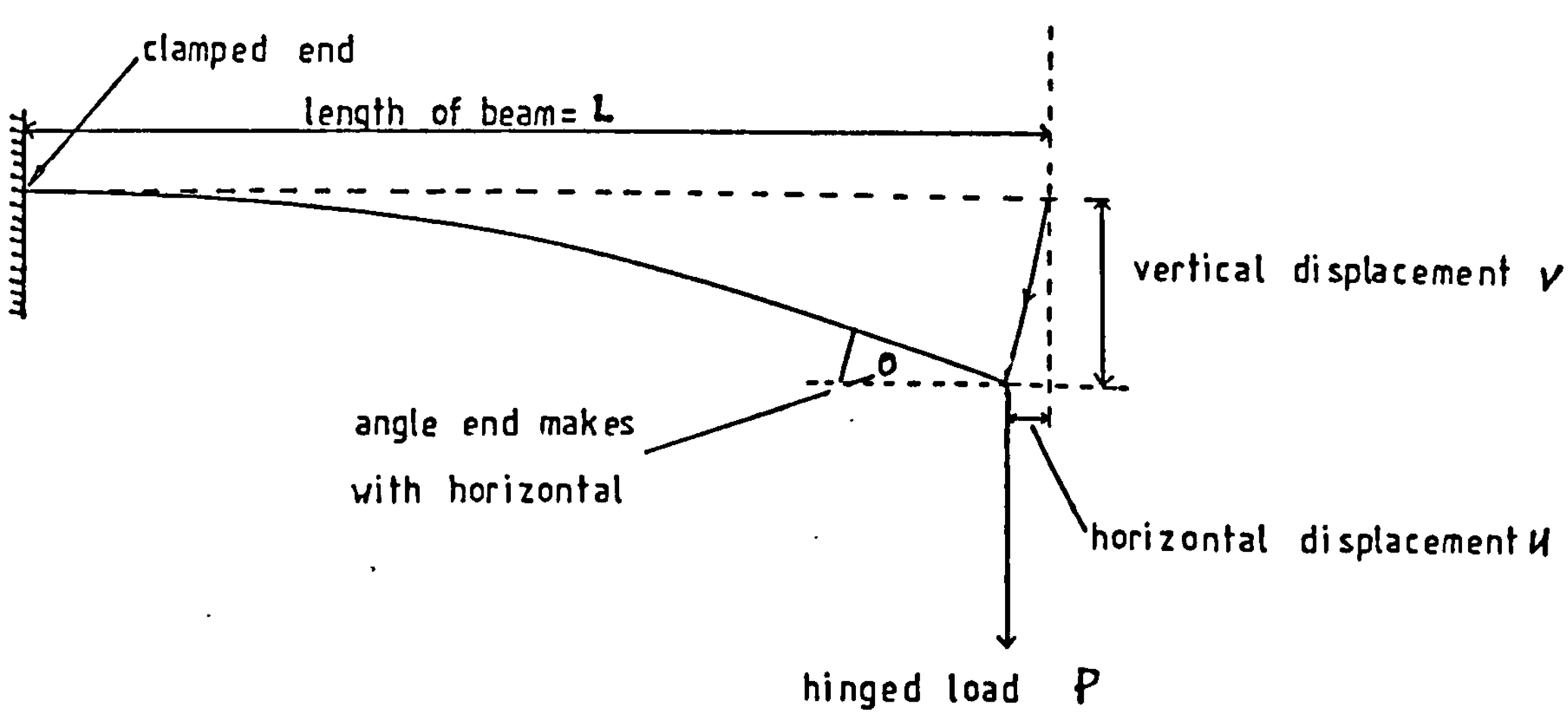

Figure 4.2.1.7(a):The Elastica Solution

Element 1 is connected to the clamped end and element 2 is connected to element 1 etc.. The 10th element is a "dummy" element. Its extensional stiffness is set equal to zero and

the bending stiffness at the two ends of the element is set equal to zero. Thus the 9th node is effectively free and the position of its point of connection to a fixed point is irrelevant.

The horizontal and vertical displacements of the end of the beam as predicted from the finite element model, for both the case when equal length elements are used are shown in figures 4.2.1.7(b),(c),(d),(e). The results achieved are remarkably accurate considering the crudity of the way in which the bending stiffness has been incorporated into the finite element model. The accuracy achieved is not dependent on the discretization used i.e. if the lengths of the elements are different. Note for the loads on the beam that have been used the behaviour of the beam is non-linear; the linear theory predictions are shown in some of the figures. In figure 4.2.1.7(f) the results are plotted for the angle of the loaded end of the beam. Once again the accuracy achieved is excellent.

In comparison against a commercial finite element package (Finite Element Analysis Limited[1986]) the results obtained are more accurate even though the finite element package used cubic elements with twice the number of degrees of freedom.

Validation is also carried out in the small displacement range for the example shown in figure 4.2.1.7(g). The uniform load always act vertically downward. The analytical solution is given in Love [1952].

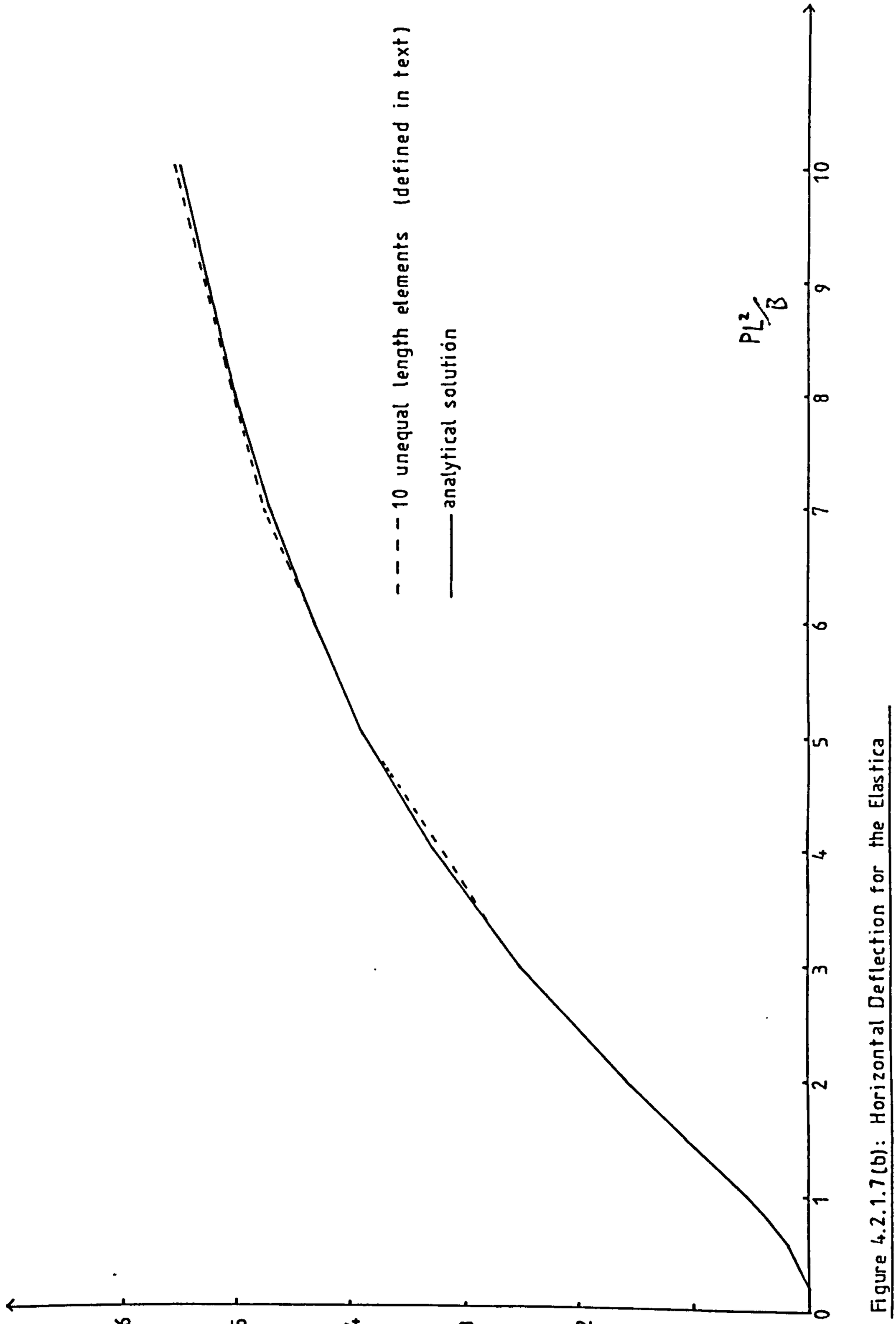

Figure 4.2.1.7(b): Horizontal Deflection for the Elastica

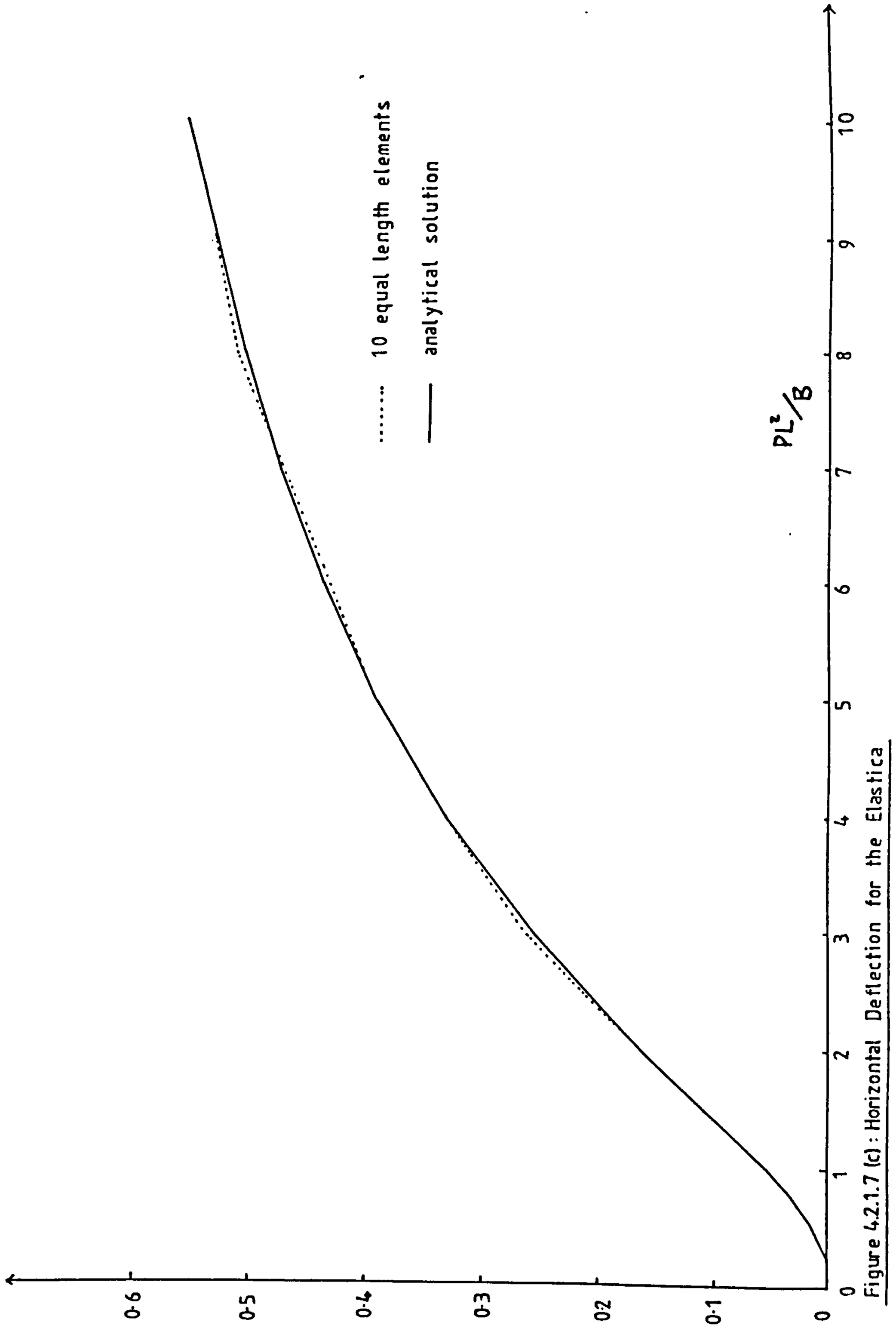

Figure 4.2.1.7 (c): Horizontal Deflection for the Elastica

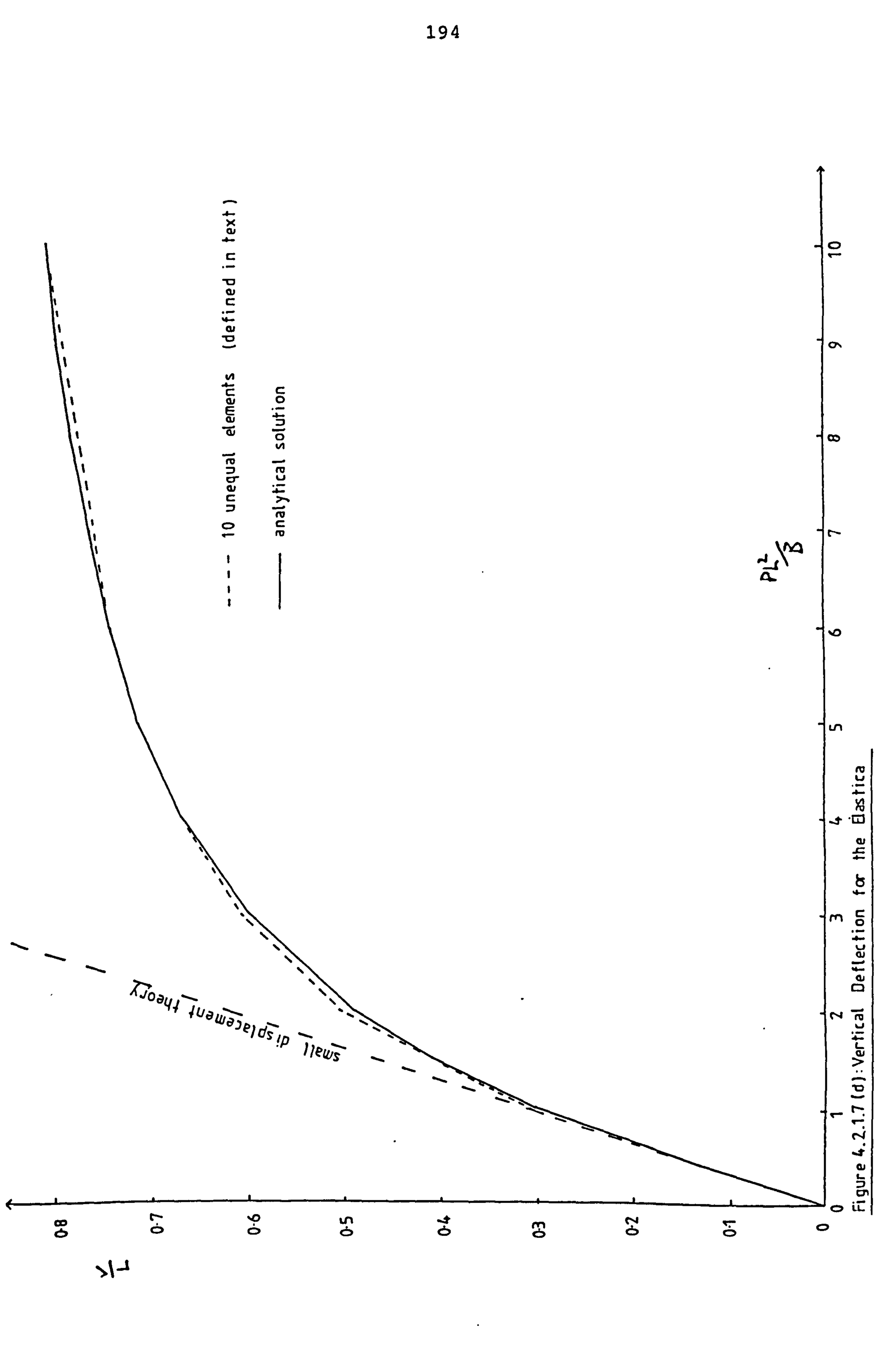

Figure 4.2.1.7 (d): Vertical Deflection for the Elastica

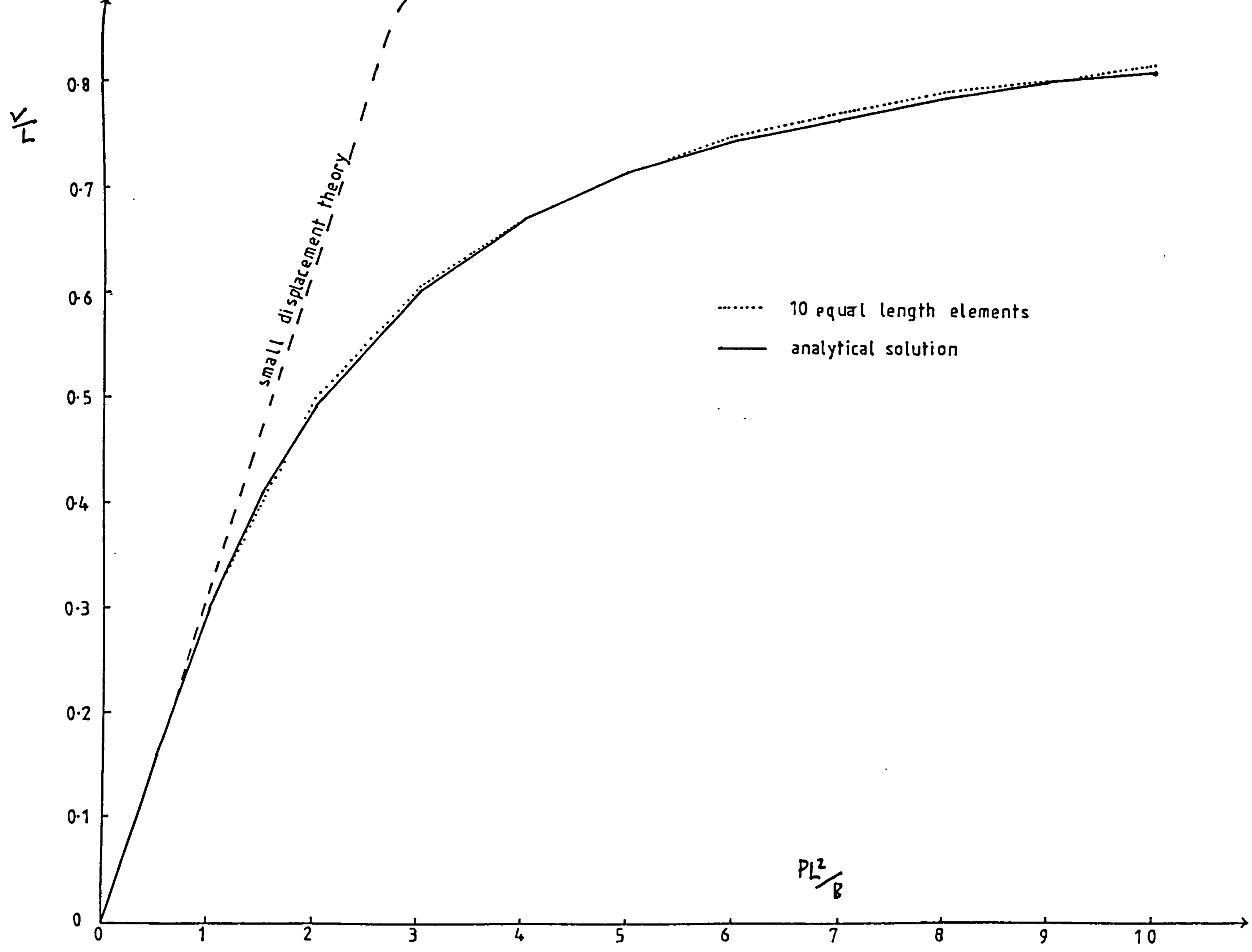

Figure 4.2.1.7 (e) : Vertical Deflection for the Elastica

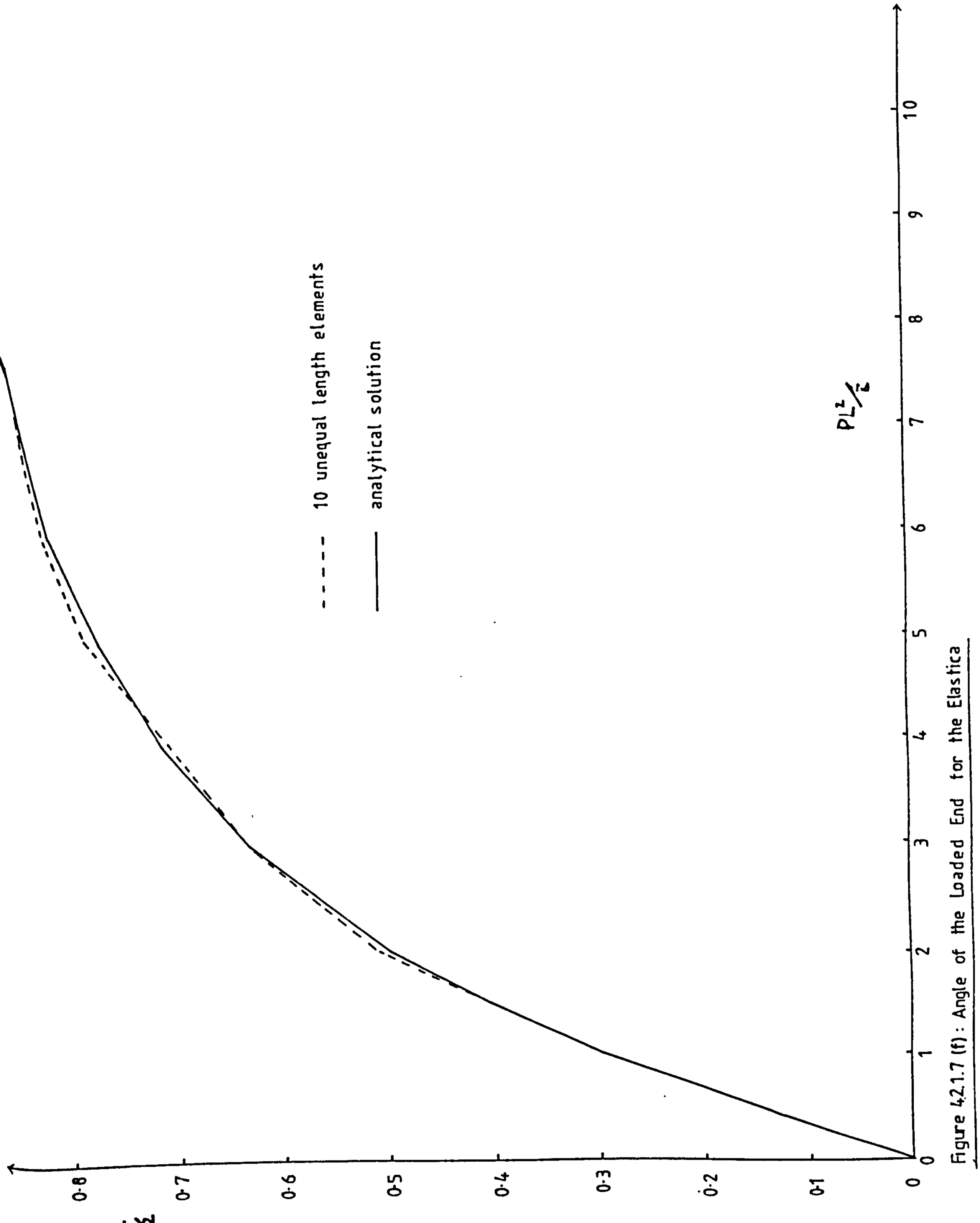

Figure 4.2.1.7 (f): Angle of the Loaded End for the Elastica

The results for the vertical displacement of the end is plotted in figure 4.2.1.7(h). Once again the accuracy achieved is excellent.

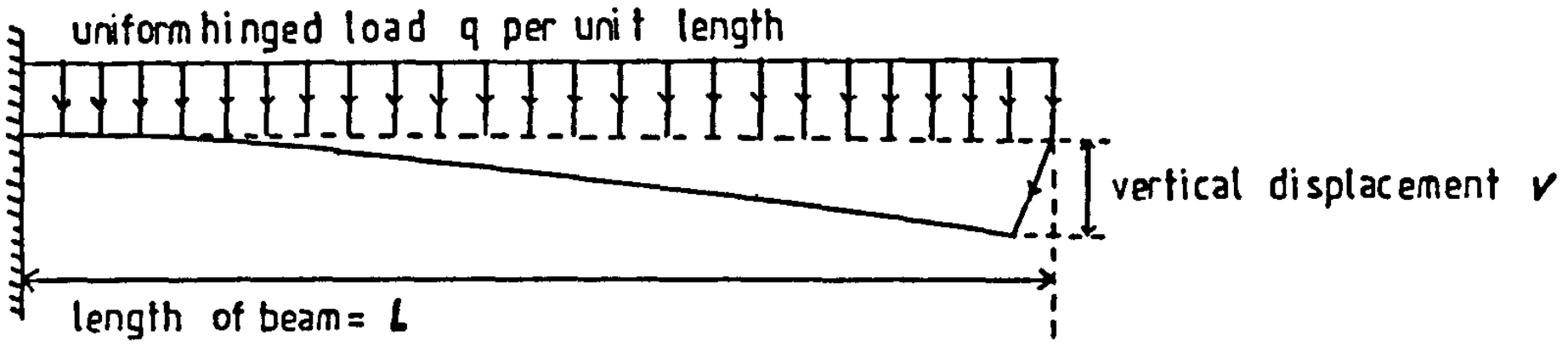

Figure 4.2.1.7 (g): Beam under uniform load (small displacements only)

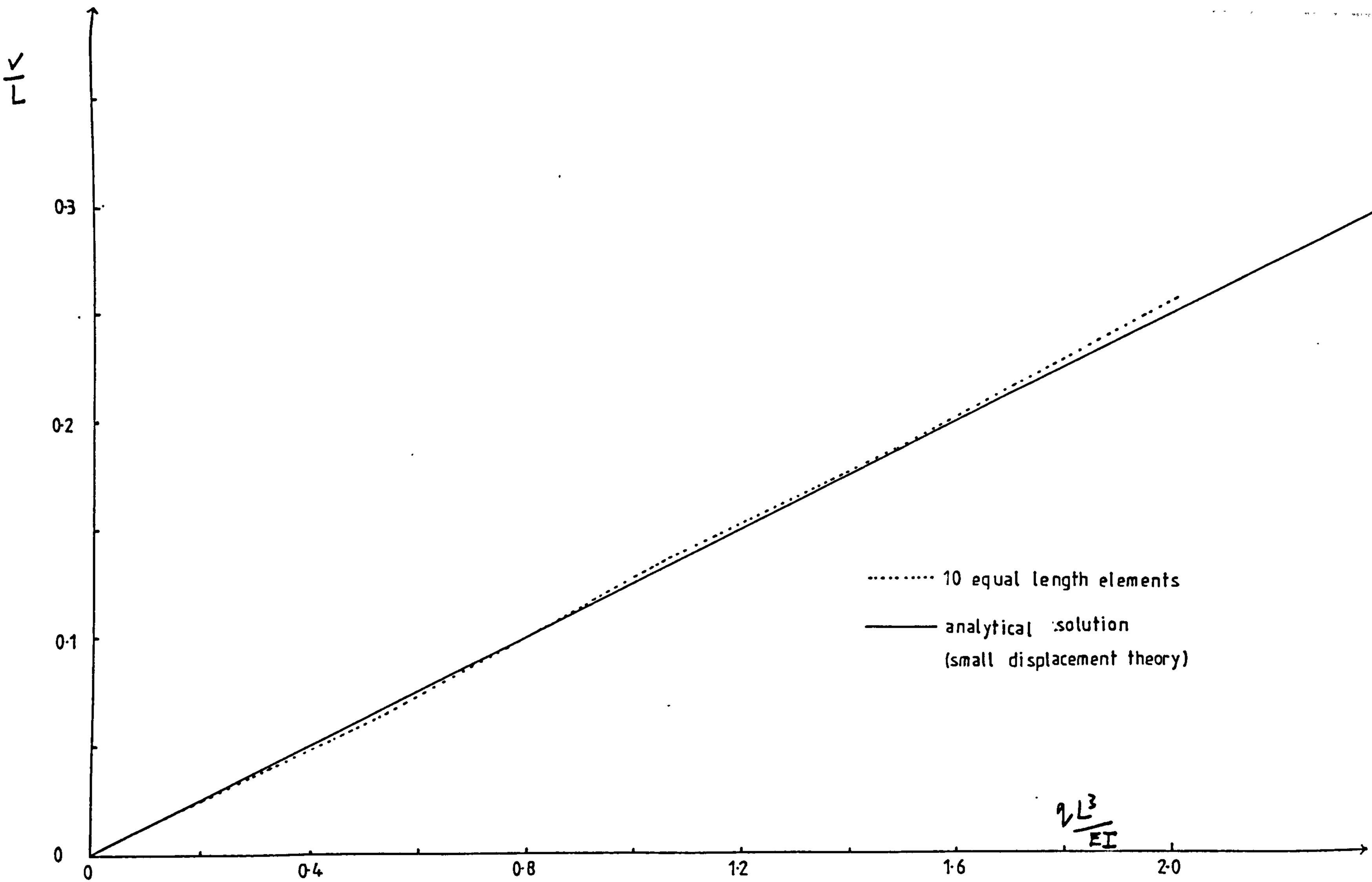

Figure 4.2.1.7 (h) : Vertical Deflection for beam under Uniform Load (small displacements only)

4.2.2:The Cubic Discretization

In section 4.2.2 it is shown how using the strain energy expression developed in section 2.6.7 it is possible to allow for the bending stiffness of the riser in the cubic discretization which was developed in section 3.7. The assembly procedure was illustrated extensively in section 3.7 and thus in section 4.2.2 only the relevant element equations are given. The strain energy V_B due to bending (section 2.6.7) is given by

$$V_B = \int_0^L \frac{B}{2} \left(\frac{\partial^2 \underset{\sim}{r}}{\partial s_0^2} \cdot \frac{\partial^2 \underset{\sim}{r}}{\partial s_0^2} \right) \left(3 - 2 \frac{\partial s}{\partial s_0} \right) ds_0 \qquad (A)$$

The strain energy expression is only valid for small strain. Using section 2.6.7

$$\delta V_B = \int_0^L B \frac{\partial^2 \underset{\sim}{r}}{\partial s_0^2} \cdot \frac{\partial^2 \delta \underset{\sim}{r}}{\partial s_0^2} ds_0 + \int_0^L \frac{B}{2} \left(\frac{\partial^2 \underset{\sim}{r}}{\partial s_0^2} \cdot \frac{\partial^2 \underset{\sim}{r}}{\partial s_0^2} \right) \left(-2 \frac{\partial \underset{\sim}{r}}{\partial s_0} \cdot \frac{\partial \delta \underset{\sim}{r}}{\partial s_0} \right) ds_0 \qquad (a)$$

If the two terms on the right hand side of this equation are discretized then the bending stiffness of the riser is effectively included.

4.2.2.2:Discretization Procedure.

The first term on the right hand side of equation 4.2.2.1(a) is a pure bending term and the second term is a coupled bending and stretching term. Using the cubic finite element characterised by equation 3.7.1(b)

$$\underset{\sim}{\Gamma} = \begin{bmatrix} \mathcal{L} & \mathcal{H} & \bar{\mathcal{L}} & \bar{\mathcal{H}} \end{bmatrix} \begin{bmatrix} \underset{\sim}{\Gamma} \\ \frac{\partial \underset{\sim}{\Gamma}}{\partial s_0} \\ \underset{\sim}{\bar{\Gamma}} \\ \frac{\partial \underset{\sim}{\bar{\Gamma}}}{\partial s_0} \end{bmatrix} \tag{A}$$

the pure bending term may be discretized

$$\int_e EI \frac{\partial^2 \underset{\sim}{\Gamma}}{\partial s_0^2} \cdot \frac{\partial^2 \delta \underset{\sim}{\Gamma}}{\partial s_0^2} \, ds_0 = \frac{(EI)_e}{H^3} \begin{bmatrix} \delta\underset{\sim}{\Gamma} & \delta\underset{\sim}{\Gamma}' & \delta\underset{\sim}{\bar{\Gamma}} & \delta\underset{\sim}{\bar{\Gamma}}' \end{bmatrix} \begin{bmatrix} 12 & 6H & -12 & 6H \\ & 4H^2 & -6H & 2H^2 \\ & & 12 & -6H \\ \text{sym.} & & & 4H^2 \end{bmatrix} \begin{bmatrix} \underset{\sim}{\Gamma} \\ \underset{\sim}{\Gamma}' \\ \underset{\sim}{\bar{\Gamma}} \\ \underset{\sim}{\bar{\Gamma}}' \end{bmatrix} \tag{B}$$

$$= (EI)_e \int_e \begin{bmatrix} \delta\underset{\sim}{\Gamma} & \delta\underset{\sim}{\Gamma}' & \delta\underset{\sim}{\bar{\Gamma}} & \delta\underset{\sim}{\bar{\Gamma}}' \end{bmatrix} \begin{bmatrix} \mathcal{L}''^2 & \mathcal{L}''\mathcal{H}'' & \mathcal{L}''\bar{\mathcal{L}}'' & \mathcal{L}''\bar{\mathcal{H}}'' \\ & \mathcal{H}''^2 & \mathcal{H}''\bar{\mathcal{L}}'' & \mathcal{H}''\bar{\mathcal{H}}'' \\ & & \bar{\mathcal{L}}''^2 & \bar{\mathcal{L}}''\bar{\mathcal{H}}'' \\ \text{sym.} & & & \bar{\mathcal{H}}''^2 \end{bmatrix} \begin{bmatrix} \underset{\sim}{\Gamma} \\ \underset{\sim}{\Gamma}' \\ \underset{\sim}{\bar{\Gamma}} \\ \underset{\sim}{\bar{\Gamma}}' \end{bmatrix} ds_0$$

in a similar manner the second term may also be discretized

$$\int_e -EI\left(\frac{\partial^2 \underset{\sim}{r}}{\partial s_0^2} \cdot \frac{\partial^2 \underset{\sim}{r}}{\partial s_0^2}\right)\left(\frac{\partial \underset{\sim}{r}}{\partial s_0} \cdot \frac{\partial \delta \underset{\sim}{r}}{\partial s_0}\right) ds_0$$

$$= -(EI)_e \left(\frac{\partial^2 \underset{\sim}{r}}{\partial s_0^2} \cdot \frac{\partial^2 \underset{\sim}{r}}{\partial s_0^2}\right)\Big|_m \int_e \begin{bmatrix} \delta\underset{\sim}{r} & \delta\underset{\sim}{r}' & \delta\bar{\underset{\sim}{r}} & \delta\bar{\underset{\sim}{r}}' \end{bmatrix} \begin{bmatrix} \mathcal{L}'^2 & \mathcal{L}'\mathcal{H}' & \mathcal{L}'\bar{\mathcal{L}}' & \mathcal{L}'\bar{\mathcal{H}}' \\ & \mathcal{H}'^2 & \mathcal{H}'\bar{\mathcal{L}}' & \mathcal{H}'\bar{\mathcal{H}}' \\ & & \bar{\mathcal{L}}'^2 & \bar{\mathcal{L}}'\bar{\mathcal{H}}' \\ \text{sym.} & & & \bar{\mathcal{H}}'^2 \end{bmatrix} \begin{bmatrix} \underset{\sim}{r} \\ \underset{\sim}{r}' \\ \bar{\underset{\sim}{r}} \\ \bar{\underset{\sim}{r}}' \end{bmatrix} ds_0$$

$$= -(EI)_e \left(\frac{\partial^2 \underset{\sim}{r}}{\partial s_0^2} \cdot \frac{\partial^2 \underset{\sim}{r}}{\partial s_0^2}\right)\Big|_m \begin{bmatrix} \delta\underset{\sim}{r} & \delta\underset{\sim}{r}' & \delta\bar{\underset{\sim}{r}} & \delta\bar{\underset{\sim}{r}}' \end{bmatrix} \begin{bmatrix} \frac{6}{5H} & \frac{1}{10} & -\frac{6}{5H} & \frac{1}{10} \\ & \frac{2}{15}H & -\frac{1}{10} & -\frac{1}{30}H \\ & & \frac{5}{6H} & -\frac{1}{10} \\ \text{sym.} & & & \frac{2}{15}H \end{bmatrix} \begin{bmatrix} \underset{\sim}{r} \\ \underset{\sim}{r}' \\ \bar{\underset{\sim}{r}} \\ \bar{\underset{\sim}{r}}' \end{bmatrix}$$

where $(EI)_e$ =value of EI evaluated at the middle of the element, H =unstrained length of the element and $\left(\frac{\partial^2 \underset{\sim}{r}}{\partial s^2} \cdot \frac{\partial^2 \underset{\sim}{r}}{\partial s^2}\right)\Big|_m$ =value of $\frac{\partial^2 \underset{\sim}{r}}{\partial s^2} \cdot \frac{\partial^2 \underset{\sim}{r}}{\partial s^2}$ at the middle of the element. $\left(\frac{\partial^2 \underset{\sim}{r}}{\partial s^2} \cdot \frac{\partial^2 \underset{\sim}{r}}{\partial s^2}\right)\Big|_m$ may be evaluated using the method given in section 3.7.7.

4.3:Moving Endpoints.

4.3.1:Introduction.

It has been assumed previously that the ends of the riser are fixed. This is an unrealistic assumption and in section 4.3 it is shown how the equations of motion must be modified for an elastic linear discretization. The same procedure can be used to obtain the modified equations of motion for the cubic discretization given in section 3.7. The modification to the force terms in the equations of motion is obvious. The only real modification is to the terms that contain the structural acceleration.

4.3.2:Additional Terms arising from the Kinetic Energy.

Allowing for the motion of the ends of the riser the kinetic energy of the riser is approximated for N elements by

$$\begin{bmatrix} \dot{\underline{r}}_0 & \dot{\underline{r}}_1 & \cdots & \dot{\underline{r}}_{N-1} & \dot{\underline{r}}_N \end{bmatrix} \begin{bmatrix} \frac{2}{6}\rho_1 H_1 & \frac{1}{6}\rho_1 H_1 & & & \\ \frac{1}{6}\rho_1 H_1 & \frac{2}{6}\rho_1 H_1 + \frac{2}{6}\rho_2 H_2 & \frac{1}{6}\rho_2 H_2 & & \\ & \frac{1}{6}\rho_2 H_2 & \frac{2}{6}\rho_2 H_2 + \frac{2}{6}\rho_3 H_3 & \ddots & \\ & & \ddots & \frac{2}{6}\rho_{N-1} H_{N-1} + \frac{2}{6}\rho_N H_N & \frac{1}{6}\rho_N H_N \\ & & & \frac{1}{6}\rho_N H_N & \frac{2}{6}\rho_N H_N \end{bmatrix} \begin{bmatrix} \dot{\underline{r}}_0 \\ \dot{\underline{r}}_1 \\ \vdots \\ \dot{\underline{r}}_{N-1} \\ \dot{\underline{r}}_N \end{bmatrix} \qquad (A)$$

all terms are defined in Chapter Three. Taking the variation gives

$$-\begin{bmatrix}\delta\underset{\sim}{r}_0 & \delta\underset{\sim}{r}_1 & \cdots & \delta\underset{\sim}{r}_{N-1} & \delta\underset{\sim}{r}_N\end{bmatrix}\begin{bmatrix}\frac{2}{6}\rho_1 H_1 & \frac{1}{6}\rho_1 H_1 & & & \\ \frac{1}{6}\rho_1 H_1 & \frac{2}{6}\rho_1 H_1 + \frac{2}{6}\rho_2 H_2 & \frac{1}{6}\rho_2 H_2 & & \\ & \frac{1}{6}\rho_2 H_2 & \frac{2}{6}\rho_2 H_2 & & \\ & & & \ddots & \\ & & & \frac{2}{6}\rho_N H_N & \frac{1}{6}\rho_N H_N \\ & & & \frac{1}{6}\rho_N H_N & \frac{2}{6}\rho_N H_N\end{bmatrix}\begin{bmatrix}\ddot{\underset{\sim}{r}}_0 \\ \ddot{\underset{\sim}{r}}_1 \\ \vdots \\ \ddot{\underset{\sim}{r}}_{N-1} \\ \ddot{\underset{\sim}{r}}_N\end{bmatrix}$$

$\underset{\sim}{r}_0$ and $\underset{\sim}{r}_N$ are known because the ends of the riser have a prescribed motion (note that it is assumed that the riser motion is uncoupled from the motion of the floating production vessel) hence $\delta\underset{\sim}{r}_0 = \delta\underset{\sim}{r}_N = \underset{\sim}{0}$. This gives the equations of motion (see Appendix C for details of manipulation)

$$\begin{bmatrix}\frac{2}{6}\rho_1 H_1 + \frac{2}{6}\rho_2 H_2 & \frac{1}{6}\rho_2 H_2 & & & \\ \frac{1}{6}\rho_2 H_2 & \frac{2}{6}\rho_2 H_2 + \frac{2}{6}\rho_3 H_3 & & & \\ & & \ddots & & \\ & & \frac{2}{6}\rho_{N-2} H_{N-2} + \frac{2}{6}\rho_{N-1} H_{N-1} & \frac{1}{6}\rho_{N-1} H_{N-1} & \\ & & \frac{1}{6}\rho_{N-1} H_{N-1} & \frac{2}{6}\rho_{N-1} H_{N-1} + \frac{2}{6}\rho_N H_N & \end{bmatrix}\begin{bmatrix}\ddot{\underset{\sim}{r}}_1 \\ \ddot{\underset{\sim}{r}}_2 \\ \vdots \\ \ddot{\underset{\sim}{r}}_{N-2} \\ \ddot{\underset{\sim}{r}}_{N-1}\end{bmatrix} = \begin{bmatrix}-\frac{1}{6}\rho_1 H_1 \ddot{\underset{\sim}{r}}_0 \\ 0 \\ \vdots \\ 0 \\ -\frac{1}{6}\rho_N H_N \ddot{\underset{\sim}{r}}_N\end{bmatrix} + \begin{bmatrix}T_2\underset{\sim}{t}_2 - T_1\underset{\sim}{t}_1 \\ T_3\underset{\sim}{t}_3 - T_2\underset{\sim}{t}_2 \\ \vdots \\ T_{N-1}\underset{\sim}{t}_{N-1} - T_{N-2}\underset{\sim}{t}_{N-2} \\ T_N\underset{\sim}{t}_N - T_{N-1}\underset{\sim}{t}_{N-1}\end{bmatrix} + \begin{bmatrix}\frac{1}{2}(\underset{\sim}{F}_{e1} + \underset{\sim}{F}_{e2}) \\ \frac{1}{2}(\underset{\sim}{F}_{e2} + \underset{\sim}{F}_{e3}) \\ \vdots \\ \frac{1}{2}(\underset{\sim}{F}_{eN-2} + \underset{\sim}{F}_{eN-1}) \\ \frac{1}{2}(\underset{\sim}{F}_{eN-1} + \underset{\sim}{F}_{eN})\end{bmatrix} \quad (A)$$

Again all terms are defined in Chapter Three. The additional inertia term on the right hand side of equation (a)

$$\begin{bmatrix}-\frac{1}{6}\rho_1 H_1 \ddot{\underset{\sim}{r}}_0 \\ 0 \\ \vdots \\ 0 \\ -\frac{1}{6}\rho_N H_N \ddot{\underset{\sim}{r}}_N\end{bmatrix} \quad (B)$$

would not be present if the ends of the riser were fixed. It has been assumed for reasons of symmetry that the right hand end of the riser has some prescribed motion however in practice it is always fixed hence the term $-\frac{1}{6}\rho_N H_N \ddot{\underset{\sim}{r}}_N$ will not be present. If a diagonal mass matrix i.e. a lumped mass matrix is used then the additional term on the right hand side of equation (a) will not be present.

4.3.3:Additional Terms arising from the Added Mass Forces.

The virtual work done on the riser by the added mass forces δW_A for N elements is approximated by

$$\delta W_A = \begin{bmatrix} \delta\underset{\sim}{r}_0 & \delta\underset{\sim}{r}_1 & \dots & \delta\underset{\sim}{r}_{N-1} & \delta\underset{\sim}{r}_N \end{bmatrix} \begin{bmatrix} \frac{1}{2}\underset{\sim}{A}_{e_1} \\ \frac{1}{2}\underset{\sim}{A}_{e_1} + \frac{1}{2}\underset{\sim}{A}_{e_2} \\ \vdots \\ \frac{1}{2}\underset{\sim}{A}_{e_{N-1}} + \frac{1}{2}\underset{\sim}{A}_{e_N} \\ \frac{1}{2}\underset{\sim}{A}_{e_N} \end{bmatrix} \qquad (A)$$

$$= -\begin{bmatrix} \delta\underset{\sim}{r}_0 & \delta\underset{\sim}{r}_1 & \dots & \delta\underset{\sim}{r}_{N-1} & \delta\underset{\sim}{r}_N \end{bmatrix} \begin{bmatrix} \alpha_1 T_1 (\ddot{\underset{\sim}{r}}_0 + \ddot{\underset{\sim}{r}}_1) \\ \alpha_1 T_1 (\ddot{\underset{\sim}{r}}_0 + \ddot{\underset{\sim}{r}}_1) + \alpha_2 T_2 (\ddot{\underset{\sim}{r}}_1 + \ddot{\underset{\sim}{r}}_2) \\ \vdots \\ \alpha_{N-1} T_{N-1} (\ddot{\underset{\sim}{r}}_{N-2} + \ddot{\underset{\sim}{r}}_{N-1}) + \alpha_N T_N (\ddot{\underset{\sim}{r}}_{N-1} + \ddot{\underset{\sim}{r}}_N) \\ \alpha_N T_N (\ddot{\underset{\sim}{r}}_{N-1} + \ddot{\underset{\sim}{r}}_N) \end{bmatrix}$$

where $4\alpha_i = \frac{1}{4}\pi\rho_w D_i^2 C_A L_i$ and

$$[T_i] = \begin{bmatrix} 1-(\underset{\sim}{t}_i)_x^2 & -(\underset{\sim}{t}_i)_x(\underset{\sim}{t}_i)_y & -(\underset{\sim}{t}_i)_x(\underset{\sim}{t}_i)_z \\ & 1-(\underset{\sim}{t}_i)_y^2 & -(\underset{\sim}{t}_i)_y(\underset{\sim}{t}_i)_z \\ \text{sym.} & & 1-(\underset{\sim}{t}_i)_z^2 \end{bmatrix} \qquad (B)$$

where $(\underset{\sim}{t}_i)_x = \underset{\sim}{t}_i \cdot \underset{\sim}{e}_x$ etc.. The added mass force is discussed in detail in section 3.2.5. δW_A may be rewritten in the form

$$-\begin{bmatrix} \delta\underset{\sim}{r}_0 & \delta\underset{\sim}{r}_1 & \cdots & \delta\underset{\sim}{r}_{N-1} & \delta\underset{\sim}{r}_N \end{bmatrix} \begin{bmatrix} \alpha_1 T_1 & \alpha_1 T_1 & & & \\ \alpha_1 T_1 & \alpha_1 T_1 + \alpha_2 T_2 & \alpha_2 T_2 & & \\ & \alpha_2 T_2 & \alpha_2 T_2 & & \\ & & & \ddots & \\ & & & \alpha_N T_N & \alpha_N T_N \\ & & & \alpha_N T_N & \alpha_N T_N \end{bmatrix} \begin{bmatrix} \ddot{\underset{\sim}{r}}_0 \\ \ddot{\underset{\sim}{r}}_1 \\ \vdots \\ \ddot{\underset{\sim}{r}}_{N-1} \\ \ddot{\underset{\sim}{r}}_N \end{bmatrix} \qquad (C)$$

Following the same reasoning as used in section 4.3.2 this gives the added mass matrix

$$\begin{bmatrix} \alpha_1 T_1 + \alpha_2 T_2 & \alpha_2 T_2 & & & \\ \alpha_2 T_2 & \alpha_2 T_2 + \alpha_3 T_3 & \alpha_3 T_3 & & \\ & \alpha_3 T_3 & \alpha_3 T_3 + & & \\ & & & \ddots & \\ & & & \alpha_{N-1} T_{N-1} + \alpha_N T_N & \alpha_N T_N \\ & & & \alpha_N T_N & \alpha_N T_N \end{bmatrix} \qquad (D)$$

which is identical to the mass matrix for the case when the ends of the riser are fixed. However there is an additional force term generated

$$\begin{bmatrix} -\alpha_1 T_1 \ddot{r}_0 \\ 0 \\ \vdots \\ 0 \\ -\alpha_N T_N \ddot{r}_N \end{bmatrix} \qquad (E)$$

Note that if a block diagonal mass matrix is used then no additional added force term will occur.

4.4:A Partially Loaded Linear Element.

4.4.1:Introduction.

When the top end of the riser lies above the water surface there exists an element that is only partially loaded. To use the conventional "lumping" process developed in section 3.4 is not correct and will lead to spurious tension transients in not only the partially submerged element but also in the adjacent elements. It is possible to reduce the tension transients by using very small elements however this is not recommended because it is very inefficient. In section 4.4 it is shown how the "lumping" process needs to be modified for a partially submerged element. The modified "lumping" on the submerged element results in alterations to the force terms and to the added mass matrix in the equations of motion.

The partially loaded element developed in section 4.4 is also used for the modelling of the ground contact of the riser with the seabed in section 4.5.

4.4.2:Derivation.

Consider the partially loaded element shown in figure 4.4.2(a). The virtual work δW_p done on the element by the partial loading is given by

$$\delta W_p = \int_e \underset{\sim}{F}.\delta\underset{\sim}{r}\,\frac{\partial \underset{\sim}{s}}{\partial s_o}\,ds_o = \frac{h}{H}\int_e \underset{\sim}{F}.\delta\underset{\sim}{r}\,ds_o = \frac{h}{H}\int_{e^*} \underset{\sim}{F}.\delta\underset{\sim}{r}\,ds_o \qquad (A)$$

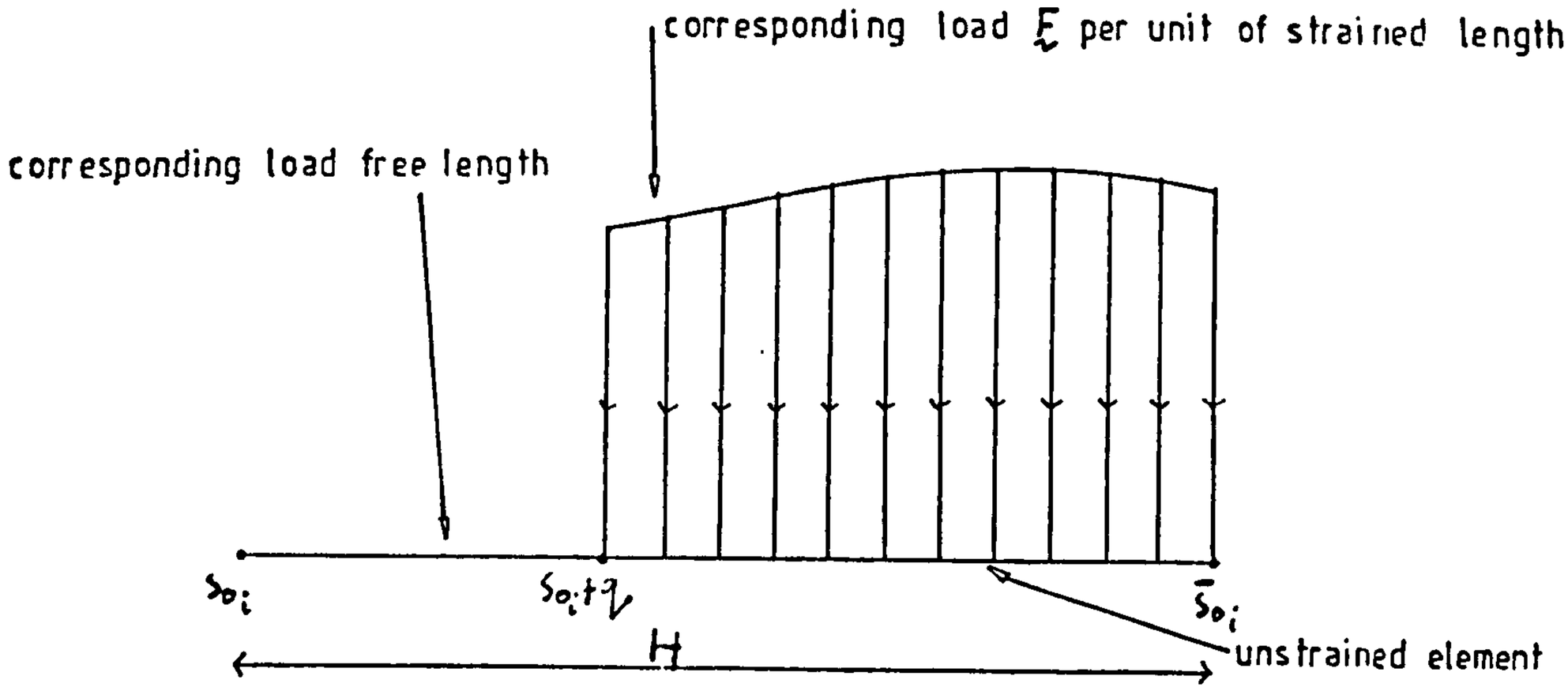

Figure 4.4.2 (a): A Partially Loaded Linear Element

where h =strained length of the element, H =unstrained length of the element, $\underset{\sim}{F}$ =force per unit of strained element length, $\underset{\sim}{r}$ =position vector of a point on the element, s =strained arc-length parameter, s_0 =unstrained arc-length parameter, e denotes integration over the whole length of the element and e^* denotes integration over the "sub-element" lying between $q + s_{0i}$ and s_{0i}. Thus

$$\delta W_p = \frac{h}{H} \underset{\sim}{F}_{me^*} \cdot \int_{e^*} \delta \underset{\sim}{r} \, ds_0 \qquad (B)$$

where $\underset{\sim}{F}_{me^*}$ denotes the value of $\underset{\sim}{F}$ evaluated at the middle of the "sub-element".

Using the standard linear interpolation defined in section 3.4.2 gives

$$\delta W_p = \frac{h}{H} \underset{\sim}{F}_{me^*} \cdot \int_{e^*} L \delta \underset{\sim}{r} + \bar{L} \delta \underset{\sim}{\bar{r}} \, ds_0 \qquad (A)$$

where L and $\bar{L}$ are the standard linear polynomials defined over the element e. By analogy it is possible to define linear polynomials L^*, $\bar{L}^*$ over the "sub-element"

$$L^* = \frac{s_o - \bar{s}_{o_i}}{-(H-q)} \quad , \quad \bar{L}^* = \frac{s_o - (s_{o_i} + q)}{(H-q)} \qquad (C)$$

L^* and $\bar{L}^*$ are useful for integrating equation (a). They may be written in terms of L and $\bar{L}$

$$L = \left(\frac{H-q}{H}\right) L^* \quad , \quad \bar{L} = \frac{(H-q)\bar{L}^* + q}{H} \qquad (D)$$

Substituting these expressions into equation (a) gives

$$\delta W_p = \frac{h}{H} \underset{\sim}{F}_{me^*} \cdot \int_{e^*} \left\{ \left[\frac{(H-q)}{H} \cdot L^*\right] \underset{\sim}{\delta r} + \left[\frac{(H-q)\bar{L}^* + q}{H}\right] \underset{\sim}{\delta \bar{r}} \right\} ds_o$$

$$= \frac{h}{H} \underset{\sim}{F}_{me^*} \cdot \left\{ \left(\frac{H-q}{H}\right)\left(\frac{H-q}{2}\right) \underset{\sim}{\delta r} + \left[\left(\frac{H-q}{H}\right)\left(\frac{H-q}{2}\right) + q\left(\frac{H-q}{2}\right)\right] \underset{\sim}{\delta \bar{r}} \right\}$$

$$= \frac{h}{H} \underset{\sim}{F}_{me^*} \left(\frac{H-q}{2}\right) \cdot \left\{ \left(1 - \frac{q}{H}\right) \underset{\sim}{\delta r} + \left(1 + \frac{q}{H}\right) \underset{\sim}{\delta \bar{r}} \right\} \qquad (F)$$

Note that q is the unstrained coordinate of the point along the element at which there is a discontinuity of loading. If the strained coordinate of the point is denoted by q_s then since the strain in a linear element is constant q_s is related to q by

$$q_s = \frac{qh}{H} \qquad (E)$$

Thus equation (b) may be written in the form

$$\delta W_p = \underset{\sim}{F}_{me^*} \left(\frac{h-q_s}{2}\right) \cdot \left\{ \left(1 - \frac{q_s}{h}\right) \delta\underset{\sim}{r} + \left(1 + \frac{q_s}{h}\right) \delta\underset{\sim}{\bar{r}} \right\} \quad (c)$$

If the element is fully submerged then equation (c) gives

$$\delta W_p = \underset{\sim}{F}_{me^*} h \cdot \left\{ \frac{1}{2} \delta\underset{\sim}{r} + \frac{1}{2} \delta\underset{\sim}{\bar{r}} \right\} \quad (F)$$

since $q_s = 0$. This is the conventional "lumping" procedure that was obtained in section 3.4.2.3. As $q_s \rightarrow h$ then more load is transfered to the correct node.

4.4.3 :Modification to the Equation of Motion.

There is no modification of the gravity load, however all the other terms must be modified if an element is partially submerged. The modification to the buoyancy force, inertia force and added mass force are described in section 4.4.1. The modifications to the other forces can similarly be deduced.

4.4.3.1:Buoyancy Force

The virtual work done on the system by the buoyancy forces is

$$\begin{bmatrix} \delta\underset{\sim}{r}_0 & \delta\underset{\sim}{r}_1 & \cdots & \delta\underset{\sim}{r}_{s-1} & \delta\underset{\sim}{r}_s & \delta\underset{\sim}{r}_{s+1} & \cdots & \delta\underset{\sim}{r}_{N-1} & \delta\underset{\sim}{r}_N \end{bmatrix} \begin{bmatrix} 0 \\ 0 \\ \vdots \\ \vdots \\ \gamma\,\underset{\sim}{U}_{es} \\ (1-\gamma)\underset{\sim}{U}_{es} + \frac{1}{2}\underset{\sim}{U}_{es-1} \\ \frac{1}{2}(\underset{\sim}{U}_{es+1} + \underset{\sim}{U}_{es+2}) \\ \vdots \\ \frac{1}{2}(\underset{\sim}{U}_{eN-2} + \underset{\sim}{U}_{eN-1}) \\ \frac{1}{2}(\underset{\sim}{U}_{eN-1} + \underset{\sim}{U}_{eN}) \\ \frac{1}{2}\underset{\sim}{U}_{eN} \end{bmatrix} \qquad (A)$$

where s denotes the submerged element and $\gamma = (h - q_s)/2h$. $\underset{\sim}{U}_{ei}$ is given by

$$\underset{\sim}{U}_{ei} = \rho_w V_i g \underset{\sim}{k} \qquad (B)$$

where ρ_w =density of seawater, g =acceleration due to gravity and V_i =submerged volume of the element. Note that since the ends execute some prescribed motion $\delta\underset{\sim}{r}_0 = \delta\underset{\sim}{r}_N = 0$. If all the elements are submerged then this result reduces to that obtained in Chapter Three.

4.4.3.2:Inertia Force

The virtual work done on the system by the inertia forces is

$$\begin{bmatrix} \delta r_0 & \delta r_1 & \dots & \delta r_{s-1} & \delta r_s & \delta r_{s+1} & \dots & \delta r_{N-1} & \delta r_N \end{bmatrix} \begin{bmatrix} 0 \\ 0 \\ \vdots \\ \gamma I_{es} \\ (1-\gamma) I_{es} + \frac{1}{2} I_{es+1} \\ \frac{1}{2} I_{es+1} + \frac{1}{2} I_{es+2} \\ \vdots \\ \frac{1}{2} I_{eN-1} + \frac{1}{2} I_{eN} \\ \frac{1}{2} I_{eN} \end{bmatrix} \qquad (A)$$

where s denotes the submerged element and $\gamma = (h-q)/2h$. I_{ei} is given by

$$I_{ei} = \frac{1}{4} \pi \rho_w D_i^2 L_i (1 + C_A) \dot{u}_{fi} |_{n_i} \qquad (B)$$

where all quantities are exactly the same as those given in section 3.2.5 except L_i and $\dot{u}_{fi}$. In this case L_i =submerged length of the element and $\dot{u}_{fi}$ is the fluid acceleration evaluated at the point on the element midway between the water surface and the submerged node if the element is only partially submerged. If all the elements are submerged then this result reduces to that obtained in

Chapter Three.

4.4.3.3:Added Mass Forces.

The virtual work done on the system due to the added mass forces is

$$\begin{bmatrix} \delta\underset{\sim}{r}_0 & \delta\underset{\sim}{r}_1 & \cdots & \delta\underset{\sim}{r}_{s-1} & \delta\underset{\sim}{r}_s & \delta\underset{\sim}{r}_{s+1} & \cdots & \delta\underset{\sim}{r}_{N-1} & \delta\underset{\sim}{r}_N \end{bmatrix} \begin{bmatrix} \frac{1}{2}\underset{\sim}{A}_{e_1} \\ \frac{1}{2}\underset{\sim}{A}_{e_1} + \frac{1}{2}\underset{\sim}{A}_{e_2} \\ \vdots \\ \frac{1}{2}\underset{\sim}{A}_{e_{s-1}} + \gamma\underset{\sim}{A}_{e_s} \\ (1-\gamma)\underset{\sim}{A}_{e_s} + \frac{1}{2}\underset{\sim}{A}_{e_{s+1}} \\ \vdots \\ \frac{1}{2}\underset{\sim}{A}_{e_{N-1}} + \frac{1}{2}\underset{\sim}{A}_{e_N} \\ \frac{1}{2}\underset{\sim}{A}_{e_N} \end{bmatrix} \qquad (A)$$

where $\gamma = (h - q_s)/2h$, $\underset{\sim}{A}_{e_i} = -4\alpha_i \ddot{\underset{\sim}{r}}_{e_i} |_{n_i}$, L_i =submerged length of an element and for reasons of simplicity for all the elements $\ddot{\underset{\sim}{r}}_{e_i} = \frac{1}{2}(\ddot{\underset{\sim}{r}}_i + \ddot{\underset{\sim}{r}}_{i-1})$. For s=1 $\underset{\sim}{A}_{s-1}$ is defined to be zero.

Now

$$
\begin{bmatrix}
\frac{1}{2}\underset{\sim}{A}_{e_1} \\
\frac{1}{2}\underset{\sim}{A}_{e_1} + \frac{1}{2}\underset{\sim}{A}_{e_2} \\
\vdots \\
\frac{1}{2}\underset{\sim}{A}_{e_{s-1}} + \gamma\,\underset{\sim}{A}_{e_s} \\
(1-\gamma)\,\underset{\sim}{A}_{e_s} + \frac{1}{2}\underset{\sim}{A}_{e_{s+1}} \\
\vdots \\
\frac{1}{2}\underset{\sim}{A}_{e_{N-1}} + \frac{1}{2}\underset{\sim}{A}_{e_N} \\
\frac{1}{2}\underset{\sim}{A}_{e_N}
\end{bmatrix}
= -
\begin{bmatrix}
2\alpha_1\, \ddot{\underset{\sim}{r}}_{e_1} \cdot \underset{\sim}{n}_1 \\
2\alpha_1\, \ddot{\underset{\sim}{r}}_{e_1} \underset{\sim}{n}_1 + 2\alpha_2\, \ddot{\underset{\sim}{r}}_{e_2} \underset{\sim}{n}_2 \\
\vdots \\
2\alpha_{s-1}\, \ddot{\underset{\sim}{r}}_{e_{s-1}} \underset{\sim}{n}_{s-1} + \gamma\, 4\alpha_s\, \ddot{\underset{\sim}{r}}_{e_s} \underset{\sim}{n}_s \\
(1-\gamma)\, 4\alpha_s\, \ddot{\underset{\sim}{r}}_{e_s} \underset{\sim}{n}_s + 2\alpha_{s+1}\, \ddot{\underset{\sim}{r}}_{e_{s+1}} \underset{\sim}{n}_{s+1} \\
\vdots \\
2\alpha_{N-1}\, \ddot{\underset{\sim}{r}}_{e_{N-1}} \underset{\sim}{n}_{N-1} + 2\alpha_N\, \ddot{\underset{\sim}{r}}_{e_N} \underset{\sim}{n}_N \\
2\alpha_N\, \ddot{\underset{\sim}{r}}_{e_N} \underset{\sim}{n}_N
\end{bmatrix}
$$

$$
= -
\begin{bmatrix}
\alpha_1 T_1 (\ddot{\underset{\sim}{r}}_0 + \ddot{\underset{\sim}{r}}_1) \\
\alpha_1 T_1 (\ddot{\underset{\sim}{r}}_0 + \ddot{\underset{\sim}{r}}_1) + \alpha_2 T_2 (\ddot{\underset{\sim}{r}}_1 + \ddot{\underset{\sim}{r}}_2) \\
\vdots \\
\alpha_{s-1} T_{s-1} (\ddot{\underset{\sim}{r}}_{s-2} + \ddot{\underset{\sim}{r}}_{s-1}) + 2\gamma\alpha_s T_s (\ddot{\underset{\sim}{r}}_{s-1} + \ddot{\underset{\sim}{r}}_s) \\
(1-\gamma)\, 2\alpha_s T_s (\ddot{\underset{\sim}{r}}_{s-1} + \ddot{\underset{\sim}{r}}_s) + \alpha_{s+1} T_{s+1} (\ddot{\underset{\sim}{r}}_s + \ddot{\underset{\sim}{r}}_{s+1}) \\
\vdots \\
\alpha_{N-1} T_{N-1} (\ddot{\underset{\sim}{r}}_{N-2} + \ddot{\underset{\sim}{r}}_{N-1}) + \alpha_N T_N (\ddot{\underset{\sim}{r}}_{N-1} + \ddot{\underset{\sim}{r}}_N) \\
\alpha_N T_N (\ddot{\underset{\sim}{r}}_{N-1} + \ddot{\underset{\sim}{r}}_N)
\end{bmatrix}
\qquad (B)
$$

$$= - \begin{bmatrix} \alpha_1 T_1 & \alpha_1 T_1 & & & & & & \\ \alpha_1 T_1 & \alpha_1 T_1 + \alpha_2 T_2 & \alpha_2 T_2 & & & & & \\ & \alpha_2 T_2 & \alpha_2 T_2 + & & & & & \\ & & \ddots & & & & & \\ & & + & \alpha_{s-1} T_{s-1} & & & & \\ & & \alpha_{s-1} T_{s-1} & \alpha_{s-1} T_{s-1} + 2\gamma_s \alpha_s T_s & 2\gamma_s T_s \alpha_s & & & \\ & & & (1-\gamma) 2\alpha_s T_s & (1-\gamma) 2\alpha_s T_s + & & & \\ & & & & \ddots & & & \\ & & & & + \alpha_{N-1} T_{N-1} & \alpha_{N-1} T_{N-1} & & \\ & & & & \alpha_{N-1} T_{N-1} & \alpha_{N-1} T_{N-1} + \alpha_N T_N & \alpha_N T_N & \\ & & & & & \alpha_N T_N & \alpha_N T_N & \end{bmatrix} \begin{bmatrix} \ddot{\underset{\sim}{r}}_0 \\ \ddot{\underset{\sim}{r}}_1 \\ \ddot{\underset{\sim}{r}}_2 \\ \vdots \\ \ddot{\underset{\sim}{r}}_{s-2} \\ \ddot{\underset{\sim}{r}}_{s-1} \\ \ddot{\underset{\sim}{r}}_s \\ \vdots \\ \ddot{\underset{\sim}{r}}_{N-2} \\ \ddot{\underset{\sim}{r}}_{N-1} \\ \ddot{\underset{\sim}{r}}_N \end{bmatrix}$$

If the top element is partially submerged this gives an added mass matrix

$$\begin{bmatrix} (1-\gamma) 2\alpha_1 T_1 + \alpha_2 T_2 & \alpha_2 T_2 & & & \\ \alpha_2 T_2 & \alpha_2 T_2 & & & \\ & & \ddots & & \\ & & & \alpha_{N-1} T_{N-1} & \alpha_{N-1} T_{N-1} \\ & & & \alpha_{N-1} T_{N-1} & \alpha_{N-1} T_{N-1} + \alpha_N T_N \end{bmatrix} \qquad (C)$$

and an additional force term of

$$- \begin{bmatrix} (1-\gamma) 2\alpha_1 T_1 \ddot{\underset{\sim}{r}}_0 \\ 0 \\ \vdots \\ 0 \\ \alpha_N T_N \ddot{\underset{\sim}{r}}_N \end{bmatrix} \qquad (D)$$

If the top element is not submerged then the added mass matrix is

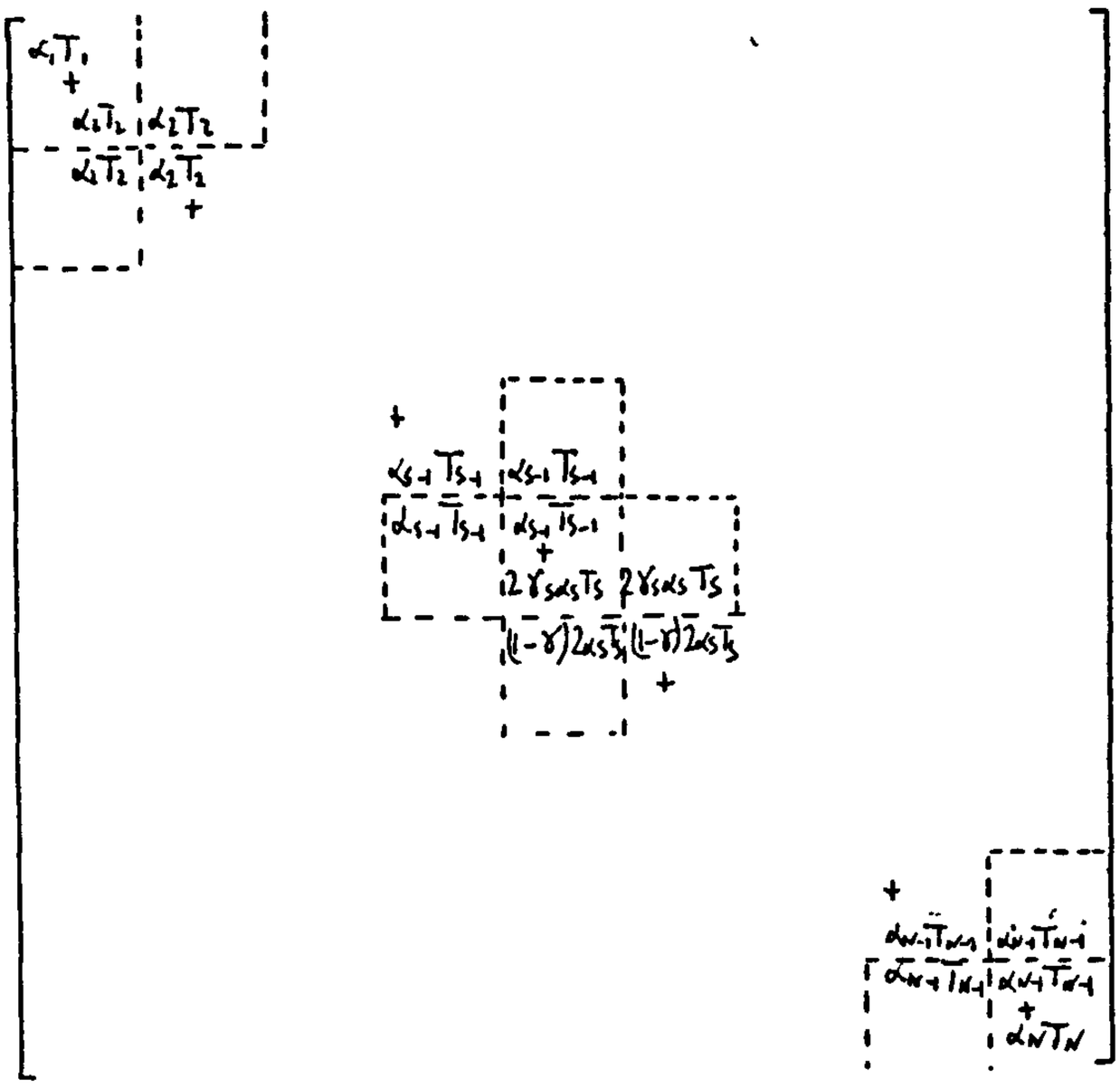

(E)

with the additional force term of

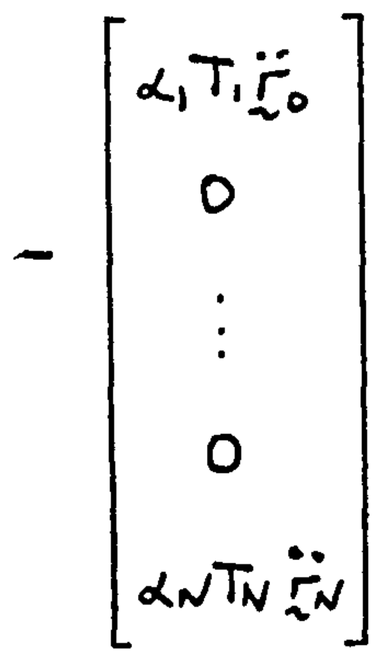

(F)

4.5:Ground Contact.

The seabed is modelled as a liquid with a density that gradually increases with depth. This is illustrated in figure 4.5(a).

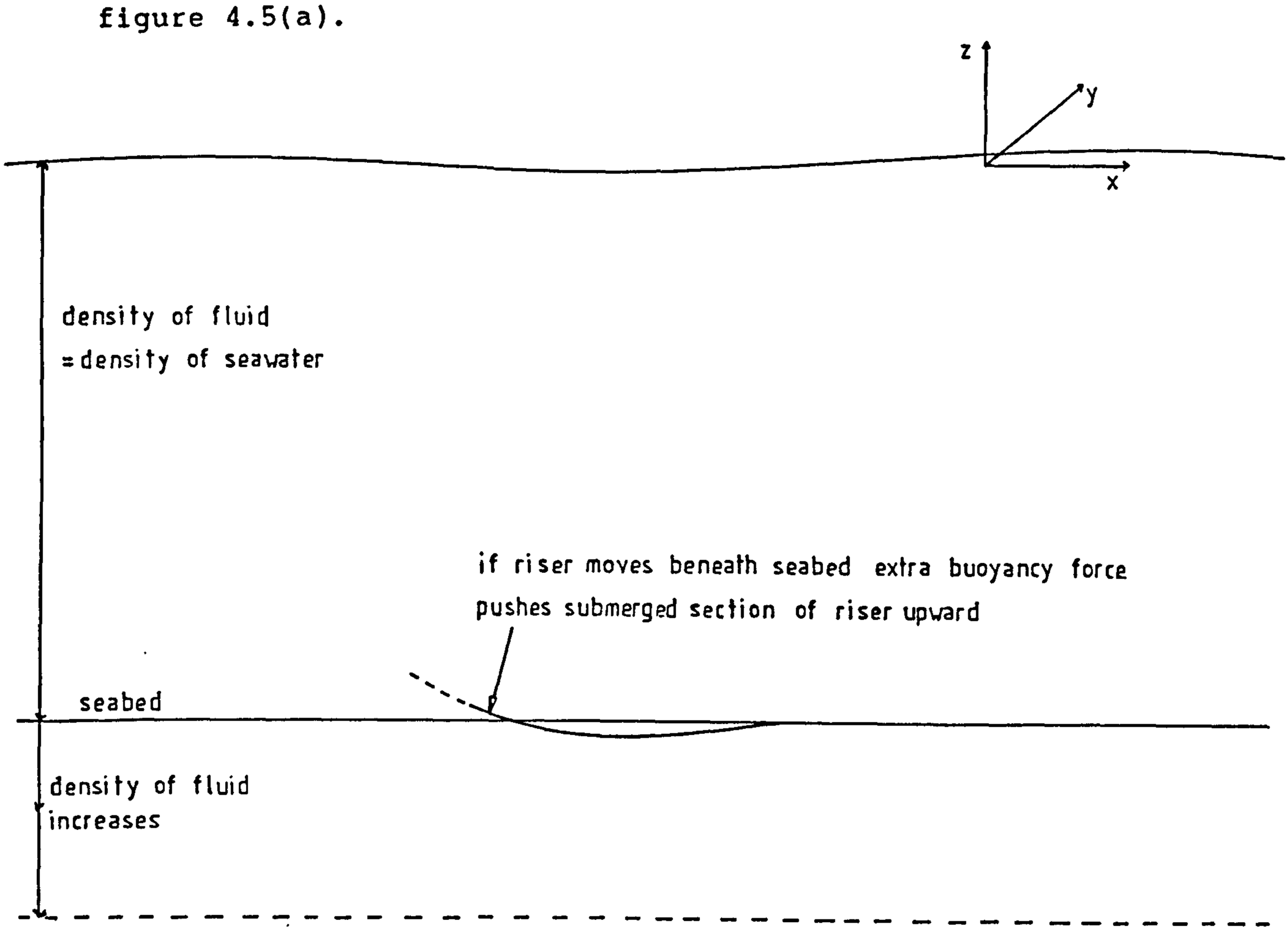

Figure 4.5(a): The Modelling of Ground Contact

The density of the seabed fluid ρ_f is given by

$$\rho_f = \rho_w \left\{ 1 + (s_d - z)(C - 1) \right\} \quad (a)$$

where z =depth beneath the sea surface, s_d =seabed depth and C =appropriately chosen constant. Equation (a) gives the result that at a distance of 1.0m below the seabed the

density of the fluid is $C\rho_w$.

Results are shown for the modelling of ground contact in figures 4.5(b),(c). Two values of the constant C are used; C =5 and C =10. The data used for this example is identical to that used in section 5.2 and S_d =-110m. The element discretization is as follows

ELEMENT	ELEMENT LENGTH[metres]
1	32
2	32
3	32
4	32
5	32
6	37.6
7	10
8	10
9	10
10	10

Note that with this element discretization if the seabed were not present then the lower part of the riser would reach a maximum depth of around -113m. With C =10 there

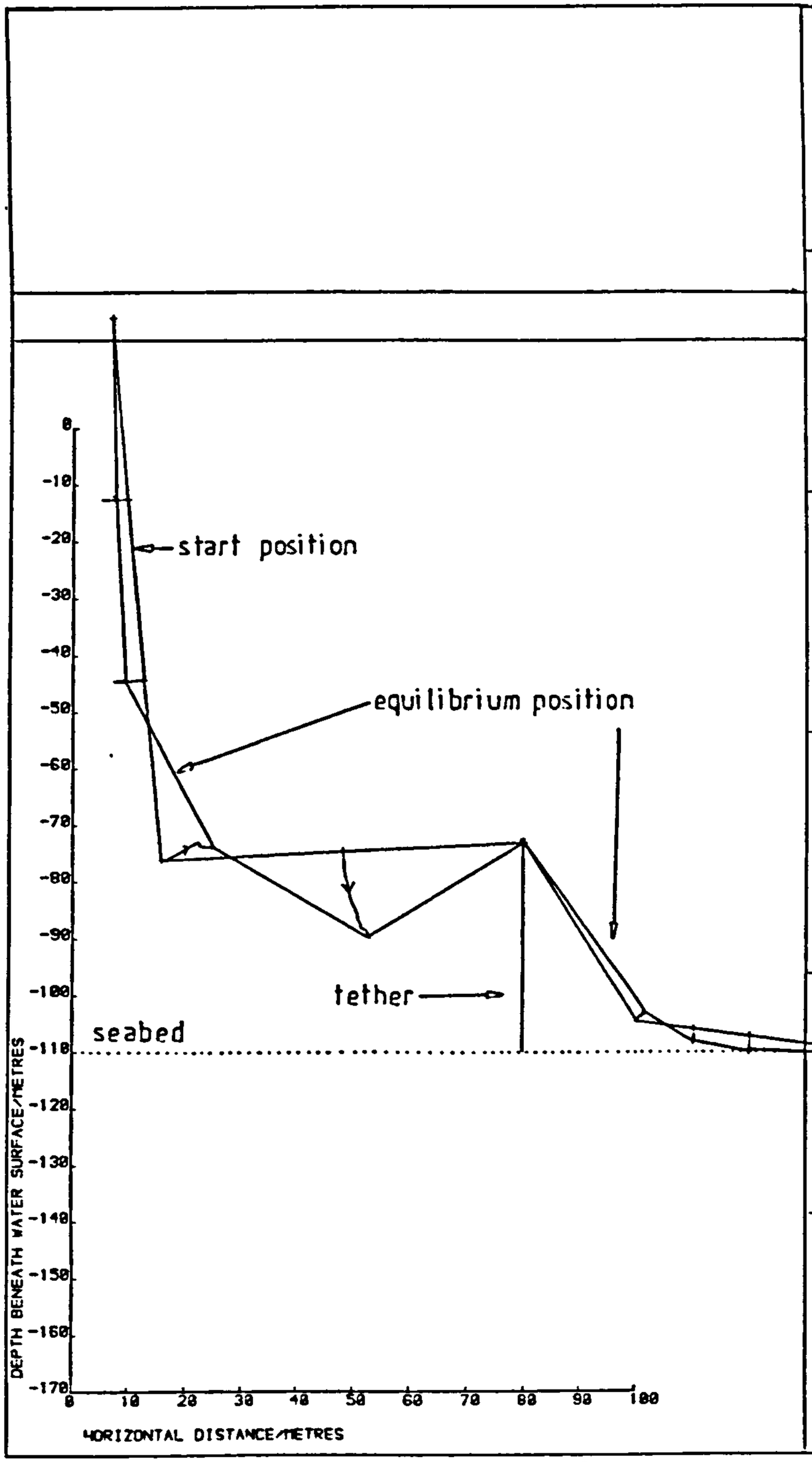

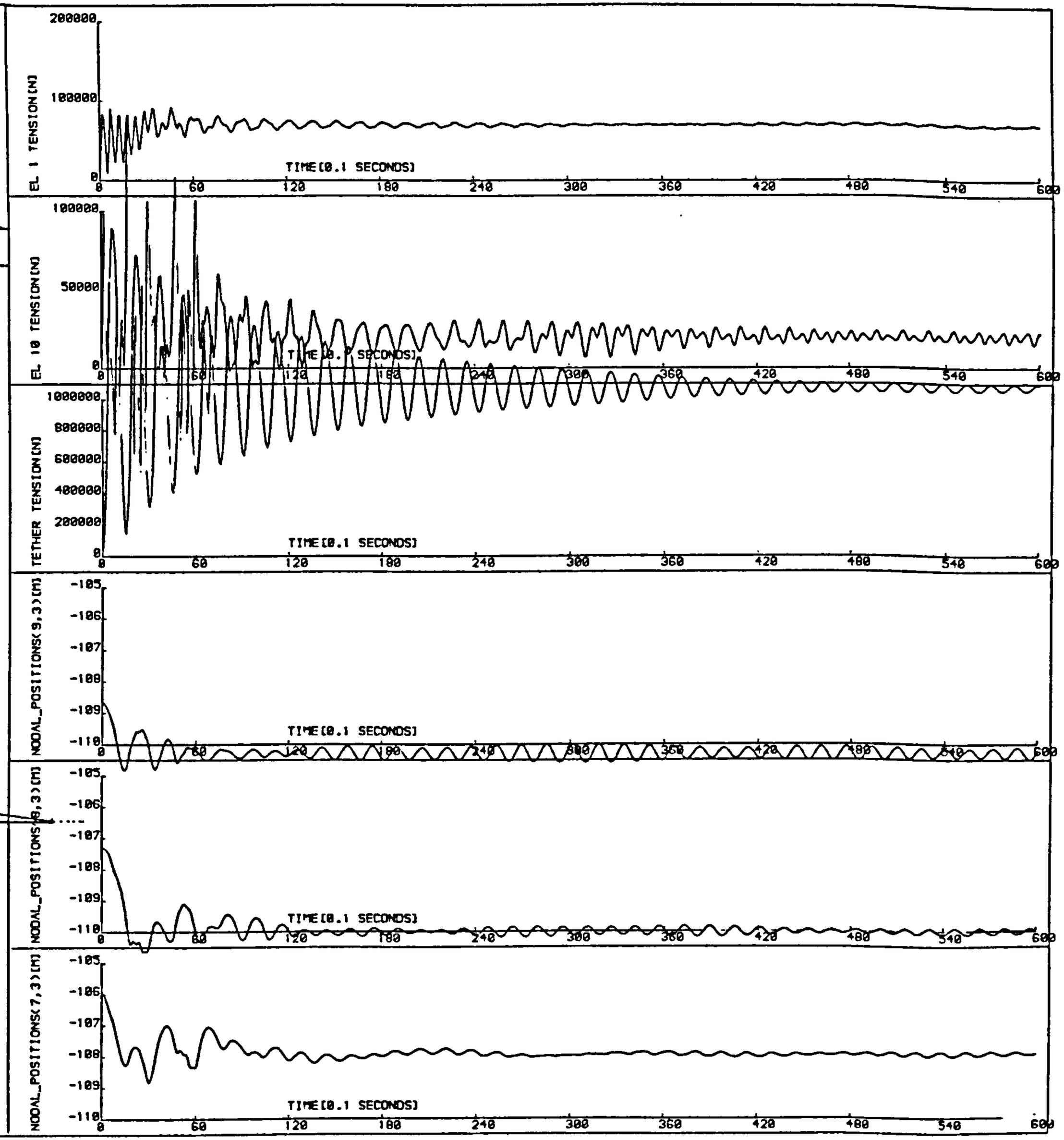

Figure 4.5(b): Ground Contact with $C = 5m^{-1}$

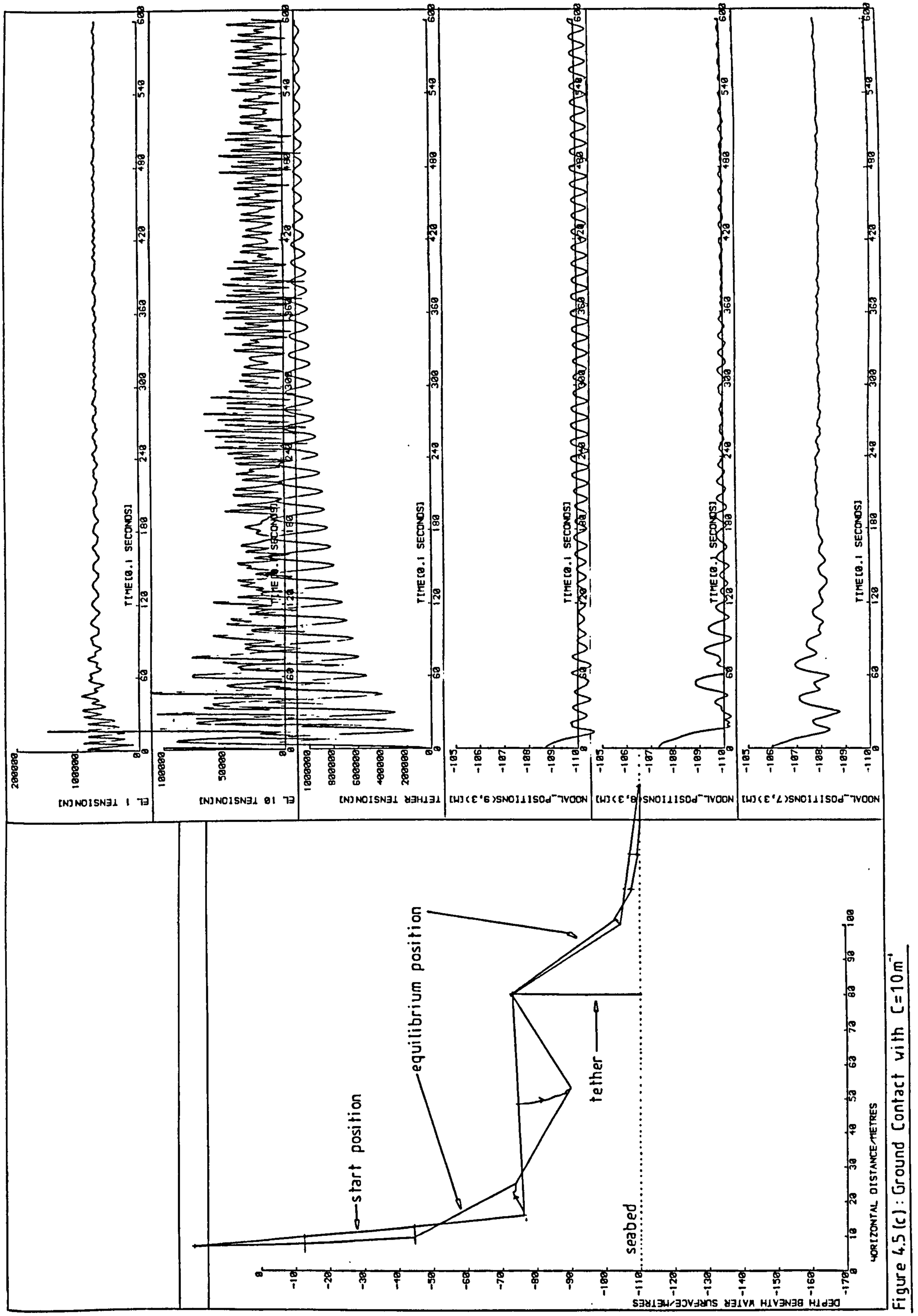

Figure 4.5 (c): Ground Contact with C=10m

are transients in the 10th element tension that are only very slowly damped out. With C =5 the transients in the 10th element tension are negligible. Note that the increase in the density of the seabed liquid are not taken account of in calculating any of the element forces apart from the element upthrust force. Better results i.e. transients of smaller magnitude would be obtained by taking account of this factor. Using more elements also improves the results. For a commercial design study many more elements are needed in the region of the seabed. Because of the way in which ground contact is modelled the ninth node lies about 0.25m beneath the seabed. This effect is of no practical consequence. Note that the eighth node lies on the seabed.

The partially loaded element developed in section 4.4 is used for the modelling of ground contact. This means fewer elements need to be used in the region of the seabed. Special care is needed to take account of the different configurations that are possible in the seabed region and to ensure that the loads are transfered to the nodes in the appropriate amounts. Examples of possible configurations are shown in figure 4.5(d).

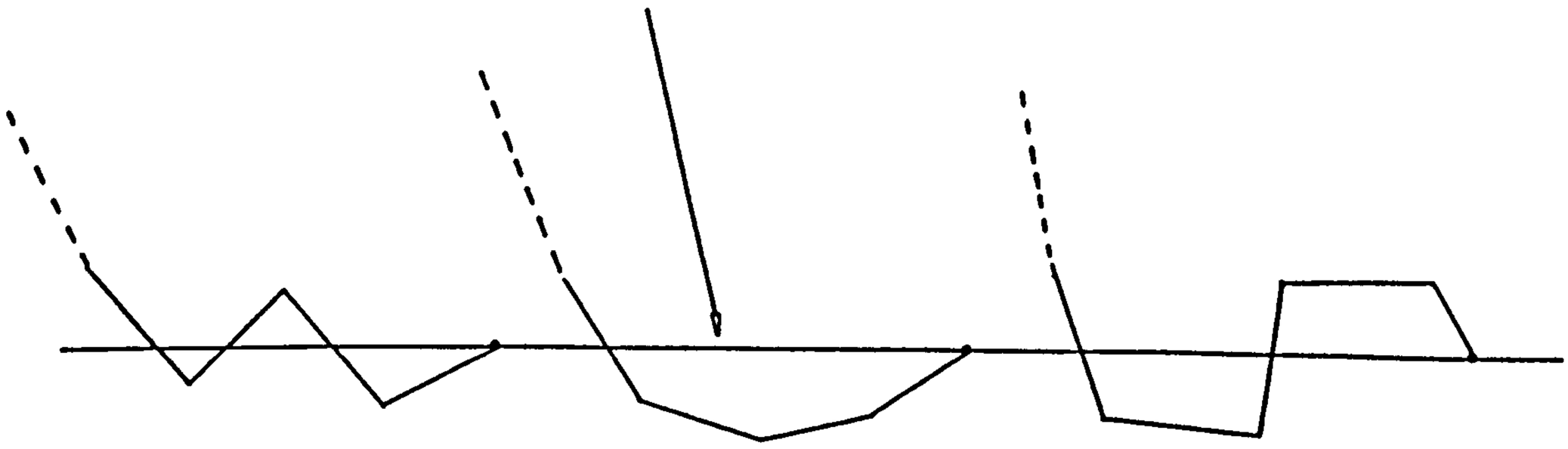

Figure 4.5 (d): Possible Seabed Configurations

4.6:Internal Material Damping.

Internal material damping may be incorporated into a linear discretization by placing dampers across the elements as shown in figure 4.6(a) Thus the virtual work done by the dampers is

$$\left[\delta\underset{\sim}{r}_0 \quad \delta\underset{\sim}{r}_1 \ldots \delta\underset{\sim}{r}_{N-1} \; \delta\underset{\sim}{r}_N\right]\begin{bmatrix} -\alpha_1[(\dot{\underset{\sim}{r}}_0-\dot{\underset{\sim}{r}}_1)\cdot\underset{\sim}{t}_1]\,\underset{\sim}{t}_1 \\ \alpha_1[(\dot{\underset{\sim}{r}}_0-\dot{\underset{\sim}{r}}_1)\cdot\underset{\sim}{t}_1]\,\underset{\sim}{t}_1 - \alpha_2[(\dot{\underset{\sim}{r}}_1-\dot{\underset{\sim}{r}}_2)\cdot\underset{\sim}{t}_2]\,\underset{\sim}{t}_2 \\ \vdots \\ \alpha_{N-1}[(\dot{\underset{\sim}{r}}_{N-2}-\dot{\underset{\sim}{r}}_{N-1})\cdot\underset{\sim}{t}_{N-1}]\,\underset{\sim}{t}_{N-1} - \alpha_N[(\dot{\underset{\sim}{r}}_{N-1}-\dot{\underset{\sim}{r}}_N)\cdot\underset{\sim}{t}_N]\,\underset{\sim}{t}_N \\ \alpha_N[(\dot{\underset{\sim}{r}}_{N-1}-\dot{\underset{\sim}{r}}_N)\cdot\underset{\sim}{t}_N]\,\underset{\sim}{t}_N \end{bmatrix} \qquad (A)$$

where α_i =damping coefficient for the ith element. Linear damping has been chosen although it would be simple to model other types of damping. There is no data available for the internal material damping of flexible risers hence it is difficult to estimate α_i . Note that the internal material damping also has an important effect on the possible vortex shedding of the riser (see section 5.4). In practice it was found that once the damping coefficient was increased past a certain value numerical instability occurred. This is identical to the situation for the extensional stiffness of the riser where past a critical value numerical instability occured when the equation $T_i = \frac{(EA)_i}{L_i^*}(L_i - L_i^*)$ was used (see Chapter Three for notation). This indicates that perhaps an incremental method of calculating the internal material damping forces is needed. Up to the point of instability the internal material damping had no noticeable effect.

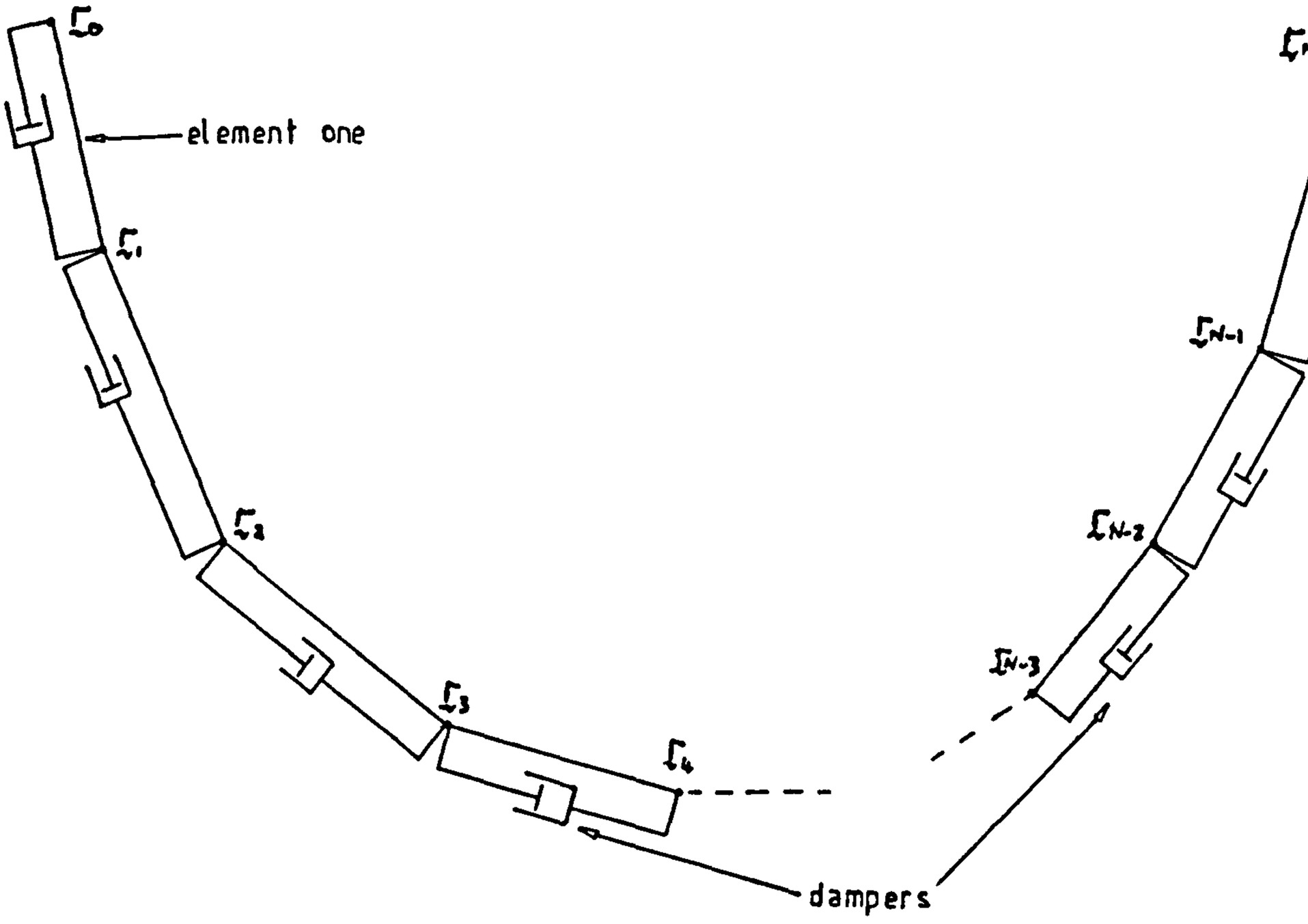

Figure 4.6 (a): The Modelling of Internal Material Damping

4.7:Internal Fluid Flow.

4.7.1:Introduction.

From section 2.5.2 the force $\underset{\sim}{R}^*$ exerted on the riser by the internal fluid per unit of strained length is given by

$$\underset{\sim}{R}^* = -\rho_f A \left(\frac{\partial}{\partial t} + v\frac{\partial}{\partial s}\right)^2 \underset{\sim}{r}(s,t) - \rho_f g A \underset{\sim}{k} \qquad (a)$$

where ρ_f =density of the internal fluid per unit volume, A =internal cross-sectional area of the riser, t =time, s =strained arc-length parameter, v =speed of internal fluid flow, $\underset{\sim}{r}$ =position vector of centre-line of riser and g =acceleration due to gravity. Note that in deriving equation (a) it has been assumed that the riser suffers small strain only. This implies that A is constant. Also note that a pressure term resulting from internal fluid flow is absorbed into the effective tension term.

It is assumed that v is constant for reasons of simplicity. Then expanding equation (a) gives

$$\underset{\sim}{R}^* = -\rho_f A \left\{\frac{\partial^2 \underset{\sim}{r}}{\partial t^2} + 2v\frac{\partial \underset{\sim}{t}}{\partial t} + v^2 \kappa \underset{\sim}{n}\right\} - \rho_f g A \underset{\sim}{k} \qquad (A)$$

The term $\rho_f A \frac{\partial^2 \underset{\sim}{r}}{\partial t^2}$ is absorbed into the acceleration term for the riser and the term $-\rho_f g A \underset{\sim}{k}$ is absorbed into the weight term for the riser. Thus the effective force $\underset{\sim}{R}_e$ per unit length of the riser due to internal fluid flow is

given by

$$\underset{\sim}{R}_e = -\rho_f A \left\{ 2v \frac{\partial \underset{\sim}{t}}{\partial t} + v^2 \kappa \underset{\sim}{n} \right\} \qquad (b)$$

$\underset{\sim}{R}_e$ is composed of two parts; one is dependent on the geometry of the riser and the other is dependent on the motion of the riser. The force on a section of a stationary riser is shown in figure 4.7(a) for various curvatures.

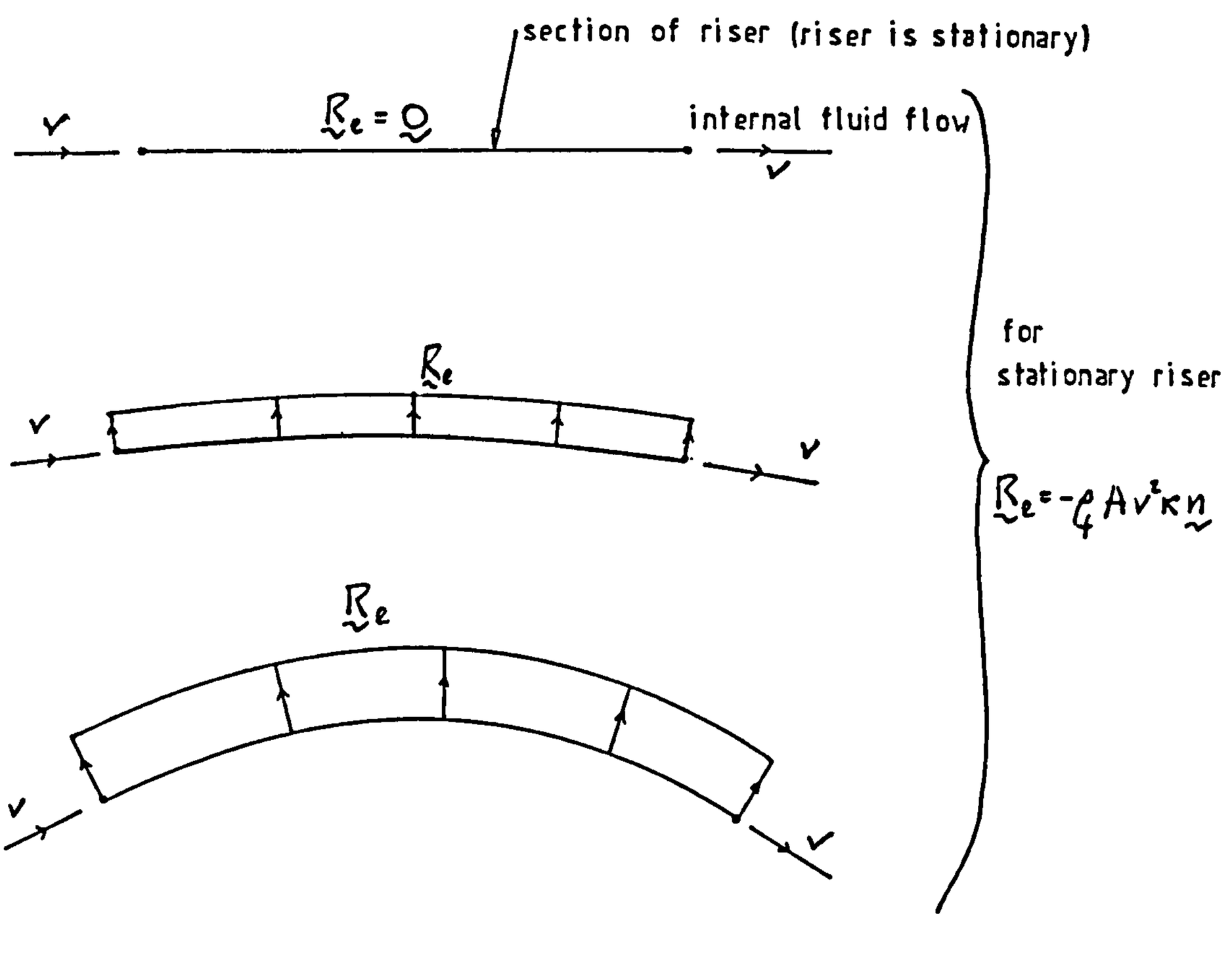

Figure 4.7.1 (a): Force on a Riser Section due to Internal Fluid Flow

4.7.2:Virtual Work done by Internal Fluid Flow.

Consider a riser modelled by N linear elements as shown in figure 4.7.2(a). An estimate is needed of the virtual work done on the riser by the internal fluid flow. This then gives the additional nodal forces that need to be added to the equations of motion.

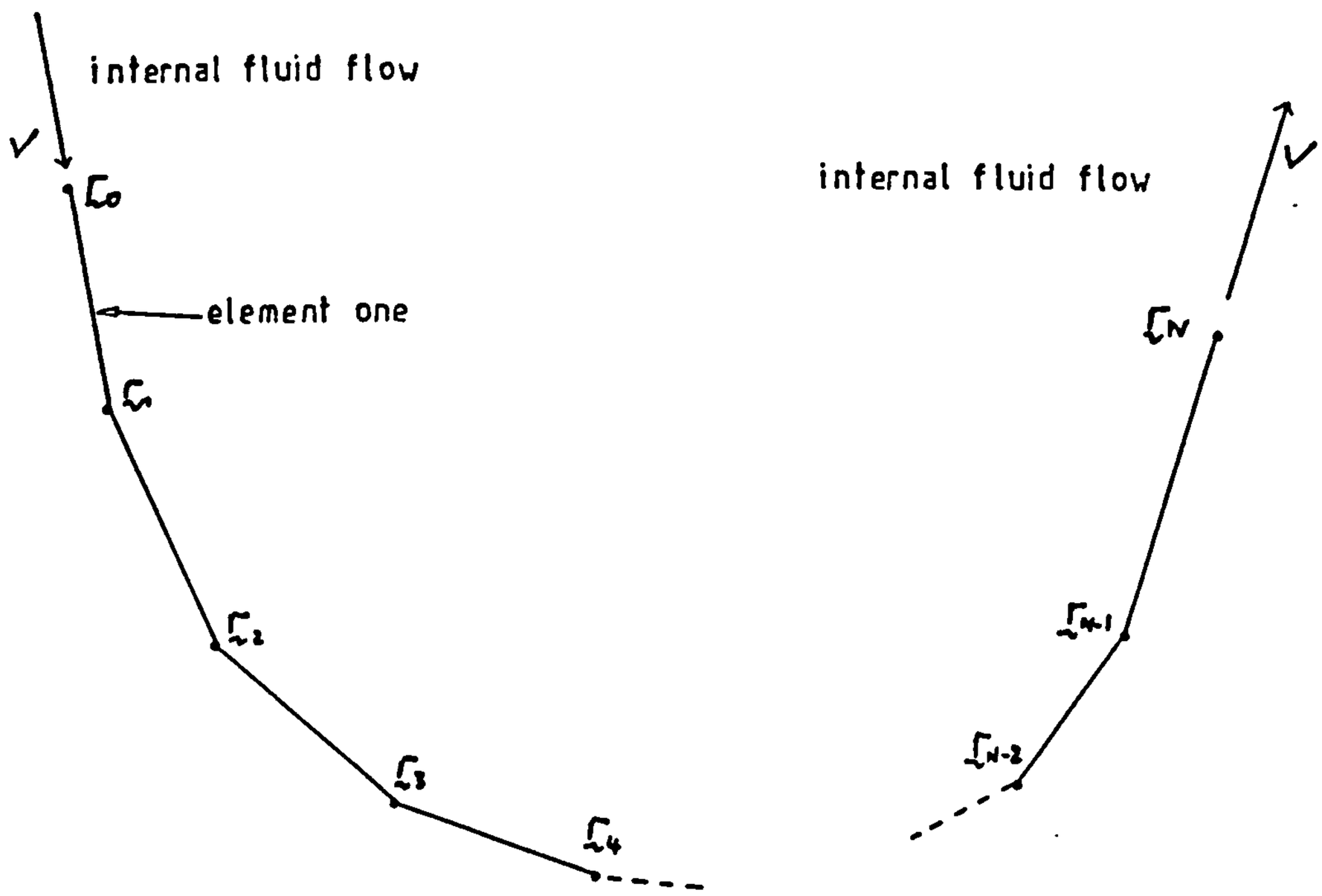

Figure 4.7.2 (a): Calculation of the Virtual Work due to Internal Fluid Flow

From section 3.4.2.3 the virtual work δW_e done on an element by the internal fluid flow is

$$\delta W_e = h \, \underset{\sim}{R}_e|_m \cdot \frac{1}{2} (\delta \underset{\sim}{\Gamma} + \delta \underset{\sim}{\bar{\Gamma}}) \qquad (a)$$

where $\underset{\sim}{R}_e|_m$=value of $\underset{\sim}{R}_e$ evaluated at the middle of the

element, h =strained length of an element and $\underset{\sim}{r}$, $\bar{\underset{\sim}{r}}$ are the appropriate position vectors (see section 3.4.2) of the ends of the element.

For a given element $\underset{\sim}{R}_e|_m$ may be evaluated as follows using equation 4.7.1(b)

$$\underset{\sim}{R}_{e_1}|_m = -\rho_f A \left\{ 2v \left.\frac{d\underset{\sim}{t}}{dt}\right|_{m_1} + v^2 \frac{1}{2}\left[\left.\frac{d\underset{\sim}{t}}{ds}\right|_0 + \left.\frac{d\underset{\sim}{t}}{ds}\right|_1 \right] \right\} \qquad (4)$$

$$\underset{\sim}{R}_{e_2}|_m = -\rho_f A \left\{ 2v \left.\frac{d\underset{\sim}{t}}{dt}\right|_{m_2} + v^2 \frac{1}{2}\left[\left.\frac{d\underset{\sim}{t}}{ds}\right|_1 + \left.\frac{d\underset{\sim}{t}}{ds}\right|_2 \right] \right\}$$

$$\vdots$$

$$\underset{\sim}{R}_{e_3}|_m = -\rho_f A \left\{ 2v \left.\frac{d\underset{\sim}{t}}{dt}\right|_{m_N} + v^2 \frac{1}{2}\left[\left.\frac{d\underset{\sim}{t}}{ds}\right|_{N-1} + \left.\frac{d\underset{\sim}{t}}{ds}\right|_N \right] \right\}$$

where $\underset{\sim}{R}_{e_i}|_m$ =value of $\underset{\sim}{R}_e$ evaluated at the middle of the ith element, $\left.\frac{d\underset{\sim}{t}}{ds}\right|_j$ =jth nodal estimate of $\frac{d\underset{\sim}{t}}{ds}$ and

$$\left.\frac{d\underset{\sim}{t}}{ds}\right|_{m_i} = \frac{\dot{\underset{\sim}{r}}_i - \dot{\underset{\sim}{r}}_{i-1}}{h_i} - \underset{\sim}{t}_i \left[\underset{\sim}{t}_i \cdot \left(\frac{\dot{\underset{\sim}{r}}_i - \dot{\underset{\sim}{r}}_{i-1}}{h_i} \right) \right] \qquad (A)$$

where h_i =strained length of the ith element and $\underset{\sim}{t}_i$ =tangent vector for the ith element. For i=1,...,N-1 the nodal estimate of $\frac{d\underset{\sim}{t}}{ds}$ is calculated in exactly the same way it was calculated in section 4.2.1.3 i.e.

$$\frac{d\underset{\sim}{t}}{ds} = \frac{\underset{\sim}{t}_{i+1} - \underset{\sim}{t}_i}{(h_i + h_{i+1})/2} \qquad (B)$$

$\frac{dt}{ds}\Big|_0$ and $\frac{dt}{ds}\Big|_N$ are dependent on the boundary conditions at the two ends of the riser. For example if the left hand end of the riser is pinned then

$$\frac{d\underset{\sim}{t}}{ds}\Big|_0 = \underset{\sim}{0} \qquad (C)$$

because of the boundary conditions derived in section 2.5.5. And if the left hand end of the riser is clamped at a tangent $\underset{\sim}{t}_L$ then

$$\frac{d\underset{\sim}{t}}{ds}\Big|_0 = \frac{\underset{\sim}{t}_1 - \underset{\sim}{t}_L}{h_1/2} \qquad (D)$$

Similarly for the right hand end of the riser; if the end is pinned

$$\frac{d\underset{\sim}{t}}{ds}\Big|_N = \underset{\sim}{0} \qquad (E)$$

and if the end is clamped at a tangent $\underset{\sim}{t}_R$

$$\frac{d\underset{\sim}{t}}{ds}\Big|_N = \frac{\underset{\sim}{t}_R - \underset{\sim}{t}_N}{h_N/2} \qquad (F)$$

From equations (a) and (b) the virtual work done on the riser by the internal fluid flow is

$$\begin{bmatrix} \delta\underset{\sim}{r}_0 & \delta\underset{\sim}{r}_1 & \cdots & \delta\underset{\sim}{r}_{N-1} & \delta\underset{\sim}{r}_N \end{bmatrix} \begin{bmatrix} \frac{1}{2} h_1 \underset{\sim}{R}_{e_1} \underset{\sim}{I}_m \\ \frac{1}{2} h_1 \underset{\sim}{R}_{e_1} \underset{\sim}{I}_m + \frac{1}{2} h_2 \underset{\sim}{R}_{e_2} \underset{\sim}{I}_m \\ \vdots \\ \frac{1}{2} h_{N-1} \underset{\sim}{R}_{e_{N-1}} \underset{\sim}{I}_m + \frac{1}{2} h_N \underset{\sim}{R}_{e_N} \underset{\sim}{I}_m \\ \frac{1}{2} h_N \underset{\sim}{R}_{e_N} \underset{\sim}{I}_m \end{bmatrix} \qquad (G)$$

Hence since in practice the ends of the riser have some prescribed motion $\delta\underset{\sim}{r}_0 = \delta\underset{\sim}{r}_N = \underset{\sim}{0}$ and the required nodal force vector that must be added to the equations of motion is

$$\begin{bmatrix} \frac{1}{2} h_1 \underset{\sim}{R}_{e_1} \underset{\sim}{I}_m + \frac{1}{2} h_2 \underset{\sim}{R}_{e_2} \underset{\sim}{I}_m \\ \frac{1}{2} h_2 \underset{\sim}{R}_{e_2} \underset{\sim}{I}_m + \frac{1}{2} h_3 \underset{\sim}{R}_{e_3} \underset{\sim}{I}_m \\ \vdots \\ \frac{1}{2} h_{N-2} \underset{\sim}{R}_{e_{N-2}} \underset{\sim}{I}_m + \frac{1}{2} h_{N-1} \underset{\sim}{R}_{e_{N-1}} \underset{\sim}{I}_m \\ \frac{1}{2} h_{N-1} \underset{\sim}{R}_{e_{N-1}} \underset{\sim}{I}_m + \frac{1}{2} h_N \underset{\sim}{R}_{e_N} \underset{\sim}{I}_m \end{bmatrix} \qquad (H)$$

4.8:Conclusions.

The power and the versatility of the finite element method has once more been illustrated. Indeed it would be difficult to use another approach to model some of the things that are necessary for a discretization to be of practical value.

The equations of motion for a riser with moving end-points have been given for the first time. If a consistent mass matrix and a consistent added mass matrix are used then extra force terms are generated. It would be unwise to use a consistent mass matrix and then to ignore the extra force terms. If the mass matrices are diagonal then no extra force terms are generated.

The bending stiffness has been incorporated into both the linear and the cubic discretization. The results from using a linear discretization are compared against the elastica solution for large displacements and against a uniformly loaded beam for small displacements. Both these problems have analytical solutions. The results obtained from using the linear finite element discretization are in remarkably close agreement with the analytical solutions. The only other reference that incorporates the bending stiffness into a linear discretization is Ractliffe[1984]. His approach is not adequately explained and no validation against analytical solutions is carried out. However the ideas that he suggests are basically correct.

Ractliffe[1984] also gives a brief sketch on the incorporation of internal fluid flow into a linear discretization. The same criticisms apply for his incorporation of internal fluid flow as for his incorporation of the bending stiffness. It is difficult to understand his approach for the inclusion of internal fluid flow effects and to reach any conclusion about its correctness. Using the theory developed in Chapter Two for the modelling of internal fluid flow and the theory developed in section 4.2 for the modelling of the bending stiffness it is simple to incorporate internal fluid flow effects into a linear discretization. Because of the accuracy achieved for the bending stiffness similar accuracy is also to be expected for the internal fluid flow.

A linear element is derived that allows for only partial loading along its length. The element is of considerable use for the modelling of ground contact and for the modelling of the loading on the elements near the water surface. It allows for longer elements to be used near the seabed and near the water surface than would otherwise be possible. A computer program using this element will need less C.P.U. time.

CHAPTER FIVE:RESULTS

For any given riser configuration there are many factors that may affect its dynamic and static behaviour such as:

1.Wave height.

2.Water depth.

3.Motion of the floating production vessel.

4.Seabed properties.

5.Length of riser.

6.Position of buoy(s) (if any), their diameters and their buoyancy.

7.Longitudinal stiffness.

8.Bending stiffness.

9.Riser diameter.

10.Internal fluid flow; force exerted by the flow on the riser will be dependent on the density of the fluid and its flow velocity.

11.The length of riser above the water surface.

12.The added mass coefficient.

13.The drag coefficient.

14.The net weight of the riser.

15.The current.

16.The wave period.

To analyse the performance of a given riser system many of these quantities must be varied. If this done then an enormous amount of data is generated and a considerable amount of C.P.U. time must be used. To compare the behaviour of different riser configurations i.e. lazy "s" against steep "s" would mean even a greater amount of data must be generated. The aim of this thesis is not to attempt such comparisons but to indicate some of the quantities that will affect the riser behaviour the most. The other aim is to show that the theory that has been derived is of considerable practical use to the design engineer.

In this chapter a riser with given properties is analysed in the steep "s" configuration. It is illustrated how complex the motion of a riser is. Several different regular waves (Brebbia and Walker[1979]) are used. The effects of top motion and current are evaluated.

Before a design engineer can have any faith in a computer program based on one of the discretizations given in this thesis the computer program must be validated. There are only three ways in which this may be done:

1.Against model tests.

2.Against analytical solutions.

3.Against full size model tests.

To use full size tests would not be practical as it would be too expensive. The disadvantage in using model tests is that scaling errors might occur. In this chapter validation is carried out both against model tests and against the analytical solution of Saxon and Cahn[1953]. In the literature there has been very little validation carried out against model tests. The model tests that are used here are for the lazy "s" configuration and thus include ground contact of the riser with the seabed. This is very useful because this allows a check to also be made on the theory for the modelling of the ground contact. The analytical solution by Saxon and Cahn[1953] is a dynamic solution and is thus very important because it allows a check on the dynamic modelling of the computer program. No validation against a relevant dynamic analytical solution has previously been carried out.

The magnitude of the bending stiffness of a typical riser is much smaller than the magnitude of the extensional stiffness of the riser. The effect of the bending stiffness of the riser is investigated in this chapter and the possibility of neglecting the bending stiffness in a dynamic analysis is discussed.

In certain circumstances a riser system might undergo vortex shedding (King[1977]). This could cause premature fatigue failure of the riser. The situations in which vortex shedding might occur are discussed. If it does occur for the steep "s" configuration then ways to reduce it

are investigated.

By studying the dynamics of a length of riser dropped from a "v" shaped configuration (see figure 5.5(b)) the effect of the longitudinal stiffness of the riser and the number of elements used is examined.

A check is made against the catenary analytical solution for a cable hanging in gravity.

5.1:Results for the Steep "s" Configuration.

The configuration that is modelled is the steep "s" configuration shown in figure 5.1(a). Because of the excellent agreement that is obtained in section 5.7 with the analytical solution of Saxon and Cahn[1956], when only 10 elements are used, only 10 elements shall be used here. More elements are however recommended for a commercial design study. The first 9 elements have an unstretched length of 20.444m and the 10th element has an unstretched length of 46.0m.

Because of the difference in the properties of commercially available buoys, the buoy at node 9 is assumed to have no volume (i.e. no drag force, no fluid inertia force and no added mass force acts on it), no mass (i.e. no inertia force acts on it). This means that the results obtained can not be swamped by the buoy properties. The net upthrust force of the buoy is set equal to 100kn.

The following data is used:

EA=0.327E+09n

Element diameters=0.28m

C_D =1.5

C_M =2.5

Density of seawater=1000Kgm^{-3}

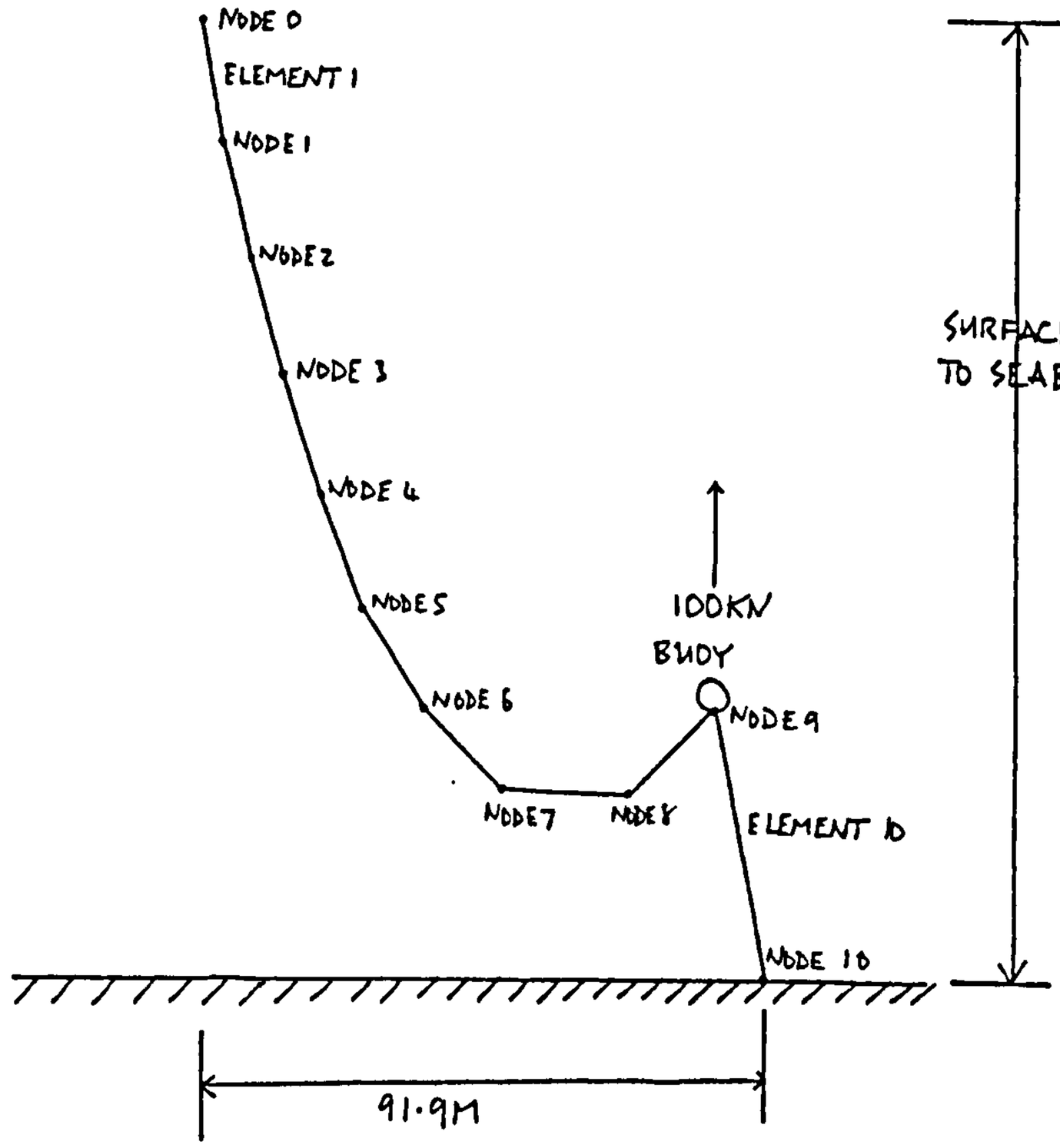

FIGURE 5.1(a) : THE EQUILIBRIUM POSITION WITH NO CURRENT

Density of riser=2000Kgm^{-3}

EI=0.0nm^{2}

Timestep=0.002s

The effect of the internal fluid flow is neglected. Only in-plane motions of the riser are considered. Various effects are investigated.

5.1.1:The Effect of Top Motion.

Various motions of the top end of the riser are prescribed to simulate the motion of a floating production vessel.

A number of runs were done with heave motion only and with surge motion only. The riser system was found to be a lot more sensitive to the heave motion than to the surge motion of the top end.

The end is constrained to move as shown in figure 5.1.1(a). The path that the end of the riser is constrained to move along is defined to be the ellipse given by the equations

$$x = a_S \sin\omega t \ , \quad z = a_H (1 - \cos\omega t) \qquad (A)$$

where a_S is the amplitude of the surge motion, a_H is the amplitude of the heave motion and ω is the frequency of the top motion.

a_S = amplitude in surge

a_H = amplitude in heave

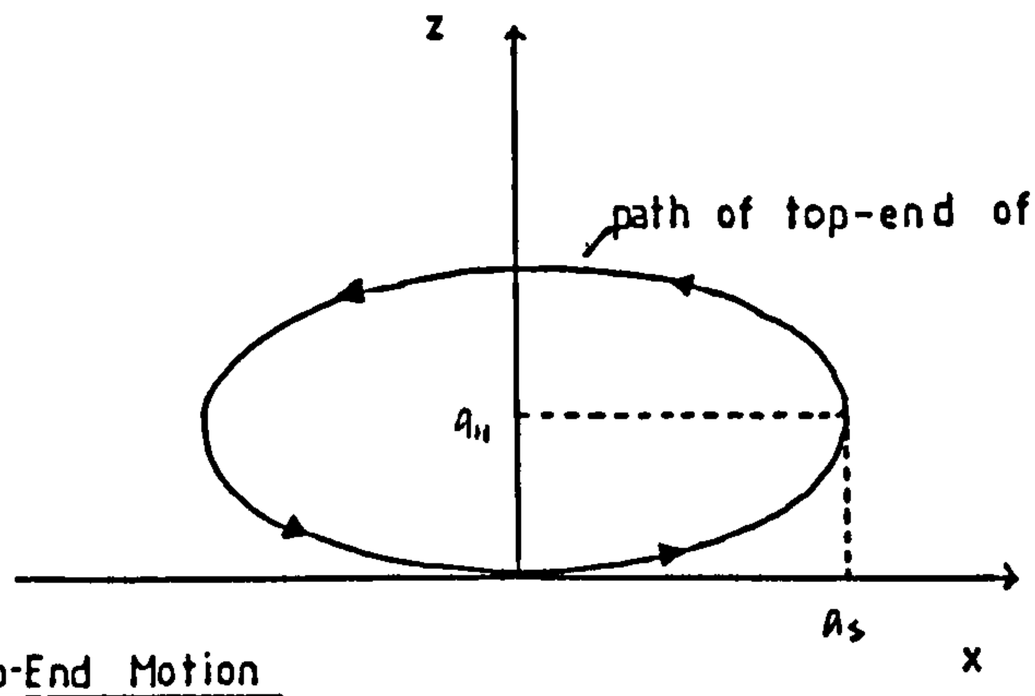

Figure 5.1.1 (a) : Top-End Motion

a_5 is set equal to 5.0m, a_4 is set equal to 1.0m and the period of the top motion is varied between 10s and 16s. The results are shown in figures 5.1.1(b)-(h). The path of node 1 is unaffected by the period of the top motion. Lower down the riser the nodal paths become more circular as the period of the top motion is reduced. However the maximum distance of the nodal path from the equilibrium position of the node is independent of the period of the top motion.

There is hardly any motion of the buoy node for any of the different period top motions. Also there is no variation in the bottom element (i.e. element 10) tension.

As the period of the top motion is reduced the tension variation in the top element and in the eighth element becomes greater.

In figure 5.1.1(i) the maximum and minimum tensions in the top element are plotted against the period of the top motion.

5.1.2:The Effect of Wave Motion

The waves travel to the right and have a wave height of either 29.0m or 14.5m. The periods of the waves range from 10s to 16s. Breaking waves occur when wave height/wave length exceeds approximately 0.1. None of the waves used here exceed this limit.

The results for a number of different waves are

given in figures 5.1.2(a)-(f). The nodal displacements decrease as the period of the waves is decreased. The element tensions increase as the period of the wave is decreased. The motion of the buoy node is negligible considering the dimensions of the riser system. The wave motion produces a considerable variation in the tensions in the first 9 elements. However the tension variation in the 10th element is not very great in comparison.

5.1.3:The Effect of Waves with Top Motion.

The wave travels to the right as before. The path of the top end of the riser is again prescribed to be an ellipse. Two different wave periods are used with the same 29.0m wave height. And two different heave amplitudes are used; 2.0m and 1.0m. The period of the wave and the period of the top motion are equal.

The results are shown in figures 5.1.3(a)-(d). With a wave and top motion the variation in the tensions is less than the corresponding case where there is wave motion only. This is still true even when the heave amplitude is doubled to 2.0m. The nodal displacements are reduced in comparison to the corresponding case where there is wave motion only. As the period is reduced the tension variation in the elements increases.

5.1.4:The Effect of Current.

A current, that is uniform with depth, of magnitude 1.2ms is used. The equilibrium position of the riser with current flowing to the right is shown in figure 5.1.4(b) and with current flowing to the left in figure 5.1.4(a). The riser suffers a greater deflection when the current flows to the left.

Note that rather than having a specialist program to find equilibrium positions of the riser it is found that it is much simpler to find the equilibrium position by using a program written to investigate the dynamics of the riser. This is done in figures 5.1.4(a),(b) where the riser is initially in the equilibrium position with no current present and is then allowed to move dynamically to the equilibrium position with the current present.

5.1.5:The Effect of Current with Wave and Top Motion.

A surge amplitude of 5.0m is used with a heave amplitude of 1.0m. The waves move to the right. Two different wave periods are used; 16s and 14s. Figures 5.1.5(a),(b) have a current of 1.2ms moving to the left and figures 5.1.5(c),(d) have a current of 1.2ms moving to the right. Note that the wave period is always set equal to the period of the top motion.

From the figures it can be seen that there is a

large difference between the cases where the current travels to the left and the cases where the current travels to the right. A typical maximum velocity of a wave is around 7.0ms which is much larger than the current velocity of 1.2ms. Hence it would not be expected that the current would have such a large effect.

An explanation of the result lies in the way the current affects the equilibrium position of the riser. The equilibrium position when the current moves to the left has a very steep top section in comparison to the case where the current flows to the right. This means that there is less length of the riser where the wave forces are greater.

Out of all the results that have been obtained in which waves have been present there is the least variation in the tensions when there is a current present that flows to the left.

5.2:Comparison with Model Tests.

In this section results are given that have been used in a comparison against model tests. For reasons of commercial security access to the model tests was restricted and the details of the model tests and the results obtained from them cannot be given here. However the computer program that has been written was shown to be in agreement with the model tests and the results obtained from the computer program are given here. Note that the computer program is run for the full scale size of the riser system. The configuration modelled is the lazy "s" configuration. The dimensions of the system and the element discretization used is shown in figure 5.2(a).

The program has also been validated against a program (R.Ghadimi[1988]) which has been shown to be in excellent agreement with model test results.

5.2.2:Data.

The unstretched lengths of the 25 elements that are used are as follows:

ELEMENT	ELEMENT LENGTH [metres]
1	11.366666
2	11.366666
3	11.366666
4	8.966666
5	8.966666
6	8.966666
7	10.866666

8	10.866666
9	10.866666
10	11.233333
11	11.233333
12	11.233333
13	10.90000
14	10.90000
15	10.90000
16	7.32
17	7.32
18	7.32
19	7.32
20	7.32
21	8.2
22	8.2
23	8.2
24	8.2
25	8.2

Thus the net length of the riser is 237.6m. The length of the riser between the top end and the buoy is 160m and the length of the riser between the buoy and the sea-bed riser connection is 77.6m. The tether length is 37.0m.

The following data is used:

Water Depth=110m

Timestep=0.001s

Element Diameters=0.312m

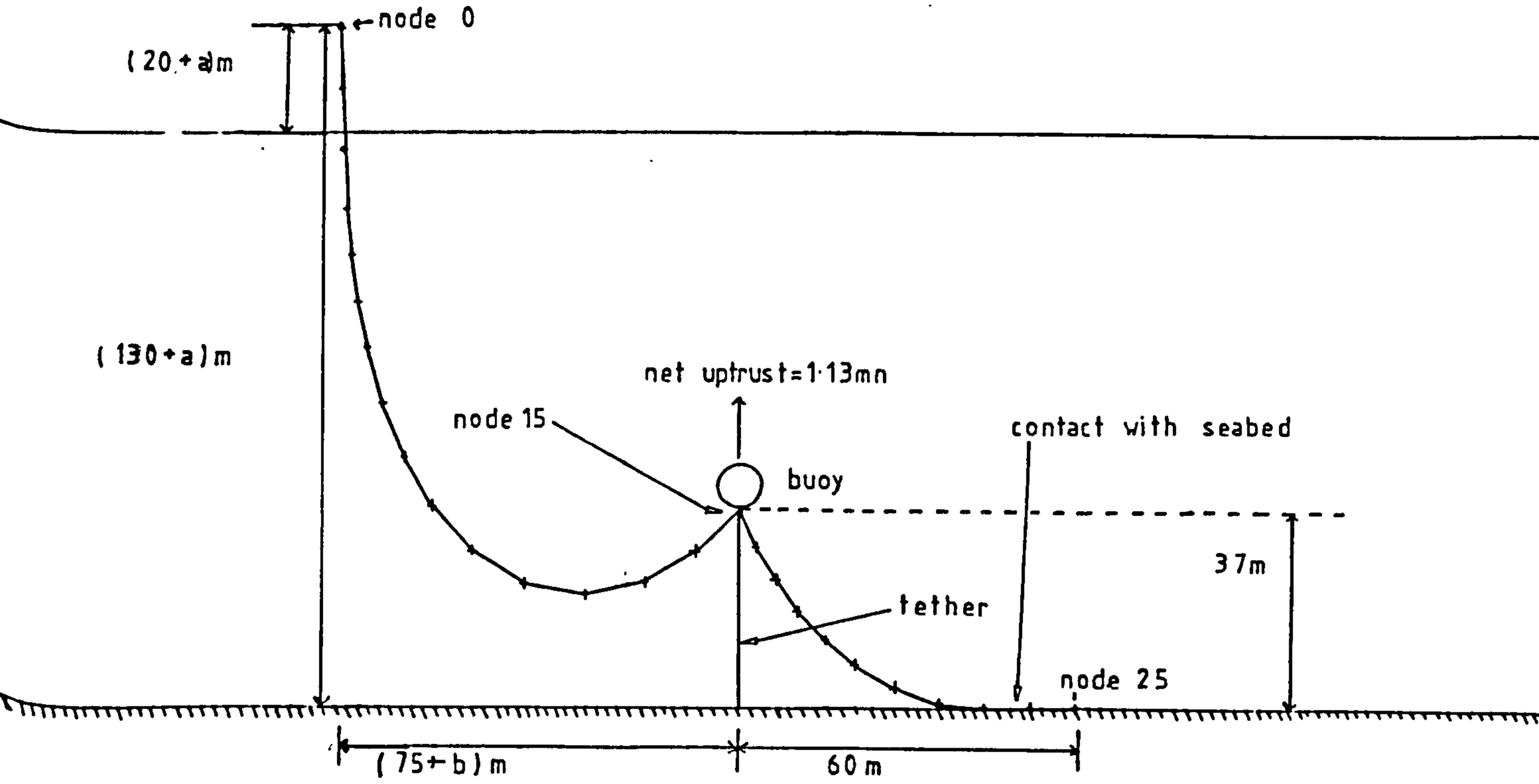

Figure 5.2 (a): Configuration used for comparison with Model Tests

EA=0.1E+09n

C_D =1.1

C_M =2.0

Density of Sea-water=1000kgm^{-3}

Density of the Riser=2000kgm^{-3}

Drag Coefficient for the Buoy=0.5

Buoy Diameter=6.9m

Buoy Mass=56780kg

Bending Stiffness=53100nm^2

The drag coefficient of the buoy can be found using Goldstein[1965]. The added mass of the buoy is equal to

$$\frac{1}{2} V_B \rho_w$$

where V_B is the volume of the buoy and ρ_w is the density of sea-water. The drag force acting on the buoy is equal to

$$\frac{1}{2} \rho_w S C_B$$

where C_B is the drag coefficient of the buoy and S is the cross-sectional area of the buoy. The fluid inertia force acting on the buoy is equal to

$$\frac{3}{2} V_B \dot{u}_f \rho_w$$

where $\dot{u}_f$ is the fluid acceleration evaluated at the buoy.

The two end connections of the riser are modelled as pinned joints. Also the connection of the riser sections at the buoy with the tether is modelled as a pinned joint.

Ground contact is modelled using the theory that was developed in earlier chapters.

The phases and amplitudes of the floating production vessel with repect to the wave motion are given by the equations:

Wave amplitude[metres]=5cos(-kx-wt)

Surge amplitude[metres]=1.95cos(-16-wt)

Heave amplitude[metres]=1.25cos(244-wt)

where k is the wave number and w is the wave frequency. At t=0 the position of the top end of the riser with respect to the axes system that will be defined later in the figures is

(5+1.95cos(-16),20+1.25cos(244))

The wave used travels to the left and has a wave height of 10m and a period of 12s. There is a current of $1.0ms^{-1}$ that travels to the left.

5.2.3:Results.

Some of the results obtained are shown in figures 5.2.3(a)-(c). Only the most important results are presented here.

The bending stiffness of the riser was found to have no discernible effect on either the static equilibrium position of the riser or on the dynamic properties of the riser. This is because the bending stiffness of the riser used here is much smaller than the extensional stiffness.

There is little variation in the tension of the tether. Note that the extensional stiffness of the tether is set equal to the extensional stiffness of the riser. No details were made available about the properties of the tether hence the forces that act on the tether e.g. drag force are not included here. There would be no problem in

including the forces that act on the tether.

The greatest tension variations do not occur at the top end of the riser. There is a considerable variation in the tension in the 10th element particularly when it is considered that only a 10m wave height is being used. The high frequency component of the tension variation in the 10th element is due to the modelling of ground contact. This high frequency component disappears as more elements are used in the region of the sea-bed.

In figures 5.2.3(a),(b) nodaldisp(a,i) denotes the nodal displacement of the ith node, with respect to the equilibrium position (with no current flowing), in the ith axis direction. 1 denotes the x axis which is horizontal and 3 denotes the z axis which is vertical.

As would be expected there is little movement of the buoy. And in the section of the riser between the buoy and the seabed there is also very little movement. Most of the movement of the riser occurs in the section of the riser that is 70m under the sea-surface. Note that the greatest variation in the tensions in the elements does not occur at the point at which the nodal displacements are the greatest.

5.3:The Effect of the Bending Stiffness.

The riser used here to investigate the effect of the bending stiffness of the riser has the same physical properties as the riser used in section 5.2. The timestep is 0.001s. The riser configuration is the steep "s" configuration and the element discretization used is identical to the one used in section 5.2. The buoy has the same properties as the buoy used in section 5.1. The bending stiffness of the riser is set equal to 55000nm^2.

The riser is released from the position shown in figures 5.3(a),(b). The motion is then followed until the equilibrium position is reached. Various quantities are plotted in the figures that illustrate the effect of the bending stiffness on the riser. In figure 5.3(b) the top end of the riser is clamped and all the other joints are pinned. In figure 5.3(a) the top end of the riser is pinned as well.

In figure 5.3(a) it is shown that when all the joints (i.e.the top end joint, the joint at the buoy and the joint at the connection with the seabed) are pinned the shear force in element 7 is negligible compared to the tension in element 7. Thus it is concluded that in this case the effect of the bending stiffness is negligible.

In figure 5.3(b) the top end of the riser is clamped at 45° to the horizontal. This means that the

bending stiffness of the riser should have the greatest effect at the top end of the riser. From the figure the shear force in the first element is only around 200n compared to the tension in the first element of 100000n. Hence the bending stiffness of the riser will have no static or dynamic effect in this case either.

Note that although the effect of the bending stiffness of a typical riser is negligible this does not mean that the inclusion of the bending stiffness in a finite element discretization is not important. This is because the evaluation of the bending moment in the riser will be necessary for fatigue life predictions.

5.4:Natural Periods, Natural Modes and Vortex Shedding.

5.4.1:Introduction.

In certain circumstances vortex shedding can cause oscillations of a riser system. These oscillations occur at the natural periods of the riser system. They reduce the fatigue life of the riser and can significantly affect the drag coefficient. The increase in the drag coefficient means that the static equilibrium position of the riser with a current present will be changed. The oscillations can occur when there is a current only, when there are waves only (particularly long period waves) and when there are waves with a current.

The object of section 5.4 is to show how it may be possible to eliminate problems caused by vortex shedding, by changing the natural periods of the riser system. As will be shown later the natural periods can be changed in several different ways, some of which are more practical than others.

The finding of the natural modes and the natural periods of the riser system also gives physical insight into the dynamic response of the riser system.

5.4.2:Description of Vortex Shedding

Vortex shedding is excellently described in Every, King and Weaver[1982] and King[1977]. And much of what follows in section 5.4.2 follows closely the descriptions

provided in these two references.

When fluid flows around a riser the flow seperates and a periodic wake is formed. The frequency f_v of pairs of vortices is a function of the velocity of the fluid V, the riser diameter d and the Reynolds number Re. The frequency f_v (measured in Hertz) is given by the equation

$$f_v = \frac{V S_t}{d} \quad (a)$$

where $S_t = S_t(Re)$ is called the Strouhal number. The relationship between S_t and Re is shown in figure 5.4.2(a). The figure shows that over a wide range of the Reynolds number ($10^2 < Re < 10^5$) the Strouhal number is equal to 0.2.

Ocean currents are typically of the order of $1.0 ms^{-1}$ and flexible riser diameters are normally in the range 0.15m-0.30m. Thus from figure 5.4.2(a) the Strouhal number for a flexible riser is equal to 0.2.

Because of the flexibility of a flexible riser interactions can occur between the vortex shedding mechanism and the riser deflections. Under certain conditions sustained oscillations can be excited and the riser oscillates at a frequency close to or coincident with its natural frequency. When these oscillations of the riser are excited (sometimes called "lock-in") equation (a) does not hold. This is shown in figure 5.4.2(b).

There are two types of oscillation that can occur;

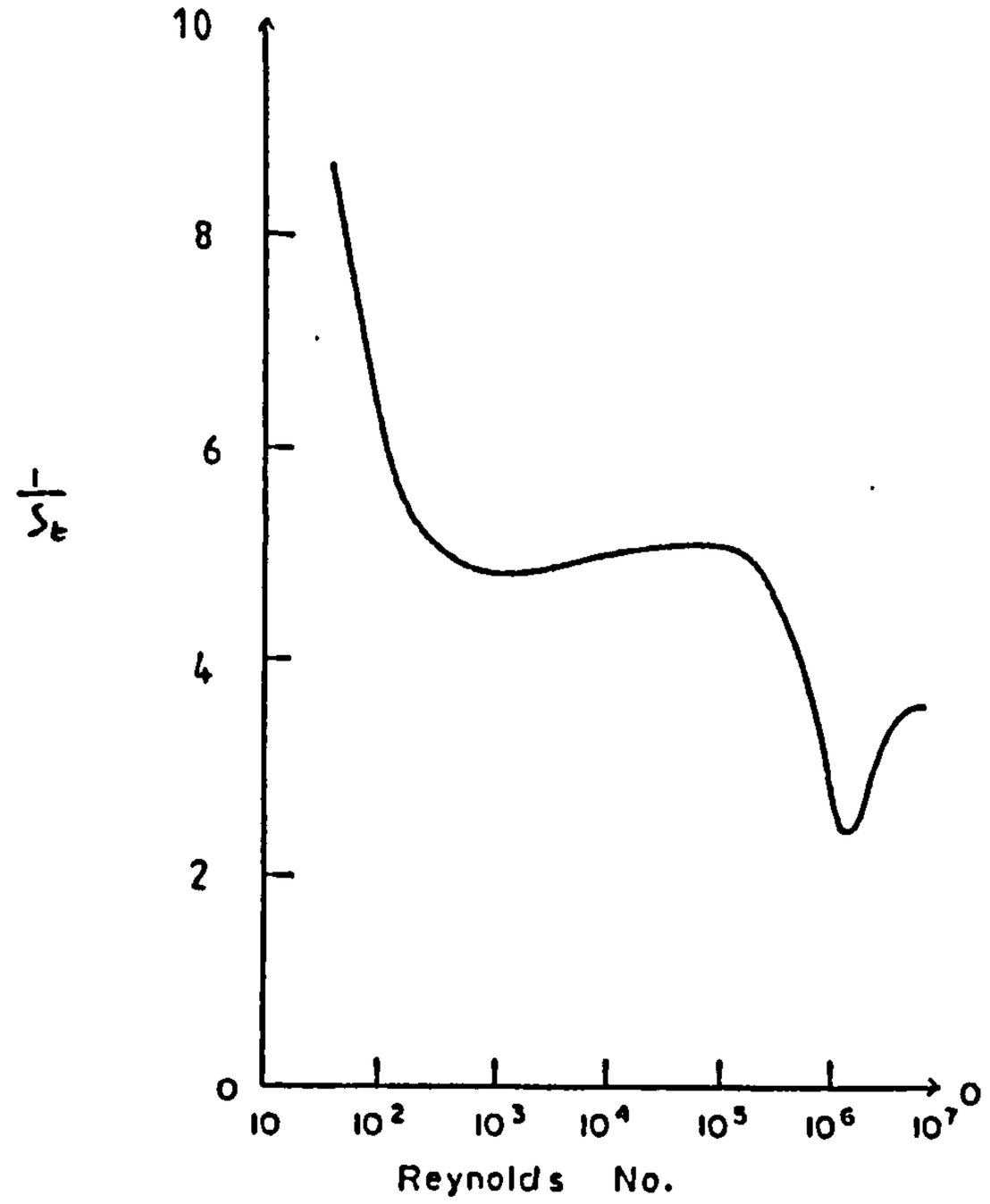

Figure 5.4.2 (a): Graph of $S_t = S_t(R_e)$ (King [1977])

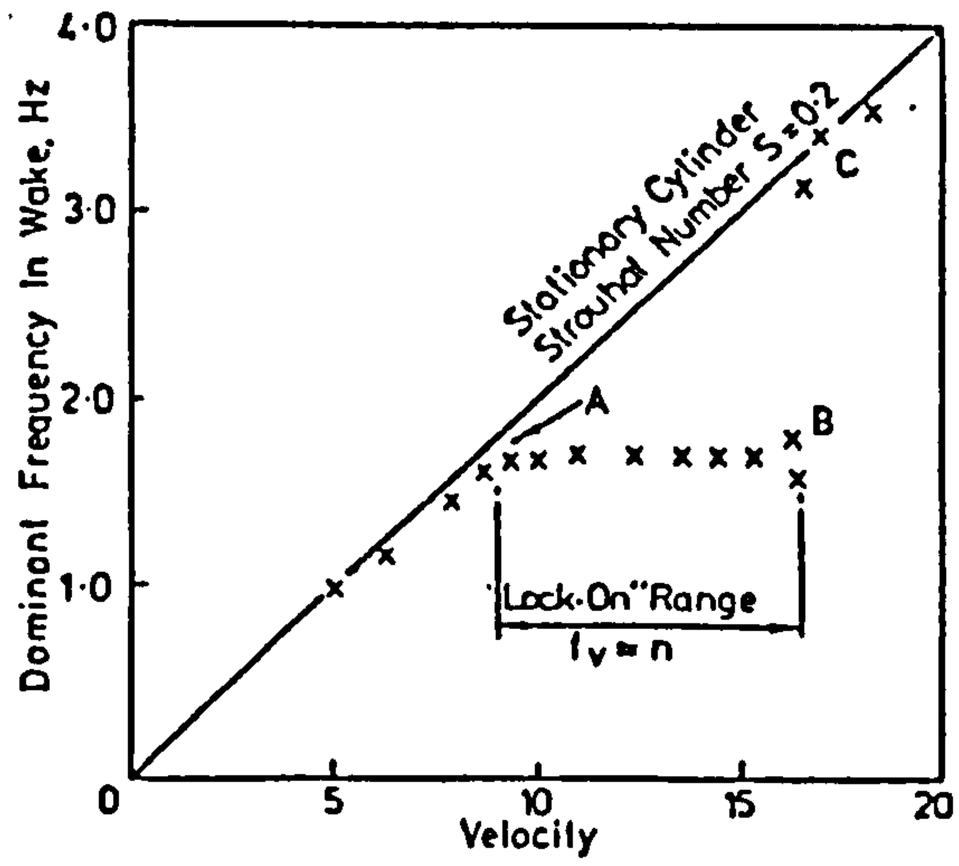

A Cross flow oscillation of cylinder starts and the vortex shedding locks-on to the cylinder oscillation.

B The upper limit of synchronisation is reached, the cylinder motion reduces and eventually ceases.

C Vortex shedding returns to a frequency described by the Strouhal relationship.

Figure 5.4.2 (b): Lock-in (Every et al. [1982])

in-line oscillation and cross-flow oscillation. Cross-flow

oscillations have larger amplitudes and can increase the drag coefficient. They are thus of more importance for a dynamic analysis of flexible riser systems. Both types of oscillation are dependent on the stability parameter K_s which is defined by the equation

$$K_s = 2m_e \delta / \rho_w d^2$$

where m_e is the equivalent mass per unit length, ρ_w is the density of sea-water and δ is the structural logarithmic decrement of the damping measured in air. The maximum in-line and cross-flow amplitudes are plotted against the stability parameter in figure 5.4.2(c).

It is known (Griffin and Ramberg[1982]) that vortex shedding can significantly affect the fatigue life of a rigid riser and can cause various other serious operational difficulties. However it is likely that the structural logarithmic decrement for a flexible riser will be greater than for a rigid riser. This is because of the muliple layer internal construction for a flexible riser which causes internal friction and dissipation of energy. Hence oscillations caused by vortex shedding might not cause any serious problems. However there is no experimental work that evaluates δ for flexible risers.

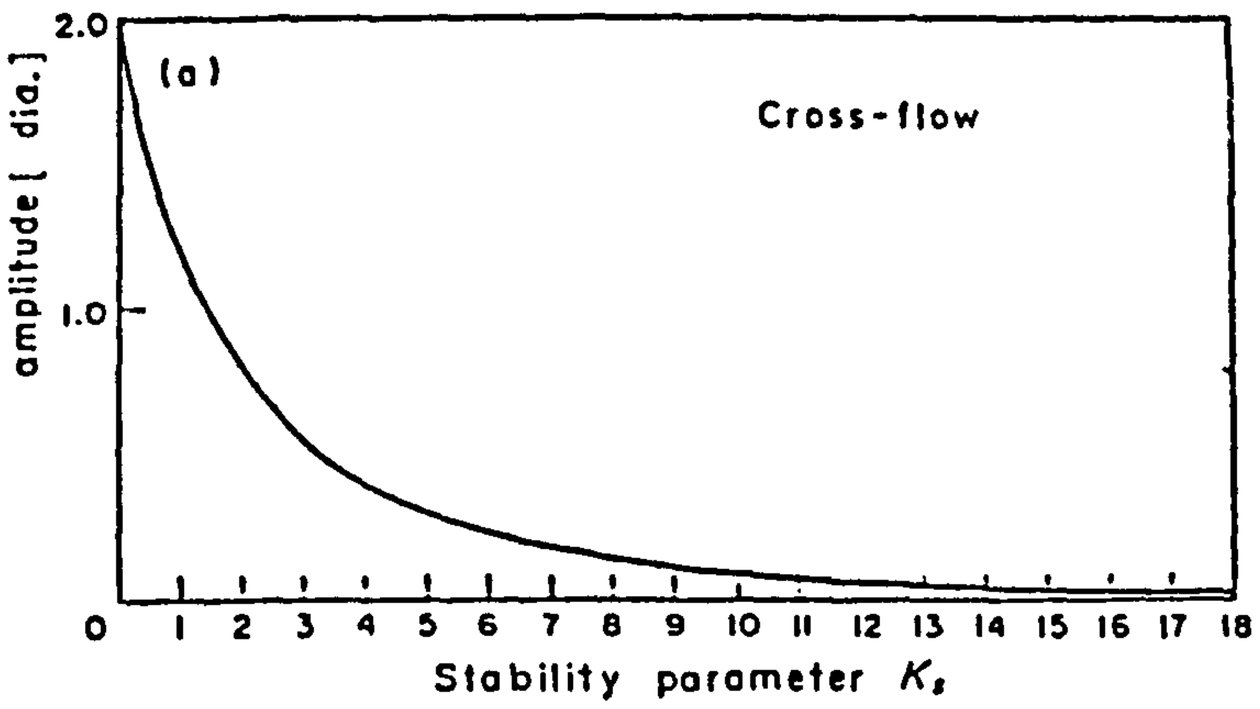

Amplitude response cross flow

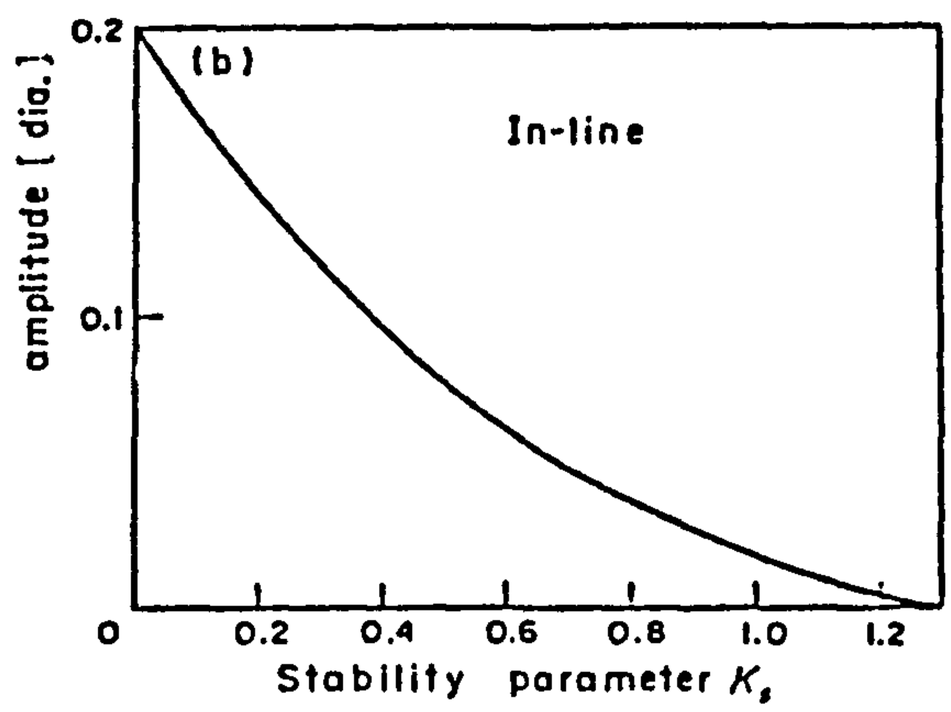

Amplitude response in line

Figure 5.4.2 (c): The Effect of K_s on the Amplitude of Vibration (Every (1982))

5.4.3: Investigation of how the Natural Periods of a Riser System may be changed.

The following quantities are changed and their effect on the natural periods of a steep "s" configuration is investigated:

1. The position of the top end of the riser.

2.The ratio of the length of the riser from the seabed to the buoy to the length of the riser from the buoy to the top end of the riser. Note that the net length of the riser is kept constant so in effect the buoy is just being moved along the riser.

3.The net length of the riser.

4.The longitudinal stiffness of the riser.

5.The buoyancy of the buoy.

The quantities that are not changed have the values given in section 5.1.

The first two in-plane mode shapes which have periods of 24.2s and 13.7s are shown in figure 5.4.3(a). The first two out-of-plane mode shapes which have natural periods of 29.8s and 16s are shown in figure 5.4.3(b). The higher mode shapes are obvious.

5.4.3.1:The Effect of Moving the Top End of the Riser.

The top end of the riser is given either a vertical or a horizontal displacement (but not a combination) with respect to the reference configuration indicated in figure 5.4.3.1(a).

In figure 5.4.3.1(b) the percentage change in the periods of the first four in-plane modes is plotted against a horizontal displacement of the top end of the riser with respect to the reference configuration. There is a greater

percentage change if the top end is moved to the left rather than to the right.

In figure 5.4.3.1(b) the percentage change in the periods of the first four out-of-plane modes is plotted against a horizontal displacement with respect to the reference configuration. The percentage changes for the first four out-of-plane modes are closer together than for the percentage changes for the first four in-plane modes. Again there is a greater percentage change if the top end of the riser is moved to the left rather than to the right.

In figure 5.4.3.1(d) the percentage change in the periods of the first four in-plane modes is plotted against a vertical displacement with respect to the reference configuration. And in figure 5.4.3.1(e) the percentage change in the periods of the first four out-of-plane modes is plotted.

The change in the period is equally affected by either a vertical or a horizontal displacement.

5.4.3.2:The Effect of Varying the Position of the Buoy on the Riser.

The net length of the riser is kept constant at 230m and the buoy is moved between the positions on the riser shown in figure 5.4.3.2(a). The percentage change in the periods of the first in-plane mode and the first out-of-plane mode (with respect to the reference

configuration shown in figure 5.4.3.2(a)) is plotted against the ratio of the lower length of the riser to the upper length of the riser in figure 5.4.3.2(b).

5.4.3.3:The Effect of Varying the Net Length of the Riser

The net length of the riser is varied between 230m and 275m as shown in figure 5.4.3.3(a). The ratio of the lower length of the riser (i.e. the length of the riser between the sea-bed and the buoy) to the upper length of the riser (i.e. the length of the riser between the buoy and the top end of the riser) is kept constant. The percentage change in the periods of the first six in-plane modes with respect to the reference configuration of 230m is plotted against the net length of the riser in figure 5.4.3.3(b). And the percentage change in the periods of the first six out-of-plane modes is plotted in figure 5.4.3.3(c).

5.4.3.4:The Effect of Varying the Longitudinal Stiffness of the Riser.

The longitudinal stiffness (i.e. the value of EA) is varied between 0.327E+09n and 0.0654E+09n. The percentage change in the periods of the first four modes with respect to the configuration with EA=0.327E+09n is plotted against EA in figure 5.4.3.4(a). Note that the range in which EA is varied covers the values of EA usually encountered for most flexible risers.

5.4.3.5:The Effect of the Net Upthrust Force Caused by the Buoy.

The net upthrust of the buoy is varied from 70kn to 100kn. The riser configurations with a net upthrust of 70kn and with a net upthrust of 100kn are shown in figure 5.4.3.5(a). In figure 5.4.3.5(b) the percentage change (with respect to the reference configuration with a buoyancy of 100kn) of the first four natural periods is plotted against the net upthrust of the buoy.

5.4.4:Conclusions.

The value of the longitudinal stiffness of the riser system in the steep "s" configuration has a negligible effect on the natural periods of the riser system. The position of the top end of the riser and the position of the buoy on the riser have a small effect on the natural periods. The biggest effects are obtained by either changing the net length of the riser or by changing the net upthrust of the buoy. Increasing the net length of the riser increases the natural periods of both in-plane and out-of-plane natural modes. Similarly increasing the buoyancy of the buoy will have the same effect.

If vortex shedding is a problem then the easiest way to overcome it would be to increase the length of the riser between the buoy and the top end of the riser since

the position of the buoy on the riser has only small effect on the natural periods. Note that from section 5.1.5 decreasing the length of the riser between the top end and the buoy might have an adverse effect on the dynamic performance of the riser system. Also note that once the riser system is installed it is impractical to change the buoyancy of the buoy.

5.5:The Effect of the Longitudinal Stiffness.

In section 5.5 the effect of the longitudinal stiffness of the riser on the dynamic and static behaviour of the riser is investigated. The data used here is identical to the data used in section 5.1 except for the timestep which is set equal to 0.005s here and for the longitudinal stiffness EA which of course is varied in this section. The riser is let go from the "v" shaped configuration shown in figure 5.5(a) and is allowed to come to rest in the equilibrium position. Ten elements are used in the discretization.

The equilibrium position of the riser is shown in figure 5.5(b) for various values of EA. The difference between the equilibrium positions of the riser for 0.01E+09n<EA<1.0E+09n is negligible. When EA=0.001E+09n, which corresponds approximately to the value for a riser made solely of rubber without any internal reinforcement, then a substantially different equilibrium position is obtained.

In figure 5.5(c) the vertical distance of the centre node of the configuration beneath the sea-surface is plotted against time as the riser is released from the "v" shaped configuration. There is practically no difference in the dynamic response of the riser for 0.01E+09n<EA<1.0E+09n particularly when the dimensions of the riser system are considered. With EA=0.001E+09n substantially different dynamic results are obtained as would be expected.

The time-histories of the tensions in the elements for different values of EA are considerably different.

It is the magnitude of EA that governs the size of the timestep that may be used before numerical instability occurs; the smaller the value of EA the bigger the timestep that may be used. Generally the use of a bigger timestep reduces the amount of C.P.U. time that must be used. Hence risers which have a smaller longitudinal stiffness will require less C.P.U. time.

5.6:The Number of Elements Needed for an Accurate Discretization

Figure 5.6(a) shows the equilibrium positions obtained with 10 elements and with 16 elements. There is a small difference between the equilibrium positions. The difference is greatest where the curvature of the riser is greatest.

In figure 5.6(b)-(d) the time-history of the distance of the centre-node beneath the sea-surface is plotted for different values of the longitudinal stiffness. For all the values of EA used there is close agreement between the results obtained using 16 elements and the results obtained using 10 elements, for the first 10s of simulation. There is a small difference in the results after the first 10s of simulation.

5.7:Check Against Known Analytical Solutions.

5.7.1:Introduction.

There are only three ways to validate a computer program that analyses the dynamics of flexible riser systems:

1.Validate against results obtained for a full size riser.

2.Validate against analytical solutions for cables (i.e. strings).

3.Validate against results from model tests.

To use full size model tests would be expensive and there are no reports in the literature of this having been done. Validation against analytical solutions has the advantage over model test validation that there are no problems resulting from scaling.

It is known that the equilibrium position of a string hanging in gravity is in the form of a catenary curve. Validation is carried out here using this analytical solution.

The known analytical solutions for the dynamics of a string are shown in figure 5.7.1(a). D.Bernoulli originally found the differential equation for system (i) shown in the figure. The differential equation was later solved by Euler who provided a power series solution. Later these power series were identified with Bessel functions. The classic vibrating string solution has also been known for a long time. The most important dynamical solution was

found by Saxon and Cahn[1953]. The elasticity of the cable is not allowed for. In the solution the natural mode shapes and natural periods are found. The solution is for a symmetrical cable only but may be easily extended to model a cable with non-symmetric supports. The Saxon and Cahn solution has been shown to be in excellent agreement with experiment for certain cable configurations and for certain natural modes. In the limit of small sag the Saxon and Cahn solution does not agree with the classical vibrating string solution. Irvine and Caughey[1974] and Simpson[1966] provide a solution that does agree with the classical solution by including the elasticity of the cable. This solution is valid for a sag to span ratio of 1:8 or less. An extension of the Saxon and Cahn solution to the case shown in figure 5.7.1(a) where a buoyant cable is in a steady current has been found by Ryan[1984].

Note that all of the analytical solutions described above assume that the string undergoes a small displacement only from the relevant equilibrium position. They all find the natural periods and mode shapes. Solutions (i) and (ii) can be demonstrated to be the result of self-adjoint (Meirovitch[1980]) boundary value problems. This means that the forced responses can be found. In the literature solutions (iii) and (iv) have not been demonstrated to be the result of a self-adjoint boundary value problem. However the equations for the natural modes for these cases are so complicated that they could not be used to find a forced response solution anyway.

Other interesting analytical solutions are described in Simpson[1972] , Pugsley[1948], Goodey[1960], Gale and Smith[1983], Smith and Thompson[1973] and Triantafyllou[1982,1983].

5.7.2:Check Against the Catenary Solution.

In figure 5.7.2(a) the equilibrium position obtained using 16 elements is compared with the relevant catenary curve. The value of the longitudinal stiffness EA is set equal to 0.1E+09n. Hence the cable can effectively be considered as inextensible and its equilibrium position will be described to a very high order of accuracy by a catenary. The finite element solution is very close to the catenary solution (Spiegal[1967]) even for only 16 elements. Using the catenary solution the tension at either of the supports of the cable is predicted to be 56557n. The tension in the top end elements of the discretization shown in the figure is 53500n. However it is not correct to compare the tension in the top elements with the top tension of a catenary. This is because the tension in one of the top elements is the average tension over that element. Hence the value of 53500n is an estimate of the catenary tension at a distance of half an element length from the top end points. The result obtained from the catenary solution is 53537n. This is in excellent agreement.

5.7.3:Check Against the Saxon and Cahn Solution.

A cable is modelled using 10 elements and is dropped from the "v" shaped configuration shown in figure 5.7.3(a). The following data is used:

Length of Cable=59.6m

Element Diameters=0.1m

Density of Water=1000kgm^{-3}

Timestep=0.001s

EA=0.2E+08n

Density of Cable=1273kgm^{-3}

The cable model predicts that the cable will almost exactly oscillate in the second in-plane mode of a catenary. This is shown in figure 5.7.3(a) where the two extreme positions of the oscillation are shown as the cable oscillates about the equilibrium position before coming to rest. In figure 5.7.3(b) as the cable approaches the equilibrium position the drag coefficient is set equal to zero in order that the amplitude of the second in-plane mode oscillation is maintained. The depth of the centre-node beneath the sea-surface is plotted against time. The curve obtained is very nearly sinusoidal. A sinusoidal curve is expected. There are two explanations for the superimposed nonlinearities on the sinusoidal curve:

1.Discretization error in the finite element model.

2.Other higher modes of oscillation could well have been excited to a smaller degree.

From figure 5.7.3(b) the period of the oscillation is measured as 3.28s.

Consider the catenary curve shown in figure 5.7.3(c), $\underset{\sim}{t}$ is the tangent vector to the catenary and ϕ is the angle the tangent vector makes with the horizontal. Then it can be shown (Saxon and Cahn[1953]) that the natural periods of oscillation of the catenary in the figure are given by the equation

$$\begin{vmatrix} C_n^{\frac{1}{4}}\bar{C}_n & C_n^{\frac{1}{4}}\bar{S}_n & C_n & \phi_n C_n \\ C_L^{\frac{1}{4}}\bar{C}_L & C_L^{\frac{1}{4}}\bar{S}_L & C_L & \phi_L C_L \\ \frac{1}{\delta}C_n^{\frac{7}{4}}\bar{C}_n & -\frac{1}{\delta}C_n^{\frac{7}{4}}\bar{C}_n & S_n & C_n+\phi_n S_n \\ \frac{1}{\delta}C_L^{\frac{7}{4}}\bar{S}_L & -\frac{1}{\delta}C_L^{\frac{7}{4}}\bar{C}_L & S_L & C_L+\phi_L S_L \end{vmatrix} = 0 \qquad (A)$$

where ϕ_n =angle the tangent makes with the horizontal at the right hand end, ϕ_L =angle the tangent makes with the horizontal at the left hand end, $C_n = \cos\phi_n$, $\bar{C}_n = \cos\{\delta f(\phi_n) + \frac{1}{\delta} g(\phi_n)\}$ etc.. f and g are defined by

$$f(\phi_n) = \int_0^{\phi_n} \frac{d\phi}{(\cos\phi)^{3/2}} \quad , \quad g(\phi_n) = \int_0^{\phi_n} \left(\frac{11}{8} + \frac{1}{32}\tan^2\phi\right)\cos^{\frac{3}{2}}\phi \, d\phi \qquad (B)$$

similarly for $f(\varnothing_L)$ and $g(\varnothing_L)$. δ (>0) is defined by

$$\delta^2 = \frac{(2\pi/T)^2 L}{g(\tan\varnothing_u - \tan\varnothing_L)} \qquad (C)$$

where T =natural period, L =length of catenary and g =the acceleration due to gravity.

The asymptotic theory used by Saxon and Cahn[1953] is only applicable when δ >1. For example for $\varnothing_u$ >70° the theory will not be applicable for the first in-plane mode and for $\varnothing_u$ >80° the theory will not be applicable for the first in-plane mode and for the second in-plane mode. Note that some of the results obtained in Saxon and Cahn's paper for δ <1 are incorrect and that the agreement that they obtain with experiment for these values is totally coincidental. For the configuration that is being used here the period of the first natural in-plane mode lies in the range δ <1. However the period of the second in-plane mode lies in the range δ >1.

In figure 5.7.3(d) the value of the determinant occuring in equation 5.7.3(a) is plotted against δ. For large δ a sinusoidal curve is obtained as predicted by theory (Ryan[1984]). Using the plot gives the period of the second in-plane mode as 3.35s. Hence the result obtained from the computer program is only in error by 2%.

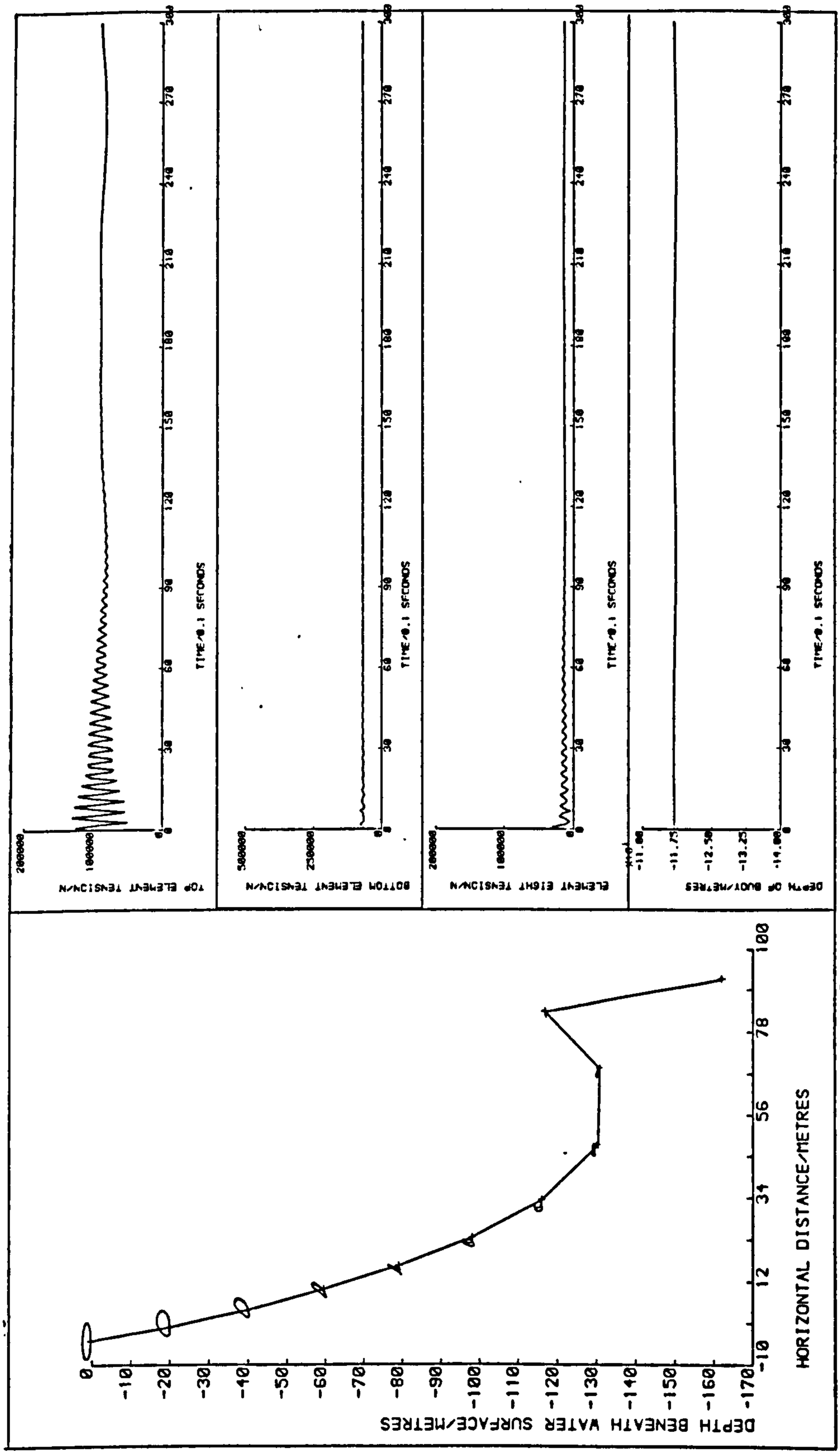

Figure 5.1.1(b): Top Motion with Period=16s

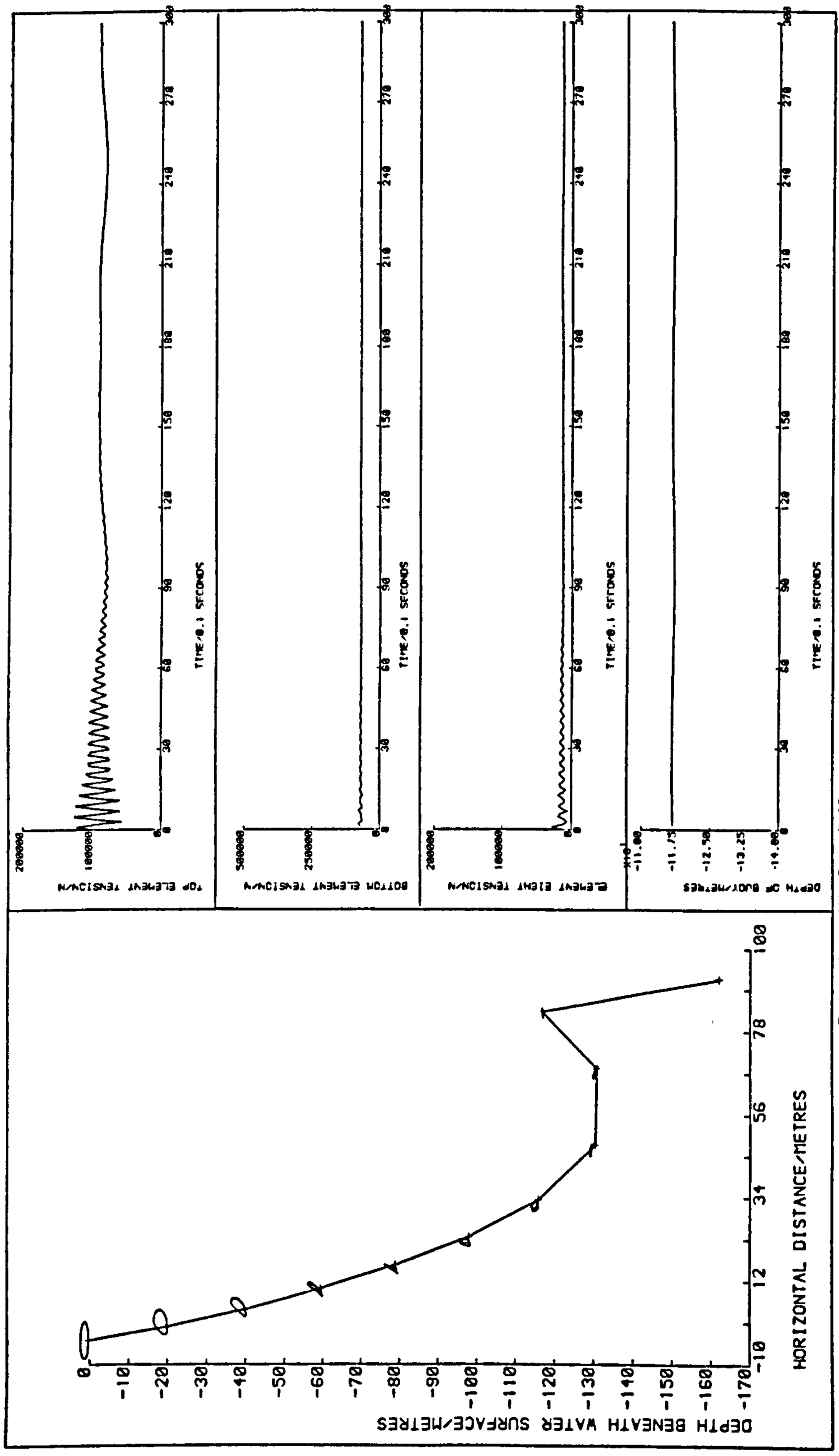

Figure 5.1.1(c): Top Motion with Period=15s

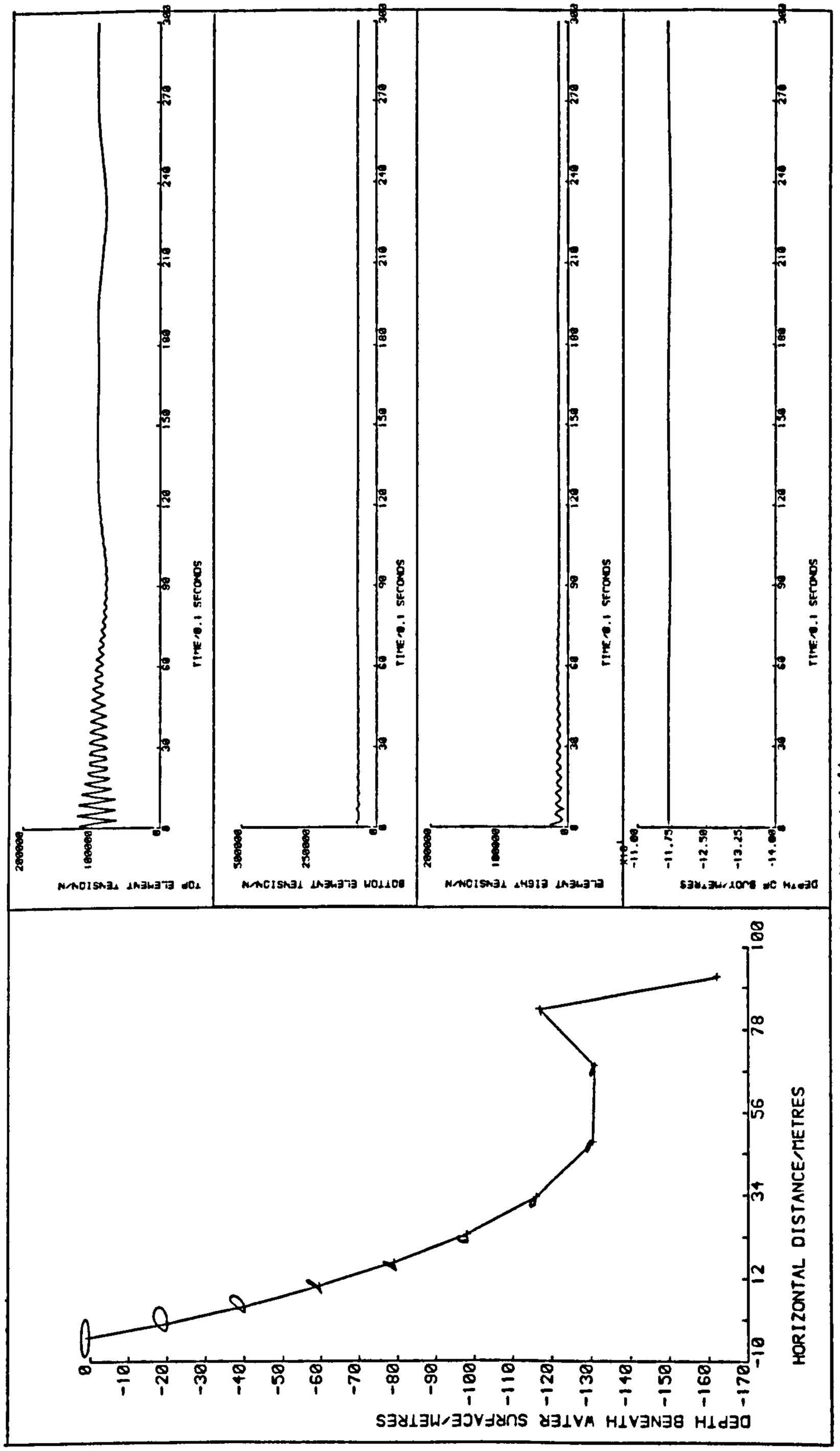

Figure 5.1.1(d): Top Motion with Period=14s

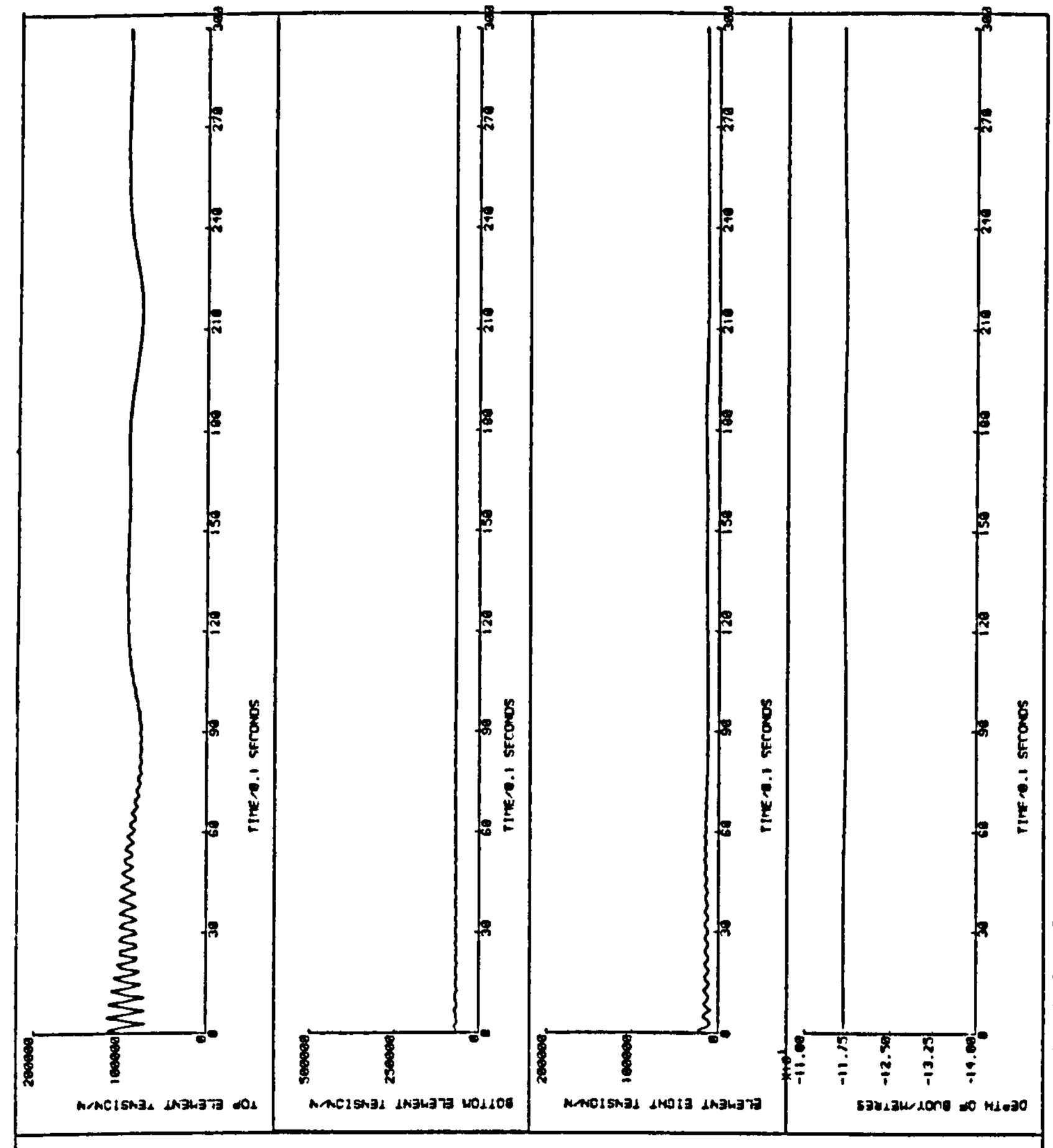

Figure 5.1.1(e): Top Motion with Period=13s

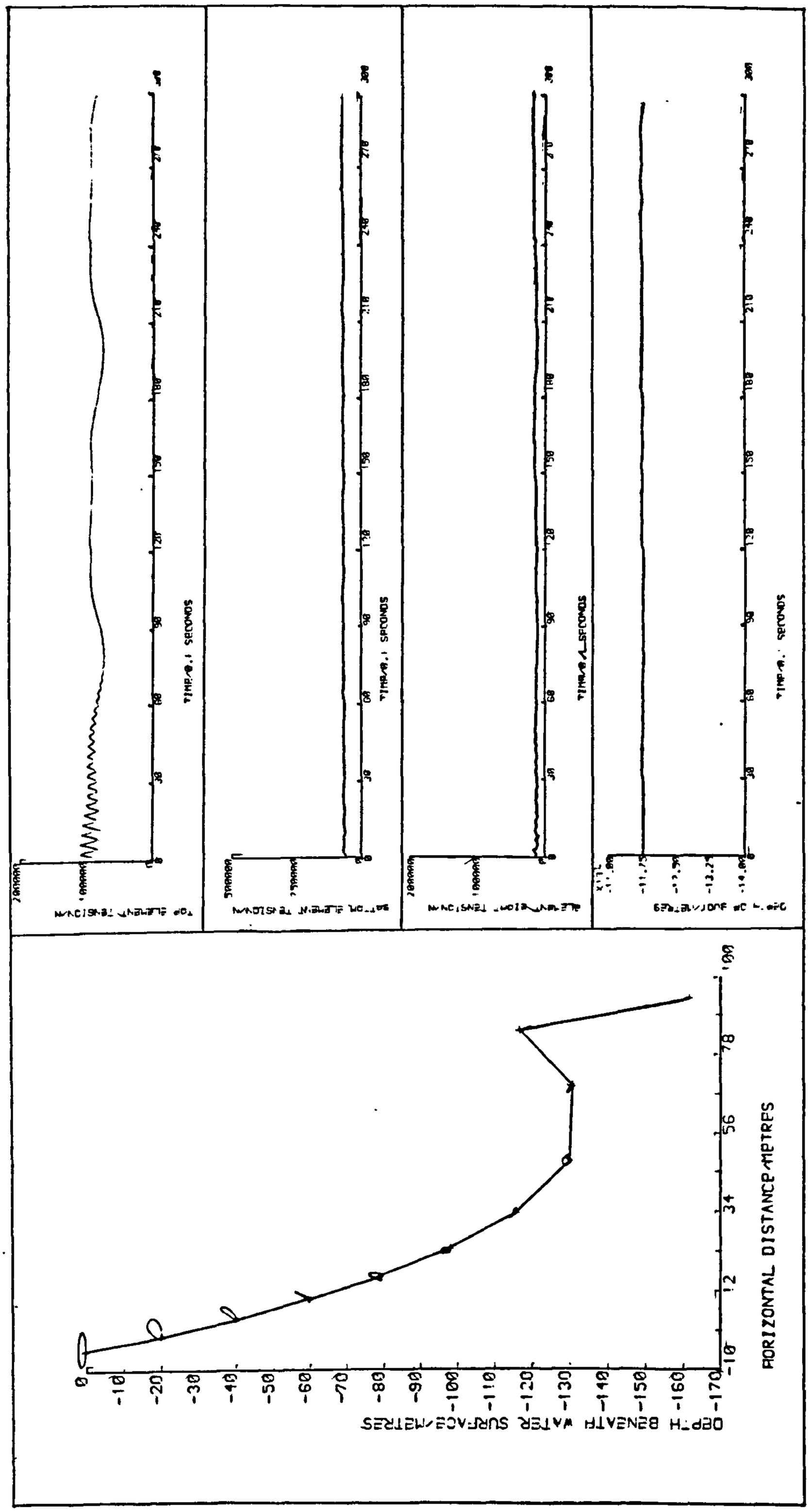

Figure 5.1.1(f): Top Motion with Period = 12 s

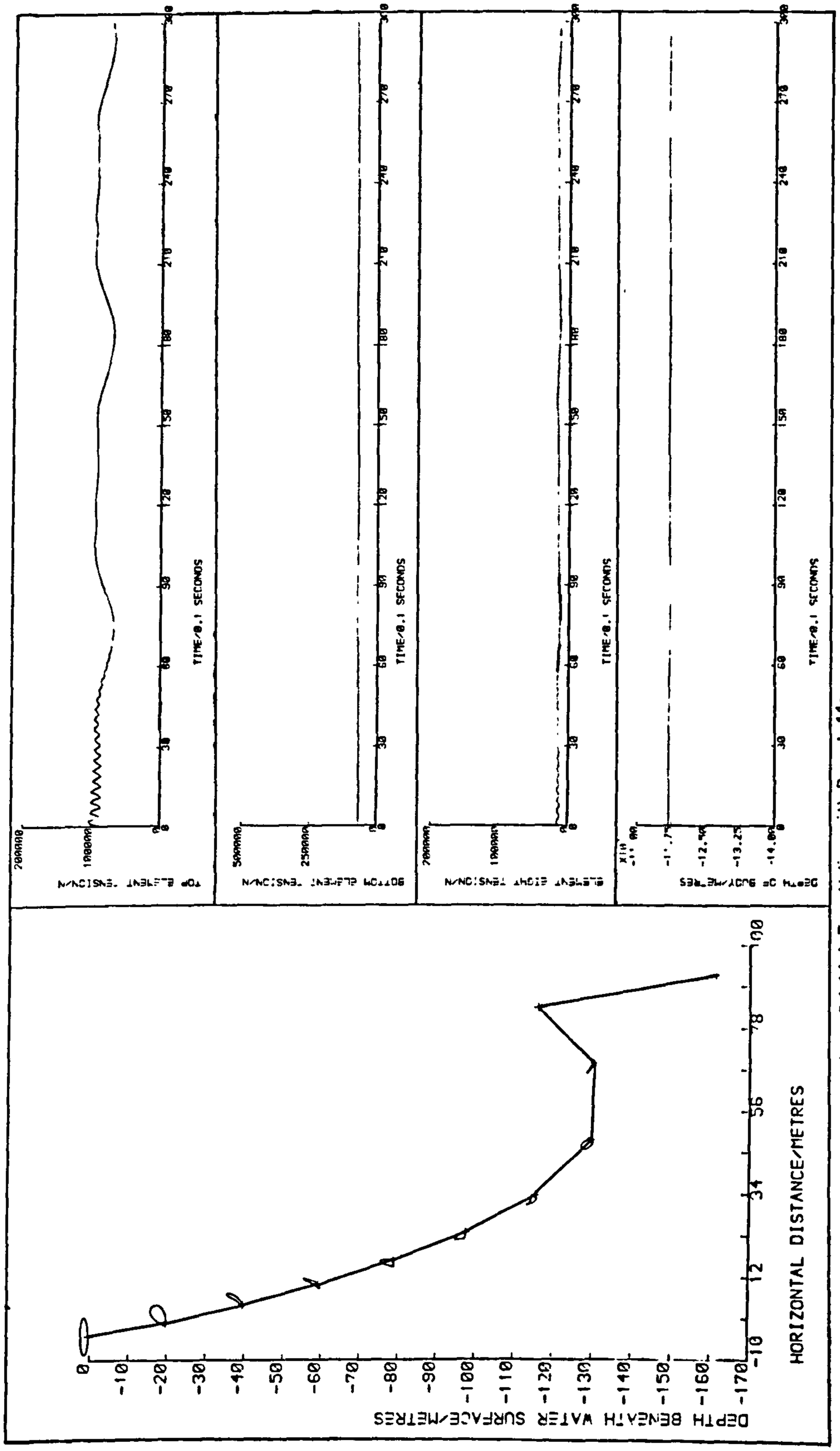

Figure 5.1.1(g): Top Motion with Period=11s

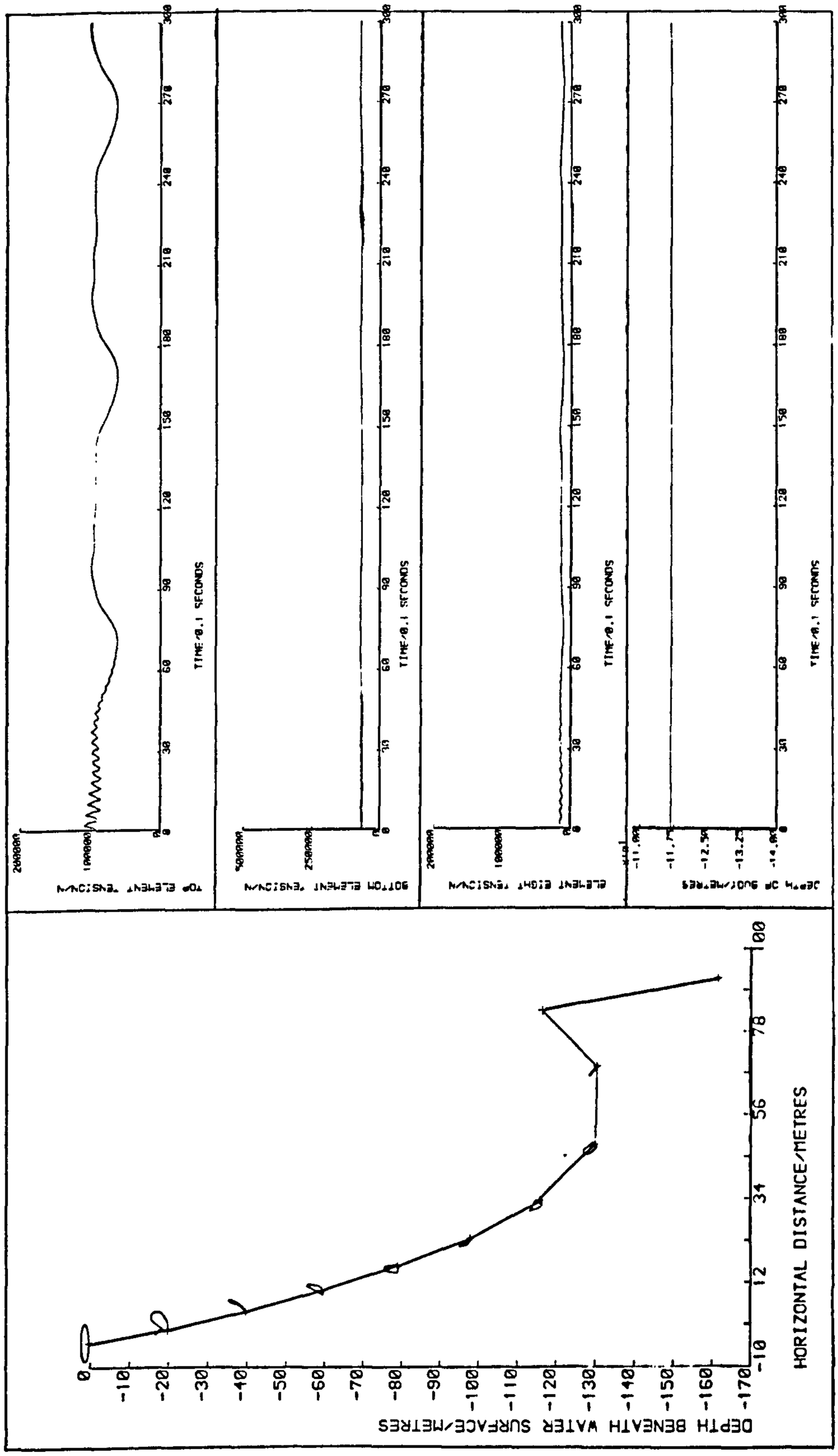

Figure 5.1.1 (h):Top Motion with Period = 10 s

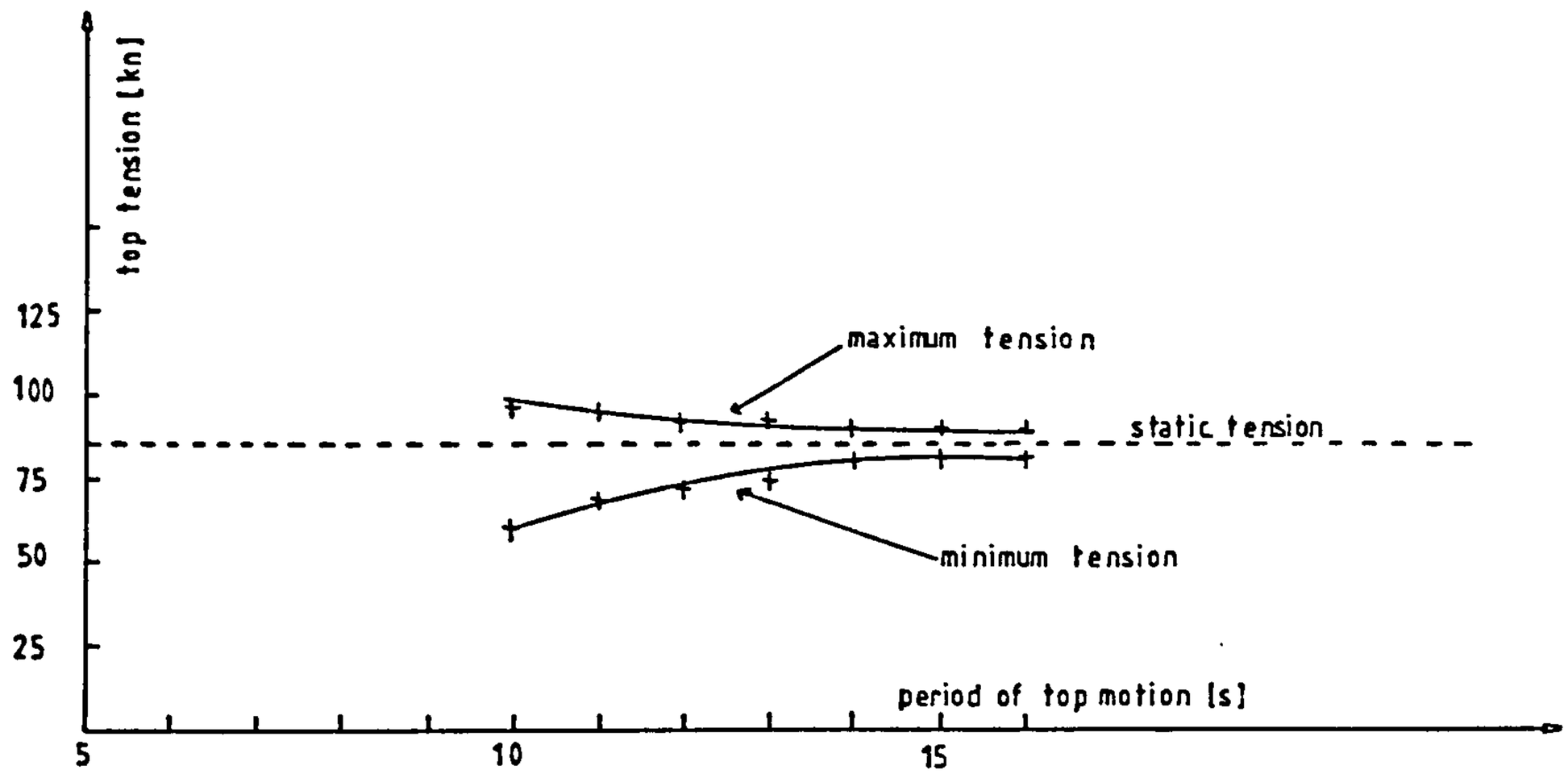

Figure 5.1.1 (i): Variation of Top Tension

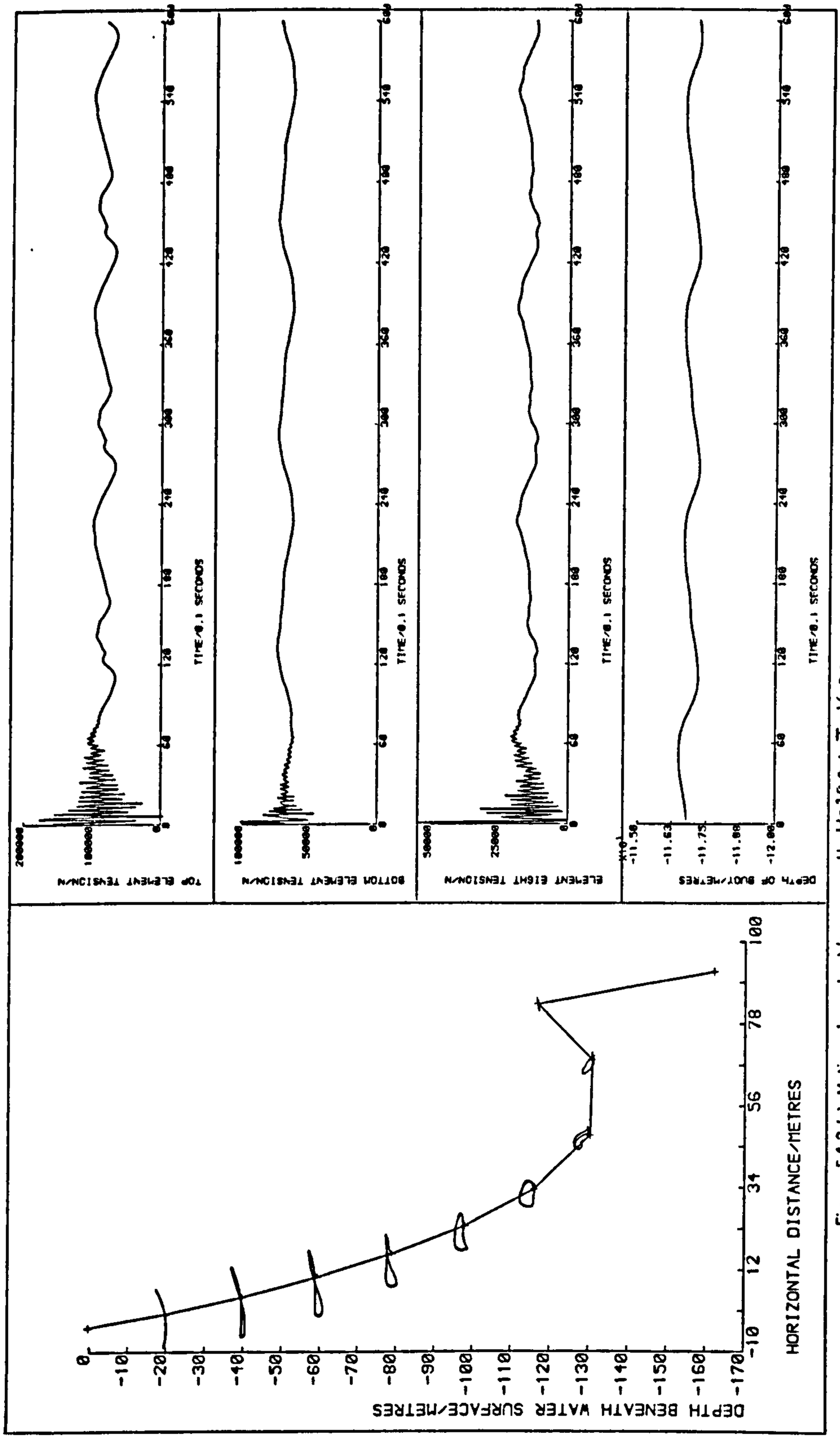

Figure 5.1.2 (a): Motion due to Wave with H=29.0m, T=16.0s

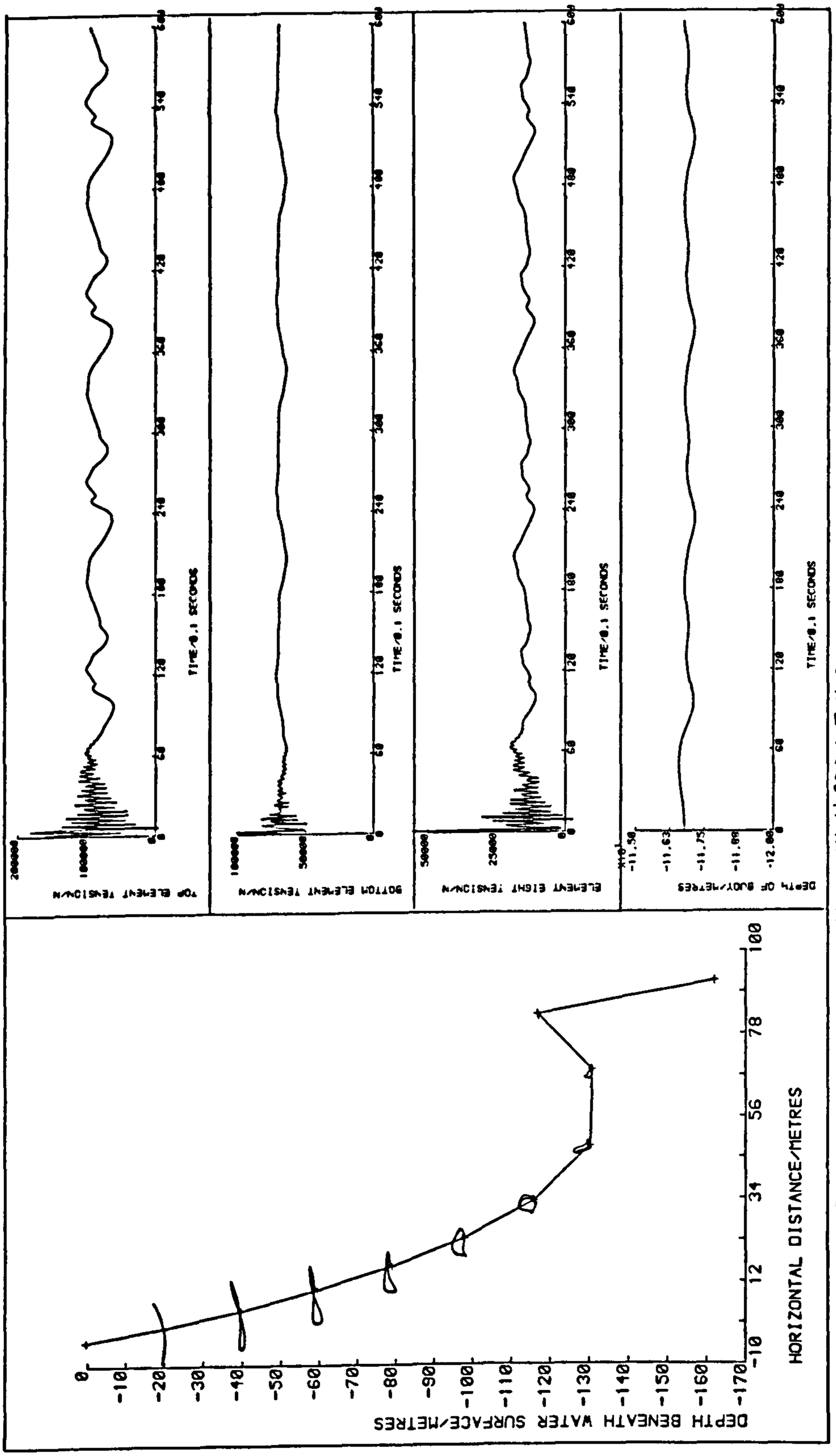

Figure 5.1.2(b):Motion due to Wave with H=29.0M, T=14.0S

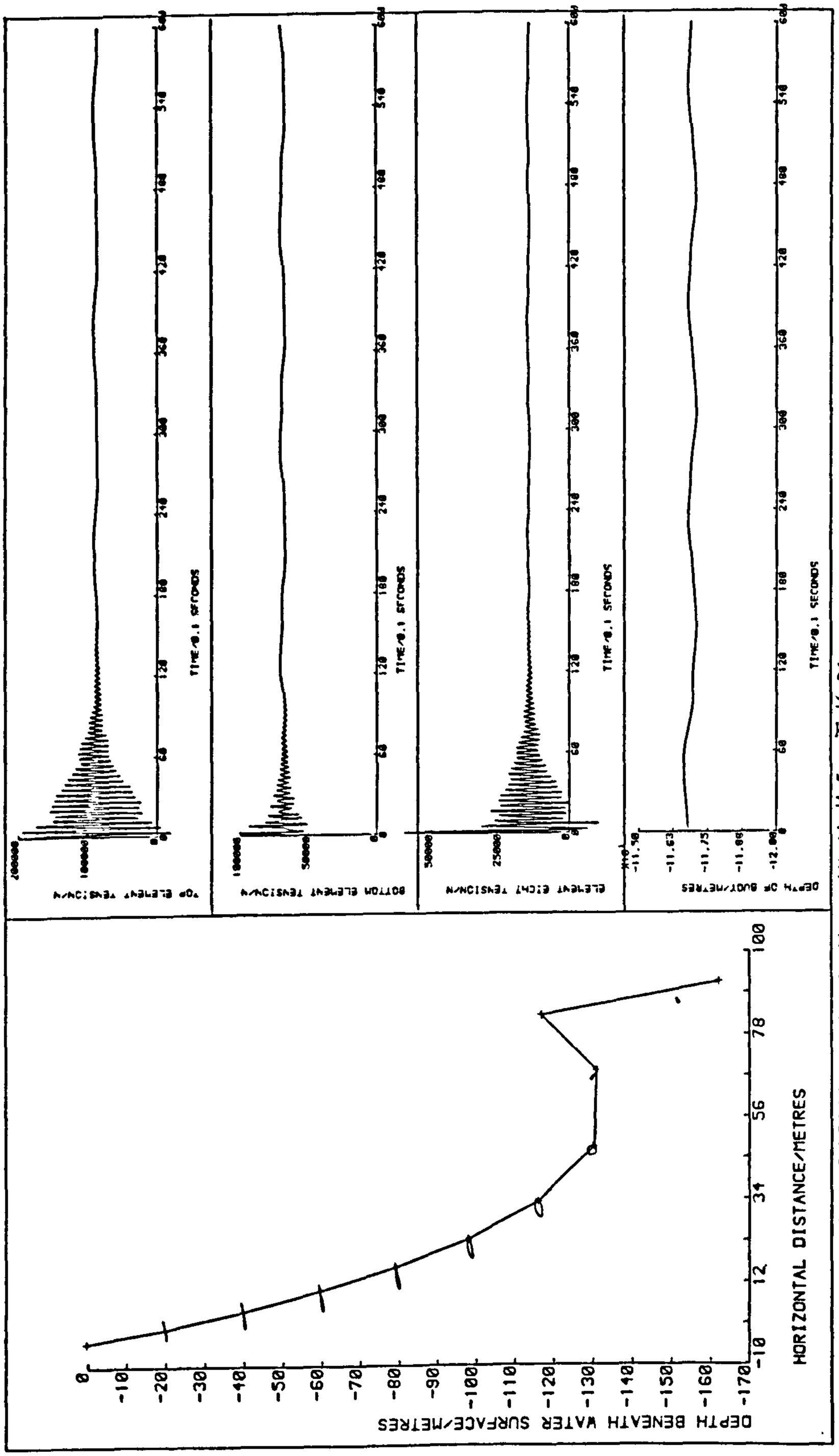

Figure 5.1.2 (c): Motion due to Wave with H=14.5M, T=16.05

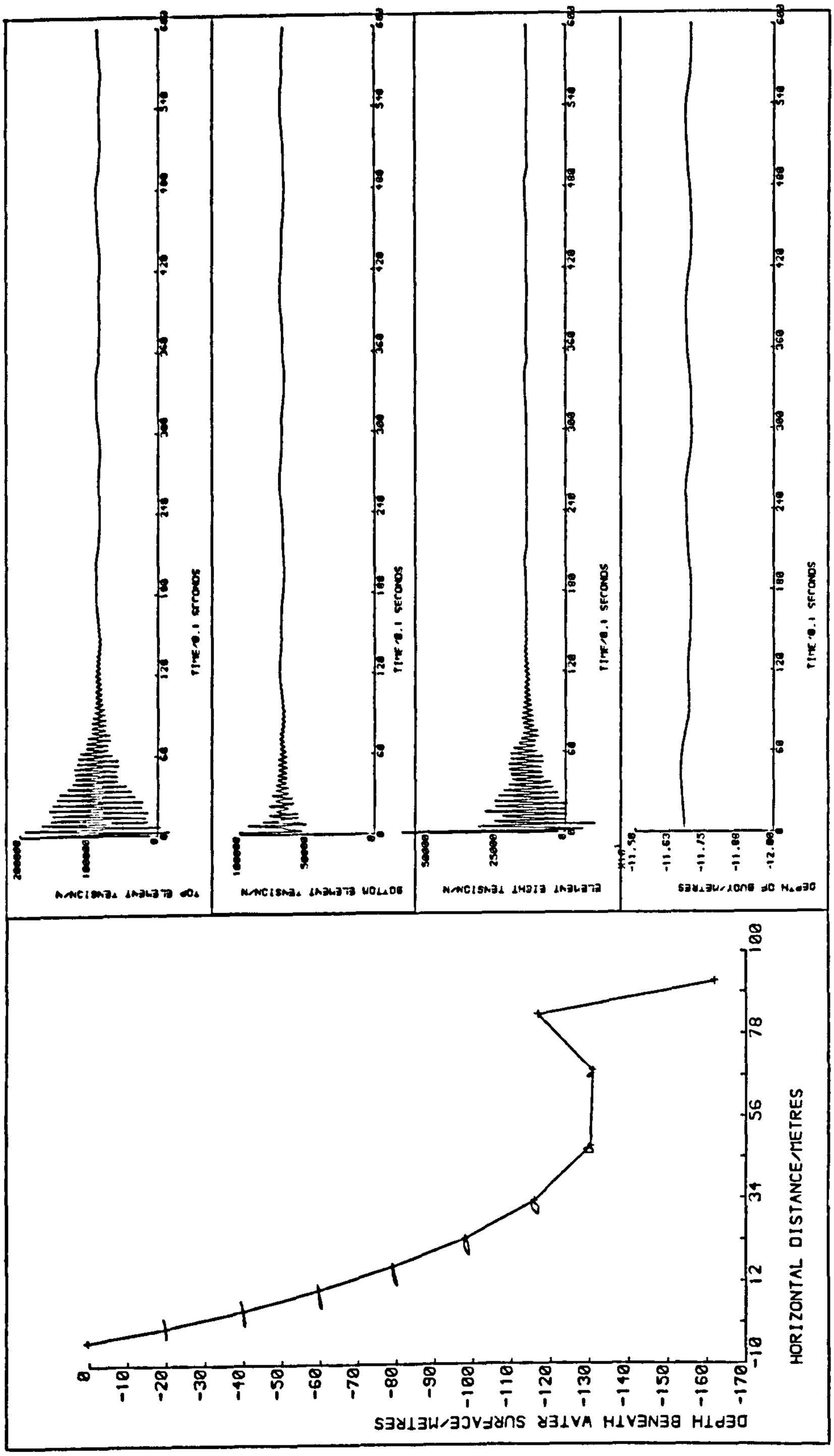

Figure 5.12 (d): Motion due to Wave with H=14·5, T=14s

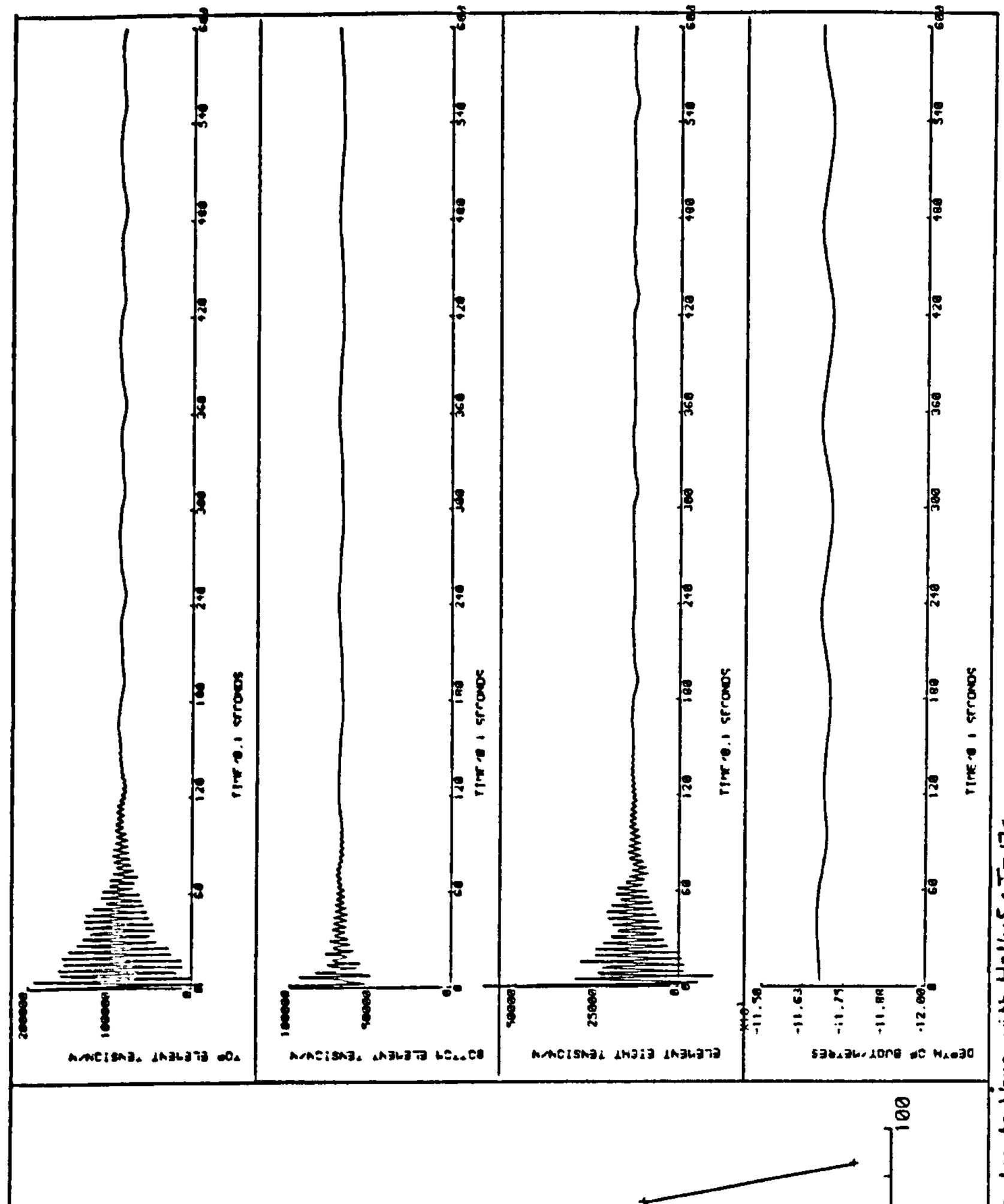

Figure 5.1.2 (e): Motion due to Wave with H=14.5m, T=17s

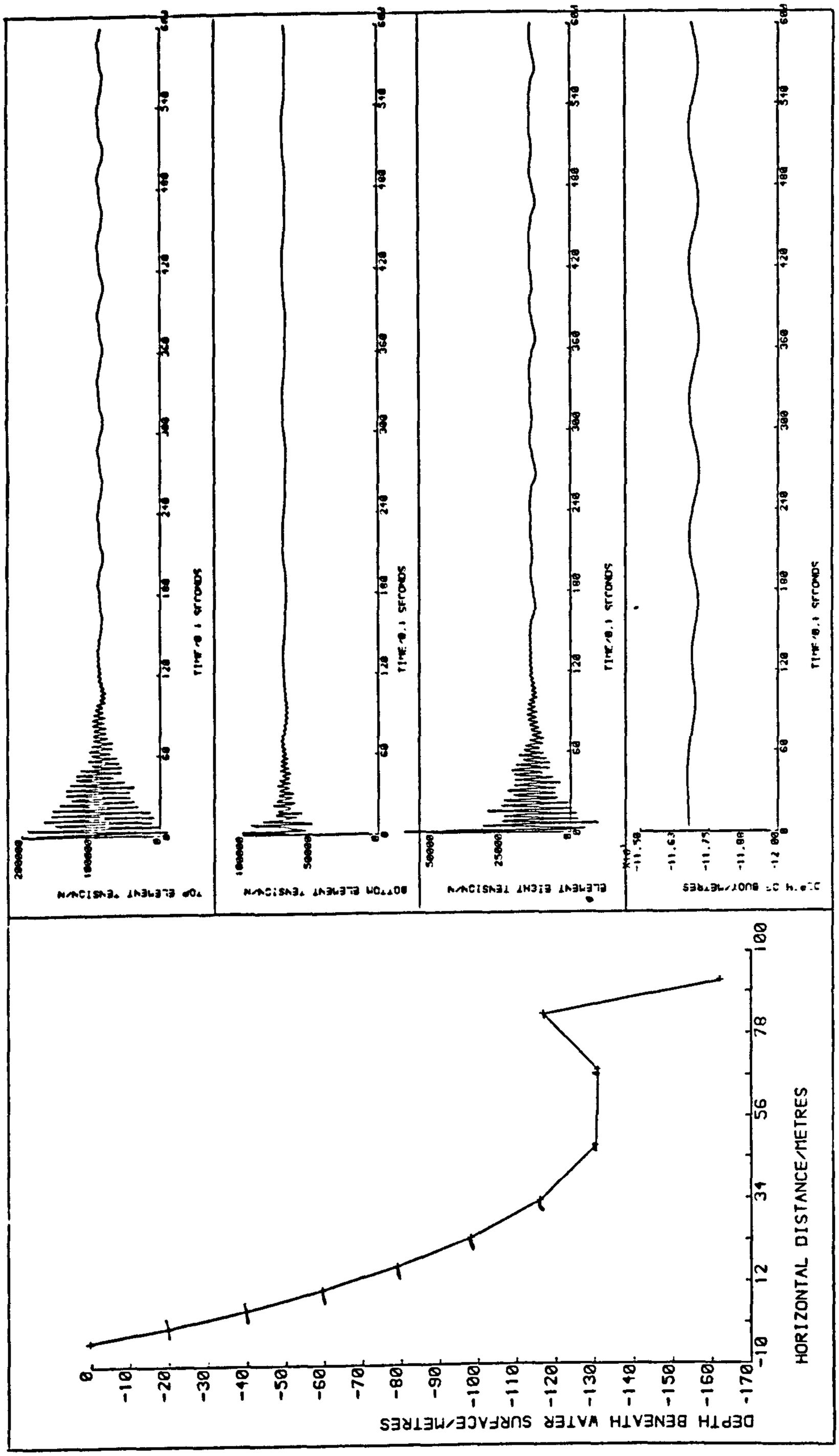

Figure 51.2 (f): Motion due to Wave with H=14·5M, T=10S

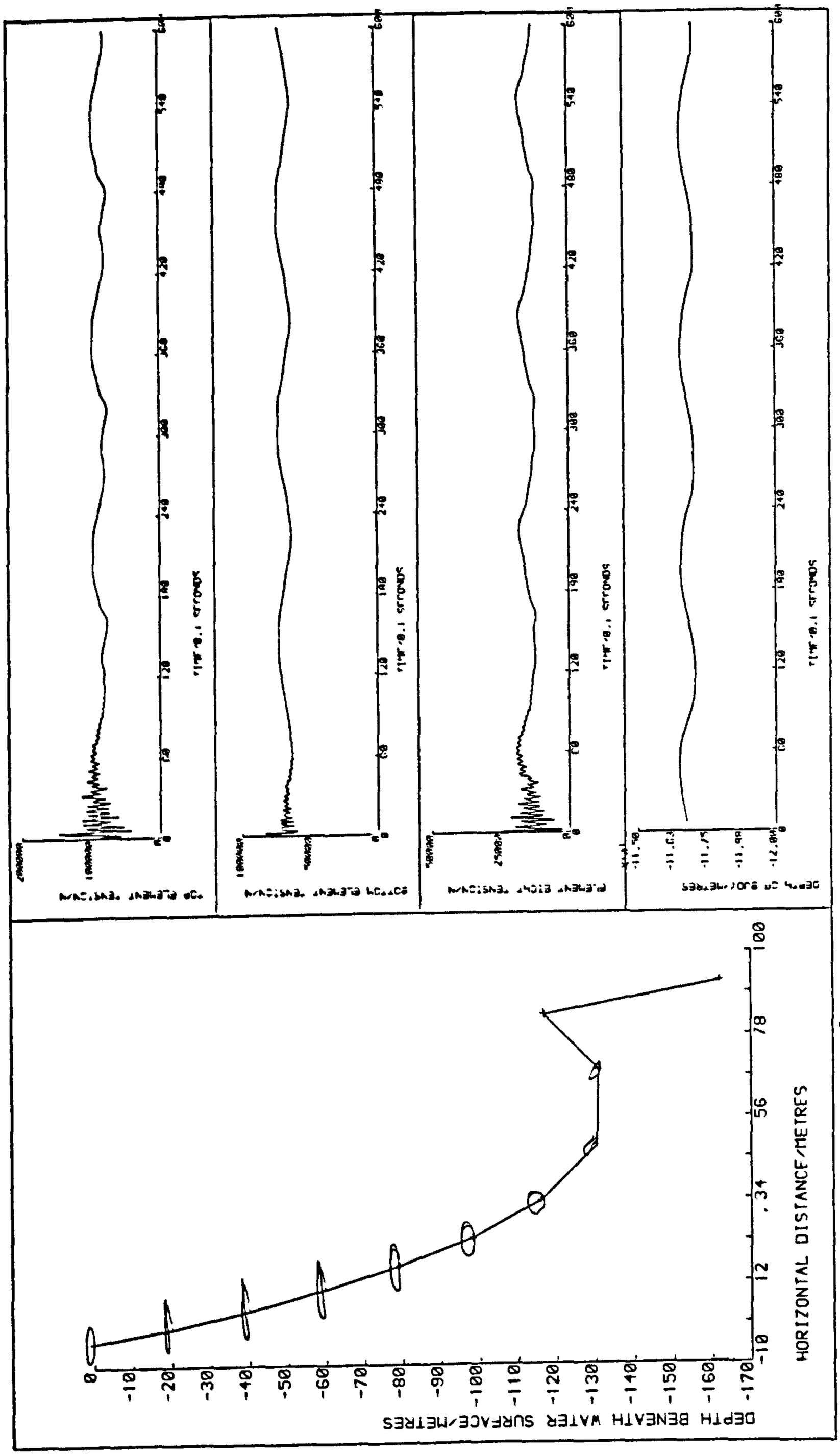

Figure 5.1.3 (a) : Wave + Top Motion H=29.0M, T=16 0s, θ_s=5.0M, θ_H=1.0M

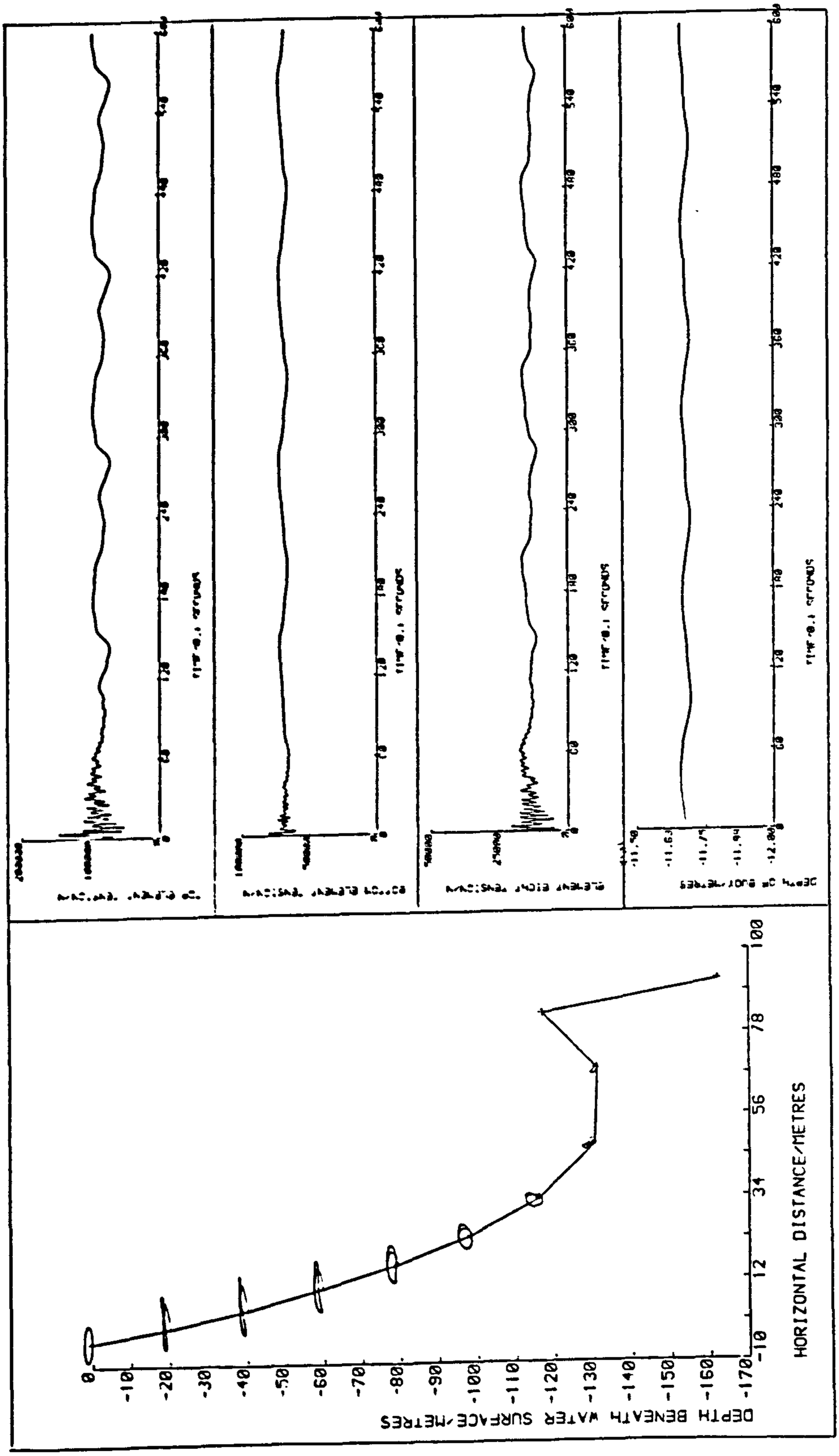

Figure 5.1.3(b). Wave + Top Motion H=29.0m, T=14.0s, a_S=5.0M, a_H=1.0M

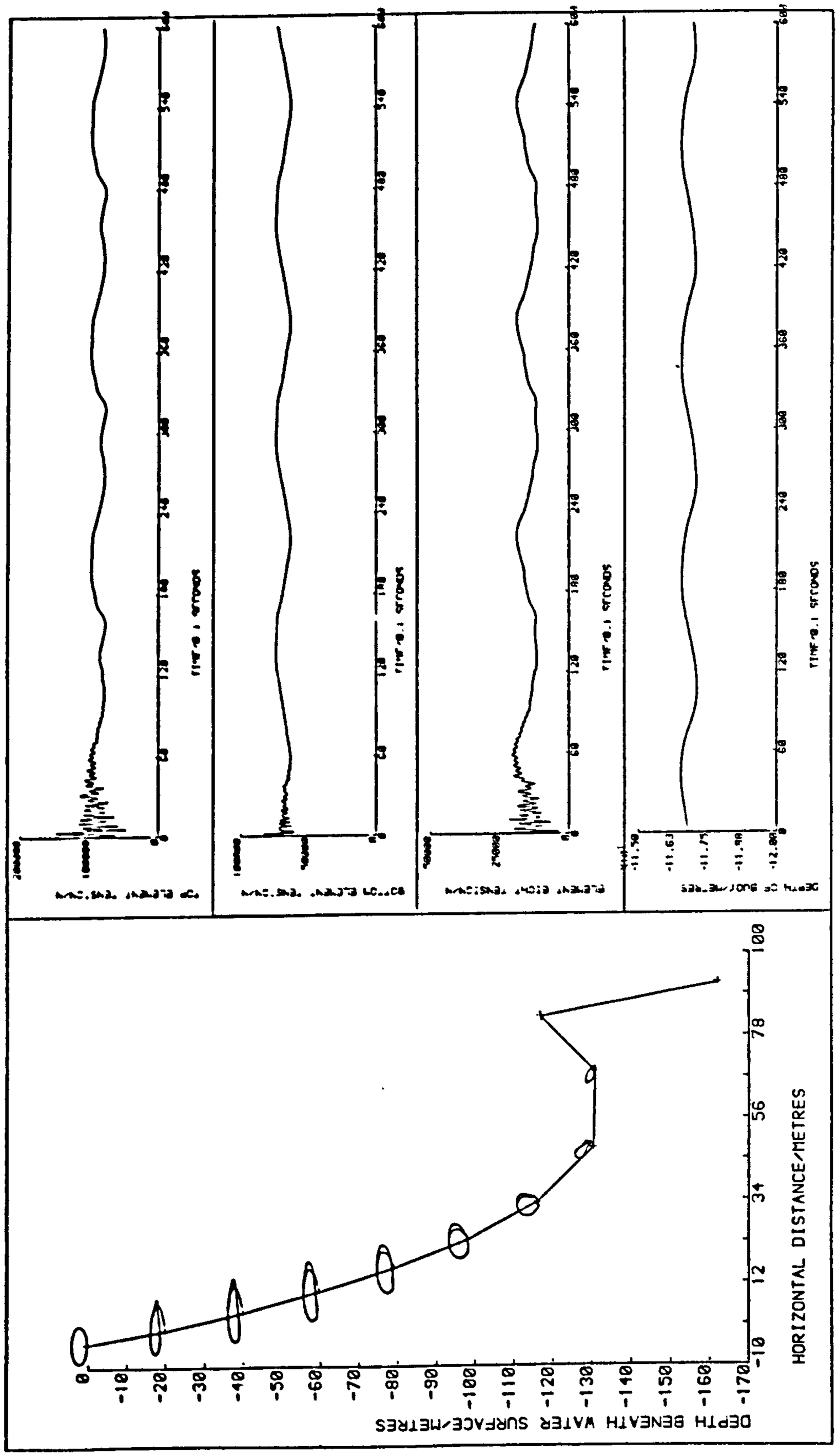

Figure 5.1.3 (c): Wave • Top Motion H=24·0M, T=16·0S, a_S=5·0M, a_H=2.0M

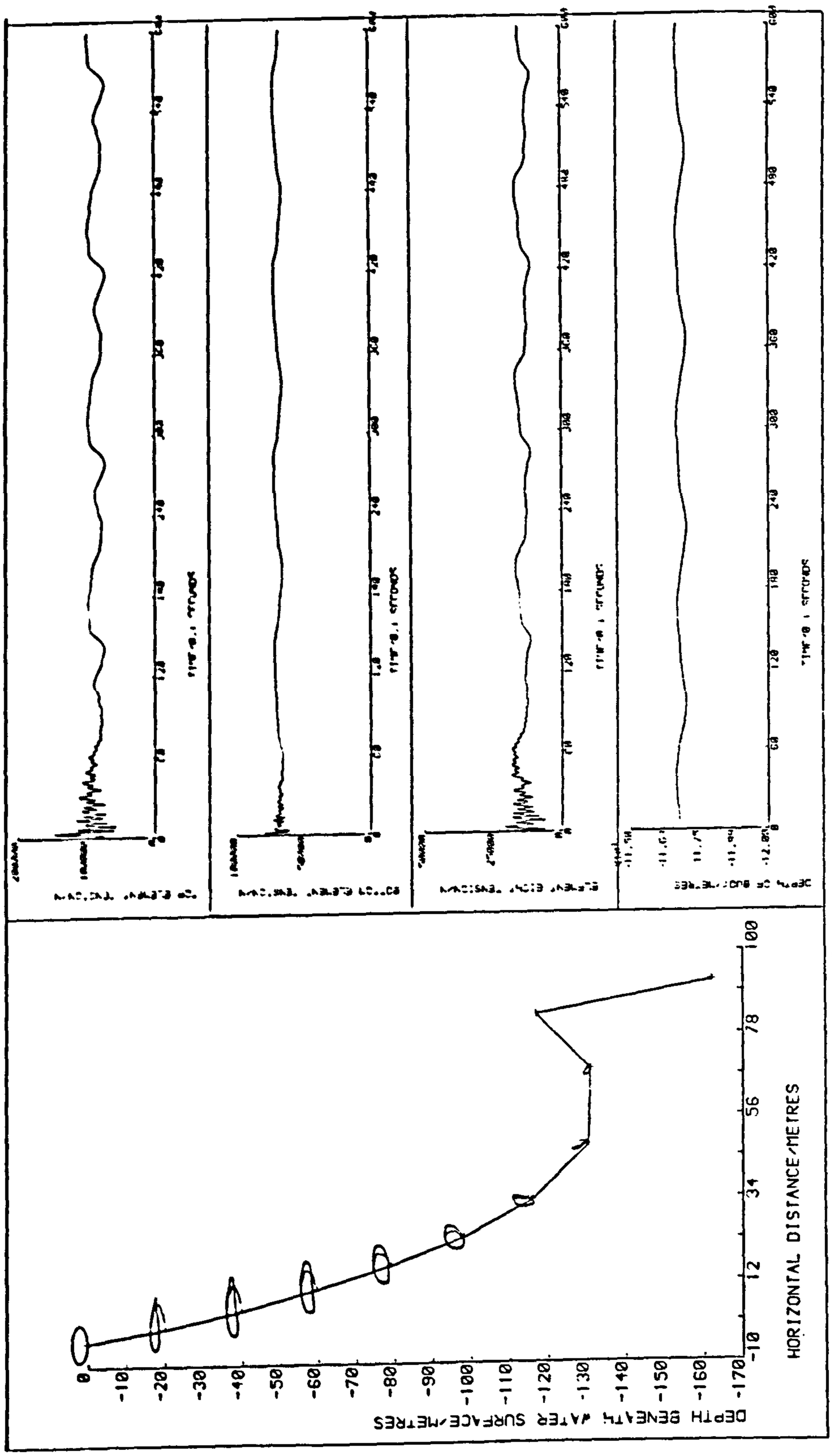

Figure 5.1.3 (d): Wave + Top Motion H=29.0M, T=14.0S, a_S=5.0M, a_H=2.0M

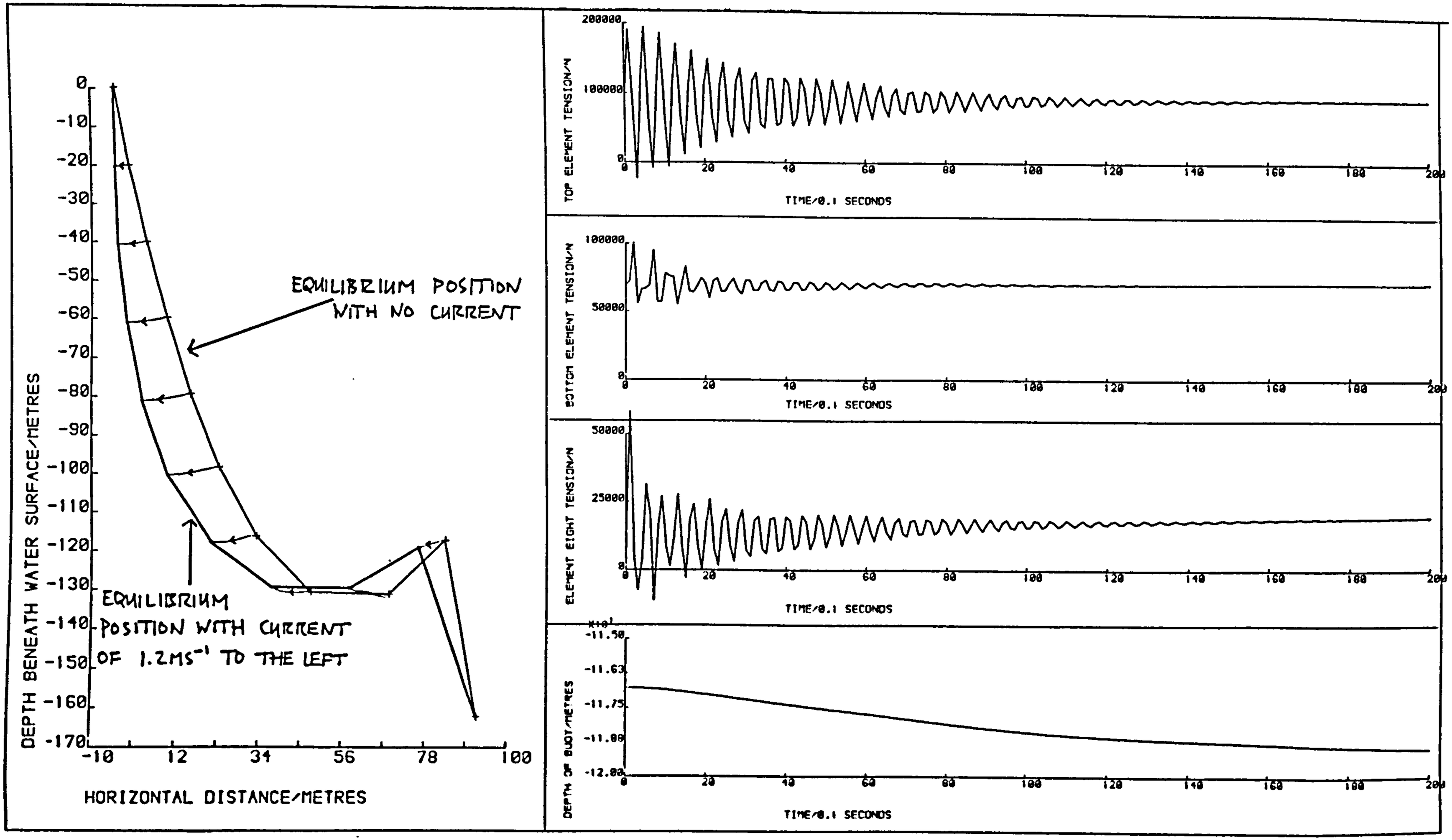

Figure 5.1.4 (a): The Effect of Current

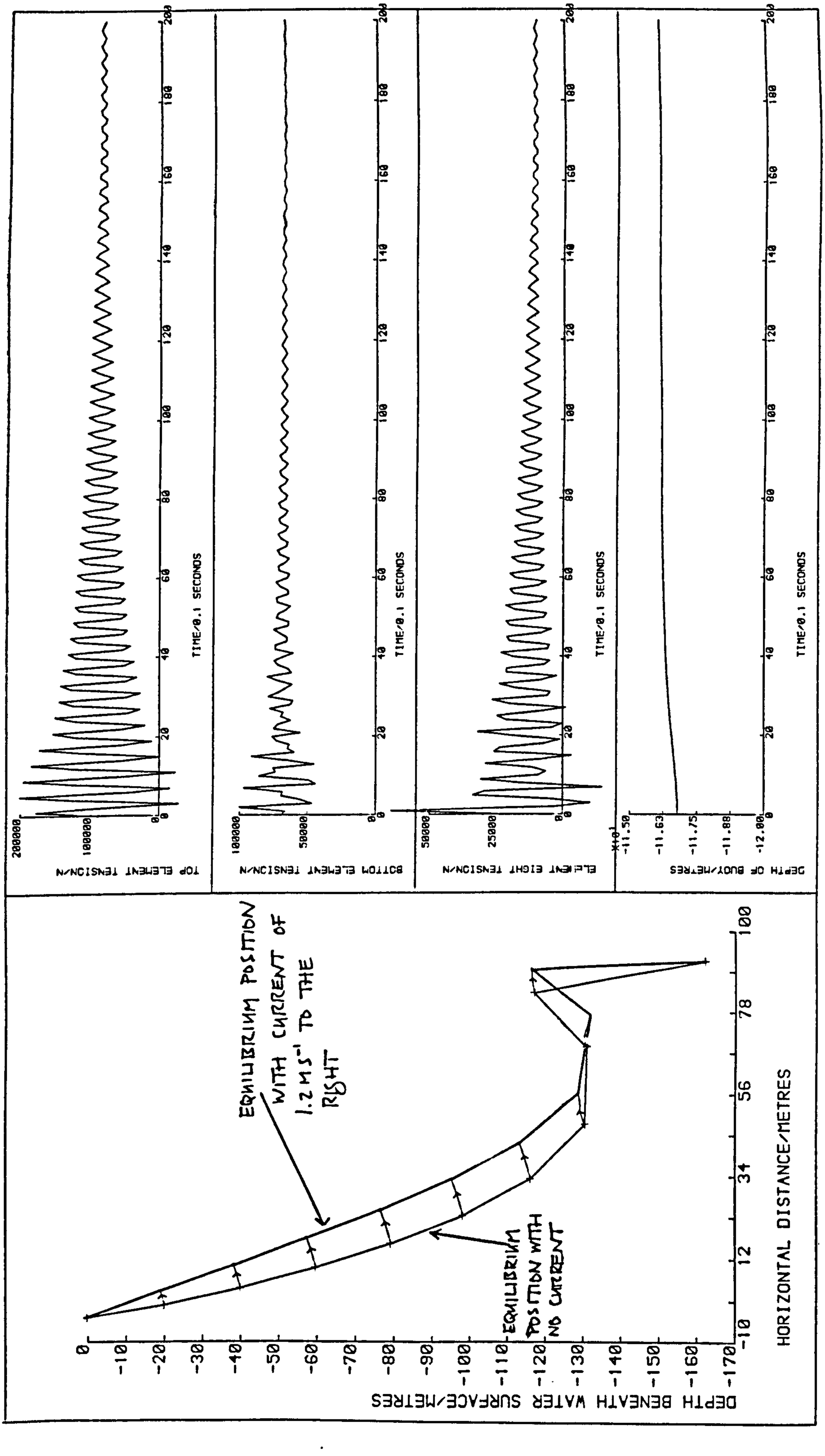

Figure 5.1.4 (b): The Effect of Current

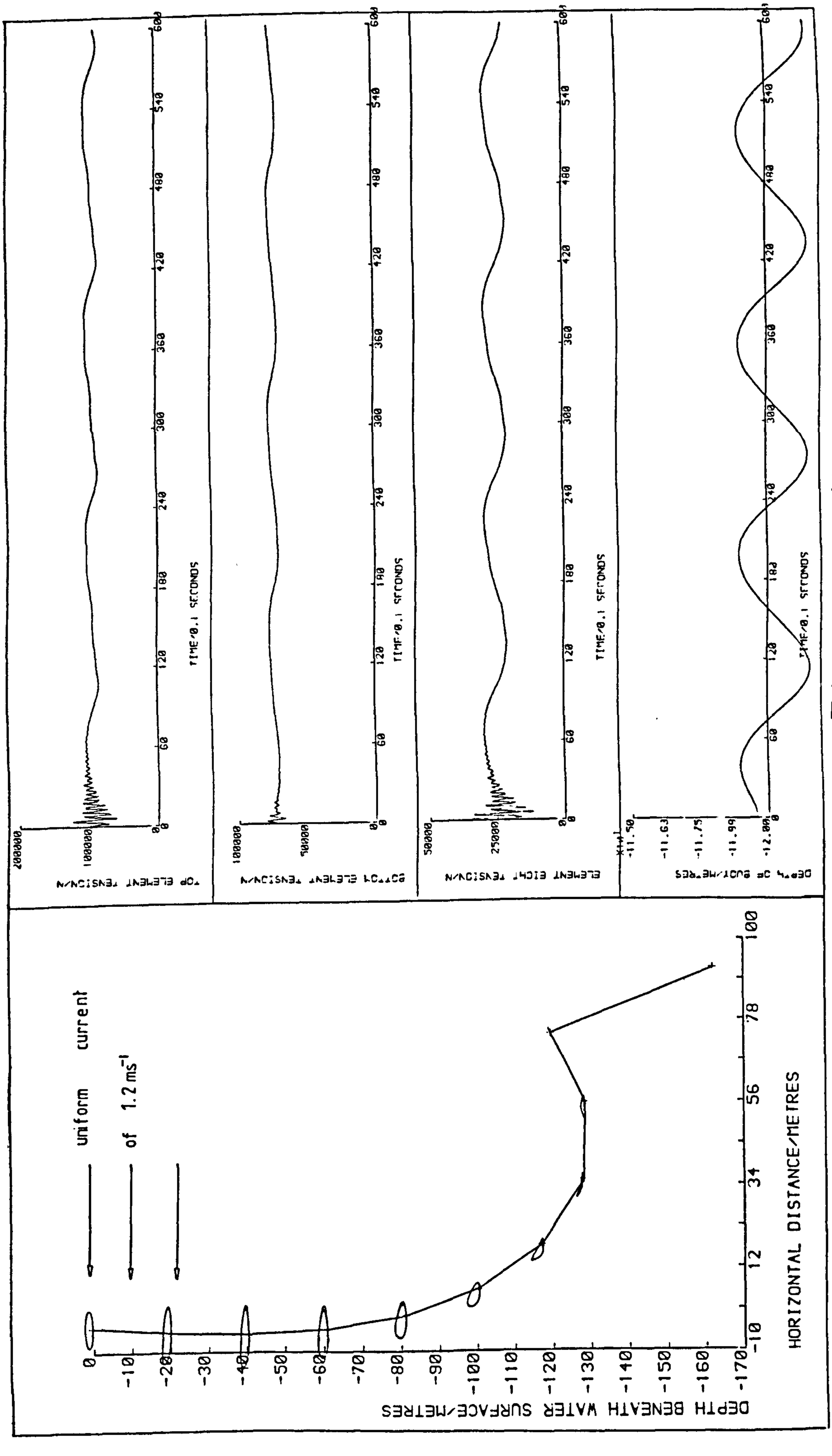

Figure 5.1.5 (a): Wave + Top Motion + Current H=24.0M, T=16.0S, a_S=5.0M, a_H=1.0M

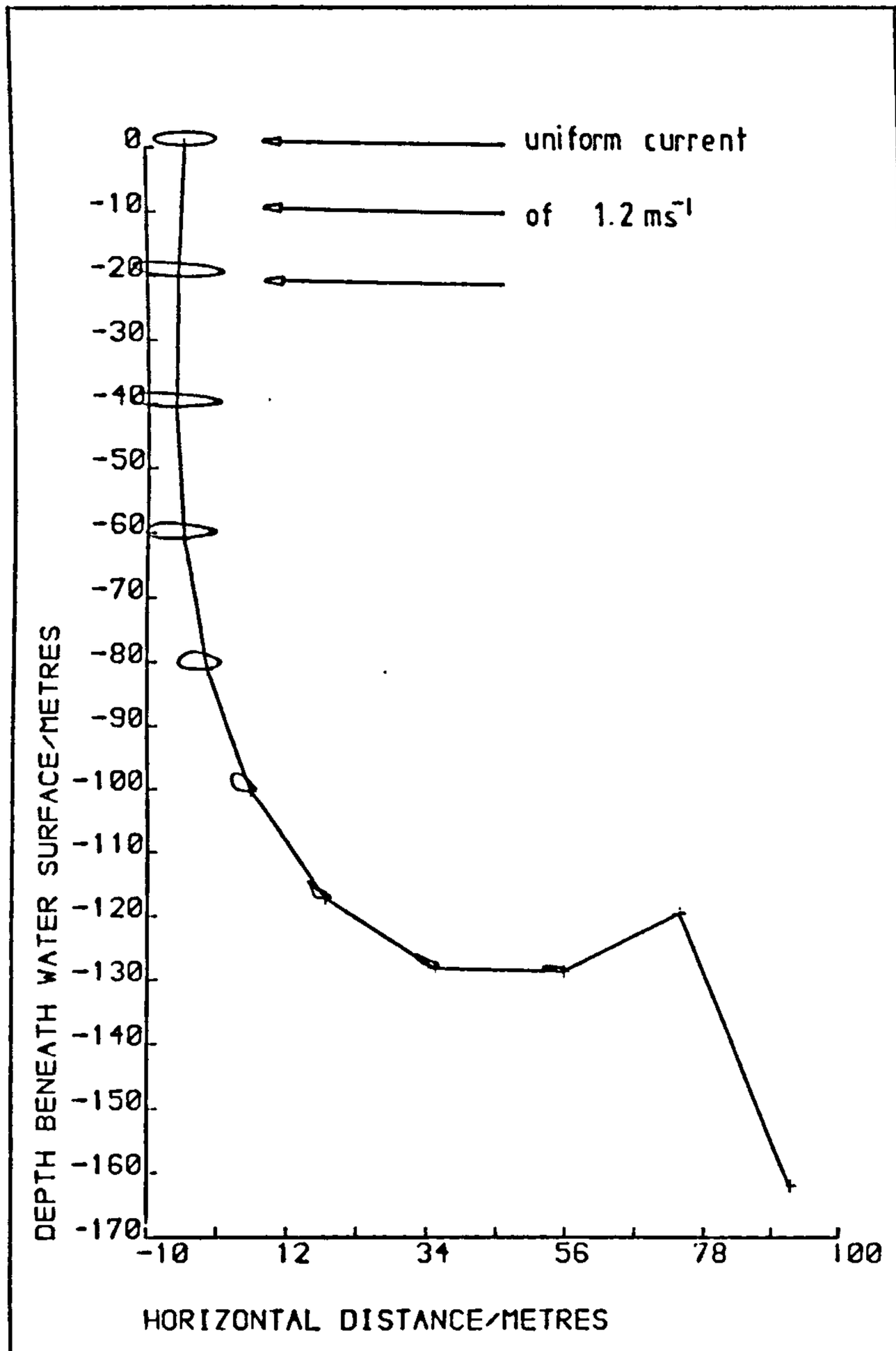

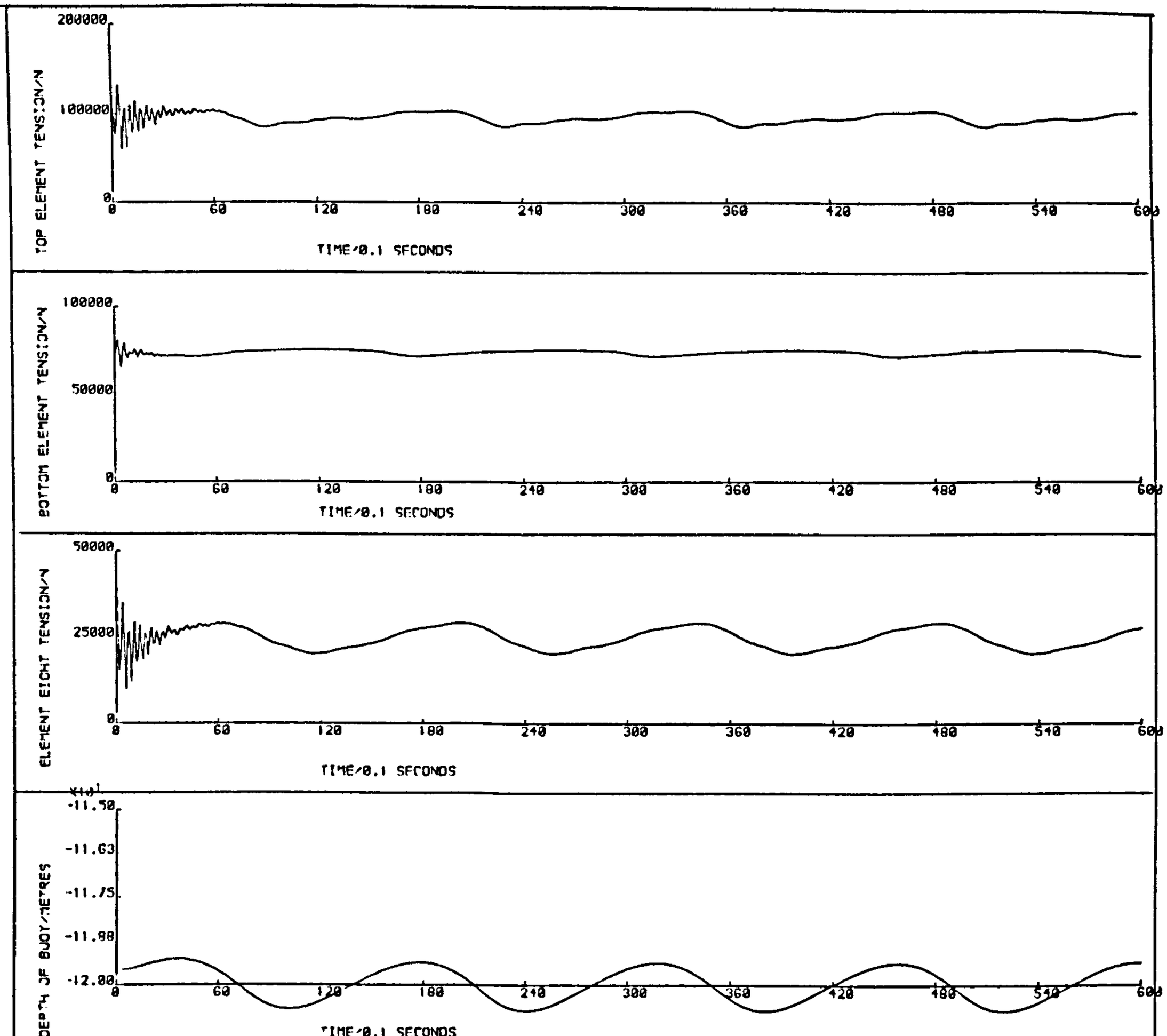

Figure 5.1.5 (b): Wave + Top Motion + Current $H = 29.0M$, $T = 14.0S$, $a_S = 5.0M$, $a_H = 1.0M$

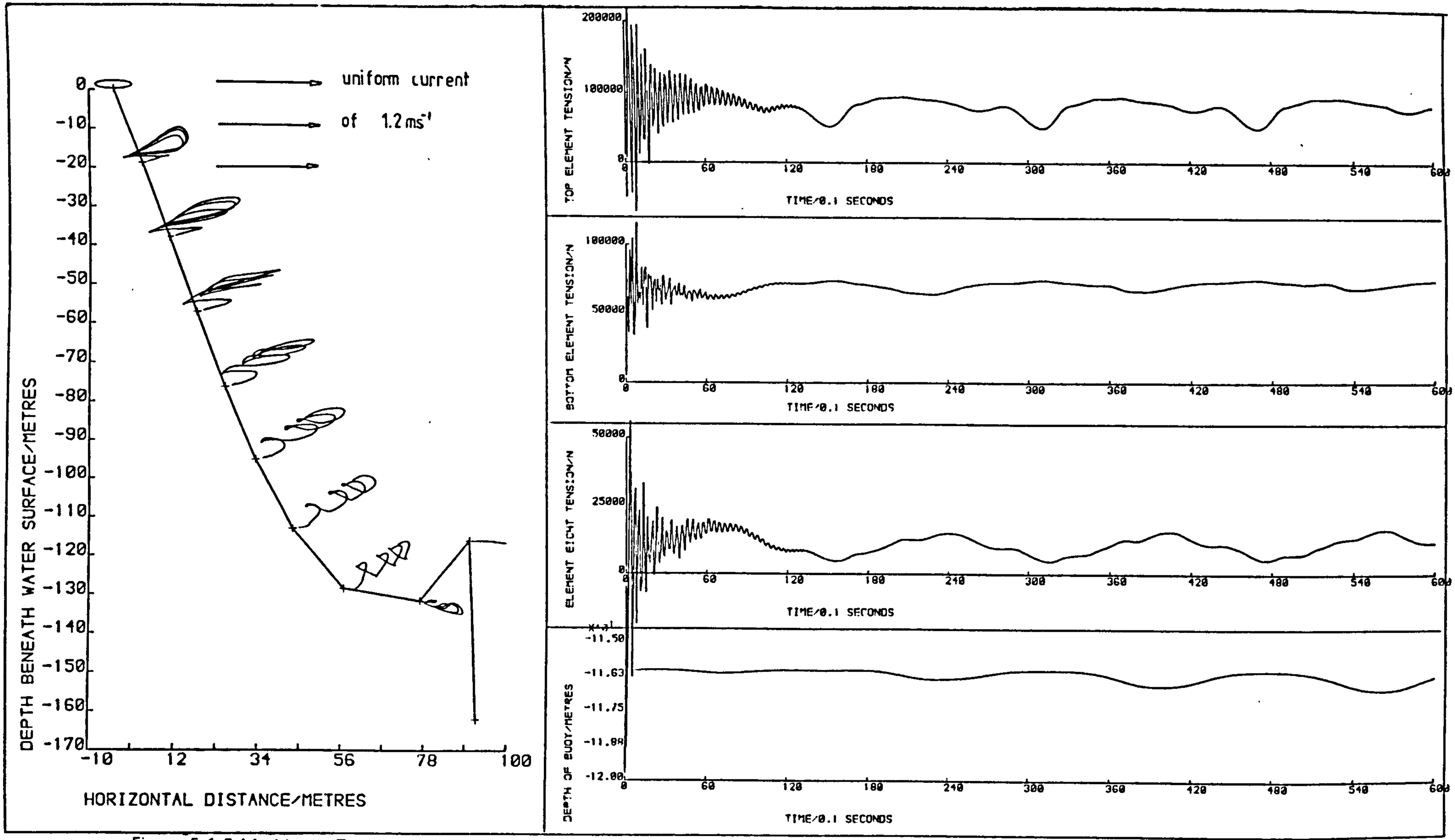

Figure 5.1.5 (c): Wave + Top Motion + Current $H = 29.0M$, $T = 16.0s$, $a_S = 5.0M$, $a_H = 1.0M$

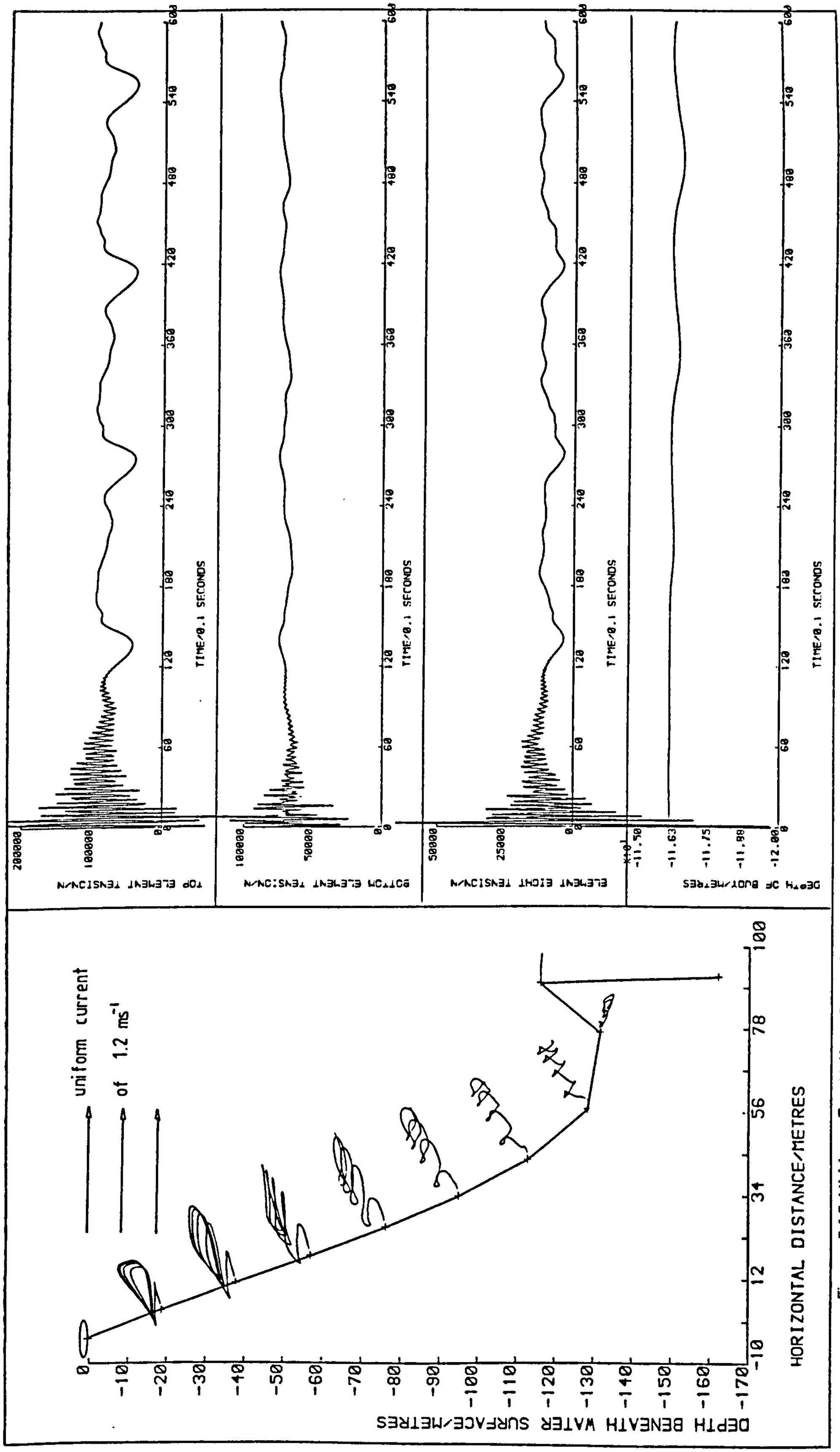

Figure 5.1.5 (d): Wave + Top Motion + Current H=29.0M, T=14.0s, a_5=5.0M, a_4=1.0M

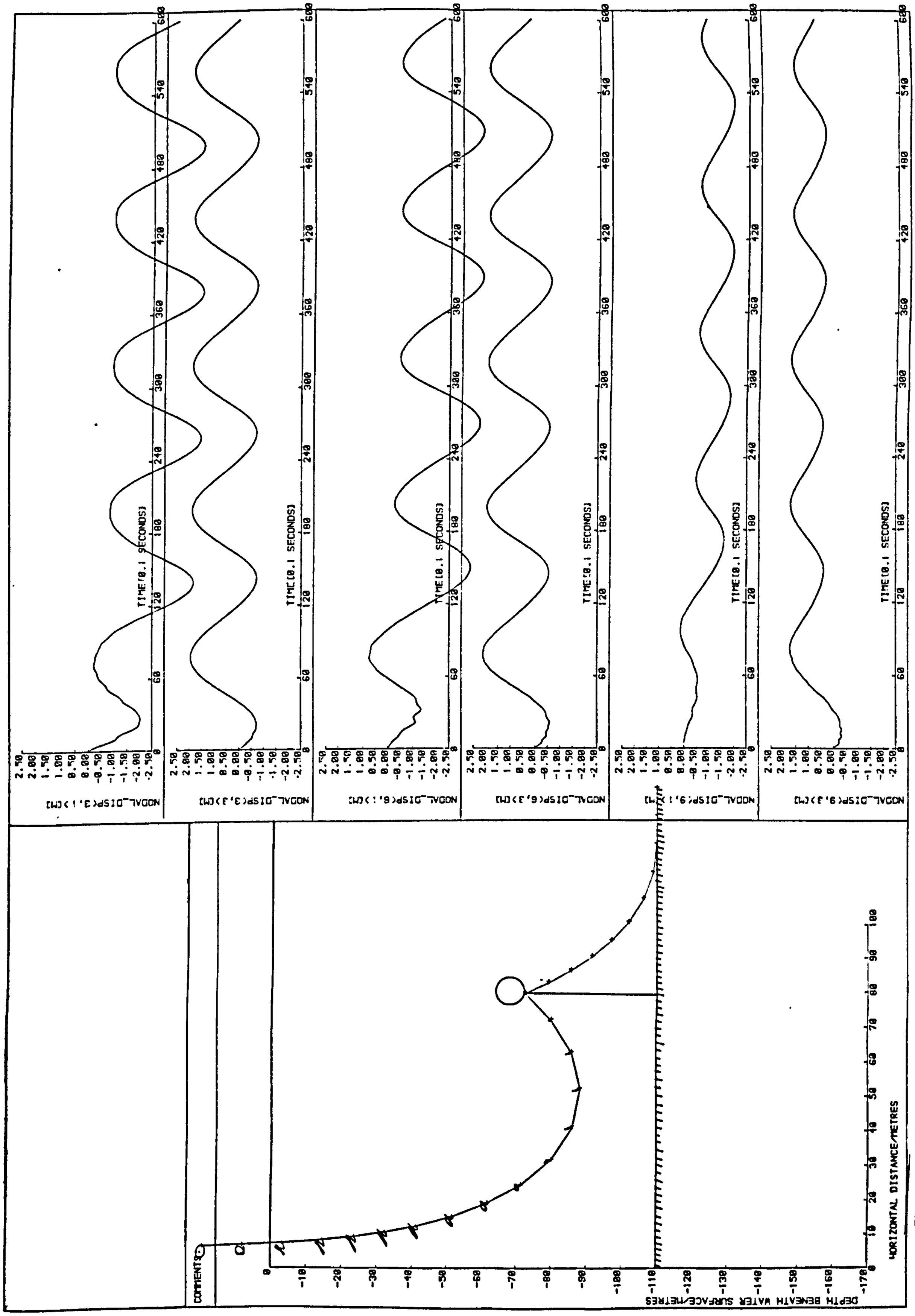

Figure 5.2.3 (a): Comparison with Model Tests

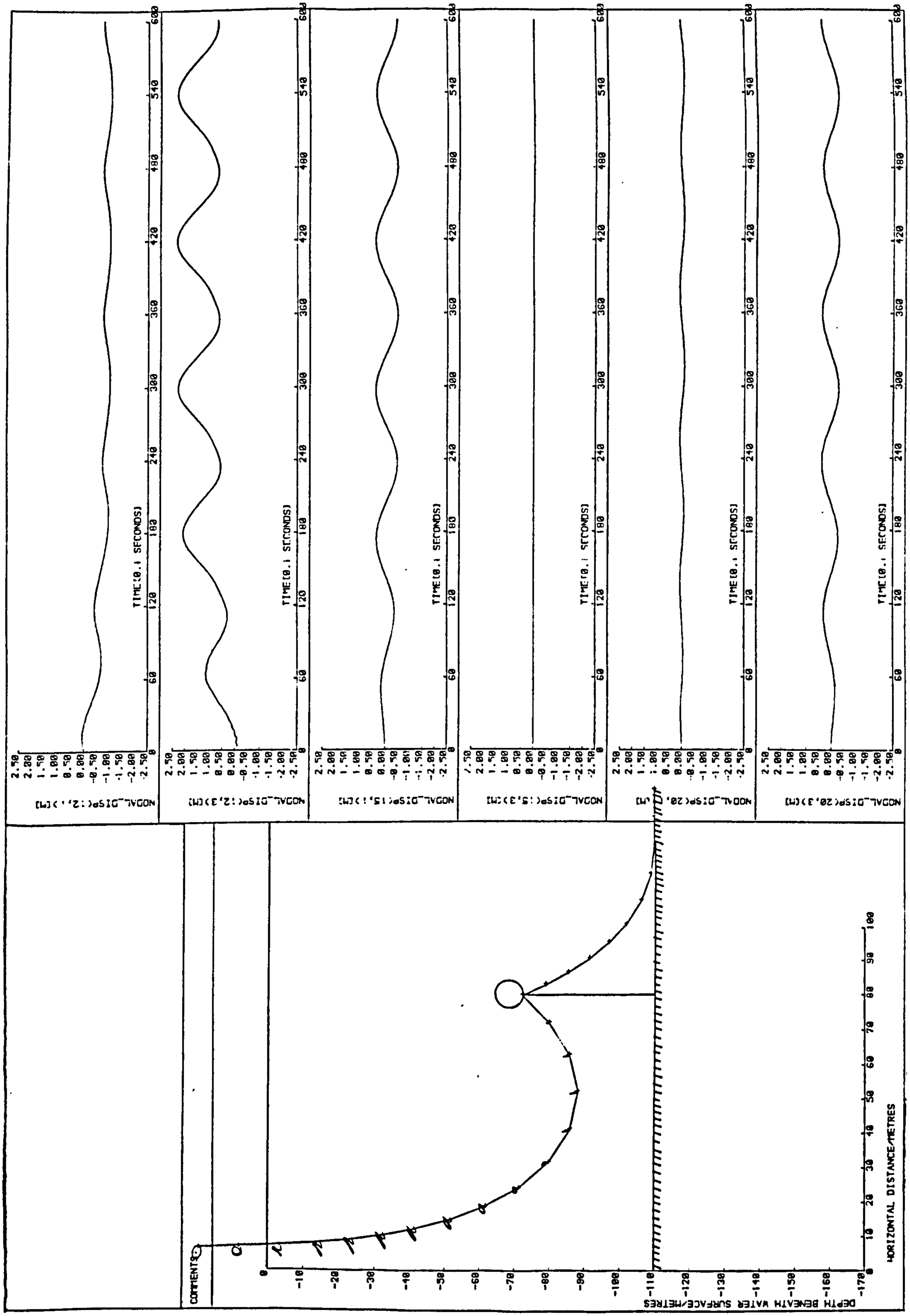

Figure 5.2.3 (b): Comparison with Model Tests

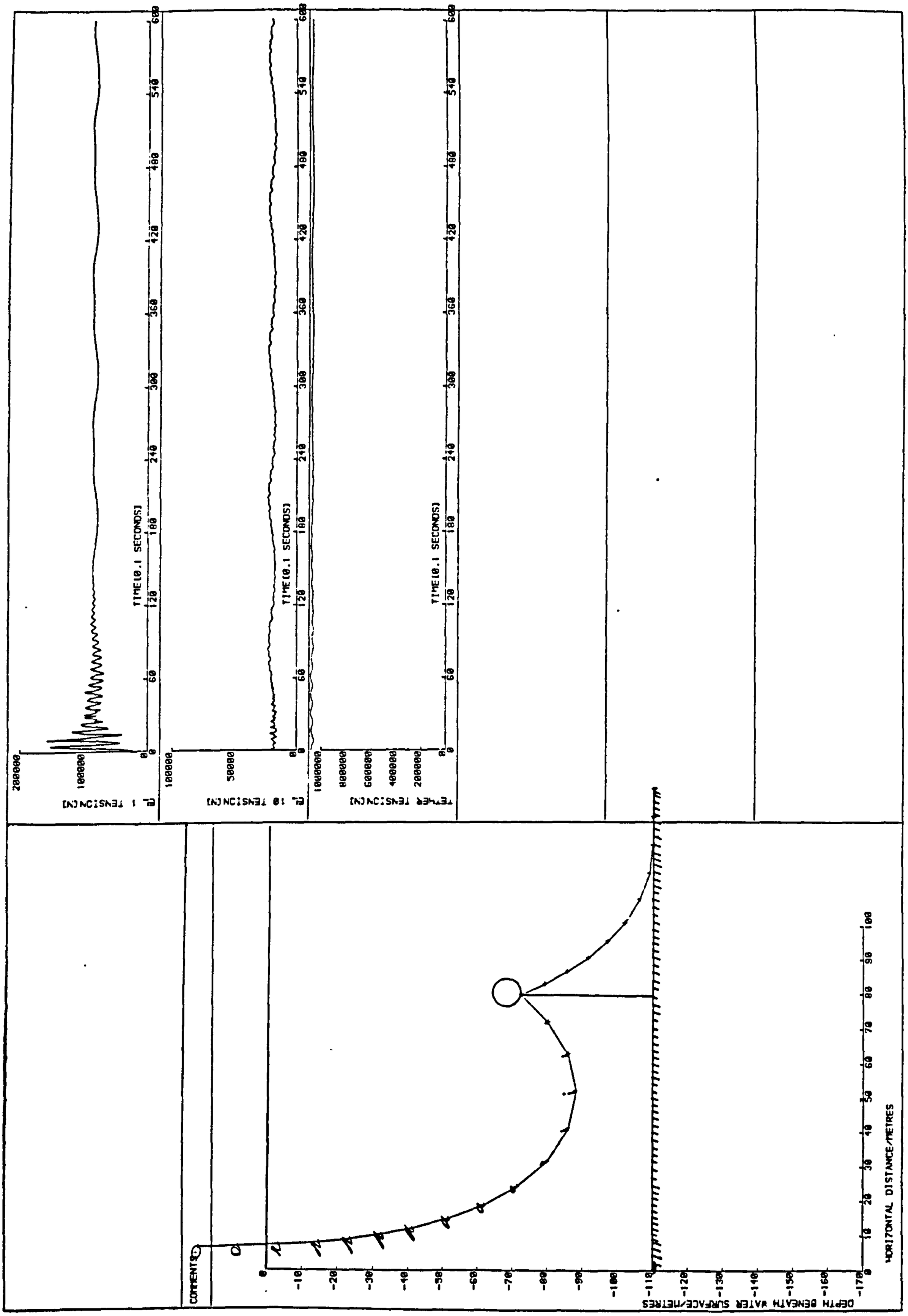

Figure 5.2.3(c): Comparison with Model Tests

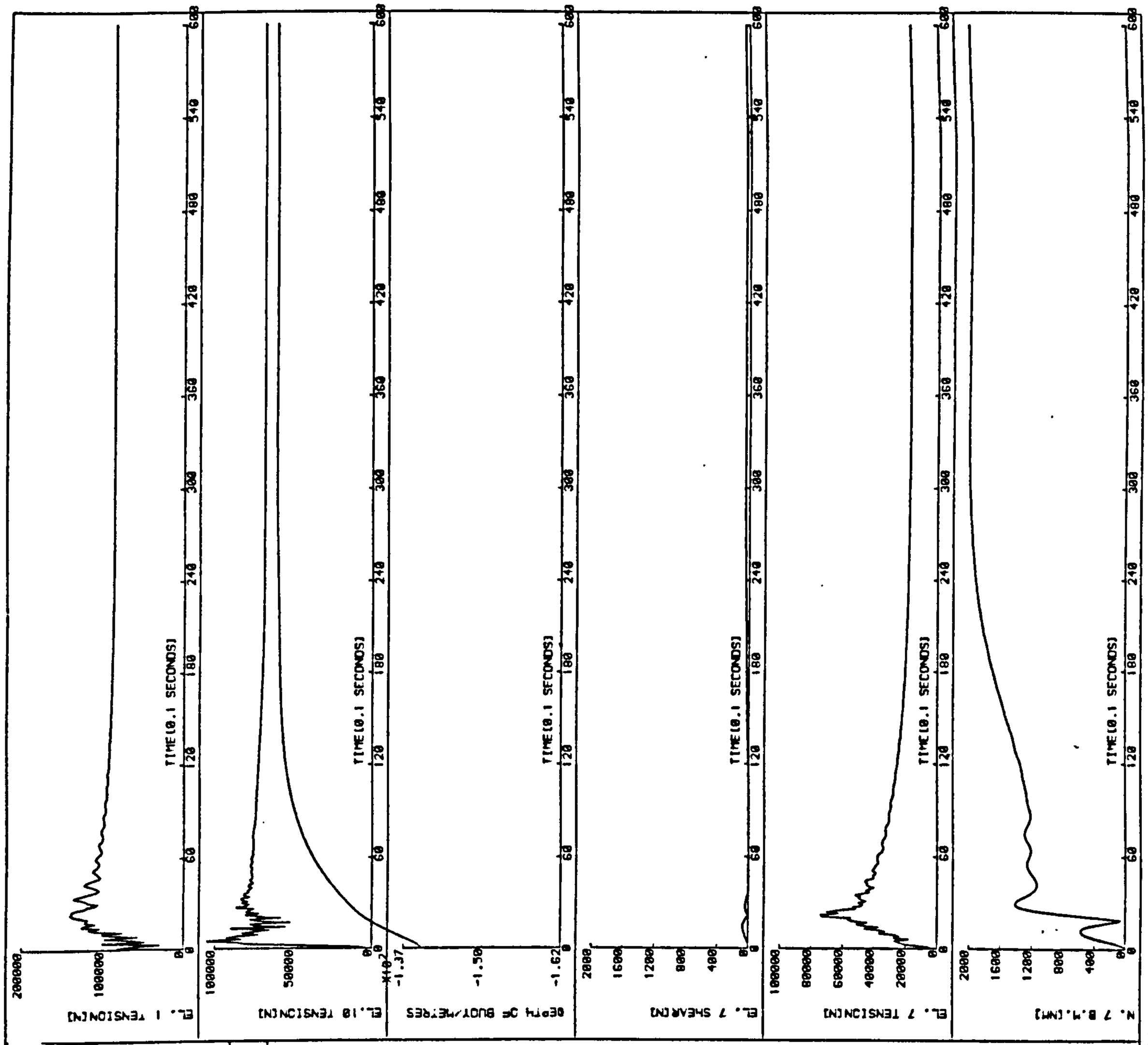

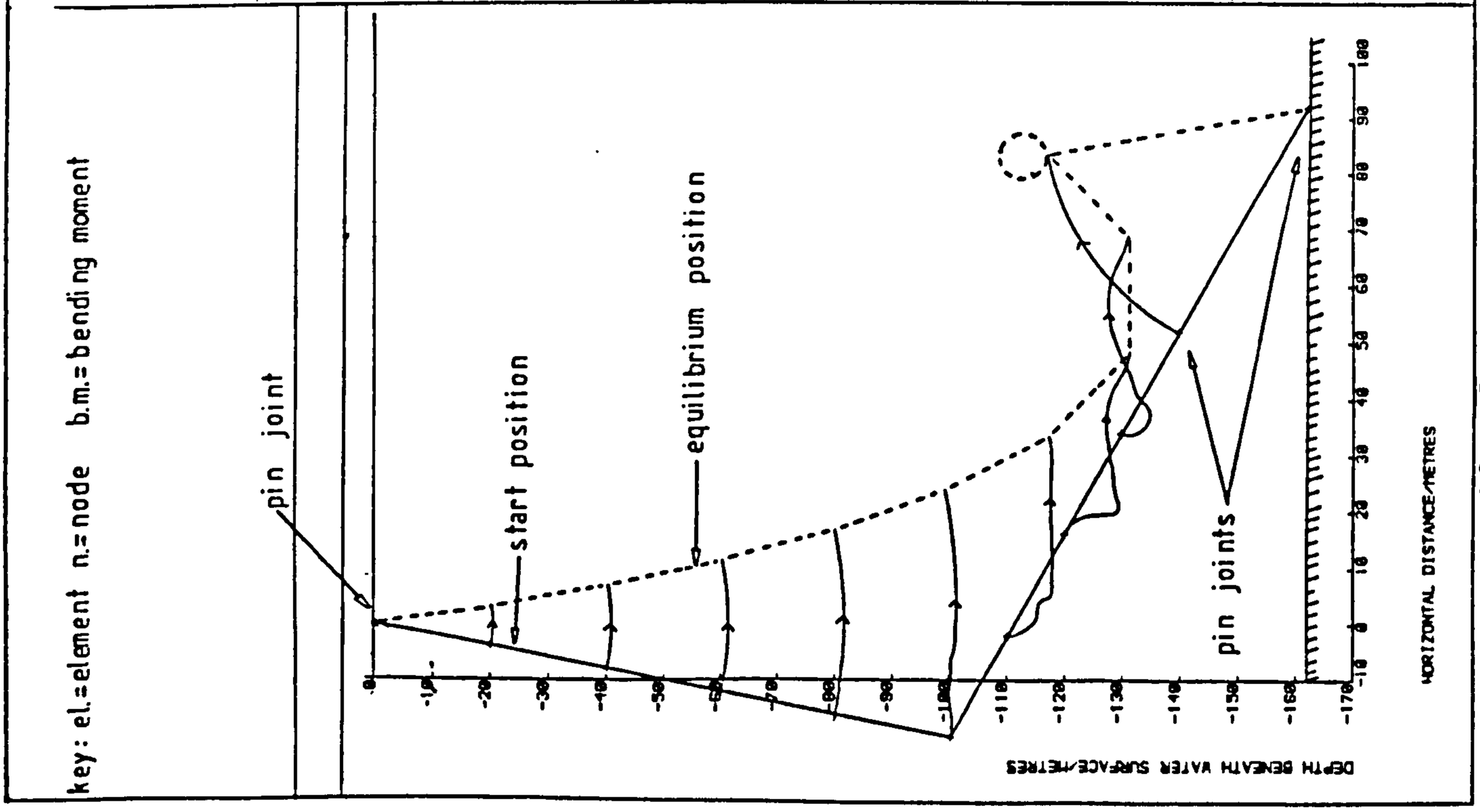

Figure 5.3 (a): The Effect of Bending Stiffness

key: el. = element n. = node b.m. = bending moment

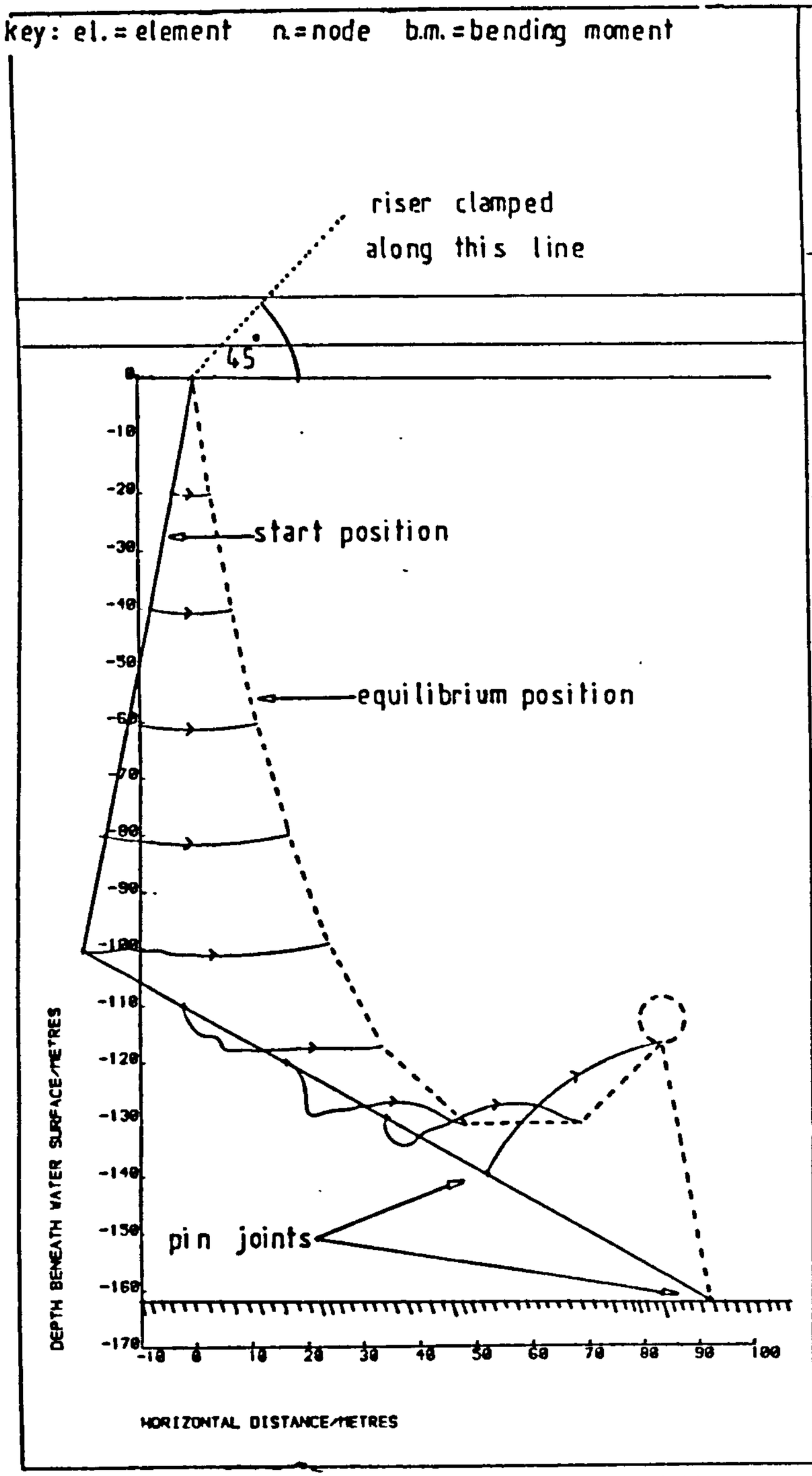

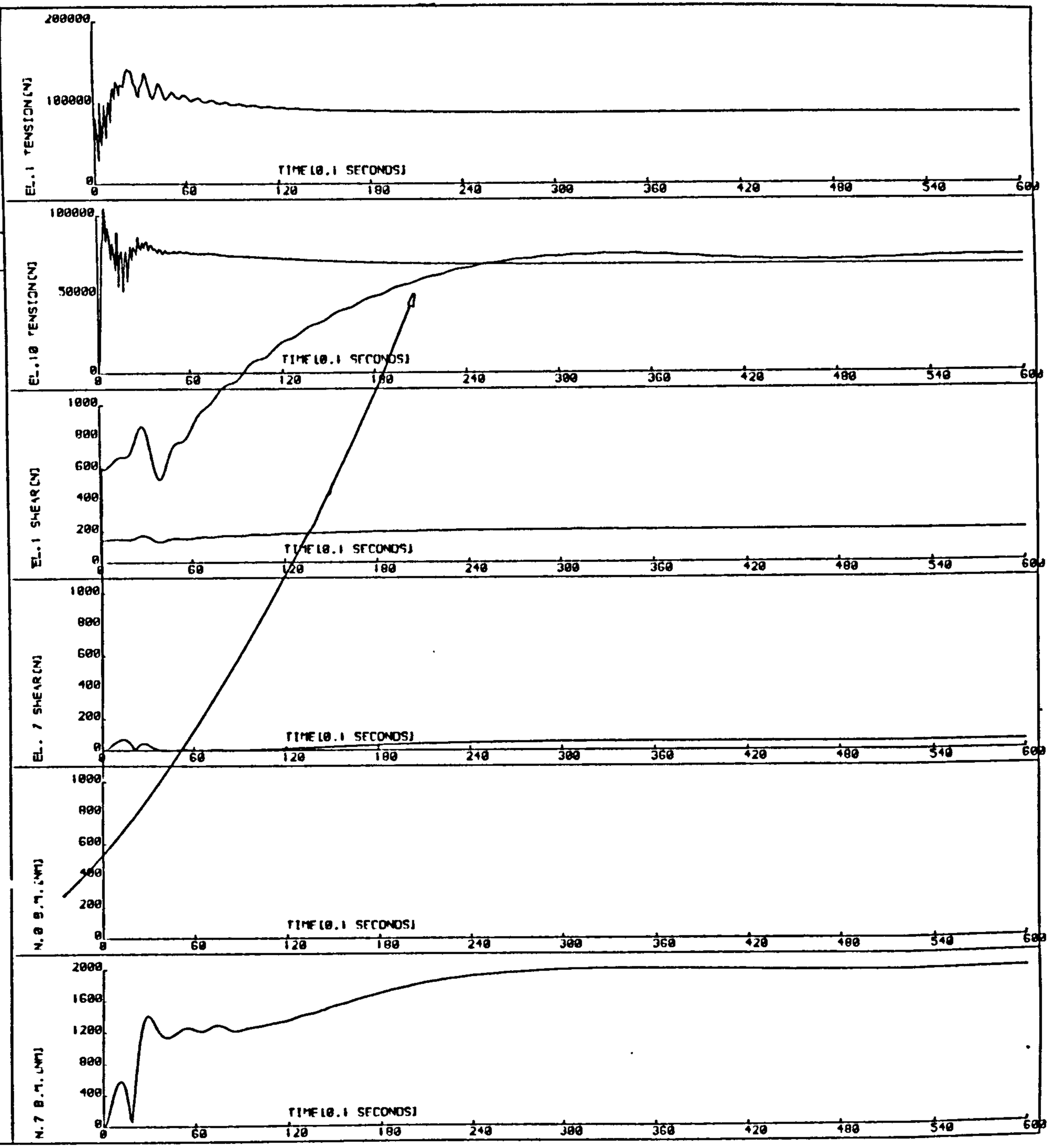

Figure 5.3(b): The Effect of Bending Stiffness

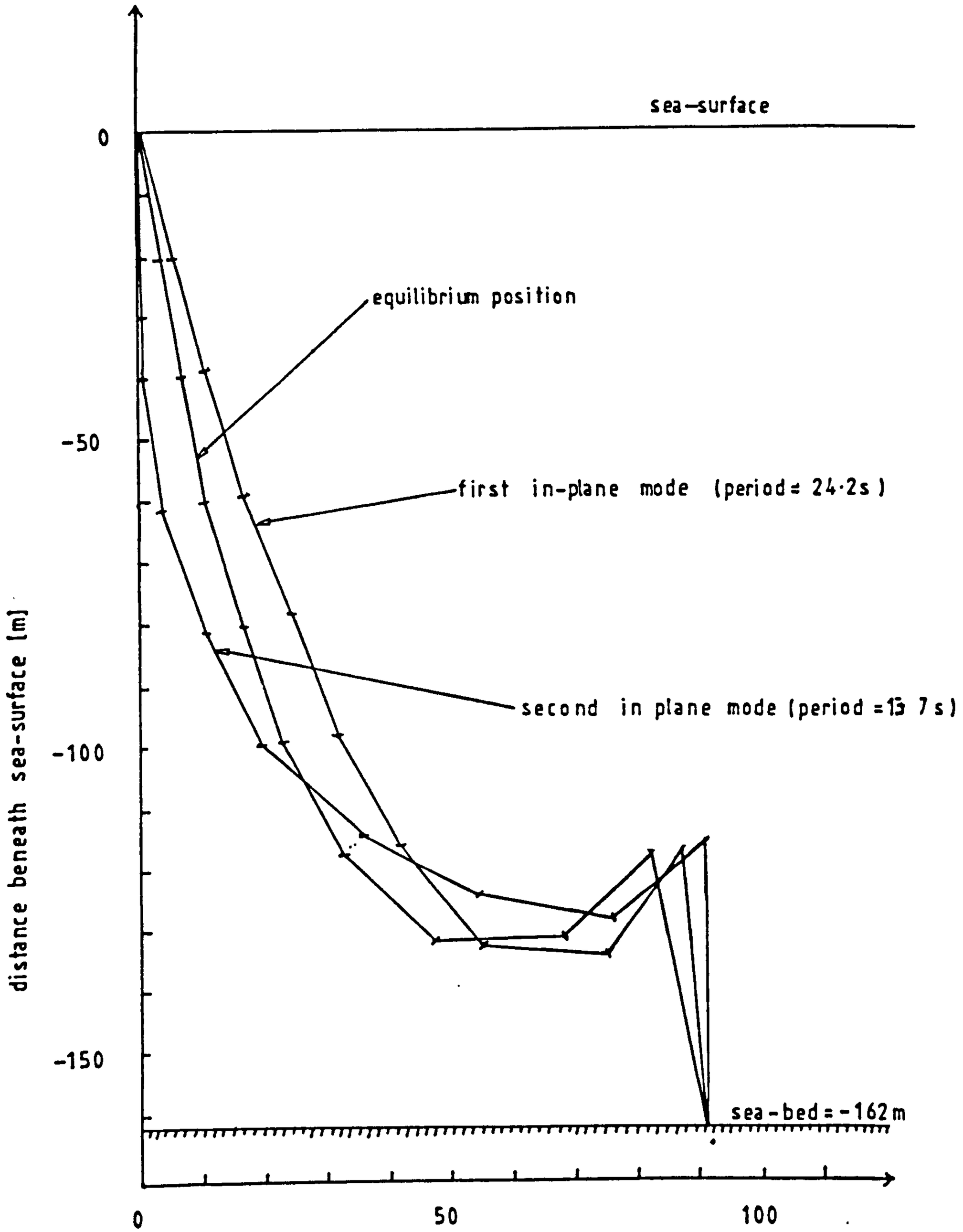

Figure 5·4·3(a): First Two In plane Modes

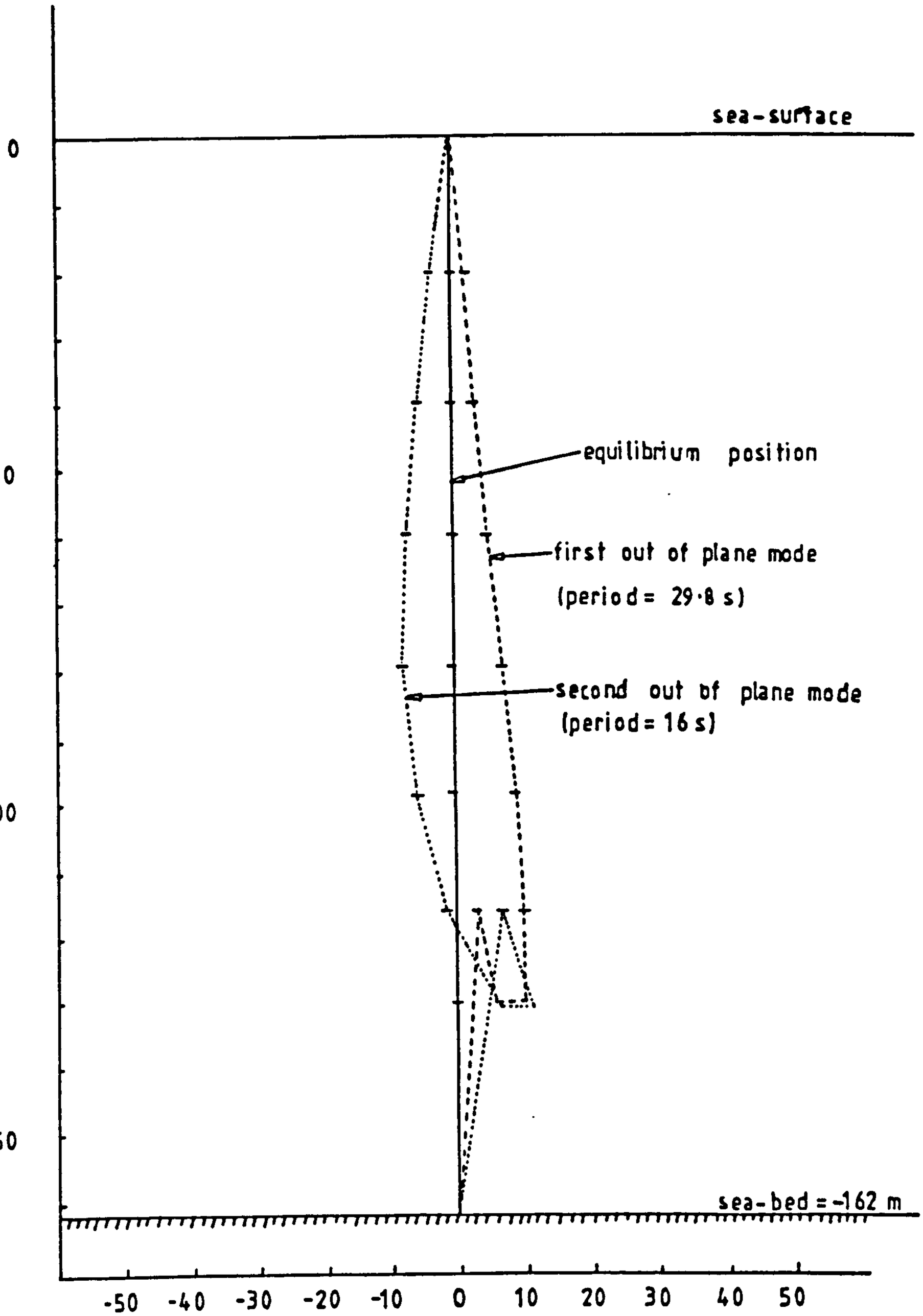

Figure 5·4·3 (b): First Two Out of Plane Modes

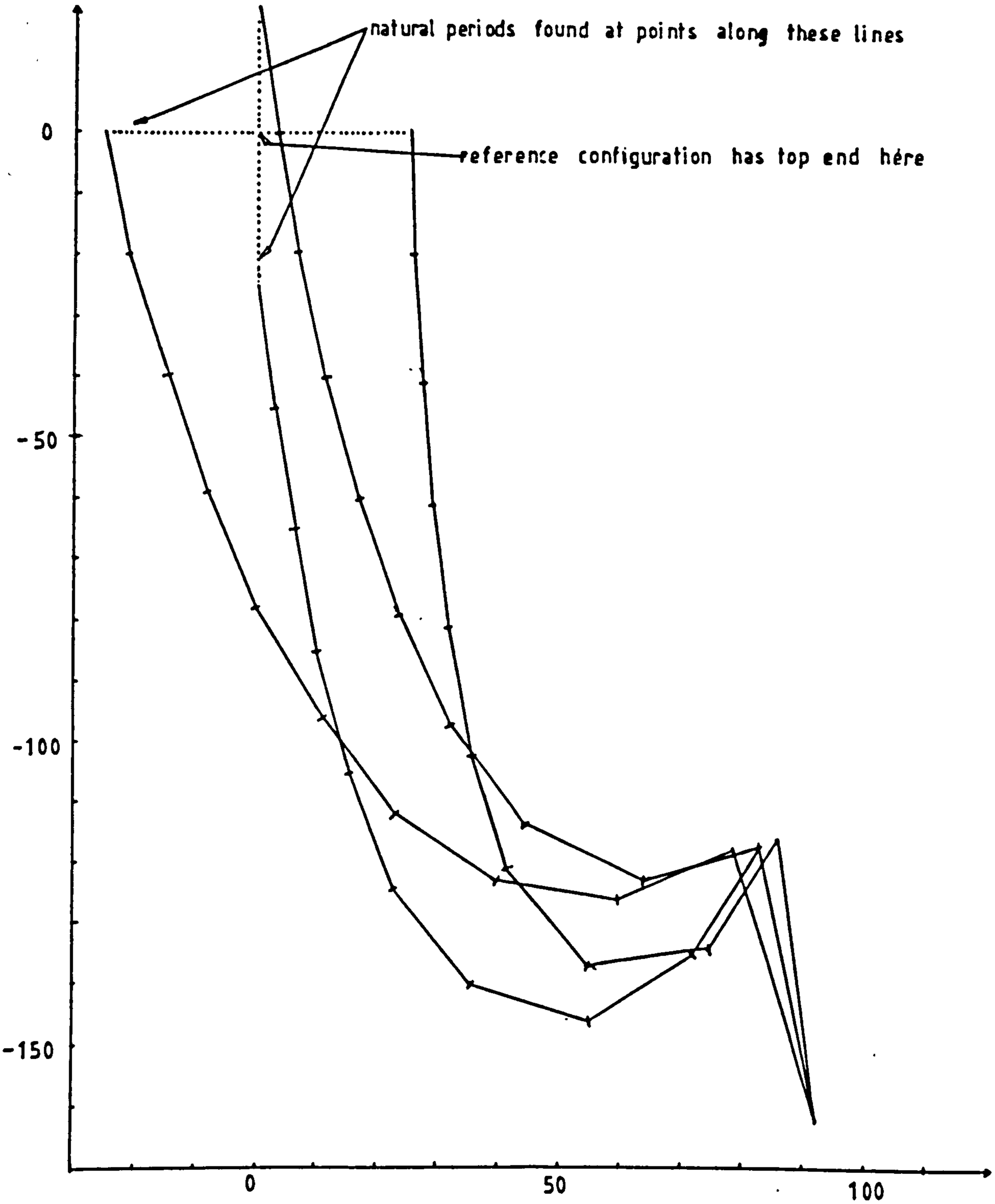

Figure 5.4.3.1 (a): Configurations for which the natural periods are found

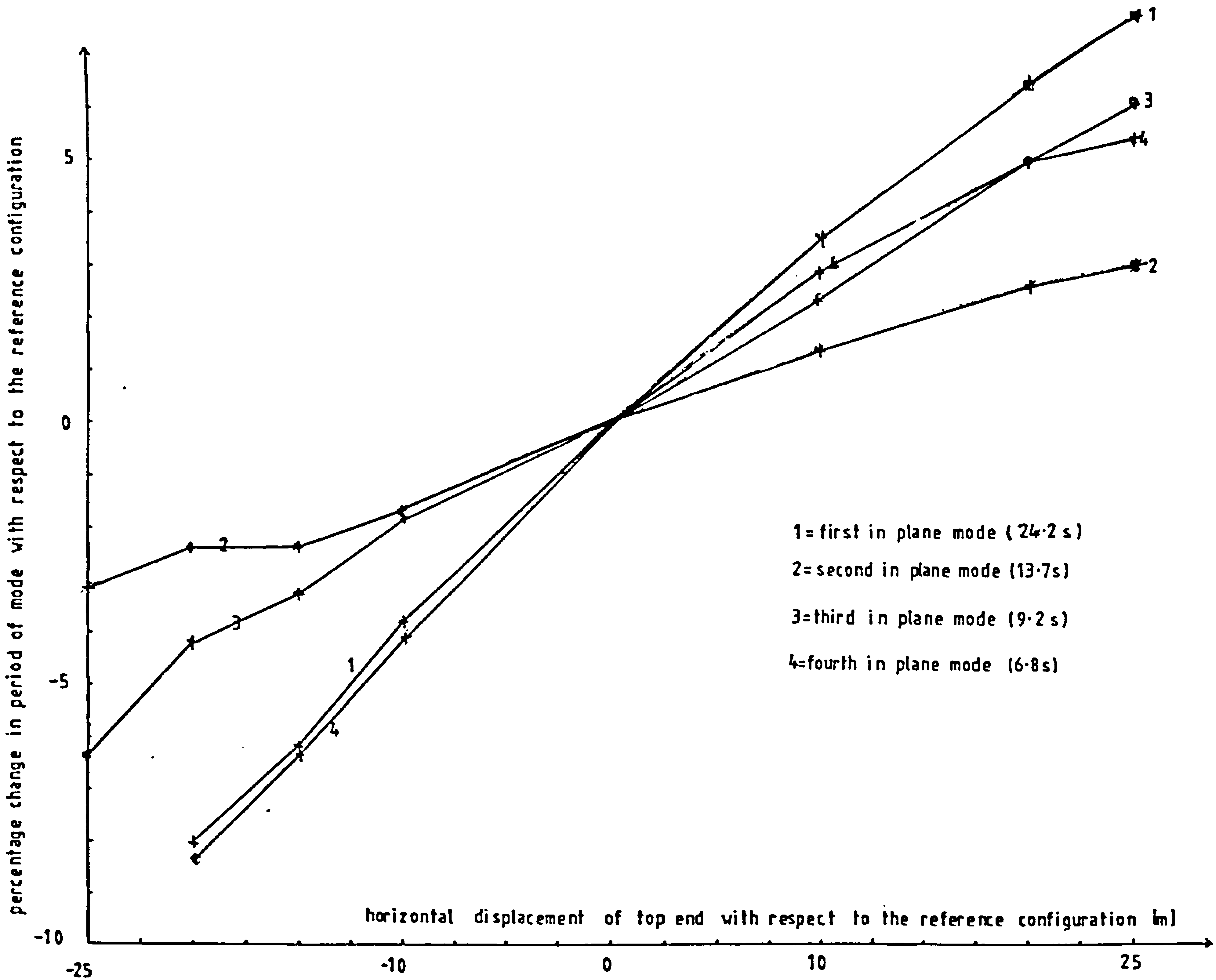

Figure 5.4.3.1 (b): Variation of In Plane Periods with Horizontal Displacement

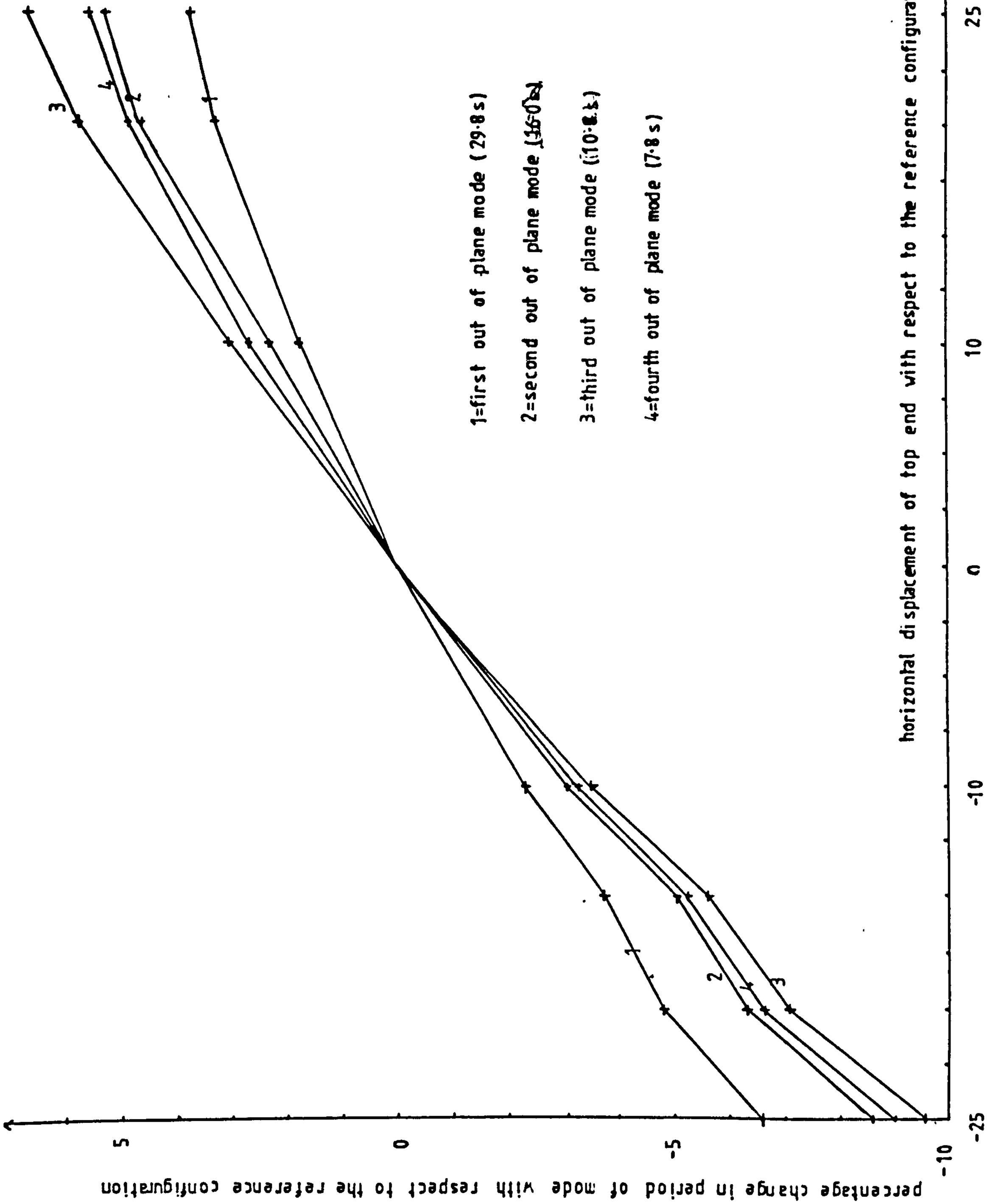

Figure 5.4.3.1 (c): Variation of

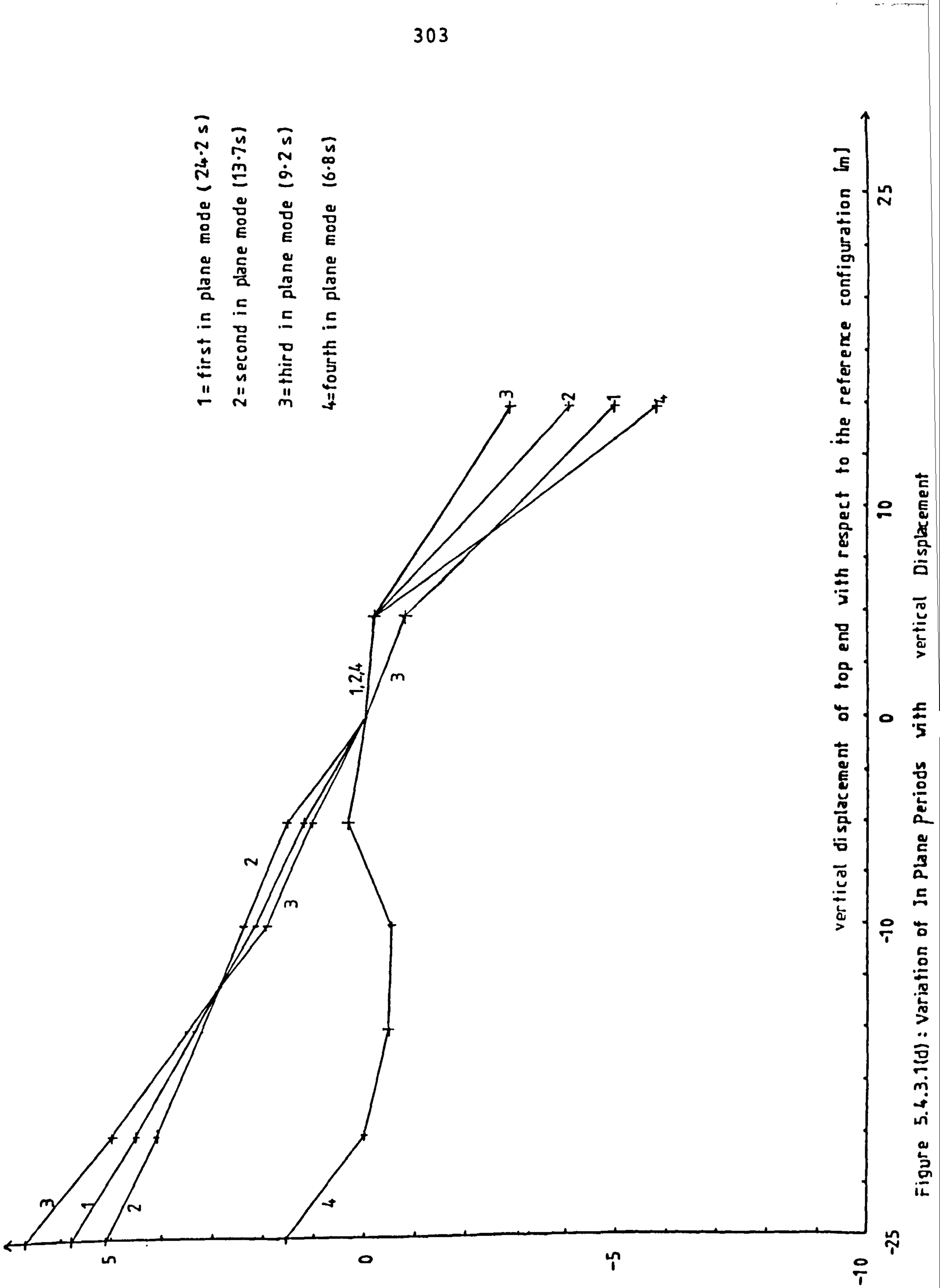

Figure 5.4.3.1(d) : Variation of In Plane Periods with vertical Displacement

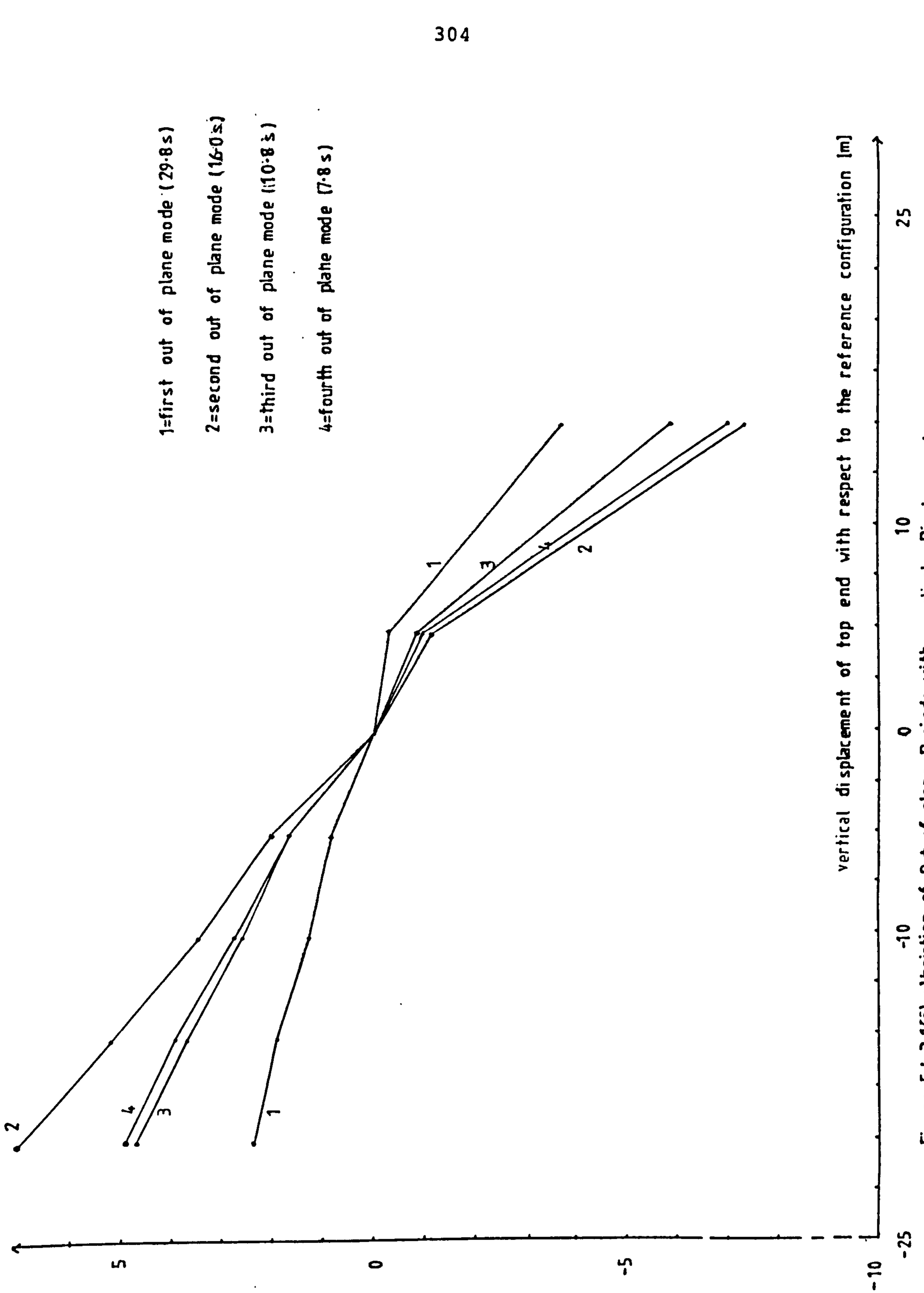

Figure 5.4.3.1(e) : Variation of

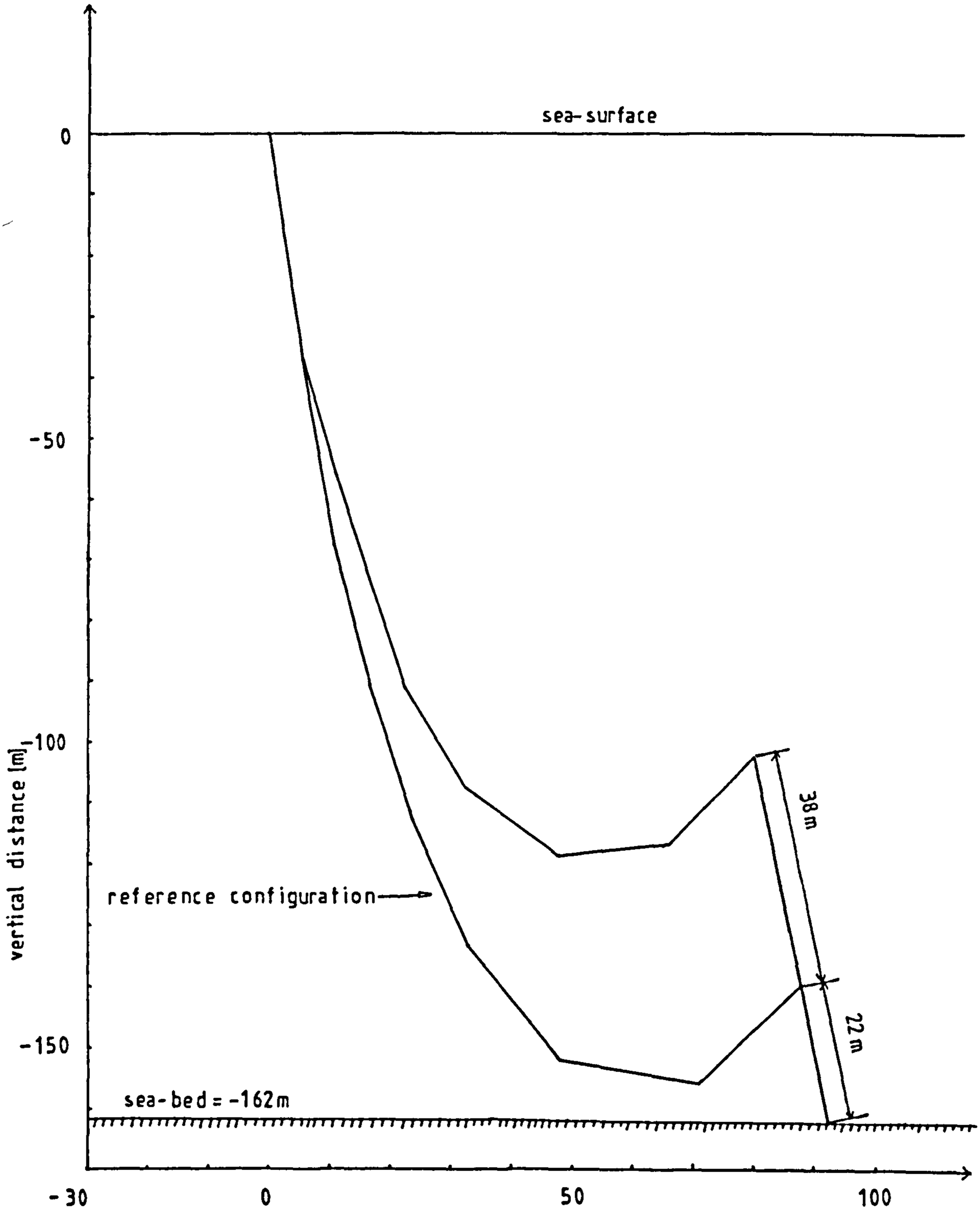

Figure 5.4.3.2 (a): Varying the Position of the Buoy

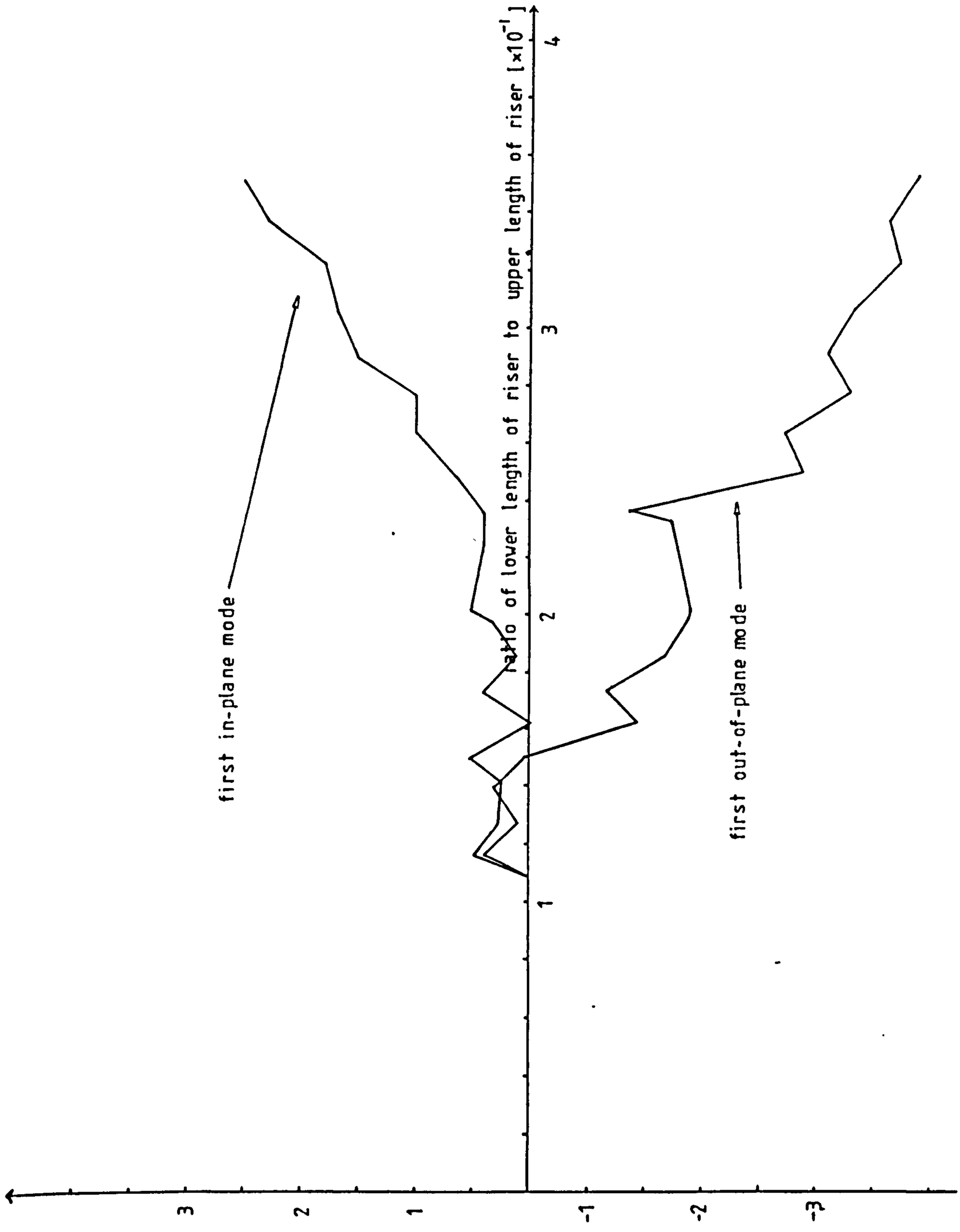

Figure 5.4.3.2 (b): The Effect of the Position of the Buoy on the First Two Modes

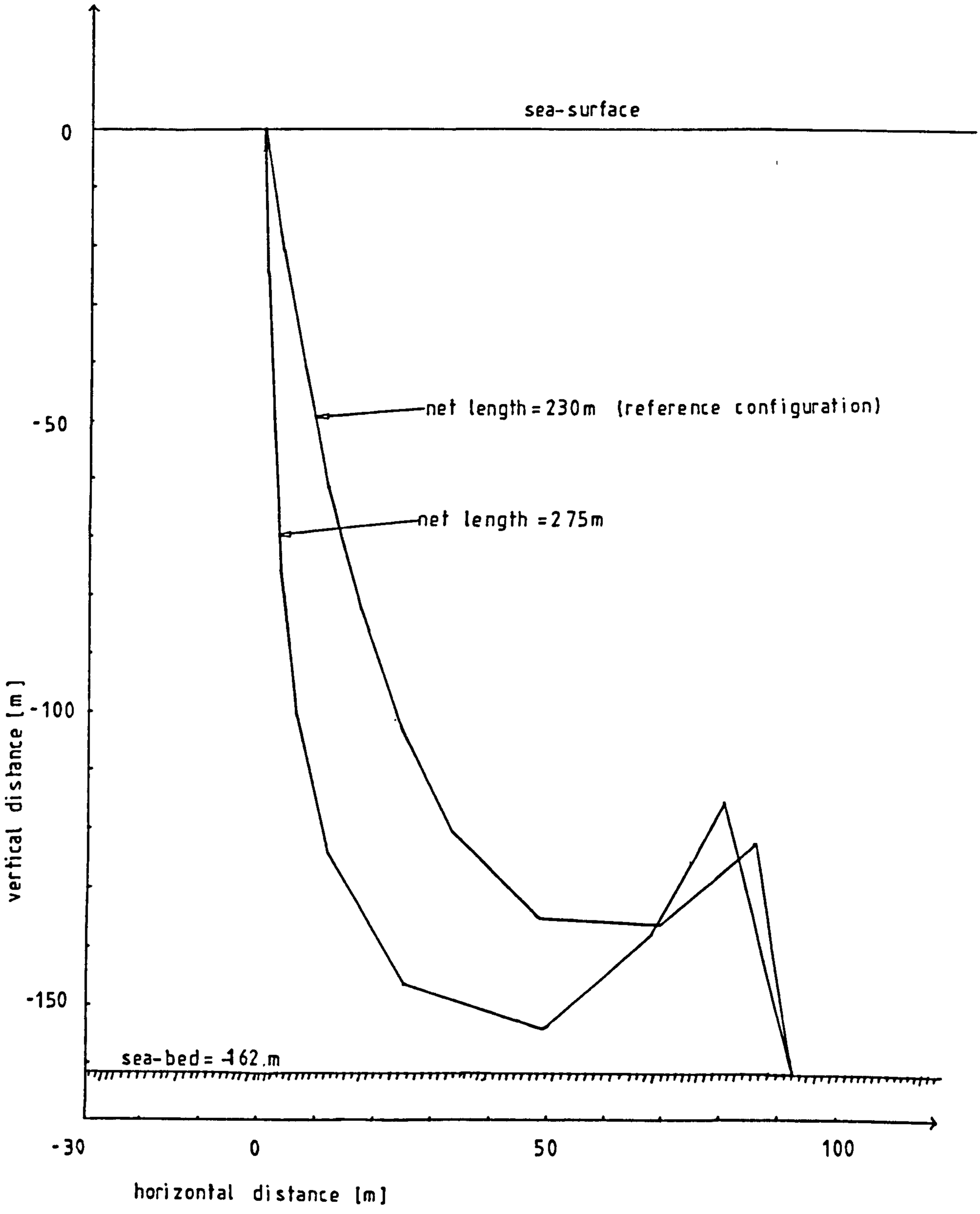

Figure 5.4.3.3 (a) : Varying the length of the Riser

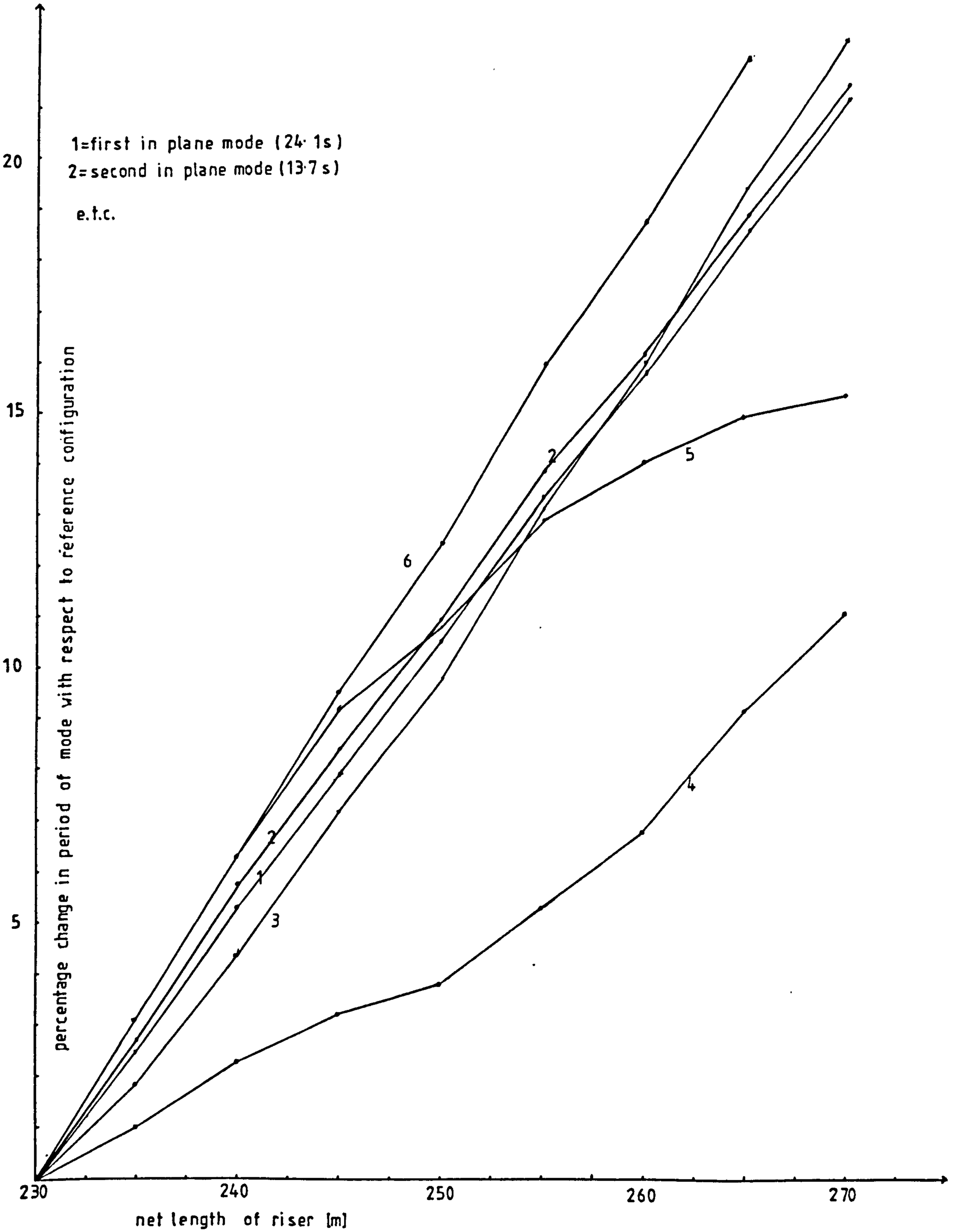

Figure 5.4.3.3 (b): The Effect of varying the length of the Riser

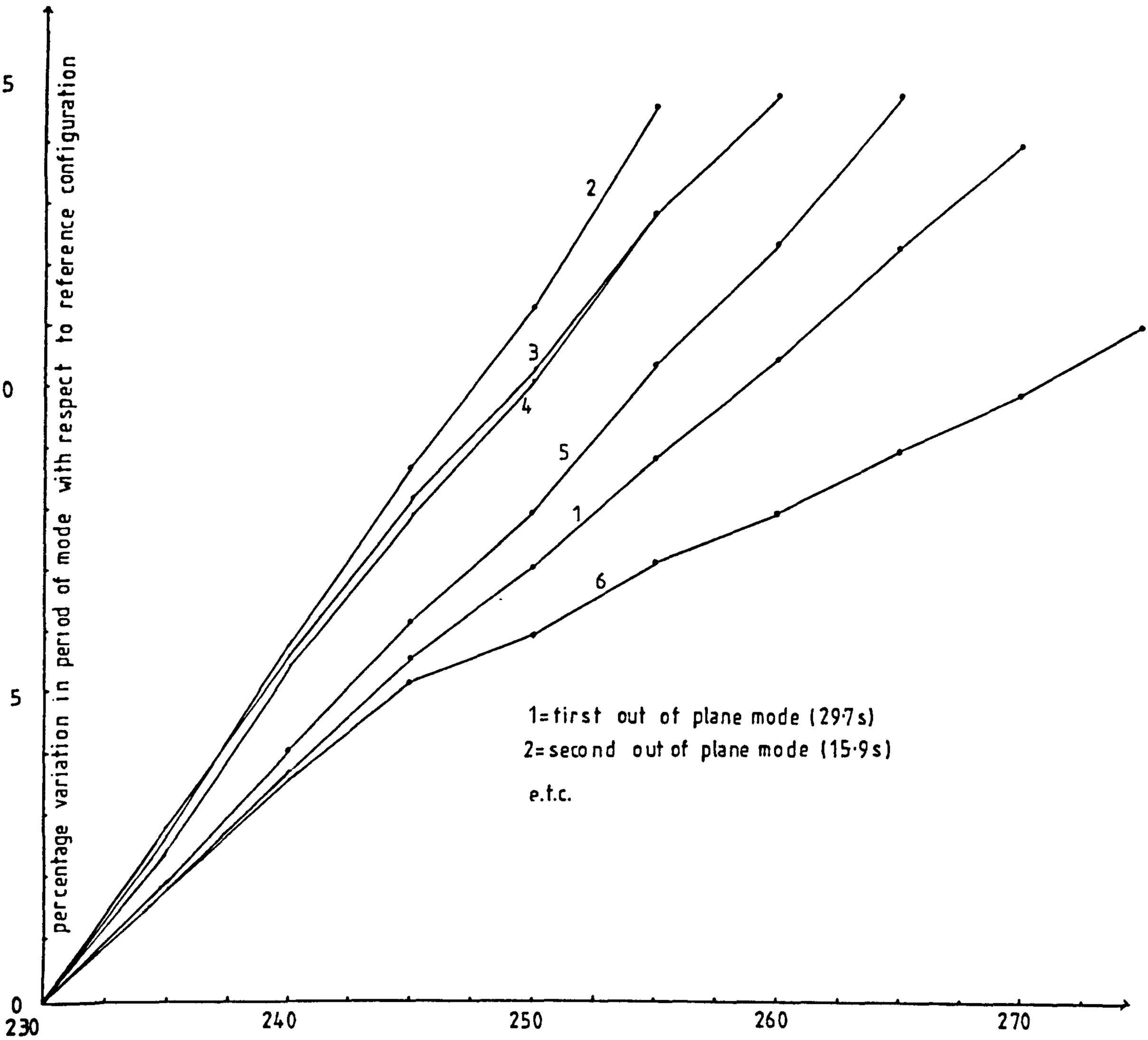

Figure 5.4.3.3(c): The Effect of varying the length of the Riser

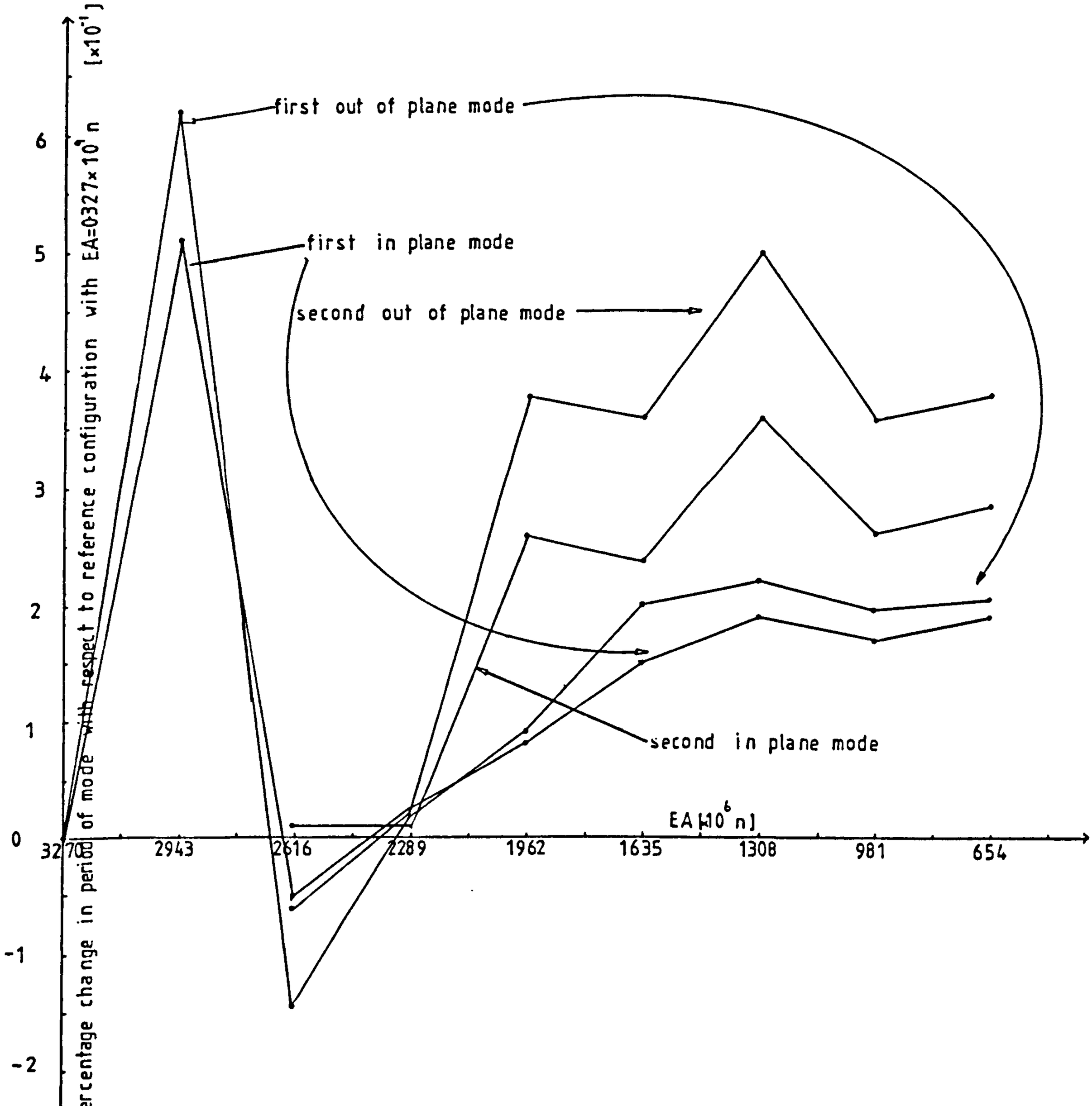

Figure 5.4.3.4 (a): The Effect of varying EA

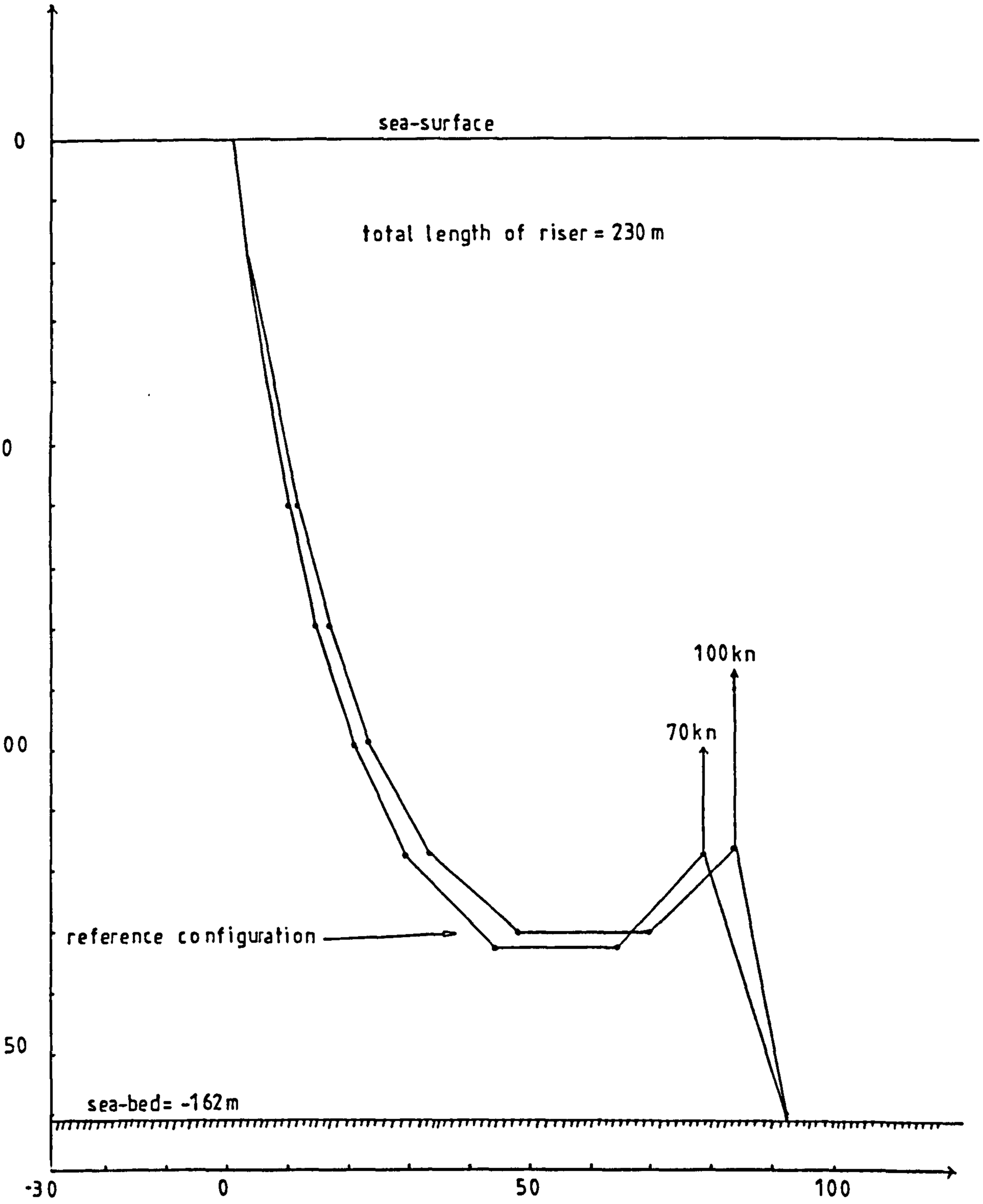

Figure 5.4.3.5 (a): Varying the Buoyancy of the Buoy

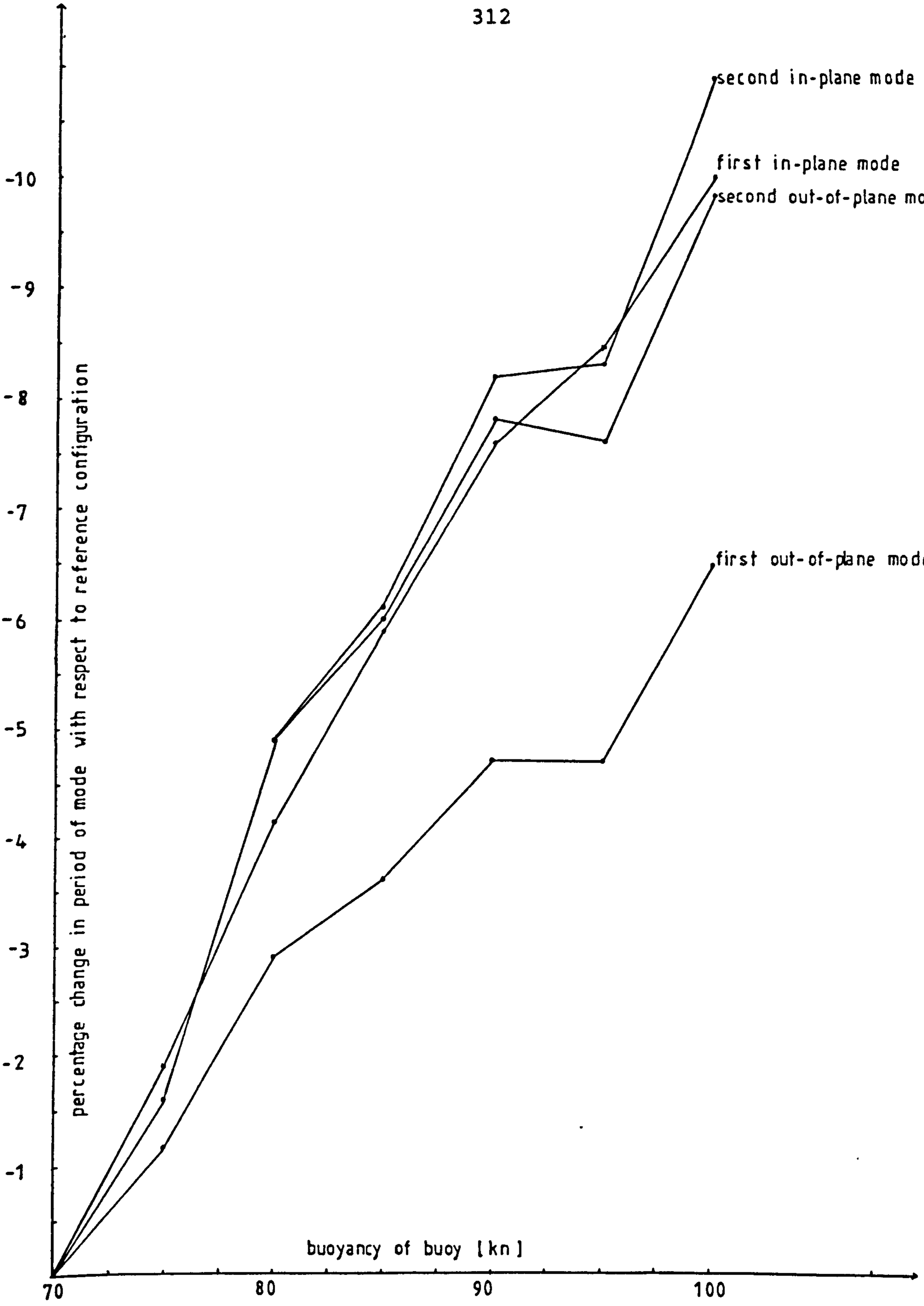

Figure 5.4.3.5(b) :The Effect of varying the Buoyancy of the Buoy

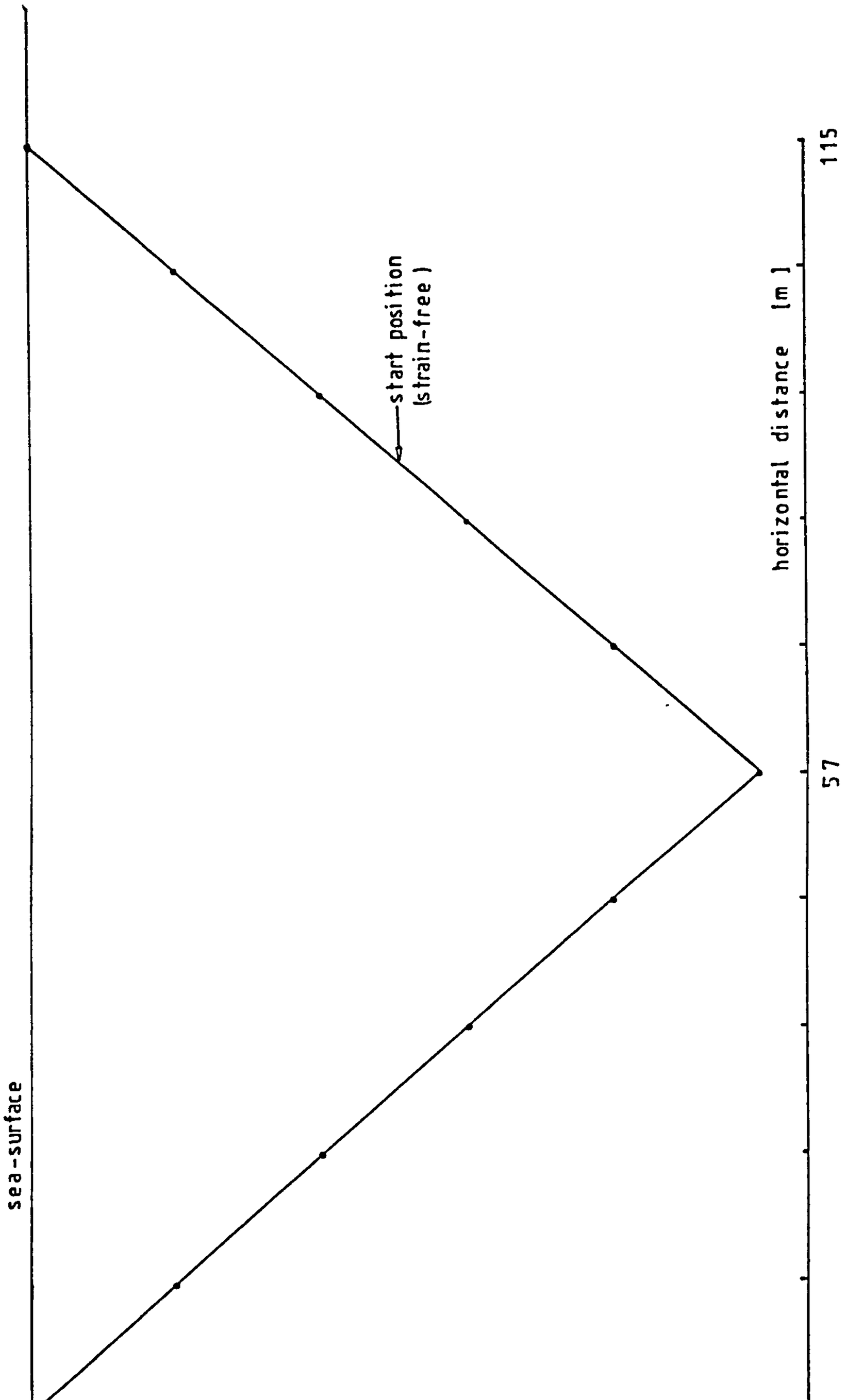

Figure 5.5 (a) : Start Position

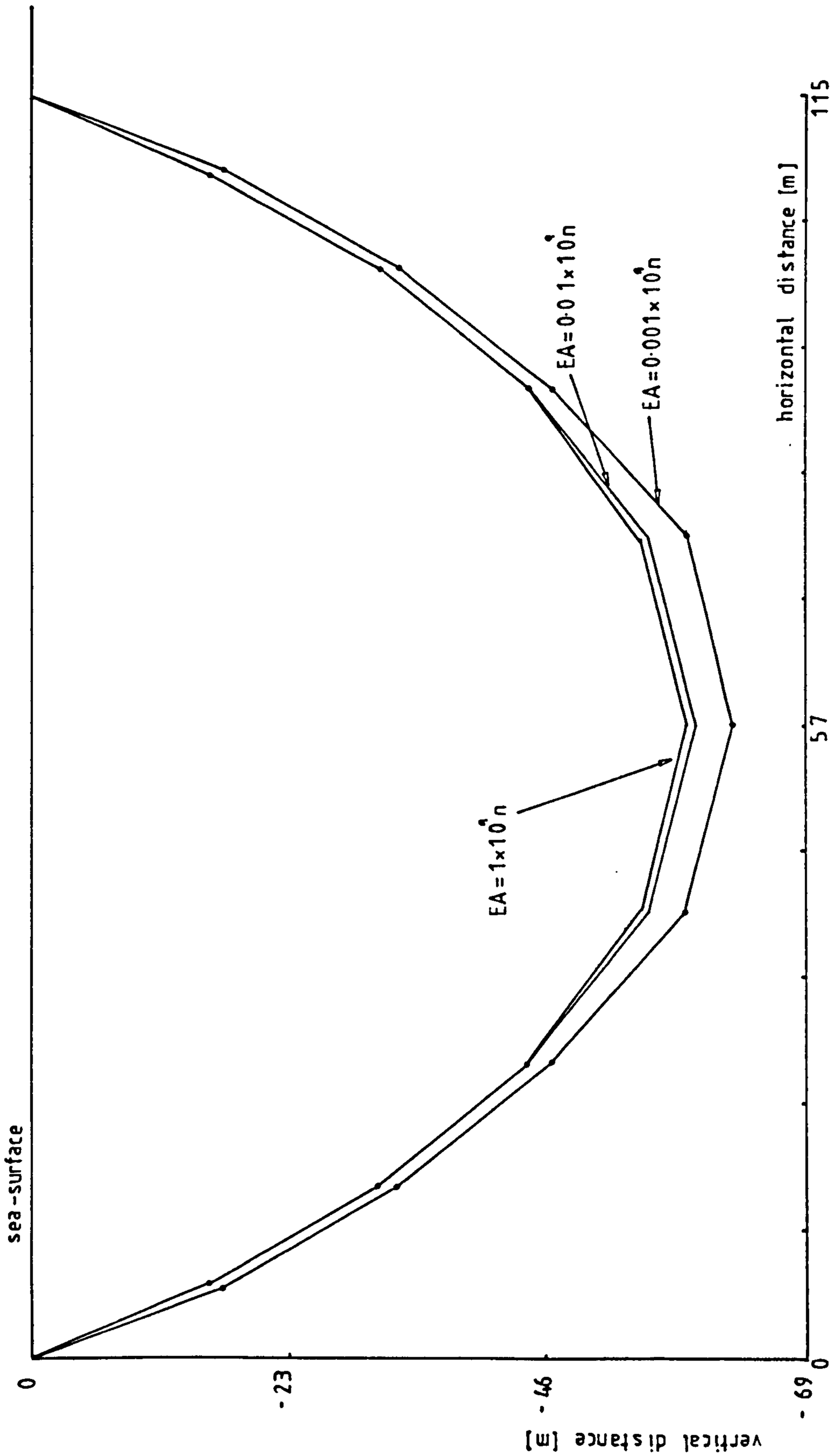

Figure 5.5(b): Equilibrium Positions for different values of EA

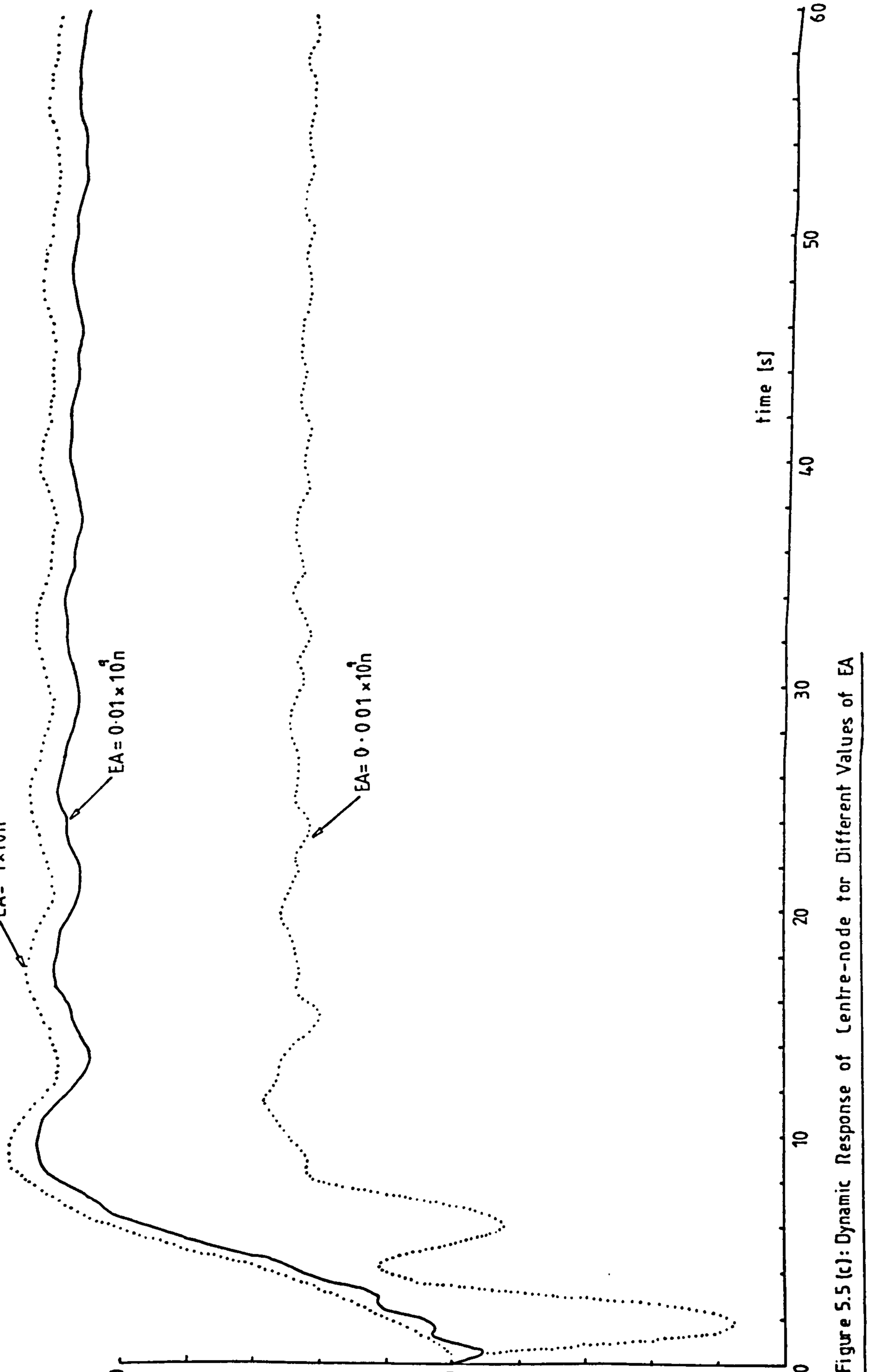

Figure 5.5 (c): Dynamic Response of Centre-node for Different Values of EA

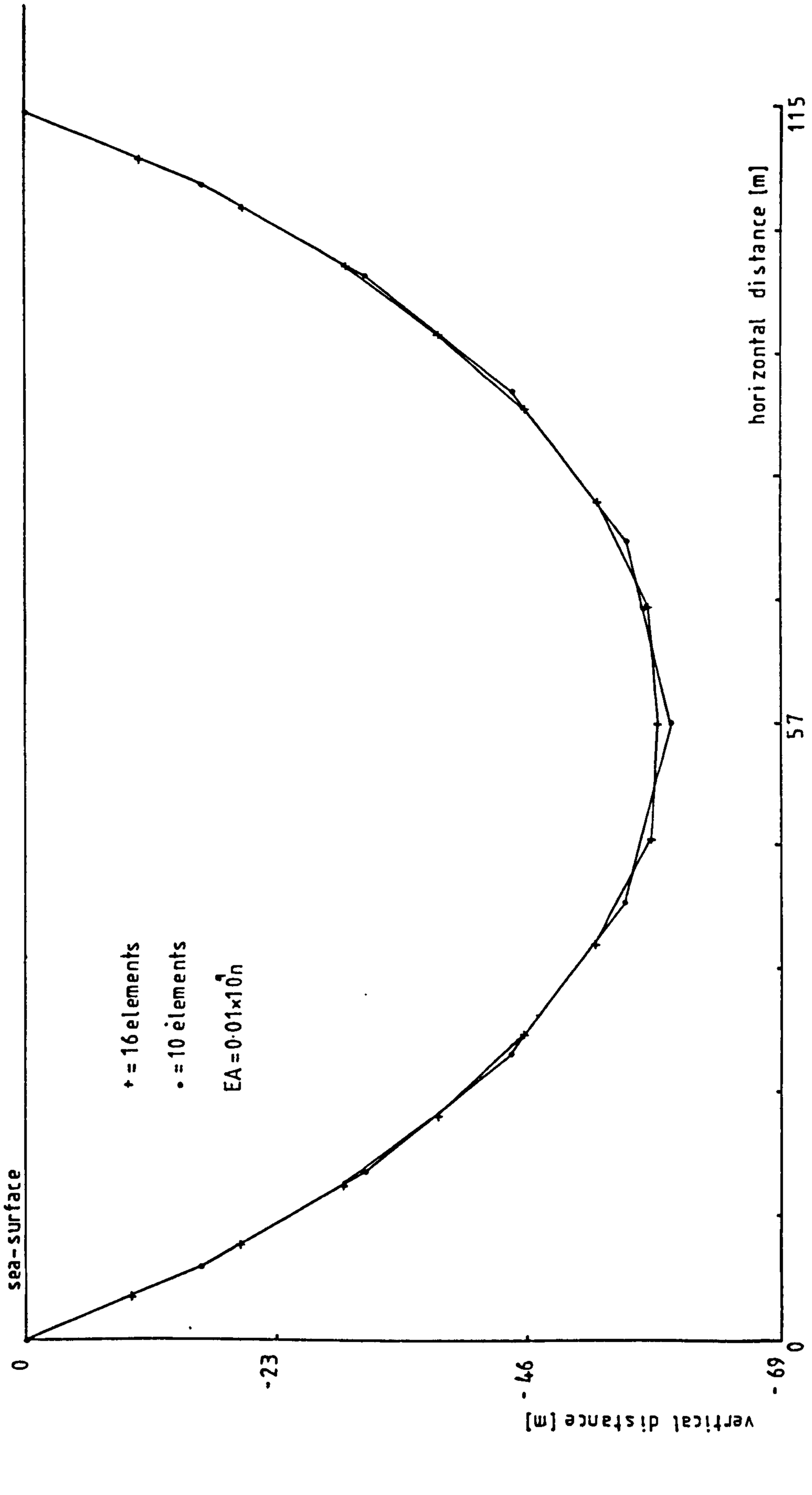

Figure 5.6 (a): The Effect of the Number of Elements on the Equi

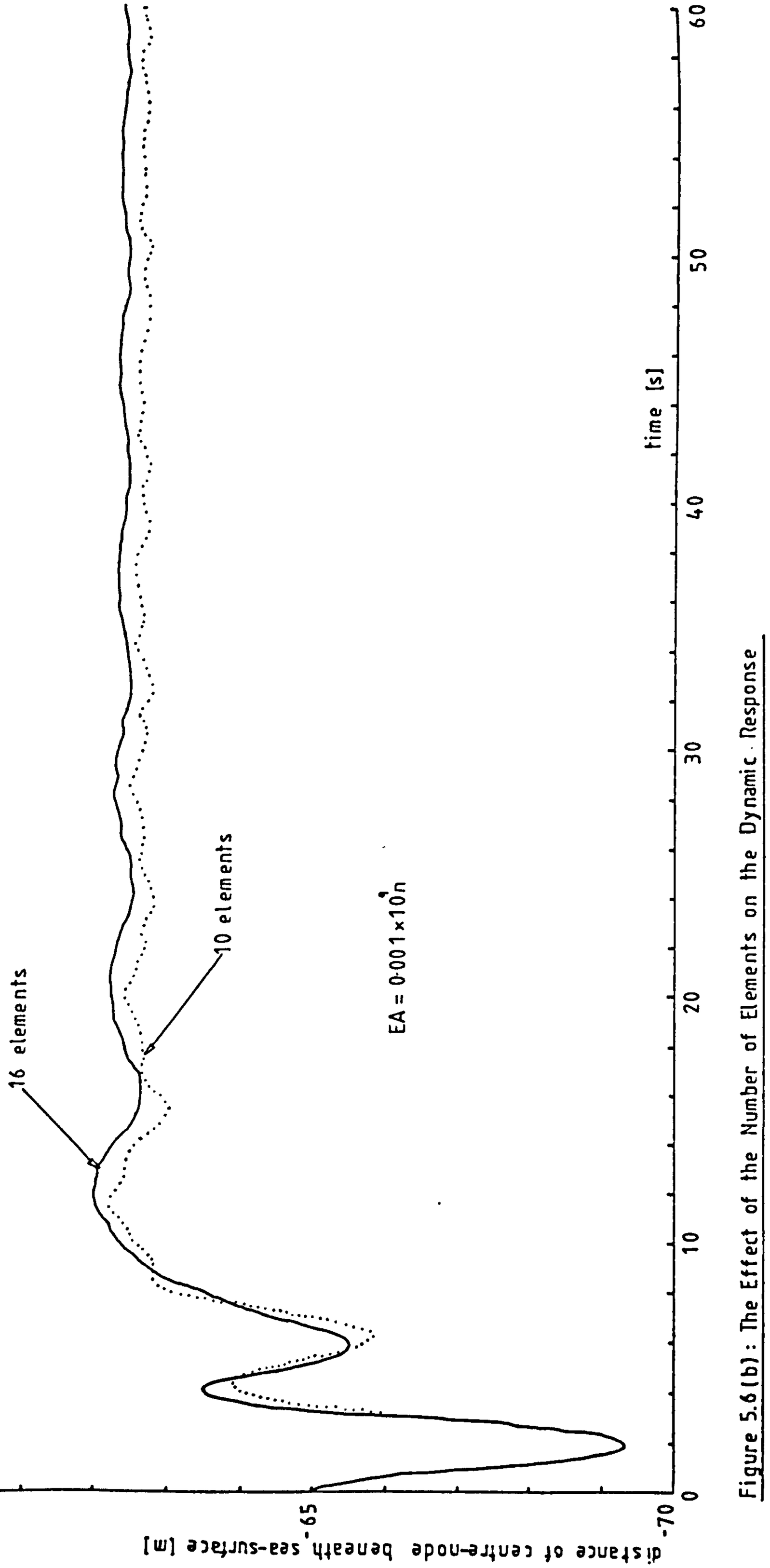

Figure 5.6(b): The Effect of the Number of Elements on the Dynamic Response

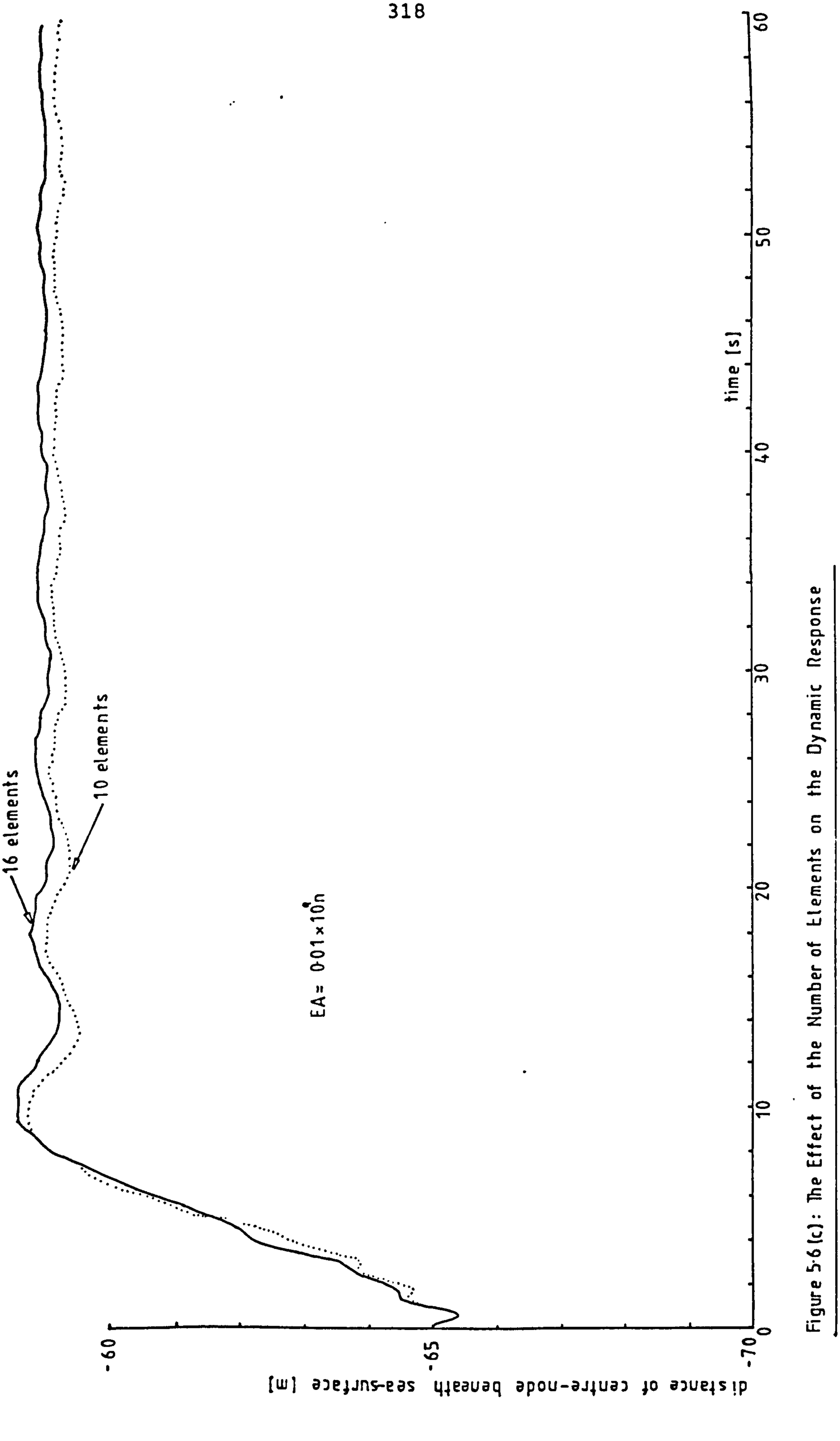

Figure 5·6(c): The Effect of the Number of Elements on the Dynamic Response

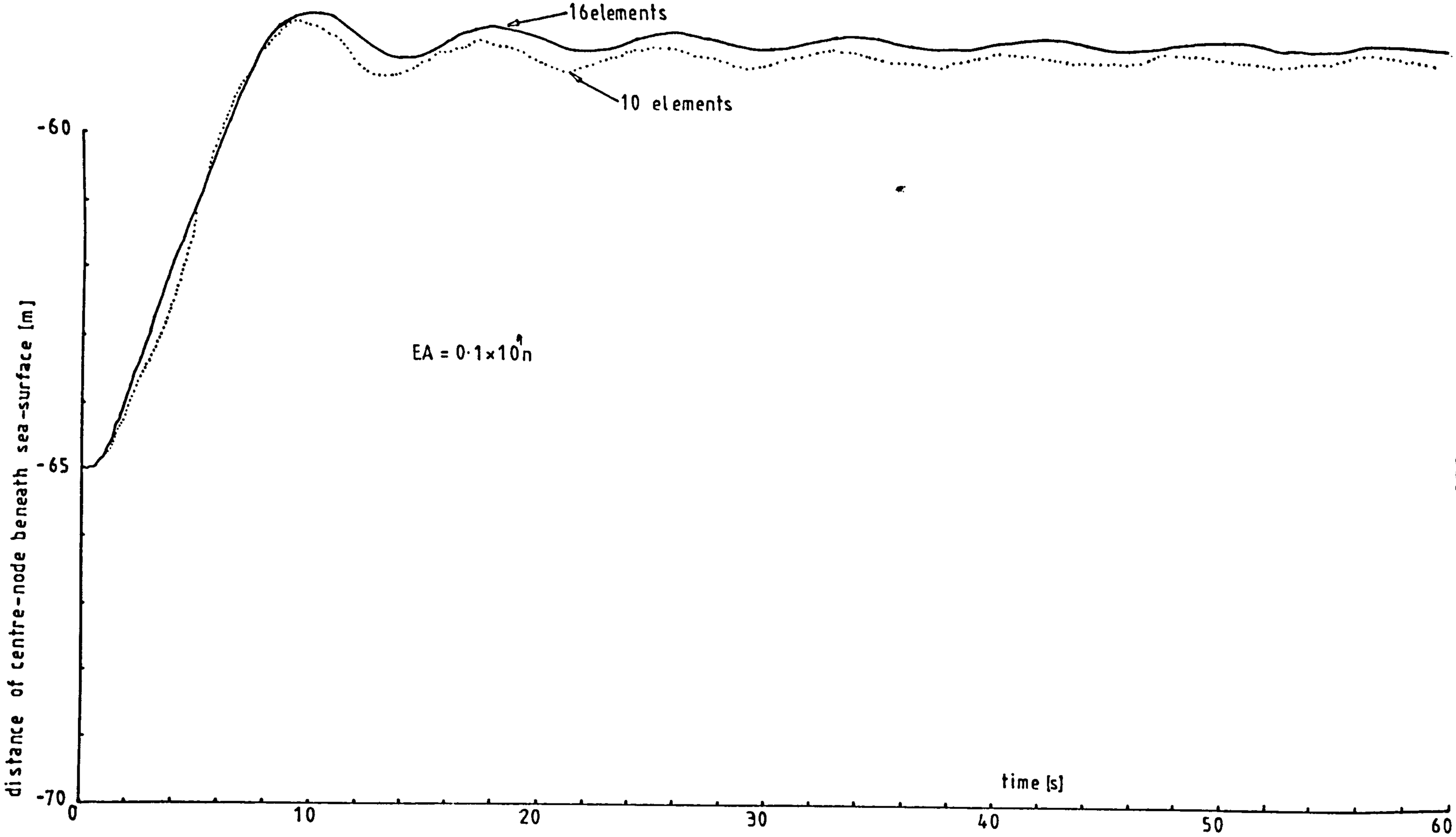

Figure 5·6(d): The Effect of the Number of Elements on the Dynamic Response

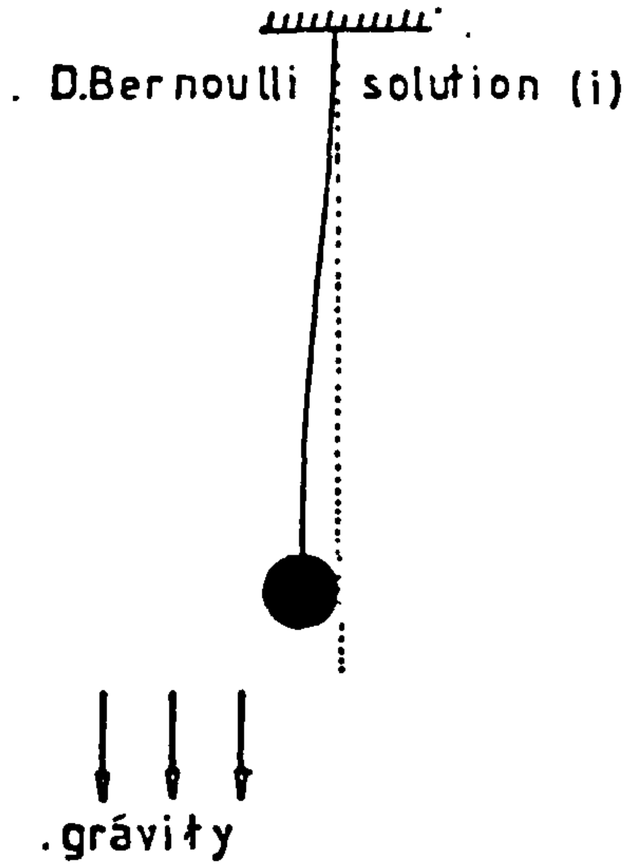

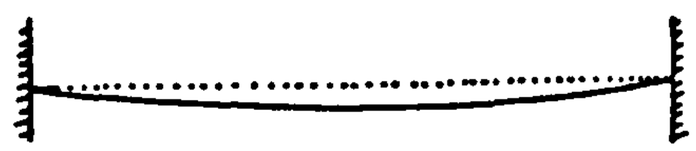

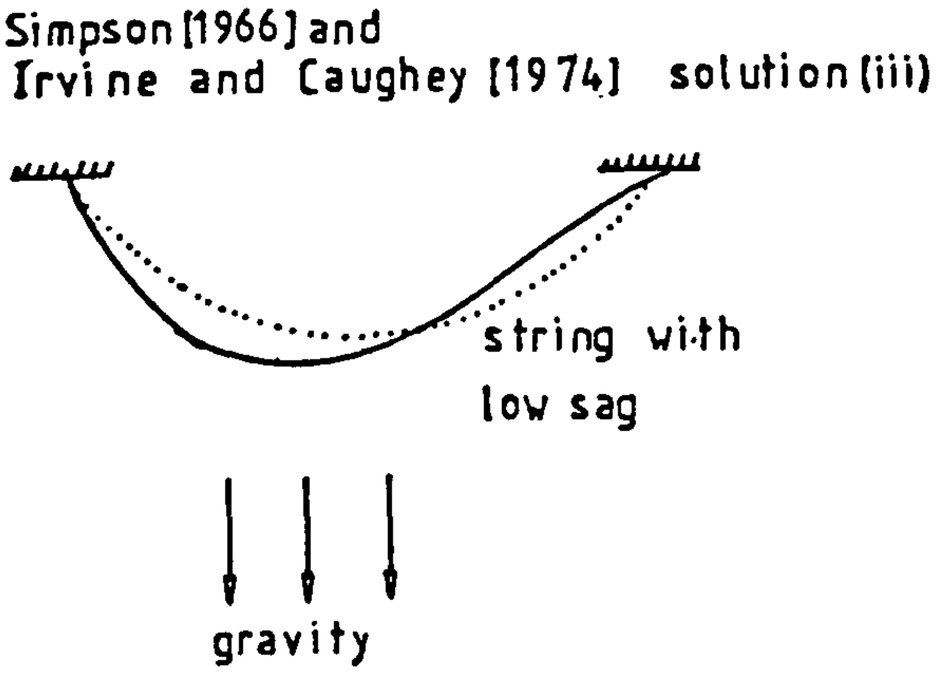

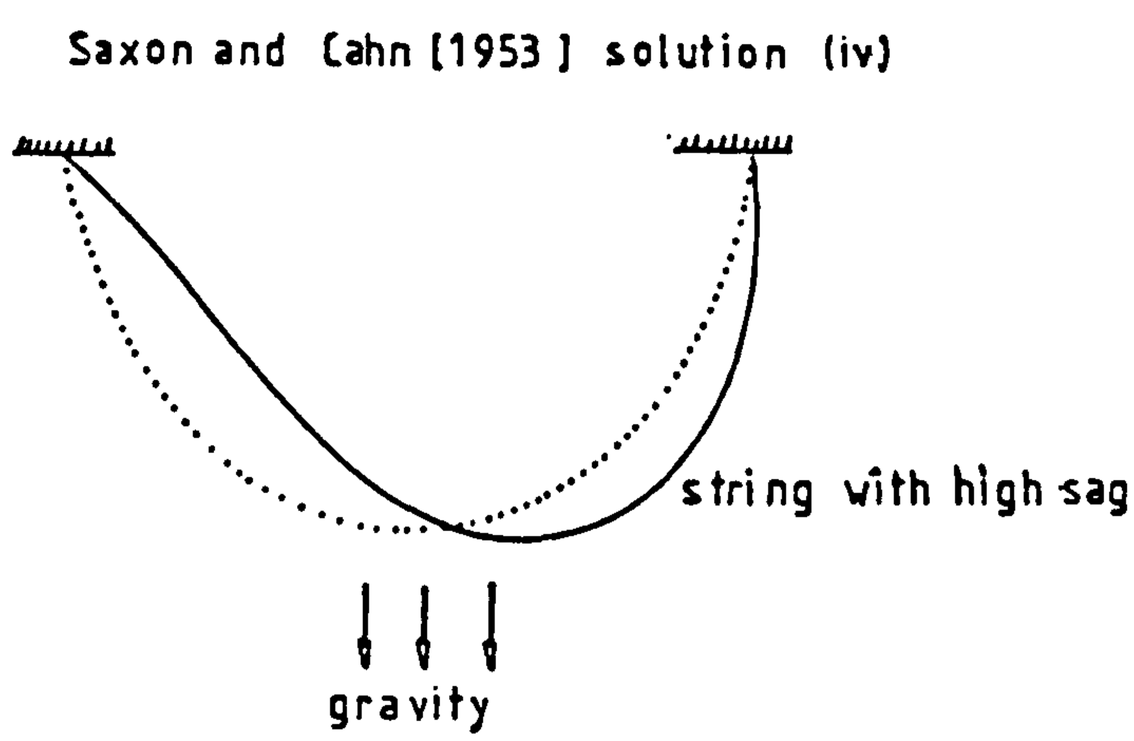

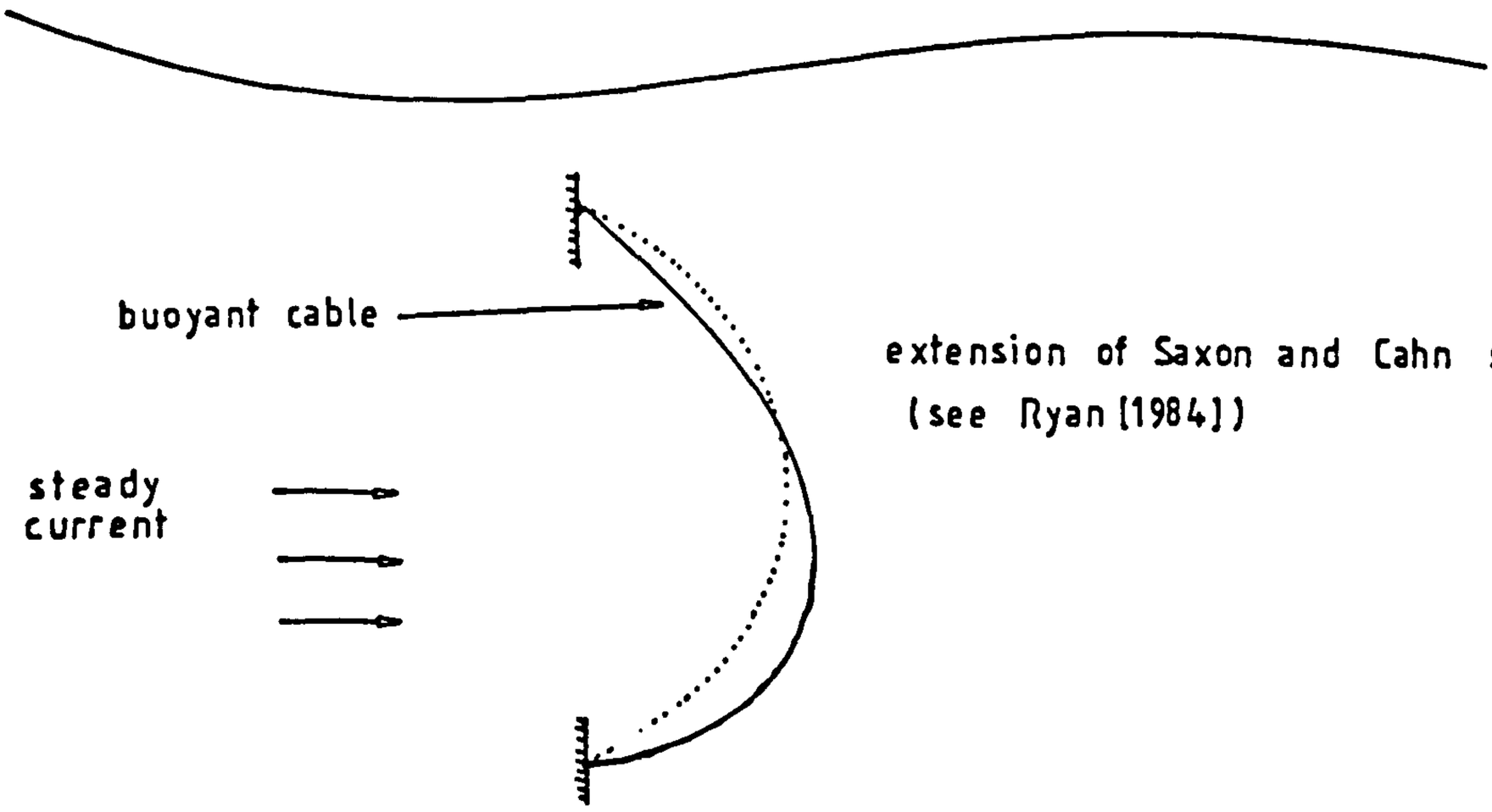

Figure 5.7.1 (a): Analytical Solutions for a Vibrating String

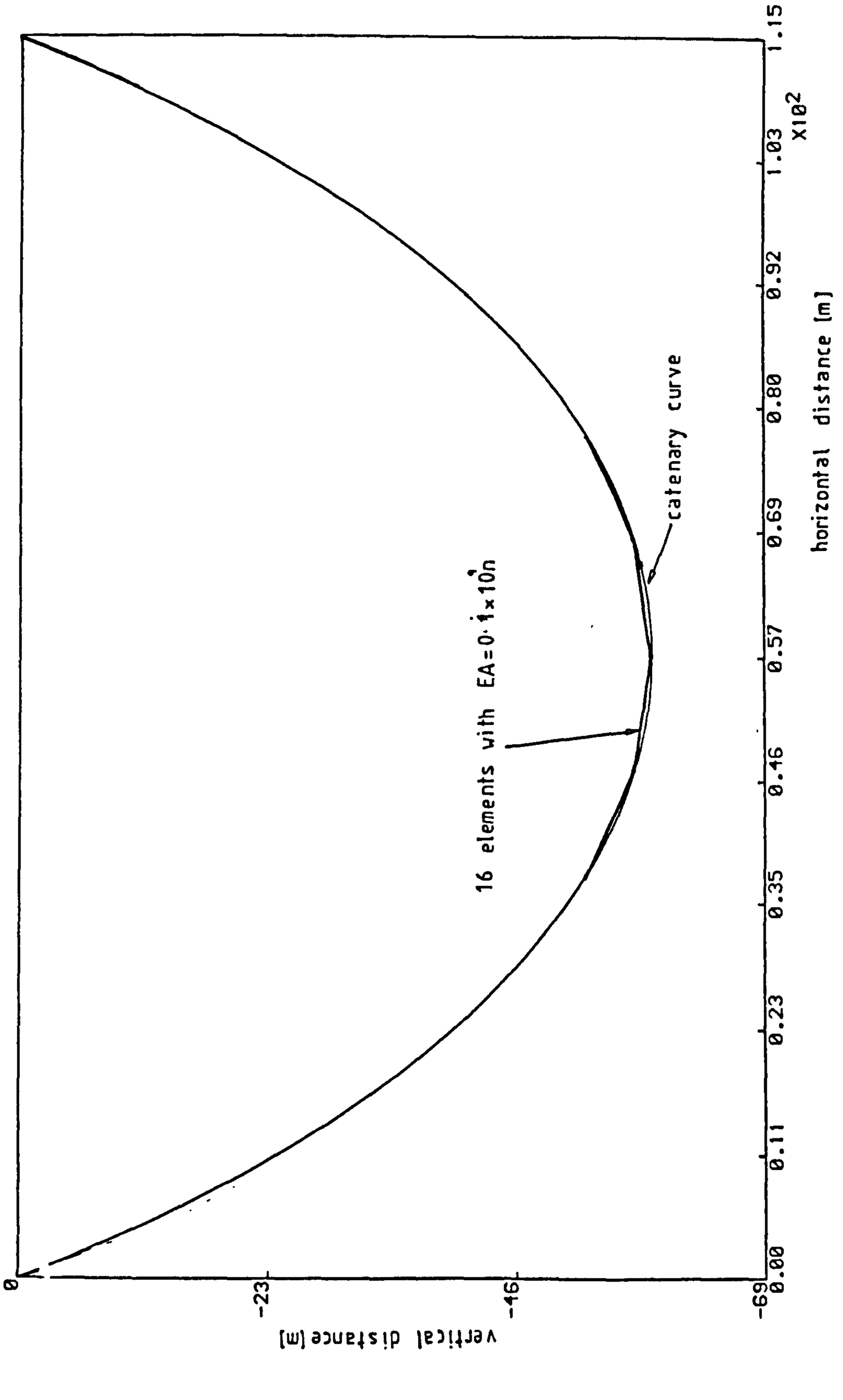

Figure 5.7.2 (b): Comparison with Catenary Curve

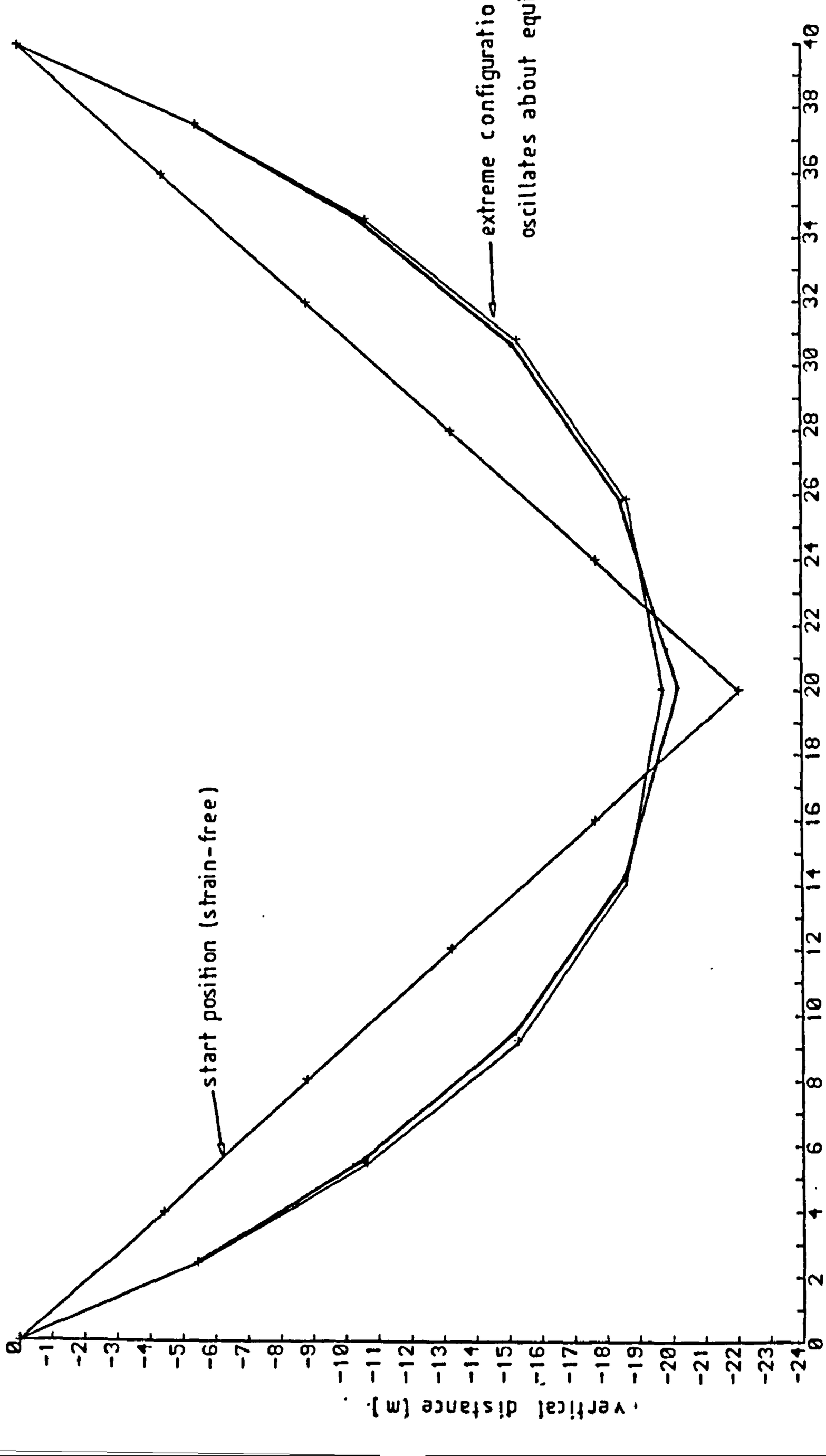

Figure 5.7.3 (a): Oscillation in the Second In-Plane Mode

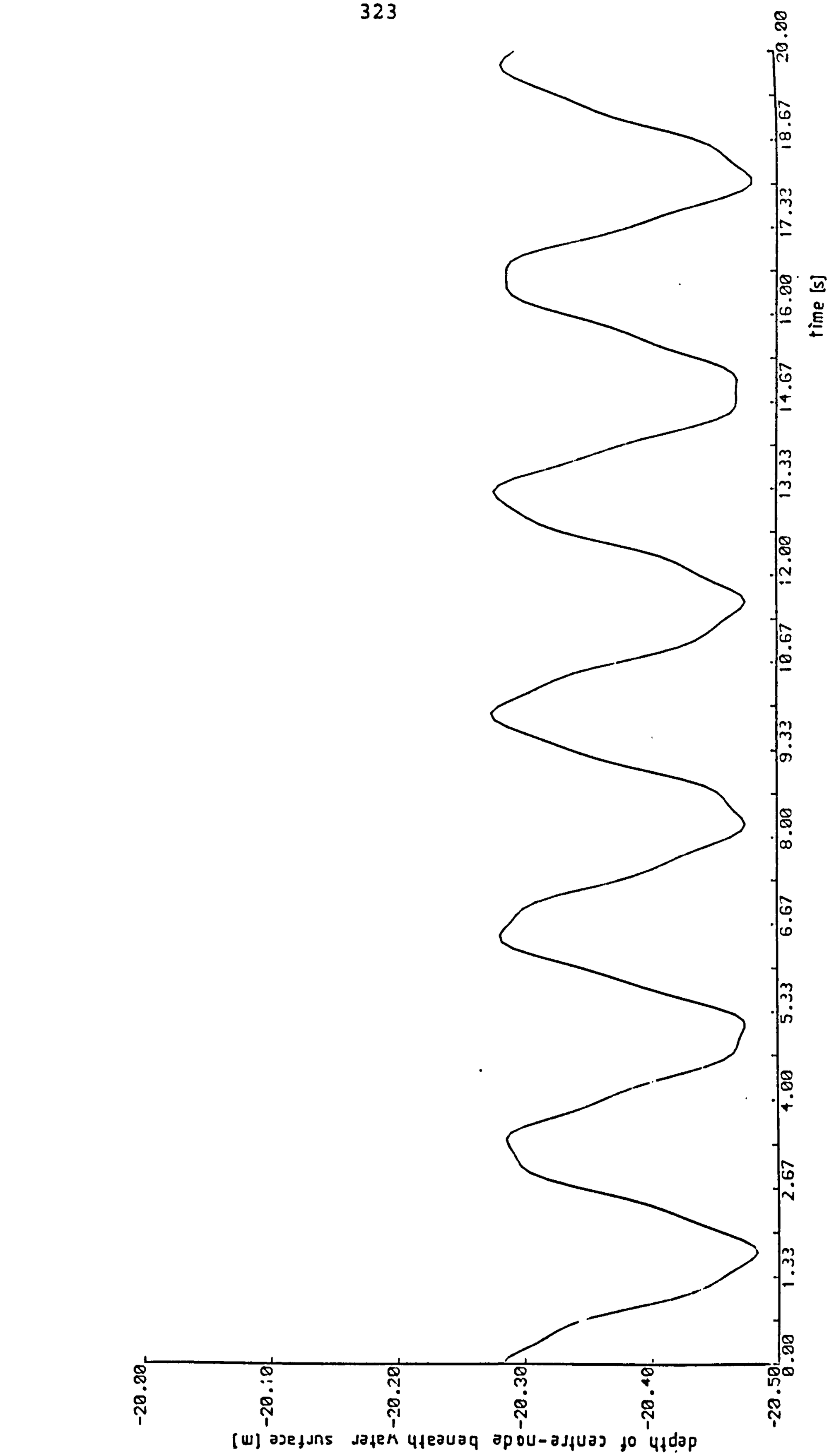

Figure 5.7.3 (b): Oscillation in the Second In-Plane Mode

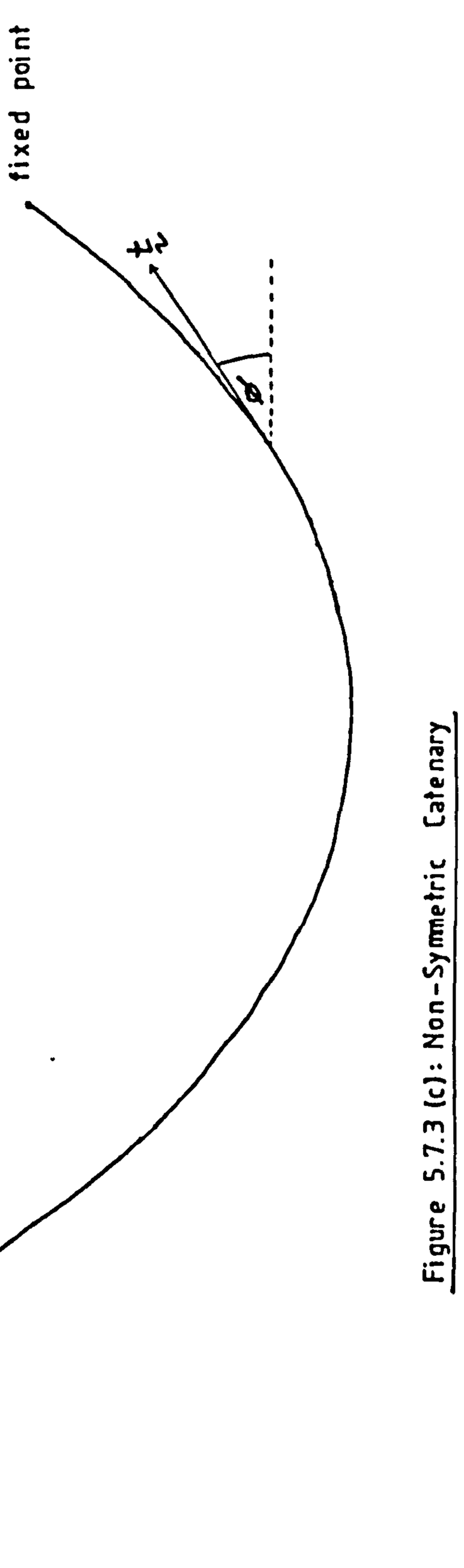

Figure 5.7.3 (c): Non-Symmetric Catenary

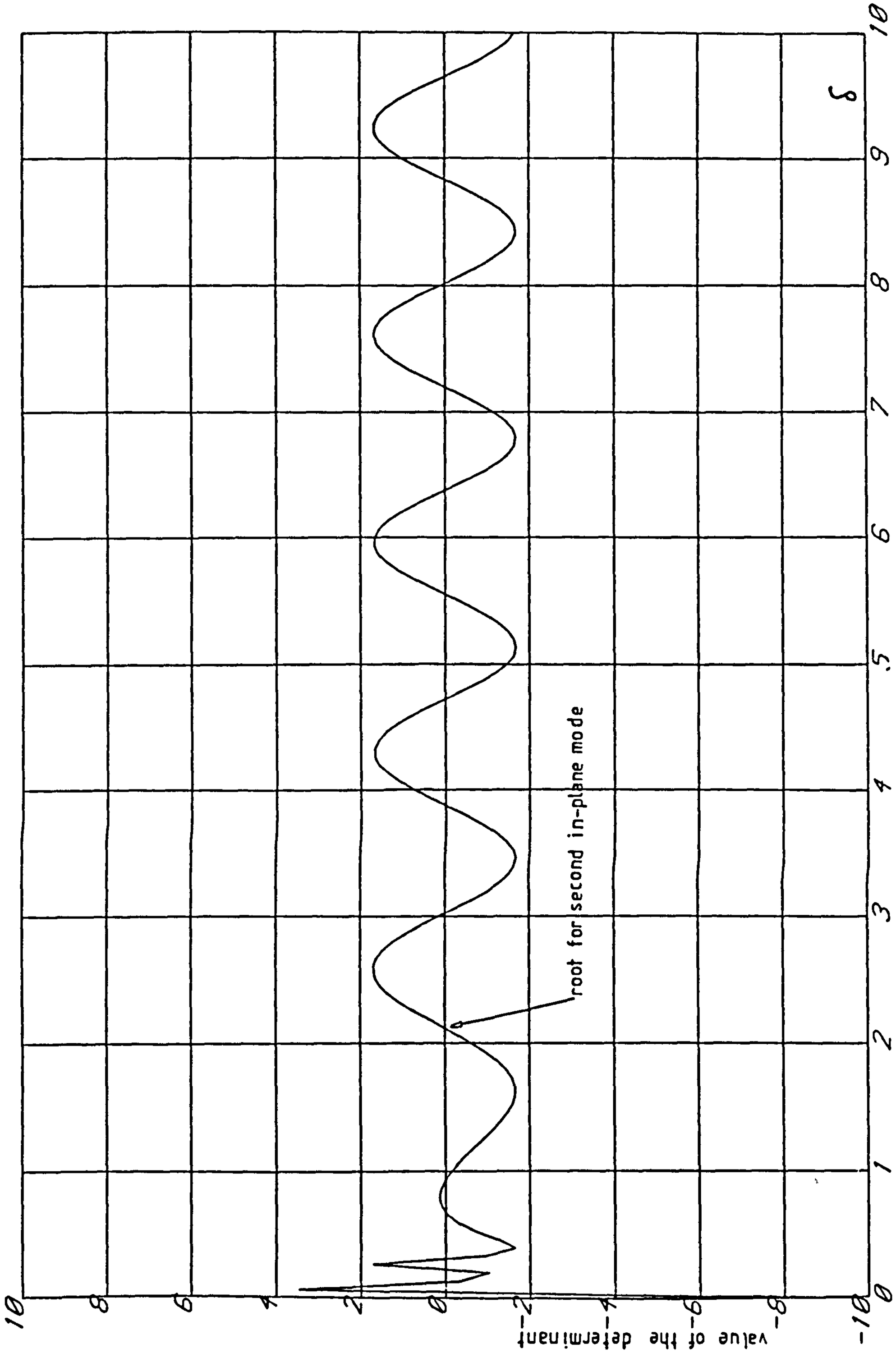

Figure 5.7.3(d): Plot of the Determinant occuring in Equation 5.7.3(a)

CHAPTER SIX:CONCLUSIONS

6.1:Introduction.

Conclusions about the work described in this thesis have been given in the relevant parts of the text. In this chapter a brief summary of the conclusions are given. Recommendations are made about possible future work.

6.2:Conclusions.

1.It is difficult to allow for large strain of the centre-line of the riser and also for the bending stiffness of the riser. However because of the present material properties of flexible risers i.e. high longitudinal stiffness they only suffer small strain anyway. All of the theory developed apart from the theory for the modelling of the bending stiffness, for reasons of generality and consistency, allows for large strain. It is possible that in the future the material properties of flexible risers may change significantly.

2.The partial differential equation (equation 2.5.4(a)) developed in section 2.5 for the dynamics of a riser reduces to all of the known relevant partial differential equations; Cristescu's partial differential equation for the dynamics of an extensible string (equation 2.5.4(c)), Nordgren's [1974] partial differential equation for an extensible riser (equation 2.5.4(b) and the standard small strain, small displacement partial differential equation (equation 2.5.6(a)) for a rigid, tensioned riser (see Kirk[1984]).

3.The strain energy expression derived in section 2.6.7 allows considerable physical insight and allows for the formulation of several versatile finite element discretizations.

4.The derivation of the variational equation for riser dynamics is more rigourous than the derivation of the partial differential equation for riser dynamics.

5.It is easy to allow for non-linear constitutive relationships for the resultant cross-sectional force. However if a non-linear constitutive relationship for the resultant cross-sectional force were used a non-standard expression for the bending moment would be obtained.

6.A mathematical model of the internal fluid flow has been found that should be adequate. In the derivation of the model it was assumed that the flow is inviscid, that over any cross-section of the riser the fluid speed is constant and that the strain in the riser is small.

7.The discretizations given in Chapter Three are perfectly adequate for a dynamic analysis of flexible riser systems and further theoretical development is not required.

8.The discretizations based on a continuum equation are to be prefered to discretizations which are based on describing the dynamics of a much simpler structural system e.g. the elastic lumped mass discretization.

9.It is possible to derive new discretizations ad infinitum.

10.For all of the discretizations that allow for the extensibility of the riser it is necessary to calculate the tensions in the elements (the elements could be either structural elements or finite elements) by using some incremental method. If this is not done then the large value of the longitudinal stiffness will cause a loss of significant digits in the calculation of the tensions. This will lead to erroneous forces which will swamp the other forces acting on the system and result eventually in numerical instability.

11.It is recommended that the longitudinal extension of the riser is allowed for. If it is not then less accurate estimates of the stress resultants are obtained and the possibility of longitudinal waves propagating along the riser is not permitted.

12.The inelastic lumped mass discretization given in section 3.3 is not recommended as it is overly complicated.

13.Many of the linear discretizations give almost identical equations of motion. However this does not imply that the choice of the discretization is not important because for example the finite element discretizations are more adaptable and simpler to use than the discretizations based on other methods.

14.Variational finite element discretizations are to be preferred over Petrov-Galerkin finite element discretizations because although in some circumstances they

are theoretically equivalent they are always considerably more simple.

15.It is possible to obtain a diagonal mass matrix and a block diagonal added mass matrix by using the finite element method.

16.It is unwise to use a numerical integration method that damps out the longitudinal waves that could propagate along the riser. This is because these longitudinal waves could significantly affect the fatigue life of the riser.

17.It is important to model the internal structural damping of the riser as it affects the vortex shedding and also the propagation of longitudinal waves.

18.Using a diagonal mass matrix (does not include the added mass matrix) introduces an unnecessary discretization error. This error is of practical significance and it is recommended that a consistent mass matrix always be used. If a consistent mass matrix is used then the use of a consistent added mass matrix is also recommended.

19.To find equilibrium positions of the riser system a specialist program is not required because the dynamics program can be used instead. For this case it is faster to neglect the added mass matrix and to use a diagonal mass matrix because the resultant diagonal mass matrix can be trivially inverted.

20.A computer program based on the cubic discretization

given in Chapter Three is considerably more complicated to write than a computer program for a linear discretization. However the resulting program for a given required accuracy is likely to need less C.P.U. time than a computer program based on a linear discretization. Because of the greater effort required for a computer program based on a cubic discretization, for a non-commercial application it is probably better to use a linear discretization. It might be thought that a linear discretization is not capable of modelling the bending stiffness of the riser however this is not the case.

21.The variational finite element discretizations that have been given are considerably more simple than any other finite element discretization for risers or cables. They are particularly suited for the analysis of structural problems.

22.An integration method that uses a timestep which is greater than around 0.1s cannot possibly follow the longitudinal wave motion in a typical riser. A timestep of 0.01s or less is recommended.

23.It is always better to use a discretization method based on a finite element method, because they are more adaptable.

24.The bending stiffness of the riser may be incorporated into a linear discretization in a very simple way that is remarkably accurate.

25.Using the theory for the modelling of the bending

stiffness the internal fluid flow effects may also be modelled accurately.

26.The cubic discretization is naturally adapted for the modelling of the bending stiffness.

27.If a consistent mass matrix is used then an additional force term in the equations of motion is generated if the top end of the riser is moving. It is unwise to neglect this additional force term.

28.Ground contact may be modelled simply by using a simple fluid model. The performance of this model could be improved by considering the extra viscosity of the seabed fluid. Special care must be taken to consider the possible riser configurations near the seabed.

29.It is important to take account of the possible discontinuities of loading on the elements near the water surface and in the region of the seabed. The necessary changes in the loading mechanism on a linear element have been found. This modified loading mechanism allows longer length elements to be used than would otherwise be possible.

30.If a consistent added mass matrix is used and the top end of the riser is moving then additional force terms are generated. It is unwise to neglect these additional terms.

31.The internal material damping of the riser may be incorporated into a linear discretization. There is no data available to estimate the internal material damping of the

riser thus its effect on the dynamics of the riser cannot be known. The forces arising from the damping may have to be calculated in an incremental way in order to avoid numerical instability.

32.The internal fluid force acting on the riser has two components; a component that is dependent on the geometry of the riser and one that is dependent on the motion of the riser.

33.A flexible riser system has complex dynamical behaviour. Considerable practical experience is needed for the design of such systems and a computer program such as the ones devised in this thesis should be of considerable help.

34.The computer program based on the linear elastic finite element is in agreement with model test results.

35.The bending stiffness of a typical riser will have no discernible effect on either the static equilibrium position of the riser or on the dynamic properties of the riser. This is because the magnitude of the bending stiffness is much smaller than the magnitude of the extensional stiffness. However the modelling of the bending stiffness is important because estimates of the bending moments of the riser will be necessary for fatigue life estimates.

36.The value of the longitudinal stiffness of a riser has a negligible effect on the natural periods of a riser in the steep "s" configuration.

37.If vortex shedding is a problem for a riser in the steep "s" configuration then the best way to overcome it would be to change the natural periods of the system by increasing the length of the riser between the top end of the riser and the buoy. A similar technique could probably be used for other riser configurations.

38.The dynamic response of the riser is not greatly dependent on the magnitude of the longitudinal stiffness of the riser.

39.The magnitude of the longitudinal stiffness controls the size of the timestep; too large a timestep results in numerical instability.

40.The Saxon and Cahn[1953] analytical solution provides an excellent check on a computer program for the dynamic analysis of flexible risers. The computer program based on a linear discretization is in very good agreement with this solution.

41.The computer program based on a linear discretization is in excellent agreement with the catenary analytical solution for a hanging string.

6.3:Recommendations for Further Work.

1.A computer program based on the cubic discretization may be written (this would be very time consuming) and a comparison could then be made with the computer program based on the linear discretization.

2.A study could be made of the dynamic responses under various different conditions (e.g. water depth and top motion) of the various different riser configurations e.g. steep "s", lazy "s". To do this would generate an enormous amount of data. It would be necessary to limit the range of parameters varied.

3.The effect of the internal fluid flow needs to be investigated (all the theoretical development has been presented in this thesis).

4.The internal material damping of the riser needs to be estimated experimentally and its effect investigated using the simple model presented in this thesis.

5.Further validation against model tests could be obtained.

6.Fatigue life predictions could be made.

REFERENCES

ANAND,G.V.: "Large-Amplitude Damped Free Vibration of a Stretched String" The Jnl. of the Acoustical Soceity of America Vol.45 No.5 1969

ANTMAN,S.S.: "The Theory of Rods" Handbuch der Physik, Mechanics of Solids vol.2 Springer Verlag 1972

BEATTY,M.F.,CHOW,A.C.: " On the Transverse Vibration of a Rubber String" Journal of Elasticity 13(1983)

BERNITSAS,M.M.,KOKARAKIS,J.E.: "Non-linear Six-Degree-of-Freedom Dynamic Model for Risers, Pipelines and Beams" Jnl.Ship.Res Sept. 1986 pp177-185

BOURGAT,J.F.,DUMAY,J.M.,GLOWINSKI,R.: "Large Displacement Calculations of Flexible Pipelines by Finite Element and Nonlinear Programming Methods" S.I.A.M. Jnl.Stat.Comput. Vol.1 No.1 March 1980

BREBBIA,C.A.,WALKER,S.: "Dynamic Analysis of Offshore Structures" Newnes-Butterworths 1979

CHANG,P.Y.,PILKEY,W.D.: "Static and Dynamic Analysis of Mooring Lines" J.Hydronautics Vol.7 No.1 Jan.1973

C.I.S.I. PETROLE SERVICES: "Flexan User's Guide" 1984

COHEN,H.: "A Non-linear Theory of Elastic Directed Curves" Int.J.Eng.Sci. 1966 vol.4 pp511-524

CONTE,S.D.,deBOOR,C.: "Elementary Numerical Analysis: An Algorithmic Approach" McGraw-Hill 1972 2nd ed.

COOK,R.D.: "Concepts and Applications of Finite Element Analysis" Wiley 1974

CRISTESCU,N.: "Dynamic Plasticity" North-Holland 1967

DO CARMO,M.: "Differential Geometry of Curves and Surfaces" Prentice-Hall 1976

EVERY,M.J.,KING,R.,WEAVER,D.S.: "Vortex-Excited Vibrations of Cylinders and Cables and their Suppression" Ocean Engineering Vol.9 No.2 pp.135-157 1982

FINITE ELEMENT ANALYSIS LTD.: "Lusas Examples Manual" Finite Element Analysis Ltd. version 86.07 July 1986

FLETCHER,C.A.: "Computational Galerkin Methods" Springer-Verlag 1984

FERRISS,D.H.: "Numerical Determination of the Configuration of an Underwater Umbilical Subjected to Steady Hydrodynamic Loading Part 2: Unsteady Aspects" N.P.L. Report D.I.T.C.2/82 March 1982

GALE,J.G.,SMITH,C.E.: "Vibrations of Suspended Cables" A.S.M.E. Jnl. of Applied Mechanics Vol.50 1983 pp.687-689

GARRETT,D.L.: "Dynamic Analysis of Slender Rods" Jnl. of Energy Resources Technology Dec 1982 Vol. 104

GHADIMI,R.:"A simple and efficient algorithm for the static and dynamic analysis of flexible marine risers" Computers and Structures 1988

GOODEY,W.J.: "On the Natural Modes and Frequencies of a Suspended Chain" Q.Jl.Mech.appl.Math. Vol.XIV Pt.1 1961

GOLDSTEIN,H.: "Classical Mechanics" Addison-Wesley 1980 2nd

ed.

GOODMAN,T.R.,BRESLIN,J.P.: "Statics and Dynamics of Anchoring Cables in Waves" Jnl. of Hydronautics Vol.104 No.4 1976

GREEN,A.E.,KNOPS,R.J.,LAWS.N.: "Large Deformations, Superposed Small Deformations and Stability of Elastic Rods" Int.Jnl.of Solids and Structures 1968 no.4 pp555-577

GREEN,A.E.,LAWS,N.: "A General Theory of Rods" Proc.R.Soc. 1966 A293 no.145

GRIFFIN,O.M.,RAMBERG,S.E.: "Some Recent Studies of Vortex Shedding with Application to Marine Tubulars and Risers"Jnl. of Energy Resources Technology A.S.M.E. Vol.104 March 1982

IRVINE,H.M.: "Energy Relations for a Suspended Cable" Q.Jl.Mech.appl.Math. Vol.XXXIII Pt.2 1980

IRVINE,H.M.,CAUGHEY,T.K.: "The Linear Theory of Free Vibrations of a Suspended Cable" Proc.Roy.Soc. A341 1974 pp.299-315

JAIN,M.K.: "Numerical Solution of Differential Equations" Wiley 1984 2nd ed.

KAMMAN,J.W.,HUSTON,R.L.: "Advanced Structural Applications: Modelling of Submerged Cable Dynamics" Computers and Structures Vol.20 No.1-3 pp623-629

KANE,T.R.,LEVINSON,D.A.: "Dynamics: Theory and Applications" McGraw-Hill 1985

KIBBLE,T.W.B.: "Classical Mechanics" McGraw-Hill 1973 2nd ed.

KING,R.: "A Review of Vortex Shedding Research and its Application" Ocean Engineering Vol.4 pp141-171

KIRK,C.L.: "Static and Dynamic Analysis of Moorings, Risers and Cables" C.I.T. Lecture Notes

LEONARD,J.W.: "Curved Finite Element Approximation to Nonlinear Cables" Fourth Annual Offshore Technology Conference 1972

LEONARD,J.W.,RECKER,W.W.: "Nonlinear Dynamics of Cables with Low Initial Tension" Jnl. of Eng. Mech. Div. A.S.C.E. Vol.98 No.EM2 April 1972

LEONARD,J.W.: "Nonlinear Dynamics of Curved Cable Elements" Jnl. of Eng. Mech. Div. A.S.C.E. Vol.99 No.EM3 June 1973

LEONARD,J.W.,NATH,J.H.: "Comparison of Finite Element and Lumped Parameter Methods for Oceanic Cables" Eng. Struct. Vol.3 1981

LOVE,A.E.H.: "A Treatise on the Mathematical Theory of Elasticity" Cambridge University Press 1952 4th ed.

MEIROVITCH,L: "Elements of Vibration Analysis" McGraw-Hill 1975

MEIROVITCH,L: "Computational Methods in Structural Dynamics " Sijthoff and Moordhoff 1980

MEGGITT,D.J.,WEBSTER,R.L.,MIGLIORE,H.J.: "Dynamic Response of Cables Subject to Ocean Forces" 12th Annual Offshore Technology Conference Houston Texas No.3854 1980

MITCHELL,A.R.,GRIFFITHS,D.F.: "The Finite Difference Method in Partial Differential Equations" Wiley 1980

MILNE,R.D.: "Applied Functional Analysis: An Introductory Treatment" Pitman 1980

MORISON,J.R.,O'BRIEN,M.P.,JOHNSON,J.W.,SCHAFF,S.A.: "The force exerted by Surface Waves on Piles" Petroleum Transactions, No. 108 TP2846 pp149-154 1950

NATH,J.H.,THRESHER,R.W.: "Anchor-Last Deployment for Buoy Moorings" 7th Annual Offshore Technology Conference Houston Texas 1975

NAKAJIMA,T.,MOTORA,S.,FUJINO,M.: "On the Dynamic Analysis of Multi-Component Mooring Lines" 14th Annual Offshore Technology Conference Houston Texas 1982

NORDGREN,R.P.: "On Computation of the Motion of Elastic Rods" Jnl.Appl.Mech. Sept. 1974 pp777-780

O'BRIEN,T.,FRANCIS,A.J.: "Cable Movements Under Two-Dimensional Loads" Jnl. of the Structural Div. A.S.C.E. Vol.19 No.ST3 June 1964

O'BRIEN,P.J.,McNAMARA,J.F.,DUNNE,F.: "Three-Dimensional Nonlinear Motions of Risers and Offshore Loading Towers" Int. Offshore Mechanics and Artic Engineering Symposium

Houston Texas 1987

O'BRIEN,P.J.,McNAMARA,J.F.,GILROY,S.G.: "Nonlinear Analysis of Flexible Risers Using Hybrid Finite Elements" Int. Offshore Mechanics and Artic Engineering Symposium Houston Texas 1986

ODEN,J.T.,REDDY,J.N.,: "Variational Methods in Theoretical Mechanics" Springer-Verlag 1976

ORTLOFF,C.R.,IVES,J.: "On the dynamic motion of a thin flexible cylinder in a viscous stream" Jnl.Fluid Mech. 1969 vol.38 part 4 pp713-720

OZEDMIR,H.: "A Finite Element Method for Cable Problems" Int. J. Solids Structures Vol.15 pp427-437 1979

PAIDOUSSIS,M.P.: "Dynamics of flexible slender cylinders in axial flow" Jnl.Fluid Mech. 1966 vol.26 part 4 pp717-736

PAIDOUSSIS,M.P.: "Dynamics of Cylindrical Structures Subjected to Axial Flow" Jnl.Sound and Vibration 1973 29(3) pp365-385

PAIDOUSSIS,M.P.,LUU,T.P.: "Dynamics of a Pipe Aspirating Fluid as Might be used in Ocean Mining" Jnl.Energy.Res.Tech. June 1985 vol.107

PETTENATI-AUZIERE,C.: "Flexible Dynamic Risers: State of the Art" The Way Forward fo Floating Production Systems Conference 16th/17th Dec. 1985 London

PEYROT,A.H.: "Marine Cable Structures" Jnl. of the

Structural Div. A.S.C.E. Vol.106 No.ST12 Dec.1980

PEYROT,A.H.,GOULOIS,A.M.: "Analysis of Cable Structures" Computers and Structures Vol.10 pp805-813 1979

PUGSLEY,A.G.: "On the Natural Frequencies of Suspended Chains" Q.Jl.Mech.appl.Math. Vol.II Pt.4 1949

RACTLIFFE,A.T.: "Dynamic Response of Flexible Catenary Risers" Int. Symp. on Developments in Floating Production Systems March 1984

RYAN,M.S.: "The Oscillations of a Neutrally Buoyant Submarine Cable in a Steady Current" M.Sc. Thesis Cranfield Institute of Technology

SARPKAYA,T.,ISAACSON,M.: "Mechanics of Wave Forces on Offshore Structures" Van Nostrand 1981

SAXON,D.S.,CAHN,A.S.: "Modes of Vibration of a Suspended Chain" Q.Jl.Mech.appl.Math. Vol.VI Pt.3 1953

SIMPSON,A.: "Determination of the Natural Frequencies of Multiconductor Overhead Transmission Lines" Jnl. of Sound and Vibration 20(4) pp.417-449 1972

SIMPSON.A: "Determination of the Inplane Natural Frequencies of Multispan Transmission Lines by Transfer Matrix Method" Proc.I.E.E. Vol.113 No.5 May 1966

SMITH,C.E.,THOMPSON,R.S.: "The Small Oscillations of a Suspended Flexible Line" A.S.M.E. Jnl. of Applied Mechanics Vol.40 1973 pp.624-626

SPIEGEL,M.R.: "Theoretical Mechanics" Schaum Series McGraw-Hill 1967

TRIANTAFYLLOU,G.S.,CHRYSSOSTOMIDIS,C.: "Stability of a string in axial flow" Proc. 4th int. O.M.A.E.S. Vol. 1 pp640-645 1985

TRIANTAFYLLOU,M.S.: "Preliminary Design of Mooring Systems" Jnl. of Ship Research Vol.26 No.1 March 1982 pp25-35

TRIANTAFYLLOU,M.S.: "The Dynamics of Taut Inclined Cables" Q.Jl.Mech.appl.Math. Vol.37 Pt.3 1984

TSINIPIZOGLOU,S.: "Three Dimensional Dynamics of Deep Sea Moorings" Dept. of Naval Architecture and Ocean Engineering, University of Glasgow Internal Report NAOE-HL-81-10 1981

TONG,P.,ROSSETTOS,J.N.: "Finite Element Method" M.I.T. Press 1977

U.K. OFFSHORE OPERATORS ASSOCIATION: "U.K. Offshore Oil and Gas" U.K. Offshore Operators Association 1986

WALTON,T.S.,POLACHEK,H.: "Calculation of Nonlinear Transient Motion of Cables" David Taylor Model Basin Report1279 1959

WALTON,T.S.,POLACHEK,H.: "Calculation of Transient Motion of Submerged Cables" Jnl. Math. Comp. No.14 1960

WAIT,R.,MITCHELL,A.R.: "Finite Element Analysis and Applications" Wiley 1985

WASHIZU,K.: "Variational Methods in Elasticity and Plasticity" Pergamon Press 1975

WEBSTER,R.L.: "Structural Response of Arbitrary Underwater Cable Systems" Ocean Engineering Mechanics A.S.M.E. O.E.D. Vol.1 1975(i)

WEBSTER,R.L.: "Nonlinear Static and Dynamic Response of Underwater Cable Structures Using the Finite Element Method" Seventh Annual Offshore Technology Conference 1975(ii)

WEN.R.K.,RAHIMZADEH,J.: "Nonlinear Elastic Frame Analysis by Finite Elements" Jnl. of Structural Engineering Vol.109 No.8 Aug.1983

WILLMORE,T.J.: "An Introduction to Differential Geometry" Oxford University Press 1983

WINGET,J.M.,HUSTON,R.L.: "Cable Dynamics: A Finite Segment Approach" Computers and Structures Vol.6 1976 pp475-480

ZIENKIEWICZ,O.C.: "The Finite Element Method" McGraw-Hill 1975

APPENDIX A:THE ELEMENTARY DIFFERENTIAL GEOMETRY OF SPACE CURVES

A.1:Introduction

In this appendix it is shown that given any space curve (i.e. a curve in three dimensional space) it is possible to define an orthonormal basis $\underset{\sim}{t}$, $\underset{\sim}{n}$, $\underset{\sim}{b}$ (as shown in figure A(a)) at each point on the space curve.

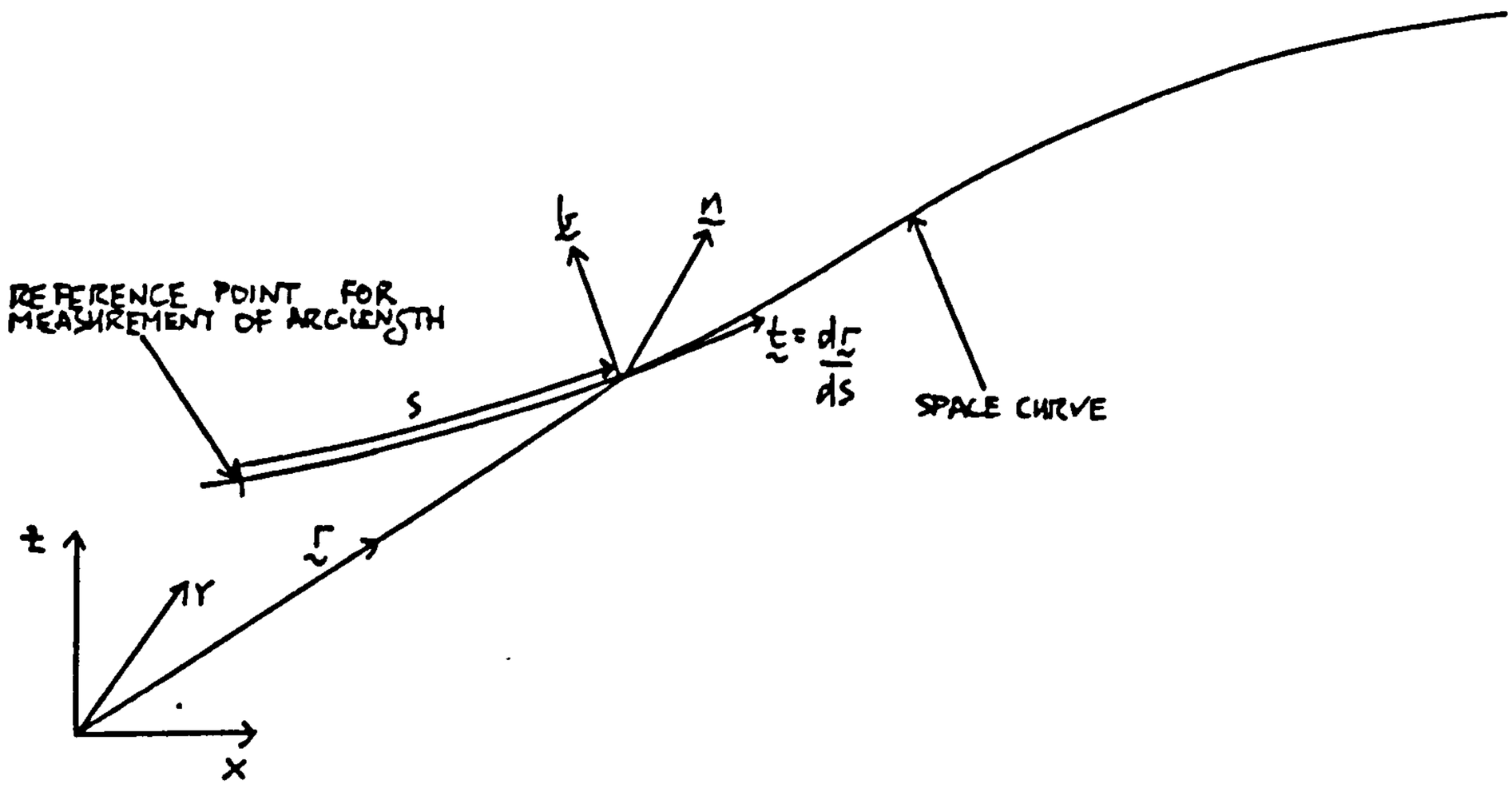

FIGURE A(a): ORTHONORMAL BASIS DEFINED AT A POINT ON A SPACE CURVE

A.2:Definition of the Tangent, Normal and Binormal Vectors

The position vector of a point on the space curve is parameterised in terms of the arc-length parameter s (which is measured from some reference point on the curve)

$$\underset{\sim}{r} = \underset{\sim}{r}(s) \qquad (A)$$

For a difference in arc-length δs along the curve

$$\delta\underset{\sim}{r} = \underset{\sim}{r}(s+\delta s) - \underset{\sim}{r}(s) = \frac{d\underset{\sim}{r}}{ds}\delta s + O(\delta s^2) \qquad (B)$$

Hence since in the limit as $\delta s \to 0$, $|\delta \underset{\sim}{r}| = |\delta s|$ the equality

$$\left| \frac{d\underset{\sim}{r}}{ds} \right| = 1 \qquad (C)$$

holds. Note that $\frac{d\underset{\sim}{r}}{ds}$ is a vector that points in the direction of increasing arc-length. The tangent vector $\underset{\sim}{t}$ to the space curve is defined as

$$\underset{\sim}{t} = \frac{d\underset{\sim}{r}}{ds} \qquad (D)$$

Now consider the second derivative of $\underset{\sim}{r}$. Since $\underset{\sim}{t}$ is a unit vector

$$\frac{d^2\underset{\sim}{r}}{ds^2} \cdot \frac{d\underset{\sim}{r}}{ds} = 0 \qquad (E)$$

Thus $\frac{d^2\underset{\sim}{r}}{ds^2}$ is a vector that is orthogonal to $\underset{\sim}{t}$. The normal $\underset{\sim}{n}$ and the curvature κ are defined by

$$\kappa \underset{\sim}{n} = \frac{d^2\underset{\sim}{r}}{ds^2} \qquad (F)$$

where $\underset{\sim}{n} \cdot \underset{\sim}{n} = 1$ and κ is restricted so that $\kappa > 0$. Note that $\underset{\sim}{n}$ is not uniquely determined if the curve is a straight line because $\frac{d^2\underset{\sim}{r}}{ds^2} = 0$. Similarly $\underset{\sim}{n}$ is not uniquely determined from this definition at points on the curve at which $\frac{d^2\underset{\sim}{r}}{ds^2} = \underset{\sim}{0}$.

The binormal vector to the curve is defined by

$$\underset{\sim}{b} = \underset{\sim}{t} \wedge \underset{\sim}{n} \qquad (G)$$

This vector is clearly only defined at those points at which the normal vector is defined.

A.3:Frenet-Serret Formulae

Since $\underset{\sim}{n}$ is a unit vector

$$\frac{d\underset{\sim}{n}}{ds} \cdot \underset{\sim}{n} = 0$$

which gives

$$\frac{d\underset{\sim}{n}}{ds} = \alpha \underset{\sim}{t} + \tau \underset{\sim}{b} \qquad (a)$$

where $\alpha = \alpha(s)$ and $\tau = \tau(s)$. Now

$$\frac{d\underset{\sim}{b}}{ds} = \underset{\sim}{t} \wedge \frac{d\underset{\sim}{n}}{ds}$$

using equation (a) gives

$$\frac{d\underset{\sim}{b}}{ds} = -\tau \underset{\sim}{n} \qquad (b)$$

The scalar τ is termed the torsion of the curve. Now

$$0 = \frac{d(\underset{\sim}{t} \cdot \underset{\sim}{n})}{ds} = \frac{d\underset{\sim}{t}}{ds} \cdot \underset{\sim}{n} + \underset{\sim}{t} \cdot \frac{d\underset{\sim}{n}}{ds} = \kappa + \alpha$$

therefore $\alpha = -\kappa$ and

$$\frac{d\underset{\sim}{n}}{ds} = \tau \underset{\sim}{b} - \kappa \underset{\sim}{t} \qquad (c)$$

Equations (b) and (c) are termed the Frenet-Serret formulae. Further details of the differential geometry of space curves can be found in Willmore[1983] or M. Do Carmo[1976].

APPENDIX B:THE PURE STRETCHING ENERGY FOR LINEAR AND NONLINEAR STRINGS

B.1:Introduction.

Consider the string shown in figure B.1(a). The ends of the string are not necessarily fixed. The string might be linearly elastic or non-linearly elastic; a linearly elastic string is defined as one that obeys the constitutive relationship 2.3.2(a) and non-linearly elastic string as one that does not. From equation 2.6.7(a) the pure stretching energy (denoted by S.E.) of the string is

$$S.E. = \int_0^L \left\{ \int T_e\left(\frac{\partial s}{\partial s_0}\right)\, d\left(\frac{\partial s}{\partial s_0}\right) \right\} ds_0 \qquad (a)$$

In this appendix this expression is evaluated for both a linearly elastic string and a non-linearly elastic string.

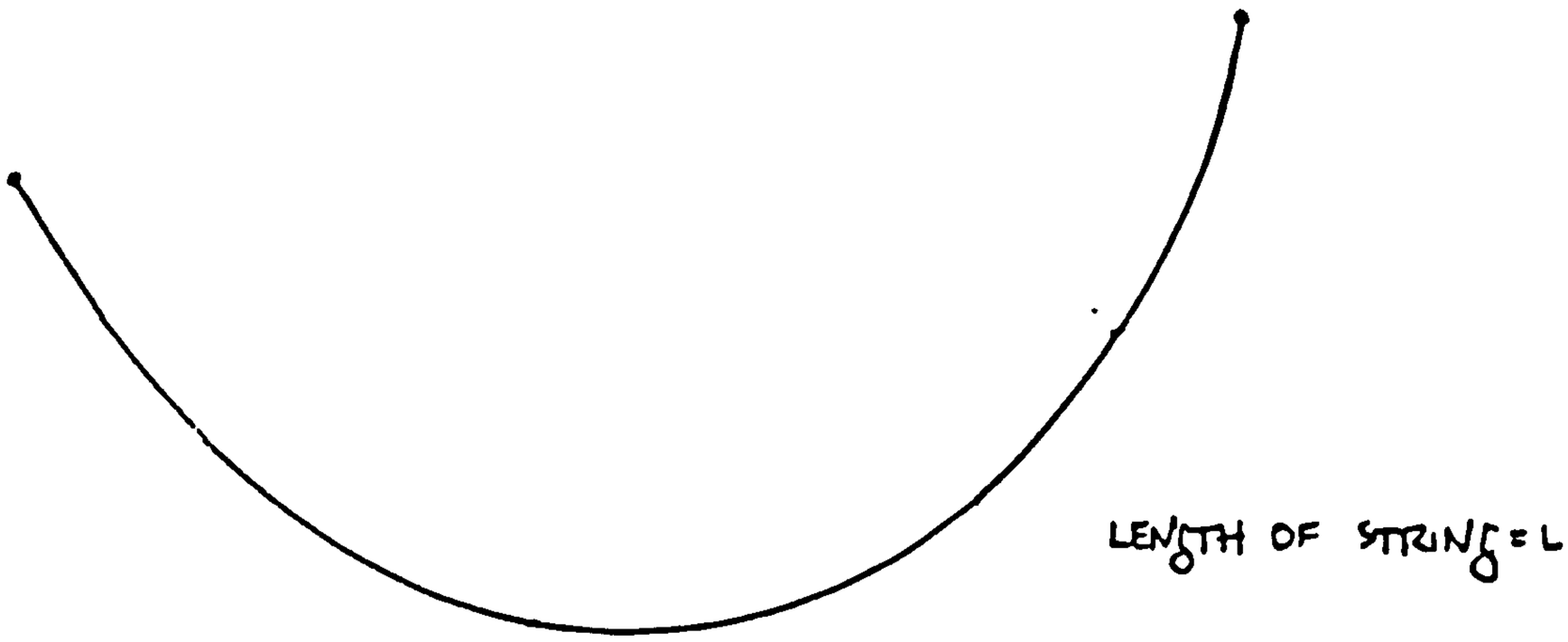

FIGURE B.1(a): MOVING ELASTIC STRINGS

B.2:Stretching Energy for a Linearly Elastic String.

For a linear string

$$T_e = A_0 E \left(\frac{\partial s}{\partial s_0} - 1 \right) \qquad (A)$$

therefore

$$S.E. = \int_0^L A_0 E \left\{ \frac{\left(\frac{\partial s}{\partial s_0}\right)^2}{2} - \frac{\partial s}{\partial s_0} \right\} + \text{constant} \quad ds_0 \qquad (B)$$

Note that the strain energy is only determined up to a constant hence with suitable choice of the constant the pure stretching energy is given by

$$S.E. = \int_0^L \frac{1}{2EA_0} T_e^2 \, ds_0 \qquad (a)$$

Compare this with the result obtained by Irvine[1980] and Anand[1969].

B.2.1:Reduction of the Strain Energy to the Result for a Straight String

Consider the string shown in figure B.2.1(a). The string is initially stretched so that the tension in the string in the equilibrium position is T_0 . If the string is subject to small displacements only then the strain energy in the string is given by the result

(Kibble[1973]) $$V = \frac{1}{2} T_0 \int_0^L \left(\frac{\partial y}{\partial x}\right)^2 dx \qquad (A)$$

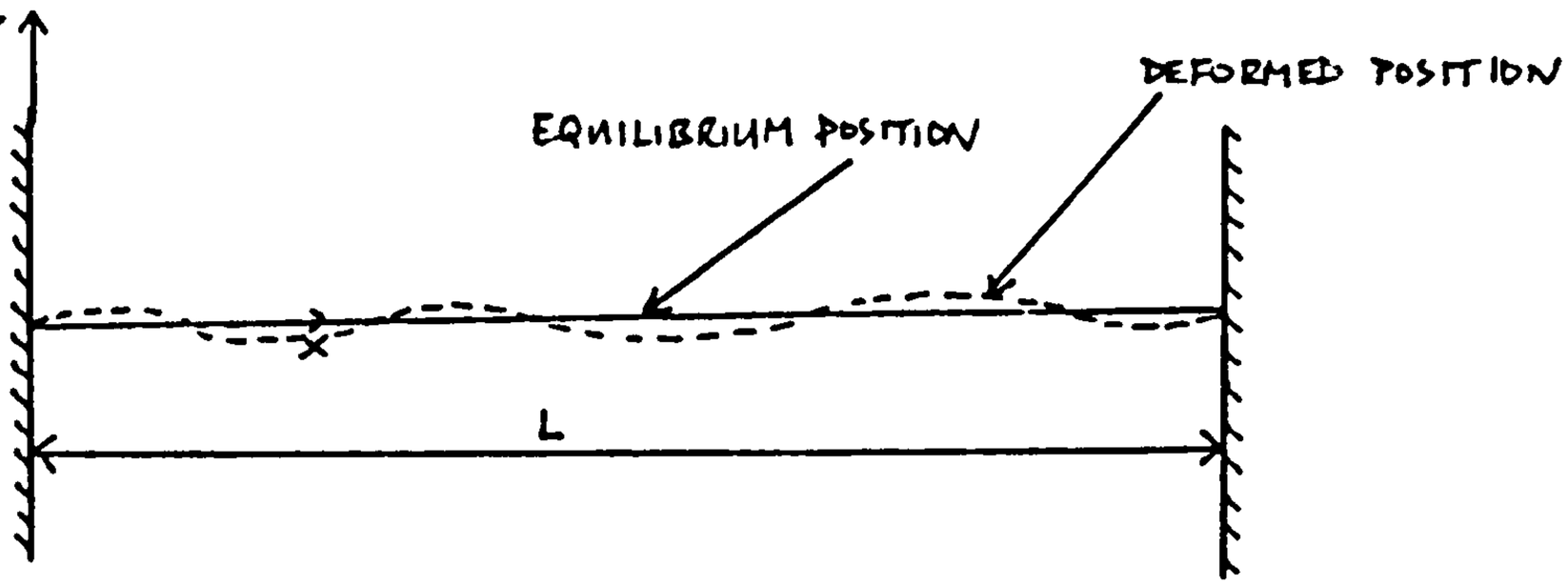

FIGURE B.2.1(4): DEFORMATION OF A STRAIGHT STRING

In this section it is shown how the strain energy expression ,equation 2.6.7(a), reduces to this result.

The position vector $\underset{\sim}{r}$ of a point on the string is given by

$$\underset{\sim}{r} = s_0 \left(1 + \frac{T_0}{EA}\right) \underset{\sim}{e}_x + y \underset{\sim}{e}_y \qquad (B)$$

for small displacements. Therefore

$$\frac{\partial \underset{\sim}{r}}{\partial s_0} \cdot \frac{\partial \underset{\sim}{r}}{\partial s_0} = \left(1 + \frac{T_0}{EA}\right)^2 + \left(\frac{\partial y}{\partial s_0}\right)^2 \qquad (C)$$

Hence the tension T in the string is given by

$$T = AE \left\{ \left[\left(1 + \frac{T_0}{EA}\right)^2 + \left(\frac{\partial y}{\partial s_0}\right)^2 \right]^{\frac{1}{2}} - 1 \right\} \qquad (D)$$

It is now assumed that the initial strain in the riser is small so that T_0/EA is a small quantity. Hence since $\frac{\partial y}{\partial s_0}$ is a small quantity also

$$T = EA \left\{ \frac{T_0}{EA} + \frac{1}{2} \left(\frac{\partial y}{\partial s_0}\right)^2 \right\} = T_0 + \frac{AE}{2} \left(\frac{\partial y}{\partial s_0}\right)^2 \qquad (E)$$

therefore

$$T^2 = T_0^2 + T_0 A E \left(\frac{\partial y}{\partial s_0}\right)^2 + \quad O\left(\left[\frac{\partial y}{\partial s_0}\right]^4\right) \qquad (F)$$

which gives using equation B.2(a)

$$V = \int_0^L \frac{1}{2} T_0 \left(\frac{dy}{dx}\right)^2 dx \qquad (G)$$

since V is only determined up to a constant and $s_0 = x$.

This is the required result.

B.3:Stretching Energy for a Non-linearly Elastic String.

From the constitutive relationship 2.3.2(d)

$$T_e = \frac{A_0 E}{3} \left\{ \frac{\partial s}{\partial s_0} - \left(\frac{1}{\frac{\partial s}{\partial s_0}}\right)^2 \right\} \qquad (A)$$

which gives using equation B.1(a)

$$S.E. = \int_0^L \frac{A_0 E}{3} \left\{ \frac{1}{2}\left(\frac{\partial s}{\partial s_0}\right)^2 + \frac{1}{\left(\frac{\partial s}{\partial s_0}\right)} \right\} ds_0 \qquad (B)$$

APPENDIX C:ALGEBRAIC MANIPULATION FOR MOVING ENDPOINTS OF THE RISER

Consider the result S of the following matrix multiplication

$$S = \begin{bmatrix} a_1 & a_2 & a_3 & a_4 \end{bmatrix} \begin{bmatrix} B_{11} & B_{12} & B_{13} & B_{14} \\ B_{21} & B_{22} & B_{23} & B_{24} \\ B_{31} & B_{32} & B_{33} & B_{34} \\ B_{41} & B_{42} & B_{43} & B_{44} \end{bmatrix} \begin{bmatrix} C_1 \\ C_2 \\ C_3 \\ C_4 \end{bmatrix} \quad (A)$$

IF $a_1 = a_4 = 0$

$$S = \begin{bmatrix} 0 & a_2 & a_3 & 0 \end{bmatrix} \begin{bmatrix} 0 & 0 & 0 & 0 \\ B_{21} & B_{22} & B_{23} & B_{24} \\ B_{31} & B_{32} & B_{33} & B_{34} \\ 0 & 0 & 0 & 0 \end{bmatrix} \begin{bmatrix} C_1 \\ C_2 \\ C_3 \\ C_4 \end{bmatrix} \quad (B)$$

$$= \begin{bmatrix} 0 & a_2 & a_3 & 0 \end{bmatrix} \begin{bmatrix} 0 & 0 & 0 & 0 \\ B_{21} & B_{22} & B_{23} & B_{24} \\ B_{31} & B_{32} & B_{33} & B_{34} \\ 0 & 0 & 0 & 0 \end{bmatrix} \left(\begin{bmatrix} C_1 \\ 0 \\ 0 \\ C_4 \end{bmatrix} + \begin{bmatrix} 0 \\ C_2 \\ C_3 \\ 0 \end{bmatrix} \right)$$

$$= \begin{bmatrix} 0 & a_2 & a_3 & 0 \end{bmatrix} \left(\begin{bmatrix} 0 \\ C_1 B_{21} + C_4 B_{24} \\ C_1 B_{31} + C_4 B_{34} \\ 0 \end{bmatrix} + \begin{bmatrix} 0 & 0 & 0 & 0 \\ 0 & B_{22} & B_{23} & 0 \\ 0 & B_{32} & B_{33} & 0 \\ 0 & 0 & 0 & 0 \end{bmatrix} \begin{bmatrix} 0 \\ C_2 \\ C_3 \\ 0 \end{bmatrix} \right)$$

$$= \begin{bmatrix} a_2 & a_3 \end{bmatrix} \left(\begin{bmatrix} C_1 B_{21} + C_4 B_{24} \\ C_1 B_{31} + C_4 B_{34} \end{bmatrix} + \begin{bmatrix} B_{22} & B_{23} \\ B_{32} & B_{33} \end{bmatrix} \begin{bmatrix} C_2 \\ C_3 \end{bmatrix} \right)$$

APPENDIX D:DATA FOR FLEXIBLE RISERS OF VARIOUS DIFFERENT DIAMETERS

DATA FOR COFLEXIP RISERS:

Inside Diameter [metres]	0.102	0.152	0.203	0.254	0.305
Outside Diameter [metres]	0.178	0.229	0.292	0.353	0.388
Minimum Bend Radius [metres]	1.16	1.50	2.00	2.30	2.55
Density of Riser per unit length [kg/m]	77.2	109	149	208	158
Maximum Pressure [Mega pascals]	4.76	3.57	2.38	2.14	1.19

DATA FOR DUNLOP RISERS:

Inside Diameter [metres]	0.152	0.203	0.254	0.392
Outside Diameter [metres]	0.214	0.265	0.326	0.362
Density per unit length [Kg/m]	48.9	64.3	102.3	116.3
Working Pressure [Mega Pa]	2.07	10.7	20.7	20.7
Test Pressure [Mega Pa]	4.14	32.1	31.0	31.0
Burst Pressure [Mega Pa]	600	475	603	536
Hydrostatic Collapse Pressure [Mega Pa]	19.3	11.7	6.48	5.90
Damaging Pull in a Straight Line [Mega N]	0.607	0.592	0.511	0.516
Minimum Bend Radius [metres]	1.5	2.0	2.4	2.9

Bending Stiffness at 293K [Nm^2]	3870	9150	17900	27200
Maximum Elongation at Test Pressure	±2%	±2%	±2%	±2%

Note: Dunlop riser of diameter 0.203m is a sweet gas lift pipe; all the other Dunlop risers are sweet diphasic crude pipes.